The cephalopod umwelt

Matthew A. Birk

December 5, 2022

Contents

Detailed Contents

List of Figures

Part I

Their physical environment

Chapter 1

Physical parameters of interest to cephalopods

1.1 Water

Water is an extremely unique molecule. Each water molecule has two H atoms covalently bonded to an oxygen atom. The two covalent hydrogens are 104.5° apart. The oxygen atoms also form hydrogen bonds with hydrogen atoms from adjacent molecules due to the uneven sharing of electrons by the oxygen (partially negative). The H-bonds are 20x weaker than the covalent O-H bonds. Liquid water has anywhere from 90% down to maybe as much as 70% of the molecules hydrogen bound to conspecifics. Because of the hydrogen bonds and the molecule's partial polarity, the molecules have a high dielectric constant (decrease the attraction of ions to each other) which is why water is such a good solvent.

Water has a high surface tension because the hydrogen bonds are more concentrated at the surface than within the water parcel because there are fewer neighbors and therefore more bonds with existing neighbors.

1.1.1 Earth's water source

It is now believed that much of Earth's water originated from asteroids rather than comets. In addition to being in a Goldilocks zone regarding temperatures for all three phases of water, water has only stayed on Earth all these billions of years because Earth is big enough that the core still hasn't cooled down and solidified. Once it does, the magnetic field will be lost and solar winds will strip away the atmosphere including all water vapor, leaving only solid ice, as on other planets.

1.1.2 Rayleigh fractionation

When water evaporates at the surface, the lighter oxygen isotope, ^{16}O is preferentially vaporized over the heavier isotope ^{18}O because it has a higher vapor pressure because it weighs less, thus leading to the evaporated water vapor and the source water being fractionated, or differing in their isotopic ratio from the original source water. For example, evaporated water vapor may have $\delta^{18}O = -8$ from its source water, meaning that the vapor's isotopic ratio, $^{18}O/^{16}O$, is 0.8% lower than the source water's ratio. As this water vapor moves towards the poles on atmospheric circulatory cells (subsection 2.1.1), each time it rains the vapor fractionates again, preferentially dumping the ^{18}O, thus further decreasing the $\delta^{18}O$ value of the remaining water vapor (Pilson, 2013). Since so much evaporation happens near the equator and the net movement of the vapor is poleward along atmospheric cells, tropical seawater is slightly enriched in ^{18}O and there's a relationship between both seawater and rainfall $\delta^{18}O$ with latitude and temperature. The fractionation of evaporation is also dependent on salinity and thus the salinity must be considered when examining a water sample's $\delta^{18}O$ (Pilson, 2013).

Mean seawater isotopic ratios are defined as SMOW: standard mean ocean water.

1.1.3 Ice

Ice has the H_2O molecules arranged in tetrahedrons (Pilson, 2013). Ice collapses into liquid water when less than 90% of its hydrogen bonds remain.

As seawater cools, the density increases. Because seawater increases in density with decreasing temperature right up to the freezing point (when $S > 24.6$; otherwise there's a density maximum before reaching the freezing point (section 1.6)), chilled seawater will sink and be replaced by warmer seawater until finally the entire water column is uniformly at the freezing point. Only then can sea ice form at the surface (Pilson, 2013). This assumes that salinity is constant, the surface water sinking rate is faster than the cooling rate, and other forms of mixing are negligible. Thus, I would expect that the temperature distribution below sea ice to be quite constant.

Table 1.1: Distribution of water on Earth. Data from Pilson 2013.

Source	Volume (10^3 km^3)	Volume (% of total)
Seawater	1,346,000	97.4
Continental ice	27,800	2.0
Groundwater	8062	0.6
Lakes and rivers	225	< 0.1
Sea ice	20	< 0.1
Vapor	13	< 0.1
TOTAL	1,386,050	100

1.1.3.1 Effect of salinity on freezing point

Seawater (S = 35 psu) freezes at around –2 °C (Pilson, 2013). This freezing point scales linearly with salinity according to $T_{freezing} = -1.922/35\,S$. The reason for this freezing point depression with increasing salinity is due to salinity's effect on vapor pressure. Salts decrease water's vapor pressure because they form hydration shells which bind more water molecules into the liquid phase, thus keeping more molecules out of the vapor phase. At the freezing point temperature of water, the vapor pressure of water and ice are equal. Salt differentially affects the vapor pressures of water and ice, lowering the vapor pressure of water relatively more than ice, thus causing ice to release more molecules into the vapor phase than water and thus cause a net shift towards water, causing the ice to melt. A colder temperature must be reached before the vapor pressure of water and ice are equal again. In addition, salts interfere with hydrogen bonding between water molecules, thus requiring a colder temperature in order for 90% of the H-bonds to stay intact for ice to form. This is why salinity affects freezing point of water.

Air can hold double the amount of water vapor with every 10°C increase in temperature (Webb).

1.2 Light

Typical PAR at the surface on a sunny summer day is 2000 μmol photons $m^{-2}s^{-1}$ (µEinsteins $m^{-2}s^{-1}$). On a cloudy winter day this decreases to ~750 μmol photons $m^{-2}s^{-1}$ (µEinsteins $m^{-2}s^{-1}$). The depth that a given wavelength of light reaches in the ocean is dependent on the angle of sunlight, cloudiness, and the water turbidity. Irradiance decreases with depth according to Lambert Beer's Law due to the electrical conductivity of seawater:

$$I_z = I_0 e^{-k\Delta z}$$

where k is the attenuation coefficient (m^{-1}) which is affected by turbidity, [POM], etc. The depth at which light of a given wavelength penetrates determines the depth of photosynthesis and thus, P_{O_2} at depth (section 1.8). Generally, in the open ocean, irradiance falls an order of magnitude every 75 meters until it is gone by 1000 m or so (Pennisi, 2012).

In the open ocean, ~474 nm light penetrates the furthest (Jerlov 1976) while in the coastal ocean light transmission is greatest at 500-550 nm (Cohen and Forward, 2009).

At sunrise and sunset, light levels change about 0.3% per second and reach a maximum rate of change of ~0.4% about 20-30 minutes after sunset or before sunrise (Cohen and Forward, 2009).

1.2.1 Vertical zonation nomenclature

The epipelagic zone, where light is sufficient for photosynthesis, can extend down to about 200 m. Below this, the mesopelagic zone extends to the absolute limit of light radiation around 1000 m. The bathypelagic zone goes deeper from 1000 m to 4000 m, the average ocean depth. Where the seafloor is deeper, the abyssopelagic zone ranges from 4000 m to the seafloor.

1.3 Sound

Sound travels through compression waves. Sound travels through seawater at around 1500 m/s compared to about 330 m/s in air. The speed is slightly variable due to temperature, salinity, and pressure. In general, warmer, saltier, and higher pressure water moves sound faster because the molecules vibrating are closer together or have more energy. Due to the thermocline and increasing pressure, sound travels slowest and therefore furthest in mid-ocean depths in a region known as the Sound Fixing And Ranging, or SOFAR channel.

Table 1.2: Major constituents in seawater. Their order can be remembered with the following pneumonic: "**C**ranchiids **N**ever **M**eet **S**epiids **Ca**use **K**illing **D**epths **Br**eak **B**ones **S**wiftly and **F**iercely".

Species	Total concentration at S = 35 psu ($mol \cdot kg^{-1}$)
H_2O	53.6
Cl^-	0.546
Na^+	0.469
Mg^{2+}	0.0528
SO_4^{2-}	0.0282
Ca^{2+}	0.0103
K^+	0.0102
DIC	$\approx 2100 \cdot 10^{-6}$
Br^-	$844 \cdot 10^{-6}$
B	$416 \cdot 10^{-6}$
Sr^{2+}	$90.6 \cdot 10^{-6}$
F^-	$68 \cdot 10^{-6}$

1.4 Temperature

Global mean oceanic temperature is 3.5 ºC with 75% of the ocean ranging from 0 to 4 ºC. Much of this is the ocean interior, however, in which few cephalopods inhabit.

The specific heat of seawater is roughly 3850 J / kg / °C.

Wind creates a mixed layer that is isothermal down to an average of 70 m (Pilson, 2013). At high latitudes where winds are strong the mixed layer depth (MLD) can get much deeper, as much as 500 m! From the bottom of the mixed layer, temperature decreases approximately exponentially with depth. The main thermocline of the open ocean that stratifies the surface waters from the ocean interior is at 200-1000 m depth depending on latitude, season, and mixing. In the summer, a diurnal thermocline of a few degrees can form in the top few meters of the open ocean due to solar radiation and little mixing, but this heat is often radiated back to the atmosphere at night.

The warmer the water, the lower the $\delta^{18}O$.

The top 3.3 m of seawater in the ocean has as much heat energy in it as the entire atmosphere above.

1.5 Salinity

1.5.1 Composition and reactivity

The oceans are salty because salts wash into the ocean from land. The residence time of water in the ocean is ~40k years. Thus, the water in the ocean has evaporated, precipitated on land, picked up ions, and washed back into the ocean many times in Earth's history.

The ionic composition of conservative ions in seawater maintain constant proportions globally (for S $\geq$ 5) (Table 1.2). Global mean salinity is 34.72 psu with 75% of the ocean ranging from 34 to 35 psu. The practical salinity scale (PSS) is slightly different from the absolute scale (S_A; g/kg) such that 35 psu seawater has 35.17 g of salt in 1 kg of seawater. Standard seawater salinity (35 psu) results in an osmolality of 1035 mOsm. Seawater is always electroneutral, such that there are just as many cation charges as anion charges (Pilson, 2013).

Each ion dissolved in seawater has anywhere from 1 to 10 water molecules surrounding it. In addition, most ions in seawater form ion pairs, or weak associations with ions of opposite charges. While ion pairing does not affect the total concentration of a given ion species, it does affect its reactivity since a proportion (sometimes a very large proportion) are paired with other ions and not as available for reactions. The "free" ions in solution that are not in ion pairs are still affected by the ionic strength of the solution because the ion of interest is surrounded by many other ions of opposite charge which decrease the central ion's reactivity. This effect is parameterized as activity coefficients. Because of ion pairing and activity coefficients, many chemical equilibria in seawater are "apparent" equilibrium constants which are adjusted numerically to account for the difference between the reactivity of the free ions and what the reactivity of the total concentration would be in fresh water.

Seawater (35 psu) has an ionic strength $\approx$ 0.7 M.

$$\text{Ionic strength} = \frac{1}{2} \sum \text{molality}_i \cdot \text{charge}_i^2$$

1.5.2 Distribution and dynamics

Salinity is a function of evaporation/precipitation (most important for open ocean surface waters), freshwater input, and ice melting. Thus there is a latitudinal pattern in salinity due to atmospheric circulation cells (subsection 2.1.1). Salinity is low at the equator and 60° where atmospheric upwelling is strong (precipitation) and salinity is high at 30° where atmospheric downwelling is strong and solar radiation causes much evaporation.

Within the ocean interior, the salinity of a water parcel changes very slowly, such that the salinity of a deep water parcel is a characteristic of its source (where it was last at the surface). In estuaries, freshwater decreases overall salinity but can also alter the proportions of the major constituents. Relative to seawater, fresh water has a much higher proportion of HCO_3^-, Ca^{2+}, and Si. When seawater evaporates, the salts do not precipitate all together. Instead, as evaporation progresses, $CaCO_3$ precipitates first followed by $CaSO_4$, NaCl, then everything else.

1.5.2.1 Atlantic vs. Pacific salinity

On average the Atlantic is more saline than the Pacific. This is due to a combination of highly saline water leaving the Mediterranean after some of the evaporated water is sent via westerlies to Pacific-bound water basins (section 4.15) and tropical easterly winds carrying evaporated water west over the Isthmus of Panama and exporting water to the Pacific (thus making the water left behind more saline) (Pilson, 2013). The Agulhas Current off the east coast of Africa also frequently spits out eddies of warm salty water from the Indian Ocean and these get carried by the Benguela Current into the south Atlantic. This is known as Agulhas Leakage.

1.6 Density

Seawater density is a function of salinity, temperature, and pressure. Typical ocean density varies from 1020 to 1050 $\mathrm{kg\,m^{-3}}$. For very rough estimates, 1 $\mathrm{kg\,m^{-3}}$ change in density can be caused by a change of 1 psu, 5 °C, or 200 dbar. Vertical gradients in density are the determining cause of seawater layering. While density is often considered with the effects of compression removed (σ_θ), the true density is the value of interest for cephalopods trying to match internal density to seawater density for buoyancy (section 53.4).

When 0 °C water freezes, it increases its volume by 10% which is why ice floats.

1.6.1 Temperature-effect mechanisms

Temperature affects density through two competing mechanisms. 1. increasing temperature increases molecular bond movement and thus increases the functional volume of each water molecule, thus increasing the total volume of the solution. 2. increasing temperature breaks more H-bonds between water molecules which allows water molecules to come closer together, thus decreasing the total volume of the solution. Typically, mechanism 1 dominates mechanism 2 and density decreases with increasing temperature. When S < 24.6 psu, however, mechanism 2 dominates over mechanism 1 at cold temperatures (T < 4 °C) and density decreases with decreasing temperature. Thus, a density maximum occurs before seawater freezes when S < 24.6 psu.

1.7 Pressure

The pressure at a given depth (z) is demonstrated by the hydrostatic approximation:

$$\mathrm{p(z)} \approx -\mathrm{g} \cdot \rho_{\mathrm{average}} \cdot \mathrm{z} + \mathrm{p_{atmosphere}}$$

where p(z) is the pressure at depth z, g is gravity, ρ_{average} is the average density of seawater between the surface and z, and $\mathrm{p_{atmosphere}}$ is atmospheric pressure.

Pressure varies from 101 kPa at the surface to 40 MPa (400 atm) on the abyssal plains (4000 m) up to 111 MPa (1110 atm) at the bottom of the Mariana Trench.

1.8 Oxygen

The average ocean oxygen concentration is ~178 $\mu\mathrm{mol\cdot kg^{-1}}$ (Keeling et al., 2010). Combined with an average ocean temperature of 3.5 °C, this is ~11.9 kPa.

On geologic timescales, atmospheric P_{O_2} has varied only slightly over time since the start of the Paleozoic. This is (at least in part) buffered by marine sediments (Table 3.2). The more O_2 in the atmosphere, the more O_2 in seawater, and the more O_2

is consumed in sediments (pulling O_2 out of the system). Inversely, when atmospheric P_{O_2} is low, there is less O_2 in seawater and less O_2 is consumed in the sediments.

In the ocean interior, the most well oxygenated waters are the north Atlantic and Southern Ocean while the lowest P_{O_2} are found in the eastern tropical Pacific.

1.8.1 Gas exchange with the atmosphere

1.8.1.1 Solubility

The atmosphere is composed of 20.95% O_2. Oxygen solubility in seawater is temperature and salinity dependent, with ≈ 5 μmol/kg less with each added °C (Pilson, 2013) and $\approx 1-2$ μmol/kg less with each added psu. The O_2-concentration of air saturated seawater is described by Henry's law. Oxygen solubility decreases with increasing salinity because ions increase O_2 molecule's activity coefficient (make O_2 more reactive than it would be in pure water) which causes a smaller proportion to have low enough energy to remain in solution. Similarly, increasing temperature decreases solubility because it provides more energy to the O_2 molecules which allows more to leave solution and remain gaseous.

1.8.1.2 Air-sea fluxes

The flux of O_2 between the atmosphere and the surface at a local region is determined by the air-sea interface, a very thin ($\approx 30-70\,\mu$m) layer which does not easily mix with the air above or the water below. Instead, oxygen fluxes through this interface by molecular diffusion alone. According to Fick's law, the rate of oxygen diffusion (flux) can be determined from the difference in $[O_2]$ between air and water, the diffusivity of the gas, and the interface thickness. However, since the interface thickness is hard to measure accurately, oxygen flux can instead be estimated by substituting interface thickness for wind speed (since the thickness is heavily dependent on wind speed) which makes predicting oxygen flux over large portions of the ocean surface much easier. Thus, oxygen flux (mol m^{-2} hr^{-1}) can be estimated as follows:

$$\text{flux} = \frac{8.0\text{u}^2}{\text{Sc}^{0.5}} \times ([\text{O}_2]_{\text{air sat.}} - [\text{O}_2]_{\text{water}})$$

where u is the wind velocity 10 m above the sea surface and Sc is the Schmidt number which varies from 200 to 2000 depending on temperature. Relative to biological processes, oxygen flux across the air-sea interface can be rather slow. Dissolved O_2 in the ocean mixed layer (100 m) takes ≈ 1 month to reach equilibrium with the atmosphere (Williams and Follows, 2011).

During storms when water and air mix, air bubbles can be trapped and pushed as far as 10 m down. At this high pressure (2 atmospheres), the bubbles implode and are "injected" into the seawater.

1.8.2 Processes driving P_{O_2}

1.8.2.1 Increasing P_{O_2}

The most common process that increases P_{O_2} is photosynthesis. Here, the O_2 produced is derived from H_2O, not CO_2. In salt marshes, P_{O_2} can reach 40 kPa (Peruzza's SEB talk)!

$P_{O_2} > 100\%$ air saturation in seawater can be formed without any biological processes merely by the mixing of water masses. Since the solubility of O_2 in seawater with temperature has a nonlinear relationship, a supersaturated water mass can form from the mixing of two masses with saturated P_{O_2} and different temperatures. While the temperatures and $[O_2]$s will mix linearly, the resulting $[O_2]$ will be higher than the $[O_2]$ in an air-equilibrated water mass at the same final temperature (Pilson, 2013).

1.8.2.2 Decreasing P_{O_2}

The primary, or maybe even exclusive, driver of P_{O_2} below air saturation is respiration (Rabalais et al., 2010).

The best explanation of P_{O_2} in the ocean interior and mid-depths is how old the water is. As deep water forms, the oxygen in the water loses contact with the atmosphere. As the water mass moves through meridional overturning circulation oxygen is lost due to respiration. Thus deep water in the Pacific and Indian Oceans have less oxygen than the newer deep water in the Atlantic.

$$[\text{O}_{2\text{ water mass}}] = [\text{O}_{2\text{ last at surface}}] - \text{MO}_{2\text{ community}} \times \text{duration}_{\text{since last at surface}}$$

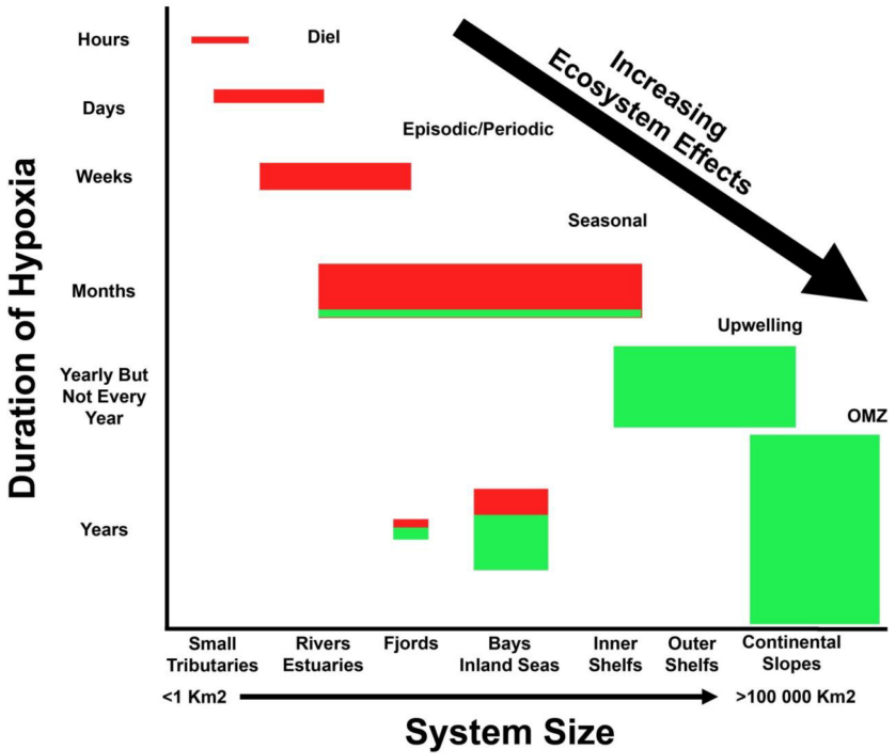

Figure 1.1: Spatial and temporal scales of hypoxic environments. Red are anthropogenic while green are natural. Figure originally from Rabalais et al. 2010.

Apparent oxygen utilization (AOU) Apparent oxygen utilization is a metric of how much oxygen is missing in a water mass compared to what would be expected if the water mass were at equilibrium with the atmosphere (air saturated). In deep water, the oxygen was last in exchange with the atmosphere at cold polar regions where solubility was high. However, high latitude storms in deep-water formation zones can cause air injection which makes the $[O_2]$ > air saturation. Since argon gas ($\approx 1\%$ of the atmosphere) has very similar solubility characteristics to oxygen, the [Ar] is an indicator of the starting $[O_2]$ and thus, the AOU. Since oxygen utilization is coupled to carbon remineralization (CO_2 production), heavily utilized water also has a more negative $\delta^{13}C$ value than the water before it (subsection 3.1.4).

Low oxygen environments are common natural phenomena in OMZs, deep basins, EBC upwelling zones, fjords, tidal zones, and eutrophicated estuaries (Rabalais et al., 2010).

Coastal hypoxic area coverage in a given region is typically largest in the summer and early fall (Rabalais et al., 2010). The longer the residence time of water in a coastal environment, the easier it is for hypoxia to develop. This is why fjords (which are typically deep with long residence times) are often hypoxic.

While respiration may consume oxygen, vertical density gradients need to be present to isolate the O_2-depleting water from the aerated surface or advected deeper water in order for a hypoxic region to develop (Rabalais et al., 2010).

1.8.3 OMZs

Oxygen-minimum zones (OMZs) are chronic (multi-decadal at least) oxygen poor regions of the water column circa 100-1000 m deep (though the depth varies by many factors) (Rabalais et al., 2010). They form most severely on the eastern margins of tropical ocean basins where upwelling induces high primary productivity up in the euphotic zone. The strongest OMZs are in the eastern tropical Pacific, northern Indian Ocean (Arabian Sea), and off the coast of northwest Africa (Benguela Current) (Rabalais et al., 2010). Weaker OMZs also exist in the north Pacific and eastern tropical North Atlantic (Gilly et al., 2013). In the Pacific and Indian Oceans OMZs are often defined as regions where $[O_2] < 20\ \mu\text{mol}\,\text{kg}^{-1}$ and oxygen limited zones (OLZ) or oxyclines (synonymous) are defined as regions where $[O_2] < 60\ \mu\text{mol}\,\text{kg}^{-1}$ (Gilly et al., 2013).

Large quantities of carbon/POM sinking below the euphotic zone from phytoplankton and their zooplankton predators cause increased bacterial respiration which greatly decreases P_{O_2} to as low as typically a few kPa or even sometimes $< 1\ \mu\text{M}\,O_2$. The rate of oxygen consumption in these areas exceeds the rate of oxygen flux through water advection.

The upper boundary of the OMZ is set by photosynthesized O_2 mixing from the surface, and the lower boundary is set by the

depth at which most of the carbon/POM has been consumed and bacterial populations diminish. Deep water advection must also be low for OMZs to form. Old upwelling deep water masses are also deprived of oxygen which further limits O_2 advection into these regions (Rabalais et al., 2010).

OMZs produce quite a few gases including N_2 (from denitrification and annamox), N_2O, H_2S, and CH_4 (Paulmier and Ruiz-Pino, 2009).

1.8.4 Eutrophication

Coastal environments such as bays and estuaries are subject to eutrophication-induced hypoxic/anoxic zones. In coastal zones, anthropogenic nutrient runoff from agricultural fertilizer, waste water facilities, and other sources and stratification of the water column (due to sunlight-induced temperature increases) lead to microbial respiration and decreased mixing of atmospheric O_2 respectively; this combination causes hypoxic/anoxic zones to develop (Diaz and Rosenberg, 2008). Bacterial respiration can come from both the water column and the sediment (Rabalais et al., 2010). When sediment-source respiration and subsequent hypoxia is strong, it can be more detrimental for benthic cephalopods than pelagic.

In addition to the lack of oxygen, when sediments become anoxic, MnO_2 in the sediment is reduced to Mn^{2+} which is bioavailable and can cause issues if concentrated in cephalopod tissue (Krang's SEB talk).

Regions with high incidences of eutrophication-induced hypoxia or anoxia are the Adriatic Sea, Baltic Sea, Chesapeake Bay, East China Sea, and the Gulf of Mexico near the Mississippi River delta (Rabalais et al., 2010).

1.8.5 Fractionation and the biological pump

^{18}O is naturally far less abundant than ^{16}O. The proportion of ^{18}O to ^{16}O in a sample is expressed relative to a standard as $\delta^{18}O$. In surface waters, primary producers fractionate the O_2 produced in photosynthesis by selectively producing the lighter ^{16}O isotope. This results in surface waters being depleted relative to the initial conditions ($\downarrow$ $\delta^{18}O$). In the ocean interior where respiration dominates O_2 conditions, heterotrophs fractionate the seawater O_2 by selectively consuming the lighter ^{16}O ($\uparrow$ $\delta^{18}O$). Thus, the biological pump causes a gradient in $\delta^{18}O$ with depth; the water's $\delta^{18}O$ value is lowest at the surface and is highest at depth. In areas where respiration is great (e.g. the OMZ) the $\delta^{18}O$ of the water is extremely high.

1.9 pH/CO_2

pH is driven by biological activity, temperature, and mixing (Hofmann et al., 2011). 95% of seawater's acid-base buffering capacity is from the CO_2 system with the remaining contributor of notable importance being the borate ($B(OH)_3$) / boric acid system ($B(OH)_4^-$) (Pilson, 2013). pH is temperature dependent, with pH decreasing by ≈ 0.01 units per °C increase (or more precisely, 0.0114 units per °C) (Pilson, 2013). pH is also pressure sensitive, with pH decreasing by ≈ 0.03 units per 1000 dbar increase in pressure again due to pressure increasing the dissociation constants of acids (Pilson, 2013).

Hydrothermal vents can reach P_{CO_2} levels of 7 kPa!

1.9.1 Pelagic

The mean modern oceanic surface pH is 8.1 units, or $[H^+] = 8$ nM. This varies zonally with pH increasing with latitude (Williams and Follows, 2011) due to the lower dissociation constants at colder temperature (Pilson, 2013). pH typically changes very slowly in the open ocean: ≈ 0.001 pH units hr^{-1} (Hofmann et al., 2011). Dissolved CO_2 in the ocean mixed layer (100 m) takes ≈ 1 year to reach equilibrium with the atmosphere (Williams and Follows, 2011). In subtropical gyres and polar regions (thus most of the open ocean), P_{CO_2} fluctuates seasonally about 50 and 130 μatm (≈ 0.05 and 0.1 pH units), respectively (Gunderson et al., 2016). Daily variability is less, with pH varying ≈ 0.02 pH units over the course of a month (Hofmann et al., 2011). However, biologically driven events like the spring bloom in the North Atlantic can cause larger and faster deviations (Hofmann et al., 2011). Additionally, along the equator where equatorial upwelling exists, pH can vary on larger scales than in other open ocean environments (Hofmann et al., 2011).

1.9.1.1 OMZs

In the ETNP, P_{CO_2} near the surface can be ≈ 50 Pa while in the core it may be over 150 Pa (Franco et al., 2014). Off the coast of Oregon, P_{CO_2} near the surface can be ≈ 40 Pa while in the core it may be over 150 Pa (Feely et al., 2016). In the north Pacific, P_{CO_2} near the surface can be ≈ 40 Pa while in the core it may be over 130 Pa (Fabry et al., 2008).

1.9.2 Coastal

In contrast to pelagic environments, coastal pH can vary largely. Some coastal regions can reach P_{CO_2} levels as high as 400 Pa (Baumann et al., 2015), though it is often much lower.

Estuaries and kelp forests typically have daily pH patterns determined primarily by the tides. pH typically changes 0.02-0.04 pH units hr^{-1} (Hofmann et al., 2011). However, heavy rainfall or high riverine output can cause pH to notably decrease in estuaries. Over the course of a month, pH can vary by 0.5 to 1 pH units (Hofmann et al., 2011). Seasonal fluctuations in pH in Narragansett Bay, RI can often be as much as 1 pH unit (Turner, 2015).

Coral reefs, in contrast, typically have very predictable daily oscillations driven by daily patterns in biological activity where pH is highest at dusk and lowest at dawn (Hofmann et al., 2011). pH typically varies $\approx$ 0.01 pH units hr^{-1} (Hofmann et al., 2011).

Coastal upwelling regions, such as those along eastern boundary currents, have high pH variance, but they vary less predictably, being driven primarily by changes in upwelling intensity and other physical forcings (Hofmann et al., 2011). pH changes in coastal upwelling regions $\approx$ 0.01 pH units hr^{-1} (Hofmann et al., 2011). Upwelling in the CCS can lead to 100 Pa CO_2 levels.

1.10 Seabed

The composition of the seabed is a function of the age of the seabed and its proximity to riverine output. The older and closer to a river, the more sediment accumulates on the seabed. Sediment thickness near major rivers like the Amazon, Mississippi, and Ganges can be up to 20 km. However, most coastal shelf is 1-2 km thick with pelagic sediment ranging from 0 to $\approx$ 700 m thick.

1.10.1 Sediment

The vast majority of the ocean floor is covered by sediment. Sediment depth is a function of the age of the underlying crust and the local sedimentation rate. Some cephalopods such as sepiids and *Octopus kaurna* inhabit sediment. This habitat can often be complexed by bioturbation (tunneling movement) and irrigation (tube maintenance). Sediment can be classified by size:

$$\text{clay (mud)} \rightarrow \text{silt} \rightarrow \text{sand} \rightarrow \text{gravel} \rightarrow \text{cobble} \rightarrow \text{boulder}$$

The interstitial water in sediment is depleted in Mg^{2+} and enriched in Ca^{2+} relative to seawater and slightly acidic compared to seawater. Within the first meter, these ions can deviate on the order of ~0.5 mM from the overlying seawater (Pilson, 2013). Interstitial water P_{O_2} is also lower due to bacterial decomposition of the biological waste in the sediment.

Sediment derives from a number of origins which are described in the following sections. On a global average, sediment composition is 50% calcareous biogenous (Pilson, 2013), 40% lithogenous clay, and 10% silicious biogenous sediment.

The grain size of sediment has a strong impact on the kind of infaunal and meiofaunal communities living there.

1.10.1.1 Biogenous sediment (derived from organisms)

Because biogenous sediments derive from organisms, they are rich in proteins, carbohydrates, lipids, and nucleic acids at least at the surface. These organic molecules do not preserve well, however, so they are not very dominant in older sediment. Biogenous sediments are also rich in inorganic shell material such as $CaCO_3$ (from foraminifera subsubsection 8.3.3.2 and coccolithophores subsection 9.1.3) and SiO_2 (from diatoms subsection 9.1.1, radiolarians subsubsection 8.3.3.1, sponge spicules, etc.). Although biological production is high in coastal environments, biogenous sediment is often still overwhelmed by riverine lithogenous sediment. Thus biogenous sediments are most dominant underlying productive pelagic habitats. The proportion of biogenic sediment is a function of biological production and preservation. $CaCO_3$ sediment is almost entirely biogenous (Pilson, 2013).

Silica (SiO_2) composition in sediment faithfully correlates with silicious plankton productivity in the overlying water column. Carbonate composition, however, is less straightforward due to the lysocline and carbonate compensation depth (subsection 3.6.1). Sea floor deeper than the CCD does not accumulate calcareous ooze because the carbonate dissolves before being buried into the sediment. If sea floor depth changes, however such as by the deepening of sea floor with age (distance from the MOR (mid-ocean ridge)) then deep sediment can contain buried biogenic calcareous material. Because of the older more acidic deep water in the Pacific compared to the Atlantic, the CCD is shallower and there are very few carbonate deposits that remain in Pacific sediments.

1.10.1.2 Lithogenous sediment (derived from land)

Lithogenous sediment is transported to the seafloor primarily via rivers but also from glaciers, wind, and gravity. They are composed often of quartz and feldspars. Larger particle sizes are found closer to shore because there is often not enough energy

Table 1.3: Typical marine sedimentation rates

Environment	Sediment source	Deposition (per 1000 years)
Neritic	Lithogenous	1 m
Pelagic	Biogenous	1 cm
	Lithogenous	1 mm

Table 1.4: Percent composition of marine rocks

Oxide	Oceanic crust	Continental crust
SiO_2	50.7	61.5
Al_2O_3	15.6	15.1
CaO	11.4	5.5
FeO	9.9	6.3
MgO	7.7	3.7

to move large particles far from shore. Because of its slow accumulation rate, pelagic lithogenous sediment is only a notable component of pelagic sediments when all other sources are lacking.

Wind-borne lithogenous sediment sinks from the surface to the sea floor at a rate dependent on the particle's size. Sand takes 2 days to sink 4 km, silt takes 6 months, and clay takes 50 years to reach the average seafloor depth.

1.10.1.3 Hydrogenous sediment (derived from dissolved chemicals)

The base layer of most oceanic sediment is metalliferous sediment which accumulates around the mid-ocean ridge.

Sediments near shore are often high in evaporites: precipitated salt from evaporated seawater. These salt domes are rich in calcite ($CaCO_3$), anhydrite ($CaSO_4$), and NaCl.

Manganese nodules Manganese nodules are 1-10 cm lumps often found on the surface of the seafloor (Pilson, 2013). They are located in regions with low sedimentation rates (areas with low overlaying biological productivity) and oxic sediment. Their name is misleading because they are composed of MnO and FeO in a roughly 1:1 ratio and grow concentrically around a bone, shark tooth, etc (Pilson, 2013). They contain lots of trace metals such as copper, cobalt, and nickel.

1.10.1.4 Cosmogenous sediment (derived from space)

Extraterrestrial particles slowly and steadily fall into the ocean and form cosmogenous sediments. Interplanetary dust particles are entering marine sediment at a constant rate.

1.10.1.5 Clathrates (gas hydrates)

Clathrates are gas-infused ice. They form when there's enough gas, pressure, and low enough temperatures. In deep marine sediments where pressure is high and temperature is low, if methane production from organic decomposition is sufficiently high, then the methane gas can mix with the water and form methane clathrates (Pilson, 2013).

1.10.2 Rock

Rocks are one of three types:

Sedimentary rocks formed from lithification of sediments

Igneous rocks crystallized from magma

Metamorphic rocks that have been changed in place by heat, pressure, or fluid

Continental rock is primarily granite.

1.10.2.1 MORBs

Oceanic rock is primarily derived from mid-ocean ridge basalt (MORB). The composition of these rocks are roughly shown in Table 1.4. As the magma is released from the ridge and cool they often form "pillow basalts". Mid-ocean ridges spread at a rate of 2-18 cm per year (Castro and Huber, 2019).

Chapter 2

Physical phenomena

World ocean currents are driven by wind patterns and horizontal seawater density gradients. Vertical density gradients determine the stability of the water column.

The Coriolis effect still bends things that are moving perfectly zonally because our coordinate system is perpendicular to the rounded surface of the Earth, while the Coriolis effect is perpendicular to the spinning axis (in line with the equator). This causes the Coriolis to bend things

2.1 Wind

Wind is caused by air masses moving down atmospheric pressure gradients.

Wind velocity is often measured on a Beaufort scale from 0 to 12.

2.1.1 Hadley, Ferrel, and Polar cells

Hadley, Ferrel, and Polar cells are the cause of the trade winds. The surface winds curl due to the Coriolis effect causing the bending of the trade winds. These atmospheric cells reach the top of the troposphere, ~10-15 km above the Earth's surface.

2.1.2 Monsoon

The monsoon phenomenon is due to high solar radiation on land in the summer which causes decreasing air density and thus low air pressure and thus storms. The opposite occurs in the winter.

2.2 Waves

2.2.1 Surface gravity waves

Shallow water waves break as they come onshore when they come in contact with the bottom. The drag from the bottom causes the amplitude, a, or wave height, to increase until the wave breaks a height to wavelength ratio of 1:7, which occurs when the bottom is 1.3x the wave height. This is at $2a \geq \lambda/7$.

Deep water waves are dispersive (larger λ waves travel faster) while shallow water waves are not.

Surface gravity waves are not perfect sine waves. As a result, objects floating at the surface do not return back to their original position with every cycle. Rather, they drift slowly in the direction the wave propagates.

Wave height is measured crest to trough.

The circular motion of surface waves can be felt (at least by humans) at a depth of about half the wave's wavelength.

Wind-driven waves typically have wavelengths of 60-150 m.

When waves come in contact with the shore at an angle, the shoreward edge of the wave slows first as it comes in contact with the bottom and this causes the whole wave to refract, or bend, towards being more parallel with the shoreline. This is why waves in a cove tend to be strongest on the edges of the cove and weakest in the middle; the waves all refract to the edges and only the trailing edges hit the middle of the cove.

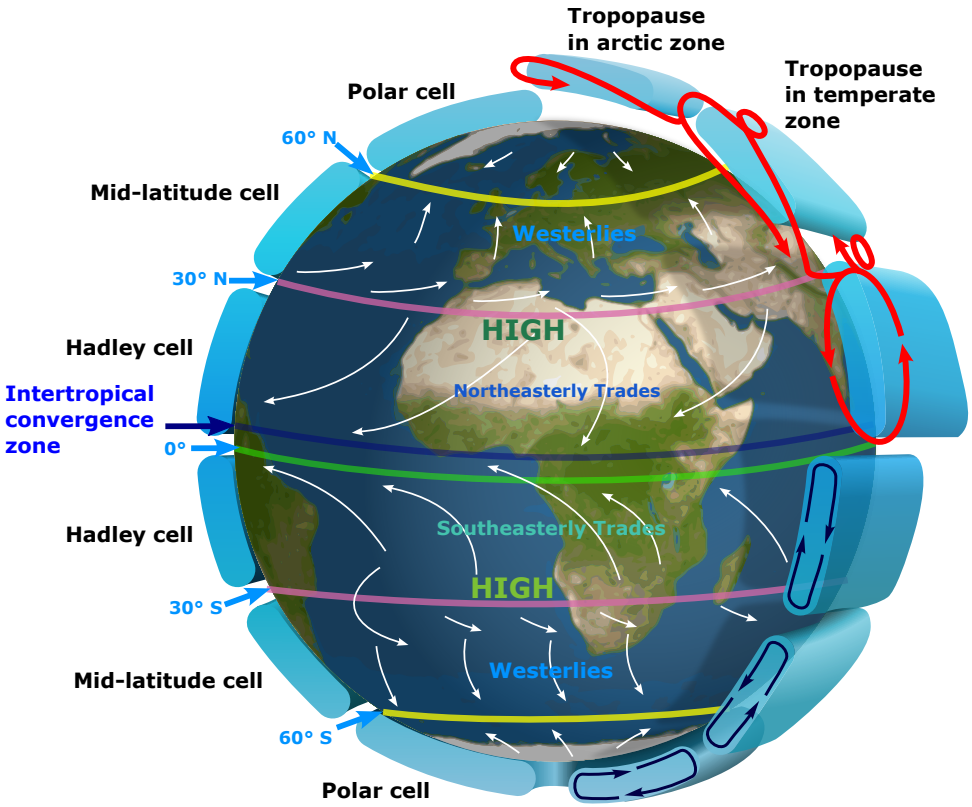

Figure 2.1: Atmospheric cells and trade winds

2.2.2 Internal gravity waves

Internal gravity waves are similar conceptually to surface gravity waves except that the difference in density between one layer of the ocean and another is much smaller than the difference in density between the ocean and atmosphere. As a result, internal gravity waves are about an order of magnitude slower than surface gravity waves and also have very large amplitudes (10^2 m). Just as in surface gravity waves, water (and the corresponding pycnocline) oscillates vertically as the wave passes. These vertical oscillations are typically 1-2 cm/sec.

Rather than being caused by winds, internal gravity waves are caused by reverberations from stratified flow hitting an abrupt change in bottom depth.

2.2.2.1 Impact on cephalopods

Internal gravity waves facilitate mixing between the nutrient-poor upper ocean and the nutrient rich ocean interior. Thus, they provide nutrients to support primary productivity and eventually cephalopod populations.

2.2.3 Tsunami waves

Tsunamis are often caused by submarine earthquakes, landslides, volcanic eruptions, icebergs, or even asteroids. Tsunamis are shallow-water waves traveling faster over deeper depths. Earthquakes are the most common source and can displace the seafloor and overlying water column by 10s to 100s of meters within seconds. This leads to very large water displacements traveling up to 760 kph.

2.3 Riverine input

Rivers flux freshwater into coastal environments. Because fresh water has lower density than salt, the incoming riverine water can form a "salt wedge" overtop of the oceanic water below. While the overall ionic strength of this fresh water is much lower than salt water, it has much larger proportions of HCO_3^-, Ca^{2+}, and Si than seawater. When the fresh water mixes with the salt water, many of the dissolved particles carried in the freshwater are precipitated out due to the addition of salt to the water

parcel. Combined with physical settling of particles from previously turbulent fresh water, this chemical precipitation causes many of the compounds fluxed into the ocean from land to be bound in the estuary rather than advecting offshore.

2.4 Tides

The gravity from both the Moon and Sun cause the tides, with the Moon exerting 2/3 of the influence. The Moon rotates around the Earth every 24 hours and 50 minutes, and the Earth-Moon system rotates around its center of mass every 27.3 days. When the Sun, Moon, and Earth are in a line (new and full moons), the gravity from the Sun and Moon combine to form a spring tide. When the Sun and Moon are at right angles (quarter moons), they compete to form a neap tide.

At a given location, the tidal cycle can be diurnal, semidiurnal, or semidiurnal with unequal phases. In general, small narrow bodies of water tend to have stronger tidal amplitudes than large wide bodies of water.

When the tide is rising, a flood current fills the body of water and when the tide is falling, an ebb current draws water away. The timing between flood and ebb is the slack tide.

As tidal waves move across ocean basins, they hit land and reflect back to sea. However, the Coriolis force drives them around. As a result, tides have, what is known as an amphidromic circulation through an ocean basin. The timing of high tides rotates counterclockwise in the northern hemisphere and clockwise in the southern hemisphere around different nodes in the middle of ocean basins.

2.5 Hurricanes

In the northern hemisphere, hurricane winds are strongest in the NE edge of the storm.

2.6 Ocean circulation

2.6.1 Upwelling

Upwelling occurs frequently along eastern boundary currents and along the equator on the eastern edge of ocean basins (Rabalais et al., 2010). They are often seasonally occurring, and input nutrients to the surface ocean, stimulating high productivity, and often hypoxia (Rabalais et al., 2010). Upwelling is predominantly caused by wind-induced Ekman transport which moves surface water horizontally, creating a pressure gradient that draws deeper water up towards the surface.

2.6.1.1 Coastal upwelling

Often, coastal upwelling draws up water from shallower depths than equatorial upwelling because coastal upwelling is much less consistent.

2.6.1.2 Equatorial upwelling

Along the equator, the trade winds are the ultimate mechanism for upwelling (subsection 2.1.1). The northeasterly trade winds in the northern hemisphere cause an Ekman transport of water 90° to the right, or towards the northwest. The mirror situation occurs in the southern hemisphere. This results in upwelling of water along the equator to replace the water moved to the poles and westward. Typically, this draws up intermediate waters (subsection 4.24.2), carrying moderate quantities of nutrients. Often, equatorial upwelling draws up water from deeper depths than coastal upwelling because equatorial upwelling is much more consistent.

2.6.2 Fronts

Fronts in physical properties are often bio-aggregators.

2.6.3 Mesoscale eddies

Other than geostrophic currents, most of the surface ocean moves through mesoscale eddies.

In the Northern hemisphere, high pressure eddies rotate clockwise and low pressure eddies rotate counterclockwise due to geostrophy. The opposite is true in the Southern hemisphere. High pressure eddies have a high sea surface height (SSH) while low pressure eddies have a low SSH. Because the pressure at great depth must be equivalent (isostatic?), high pressure eddies which have a higher SSH must have a lower average density and thus they accumulate deeper thermoclines since the warm water

Table 2.1: Characteristics of mesoscale eddies.

High pressure eddies	Low pressure eddies
Clockwise*	Counterclockwise*
Wam-core	Cold-core
High SSH	Low SSH
Deep thermocline	Shallow thermocline
High SST	Low SST

* In the Northern hemisphere.

has lower density. The opposite is true for low pressure eddies which have shallower thermoclines. In order to stabilize a deeper thermocline, SST must be warmer than average so a continual temperature gradient with depth is maintained. Likewise, low pressure eddies have slightly cooler SST.

Surface water in eddies typically moves around 10-20 km/day (cm/s).

2.6.4 Geostrophic currents

All the major surface ocean currents involved in ocean basin gyres are geostrophic currents (including the ACC) (Figure 2.2).

Geostrophic currents are currents which are in balance between two forces acting in opposing directions, both perpendicular to the direction of the current. Prevailing winds blow a current in a given direction. In the Northern Hemisphere, the Coriolis force drives the water to the right of the wind direction, causing it to build up. This buildup of water on the right, however, creates a horizontal pressure gradient such that water also has a tendency to go down its pressure gradient to the left. Thus when the forces from the Coriolis effect and horizontal pressure gradient are balanced, the current flows parallel to the prevailing winds and is considered in geostrophic balance. In the Southern Hemisphere, Coriolis pushes water to the left, then the pressure gradient counteracts to the right. In geostrophic currents, the prevailing winds have already setup the SSH gradient so it's only the horizontal pressure gradient that is actually creating movement at the present.

Currents are only geostrophic on large scales where flow is steady, friction is negligible, and the Coriolis force is much more influential than advection (i.e. Rossby ratio $<<1$).

Western boundary currents (WBCs) are stronger, deeper, and narrower than eastern boundary currents (EBCs).

Water velocity along geostrophic currents can be estimated as:

$$v = -\frac{g}{f}\frac{\delta n}{\delta x}$$

where v is the velocity (m/s), g is gravity (9.8 m/s^2), f is the Coriolis force (typically ~10^{-4} s^{-1}), and $\frac{\delta n}{\delta x}$ is the SSH gradient which can be obtained from satellite data. The resulting velocity is perpendicular to the SSH gradient; the high SSH is on the right of the direction of flow in the Northern hemisphere and to the left of the flow in the Southern hemisphere.

2.6.4.1 Antarctic Circumpolar Current

The ACC is the largest current in the world, with flow rates around 180 Sv (Pilson, 2013)! It runs east around Antarctica.

2.6.4.2 The Gulf Stream

The Gulf Stream is the western boundary current of the North Atlantic. It is ~50-100 km across and averages 2 ms^{-1} (~170 km / day). Its typical flow is about 30-100 Sv (million m^3/s) (Pilson, 2013). It follows the eastern margin of the US from Florida north to Cape Hatteras, where it diverges from the continental shelf. Its location is very stable south of Cape Hatteras, but a geological feature known as the Charleston Bump offshore from Charleston, SC creates a disturbance which pushes the Gulf Stream offshore and also creates much more variability.

2.6.4.3 Peru (Humboldt) Current

The Peru Current is the eastern boundary current (EBC) along the south Pacific gyre. Productivity is high along the Peru Current because of Ekman transport induced upwelling along the steep continental slope of the west coast of South America. The water column along the Peru Current (and California Current) has a characteristically shallow thermocline because the SSH is so low relative to the western Pacific where trade winds push lots of water (subsection 2.1.1). The thermocline-SSH relationship exists for the same reason as it does in mesoscale eddies (subsection 2.6.3). This shallow thermocline permits high

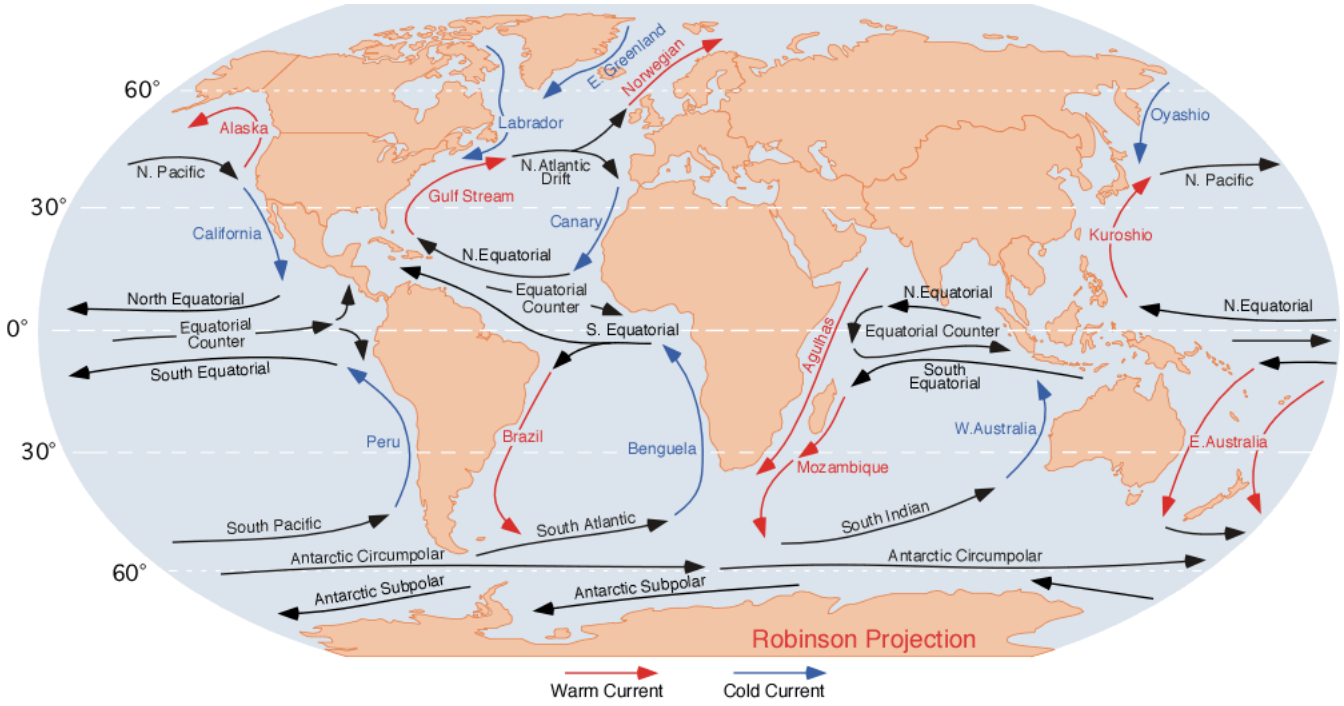

Figure 2.2: Surface ocean currents

quantities of nutrient flux with only moderate upwelling which is why such large cephalopod populations can be supported (as well as other stocks).

2.6.5 Subtropical gyres

2.6.5.1 Ekman dynamics and Sverdrup circulation

Subtropical gyres are characterized by being regions of downwelling (Ekman pumping) flanked by the equatorial tropics and high latitudes which are both upwelling regions (Ekman suction). These Ekman pumping/suction patterns are due to predominant winds driving Ekman transport. Currents around the gyre all direct surface water towards the center of the gyre which pushes surface water downward. Decreasing winds and an increasing Coriolis force with increasing latitude in the high latitude regions cause slightly more equatorial water to move faster towards the equator than the extreme polar waters. This difference leaves a suction, drawing interior water from below.

The Ekman pumping in the center of the gyre vertically compresses the ocean interior underneath it. This compression decreases the water column's angular velocity, thus causing it to move slowly towards the equator. Western boundary currents are formed to return the slowly moving equatorward water across the whole gyre back towards the poles. By having the continent on its western margin, the WBC has a gradient in horizontal velocity due to friction with the continent. This gradient in friction creates a torque which increases the water column's angular velocity again allowing it to move towards the pole.

2.6.6 Meridional overturning (thermohaline) circulation

In the North Atlantic east of Greenland and a few regions around Antarctica, cooling and evaporation increase surface water's density causing it to sink and form deep water (Pilson, 2013). This does not occur in the North Pacific very much because the Pacific is not as salty as the Atlantic, and water cools to ice before being dense enough to sink (Pilson, 2013).

Since these are focal points of downwelling water, the returning upwelling water is spread over much of the ocean. This upwelling from depths causes a vertical stretching of the water column, thus increasing its angular velocity, and driving the water poleward again. The majority of meridional movement of deep water along the "deep water conveyor belt", therefore, is in deep, narrow, and strong western boundary currents. From the North Atlantic, a DWBC goes southward underneath the Gulf Stream and along the eastern margin of the Americas.

Sinking around Greenland due to cooling temperature forms North Atlantic Deep Water (NADW) and sinking around Antarctica due to salinity increase (from ice formation) forms Antarctic Bottom Water (AABW). Once NADW makes its way to Antarctica, it mixes with AABW and Antarctic Intermediate Water (AAIW). The resulting Common Water moves into the

Pacific and Indian Oceans (Pilson, 2013). Upwelling occurs here (and elsewhere) bringing deep water back to the surface. From here, the water makes its way west to the Atlantic, Carribean, Gulf of Mexico and then to the North Atlantic to sink again. The circulation takes ~1000-1500 years (Pilson, 2013).

Global thermohaline circulation has a flow rate of about 30 Sv (Pilson, 2013).

Because CO_2 is more soluble at the cold polar waters where deep water formation occurs and less soluble at the warm low latitude waters where much of deep water upwells, the MOC functions as a "solubility pump" to transport CO_2 from the poles to the tropics (Pilson, 2013).

2.6.6.1 Impact on cephalopods

The path of this circulation pattern is relevant for cephalopods because deep seawater loses oxygen (to respiration) as it ages in the ocean interior. Thus deep water is most oxygenated at downwelling regions and decreases in P_{O_2} in older deep water (e.g. in the Pacific and Indian Oceans).

2.7 Climate oscillations

2.7.1 ENSO

The Eastern Tropical Pacific Ocean (ETP) is a dynamic region of the ocean on the western coast of Americas. It is characterized by inter-annual oscillations in atmospheric pressure between the western and eastern basins (Walker, 1924). The atmospheric pressure gradient drives surface winds over the equator. Because there is no Coriolis force at the equator to deflect the water towards the poles, the equatorial winds drive equatorial surface currents straight across the ocean basin. Normally, the predominant winds are easterlies, driving the surface currents westward. As water moves westward, according to the conservation of mass, new water must replace it. This water is drawn from the ocean interior through upwelling.

Every 2-7 years, the atmospheric Southern Oscillation changes phase, which moves air mass westward causing high atmospheric pressure in the western Pacific and low atmospheric pressure in the ETP according to the hydrostatic equation. This reversal of the surface atmospheric pressure gradient across the Pacific basin leads to a weakening and even reversal of equatorial currents. The anomalous movement of warm water eastward across the basin towards the western coast of South America is known as El Niño. Upwelling water mass flux decreases somewhat during these events. The movement of water towards the east also increases SSH in the eastern Pacific which deepens the thermocline (subsection 2.6.3) which in turn makes nutrient reserves deeper and thus decreases coastal upwelling productivity characteristic of the California and Peru Currents.

Often, after an El Niño event, the Southern Oscillation overcompensates in its reversal, leading to a La Niña event where surface water in the ETP is anomalously cool (Clarke, 2014).

The ENSO phase can be quantified by the Multivariate ENSO Index (MEI), which incorporates sea-level atmospheric pressure, surface wind, SST, and longwave radiation into space into a single quantitative value (Wolter and Timlin, 1998).

2.7.2 NAO

The North Atlantic Oscillation is a variation in the difference in atmospheric pressure measured between the Icelandic Low and the Azores High. The position of these centroids also shifts somewhat. When the difference is greatest (NAO+), the westerlies are strongest, bringing ocean air to provide cool summers and warm winters to central Europe. When the difference is lesser (NAO-), the westerlies are weaker and therefore central Europe has more severe winters. The NAO is most influential on conditions in the Atlantic during the winter, as opposed to the summer.

In the waters off New England, NAO+ causes increased temperature and rainfall which makes the surface waters warmer and less saline, both contributing to lower density water and thus less upwelling and associated primary productivity. This has been linked to lower cod catches on Georges Bank.

2.7.3 PDO

During a positive phase, the northwestern Pacific cools while the northeastern and equatorial-eastern Pacific warms.

During a negative phase, the northwestern Pacific warms while the northeastern and equatorial-eastern pacific cools.

OMZ depth is impacted by the PDO, shoaling and deepening (Deutsch et al., 2011).

During negative PDO phases, the midwater (50-300 m) ETP sees a rise in oxygen and decline in nutrients (Stramma et al., in review at Biogeosciences Discussion).

2.7.4 Glacial-interglacial oscillations

Glacial-interglacial cycles are caused predominantly by Milankovitch cycles which are wobbles in the tilt of the Earth's axis. For the last ~1 Ma, oscillations have had a period ~100 ky. The last glacial maximum (LGM) was about 20 ka (Pilson, 2013). During the LGM, sea level was ~125 m lower than the current level (Pilson, 2013). Recent glacial P_{CO_2} levels were ~180 μatm and interglacial levels ~280 μatm.

2.7.4.1 Continental ice volume

Currently, about 10% of continental ice is on Greenland and the rest is on Antarctica (Pilson, 2013). If all continental ice melted, sea level would be ~200 m higher than during glacial periods. Ice melting/freezing also changes mean ocean salinity by ~2 psu (Pilson, 2013).

When continental ice melts it raises sea level and covers larger portions of continental margins worldwide. Since water has a lower albedo than land, the increased proportion of aquatic surface area worldwide causes more heat to be absorbed and less to be reflected, thus warming the climate further. Thus, the albedo-impact of continental ice melting is a positive feedback effect on glacial-interglacial cycling.

Past changes in continental ice volume can be reconstructed due to the different $\delta^{18}O$ of snowfall-derived continental ice and seawater (subsection 1.1.2). During glacial periods when the continental ice volume was highest, there was lots of ^{18}O depleted water caught up in ice and thus seawater had a higher $\delta^{18}O$. During interglacial periods, however, all of the ^{18}O depleted water returned to the sea, thus lowering seawater $\delta^{18}O$ relative to glacial periods (Pilson, 2013).

2.7.4.2 Marine calcifiers and oxygen fractionation

When calcifying organisms create their shells from $CaCO_3$, the oxygen molecules they used have a $\delta^{18}O$ related to the $\delta^{18}O$ of the ambient seawater in which they lived. Thus, due to the relationship between paleotemperature and seawater $\delta^{18}O$ (subsubsection 2.7.4.1), paleotemperature can be inferred from the $\delta^{18}O$ of shells (Pilson, 2013).

2.7.4.3 Alkenone ratios

Some coccolithophores produce alkenones, long hydrocarbons with a ketone group on one end. The ratio of C-37:2 to C-37:3 produced varies depending on the surface temperature at which the coccolithophores grow. Thus, sediment examination of alkenone ratios in coccoliths provides a proxy of paleotemperature at the surface (Pilson, 2013).

2.7.5 Long-term climate changes

There are two leading hypotheses for the drivers of long-term climate changes, i.e. throughout the Cenozoic:

- BLAG hypothesis states that faster rates of spreading of tectonic plates causes increased CO_2 emissions from the mantle at the MOR and subduction zones. This increases temperature which in turn increases precipitation and vegetation, both of which increase chemical weathering of rocks. Increased weathering draws CO_2 out of the atmosphere cooling the climate.
- Uplift-weathering hypothesis asserts that rising mountain ranges expose large quantities of rock to the atmosphere. These rocks readily react with atmospheric CO_2 drawing it out of the atmosphere and thus cooling climate.

2.8 Historical phenomena and events

2.8.1 Ocean acidification events

Historical records of pH can be inferred from pH-sensitive boron speciation. Atmospheric P_{CO_2} can be inferred (at least in the recent past) from ice cores.

In the recent past glacial-interglacial cycles, pH only changed 0.1-0.2 units. The Holocene (past 10k years) has had extremely stable atmospheric P_{CO_2} (260-280 μatm) and surface ocean pH (Δ0.04 units). The Pleistocene (2.6 - 0.01 Ma) and Pliocene (5.3 - 2.6 Ma) before it had gradual changes in carbonate chemistry that varied over 10,000s of years between 200-500 μatm P_{CO_2}.

From the beginning of the Cenozoic (66 Ma) until the Pliocene, atmospheric P_{CO_2} decreased and surface ocean pH increased from ca. 1000 μatm and 7.7 units to Pliocene values near 350 μatm and 8.1 units respectively (Zeebe, 2012).

Before, in the rest of the Phanerozoic (541 Ma - present), there have been 7 major perturbations in oceanic carbonate chemistry. Table 2.2 provides some most extreme conditions cephalopods have had to face throughout their evolution.

Table 2.2: Most extreme carbonate chemistry parameters throughout cephalopod history.

Time	Atmospheric P_{CO_2} (μatm)	Surface ocean pH
Cambrian - end-Devonian (541 - 359 Ma)	6000	7.4
Carboniferous - end-Triassic (359 - 201 Ma)	2600	7.7
Jurassic - end-Cretaceous (201 - 66 Ma)	4200	7.6
Cenozoic (66 Ma - present)	1000	7.7

2.9 Anthropogenic climate change

The average rate of climate-driven change in marine species distribution is 72 km per decade (Pecl et al. 2017, Science).

It should be noted that burning fossil fuels has released lots of low $\delta^{13}C$ carbon into the atmosphere. Therefore, measured baseline $\delta^{13}C$ has also changed over time since the Industrial Revolution; this is known as the Suess effect.

2.9.1 Global warming

Carbon dioxide, as well as water vapor, methane, nitrous oxide, and other gases, reflect infrared radiation leaving the Earth back towards the Earth. Thus, the higher the concentration of these "greenhouse gases" in the atmosphere, the more radiation will be retained within the atmosphere and the Earth will warm (Pilson, 2013). Atmospheric P_{CO_2} was 18 Pa at the LGM and was 28 Pa at the start of the industrial revolution.

Mean global seawater surface temperature (SST) is expected to rise by 1-3 °C (Collins et al., 2013). Under the RCP8.5 CO_2 emission model, SST around North America is expected to increase 3-4 °C by the end of the century (IPCC, 2014). Warming is expected to increase SST at low latitudes and increase precipitation/ice melt at high latitudes. Both of these effects will likely induce stratification.

In coastal systems, increased stratification may decrease subsurface P_{O_2}. Increased rainfall in a coastal region's watershed may be a stronger driver of stratification than merely increased temperature alone (Rabalais et al., 2010). Coastal rainfall also flushes nitrogen, phosphorus, and silica into coastal waters which may trigger a hypoxic event (Rabalais et al., 2010).

2.9.2 Ocean acidification

Atmospheric and oceanic P_{CO_2} have been increasing ~1.7 μatm/year (Church et al., 2013) leading to a average yearly decline of 0.0017 pH units (Hofmann et al., 2011). The oceans take up ~3 Gt C / year from the atmosphere (Pilson, 2013). While polar regions still remain supersaturated with $CaCO_3$ ($\Omega > 1$)(subsection 3.6.1), they will start to become undersaturated even at the surface at P_{CO_2} = 600 μatm (Pilson, 2013). Ultimately, OA will actually increase ocean alkalinity because the increased acidity will raise the carbonate compensation depth (subsection 3.6.1) which will dissolve more $CaCO_3$ thus adding more CO_3^{2-} to seawater (Pilson, 2013).

2.9.3 Deoxygenation

The oceans are losing on average 2% of the dissolved O_2 every 50 years (Schmidtko's OSM talk).

Oxygen minimum zones worldwide are expected to increase in intensity and size (both horizontally and vertically) for the following reasons: 1. increased temperature decreases seawater [O_2] at air saturation (Weiss, 1970), 2. advection of O_2 rich water is expected to decrease due to increased stratification, 3. increased temperature increases microbial MO_2 which drives down seawater [O_2] (Devol, 1978), and 4. increased North Atlantic temperatures will slow MOC, increase deep water residence time, and result in lower [O_2] upwelling water (Stocker and Schmittner, 1997). On average, OMZ cores have become more hypoxic by ~0.2 μM/year (Stramma et al., 2008). This will have impacts on biogeochemical cycles.

Chapter 3

Biogeochemistry

The consumption of nutrients is primarily conducted by phytoplankton in the euphotic zone. Much of the remineralization of nutrients is physically separated, occurring in the ocean interior via bacterial respiration.

The following nutrients are nearly invariant throughout the ocean breadth and depth: Na, Mg, K, Ca, S, Cl, Br, and some trace elements. The other nutrients relevant to cephalopods and their communities have distinct patterns spatially and temporally and are thus examined in this chapter.

3.1 The carbon cycle

When considering masses of carbon, it is helpful to remember 1 gigatonne (Gt) = 1 petagram (Pg).

In a year, local perturbations in atmospheric P_{CO_2} are mixed and diluted to a homogenous atmospheric P_{CO_2} (Pilson, 2013). Additionally, it takes ~1 year for CO_2 dissolved in the surface ocean to equilibrate with the atmosphere (Williams and Follows, 2011).

In 10s to 100s of years, carbon exchanges between the atmosphere, biosphere, soils, and the surface ocean. Combined, these systems hold ~4,000 Pg C (Zeebe, 2012).

In 1000s of years, carbon in the surface ocean can mix with the ocean interior which contains ~38,000 Pg C (Zeebe, 2012; Pilson, 2013).

In 1000s to 100,000s of years, much of the anthropogenic CO_2 will eventually be absorbed by the ocean, shuttled to deep sediments and be neutralized by carbonate sediments in this timescale. At this scale, oceanic carbon equilibrium is reached between mineral weathering from terrestrial sources (C input) and precipitation of $CaCO_3$ to marine sediments (C output) (Zeebe, 2012).

In >100,000s of years, carbon fluxes between the ocean and the carbonate-rich rock reservoirs that compose the Earth's crust. This rock reservoir dwarfs the atmospheric and oceanic carbon sources with ~10^8 Pg C (Zeebe, 2012).

On timescales relevant to cephalopod populations, carbon from the atmosphere is "fixed" into biologically usable forms by primary producers. Much of this carbon is shuttled up trophic links to higher order taxa. Eventually, some of the carbon sinks into the ocean interior and is stored in deep ocean sediments. Phytoplankton contribute 50% of global C fixation (~50 $\mathrm{Pg\,C\,yr^{-1}}$) (Pilson, 2013) with diatoms contributing 50% of this.

Weathering of rocks consumes atmospheric CO_2.

Carbon input into the oceans from rivers is quite small compared to net primary production carbon flux from phytoplankton (<1%), but can still be a notable contributor in coastal systems (Pilson, 2013).

3.1.1 Forms of carbon

Carbon in marine systems can be held in five forms in decreasing abundances in the ocean:

Mineral Large carbon stores exist in the form of minerals.

DIC Dissolved inorganic carbon.

DOC Dissolved organic carbon. Arbitrarily defined as material passing through a 0.5 μm filter.

POC Particulate organic carbon. Carbon is held in this form as detritus, fecal pellets, marine snow, etc. Arbitrarily defined as material collected on a 0.5 μm filter.

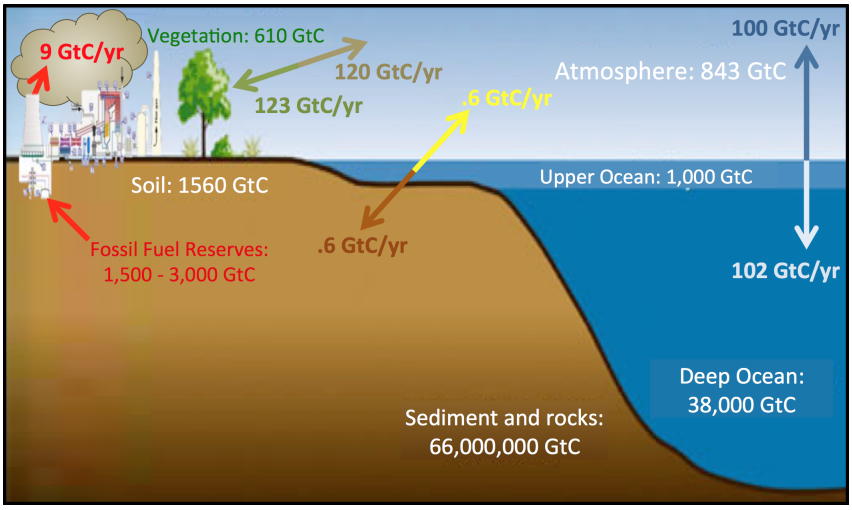

Figure 3.1: Carbon cycle

Table 3.1: Dissociation constants of DIC species in seawater (T = 25 °C, S = 35). CO_2^* indicates dissolved CO_2 and H_2CO_3. The $'$ indicates these are "apparent" dissociation constants whose values are adjusted for $[H_2O]$, activity coefficients, and ion pairing of the species involved.

K_0'	$P_{CO_2}(g) \rightleftharpoons CO_2^*$	$K_0' = \frac{[CO_2^*]}{P_{CO_2}}$	≈ 1.5
K_1'	$CO_2^* + H_2O \rightleftharpoons HCO_3^- + H^+$	$K_1' = \frac{[HCO_3^-][H^+]}{[CO_2^*]}$	≈ 5.8
K_2'	$HCO_3^- \rightleftharpoons CO_3^{2-} + H^+$	$K_2' = \frac{[CO_3^{2-}][H^+]}{[HCO_3^-]}$	≈ 8.9

Organisms Much carbon is held in the biomass of living organisms.

Biological carbon vectors take the forms of POC as detritus, DOC emitted from living and dead organisms, DIC emitted through respiration, and nekton moving between habitats (Hyndes et al., 2014).

3.1.1.1 DIC

Currently, DIC is roughly composed of 90% HCO_3^-, 9% CO_3^{2-}, and 0.9% CO_2/H_2CO_3. Of the CO_2/H_2CO_3 component, only about 0.1% is H_2CO_3; the vast majority is dissolved CO_2 gas. CO_2 at the surface takes weeks to months to equilibrate with the atmosphere. Surface DIC varies zonally, with DIC increasing with latitude due to the high gaseous CO_2 uptake at the colder poles (Williams and Follows, 2011). $[CO_3^{2-}]$, however, is inversely related to latitude (higher $[CO_3^{2-}]$ in the tropics). DIC generally increases with depth for the following reasons: sinking of CO_2 rich polar waters, the biological pump, and sinking of $CaCO_3$ (carbonate pump). $CaCO_3$ precipitation (formation) decreases pH (Pilson, 2013). The dissociation of H_2CO_3 into HCO_3^- and H^+ is quite fast (milliseconds) but the conversion of CO_2 to H_2CO_3 is a rather slow process that can take minutes to reach equilibrium. The half-life of the reaction ranges from 30 seconds to 5 minutes as the temperature falls from 25 to 0 °C (Kern, 1960).

The Revelle ratios are the ratios of the proportional difference in inorganic carbon species in seawater with a change in the system.

$$R = \frac{\Delta P_{CO_2}}{P_{CO_2}(\text{initial})} \Big/ \frac{\Delta DIC}{DIC\ (\text{initial})} \approx 10$$

$$R = \frac{\Delta[H^+]}{[H^+]\ (\text{initial})} \Big/ \frac{\Delta DIC}{DIC\ (\text{initial})} \approx 10$$

For example, a 1% change in DIC creates a 10% change in $[H^+]$.

pH See section 1.9.

Total alkalinity (TA) TA is the charge balance of the seawater. Because the conservative cations slightly exceed the conservative anions in charge concentration, nonconservative ions must have a slight negative charge concentration. As such, TA is often expressed as the excess of proton acceptors over proton donors as follows:

$$TA = [HCO_3^-]+2[CO_3^{2-}]+[B(OH)_4^-]+[OH^-]+[HPO_4^{2-}]+2[PO_4^{3-}]+[H_3SiO_4^-]+[NH_3]+[HS^-]+...-[H^+]-[HSO_4^-]-[HF]-[H_3PO_4]-[HNO_2]-...$$

TA follows salinity closely. Therefore, it is highest in the subtropical gyres and lowest at high latitudes (Williams and Follows, 2011). Also, it decreases with depth in the Atlantic where surface water has high salinity, and it increases with depth in the Pacific where surface water has lower salinity. Photosynthesis and respiration have a slight impact on TA due to their impact on ammonia and nitrate but otherwise do not affect TA. This is because respiration releases CO_2 in a dissolved state. Every HCO_3^- and CO_3^{2-} ion produced from this respired CO_2 is matched by an equimolar quantity of H^+ produced, thus balancing out the bases. $CaCO_3$ precipitation also decreases TA since it removes CO_3^{2-} from seawater (Pilson, 2013). Each mole of $CaCO_3$ precipitation reduces TA by 2 moles.

3.1.1.2 DOC

Since DOC includes everything smaller than 0.5 μm, then it includes viruses and small bacteria. DOC concentrations can vary from ~40 μmol/kg in deep water to 80 μmol/kg in productive surface water. [DOC] are highest in the tropical surface waters because stratification prevents too much downward flux. Rivers carry a lot of DOC into the marine system. Much of the DOC in deep water is somehow nonreactive with biological mechanisms and thus can avoid reaction for thousands of years (Pilson, 2013). Examples of DOC are humics , fatty acids, sugars, amino acids, vitamins, small hydrocarbons (e.g. methane), carbon-containing gases (e.g. carbon monoxide, DMS), halocarbons, and alkenones (long hydrocarbons with a ketone at one end). Fatty acids, sugars, and amino acids cumulatively compose about 25% of all DOC while humics (hydrocarbons with many oxygen functional groups) compose ~20% of DOC. The rest of the known compounds are in the nM or pM range. The rest is an as of yet unknown composition.

3.1.1.3 POC

$<$ 1 μmol/kg in deep water and ~100 μmol/kg in productive surface water (Pilson, 2013).

Marine snow composes most POC.

Marine snow Marine snow is particulate organic matter (POM) typically composed of biological "junk" such as mucus secretions, larvacean houses, fecal pellets, plankton carcasses, crustacean molts, etc. As marine snow sinks, it supports bacterial consumption and proliferation, thus increasing bacterial respiration. Since aggregations can become sizable, they sink faster than individual components, thus accelerating carbon transport to the sediment. Marine snow is food for not only bacteria, but pelagic and benthic animals as well.

3.1.2 Spatial differences

Coastal ecosystems have some of the highest primary productivity rates in the ocean. In fact, the NPP of coastal ecosystems like saltmarshes, mangroves, and seagrass beds can incorporate more than 80 mol C/m^2/year (Hyndes et al., 2014). Some of carbon imported into coastal ecosystems, however, is not from primary producers but from externally derived detritus (Hyndes et al., 2014).

Coastal sandy shorelines have low NPP but they are important ecosystems for nutrient recycling which occurs by degradation of detritus that is transported into these systems (Hyndes et al., 2014). According to Pilson (2013), subtropical gyres often have quite low NPP (~5 mol/m^2/year) while coastal areas have higher NPP (~20 mol/m^2/year) and eastern boundary currents with strong upwelling can have very high NPP (~150 mol/m^2/year).

Nekton are the primary vectors of carbon export from mangroves and saltmarshes due to the low advection and nursery function of these habitats (Hyndes et al., 2014).

The Southern Ocean exports 80 Tmol of carbon each year (Schlitzer 2002 cited in (Lavery et al., 2010)).

Because CO_2 is more soluble at the cold polar waters where deep water formation occurs and less soluble at the warm low latitude waters where much of deep water upwells, meridional overturning circulation functions as a "solubility pump" to transport carbon from the poles to the tropics (Pilson, 2013).

While primary production may be high in the euphotic zone, only ~10% of carbon from net primary production is exported below the euphotic zone. Of that exported carbon, ~10% makes its way to the sediment without being consumed (depending on depth), and of that settled carbon, only ~10% gets incorporated in the sediment rather than being consumed by bacteria or other biota. Thus, only about 0.1% of net primary production is stored into the sediment where it can stay for any notable

length of time on a geologic scale. Very high primary productivity rates, however, can overwhelm bacterial consumption rates and result in larger proportions of particulate carbon export, sometimes exponentially more. The flux of particulate carbon from the surface decreases exponentially with depth (Pilson, 2013).

3.1.3 ^{14}C and age

Most carbon on Earth has six neutrons ($^{12}_{6}$C), but radioactive carbon-14 has eight neutrons ($^{14}_{6}$C). It is formed in the atmosphere when cosmic rays produce neutrons which collide with nitrogen-14 to remove protons:

$$^{14}_{7}\mathrm{N} + \text{neutron} \rightarrow ^{14}_{6}\mathrm{C} + \text{proton}$$

Carbon-14 has a half-life of 5730 years. Cephalopods (and all living things) incorporate carbon-14 into their tissues in proportion to the carbon-14 in the atmosphere. While the proportion can vary slightly due to variation in cosmic radiation or P_{N_2}, currently the ^{12}C : ^{14}C is $1^{12} : 1^{0}$. Once an object is chemically inert, the ^{14}C input ceases and its concentration decreases logarithmically following its mean lifetime, τ, 8267 years (but adjusted to match historical measurements):

$$\text{age}\,(\text{in}\,^{14}\text{C}\,\text{years}) = -8033 \cdot \ln(^{14}\text{C}/^{12}\text{C})$$

Since absolute ages require calibration due to variation in [^{14}C] over time, the loss of ^{14}C over time is often expressed as Δ^{14}C:

$$\Delta^{14}\mathrm{C} = \left(\frac{^{14}\mathrm{C}/^{12}\mathrm{C}_{\text{sample}}}{^{14}\mathrm{C}/^{12}\mathrm{C}_{1950\text{s wood}}} - 1\right) \times 1000$$

3.1.4 Fractionation and the biological pump

^{13}C is naturally far less abundant than ^{12}C. The proportion of ^{13}C to ^{12}C in a sample is expressed relative to a standard as δ^{13}C. In surface waters, primary producers fractionate the DIC available for photosynthesis by selectively preferring the lighter ^{12}C isotope. This results in surface waters being enriched relative to the initial conditions ($\uparrow \delta^{13}$C) and the body composition of the primary producers deplete relative to the water from which they were formed ($\downarrow \delta^{13}$C). As dead phytoplankton sink into the ocean interior, remineralization of their cells results in the release of this deplete δ^{13}C source into the deep water. Thus, the biological pump causes a gradient in δ^{13}C with depth; the water's δ^{13}C value is highest at the surface and is lowest at depth. In areas where remineralization is great (e.g. the OMZ) the δ^{13}C of the water is extremely low.

3.1.4.1 Spatial patterns of δ^{13}C

There is a strong latitudinal gradient of δ^{13}C such that the poles have a more negative value than the tropics.

δ^{13}C also various by distance from the coast and also pelagic versus benthic somehow...

It should be noted that burning fossil fuels has released lots of low δ^{13}C carbon into the atmosphere. Therefore, measured baseline δ^{13}C has also changed over time since the Industrial Revolution; this is known as the Suess effect.

3.2 The nitrogen cycle

N_2 gas in seawater is quite inert other than the biota which utilize it for nitrogen fixation. Thus, it is often close to air saturation throughout the ocean (Pilson, 2013). NH_3 is usually ~5% of [$NH_3 + NH_4^+$] depending on pH, temperature, and salinity. ^{14}N and ^{15}N are both stable isotopes in the atmosphere and ocean and are fractionated in biological processes.

Important dissolved inorganic nitrogen (DIN) species: NH_4^+ (ammonium), NH_3 (ammonia), N_2 (dinitrogen gas), N_2O (nitrous oxide), NO (nitric oxide), NO_2^- (nitrite), NO_3^- (nitrate)

Concentration range: ~48 μmol/kg NO_3^- in deep N. Pacific water (16x [DIP]; (subsection 3.3.1)), ~10 μmol/kg NO_3^- in estuaries, to 1 μmol/kg NO_3^- maximum in open ocean (but often much less)

According to the Redfield equation, 166 μmol O_2 (AOU) yields 16 μmol DIN (subsection 9.0.1).

Most cephalopods are similar to most marine animals and can tolerate <0.1 mg/l un-ionized NH_3 (5 μM NH_3), <0.1 mg/l NO_2 (2 μM NO_2^-), and <20 mg/l NO_3 (300 μM NO_3^-) (von Boletzky and Hanlon, 1983).

3.2.1 Nitrogen fixation ($N_2 \rightarrow$ PON)

Nitrogen fixation in the marine system is done almost exclusively by cyanobacteria, particularly *Trichodesmium* spp. (Pilson, 2013) which flourish in the nitrate-poor subtropical gyres. They convert gaseous N_2 to particulate organic nitrogen (PON) (i.e. their tissues) and as such, they have a much higher N:P ratio than the Redfield ratio. This process occurs only near or at the surface because of cyanobacterias' need for solar radiation and iron; iron is a key element in nitrogenase, their N_2-fixing enzyme. Bacteria which can fix nitrogen are diazotrophs.

3.2.2 Assimilation ($NH_4^+/NO_3^- \rightarrow$ PON)

Other than nitrogen fixing bacteria, all other primary producers acquire their nitrogen through assimilation. These phytoplankton are dependent on NH_4^+ or NO_3^- dissolved in seawater from which they input to their tissues. Most assimilation occurs in the euphotic zone, but some archaea can assimilate in aphotic deep water.

Phytoplankton grow best on NH_4^+ but their growth keeps concentrations of it low. When sufficient ammonium is not available, they utilize nitrite or nitrate instead (Pilson, 2013). They also keep these species sparse at the surface where $[NO_3^-]$ is rarely above 1 μmol/kg. This is a key reason why upwelling stimulates productivity: it brings nitrate rich deep water to the surface which allows phytoplankton to grow. The pathway is the same regardless of which DIN species is assimilated; if NO_3^- is assimilated, it first undergoes reduction to NH_4^+ before going through the rest of the pathway. Since almost all NH_4^+ assimilated comes from euphotic sources, its assimilation goes towards recycled production. In contrast, since almost all NO_3^- assimilated comes from deep water, its assimilation goes towards new production.

3.2.3 Remineralization (PON $\rightarrow NH_4^+$)

Remineralization is achieved by respiring metazoans as well as bacteria that break down PON in the form of detritus (Von Brand et al., 1937).

Remineralization of PON is conducted by respiration and thus, is the only direct influence cephalopods have on the nitrogen cycle. Here, proteins are metabolized (Figure 34.3) to produce NADH and $FADH_2$ in the Kreb's cycle and the resulting waste product is NH_4^+.

3.2.4 Nitrification ($NH_4^+ \rightarrow NO_2^- \rightarrow NO_3^-$)

A population of NH_4^+ molecules take on average about 3 months to be completely oxidized to NO_3^- in pelagic environments. This is why the ocean interior is relatively rich in nitrate. However, the bacterial oxidations of the NH_4^+ are rather slow processes and are pretty negligible in productive surface waters. Nitrification can only occur in oxic water; in suboxic and anoxic water (Table 3.2), NH_4^+ accumulates as PON remineralizes.

3.2.4.1 Ammonia oxidation

Below the euphotic zone, remineralized ammonium fuels populations of archaea (ammonia oxidizing archaea, AOA) and also some bacteria (AOB) which convert NH_4^+ to NO_2^- (Von Brand et al., 1937). Archaea seem to be the dominant players in the water column compared to bacteria for ammonia oxidation (Wuchter et al., 2006). In fact, up to 40% of the microbial community can be ammonia oxidizing archaea (from the Thaumarchaeota subgroup), but they can also process DON so their populations are not completely coupled to water ammonium levels. In the sediment, however, AOBs are most dominant. In shallow coastal sediments, *Nitrosomonas* spp. are the most abundant AOBs.

3.2.4.2 Nitrite oxidation

As nitrite concentration builds, it fuels a population of nitrite oxidizing bacteria (NOB) and also some archaea (NOA) which convert NO_2^- to NO_3^- (Von Brand et al., 1937) where it remains as long as $[O_2]$ remains too high for denitrifying bacteria to convert it to N_2 (Pilson, 2013). Interestingly, the nitrite oxidizing bacteria and archaea make up only up to 1% of the microbial community in the pelagic water column, unlike the abundant ammonia oxidizing microbes. However, the most abundant NOBs in the pelagic water column are of the genera *Nitrospina*, *Nitrococcus*, and *Nitrospira*. In shallow coastal sediments, *Nitrobacter* spp. are the most abundant NOBs.

3.2.5 Denitrification ($NO_3^- \rightarrow N_2$)

Denitrification occurs by bacteria, archaea, and some benthic foraminifera. These organisms inhabit anoxic or severely hypoxic regions of the ocean such as sediments and also OMZs. Most of the ocean's denitrification occurs in sediment on continental

shelves. Denitrification only occurs when $O_2 < 4.5 - 10\,\mu$mol/kg (Stramma et al., 2008) because it is less efficient than O_2 reduction (section 3.7). Here, these organisms utilize NO_3^- as a terminal electron accepter rather than O_2. Through a complex of enzymes they convert NO_3^- first to NO_2^- then to NO then to N_2O followed finally by N_2. Since N_2O is nonpolar, it easily escapes the cells and is typically produced whenever N_2 is produced.

Denitrification fractionates the available nitrogen, preferentially removing ^{14}N and leaving the remaining NO_3^- enriched in ^{15}N which increases the "baseline" $\delta^{15}N$ in trophic relationships.

The Pacific surface waters have a lower N:P ratio than in the Atlantic (but they still average out to the global 16:1 average). This is probably due to denitrification. The Pacific has larger OMZs which increases the ocean-wide rates of denitrification compared to the Atlantic. Thus, the Pacific is a net sink in oceanic N while the Atlantic is a net source of N (Pilson, 2013).

3.2.5.1 Anammox denitrification ($\mathbf{NO_2^- + NH_4^+ \rightarrow N_2}$)

The anammox denitrification process is another form of denitrification. It is conducted by anoxic bacteria and may play a sizable role in the total denitrification process globally.

3.2.6 Dissolved organic nitrogen (DON)

A fair amount of nitrogen in seawater (especially surface waters where phytoplankton keep all the DIN species low) is dissolved organic nitrogen. This nitrogen is held mainly in animal waste such as urea or pieces of bacterial cell walls. [DON] in the euphotic zone is often ~10 μmol/kg.

3.3 The phosphorus cycle

Phosphorus fluxes into the marine system via rivers (Pilson, 2013). Phosphorus is somewhat often the limiting element for phytoplankton growth (Pilson, 2013). DIP are the most abundant forms of phosphorus, typically about 10x more concentrated than DOP.

3.3.1 Dissolved inorganic phosphorus (DIP)

Important species: H_3PO_4, $H_2PO_4^-$, HPO_4^{2-}, PO_4^{3-}

In seawater, almost no phosphoric acid is undissociated ($[H_3PO_4] \approx 0$). The remaining three anions are distributed as 90% HPO_4^{2-}, 9% PO_4^{3-}, and 0.9% $H_2PO_4^-$ (coincidentally very similar to DIC's species distribution). The total concentration of DIP ranges between 0 at the surface and ~3 μmol/kg in deep N. Pacific water (Pilson, 2013) with phosphorus depleted at the surface where phytoplankton have consumed much, peaking around 1000 m or so when detritus is mainly consumed, and lowering somewhat with depth to the bottom. Because Pacific deep water is older, it has almost twice the concentration of DIP as the Atlantic (Pilson, 2013). In coastal temperate regions, total DIP varies seasonally with the highest concentrations in the summer and lowest in winter. During these seasonal patterns, DIP is exchanged between the sediment and water column (Pilson, 2013).

According to the Redfield equation, 166 μmol O_2 (AOU) yields 1 μmol DIP (subsection 9.0.1).

3.3.2 Dissolved organic phosphorus (DOP)

Phosphorus can also occur in seawater as part of organic molecules such as phospholipids or nucleic acids. DOP concentration is typically around 0.1-0.2 μmol/kg (Pilson, 2013).

3.3.3 Polyphosphates

Polyphosphates are polymers of phosphates which are produced by bacteria and phytoplankton. They are produced as storage molecules but are excreted into the water when cells lyse. They are not very concentrated in most areas of the ocean.

3.4 The silicon cycle

3.4.1 Species

Silicon (Si) is always bound to oxygen, typically as silica, SiO_2 (Pilson, 2013). Diatoms, radiolarians, and silicoflagellates make their shells out of opal, an amorphous precipitate of silica (Pilson, 2013). Most of the silica on Earth, however, is in minerals such as quartz. In seawater, however, silica is most abundant in the form of silicic acid, $Si(OH)_4$ which varies from ~1 μmol/kg in productive surface water (where it is taken up by plankton) to ~200 μmol/kg in deep Pacific water (Pilson, 2013). Silicic

acid, however, has an equilibrium concentration somewhere between ~1000 and 2000 μmol/kg depending on structure, organic coatings, and of course temperature and pressure. Silicic acid is undersaturated everywhere in the ocean, therefore, but this is maintained because equilibrium is reached so slowly. It can take many weeks or months for aqueous and precipitated silica (e.g. opal) to reach equilibrium.

3.4.2 Fluxes and distribution

Most of the silicon entering the oceans comes in through rivers and leaves through sediment deposition. Riverine water has a much higher proportion of Si relative to ionic strength than seawater. This is due to rock weathering. While much of diatom and radiolarian tests are dissolved before they are buried, there is certainly a net flux of silicon through sedimentation. Even once it's buried, however, the tests can still move towards equilibrium with the interstitial water in the sediment and this water can diffuse towards the sediment surface and flux back out into the water column.

The fluxes of silicon into and out of the oceans may not be in steady state. Due to anthropogenic nitrogen and phosphorus enrichment in rivers and lakes, freshwater diatoms are precipitating much of the silica that use to flow freely to the ocean. Now instead, there may be less silica entering the oceans and thus a net decrease in the ocean's silica budget.

Si distribution varies from nitrogen and phosphorus because silicon remineralizes at a deeper depth than nitrogen and phosphorus are respired. While respiration can happen quickly, silica remineralizes slowly and thus tests reach deeper depths before the silica remineralizes. Dissolution is also more favorable under higher pressure which dissolves even more silica at depth.

Diatoms utilize silica heavily. In fact, healthy diatoms are composed of 1:1 Si:N.

3.5 Trace metal elements

Trace elements are nutrients with concentrations <1 μmol/kg. They often have conservative, nutrient-like, or scavenged vertical distributions (Pilson, 2013). Iron, zinc, and manganese are the three most concentrated trace elements in organisms (at least phytoplankton). Metal toxicity is typically caused by a molecule mistaking a toxic metal for the intended nutrient metal. Many metals in seawater are highly reactive and are present in a variety of species. Three important equilibria that metal ions establish are 1. ion hydration ($M + n\,H_2O \rightleftharpoons M(H_2O)_n$), 2. hydrolysis ($M + H_2O \rightleftharpoons MOH^- + H^+$), and 3. anion binding (e.g. Cl^-, SO_4^{2-}, F^-, or OH^-). The smaller and more highly charged a metal cation, the more it hydrolyses.

Heavy metal concentrations in cephalopod tissues are often highest in the digestive gland and branchial hearts (Lischka and Roldan-Wong's 2018 CIAC talks).

3.5.1 Aluminum

Aluminum has its highest concentration at the surface where wind-borne dust fluxes Al into seawater. From there, Al seems to be scavenged, leading to a declining [Al] with depth, although [Al] increases again in very deep water due to remineralization (Pilson, 2013). [Al] is higher in the Atlantic than Pacific since almost all Al is scavenged by the time water reaches the Pacific basin and there is less dust input than in the Atlantic (Pilson, 2013). Al is quite insoluble, but its solubility is pH-dependent, increasing with decreasing pH in normal seawater ranges.

3.5.2 Cadmium

Cadmium has been found to be used in carbonic anhydrase isoforms in some phytoplankton especially when zinc is scarce. There is no evidence that it is utilized by any cephalopods, but I do not see any reason why it couldn't be used for the same purpose.

Cadmium has a nutrient-like distribution, and is quite strongly correlated with phosphorus (Pilson, 2013). Concentrations in deep water can reach 1 nmol/kg (Pilson, 2013).

3.5.3 Cobalt

Mean [Co] is ~50 pmol/kg at the surface but it is scavenged with depth. Much cobalt is bound to organic ligands.

3.5.4 Copper

Copper is utilized in many enzymes, including, notably, hemocyanin. 85% of copper in cephalopods is part of hemocyanin. Its concentration in seawater is problematic for phytoplankton if too low (unavailable) or too high (toxic). Copper is toxic at high concentrations because it outcompetes manganese at manganese uptake sites. There is lots of anthropogenic Cu pollution in developed coastal regions which can be toxic to phytoplankton and some zooplankton.

99.9+% of Cu in seawater is not free ion form but bound to organic ligands and not bioavailable (Pilson, 2013). It is likely that these ligands are produced by phytoplankton to keep environmental [Cu] at reasonably low levels. Some bacteria can utilize this ligand-bound Cu and thus make it bioavailable to higher trophic levels including cephalopods through their diet. Otherwise, copper availability to cephalopods only comes through the small proportion that are free and utilized by phytoplankton. Mean oceanic [Cu] is ~4 nmol/kg and is more abundant with increasing depth. At deep depths where organic ligands are much more scarce, as much as 1% of total [Cu] may be free Cu^{2+}; the remaining is complexed with anions such as CO_3^{2-} or bound to inorganic ligands.

3.5.5 Germanium

Germanium is utilized by phytoplankton that create silicious tests. Germanium has very similar chemical properties to silica and thus, is incorporated into tests (Pilson, 2013).

It is distributed in three forms: 1. inorganic Ge, 2. $CH_3Ge(OH)_3$ (monomethylgermaninum), and 3. $(CH_3)_2Ge(OH)_2$ (dimethylgermanium). The inorganic form has a distribution very similar to silica but just lower in abundance. The organic forms are conservative, closely following salinity patterns (Pilson, 2013).

3.5.6 Iron

Iron is an essential nutrient for all biota because of its importance in key enzymes. Nitrogen fixing bacteria such as *Trichodesmium* require much more iron than most because nitrogen fixing and reducing enzymes need Fe (Pilson, 2013). In fact, even phytoplankton that utilize NO_3^- require more Fe than when utilizing NH_4^+ since there are enzymes which reduce nitrate to ammonium before it is incorporated into the rest of metabolism (Pilson, 2013).

Iron enters marine systems primarily through inorganic wind dispersal and leaching from rocks (and subsequent input through rivers) (Pilson, 2013). Lots of iron blows off the Sahara Desert into the Atlantic.

In most of seawater, where oxygen is present, Fe is in the ferric form, Fe^{3+}, which is quite reactive. The ferrous form, Fe^{2+}, is much less reactive but only found in anoxic regions (section 3.7). Inorganic iron, ferric hydroxide, is quite insoluble in seawater (Pilson, 2013), though its solubility is pH dependent, becoming more soluble with lower pH in the natural seawater range. However, 99+% of Fe in seawater is not free inorganic molecules but bound to an organic ligand such as siderophores. Siderophores are complex organic molecules produced by bacteria that have an extremely high affinity for iron (Pilson, 2013). Because it is an essential nutrient, [Fe] in seawater has a nutrient-like distribution and a mean concentration ~1 nmol/kg (Pilson, 2013). Manganese nodules actually contain just as much iron as manganese and thus are a notable store of iron in sediment (section 1.10.1.3).

Fe^{3+} is utilized by some bacteria as a replacement for oxygen in anoxic sediments section 3.7.

3.5.6.1 High-nitrate low chlorophyll (HNLC) regions

In some regions of the ocean (e.g. Southern Ocean, north Pacific, ETP) nitrate, which is typically the limiting nutrient, is abundant but phytoplankton stocks are still low. These HNLC regions are limited instead by iron. These regions tend to be in regions of the ocean that are isolated from land and have low fluxes of Fe through desert winds or riverine input. These regions may be part of the glacial-interglacial system: when iron enters these systems, carbon export increases which drives down atmospheric P_{CO_2} which in turn decreases atmospheric temperature. As the climate cools, regions of land become more arid and weathered by growing glaciers which in turn releases more iron to the system. Thus, HNLC regions can be positive feedback mechanisms for climate change.

3.5.7 Lead

Lead has a strange depth distribution because it is overwhelmed by contamination from leaded gasoline. Thus, concentrations are highest at the surface in the Atlantic. They are decreasing over time in surface waters because of the phasing out of leaded gasoline (Pilson, 2013).

3.5.8 Manganese

Mean [Mn] is 500 pmol/kg (Pilson, 2013) and has an enigmatic distribution with depth. The main form, Mn(IV), or Mn^{4+}, is quite insoluble and precipitates easily, often forming manganese nodules (section 1.10.1.3). Mn^{4+} is utilized by some bacteria as a replacement for oxygen in anoxic sediments section 3.7. Mn^{2+} is only found in anoxic water (section 3.7).

3.5.9 Mercury

Mercury accumulation in cephalopods and other high-trophic animals can be notable. Deep living fishes often have higher accumulations of Hg than shallow living taxa (Bustamante's 2018 CIAC talk). Within a given cephalopod, typically ~70% of the Hg is in the muscle (Bustamante's 2018 CIAC talk) and the vast majority of the Hg in this mantle is methylmercury (Lacoue-Labarthe's 2022 CIAC talk). Similarly, most of the mercury in the brain is methylmercury (Minet's 2022 CIAC talk).

Mercury exists in three oxidation states: Hg^0, Hg^+, and Hg^{2+}. The accumulated forms of Hg which are toxic at high concentrations are monomethylmercury, $HgCH_3^+$ and dimethylmercury, $Hg(CH_3)_2$ (Pilson, 2013). Bacteria produce $HgCH_3^+$ from Hg^0. One interesting aspect of Hg^0 is that it can behave like a gas, with a vapor pressure and saturation concentration in seawater (Pilson, 2013). It appears to be supersaturated in seawater and fluxes through the atmosphere rapidly. Most Hg, however, is in the form of $HgCl_4^{2-}$ (Pilson, 2013). Total [Hg] varies from 1-5 pmol/kg (Pilson, 2013).

3.5.10 Nickel

Nickel is an essential element for a number of enzyme active sites (Pilson, 2013). It follows a nutrient-like distribution reaching ~10 nmol/kg in deep water (Pilson, 2013).

3.5.11 Selenium

Selenium is an essential nutrient for many phytoplankton. There are two oxidation states in seawater, Se(IV) and Se(VI). Both forms have a nutrient-like distribution even though only Se(IV) is utilized by phytoplankton (Pilson, 2013). At depth, total [Se] can reach 2 nmol/kg (Pilson, 2013).

3.5.12 Zinc

Mean [Zn] is 6 nmol/kg but it has a nutrient-like distribution so it is more deplete at the surface (Pilson, 2013). Most zinc is bound to organic ligands.

3.6 Calcium carbonate

Cephalopods utilize $CaCO_3$ to create their statoliths and cuttlebones.

Roughly 21 trillion moles of calcium flux through the oceans yearly (Pilson, 2013). Calcium enters the ocean through riverine input, the result of dissolving away limestone. Riverine water has a much higher proportion of Ca^{2+} relative to ionic strength than seawater. Most calcium precipitates out of the ocean as $CaCO_3$ which is almost entirely biogenic (Pilson, 2013). $CaCO_3$ precipitation is conducted primarily through forams, coccolithophores, and corals. Coral reefs precipitate ~9 trillion moles of calcium each year, or about 40% of all Ca export from the ocean (Pilson, 2013). Some quantity of $CaCO_3$ is also precipitated via whiting events in shallow warm waters when the water gets too warm for CO_3^{2-} to stay in solution (Pilson, 2013).

Precipitation of $CaCO_3$ decreases seawater alkalinity and increases P_{CO_2} (Pilson, 2013). The increase in P_{CO_2} with $CaCO_3$ precipitation is due to the following mechanism: as CO_3^{2-} fluxes out of the seawater system, HCO_3^- must dissociate into CO_3^{2-} and H^+ in order to maintain K_2 (Table 3.1). However, since CO_3^{2-} is constantly fluxing out of the system, this constant dissociation causes $[H^+]$ to increase. The increase in $[H^+]$ results in a shift towards H_2CO_3 in order for K_1 to be maintained. This is how $CaCO_3$ precipitation results in higher seawater P_{CO_2}. The equilibrium between solid $CaCO_3$ and its ion products, Ca^{2+} and CO_3^{2-}, can take months to be reached. This is why the saturation state can vary from 1 in most parts of the ocean.

3.6.1 Saturation state (Ω)

The dissociation constant for $CaCO_3$, K_{sp}, is temperature, salinity, and pressure sensitive (Pilson, 2013). The saturation state of a water mass can be defined as:

$$\Omega = \frac{[Ca^{2+}][CO_3^{2-}]}{K_{sp}}$$

Almost all warm surface waters are supersaturated with $CaCO_3$, typically Ω = 2-3. At greater depths, however, saturation decreases. This is due to a number of factors: 1. unlike most salts, $CaCO_3$ becomes more soluble at colder temperatures (K_{sp} increases), 2. greater pressure increases K_{sp} as well as K_1 from carbonic acid which decreases pH thus driving $[CO_3^{2-}]$ down, 3. at depth pH is lower due to respiration which decreases $[CO_3^{2-}]$ (Pilson, 2013).

Table 3.2: Redox processes. A Redfield molecule is defined in subsection 9.0.1 on page 81.

Zone nomenclature	Process	Oxidant (e^- acceptor)	Product	Concentration in seawater (μM)	Energy
"Oxic"	Aerobic respiration	O_2	H_2O	200-300	
"Suboxic"	Mn reduction	MnO_2 (solid) / Mn^{4+}	Mn^{2+}	<0.001 (~10 in sediment)	
	Denitrification	NO_3^-	N_2	10-40	
	Fe reduction	Fe_2O_3 (solid) / Fe^{3+}	Fe^{2+}	<0.001 (~10 in sediment)	
"Anoxic"	Sulfate reduction	SO_4^{2-}	HS^-	28,000	
	Methanogenesis	CO_2	CH_4	Very high. produced by all reactions above	

The lysocline is the water column depth below which dissolution of CO_3^{2-} begins. The carbonate compensation depth (CCD) is deeper, the depth at which the rate of dissolution is equivalent to the rate of downwelling carbonate flux from the surface.

Since aragonite is more soluble than calcite, often when aragonite dissolves, it reprecipitates as calcite (Pilson, 2013).

3.7 Redox processes

Oxidation $\mathbf{CH_2O}$ (glucose) $+ H_2O \rightarrow \mathbf{CO_2} + 4H^+ + \mathbf{4e^-}$

Reduction $\mathbf{O_2} + 4H^+ + \mathbf{4e^-} \rightarrow \mathbf{2H_2O}$

Oxygen may be the most frequently utilized terminal electron acceptor in biological metabolism, but it is not the only one. $[O_2]$ can often become extremely low or non-existent in sediments or even deep water columns where production above is high and advection is low (e.g. fjords, trenches, Black Sea). In these regions, some forms of bacteria, archaea, and a few protozoa utilize other substrates to oxidize glucose (or other substances) to CO_2. These processes all utilize redox reactions, which involve electron transfer from a reductant (e.g. glucose) to an oxidant.

Table 3.2 shows the order (and sediment depth) in which these anoxic oxidations occur. Mn and Fe reduction are negligible in the water column because they are both so insoluble in seawater and therefore present in extremely small concentrations. Although sulfate reduction is near the bottom of the redox tower, SO_4^{2-} is much more concentrated than NO_3^-, Mn, Fe, or even O_2 concentrations and thus its reduction to H_2S is the most obvious characteristic of anoxic sediments or water (Pilson, 2013). Because of the abundance of sulfate in seawater, methanogenesis is only reached in sediments (rather than the water column). The redox tower is arranged in the order it is because each process produces less energy per unit of organic material than the process above it. Thus, it is less efficient and only resorted to when other substrates have been exhausted (Pilson, 2013). Sediment (as well as anoxic water columns like in the Black Sea) that is $<$ 4.5-10 μM O_2 is the threshold where denitrification begins (subsection 3.2.5).

Chapter 4

Geographic locations of interest

4.1 Earth

The Earth is ~4.5 billion years old and the oceans are ~4.4 billion years old.

Total ocean surface area: ~360×10^6 km^2.

Total ocean volume: about 1 billion km^3 or 1 trillion m^3 (or more precisely: 1.35×10^{12} m^3). The total volume has been roughly constant over geologic history (Pilson, 2013).

One degree latitude = 111 km. Longitude is similar at the equator but shortens with higher latitude.

Earth radius: ~6400 km

The oldest oceanic crust on Earth is ~150 MY old in the northwest Pacific.

4.2 Arctic Ocean

Traditionally, sea ice ages and grows thicker in the Beaufort Sea north of Alaska and sea ice is lost from the Arctic through the Fram Straight heading south along the east coast of Greenland.

There are 10-12 cephalopod species that are endemic to the Arctic (Golikov's 2015 CIAC talk) but 32 species are known to inhabit it (Rosa's 2018 CIAC talk). However, there are no sepiids nor myopsids in the Arctic (Rosa's 2018 CIAC talk). *Gonatus fabricii* are the most abundant pelagic cephalopod in the Arctic.

4.3 Baltic Sea

The Baltic Sea has had lots of issues with eutrophication.

4.4 Bering Sea

The net water movement through the Bering Sea is from the Pacific to the south through the Bering Strait up into the Arctic.

Pollock remains an important fishery here but the historical crab fishery is in decline.

4.5 Bermuda Atlantic Time-series Study (BATS)

The plankton community at BATS has been shifting in recent years away from diatoms and towards more cyanobacteria.

4.6 Black Sea

The Black Sea has essentially zero tidal amplitude!

Due to lots of freshwater input as well as extremely salty input from the Med, the Black Sea is highly stratified and anoxic below about 100 m.

4.7 California Current System (CCS)

The California Current is the eastern boundary current (EBC) along the north Pacific gyre. Productivity is high along the CCS because of Ekman transport induced upwelling along the steep continental slope of the west coast of North America. The water column along the CCS (and Peru Current) has a characteristically shallow thermocline because the SSH is so low relative to the western Pacific where trade winds push lots of water (subsection 2.1.1). The thermocline-SSH relationship exists for the same reason as it does in mesoscale eddies (subsection 2.6.3). This shallow thermocline permits high quantities of nutrient flux with only moderate upwelling which is why such large cephalopod populations can be supported (as well as other stocks).

Coastal regions along the CCS can often encounter numerous or long-duration hypoxic events (Low et al., 2021). Oxygen at 20 m depth off San Diego gets down to ≈7 kPa (Low et al. 2021).

Octopus californicus is the most abundant deep water octopod off the California coast (Hochberg 1997 cited by Seibel Childress 2000).

4.8 Caribbean Sea

The Caribbean has 129 species of cephalopods (Judkins dissertation). *Opisthoteuthis agassizii* and *Stauroteuthis syrtensis* are by and large the two most abundant cirrates in the Caribbean (Pratt's 2022 CIAC talk).

Coral diversity is lower in the Caribbean than the Indo-Pacific because the Caribbean got too cold during the recent ice ages to support corals. At least parts of the Indo-Pacific remained warm enough to support high diversity and recolonization from the Indo-Pacific was impeded by the closing of the Isthmus of Panama < 10 MYA (Castro and Huber, 2019).

4.9 Chesapeake Bay

The Chesapeake Bay is the largest estuary in the United States and one of the largest in the world (Rabalais et al., 2010).

Average depth is 6 m (Rabalais et al., 2010).

Eutrophication is a major problem for the bay (Rabalais et al., 2010). Typical summer hypoxic water volume is 10 km^3 (Rabalais et al., 2010).

4.10 Delaware Bay

The Delaware Bay watershed covers all of eastern Pennsylvania, western New Jersey, and into southern New York. The bay is home to *Doryteuthis pealeii* (Haefner Jr., 1964).

4.11 Eastern Tropical North Pacific (ETNP)

4.11.1 OMZ

The ETNP OMZ was first discovered by the Dana expedition in 1922. The ETNP has an extensive oxygen minimum zone which has one of the lowest minimum $[O_2]$ values: 1.8 μM (Wishner et al., 2013). The OMZ depth typically spans from 300 m to 600 m (Wishner et al., 2013). Much of the OMZ in this region is composed of water masses that have moved from the highly productive California Current and Peru Current. The western boundary of the ETP OMZ is restricted near the equator. This is due to easterly flowing currents from the relatively oxygenated western Pacific (Stramma et al., 2008).

In the ETNP, P_{CO_2} near the surface can be ≈ 50 Pa while in the core it may be over 150 Pa (Franco et al., 2014).

4.12 Gulf of California

The most abundant cephalopod paralarvae in the GoC are pyroteuthids (exclusively *Pterygioteuthis hoylei*; De Silva-Dávila et al. 2013) and ommastrephids, but argonauts are also commonly found in the spring. *Abraliopsis* spp. are frequently caught but not very abundant (De Silva-Dávila et al., 2015).

- The GoC is an evaporative basin. Thus, generally, salinity increases with latitude.
- Wind is NWerly in the winter and SEerly in the summer. This leads to coastal upwelling on the western margin in the summer and eastern margin in the winter.

- There are two predominant surface water masses: in the north is the Gulf of California Water Mass (GCW) characterized by salinity > 35 psu and in the south is the Tropical Surface Water (TSW) with salinity < 35 psu. Cephalopod paralarvae assemblages follow these masses. Below the GCW are the Pacific Intermediate Water (PIW) and Pacific Deep Water (PDW).
- SST ranges from 15 °C in the winter to 30+ °C in the summer.
- The OMZ in Guaymas Basin is quite shallow: ~150-200 m down to 800 m (Trübenbach et al., 2013). The upper margin of the OMZ is often near the deep scattering layer where prey (e.g. myctophid) abundance is high.
- San Pedro Martir Basin is the northern extent of the OMZ
- Guaymas Basin is 2000 m deep (Gilly et al., 2012)

4.13 Gulf of Mexico

The Gulf of Mexico is bordered on three sides by North America. The continental shelf width averages roughly 200 km except along mainland Mexico where the shelf width is only ~50 km. At the center of the Gulf, typical bottom depths are in the mid-3000 m range. Although there is a wide distance between Florida and the Yucatan Peninsula, their shelves are both quite wide which leaves only ~130 km wide gap of deep water (i.e. 2000+ m) for deep water to flow into or out of the Gulf. The Gulf of Mexico Loop Current brings water up from the Caribbean and then east through the Florida Straights into the Gulf Stream. This Loop Current can often spin off eddies into the Gulf.

The Mississippi River flows ~0.02 Sv of water into the Gulf.

The Isthmus of Panama, determining current flow dynamics in the Gulf of Mexico, did not form until < 10 MYA.

The Gulf of Mexico contains biological communities that are a mix of temperate Atlantic species and tropical Caribbean species, depending on how water advects through the region (Hixon, 1980).

There are 138 cephalopod species in the pelagic Gulf of Mexico (Heather Judkins). *Lolliguncula brevis* are the dominant squid species along west Florida estuaries (Dragovich and Kelly Jr., 1967). Along an offshore gradient on the continental shelf, *Lolliguncula brevis* are found in the shallowest regions, *Doryteuthis pleii* are found in the 10s of meters depth range, and *Doryteuthis pealeii* are found in the 50+ depth ranges furthest off the coast along the continental shelf (Hixon, 1980).

In the pelagic environment, some of the most abundant families are enoploteuthids, cranchiids, pyroteuthids, and ommastrephids (Judkins et al., 2017). *Japetella diaphana* are quite abundant in the Gulf of Mexico (Judkins' 2022 CIAC talk). *Opisthoteuthis agassizii* and *Stauroteuthis syrtensis* are by and large the two most abundant cirrates in the Gulf of Mexico (Pratt's 2022 CIAC talk).

4.13.1 West Florida Shelf

The West Florida Shelf is on the west coast of Florida in the northeastern Gulf of Mexico. It is ~200 km wide.

While both *Doryteuthis pealeii* and *Doryteuthis pleii* are found on the West Florida Shelf, the latter is much more abundant (Hixon, 1980).

4.13.2 Eutrophication from the Mississippi River delta

The Mississippi River creates a highly salinity-stratified plume that travels west from the delta (Rabalais et al., 2010). This causes a eutrophication-induced dead-zone in the Northern Gulf of Mexico that typically forms in the early spring, lasts through the summer, and dissipates in the late autumn. The dead zone is typically very large, the second largest anthropogenic hypoxic zone in the world after the Baltic Sea (Rabalais et al., 2010). Typically, at its yearly peak, about 13,500 km^2 of the Gulf of Mexico is hypoxic (< 60 μM) but it can exceed 22,000 km^2 some years (Rabalais et al., 2010).

4.14 Macaronesia

Macaronesia is a collection of island groups off the west coasts of Africa and Europe including Cape Verde, the Canary Islands, Madeira, and the Azores. The marine ecosystems are similar in the later three island groups but Cape Verde has a distinct ecosystem (Merten's 2022 CIAC talk).

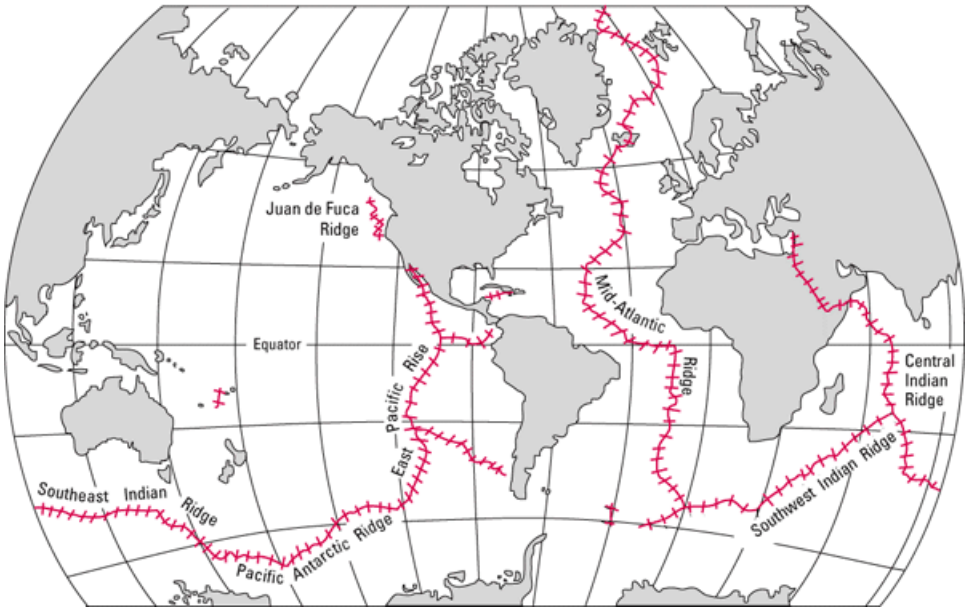

Figure 4.1: Mid-ocean ridge system.

4.15 Mediterranean Sea

The Mediterranean is characterized by eastward surface currents and westward bottom currents. Salinity is high (38-39 psu) compared to oceanic waters due to the high evaporation rate (Pilson, 2013). Over time, this has led to high abundance of evaporitic sediment (over 1 km thick!) that is rich in $CaCO_3$, $CaSO_4$ and NaCl subsubsection 1.10.1.3. Seawater residence time is about 70 years.

Late in the Miocene epoch (6 Ma), the Strait of Gibraltar closed up and created the Messinian Salinity Crisis for about 600k years as water levels dropped by a few hundred meters and the resulting salinity became so high the entire Med was uninhabitable for marine life. Thus, all extant marine life in the Med migrated back into the Med when the Strait of Gibraltar opened back up and the Atlantic refilled the Med to its present-day level.

4.16 Mid-Ocean Ridge System

The Mid-Ocean Ridge System (MORS) spans 60,000 km and has an average depth of 2500 m. Depending on location, 2.5-15 $cm \cdot yr^{-1}$ of new oceanic crust is formed along the ridge. The fastest spreading is along the East Pacific Rise, while the Mid-Atlantic Ridge is much slower. The global average spreading rate is ~5 cm / year (Pilson, 2013). MORS occur where tectonic plates diverge and underlying mantle is excreted to form new crust.

4.16.1 Hydrothermal vents

Seawater cools new basalt, cracks it, and infiltrates the new crust. As seawater gets deeper, it warms until it is released through hydrothermal vents. Black smokers emit acidic water up to 350 °C, while white smokers are cooler (30-330 °C). Vents are hot while seeps are ambient temperature. Chimneys are formed from $CaSO_4$ (anhydrite) but are layered with other precipitates from the plumes as well. At a given location on a vent, temperature, O_2, pH, and [sulfide] are very ephemeral, changing on the order of minutes. Compared to normal seawater (Table 1.2), the water coming out of hydrothermal vents has no Mg^{2+}, no SO_4^{2-}, 1000-fold increase in silica, high concentrations of trace metals (e.g. Mn), lots of methane, sulfide, and CO_2 (Pilson, 2013). Vent-water pH is often <4 (Pilson, 2013) with P_{CO_2} of 7 kPa. $[Na^+]$ and $[Cl^-]$ are very strange coming out of vents due to strange physics of how at high pressure and temperature the liquid and gas phases blend and it causes salt solubility to do strange things. Black smokers are black because of the dissolved iron immediately precipitating when the water hits cold ambient seawater.

Most vent fields are only active for years to decades. They cease activity due to tectonic changes in the fracture pattern, clogging from mineral precipitates, or extinguishment of the magma source.

4.17 Narragansett Bay

- Typical depth ranges from 8 meters in the north, to ~37 m at the mouth of the bay with a maximum depth of 56 m.
- Temperature varies from 0.8 to 26.4 ^{o}C with daily ranges around 5 ^{o}C (Turner, 2015).
- Water residence time is 30 ± 9 (s.d.) days.
- Daily pH fluctuations can be on the order of 0.4 units and are driven by DIC (respiration-photosynthesis balance). pH ranges from 8.2-8.6 during February/March to 7.7-8.1 during June/July (Turner, 2015). O_2 equilibrates with the atmosphere before the bay flushes, but CO_2 is flushed before equilibrating with the atmosphere (Turner, 2015).

Narragansett Bay is ~20,000 years old. It was a freshwater lake initially carved from glaciers. When they melted, sea level rise flooded it with seawater.

Doryteuthis pealeii are the only squid that occur in Narragansett Bay, typically inhabiting the bay from May/June through October/November.

4.18 North Sea

The North Sea is quite shallow especially in its southern regions, averaging only 94 m deep and maxing out at ~700 m.

4.19 Red Sea

The Red Sea has an average depth of only 500 m and a maximum depth of 3000 m.

The SST varies from 26-30 °C year-round. Due to its highly-evaporative climate and poor convection with neighboring bodies of water, has a very high salinity: 36-41 psu.

4.20 South China Sea

The dominant surface currents change seasonally with the monsoon.

4.21 Southern Ocean

If a hard boundary is needed, the Southern Ocean is most often defined as water south of 60 °S or alternatively as that south of the Southern Subtropical Front (defined as the boundary where salinity at 100 m depth first drops below 34.9 psu.

Within a month, pH can vary 0.05 to 0.1 pH units (Hofmann et al., 2011).

Just north of the ACC, Subantarctic Mode Water (SAMW) is formed (sinks to mid-depths) and spreads to near the equator in the Pacific and to the northern subtropics in the Atlantic.

54 species of cephalopods inhabit the Southern Ocean including 42 squids, however no myopsids or sepiids inhabit the Southern Ocean (Rosa et al., 2017). The single most diverse and abundant genus is *Pareledone*. There are 33 endemic octopod species and 1 endemic squid species known (Xavier's 2022 CIAC talk).

Squids in the Southern Ocean in general migrate southwards as they grow (Queiros et al. 2021, MEPS).

Antarctic predators (birds and mammals) often spend much of their time near the South Atlantic and South Indian oceans by comparison to the South Pacific (Xavier's 2022 CIAC talk).

4.21.1 History

In the early Eocene, Antarctica was a very warm tropical place when it was still connected to Australia and South America. Antarctica was separated with the Antarctic Circumpolar Current (ACC) by the formation of the Drake Passage off South America 30-50 Ma. Subsequently, glaciers started forming on the continent 36.5 Ma. The continent is currently under 3-5 km of ice.

4.22 Subtropical gyres

Subtropical gyres are formed by the geostrophic currents (subsection 2.6.4).

Subtropical gyres are oligotrophic and thus have low primary productivity, but the phytoplankton that do exist there are predominantly cyanobacteria rather than eukaryotic phytoplankton like diatoms. This is because cyanobacteria are smaller and thus advantaged in nutrient-limited waters. The most abundant cyanobacteria in these gyres are *Prochlorococcus* spp., *Synechococcus* spp. and *Trichodesmium* (N_2-fixing).

Atlantic subtropical gyres have slightly higher [Chl a] than Pacific gyres because they are not Fe-limited like Pacific gyres are.

4.22.1 Atlantic subtropical gyres

The Atlantic subtropical gyres are low in N and Si but have plenty of Fe from Saharan dust deposition. They are N-limited because the deep water is new NADW.

4.22.2 Pacific subtropical gyres

The Pacific subtropical gyres are low in Fe and thus are HNLC environments.

Because the Pacific has a low pH generally, the carbonate saturation state (Ω) is < 1 in much of the water column (subsection 3.6.1), and thus there are very few calcareous sediments in the Pacific.

4.23 Tampa Bay

Tampa Bay is an estuary along central western Florida. In the 1960s Tampa Bay had a large eutrophication problem, but nutrient input reductions were made in the 1980s and hypoxia has been depressed (Rabalais et al., 2010).

- 900 km^2 area and 341 km of shoreline (Dragovich and Kelly Jr., 1964).
- Mean depth is 3 m, with 90+% of the bay < 7 m (Dragovich and Kelly Jr., 1964).
- Circulation is primarily tidally driven, with riverine output playing a minor role. Tidal range varies from 58 to 68 cm (Dragovich and Kelly Jr., 1964).
- Because it is so shallow, water temperatures follow air temperatures, with a yearly range from as low as 10 ^{o}C in Dec/Jan to 32 °C in Jul/Aug (Dragovich and Kelly Jr., 1964).
- Salinity can become nil in some areas of the bay after heavy rainfall (Dragovich and Kelly Jr., 1964).
- Hypoxia was a major issue in the 1960s - 1980s but now hypoxia only occurs in the dredged channels in summer (Rabalais et al., 2010).
- Phytoplankton in the bay are strongly nitrogen-limited. The nearby Bone Valley provides high phosphorus inputs which leave nitrogen as the limiting element (Rabalais et al., 2010).

Lolliguncula brevis and *Octopus* sp. are the only two cephalopod species known in Tampa Bay (Dragovich and Kelly Jr., 1964). *L. brevis* is the second most abundant invertebrate in Tampa Bay.

4.24 Water masses

Water masses are characterized by T-S curves (temperature-salinity characteristics) (Emery, 2003).

4.24.1 Upper waters (0-500 m)

4.24.2 Intermediate waters (500-1500 m)

4.24.2.1 Antarctic Intermediate Water (AAIW)

4.24.3 Deep waters (1500+ m)

4.24.3.1 North Atlantic Deep Water (NADW)

NADW lies in the 2000-4000 m depth range in the Atlantic.

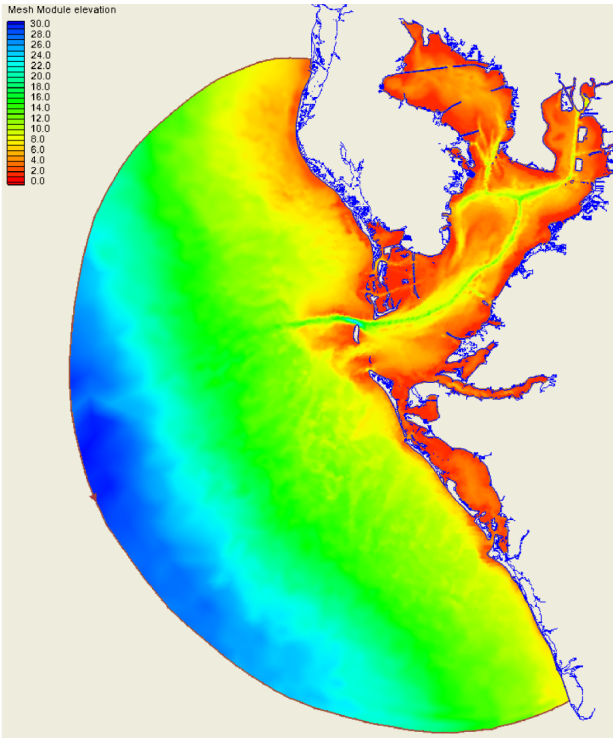

Figure 4.2: Tampa Bay bathymetry. From the Tampa Bay Operational Forecast System.

4.24.3.2 Antarctic Bottom Water (AABW)

AABW is characterized by an anomalous quantity of Si relative to NO_3^-. This is because when diatoms in the surface Southern Ocean are Fe limited, they don't assimilate NO_3^- because they can't process it, but they still take up Si to form their frustules. Thus, they form their frustules but do not develop their bodies proportionally, and therefore become negatively buoyant and sink into the AABW. Here, due to the greater depth, the silicious frustules remineralize (section 3.4) and flux a much higher proportion of Si relative to NO_3^- into this water mass than in most water masses.

4.25 Paleolocations

4.25.1 Pangaea and Panthalassa

Pangaea broke apart in the late Cretaceous.

Chapter 5

Generalized locations of interest

All of the following information is stereotyped generalizations of these environments.

5.1 Reef

5.1.1 Categories

$$\text{Open ocean} \rightarrow \text{Reef slope} \rightarrow \text{Reef crest} \rightarrow \text{Reef flat}(\rightarrow \text{Lagoon}) \rightarrow \text{Shore}$$

Reefs can be categorized by three rather porous and overlapping groups: fringing reefs, barrier reefs, and atolls (Castro and Huber, 2019).

- Fringing reefs are the most common and are composed of a reef slope (fore reef), reef crest, and reef flat (back reef) before reaching the shore.
- Barrier reefs are similar to fringing reefs except between the reef flat and shore is an extended sandy or muddy lagoon.
- Atolls are similar to barrier reefs but there's no shore anymore so the lagoon just continues to the reef flat on the other side.

5.1.2 Composition

Reefs are built up by a combination of mainly corals and coralline algae, but also some other calcifiers.

Reef flats are exposed to sediment and freshwater so they tend to be less diverse since only hardy species can endure these stressors (Castro and Huber, 2019). However, these must not be the only contributors since atoll reef flats are also low in coral abundance and diversity and they do not have any sediment or freshwater contributors.

Reef crests may be diverse or an algal ridge if waves are intense. Coralline algae generally makes stronger and less porous carbonate rocks and thus withstands wave action better than coral carbonate (Castro and Huber, 2019). For this reason, reef crests are often built up mainly by coralline algae because they can withstand the waves. In fact, on the windward side of atolls, the reef crests tend to be dominated by coralline algae while on the leeward side, there are comparably fewer algae (Castro and Huber, 2019).

Reef slopes can often be the most diverse because pelagic water brings nutrients and zooplankton (Castro and Huber, 2019).

Tropical reefs can be extremely productive, fixing up to 1500-3500 g C / m2 / year.

Corals are constantly competing for space and light. They utilize toxic attacks to form "demilitarized zones" between individuals.

The high diversity is in part due to frequent catastrophic events such as storms that prevent few species from dominating.

Table 5.1: Seafloor regions. Based on Nixon and Young, 2003.

Region	Depth range (m)	Slope ratio
Continental shelf	20-550	1:1000
Continental slope	550-2000	1:40
Continental rise	2000-5000	1:100 - 1:700
Abyssal plains	~4000	0

5.1.3 Nutrient cycling

Coral reefs can survive in nutrient poor waters because the coral - *Symbiodinium* mutualism allows corals to get their nutrients and serve as the base of the ecosystem. In general, there is high nutrient recycling in coral reefs. Predators return nutrients back to the reef through their excrement.

5.2 Barrier island

Barrier islands shift perpendicularly to shore following sea level. They form on wave-dominated coastlines where waves deposit large quantities of sediment. Sediment moves frequently along barrier islands via longshore drift. There are less barrier islands at high latitudes because post-glacial rebound prevents localized rising sea level. This movement of the island can be demonstrated by the finding of blackened oyster shells on an ocean-facing beach. These shells have been buried deep in anoxic sediment and the location where found used to be salt marsh.

5.3 Deep sea

Biomass decreases an order of magnitude per km in depth.

5.4 Hot seeps

5.5 Cold seeps

Cold seeps are fed by methane-ice and often form above oil and gas deposits.

5.6 Salt marsh

Salt marshes in the mid-Atlantic of the USA are filled with *Spartina alterniflora* (saltmarsh cordgrass) in the low marsh.

Low marsh region between median low tide and median high tide. This region is covered in seawater once or twice a day.

High marsh region between median high tide and spring high tide. This region is covered in seawater twice a month.

The plankton in saltmarshes is dominated by diatoms, copepods, and polychaete larvae.

5.7 Open ocean

Cephalopods that inhabit open pelagic environments are faced with stressors that vary over a longer timescale than those in coastal systems. Most large scale pelagic changes occur on seasonal or interannual cycles rather than the diel or even hourly changes that are frequent in coastal systems. However, small diel changes in pH and temperature have been observed (BATS and HOT) but they are orders of magnitude smaller than the changes in coastal systems (Gunderson et al., 2016).

5.8 Marine caves

Some marine caves can be quite physiologically demanding: having very low oxygen and also high temperature (e.g. >25 °C) (Bishop et al., 2004).

Troglobitic (permanently cave-dwelling) organisms have similar hypoxic adaptations as OMZ-adapted species (Bishop et al., 2004).

5.9 Polar (high latitude)

Many kinds of algae can accumulate on the underside of sea ice, forming algal mats that can be large proportions of primary productivity during certain times at high latitude.

Part II

Their community

Chapter 6

Plants

Among the marine-associated plants, seagrasses are the only truly marine organisms. The rest are merely extremely salt-tolerant but cannot be completely submerged indefinitely.

Cellular traits Plant cells often have their cytoplasms connected through tiny ports in the cell wall known as plasmodesmata (plasmodesma, singular).

The middle lamella is a substance that connects the primary cell walls of two plant cells together.

Plant cells often also have a secondary cell wall between the primary and plasma membrane.

As a generality of plants in general, above ground structures tend to only respire at night, while the roots are constantly respiring.

In most C3 plants, the Calvin cycle slows down as NADPH stock declines in the night.

Reproduction Similarly to macroalgae reproduction section 7, angiosperms alternate generations between a diploid sporophyte that produces haploid gametophytes. In angiosperms, the main plant is the sporophyte and the gametophytes are reduced to small structures known as pollen and eggs. Once fertilized, the diploid zygote is in a seed within the fruity body of the plant.

6.1 Seagrasses

There are only 60-70 known species of seagrasses.

Seagrasses can form extensive meadows which provide important habitat for animals. They primarily occur in sheltered areas where wave action is sufficiently weak. Sometimes these meadows can be one giant individual.

They are angiosperms and can reproduce sexually or asexually. Although they do produce flowers, they are very small, likely because they rely mainly on currents rather than insects to pollinate.

Although they look like terrestrial grasses, they are not very closely related to them.

Seagrasses can suffer from epiphytes blocking sunlight to their leaves.

Seagrasses have horizontal stems known as rhizomes that are typically buried in the sediment. From these stems grow both the leaves and the roots.

6.2 Salt-marsh grasses

Salt-marsh grasses such as *Spartina* spp. have salt glands in their leaves to excrete salt. They grow in the intertidal, so their roots are submerged frequently but not constantly. These plants only grow in wave-protected areas in temperate climates (those that experience frost).

6.3 Mangroves

Mangrove forests are known as mangals. These plants only grow in wave-protected areas in (sub)tropical climates (those that do not experience frost).

Mangrove trees are a polyphyletic group.

Mangrove trees are viviparous, giving birth to new seedlings directly from the parent tree, without any independent seed stage.

There is often a distinct range pattern where red mangroves are closest to the ocean, followed by black mangroves, and finally white mangroves.

6.3.1 Red mangroves

Red mangroves are the seaward-most of the three major groups of mangroves. These plants have huge roots above the group that hold the plant up on stalks. They tolerate the salt by avoiding taking it up in the first place.

6.3.2 Black mangroves

Black mangroves have many vertical protrusions from the sediment that they use to acquire oxygen for their metabolism (to supplement their O_2 derived from photosynthesis).

Chapter 7

Macroalgae

Algae are a polyphyletic group of eukaryotes that can be organized into micro- and macro-algae depending on if they are uni- or multi-cellular, respectively. This section covers macroalgae while microalgae are covered in section 9.1. Macroalgae are traditionally split up into red, green, and brown algae but any individual species or individual in a species can vary in color based on pigments, sun exposure, age, etc.

Reproduction Broadly, asexual reproduction is very commonly used in macroalgae since the thallus can split since it is not dependent on roots for nutrients (Castro and Huber, 2019). However, during sexual reproduction, macroalgae can have two different categories of life history strategies: either with or without alternation of generations.

Without alternation of generations This strategy is not very common, being seen only in some brown and green algae, albeit in some very abundant species on the western Atlantic coast (e.g. *Fucus* and *Codium*).

Similarly to animals, the diploid thallus undergoes meiosis to form haploid gametes that fertilize to form a diploid zygote which grows into a diploid thallus again.

With alternation of generations Alternating generations is the most common strategy of sexual reproduction in macroalgae. A diploid thallus known as a sporophyte undergoes meiosis to form haploid spores. Unlike gametes that must fertilize to grow, the haploid spore divides on its own and forms into a haploid thallus known as a gametophyte. This gametophyte produces gametes which are released, fertilized to form a diploid zygote, which in turn grows into another diploid sporophyte thallus.

In some species, the sporophyte and gametophyte thalli are morphologically identical, while in other species the sporophyte is huge relative to a diminished gametophyte. Red algae also have third stage that is described below.

7.1 Red algae (Rhodophyta)

Red algae are quite specious, with over 10k species, the vast majority being marine. In fact, there are more marine red alga species than green or brown algae combined. Most red algae are macroalgae. In addition to chlorophyll a, they also contain phycobilin accessory pigments such as phycocyanin or phycoerythrin (Castro and Huber, 2019).

Unique sexual reproductive life history strategy Unlike other macroalgae, red algae gametes are not motile and are instead excreted in slime (Castro and Huber, 2019). These haploid gametes are fertilized to form a diploid zygote that grows into a diploid thallus known as a carposporophyte. This carposporophyte produces diploid spores known as carpospores that divide to form a diploid sporophyte. Then, as in the other macroalgae with alternating generations, the sporophyte undergoes meiosis to form haploid spores which grow into haploid thalli known as gametophytes, which in turn produce more haploid gametes.

7.1.1 Coralline algae

Coralline algae deposit very sturdy calcium carbonate deposits within their cell walls that help form reefs. This $CaCO_3$ also discourages grazing, which helps them be more abundant more fleshy macroalgae on reefs (Castro and Huber, 2019).

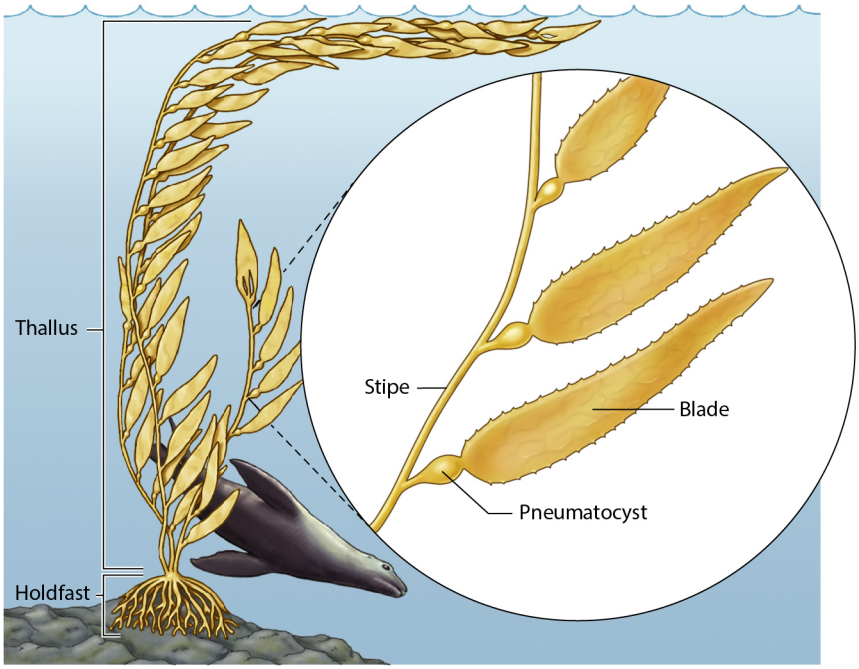

Source: Bill Ober

Figure 7.1: Macroalgae morphology

7.2 Green algae ("Chlorophyta")

This is a polyphyletic group when referring to all green algae. The taxonomic grouping of Chlorophyta still exists but is much more narrow in scope. They are mainly microalgae (unicellular) but there are still a fair number of macroalgae species and these can sometimes dominate habitats (Castro and Huber, 2019).

Some species of green algae form symbioses with fungi to form lichens. The fungal hyphae provide the structure and the algae provide the food. These lichens are very common at the upper reaches of rocky intertidal zones.

7.3 Brown algae (Phaeophyta)

Brown algae are exclusively macroalgae. Their cells are rich not only in chlorophyll a but also in the accessory pigment fucoxanthin, which gives them their brown color (Castro and Huber, 2019). They tend to be most abundant in temperate and polar regions.

Brown algae are unique among organisms in their secondary endosymbiosis of red algae.

Kelp beds become "kelp forests" when their thalli float on the surface in a thick mat.

Kelps typically can only grow down to 25 m or so depth before sunlight is insufficient.

7.3.0.1 *Macrocystis* spp.

Giant kelp is the largest benthic organism in the ocean.

7.3.0.2 *Sargassum* spp.

Sargassum is one of the few floating brown macroalgae. It is most abundant off the eastern coast of the United States and also in the Gulf of Mexico.

Chapter 8

Microbes

Microbes are not found homogeneously throughout the ocean volume, but rather are aggregated around particles like marine snow, phytoplankton, and protists.

8.1 Viruses

Viral abundance in seawater ranges from 10^3 to 10^7 viruses per ml. 90% of viruses infect prokaryotes where they are important vectors of horizontal gene transfer. They reproduce prolifically with a turnover rate on the order of hours. Viral genomes can be DNA or RNA and can be single- or double-stranded. Most viruses are 20-200 nm in diameter (Castro and Huber, 2019). Because they cause the lysis of so many bacteria and plankton cells, they are a notable driver of DOM formation (when the cells burst out their contents) (Castro and Huber, 2019).

8.2 Prokaryotes

Prokaryotes are an important component of the microbial loop: they recycle dissolved and particulate organic matter (DOM and POM) to make it biologically available for their predators.

Unlike animal cells, prokaryotes have a cell wall in addition to their cell membrane.

Archaean chromosomes have introns and histones, unlike bacteria. Archaean cell membranes can have branched phospholipids.

8.2.1 Bacteria

Since cyanobacteria are photosynthetic, I have included them in phytoplankton (subsection 9.2.1).

Bacterial abundance in seawater is on the order of 1 million bacteria ml^{-1} but often 90% of these bacteria are in an inactive dormant state. Bacterial respiration is highest at the surface ($\tilde{}$20 nmol $O_2 \cdot l^{-1} \cdot hr^{-1}$; open ocean; Robinson, 2008) and decreases exponentially with depth due to temperature and food decreases.

Different strains of bacteria have vastly different nutritional and metabolic requirements (e.g. photoautotrophy, heterotrophy, chemoautotrophy, etc.).

Most bacteria are 0.5 to a few μm in diameter. However, a new record-breaker was recently discovered living in Caribbean mangroves and is 2 cm long and even stores its DNA inside a membrane like eukaryotes! Giant bacteria like this tend to have a giant water sac in their middle taking up most of their volume so that SA:V ratio is still manageable by diffusion.

8.2.1.1 *Vibrio fischeri*

Vibrio fischeri are gram-negative bacteria. They typically compose about 0.1% of the bacterioplankton (McFall-Ngai's 2022 CIAC talk). In seawater, *V. fischeri* cannot survive well above 28°C but within the *Euprymna* light organ they can better survive warmer temperatures (McFall-Ngai's 2022 CIAC talk).

8.2.2 Archaea

There are some archaea which inhabit anoxic sediments that utilize terminal electron acceptors other than oxygen. They contribute to the redox tower in sediment (section 3.7).

Thaumarchaeota are the ammonia-oxidizing archaea.

8.3 Protists

Protists are single-celled eukaryotes. There is very high diversity in this group but many are dependent on hosts in some way either as symbionts or parasites. Some protists are heterotrophic (ingest food), while others are photosynthetic.

Many protists osmoregulate with a contractile vacuole: a structure that slowly accumulates water and then expels it periodically. Naturally, these are most common in freshwater taxa but some marine taxa also have them.

8.3.1 Alveolates

Alveolates are one of the major clades of eukaryotes.

8.3.1.1 Apicomplexans

Apicomplexans are all parasitic and are known to infest cephalopods.

8.3.1.2 Ciliates

Ciliates are an entire phylum of alveolates and contain over 10,000 species! Ciliates are named after their cilia that they use for locomotion. Some are planktonic and some are found all over such as inside intestines, in gills, on macroalgae, in the sediment, on ommastrephid egg masses, etc.

All ciliates have a polyploid macronucleus that is utilized for gene regulation, and one or more diploid micronuclei that contains the germline DNA.

Paramecium is a genus of ciliates.

Ciliates may be parasites of cephalopod eggs (Birk et al., 2017).

8.3.1.3 Dinoflagellates

See subsection 9.1.2.

8.3.2 Amoebas

Amoebas are technically any unicellular organism that can alter its shape with pseudopods. Therefore it is a polyphyletic term that encompasses a wide diversity of taxa.

8.3.3 Rhizarians

All rhizarians are non-photosynthetic but some (such as many radiolarians and foraminiferans) harbor symbiotic algae.

8.3.3.1 Radiolarians

Radiolarians are planktonic and form silica skeletons. They are the second most important silicious plankton after diatoms. Their skeletons are typically 100-200 μm spheres with spines. There are ~2,500 known species. They have very thin pseudopodia just like forams.

8.3.3.2 Foraminifera

Foraminifera first evolved in the mid- to late-Mesozoic. There are ~6-10k species. Species inhabit specific depth ranges from the surface to the deep and temperature ranges. Most species live in sediment but some are planktonic. The benthic species have larger and thicker tests than the planktonic ones. Although the planktonic forms are not very specious, they can be abundant and contribute substantially to calcareous biogenous sedimentation.

The size and porosity of the tests are used as a marker for paleotemperature in marine sediments.

Defining characteristic(s) Forams have a calcite $CaCO_3$ test that, interestingly, is excreted inside the cell membrane. Their tests can have several chambers and the chambers grow as the cell grows. Pseudopodia stick out through pores in the test to grab prey, move about, or anchor to the substrate. The pseudopodia can be extremely long and narrow, looking like spines radiating from the test rather than the bulbous pseudopodia of amoebas, for example.

8.3.4 Algae

Technically, algae are protists, but they are covered in chapter 7 and section 9.1.

8.4 Fungi

Fungi are heterotrophs that have cell walls made of chitin. There are over 1,500 marine fungal species and most live in or on other organisms. Fungi feed by excreting digestive enzymes and absorbing the resulting nutrients. While most bacteria cannot digest cellulose, fungi can and thus are important decomposers of marine plants such as seagrasses and mangroves.

Some species of fungi form symbioses with cyanobacteria and/or green algae to form lichens. The fungal hyphae provide the structure and the cyanobacteria / algae provide the food. These lichens are very common at the upper reaches of rocky intertidal zones.

Fungal filaments are known as hyphae.

Fungi can often be parasitic to various marine organisms. Fungi can biofoal cephalopod eggs and prevent hatching (Nyholm's MBL talk).

8.4.1 Yeast

Yeast are a few up to a few tens of μm in diameter.

Chapter 9

Phytoplankton

All phytoplankton use C3 photosynthesis.

Different phytoplankton taxa attain sizes in different orders of magnitude. This size difference gives them very different nutrient characteristics and roles in the food web.

Plankton cells on average contain the Redfield C:N:P ratio of 106:16:1 which causes these nutrients to exist in this ratio in the deep ocean where phytoplankton cells are remineralized. This ratio varies in individual phytoplankton cells and species based on its composition of resource-capturing machinery (high N:P) or growth machinery (low N:P) (Arrigo, 2005). The Redfield ratio holds generally true worldwide, but there are variations between ocean basins (see subsection 3.2.5) and also can be large variations nearshore where the fluxes of elements via riverine input and mixing with sediment can outpace the rate of mixing.

Phytoplankton biomass is commonly estimated by measuring [Chl a] via satellites. To demonstrate rough distributions of phytoplankton, [Chl a] is typically ~0.05 $\text{mg} \cdot \text{m}^3$ ($\text{nmol} \cdot \text{l}^{-1}$) in the subtropical gyres, 1 $\text{mg} \cdot \text{m}^3$ ($\text{nmol} \cdot \text{l}^{-1}$) in coastal areas, and up to 10 $\text{mg} \cdot \text{m}^3$ ($\text{nmol} \cdot \text{l}^{-1}$) in extreme blooms. While the life history and phylogeny of phytoplankton are diverse, most forms have generation times ranging from 5 hours to 10 days.

Phytoplankton produce 50% of the Earth's O_2 flux and thus 50% of C fixation. 50% of oceanic primary production is due to diatoms, and a large proportion is through cyanobacteria as well.

Unintuitively, phytoplankton stock (i.e. [Chl a]) is not well correlated with primary productivity rates (Menden-Deuer). This is because there are other limiting factors at play such as limiting nutrients, PAR, predation rates, etc.).

9.0.1 Nutrient requirements

The most common limiting factors for primary productivity are (in no particular order) light levels, temperature, nutrients, grazing, and viral infection. The three most common limiting nutrients are NO_3^- (especially at low latitudes and nearshore), phosphorus, and iron (especially at high latitudes). Nitrogen limitation is so common at low latitudes because stratification prohibits NO_3^- rich deep water from reaching the euphotic zone. Nitrogen limitation is common nearshore because high rates of denitrification in anoxic sediments reduce its concentration relative to phosphorus (subsection 3.2.5). Iron is limiting at high latitudes because not much iron is carried from desert winds to the high latitudes and because N and P are sufficiently provided from deep upwelling water. Once nutrients sink from the euphotic zone down to the main thermocline, their residency there can last days to tens of years. Once below the thermocline in the ocean interior, it can take hundreds to thousands of years for it to reach the surface again (Moore et al., 2013).

While NO_3^- is typically the N-containing nutrient species that phytoplankton rely upon, they actually preferentially uptake NH_4^+ over NO_3^- because it is more efficient. When NO_3^- is consumed, it is first converted to NH_3 before entering the biosynthetic pathway.

The productivity potential (grams of phytoplankton supported) of a given volume of water mass can be estimated by examining its concentrations of nutrients and plugging the limiting nutrient into a generic photosynthesis equation to produce a "Redfield molecule" (Pilson, 2013):

$$124\,CO_2 + 140\,H_2O + 16\,HNO_3 + H_3PO_4 \rightleftharpoons (CH_2O)_{104}(CH_2)_{20}(NH_3)_{16}H_3PO_4 + 166\,O_2$$

If, however, the phytoplankton are utilizing NH_4^+ rather than NO_3^-, then the expected relationship becomes:

$$124\,CO_2 + 124\,H_2O + 16\,NH_3 + H_3PO_4 \rightleftharpoons (CH_2O)_{104}(CH_2)_{20}(NH_3)_{16}H_3PO_4 + 144\,O_2$$

where the limiting nutrient is supplied on the left. Each time this pseudo-reaction occurs, 124 units of carbon are produced, and phytoplankton biomass can be estimated by a quantity of carbon. Often, carbon composes 45% of phytoplankton dry weight

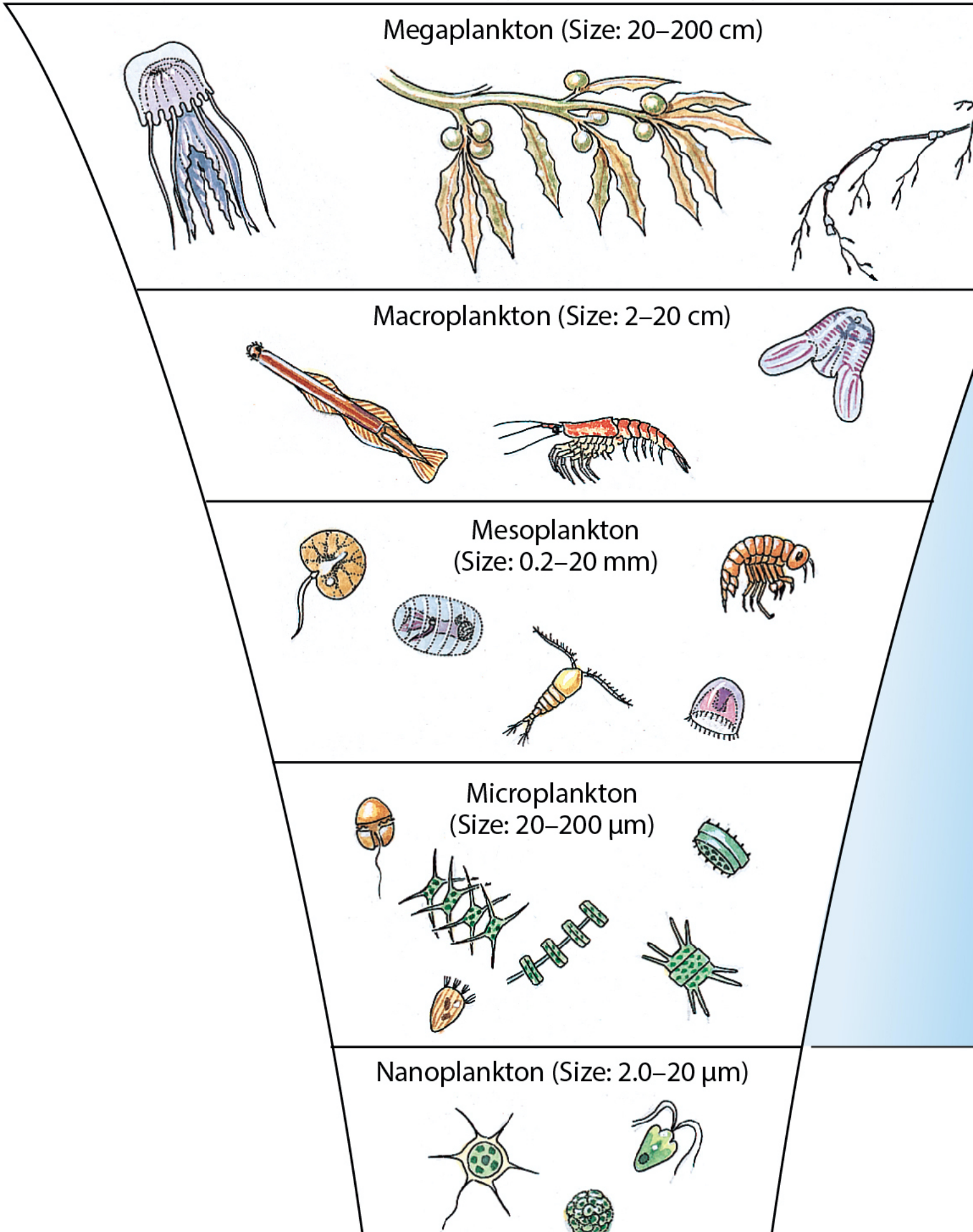
Megaplankton (Size: 20–200 cm)
Macroplankton (Size: 2–20 cm)
Mesoplankton
(Size: 0.2–20 mm)
Microplankton
(Size: 20–200 µm)
Nanoplankton (Size: 2.0–20 µm)

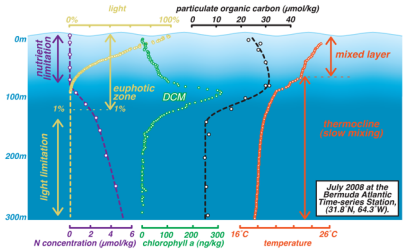

Figure 9.2: Various physical and chemical requirements for phytoplankton growth.

(Pilson, 2013). The generic organic molecule (the "Redfield molecule") on the right represents the appropriate oxidation states of carbohydrates, lipids, proteins, and phosphate molecules.

Nutrients may limit phytoplankton in two ways:

1. According to Liebig's law of the minimum, whichever nutrient is most limiting (lowest compared to the Redfield ratios expected) limits phytoplankton biomass.

2. According to the Blackman limitation hypothesis, whichever nutrient is most limiting limits phytoplankton growth rate.

9.0.1.1 Preformed nutrients and deep-water nutrient accumulation

When deep water is formed, there is some quantity of N and P that are in the high latitude surface water (unused since deep water formation is typically in winter when sunlight limits growth). This initial nutrient concentration (preformed nutrients) is added to once it sinks only by biological processes. According to the Redfield ratio, for every 166 or 144 μmol of O_2 consumed (AOU, (section 1.8)) there are 16 μmol NO_3^- or NH_4^+ and 1 μmol DIP produced.

9.0.1.2 Micronutrient needs

The three most concentrated micronutrient metals in phytoplankton are iron, manganese, and zinc. In addition, some phytoplankton require trace quantities of cadmium in order to form their carbonic anhydrase enzymes.

9.0.2 Primary production

Gross primary production quantity of organic matter produced per unit area and time

Net primary production (NPP) quantity of organic matter produced minus quantity respired by producers per unit area and time

New production quantity of organic matter produced from nutrient inputs from the ocean interior (sourced mainly by NO_3^-)

Recycled (regenerated) production quantity of organic matter produced from nutrients already in the euphotic zone (sourced mainly by NH_4^+)

Export production quantity of organic matter transported out of the system into the ocean interior

f-ratio proportion of NPP that is new production (supports cephalopod populations). Global average f-ratio is 0.16 but it varies from ~0.1 to 0.5 in different regimes.

PP is not highest at the surface even though PAR is highest there because nutrients are limiting at the stratified surface. Maximal PP, therefore, is typically a few 10s of meters below the surface where both light and nutrients are high. Below this peak, PP decreases reaching the compensation depth, where PP = respiration and thus, net PP = 0.

Sverdrup's critical depth model is a model that predicts that a spring phytoplankton bloom will occur when the mixed layer shoals above the critical depth (0.1-1% surface PAR). Only when phytoplankton stay at this depth or shallower can they stay in a zone where growth rates outweigh loss rates to dark depths. The compensation depth is the depth at which photosynthesis rate = respiration rate, but this is shallower than the critical depth because phytoplankton can move into light-limited depths for a time as long as they can return to the light shallows to "burn off" photosynthetic "debt".

60-80% of PP product is consumed quickly by predatory zooplankton and recycled within the euphotic zone. The rest is lost to either sinking, fecal excretions, parasites, or viruses.

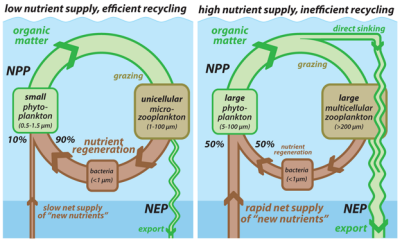

Figure 9.3: Effect of nutrient supply on nutrient recycling.

Much of the PP that occurs in the ocean is often regenerated production where energy and biomass merely loop between phytoplankton and zooplankton (Eppley and Peterson, 1979). New nutrients are required to support new production which can support cephalopod populations. Over a yearly timescale, export production balances new production when the system is in steady state.

According to Pilson (2013), subtropical gyres often have quite low NPP (~700 μmol C/m^2/hr) while coastal areas have higher NPP (~2000 μmol C/m^2/hr) and eastern boundary currents with strong upwelling can have very high NPP (~17,000 μmol C/m^2/hr). The ocean in total produces ~ 4000 Tmol C/year (Pilson, 2013). Typically, ~10% of this POC makes it below the euphotic zone.

9.0.2.1 Support of cephalopod populations

A given rate of primary production does not always support the same size cephalopod population. Primary productivity (PP) occurs in three generalized locations: 1) open ocean oligotrophic gyres, 2) coastal regions, and 3) upwelling zones. The PP in oligotrophic gyres has a lower f-ratio (0.1) than coastal (0.3) or upwelling regions (0.5). Thus, a larger proportion of the PP rate goes out of planktonic cycle into higher trophic levels.

Another related reason that a given PP rate can support different sized cephalopod populations is trophic efficiency. Since only ~10% of energy is moved from one trophic level to the next, the length of the food chain below cephalopods will affect how the PP rate determines cephalopod stocks. In oligotrophic regions cyanobacteria contribute more to PP than diatoms because they are more competitive in nutrient-limited conditions. Since cyanobacteria are smaller, the food chain is longer before cephalopods can gain energy from cyanobacterial PP. In coastal and upwelling regions, however, diatoms contribute more to PP than cyanobacteria. Since diatoms are larger, they support shorter food chains for cephalopod and fish stocks to grow. Thus, PP rates in oligotrophic gyres must be higher than in coastal or upwelling regions to support the same quantity of cephalopods.

PP rates are typically 2-4x higher in coastal and upwelling regions than gyres which, combined with the diatom-cyanobacterium difference and different f-ratios, is why cephalopod populations can become so abundant in these regions.

9.1 Eukaryotic phytoplankton (microalgae)

Other than diatoms, all the main microalgae (dinoflagellates, coccolithophores, silicoflagellates, cryptophytes) have at least one flagellum for motility.

Many kinds of algae can accumulate on the underside of sea ice, forming algal mats that can be large proportions of primary productivity during certain times at high latitude.

9.1.1 Diatoms

Ecological importance Diatoms first evolved in the Triassic.

There is nearly an order of magnitude variation in estimations of species diversity. A low-end estimate is roughly 6,000 marine diatom species (with another ~6,000 freshwater species). Most are planktonic but some adhere to solid surfaces. Most are abundantly photosynthetic but a few species have no pigments and are heterotrophic. Diatoms contribute 40-50% of global oceanic primary production and 50% of deep carbon export. Diatoms are notable contributors to the silicious component of biogenous sedimentation. Diatoms are relatively recently dominant phytoplankton. They did not become cosmopolitan until 40-50 Ma in the Paleogene.

Diatoms often aggregate together in chains. They are most abundant in temperate and polar regions. Diatoms and cyanobacteria are the most abundant phytoplankton in the ocean. However, cyanobacteria are dominant in subtropical gyres while diatoms

are dominant in coastal regions since they are larger and can thus avoid more predators. Some diatoms can horde nutrients when they are available and use their stores when nutrients are limiting. This is in part how they can form such large spring blooms.

Shellfish poisoining is often due to a domoic acid toxin that is produced by some diatom species.

Defining characteristic(s) Diatoms are enclosed by a silica shell known as a frustule. This frustule is composed of two partially-overlapping halves known as thecae (or valves). The frustule contains pores to allow light, nutrients, and gas exchange and also spines and ribs to slow sinking. In addition to the spines, the cells and even frustule also sometimes contain oil droplets to increase buoyancy. Diatoms are often a golden color due to carotenoid pigments (in addition to Chl a and c). Their silica frustule makes diatoms the most silica dependent of all phytoplankton, but it provides them with protection from predators and also might angle ambient light to optimize photosynthesis. Silica is also cheaper to make than $CaCO_3$. Diatoms require lots of silica. A healthy diatom is composed of 1:1 Si:N.

They can be subdivided based on their axis of symmetry: either centric (radial) or pennate (bilateral).

Typically, diatoms reproduce asexually, with the upper and lower thecae separating, taking half the cell with it, and then forming a new, smaller half. The daughter cell from the upper (larger) theca is the same size as the parent cell, but the daughter cell of the lower (smaller) theca forms an even smaller (now the new lower) theca. As a result, diatoms gradually get smaller with each generation until a specialized stage known as an auxospore is produced that produces full-size daughter cells. The auxospore can also be produced to withstand nutrient-poor conditions and can also be formed through sexual reproduction.

Diatoms can grow up to about 1 mm in diameter, making them some of the largest phytoplankton.

9.1.2 Dinoflagellates

Ecological importance There are ~2,000 species of dinoflagellates and almost all are marine. Dinoflagellates are most abundant in low-latitudes.

Dinoflagellates are one of the phytoplankton taxa that can form harmful algal blooms (HABs). In fact, a single species, *Karenia brevis* is responsible for red tides in the Gulf of Mexico. About 100 species of dinoflagellates produce neurotoxins that may be poisonous to cephalopods.

Quite a few dinoflagellates are symbiotic with other organisms such as sponges, sea anemones, giant clams, and of course corals. The genus *Symbiodinium* are common coral symbionts. These symbionts provide fixed carbon to their hosts and utilize the nutrients released by their hosts. Still other kinds of dinoflagellates are parasitic.

Dinoflagellates are the main taxa causing bioluminescent blooms in tropical surface waters.

Defining characteristic(s) Dinoflagellates have two flagella: one wraps around a groove in the middle of their theca (transverse flagellum) and another is free (longitudinal flagellum). They both help the dinoflagellate move. Their theca (when present) is composed of cellulose. In some species, their theca has prominent horns. The presence or absence of the theca shell makes dinoflagellates either "armored" or "naked".

About half of all dinoflagellates photosynthesize but about half also ingest food particles for energy too. A few, but certainly not most, dinoflagellates have a light-sensitive pigment spot that functions as a very simple eye. They reproduce almost exclusively asexually.

Some dinoflagellates have weird cell nuclei with the chromosomes attached to the nuclear membrane and without histones.

Most dinoflagellates are 15-40 μm or so in diameter.

9.1.3 Coccolithophores

Coccolithophores first evolved ~230 Ma.

Defining characteristic(s) Coccolithophores are round cells with two flagella. They cover their cell with multiple calcite $CaCO_3$ coccoliths which compose a coccosphere. Since $CaCO_3$ is transparent, photosynthesis is not impaired by the coccosphere.

The White Cliffs of Dover were formed primarily from coccoliths.

Coccolithophores are typically 5-100 μm wide.

9.1.3.1 *Emiliania huxleyi*

These coccolithophores are cosmopolitan and can form extensive blooms.

9.1.4 Silicoflagellates

Silicoflagellates have an internal silica skeleton and a long flagellum. Their skeletons compose 1-2% of silicious biogenous marine sediments worldwide.

9.1.5 Cryptophytes

Cryptophytes have two flagella and are only 10-50 μm in diameter.

9.1.6 Other algae

9.2 Prokaryotic phytoplankton

9.2.1 Cyanobacteria (inaccurately, "blue green algae")

Second to diatoms, cyanobacteria contribute 25% of oceanic primary production (at least in pelagic environments) and are the most abundant autotrophs on Earth.

One of the characteristic traits of cyanobacteria (as opposed to other bacteria) is the presence of a mucilaginous sheath outside the cell membrane. This mucilaginous sheath is composed of cellulose and facilitates intercellular binding (i.e. colony formation). The blue-green coloration of this sheath is cyanobacteria's namesake. Cyanobacteria also have a second sheath known as the gelatinous sheath that is composed of collagen that also facilitates intercellular binding (i.e. colony formation).

Cyanobacteria have chlorophyll a and other accessory pigments they store in thylakoid membranes.

Cyanobacteria, particularly *Trichodesmium*, are also the only major vector of nitrogen fixation. They convert dissolved N_2 gas into NH_3 via the enzyme nitrogenase. Most of this NH_3 is incorporated directly into amino acids for their proteins. They are abundant in warm oligotrophic waters because they are not nitrogen-limited like all other phytoplankton that rely on aqueous NO_3^-. *Trichodesmium* blooms can form long filaments visible on the surface!

Other than *Trichodesmium*, there are two abundant cyanobacterial genera in subtropical gyres: *Prochlorococcus* and *Synechococcus.* Cyanobacteria are smaller than eukaryotic plankton like diatoms and thus have an advantage in oligotrophic waters because they have a smaller SA:V and there is less distance for nutrients to travel from the center of the cell to the surface, thus providing a higher nutrient concentration gradient.

Some kinds of cyanobacteria produce siderophores, which are large organic molecules which have a high affinity for iron (Pilson, 2013). The bacteria release these into the water and then absorb iron-bound siderophores to acquire iron (Pilson, 2013). Competing bacteria produce their own strains of siderophores and can compete with each other intensely for iron (Pilson, 2013).

9.2.1.1 *Prochlorococcus* spp.

These are some of the most abundant phytoplankton in subtropical gyres.

9.2.1.2 *Synechococcus* spp.

These are some of the most abundant phytoplankton in subtropical gyres.

9.2.1.3 *Trichodesmium* spp.

These are some of the most abundant phytoplankton in subtropical gyres. Especially in the Atlantic gyres, they use nitrogen-fixation to gain advantage over N-limited competitors. They are more abundant in Atlantic than Pacific gyres because they have high iron requirements which can be sustained much better by Saharan winds in the Atlantic.

Chapter 10

Invertebrates

The sections are the 30 marine animal phyla other than molluscs, which are outlined in chapter 14.

General invertebrate knowledge Due to boundary layers and local respiration rates, sessile benthic animals may be oxygen-limited for space even in mild conditions (Ferguson et al., 2013). Flat forms of bryozoans, sponges, barnacles, and tunicates have lower P_{crit}s than erect forms (Ferguson et al., 2013).

Many burrowing animals come out of their burrows and stay on the sediment surface under severe hypoxia (Wu, 2002).

10.1 Acanthocephala

These are all worm-like endoparasites.

10.2 Annelida

Annelids are known as "segmented worms". There are over 14,000 species. In most groups (see below), the segments are separated by a wall known as a septum. Not all have clear external markings of their segmentation like earthworms do.

Most groups (see below) have chitinous bristle-like structures known as setae.

Annelids have a closed (distinct blood vessels) and segmented circulatory system but their digestive system is not segmented. Their excretory system is segmented and composed of a nephridium (kidney equivalent) for each segment. Each segment also has ganglia to control that segment's portion of both the longitudinal and circular muscles.

Most annelids move by vibrating the sediment in front of them to liquify it, then extending forwards, before anchoring the front in place and pulling the back forwards as well.

Annelid eyes are rhabdomeric (Figure 52.1.2.1) but can also have ciliary eyes. Their eyes can generally function for directional photoreception (McCormick and Levin, 2017).

Annelids may feed by deposit feeding, muco-suspension feeding, suspension feeding with a trap, predation, or parasitism.

Similarly to some other phyla, their larvae are known as trochophores.

Taxon	Parapodia	Setae	Hermaphroditic	Septa
Polychaeta	Yes	Many	Few	Yes
Oligochaeta	No	Few	Yes	Yes
Hirudinea	No	None	Yes	No

10.2.1 Polychaetes

Most marine annelids are polychaetes. There are ~15,000 describes species of polychaetes and ~95% of them are marine. They are abundant in soft sediments in both shallow and deep sea bottoms as well as hydrothermal vents. They also inhabit crannies within rocks and corals. Different species have different reproductive strategies such as asexual and simultaneous hermaphroditism.

Polychaetes have parapodia that are used for respiration, sensation, and movement. Their parapodia each have many setae (bristles). Their parapodia are vascularized with many capillaries and function kind of like gills.

10.2.1.1 *Arenicola marina*

These are known as lugworms or sandworms and are rather similar to terrestrial earthworms. They can be abundant in the sand in the intertidal zone of a beach. Their castings can be commonly seen as coiled piles of sediment.

10.2.1.2 *Eunice aphroditois* (Sand striker)

Sand striker worms, as they are known, are burrowing ambush predators that can grow up to 3 m long (the longest polychaete recorded) in the Atlantic. They have five antennae that sense prey and mandibles that can capture fishes, cephalopods, and other relatively large prey.

10.2.1.3 Feather duster worms

Feather duster worms are from the order Sabellida and are named after their protruding feathery cilia-lined tentacles. They form hard tubes in which they live. They have lost their parapodia. This group includes the Christmas tree worms.

10.2.1.4 Giant tube worms (Siboglinidae)

Giant tube worms are almost all deep-water either near hydrothermal vents, whale falls, or methane seeps. These lack a mouth and gut (very rare in animals) and instead acquire nutrients straight from their long tentacles. They often harbor symbiotic bacteria for food as well.

10.2.1.5 *Spirorbis* spp.

Spirorbid worms are small (2-5 mm) worms that form small coiled white shells in which they hide. They biofoul lots of surfaces and are quite common.

10.2.1.6 *Tomopteris* spp.

These are holoplanktonic deep sea polychaetes with yellow bioluminescence from their parapodia. They can also rapidly swim in reverse!

10.2.2 Oligochaetes

10.2.3 Hirudineans (leeches)

Hirudineans have two suckers (one on each end) and a large gut for storing blood. They lack parapodia.

10.3 Arthropoda

Most arthropods have high-resolution image forming eyes (McCormick and Levin, 2017). Arthropod eyes are rhabdomeric (Figure 52.1.2.1).

10.3.1 Insects

Insects are the only animals I know of that do not circulate respiratory gases in their blood. Insect hemolymph ranges from 6.4 to 7.5 (Harrison 2001).

10.3.2 Crustaceans

10.3.2.1 Copepods

Copepods are abundant animals in the shallow marine environment. In fact, it has been estimated that they consume 10-15% of global primary productivity (Melzner's SEB talk).

Copepods have a complex life history with many stages.

Copepods spawn daily in shallow water.

Most copepods do not possess any gills, and non-calanoid copepods do not have any heart or blood vessels either. They instead rely on diffusion through pits in their cuticle.

When escaping predators, some copepods have been measured to swim over 1000 body lengths per second!

Diapause Copepods diapause (Stage V) in deep water when conditions become unfavorable. In the Southern Ocean, shortening day length can also trigger diapause in Antarctic copepods in expectation of worsening phytoplankton stocks (Melzner's SEB talk). Diapausing copepods undergo many physiological changes. They can be composed of up to 50% wax esters by body mass (Melzner's SEB talk), making diapausing copepods a nutritious prey item for cephalopods. In addition, their blood can accumulate as much as 200-300 mM NH_3 (Melzner's SEB talk).

10.3.2.2 Krill

There are about 80 species of krill. Krill (or euphausiids) are different from shrimp in that they have external gills. Krill are omnivorous but predominantly eat phytoplankton as well as copepods, algae, and fish larvae. They are an abundant component of nearly all pelagic communities. They Antarctic krill reproduce seasonally. They have a typical lifespan of 2 years for tropical species up to 7 years for Antarctic krill.

Legs can be used for either feeding, grooming, or swimming. The number of thoracic legs is species-specific.

10.3.2.3 Shrimp

Shrimps can be divided into two groups. They are separated by the overlap of some abdominal sections of their shell that give one group the appearance of a "broken back".

10.3.2.4 Amphipods

Amphipods are laterally compressed.

10.3.2.5 Isopods

Isopods are dorsoventrally compressed.

10.3.2.6 True crabs (Brachyurans)

10.3.2.7 False crabs (Anomurans)

This includes squat lobsters, mole crabs, king crabs, hermit crabs, and coconut crabs.

10.3.2.8 Lobsters

Lobster larvae are known as zoea.

10.3.2.9 Barnacles

Barnacles can be either stalked (gooseneck barnacles) or unstalked (acorn barnacles).

Since barnacles are entirely sessile, in order to mate with their neighbors, male barnacles grow penises up to 8x their body length, the longest relative to body size in the animal kingdom.

Barnacles (at least some subgroups) do not contain any of the three key proteins involved in the HIF pathway (HIFa, PHD, or VHL) (Graham and Barreto, 2020).

10.3.3 Sea spiders (pycnogonids)

Pycnogonid abdomens are so small that many of their internal organs (including their GI tract) are in their legs. Male sea spiders carry around his fertilized eggs in specialized appendages until they hatch.

Most pycnogonids are small, with leg spans < 1 cm, but deep sea polar ones can reach 70 cm!

They have a long proboscis with which they feed on sessile organisms such as sponges and cnidarian polyps.

Sea spiders transport oxygen through their bodies via peristalsis of their gut (Woods et al. 2017). They also utilize cutaneous respiration through pores in their cuticle (Lane et al., 2018).

10.3.4 Horseshoe crabs

10.4 Brachiopoda

There are about 400 known species of brachiopods. They used to be extremely abundant in the Paleozoic but were decimated at the end of the era.

Brachiopods, known as "lamp shells", are morphologically distinct from bivalve molluscs in that their shells are on the upper and lower surfaces unlike the left-right orientation of bivalve shells. Also unlike bivalves, the two valves of brachiopods are often different sizes. They are also "stalked" but different from stalked barnacles in that they only have 2 shells. The two major groups can be differentiated based on if their valves connect with a hinge or are just held together solely with muscles.

They filter feed with a lophophore. The lophophore structure looks like a U-shaped fleshy extension off of which many ciliated tentacles grow. The cilia draw a current through their shell.

They attach to either rocky or sediment substrate (depends on the species) with their stalk. They are typically found in cold water at high latitudes or deep depths.

Brachiopods are solitary and most known species are broadcast spawners.

Brachiopods utilize hemerythrin in their blood which makes it purple!

10.5 Bryozoa

There's over 6000 known species of bryozoans and most are marine. Along with brachiopods, bryozoans have a lophophore. They will withdraw their lophophores and close their operculum when disturbed.

Bryozoan colonies are often formed by asexual reproduction of a single settled larva, known as an ancestrula.

They will grow on just about any surface from rocks to exoskeletons, shells, macroalgae, and even ice!

Individual animals are known as zooids. Individual zooids are small, only a few millimeters at most. Some are "normal", known as autozooids, while others are specialized zooids for attaching to substrate, cleaning, defense, or brooding eggs. The zooids are interconnected and share food and waste products.

Only some bryozoans are calcifying.

Rather than having an excretory system, when waste products accumulate within a zooid, the viscera and lophophore are removed and reformed by the body wall!

Bryozoans are mainly hermaphroditic.

Larvae start off positively phototaxic but become negatively phototaxic before settling and metamorphosis.

Some bryozoan species encrust surfaces while others form erect structures like a sea fan. Flat forms of bryozoans have lower P_{crit}s than erect forms (Ferguson et al., 2013).

10.6 Cephalorhyncha

Cephalorhynchs have an eversible proboscis covered in spines with which they feed. They are related to the nematodes and arthropods due to their ecdysis.

10.7 Chaetognatha

Chaetognaths (or arrow worms) are voracious transparent predators. In fact, they are the most abundant predators in the ocean. They have sensory cilia all over the upper third of their body that they use to detect mechanical vibrations from prey. They also have eyes, fish-like fins and a tail. They feed principally on crustacean zooplankton (Robison, 2004), especially copepods but also larvae and other arrow worms. Some chaetognaths harbor tetrodotoxin in their mouths to help subdue prey. They do not swim often but can dart fast to grab prey or escape predators.

There are about 130 species, all of which are marine. They range in size from 1 to 10 cm.

Chaetognaths occupy a similar ecological niche as ctenophores.

They have a hydrostatic skeleton powered exclusively by longitudinal muscles.

Chaetognaths are hermaphroditic with the ovaries in the trunk and sperm in the tail but it makes its gametes at different times to avoid self-fertilization.

10.8 Chordata

The defining traits of chordates are that at least at some point during development they all possess:

1. a single hollow dorsal nerve cord
2. gill slits near the anterior part of the gut (known as a pharynx in some groups)
3. a notochord: a flexible support rod between the nerve cord and gut
4. a post-anal tail

10.8.1 Tunicates

All 3000 known species of tunicates are filter feeders. Tunicates are the only known animals to synthesize cellulose. They are also known as urochordates.

10.8.1.1 Sea squirts (Tunicata: Ascidiacea)

Ascidians are the only sessile chordates and attach to their hard or soft substrates. Their bodies are protected by a gelatinous or tough outer covering known as a tunic. They feed with a large ciliated sieve known as a pharynx that leads straight to the stomach. Water enters the pharynx through an incurrent siphon and filtered water leaves through a separate excurrent siphon. They are known as sea squirts because they can forcefully expel water through either siphon when disturbed.

Although the adult form has no dorsal nerve cord or notochord, the larvae resemble frog tadpoles and have all four key traits.

10.8.1.2 Salps (Tunicata: Thaliacea: Salpida)

Salps are transparent barrel-shaped animals. Salps pump water through their bodies with muscle bands to filter feed. This pumping also allows them to move horizontally and vertically quite easily. This muscular mechanism of water flow differentiates them from doliolids. Water flows anteriorly to posteriorly through the body. The brown/orange ball is their stomach. Water enters on the far side of the stomach and exits on the side near the stomach.

Salps are most abundant in warm shallow waters.

10.8.1.3 Doliolids (Tunicata: Thaliacea: Doliolida)

Doliolids alternate through sexual and asexual generations. Gonozooids are individual barrel shaped transparent animals that resemble salps in many ways. However, when these gonozooids release their gonads, the fertilized eggs become oozoids (known as "nurses") that asexually make many other zooids in a long tail. These attached zooids function to feed the oozoid and keep her making more zooids in the chain.

Doliolids pump water through their bodies with cilia to filter feed. This pumping also allows them to move horizontally and vertically quite easily. This ciliary mechanism of water flow differentiates them from salps.

10.8.1.4 Pyrosomes (Tunicata: Thaliacea: Pyrosomatida)

Pyrosomes are a colonial meta-individual made of zooids. They are tube shaped with an opening at one end through which all the zooids propel their water to move the colony forward. They filter feed and bring water in through individual pharynxes. In this way, their mechanism of water flow is not unlike that of sponges.

10.8.1.5 Larvaceans (Tunicata: Appendicularia)

Larvaceans are euphotic filter feeders. They have a small tadpole-like body plan and can vary in color from transparent to bright yellow! This body is similar to the larval stages of sea squirts. They create a proteinaceous and fiberous "house" where they can filter the water to feed by pumping their tail to generate a current. These houses compose a large proportion of marine snow (section 3.1.1.3) which has been documented to be eaten by *Vampyroteuthis infernalis*. Giant larvacean houses have been documented to be over 1 m wide and are actually quite complex and not all that amorphous. Once houses clog up after a day or two, the larvacean abandons it and makes a new one within a few hours.

10.8.2 Lancelets (Cephalochordates)

Lancelets look like headless fishes and can grow up to 7 cm in length. The adult form has all four of the core chordate traits and is basically a vertebrate without a backbone. They often bury themselves tail-first in sediment and filter feed.

They have gill slits in their pharynx but are used only for feeding and not respiration.

Circulatory system has no hemoglobin or RBCs.

10.8.3 Vertebrates

See chapter 11.

10.9 Cnidaria

All cnidarians have radial symmetry (repeating body parts around their central axis) and oral and aboral surfaces. They have many tentacles that surround their mouth, which in turn leads to a "blind" gut (no anus). Cnidarian body plans are composed of an epidermis cell layer on the outside, a gastrodermis cell layer on the inside, and a generally cell-less jelly-like collagenous mesoglea in between. This makes them diploblastic.

A given individual at a given life stage is always going to be either a polyp or a medusa. Polyps attach to substrate with their oral surface upwards, while medusa are unattached with their oral surface downwards. Polyps are often, but not always, colonial. Many colonies have specialized polyps that serve specialized needs. In these taxa, the polyps may be referred to as "zooids".

Medusa stages often possess statocysts all along the bell rim for balance. A calcium sulfate rock sits within a hair-lined cavity and depression of the hairs provides nervous input to orientation.

Altogether, there are nearly 12,000 known species of cnidarians (WoRMS).

Asexual reproduction by budding is common among the polyp stage and sexual reproduction is more common in the medusa stage (except in anthozoans that lack medusae). Cnidarian larvae are known as planula larvae and swim with cilia.

Bell shape in medusae vary from prolate (stretched axially) to oblate (squished axially). The former tend to utilize jet-propulsion (at least at small sizes) while the later utilize a drag-based rowing locomotion

Cnidarians reproduce many different ways but a common strategy is for male and female medusae to produce a zygote which becomes a planula larva that settles to form a benthic polyp. This polyp multiplies to form a colony. This colony, in turn, can asexually bud off new medusae. Though some taxa have no medusa stage and others have no polyp stage.

Digestion of food begins within the gastrodermal cavity and continues within the gastrodermal cells themselves.

The gastrodermal cavity has multiple functions (not just digestion). It also stores gametes among other functions.

Cnidarians are osmoconformers.

Nematocysts Nematocysts are stored inside specialized cells known as cnidocytes. Depending on the taxon, the nematocysts fire with a hydrostatic pressure of nearly 200 bar! The nematocyst contains a thread that can be ejected onto prey. This thread may be toxin-bearing, spiny, sticky, or just really long to wrap around prey, depending on the taxon.

Cnidocytes can be found in both the epidermis and the gastrodermis.

To be fired, the nematocyst must be mechanically stimulated by depressing a small projection on its surface known as a cnidocil. This releases a hinged lid and releases the pressurized thread inside.

10.9.1 Anthozoans

Anthozoans lack a medusa stage and, thus, are all exclusively polyps. The polyps release gametes into the water directly to form planktonic planula that settle as more polyps. Unlike the small polyps of other cnidarian taxa, anthozoan polyps possess septa (partitions) in their gastrodermis which 1) increase gut surface area, 2) provide structural support, and 3) support calcification (in those that calcify).

Anthozoans are the most specious group of cnidarians by far. The two main groups of Anthozoa are Hexacorallia (6-fold symmetry) and Octocorallia (8-fold symmetry).

Octocorals are known to be good substrate for cuttlefish egg deposition (Gaikwad et al., 2021).

10.9.1.1 Sea anemones (Hexacorallia: Actiniaria)

Anemones have a pedal disc with which they attach to substrate. Their body column connects to the oral disc that bears the tentacles. Although they appear entirely sessile, they can detach and reattach to substrate at will.

Just like some corals, sea anemones can harbor symbiotic zooxanthellae (Castro and Huber, 2019).

Some anemones (those of the Acontiaria taxon) have specialized white coiled thread-like tissues known as acontia that are stored within the gastrodermal cavity. These acontia are full of toxin-bearing nematocysts and are used as self-defense from neighboring competitors or predators.

10.9.1.2 Hard corals (Hexacorallia: Scleractinia)

Coral reefs are composed of individual polyps but polyps in a colony are all interconnected in their nervous systems and often digestive systems as well (Castro and Huber, 2019). The colony forms by an individual planula larva settling on a hard bottom and then metamorphosing into a polyp and this founder polyp divides to form a colony (Castro and Huber, 2019). Reef-building corals are typically from the order Scleractinia and almost always have symbionts (Castro and Huber, 2019). Hard corals have hexaradial symmetry so their tentacles and mesenteries (internal walls) are always in multiples of six.

A thin layer of tissue known as the coenosarc overlies the stony skeleton and connects the polyps and provides a means of inter-polyp coordination.

Inside the coral polyp body are mesenterial filaments covered in nematocysts that can be extruded to attack prey or neighboring competitors. These are different but functionally similar to the acontia of some anemones.

A fair number of coral taxa are nocturnal, with their tentacles retracted during the day.

All hard corals that have been studied are oxyregulators, with Pcrit values around 20-40% air saturation or so (Hughes et al., 2022).

Symbioses Shallow-water corals maintain symbioses with dinoflagellates, most commonly *Symbiodinium*. These dinoflagellates provide the majority of food to corals under the majority of conditions and coral species. The term "zooxanthellae" is a colloquial taxonomic group of any coral symbionts (dinoflagellates, diatoms, etc.) that is now discouraged use in some circles due to its over-generality. When stressed, corals bleach when their symbionts leave the polyps. Sometimes, the corals turn vibrant colors within a few weeks after bleaching as pigment production increases to protect the polyps. This pigment production also facilitates symbiont re-colonization (Bollati et al., 2020).

Calcification Corals form aragonitic $CaCO_3$ skeletons under their base using their calicoblastic cells. They do this by isolating seawater parcels and increasing the pH at the calcification site to 8.2 to 10.2 (Tambutte's SEB talk). They also pump in Ca^{2+} and HCO_3^- to further encourage $CaCO_3$ formation. The calcifying cells are rich in mitochondria and form septate junctions to prevent ions escaping from the calcification site (Tambutte's SEB talk). The calcifying cells possess high levels of Ca-ATPase and Cl-HCO_3 transporters as well as extracellular carbonic anhydrase (Tambutte's SEB talk). Interestingly, they have not been found to have high levels of NKA (Tambutte's SEB talk).

Synchronous spawning In many reefs, hard corals spawn their gametes synchronously once a year based on lunar phase and water temperature.

10.9.1.3 Soft corals (Octocorallia: Alcyonacea)

This clade is monophyletic but contains numerous subgroups that are traditionally treated rather separately. Unlike hard corals, each polyp has eight feather-like tentacles and no extant species form a hard skeleton (with a single exception).

Soft corals have pointy calcite calcium carbonate structures in their tissues known as sclerites that help them avoid predation (Castro and Huber, 2019). These sclerites are extremely morphologically diverse, which makes them useful for taxonomy.

All soft corals that have been studied are oxyregulators, with Pcrit values around 20-40% air saturation or so (Hughes et al., 2022).

Gorgonians ("sea fans and sea whips") Gorgonian bodies are branching and mainly proteinaceous. They are not calcifiers (Castro and Huber, 2019). Sea fans often grow perpendicular to the prevailing current to get the most efficient filter feeding.

10.9.1.4 Sea pens and pansies (Octocorallia: Pennatulacea)

10.9.2 Cubozoans ("box jellyfishes")

Cubozoans have a square shaped medusa with a stalk bearing one or more tentacles attached to each corner of the medusa. As with all cnidarians, they possess nematocysts. Some species are venomous and can be fatal to humans. These taxa are very different from other jellies (i.e. scyphozoans) in that their nervous system is much more complex. They have a nerve ring around their medusa that coordinates contractions for efficient swimming. They also have image forming eyes that help them swim towards prey! These are often located along the rim of the bell alongside the statocysts.

They are primarily limited to low latitudes and inhabit both coastal and pelagic environments.

As in scyphozoans, they also have very tiny polyps.

They are fast swimmers that actively hunt fishes and invertebrates. Sea turtles are putatively immune to their toxins since they are such common predators.

Sea wasp (*Chironex fleckeri*) Sea wasps of the Indo-Pacific can have fatal stings to humans. Their bells can be 25 cm across with up to 4 m tentacles.

10.9.3 Hydrozoans

The medusa stage of hydrozoans tend to be very small and have an inward extension of the bell, known as a velum, that supports swimming efficiency, unlike other cnidarians. The polyps are often colonial and sometimes bushy or feathery. Long and slender (prolate) hydromedusae utilize jet-propulsion by contracting the entire bell simultaneously, while the flat wide (oblate) hydromedusae contract mainly just the bell margin, which produces a drag-based rowing propulsion (Colin and Costello, 2002). Prolate medusae tend to be ambush predators that wait for prey to be ensnared by their tentacles, whereas oblate medusae create vortices through their tentacles that allow prey to be caught in the vortices and be entangled (Colin and Costello, 2002).

10.9.3.1 Hydroids

Hydroids are colonial benthic cnidarians. They form from a single settled polyp which buds additional polyps in a species-specific branching pattern. They can form large colonies which rather resemble terrestrial ferns. Morphologically they are distinct from corals in that the individual polyps are often on long slender stalks.

Freshwater *Hydra* are hydroids but they are unique in that they are not colonial but solitary.

Fire coral (*Millepora*) Fire coral is not a true coral but rather is a kind of hydroid.

10.9.3.2 Siphonophores

Siphonophores are colonial polyps (though they superficially resemble a single individual medusa). In fact, their individual organisms (zooids) are functionally specialized and interdependent on each other. Some may be floats and others may be long tentacles. They are different from other jellies in this colonial "meta-individual" existence.

Small siphonophores can be active hunters while larger ones tend to be more passive hunters (Robison, 2004).

Portuguese man-of-war (*Physalia*) *Physalia* is cosmopolitan in warm surface waters. Its tentacles can reach 50 m long! It possesses a gas bladder known as a pneumatophore that contains up to 90% CO_2.

10.9.4 Myxozoa

These are all obligate parasites.

10.9.5 Scyphozoans ("true jellyfishes")

Scyphozoans are predatory, feeding on fishes and zooplanktonic invertebrates with their nematocysts on their tentacles. The nematocysts fire with a hydrostatic pressure of nearly 200 bar! They are meroplanktonic; that is, they have a benthic stage in their life cycle as a polyp that buds off medusae. The often tiny polyps can live for years to decades while the medusae only live a few months generally.

They possess a nerve net that they use for semi-coordinated contraction of their medusa for propulsion. Very small medusae can move by jet-propulsion but any medusae larger than about a centimeter uses a rowing propulsion. They "row" by contracting and expanding their bell to create pressure differences on top and below their bell. Alternating suction forward and heightened pressure backwards moves the medusa forward. Although this motion helps, it is slow and weak and they remain pretty bound to ambient water movement.

Some scyphozoans have rather primitive, light-sensitive eyes. These are often located along the rim of the bell alongside the statocysts.

Jellyfish abundance has been on the rise in recent years for unagreed-upon reasons.

10.9.6 Staurozoa

These are the stalked jellyfishes.

10.10 Ctenophora

Ctenophores, known as "comb jellies" or "sea gooseberries" use 8 rows of ciliated "combs" for propulsion. In fact, they are the largest organism that uses this form of locomotion. They are called "combs" because the cilia are all fused at the base like a comb or like eyelashes. As the cilia beat in a synchronized pulse running down the comb, they refract light which is what gives ctenophores their iridescent look.

The 8 comb rows are controlled by 4 nerve tracks that meet together at the aboral end. A statocyst here connects to the four tracks and when the statolith presses on one of the four hair cells, the corresponding nerve increases ciliary beating to right the animal.

There are roughly 100 known species.

Unlike cnidarians, ctenophores are triploblastic.

They are predatory, feeding on other zooplankton such as fish larvae, small crustaceans or rotifers. They are common in coastal environments but also pelagic environments.

Some ctenophores can be active hunters while larger ones tend to be more passive hunters (Robison, 2004). Their tentacles possess specialized prey-capture mechanisms known as "colloblasts" similarly to the nematocysts of cnidarians but instead they utilize adhesives rather than toxins to capture their prey. Upon capture, the tentacles move prey up towards the mouth for consumption.

Venus's girdle (*Cestum veneris*) This ctenophore looks like a long transparent ribbon up to a meter long, unlike most more circular ctenophores.

10.11 Cycliophora

These critters have been found exclusively in the mouthparts of lobsters.

10.12 Dicyemida

This phylum contains exclusively parasites in benthic cephalopod renal appendages. They range in length from 0.5 to 7 mm.

Their mitochondrial genes (at least three cytochrome oxidase genes (COI, COII, and COIII) are split up into minicircles, rather than one circular mtDNA genome (Watanabe et al., 1999). They have not been found in oceanic cephalopods, just ones that have some association with the benthos.

10.13 Echinodermata

Echinoderms have a 5-pointed symmetry.

Echinoderms circulate oxygen through both their coelomic fluid and water vascular system.

Echinoderms are osmoconformers.

Inside their central disk, echinoderms have a nerve ring that coordinates the arms.

Echinoderm eyes have low-resolution vision and can form fuzzy images (McCormick and Levin, 2017).

Echinoderms have a ciliated epidermis that covers their endoskeleton. It is considered an endoskeleton because of this epidermal layer above it, but it functions similarly to an exoskeleton.

Echinoderms are generally dioecious (separate sexes) and possess at least 5 gonads. Most broadcast spawn their gametes sometimes in a coordinated manner after aggregating and the resulting larvae are bilaterally symmetrical, not attaining pentaradial symmetry until metamorphosis. Alternatively, some asteroids, ophiuroids, and holothuroids can reproduce asexually through splitting their central disk and regenerating the missing components.

In general, regeneration is highly developed in echinoderms (except echinoids), which makes them promising model organisms.

The endoskeleton of echinoderms is composed of a special kind of calcium carbonate known as stereom.

Water vascular system The defining characteristic of echinoderms is their water vascular system. Water enters through the madreporite on the aboral surface, through the stone canal, and fills the ring canal and radial canals in each arm. All along the arms are lateral canals extending to tube feet, sometimes with internal muscular ampullae that look like turkey basters. The tube feet are muscular with suckers on the ends (in most taxa) and are controlled by this hydrostatic system. One-way valves in the lateral canals prevent water from flowing out of the tube feet when muscles contract. By alternating relaxation and contraction of tube feet and ampullae, the tube feet can move.

Pedicellaria Pedicellariae are tiny muscular jaws all over the aboral surface of sea stars and sea urchins. They seem to play some sensory function given their neural complexity but also seem to be used to keep the animal clear of epibionts. There have been reports as well of these pedicellariae cutting the gut opening of other predatory sea stars.

10.13.1 Sea stars (Asteroidea)

On the oral surface of the arms, the tube feet are lined within channels called ambulacral grooves.

Sea stars are active predators, consuming their prey by everting their stomachs and excreting digestive enzymes from their large digestive glands. They are famous for using this strategy to prey on bivalves by digesting the bivalve alive before its muscles weaken to open its valves.

Sea stars use their tube feet to move, not their whole arms (unlike ophiuroids).

Most juvenile sea stars feed on

Crown-of-thorns sea star (*Acanthaster planci*) The crown-of-thorns sea star is found throughout the Indian and Pacific Oceans. Population outbreaks are natural phenomena (though enhanced by eutrophication providing nutrients to support their larvae) (Castro and Huber, 2019). These outbreaks can be problematic because they feed upon hard corals and can cause major damage to reefs that lasts for at least a decade (Castro and Huber, 2019).

10.13.2 Brittlestars (Ophiuroidea)

Brittlestars lack many structures found in asteroids. They lack suckers on their tube feet, organs in their arms, and an anus.

Their arms are elongate and skinny, used for locomotion. The lack of organs in their arms makes them more dispensable than in asteroids, which is good since the arm tips are often eaten by fishes.

Brittlestars typically feed on detritus but have been observed to predate on cephalopods.

10.13.3 Sea urchins and sand dollars (Echinoidea)

Unlike the other echinoderms, echinoids cannot regenerate.

10.13.3.1 Sea urchins

The sea urchin body plan is similar to a sea star with its arms curled up. The ambulacral grooves run along the aboral surface of the sea urchin.

The sea urchin's test is composed of various tessellated plates of calcite.

Unlike sea stars, sea urchins have a long winding digestive system, which is needed for their plant-based diet.

Sea urchins move with both their tube feet and their mobile spines that are embedded in ball-and-socket joints within the test.

Sea urchins are mainly herbivores on macroalgae and seagrasses, but they also end up eating sponges and bryozoans and similar epibionts on their main prey.

The mouth of sea urchins is known as Aristotle's lantern and possesses a complex array of muscles and plates to form the jaw-like assembly with 5 teeth.

Sea urchins are oxyconformers (Spicer, 1995).

Sea urchins inhabit rocky substrates with nooks to hide in.

10.13.3.2 Sand dollars

Sand dollars are basically dorsoventrally flattened sea urchins. Unlike urchins, they inhabit sandy habitats. Wave action in these environments can be intense. Some sand dollars have slots in their tests known as lunules. These are thought to allow water to flow through which prevents the sand dollar from being lifted up by wave action (interrupts Bernoulli effect). Sand dollars with

lunules can live in higher wave action environments than those without. To stay on the benthos, it is thought that some sand dollars (those without lunules) eat the densest sand grains to weigh them down.

They are coated in thousands of tiny spines along with suckered tube feet. They graze microbes and algae off sand grains. Species without lunules also sometimes stand on end to filter feed with their spines.

The 5-pointed flower-looking structure in their tests is known as the petaloid and is composed of many small holes through which specialized respiratory tube feet extend for gas exchange.

10.13.4 Sea cucumbers (Holothuroidea)

In sea cucumbers, the oral and aboral surfaces are at the ends of the cylindrical body and the five arms are concentrated towards the bottom (in some species). The uppermost arms still don't make contact with the substrate very often and the tube feet here often vestigial or absent altogether. They respire through a pair of branching structures known as "respiratory trees" that are located just inside their anus. Their respiration occurs as water moves tidally through their anus.

Their skin can be very soft but once disturbed, can be quickly morphed into being warty and tough. Unlike the solid test structure found in some other echinoderms (e.g. echinoids), sea cucumbers have microscopic spicules throughout their skin.

Some sea cucumbers are deposit feeders, eating POM off the bottom and often sediment along with it. Others have feathery branching tentacles (modified tube feet) that radiate all around the mouth that they use to filter feed plankton. Sea cucumbers have rather long digestive tracts compared to other echinoderms, which is needed to process all the sediment they consume.

Due to their lack of a hard test, some sea cucumbers form toxins and others resort to eviscerating their guts through the mouth or anus to distract a predator and regenerate the structure within a few days. This regeneration happens through the de-differentiation of existing cell types (a rather novel capability). Still others can excrete structures known as Cuvierian tubules from the base of their respiratory tree through their anus. These tubules expand up to 20x their length upon contact with seawater and are very sticky, to stick onto a predator.

10.13.5 Feather stars and sea lilies (Crinoidea)

Crinoids evolved (or at least were specious) well before the other extant echinoderm classes.

The crinoid body plan is basically an upside down brittlestar with the mouth and ambulacral grooves facing upwards. Similarly to the brittlestars, the major organs are absent from the spindly arms. Crinoids suspension feed with their feathery arms that can branch up to 200 in number. Specialized tube feet on the arms can secrete mucus to aid in prey capture. Food is transported down the ambulacral grooves to the mouth. The gut is U-shaped, with the anus on the oral surface as well.

Stalked crinoids are known as sea lilies while un-stalked crinoids are known as feather stars. Sea lilies mainly live in the deep sea and can be very abundant on sea mounts. Sea lilies can move very slowly on the sea floor while feather stars can move much faster with their long cirri. At times, they will even swim by "dog paddling" all their arms.

10.14 Entoprocta

These animals resemble bryozoans in many ways. Whether or not these are lophophorates (like the bryozoans) seems to be a matter of how you define a lophophore.

10.15 Gastrotricha

These are common meiofaunal worms.

10.16 Gnathostomulida

These are known as "jaw worms" and they are meiofaunal.

10.17 Hemichordata

Hemichordates are deuterostome worms with a dorsal hollow nerve cord. Some live in tubes and others move about freely. Most are deposit feeders, eating POM out of sand just like sea cucumbers.

10.17.1 Acorn worms

10.18 Mollusca

See chapter 14.

10.19 Nematoda

Nematodes, or round worms, are some of the most abundant multicellular organisms in the ocean. It is thought that 4 out of every 5 animals on Earth are nematodes! Some are free living and some are parasitic. Free living species are most abundant in sediments and feed on *in situ* bacteria. You can find nematodes as parasites of just about any other living thing (plant and animal). This includes the pinworms and hookworms. Most marine species are thought to have at least one nematode parasite species specific to them.

They are known as round worms because their cross section is perfectly round because they are slightly pressurized (~0.5 atm). Their mouth even has a sphincter to prevent them from deflating when the mouth opens.

They have a complete digestive system with both a mouth and anus. They have no respiratory structures so all gas exchange is through diffusion (which forces the body to stay thin).

Nematodes are mostly dioecious (separate sexes).

They are unique amongst other worms in that they have a hydrostatic skeleton powered exclusively by longitudinal muscles. This results in their "writhing"-like form of locomotion.

The skin of at least some parasitic nematodes is resistant to digestive enzymes, an adaptation that helps them inhabit GI tracts.

10.20 Nematomorpha

These are known as "horsehair worms". There are only 5 described species in this phylum.

10.21 Nemertea

Nemerteans are known as "ribbon worms". There are ~1,300 described species. They can be found all over but are most abundant in shallow temperate waters.

Nemerteans are known for their eversible proboscis that can inject toxins into their prey. The proboscis can be sticky, possess suckers, or even have a spike. Once caught, the proboscis and prey must be pulled inside the body and eating can take multiple days to complete.

Nemerteans have a complete digestive system with both a mouth and anus. They also have a circulatory system.

10.22 Orthonectida

These are all parasites that kill their hosts.

10.23 Phoronida

Phoronids are lophophorates. There are only 13 known species. They are tube-building worms. Unlike similarly looking polychaetes such as feather duster worms, they have a U-shaped gut, with the anus near the mouth. They burrow in sand or attach their tubes to rocks.

10.24 Placozoa

These are considered the simplest free-living animals.

10.25 Platyhelminthes

Platyhelminths, or flatworms have no internal body cavity (they are acoelomates). They also have a "blind" gut with no anus. Many are parasitic but some are free living.

Flatworms are so flat, they have no circulatory or respiratory organs and instead gas exchange by simple diffusion.

10.25.1 Turbellaria

Turbellarian flatworms are the most commonly encountered since they are mostly free living. *Dugesia* spp. is the typical model species for platyhelminths but many species are extremely bright and colorful. They are carnivorous. Turbellarians are hermaphroditic and undergo penis fencing. The first to be stabbed acts as the female and has to bear the cost of healing their wound and developing expensive eggs. They typically have direct development and no larval stage.

10.25.2 Monogenea

These are ectoparasites on the skin, gills, and fins of fishes. They typically just have one host in their lifecycle. Monogeneans are hermaphroditic.

Their main attachment point is a hook/clamp/sucker (depends on the taxon) known as a "haptor".

10.25.3 Trematoda (flukes)

These are endoparasites with 2-3 hosts in their lifecycle. The larvae can infect a variety of marine animals but the adult lifestage exclusively infects vertebrates such as fishes, seabirds, and cetaceans.

10.25.4 Cestoidea (tapeworms)

These are endoparasites with 2+ hosts in their lifecycle. Adults live inside the intestines of most vertebrate species and larvae can be found in any marine animal. The record longest found was a 40 m tapeworm inside a whale.

Their bodies are formed of repeating units similarly to annelids. They are very degenerate with no head, sensory structures, or brain. They attach to their host's intestines with suction cups / hooks known as a "scolex" and absorb nutrients directly across their body wall.

10.26 Porifera

Morphology / physiology Sponges are the most primitive animals because their cells are pretty independent and do not form tissues with specialized cell types. Individual cells are very plastic and even after differentiating can change into other cell types when needed. In fact, at least in some species, if an individual is split into multiple pieces, those pieces can become new individual sponges.

Their outer surface is formed by pinacocyte cells along with porocyte cells (described later).

The sponge feeds by drawing water in through many small pores known as ostia on their surface then expelling filtered water through one or a few central large openings known as an osculum (oscula, plural). In many sponges, these ostia run through porocytes, specialized cells that can close when needed.

The water flow is generated by collar cells known as choanocytes that line the inside feeding chamber(s) of the sponge. The choanocytes each have a large flagellum that beats to move the water and also "collars" formed from microvilli (cellular protrusions) that filter out the food particles from the current. These collars have only about a 0.1 μm opening so even bacteria are captured. Once captured, the food particles are phagocytosed.

Since the oscula are typically protruding out the top where water movement is greater, a slight Bernoulli effect actually helps to make a bit of suction to help aid the choanocytes in circulating water.

In addition to the choanocytes, the external pinacocytes can also phagocytose food particles too large to fit through the ostia.

In between the pinacocytes on the outside and the choanocytes on the inside lies a jelly-like collagenous matrix known as mesohyl. Within this mesohyl are "wandering cells" known as amebocytes that secrete either silicious or calcareous spicules and, in some classes (see below) also a protein matrix known as spongin. Together, the spongin (when present) and spicules (when present) provide structural support for the sponge. The number of rays in the spicules are a key taxonomic character for species identification. The amebocytes also serve a role in food transport within the body.

The overall body shape can be branching, tubular, round, volcano-like, or encrusting. In small ($<$ 1mm) simple sponges, the whole inside is one large feeding chamber with one osculum exit, but in larger more complex sponges, there are canals that pipe water into multiple feeding chambers and multiple oscula exits.

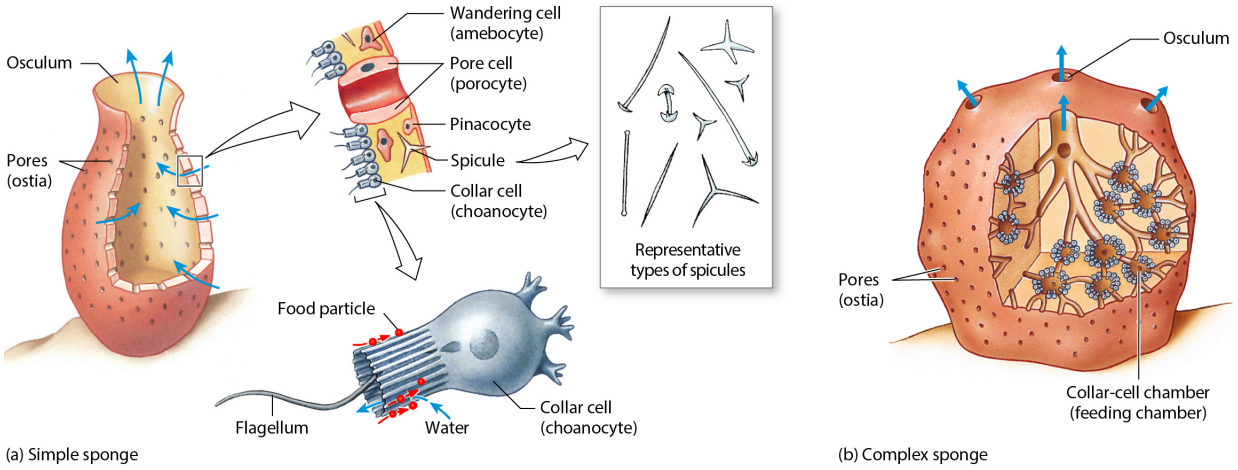

Figure 10.1: Sponge morphology

Reproduction Sponge reproduction is sometimes asexual, with fragments breaking off and forming new individuals. In a few marine species (and many freshwater ones), the sponge can also form environmental-stress-resistant structures known as gemmules that can form new sponges after conditions improve.

However sexual reproduction also occurs. Most sponges are hermaphroditic but some have separate sexes. Regardless, sponges do not have specialized gonad tissues. Instead, choanocytes and amebocytes change directly into sperm and eggs, respectively. As in other animals, there are clearly differentiated eggs (large nutrient rich gametes) and sperms (small flagellar gametes). The sperm are released in broadcast spawning events but the eggs are typically withheld and fertilized internally after, presumably, filtering out sperm that enter through the ostia.

Once the zygote forms and develops into an embryo of flagellated cells, the embryo is released into the water and is now known as a larva that can settle in a new place.

Ecology Almost all of the nearly 10,000 known sponges are marine and all are sessile. Sponges can be found at all latitudes and depths. There are some deep-sea sponges that even attach to manganese nodules when there is only sediment everywhere else (section 1.10.1.3)(Purser et al., 2016). They tend to do best in clear water since suspended sediment can easily clog their ostia.

Some deep incirrates have been observed to lay their eggs on stalked sponges (Purser et al., 2016).

Sponges filter feed on bacteria, plankton, and POM. Some are carnivorous.

Most species are capable of closing their ostia and oscula.

Their lifespan can range from a few years in temperate species to hundreds or possibly thousands of years in the tropics or deep.

Sponges avoid predation both with their spicules and by producing toxins. There's been a lot of research on putatively noxious chemical production by sponges to deter fishes but there's still some debate about its function. These deterents may also be effective at competing for space, a key skill for any sessile reef organism.

10.26.1 Demosponges (Porifera: Demospongiae)

The demosponges (aka sclerosponges or coralline sponges) represent about 75% of all known sponges. They are most abundant in shallow temperate and tropical waters but a few species can be very deep. They can settle on hard substrate or sediment.

10.26.1.1 *Spongia officinalis*

This is the traditional bath sponge.

10.26.2 Homoscleromorph sponges (Porifera: Homoscleromorpha)

This class is closely related to the demosponges and is similar in many characteristics.

10.26.3 Calcareous sponges (Porifera: Calcarea)

Calcareous sponges are most abundant in shallow (< 100 m) temperate and tropical waters. There are ~500 known species. The only simple body plans (with a single feeding chamber) are all calcareous sponges.

10.26.4 Glass sponges (Porifera: Hexactinellida)

Glass sponges are polar and deep-dwelling taxa that grow within sediments rather than hard substrate. Their silicious spicules often fuse together to form a lace-like skeleton.

Unlike the other Poriferan classes, glass sponges have multi-nucleated cells.

10.26.4.1 *Euplectella aspergillum* (Venus' flower basket)

This particular species is unique in that it has a symbiotic relationship with boxer shrimp that are "imprisoned" inside the sponge for life (once they grow to big to get out). A male and female will both live their lives inside the sponge and their larvae only can escape out to find a new sponge.

Class	Cells	Spicule composition	Spongin?	Substrate preference
Demospongiae	Mononuclear	Silica	In most species	Either
Homoscleromorpha	Mononuclear	Silica	In most species	Either
Calcarea	Mononuclear	Calcite	No	Hard
Hexactinellida	Multinuclear	Silica	No	Sediment

10.27 Priapulida

There are only 22 described species of priapulid worms.

10.28 Rotifera

Most rotifers are freshwater but a few are marine.

10.29 Sipuncula

Sipunculans, or "peanut worms", are unsegmented worms. Their digestive system is U-shaped, with the anus exiting anteriorly.

They have very high anaerobic capacity that they utilize for burrowing in the hypoxic/anoxic benthos.

10.30 Tardigrada

10.31 Xenacoelomorpha

These are small bilaterally symmetrical things.

Chapter 11

Vertebrates

11.1 Jawless fishes (Agnatha / Cyclostomata)

The clade Agnatha includes extinct lineages of jawless fishes while Cyclostomata refers to just these two living clades.

Agnathans have no jaws and no paired fins or scales but they do protect their brains with skulls.

They feed with suction through a round mouth lined with rows of teeth. They have cylindrical bodies.

11.1.1 Lampreys

Lampreys start their lives in freshwater but some species live in the ocean as adults. They suck the blood of other fishes or feed on benthic animals.

11.1.2 Hagfishes

Hagfishes, or slime eels, are not closely related to other eels. They feed on dead or dying fishes and bury themselves in muddy sediment.

They have rudimentary vertebrae but no vertebral column. There's debate whether hagfishes belong with lampreys as early-branching fishes or whether they are secondarily degenerate fishes that lost their jaws and vertebrae.

They have no image-forming eyes but just photosensitivity. Instead their olfaction is great thanks to their pair of barbels.

When caught, they can release copious amounts of slime to evade predators grasps and clog a predatory fish's gills. They can also tie themselves in an overhand knot which helps them get out of their own slime and helps them rip themselves off of prey to get a mouth-full of food.

They can make 400x their own volume in slime and make extreme amounts in seconds thanks to seawater mixing with it rapidly to expand it.

11.2 Cartilaginous fishes (Chondrichthyes)

These fishes have skeletons made of cartilage, lighter and more flexible than bone. Unlike the jawless fishes (which also have cartilaginous skeletons), this clade differs in its jawed mouths and paired fins.

These fishes have placoid (pointed tipped) scales that point backwards so they're smooth to the touch moving posteriorly but sandpaper moving anteriorly.

Elasmobranchs do not have Bohr effects in their hemoglobins (Johansen and Weber, 1976).

Benthic elasmobranchs have a spiracle, or small opening, behind the eye that leads to the mouth and gills. This is especially important for skates and rays whose gills are often pressed against the substrate.

11.2.1 Chimaeras

Chimaeras are the only group of Chondrichthyes that are not elasmobranchs. They are an outgroup to the rest due to their having only one pair of gill slits rather than 5-7. They are mostly deep-water species.

11.2.2 Sharks

There are ~500 known species of sharks.

Shark tails are usually heterocercal (upper lobe bigger than lower lobe) as the greater propulsion on the top portion of the tail forces the tail down and head up, which gives lift when they swim. They typically have 2 dorsal fins. They have 5 to 7 gill slits on each side of the body.

Teeth are counted in rows along the edge of the jaw and in series going from the front to the back of the mouth. Lost teeth are common since they do not have roots. Teeth are replaced by backups further in the mouth from 2-15 series.

Some shark species are oviparous while others are ovoviviparous. In oviparous species, the embryos often move around to help oxygenate the egg but will stop moving when sensing an electrical field from a potential predator nearby.

Mako sharks are the fastest sharks.

Thresher sharks use their exaggerated heterocercal tail to corral and stun fish prey.

Whale and basking sharks are filter feeders.

Bull sharks, *Carcharhinus leucas*, can travel far up rivers into lakes!

11.2.2.1 Hammerhead sharks

Eyes and nostrils are both on the lateral tips of the head which gives them binocular vision and olfaction.

11.2.2.2 *Hemiscyllium ocellatum* (Epaulette shark)

This species of shark inhabits tide pools in northern Australia and New Guinea and is extremely hypoxia tolerant due to its adaptation to this environment.

11.2.3 Rays and skates (Batoidea)

Taxon	Reproduction	Tail shape	Nose	Teet
Rays	Ovoviviparous	Long whip-like sometimes with 1-2 venomous barbs	Often relatively blunt	Form p
Skates	Oviparous ("mermaid's purse")	Short broad often with midline thorny spines	Often relatively pointy	Small and

There are about 300 skate species worldwide.

All batoids have 5 gill slits and they are on the ventral side of the body.

Rays tend to eat benthic animals by crushing they with their plate-like jaws.

Eagle rays feed on the bottom while manta rays feed on plankton.

11.2.3.1 Manta rays and devilfishes (Mobulidae)

Manta rays have complex courtship behavior, where the female is tailed by multiple males, forming a "mating train" where she selects a suitable individual to mate.

11.2.3.2 Electric rays (Torpediniformes)

Electric rays can shock up to 200 V depending on the species.

11.3 Bony fishes (Osteichthyes)

Most bony fishes, or osteichthyans, have cycloid or ctenoid scales, unlike the placoid scales of cartilaginous fishes. These scales are made of bone covered in skin and protected by mucus. Bony fishes also have a bony operculum, unlike cartilaginous fishes. Most bony fish caudal fins are homocercal, unlike the heterocercal fins common in cartilaginous fishes.

The fins of ray-finned fishes (Actinopterygii) are thin membranes spanning bony spines known as fin rays.

Bony fishes have protrusible jaws that can extend forwards.

Many bony fishes have a swim bladder just above the GI tract that helps compensate for the dense bones in their bodies.

There are currently over 18,000 accepted marine teleost species worldwide.

Marine fishes acquire the water they need by swallowing seawater and absorbing just the water across the intestinal wall (Heuer and Grosell, 2014). This is facilitated by $CaCO_3$ precipitation in the intestinal lumen which draws Ca^{2+} out of solution thus lowering osmotic pressure which facilitates osmosis out of the lumen into the blood (Heuer and Grosell, 2014).

Marine fishes have a highly developed branchial acid-base mechanism (Heuer and Grosell, 2014; Figure 11.2).

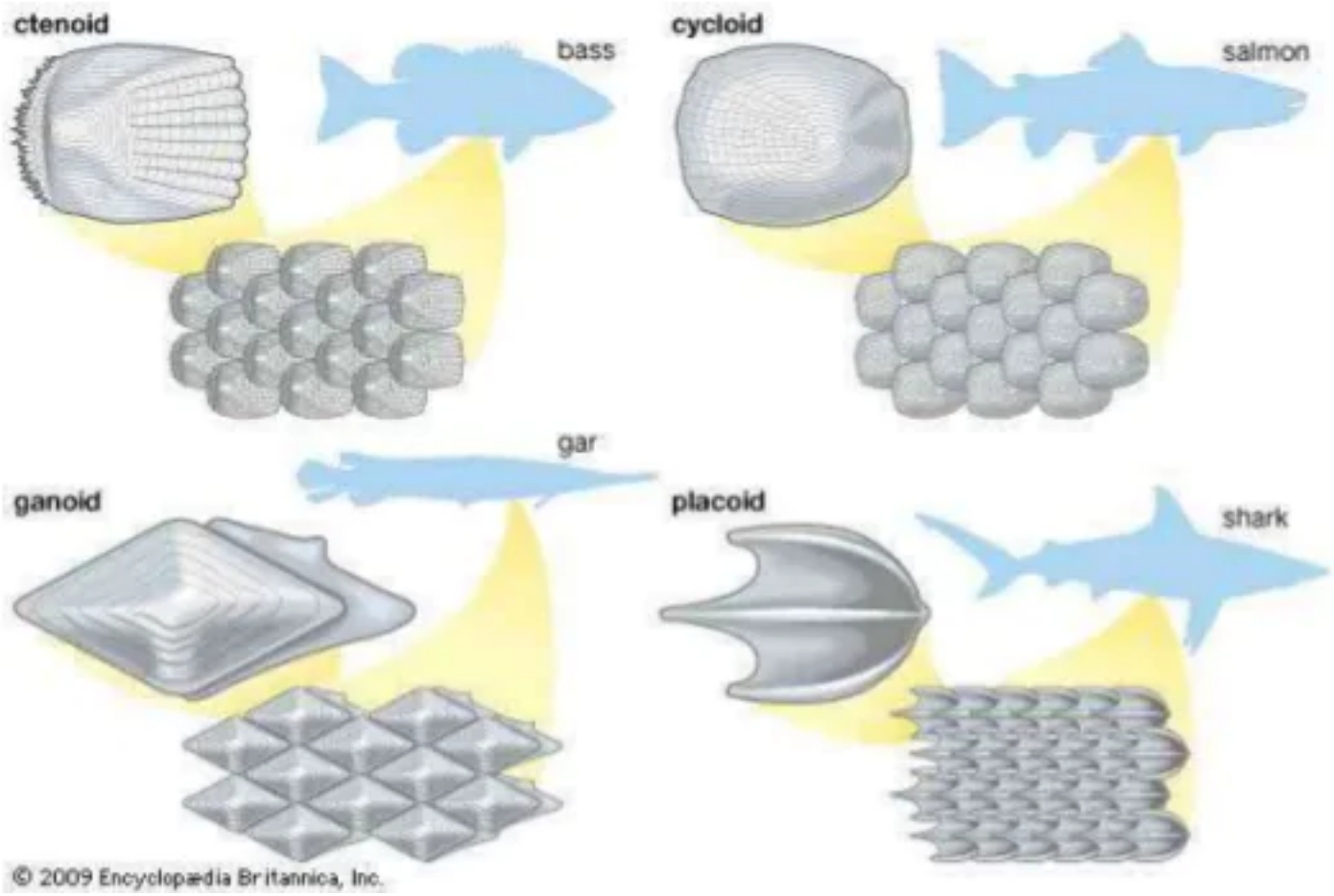

Figure 11.1: Fish scales

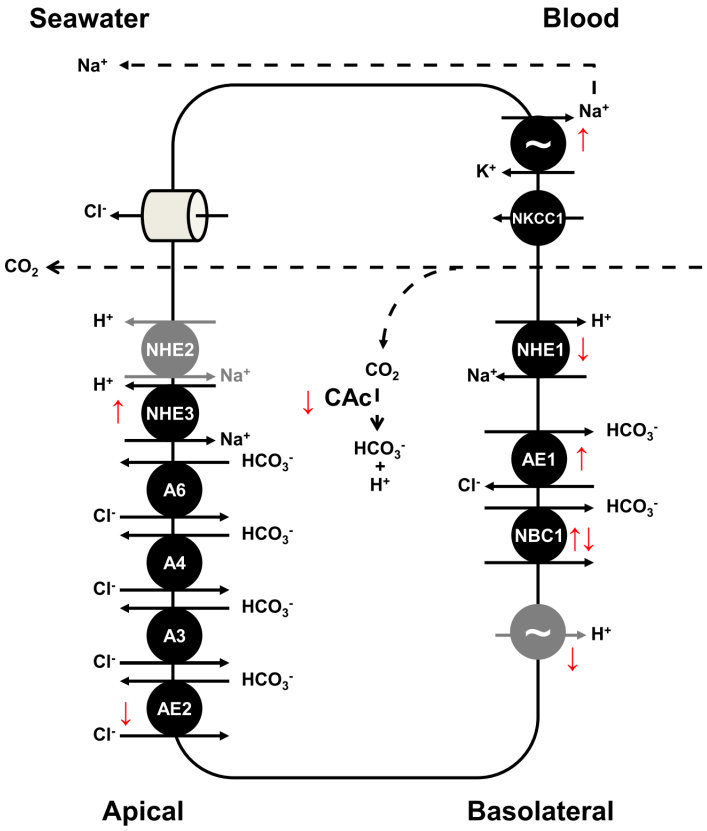

Figure 11.2: Acid-base relevant transporters in marine fish gills. Red arrows indicate documented responses to environmental hypercapnia. Figure from Heuer and Grosell (2014).

How fishes are better equipped than cephalopods for an active lifestyle

- Fishes can have much higher [Hb] than cephalopod [Hc] because they have red blood cells and therefore no viscosity limitation. This means active fishes can have as much as 7 mmol $O_2 \cdot L^{-1}$ (Root, 1931), compared to squids' 2 mmol $O_2 \cdot L^{-1}$.
- Fish hearts are able to deal with low O_2 in blood (venous blood supply), but cephalopod heart tissue has low anaerobic capacity (arterial blood supply).
- Fish muscle fibers have 3-7 capillaries around each muscle fiber. Squid muscle fibers are much more sparsely supplied. In the outer aerobic layers of circular tissue, capillaries are found every 5-8 muscle fibers and in the central anaerobic layers, capillaries are found 20+ muscle fibers apart (Bone et al., 1981). However, fish myocytes are quite a bit larger (Kinsey et al., 2007), so the gaseous diffusion distances may not be so different.
- Fishes use undulatory fins which are much more efficient than cephalopod jet propulsion (subsection 54.2.1).
- Fishes use much less muscle mass for ventilation than cephalopods, especially decapodiforms.

Fish choroid rete and retinal oxygen supply Some teleosts have a choroid rete, which utilizes the Root effect of fish hemoglobin to raise arterial P_{O_2} up to nearly 80 kPa! This is necessary in order to supply sufficient oxygen to the highly demanding retina.

11.3.1 Disks & Ovals / Colorful

Angelfishes and butterflyfishes are laterally compressed coral reef fishes. Angelfishes are different from butterflyfishes in that they have spines on their operculum. Angelfishes also *tend* to have convex foreheads and pointed posterior trails on their dorsal and anal fins. In contrast, butterflyfishes *tend* to have concave foreheads with pointed snouts and rounded posterior ends of their dorsal and anal fins. These taxa are strictly found in shallow coral reefs and are diurnal.

They may be predators of cephalopod paralarvae in coral reef ecosystems.

11.3.1.1 Angelfishes (Pomacanthidae)

Angelfishes are generalist predators, feeding on zooplankton, algae, sponges, benthic invertebrates, etc.

11.3.1.2 Butterflyfishes (Chaetodontidae)

Most butterflyfishes are coralivores but some consume zooplankton.

11.3.1.3 Surgeonfishes (Acanthuroidei)

Surgeonfishes are also known as tangs and are algavores. Most have a rather prominent spine sticking laterally out from their caudal peduncle.

11.3.2 Silvery

11.3.2.1 Barracudas (Sphyraenidae)

This family is monogeneric with all species in the genus *Sphyraena*.

Large species tend to be solitary, while smaller species can be somewhat gregarious and school.

11.3.2.2 Chub

Chub tend to stay in the water column well above the reef.

11.3.2.3 Jacks (Carangidae)

Jacks tend to be seen in the water column around the edges of the reef.

11.3.2.4 Porgies

Porgies are also known as sea bream.

They have strong sloping foreheads.

11.3.2.5 Scombroids (tunas, mackerels, bonitos) (Scombroidei)

11.3.3 Sloping Head / Tapered Body

Snappers have dorsal canine teeth, while grunts do not.

11.3.3.1 Grunts (Haemulidae)

Grunts are named after the grunting noise they make when captured.

Grunts are nocturnal bottom-feeding fishes.

11.3.3.2 Snappers (Lutjanidae)

Snappers are carnivorous.

11.3.4 Small Ovals

These fishes tend to dart in and out of small crevices in the reef.

11.3.4.1 Damselfishes, chromis, and clownfishes (Pomacentridae)

Damselfishes are rather small brightly-colored reef fishes. Most live in shallow tropical coral reefs but some live in temperate reefs. They are notoriously territorial.

They are omnivorous, feeding on crustaceans (mainly shrimp and copepods) and phytoplankton.

They may be prey for cephalopods.

Chromis are less territorial than other damselfishes.

11.3.5 Heavy Body / Large Lips

These fishes often hide in the shadows and are predatory.

11.3.5.1 Grouper (Epinephelinae)

Grouper swallow their prey whole with suction. They are large predators of octopuses.

11.3.6 Swim With Pectoral Fins / Obvious Scales

11.3.6.1 Parrotfishes (Scaridae)

Parrotfishes have plate-like teeth that they use to scrape algae.

11.3.6.2 Wrasses (Labridae)

Wrasse are smaller and more elongated than parrotfishes. Color changing throughout the maturation process is common.

11.3.7 Reddish / Big Eyes

These fishes have very large eyes, matching their nocturnal behavior.

11.3.7.1 Squirrelfishes (Holocentridae)

Squirrelfishes are named as such based on the prominently large posterior end of their dorsal fin, with large rays that stick up resembling a squirrel's tail.

11.3.8 Small, Elongated Bottom-Dwellers

Blennies and gobies are small elongate fishes that are rather eel-like except for their head. They are benthic burrowing animals, often inhabiting reef crevices or burrowing in sand.

They are herbivorous.

Blennies or gobies may be prey for cephalopods.

11.3.8.1 Blennies (Blennioidei)

Blennies often have cirri above their eyes.

11.3.8.2 Gobies (Gobiidae)

Gobies are different from blennies in that their pelvic fins are fused to form a disc-shaped sucker which helps them adhere to the substrate.

11.3.8.3 Jawfishes (Opistognathidae)

Jawfishes typically dig burrows in the sand with their mouths.

11.3.9 Odd-Shaped Bottom Dwellers

11.3.9.1 Flatfishes (Pleuronectiformes)

There are a variety of commercial flatfishes such as flounder, halibut, plaice, and sole.

11.3.9.2 Frogfishes

Frogfishes tend to walk on their pectoral fins.

11.3.9.3 Lizardfishes (Aulopiformes)

11.3.9.4 Seahorses (Syngnathiformes)

11.3.9.5 Toadfishes (Batrachoididae)

11.3.10 Odd-Shaped Swimmers

11.3.10.1 Drums/croakers (Sciaenidae)

Croakers are benthic fishes which make drumming noises by utilizing abdominal muscles to beat their swim bladders (especially male mating calls). They inhabit tropical and temperate estuaries and bays worldwide. They prefer poor visibility environments with the exception of a few species.

They eat invertebrates and small fishes.

11.3.10.2 Pufferfishes (Tetraodontiformes)

11.3.10.3 Remoras (Echeneidae)

11.3.10.4 Triggerfishes (Balistidae)

Triggerfishes have three dorsal spines, while filefishes have two.

11.3.10.5 Filefishes (Monacanthidae)

Filefishes have two dorsal spines, while triggerfishes have three.

11.3.11 Eels

11.3.11.1 Eels (Anguilliformes)

Eels are elongate fishes with both the dorsal and anal fins fused to the caudal fins. They can swim backwards.

They inhabit shallow water sandy, muddy, rocky, or coral environments. A few species inhabit deeper water along continental slopes as well. They lay their eggs in seawater but grow as juveniles in freshwater environments. Thus, it is only hatchlings and adults that encounter cephalopods.

They are nocturnal carnivores.

11.3.12 Other

11.3.12.1 Anglerfishes (Lophiiformes)

Anglerfishes are deep-sea fishes; some are pelagic and some are benthic. They have a bioluminescent lure which they use to attract and distract prey. Some are sexually dimorphic, with males even parasitic mates.

They are opportunistic feeders and thus eat what they encounter, often crustaceans and fishes.

They may be predators or prey of cephalopods.

11.3.12.2 Billfishes (Istiophoriformes)

Swordfishes (Xiphiidae)

Marlins (Istiophoridae)

***Makaira nigricans* (blue marlin)** The blue marlin is one of the predators of *Dosidicus gigas* in the ETP (Jereb and Roper, 2010). *Dosidicus* are one of its top three prey items.

11.3.12.3 Bristlemouths (Gonostomatidae)

Bristlemouths, or gonostomatids, are meso- and bathypelagic fishes. They are an abundant component of the mesopelagic community. *Cyclothone* may be the most abundant vertebrate genus in the world.

11.3.12.4 Catfishes (Siluriformes)

Although most catfishes are freshwater, some are marine.

11.3.12.5 Cods, polluck, haddock, hakes, whiting (Gadidae)

There are several commercially important cods including cod, haddock, whiting, and pollock.

Cods are generally moderately sized and can be diagnosed by three dorsal fins and two anal fins. Most species also have a barbel on their chin.

Cods predominantly inhabit temperate and higher latitude regions on continental shelves.

Their diet includes benthic fishes and crustaceans.

They may be prey, competitors, or predators of cephalopods.

***Theragra chalcogramma* (Alaska / walleye pollock)** This species supports the largest fishery in the United States.

11.3.12.6 Dragonfishes and hatchetfishes (Stomiiformes)

These are fishes that inhabit deep pelagic waters worldwide. They have large elongate teeth, a large mouth, and a chin barbel. All stomiiforms have one or two rows of ventral photophores from the head to the tail.

11.3.12.7 Herrings, anchovies, menhadens, and shads (Clupeiformes)

Clupeoid fishes support a very large fishery but 90% of the catch is used for fish meal.

11.3.12.8 Lanternfishes (Myctophiformes)

Myctophids are some of the most abundant fishes in the deep pelagic.

11.3.12.9 Perches

11.3.12.10 Salmonids (salmon, trout) (Salmonidae)

Unlike the famous Pacific salmon species that are all semelparous, the Atlantic salmon (*Salmo salar*) is iteroparous.

11.3.12.11 Sculpins (Cottoidei)

Sculpins are benthic fishes inhabiting coastal regions.

11.4 Reptiles

All marine reptiles must come to the surface to breathe.

11.4.1 Crocodilians (Crocodilia)

11.4.1.1 Saltwater crocodile (*Crocodylus porosus*)

Saltwater crocodiles are native to the Indo-Pacific and Australia and are the most aggressive and dangerous marine animals to humans.

11.4.2 Sea snakes (Squamata)

There are about 70 species of sea snakes, all of which in the Indo-Pacific.

As with other marine reptiles, sea snakes must surface periodically to breathe.

Sea snakes have a flattened tail that acts like a paddle and lack ventral scales on their belly, thus prohibiting them from moving on land.

Sea snakes are ovoviviparous.

11.4.3 Marine iguana (*Amblyrhynchus cristatus*)

The only extant marine iguana is endemic to the Galapagos. There are various subspecies with variations in appearance between the islands.

Marine iguanas have laterally compressed tails to help with propulsion.

It feeds almost exclusively on macroalgae. Some males dive into the ocean for food while others and females only forage during low tide in the intertidal zone.

11.4.4 Turtles (Testudines)

There are 9 extant species of marine turtles, 7 of which are what we typically think of as "sea turtles", while the others live in brackish marshes and other coastal habitats.

Sea turtles first evolved in the late Jurassic.

Most species of sea turtles have average clutch sizes of 100-200 eggs. Typically only about 80% of laid eggs will hatch. Of those that hatch, 50% don't make it to the water. Of those that make it to the water, 50% die rather early on. Many young turtles after making it off the beach will spend time in floating habitat (like *Sargassum*) while they grow. Of those that survive the first few days/weeks, only about 10% survive to sexual maturity, which in most species is around 20 years.

11.4.4.1 Flatback

11.4.4.2 Green

11.4.4.3 Hawksbill

11.4.4.4 Kemp's Ridley

11.4.4.5 Leatherback

Leatherback turtles are heterotherms!

11.4.4.6 Loggerhead

11.4.4.7 Olive Ridley

11.4.5 Ichthyosaurs

Ichthyosaurs evolved early in the Triassic and became as big as sperm whales (first known giant animal ever evolved in ocean or land). The record largest were 17-25 m long and 40 metric tons. They had quite large eye:body size ratio, suggesting highly visual predation. In fact, they hold the record for largest vertebrate eye ever found.

Most ichthyosaur lineages went extinct by the end of the Triassic but some continued on into the Jurassic despite competition from the new plesiosaurs that had evolved during Jurassic, though the ichthyosaurs were never as dominant as during the Triassic. All ichthyosaurs finally died by 95 Ma.

11.5 Birds

All birds have waterproof feathers thanks to an oil excreted from a gland just above the base of their tail, and rubbed over their feathers during preening.

Seabirds are dependent on the ocean for at least a portion of their life history. They have salt glands which allow them to drink seawater and excrete the salt.

Many seabirds are rather monogamous.

Some seabirds can dive as deep as 30 m.

All birds have oxygen supply improvements relative to vertebrates and high-altitude birds in particular have even further adaptations (Scott, 2011).

Amongst birds, those with large hearts and large flight muscles have smaller genomes than less athletic birds, presumably to reduce metabolic costs of cell division (Wright et al. 2014).

Some seabirds can fly long distances without much effort thanks to dynamic soaring: a flying technique of repeatedly moving between fast and slow moving air masses that helps them generate lift without flapping their wings.

11.5.1 Albatrosses, petrels, and shearwaters (Procellariiformes)

This group of seabirds are sometimes known as tubenoses because they have tube-like nostrils and broad heavy beaks.

Albatrosses live to an extremely long age; some at least 60 years. They can grow to wingspans up to 3.4 m (the longest of any extant bird).

The wandering albatross consumes lots of squids in the Southern Ocean but consumption is mostly scavenging (Abreu's 2022 CIAC talk).

11.5.2 Boobies and gannets (Suliformes)

Gannets and boobies (Sulidae) make plunge-dives at high speeds >20 m/s.

11.5.3 Divers and loons (Gaviiformes)

11.5.4 Grebes (Podicipediformes)

11.5.5 Gulls, terns, auks, waders, and other shorebirds (Charadriiformes)

At least some species of terns forage ~1 m or so from the surface.

11.5.6 Herons (Ciconiiformes)

11.5.7 Pelicans and cormorants (Pelecaniformes)

When cormorants dive, they propel themselves with their feet.

11.5.8 Penguins (Sphenisciformes)

Penguins evolved 60-70 million years ago. Their closest living relatives are the tubenoses. There are 18 extant penguin species. The Antarctic species feed mainly on krill but also lots of squids. They can swim more than 16 kph.

Emperor penguins are the deepest diving seabird, reaching 500+ m, while other species often can reach 200-300 m. They can live up to 20-30 years.

Compared to other seabirds, penguins have evolved high Hb-O2 binding affinity and a large Bohr effect, which both improve oxygen transport from the lungs to the systemic tissues (Signore et al. bioRxiv). They also have high RBC, Hb, and myoglobin concentrations relative to other birds.

Penguins are common prey for orcas, leopard seals, and other apex marine predators.

Adaptations to aquatic living Penguin wings are short, broad, and firm, which help them push through the water. Penguins can produce thrust on both the up and downstrokes, unlike flying birds that only produce thrust on the downstroke. This helps them move through the much denser medium.

Penguins have rete mirable to warm venous return, helping to keep them warm in cold waters.

Penguins have a flattened cornea to minimize refraction and muscles that can change the shape of their very flexible eye lens. These two adaptations allow them to see clearly in both air and water.

Their bones are denser than flying birds, making them less buoyant when diving.

11.5.9 Rails and coots (Gruiformes)

11.5.10 Waterfowl (Anseriformes)

Ducks, geese, and swans will commonly inhabit coastal marine waters.

11.6 Mammals

Land mammals first evolved in the Jurassic. At some point in time, at least five groups of terrestrial mammals independently adapted back to a marine lifestyle.

Unlike in other vertebrates, mature mammalian erythrocytes (RBCs) do NOT have nuclei (Kardong, 2012).

Marine mammal tissues have lower P_{O_2} compared with human tissues (Fahlmann's USF CMS talk).

Most marine mammals have unihemispheric slow wave sleep.

To overcome the high thermal conductivity of water, all marine mammals (except otters) have evolved a thick layer of blubber. Their blubber serves three benefits: 1) insulation, 2) energy reserve, and 3) buoyancy.

Most marine mammals have higher hemoglobin and myoglobin concentration than terrestrial mammals, to function as oxygen reserves for longer dives.

Amongst all the marine mammals, cetaceans and sirenians are the only ones that never leave the water their whole lives.

11.6.1 Cetaceans

There are currently 86 extant species of cetaceans.

To overcome the high thermal conductivity of water, cetaceans have evolved counter-current heat exchange in the flippers and dorsal fins such that chilled venous blood leaving these appendages runs nearby and countercurrent to warm arterial blood, thus warming the venous blood before reaching the body core. Not only does this help warm the venous return but it is also perhaps an exaptation that cools the arterial blood before reaching the testes. In this case, venous return from the dorsal fin runs along the surface of the body down to the testes to cool them closer to the 34°C optimal temperature for mammalian spermatogenesis.

When cetaceans first evolved in the Paleogene, their evolution of echolocation may have been driven at least in part by cephalopods. Shells provide strong echolocation signal and would have been a strong selective factor favoring this behavior.

Their tail fins are known as flukes and the pattern and shape of the flukes are an individual diagnostic.

Cetaceans have modified their nostrils to be on top of the head and this "blowhole" can have one or two separate openings, depending on the species. The shape of the blowhole spray when they surface is one of the species diagnostics people use.

Whales return to the same breeding and feeding grounds annually during their semiannual migrations.

Whales tend to have very lipid-rich bones to help with buoyancy, which makes their whale falls particularly energy-rich for deep sea communities.

11.6.1.1 Toothed whales (Odontocetes)

Sperm whales excrete ambergris, which is an extremely valuable comodity in the perfume industry. It is a waxy excretion that is thought to be a substance excreted by the whale's intestine to protect against the sharp pointy edges of giant squid beaks that they often consume.

Orcas Orcas in different parts of the world have different prey preferences. For example, those in New Zealand prefer stingrays while those around Patagonia prefer sea lion pups.

Sperm whales Sperm whales have family units of 6 to 15 individuals, and nearby family units communicate in a similar "dialect" unlike genetically identical individuals from other "cultures".

Sperm whales eat lots of squids. In the subtropics, they eat mostly histioteuthids, octopoteuthids, cranchiids, and onychoteuthids (based on proportions of beaks in stomachs) (Cherel's 2022 CIAC talk). In whales harvested from the Southern Ocean, however, onychoteuthids dominate their squid prey composition (Cherel's 2022 CIAC talk).

Dolphins Dolphins are distinguished from porpoises by their longer snouts, cylindrical teeth, and crescent shaped dorsal fins. Many dolphin species that dive to depths have large myoglobin stores in their muscles, especially their locomotor muscles (Arregui et al. 2021, Animals).

Dolphins hear in the 8-12 kHz range.

Porpoises Porpoises are distinguished from dolphins by their very short snouts, and flattened teeth. Some don't have a dorsal fin at all and others have very triangular rather than crescent shaped fins.

Narwhals Narwhals' tusks have a spiral that is driven by their microtubules!

11.6.1.2 Baleen whales (Mysticetes)

The only cetaceans to sing "songs" are all male baleen whales. In this case a "song" is not just any vocalization but a complex, long, and repeatable pattern of vocalizations. Unlike us, they don't have to exhale air to sing; they can move the same air back over their "vocal cord equivalents" in repetition. Different populations have different songs and there is cultural transmission when individuals from different populations interact.

We don't know why they sing but it could be to mark their territory, attract mates, coordinate migration, communicate with offspring, or for fun.

Baleen whales have been known to travel down to the SOFAR channel (section 1.3) to propagate their vocalizations long distances.

Baleen whales (or at least one species sampled) hear in the 2-6 kHz range.

Gray whales Unlike other baleen whales, gray whales don't filter feed in the water but instead through the sediment!

11.6.2 Pinnipeds

All pinnipeds need to periodically return to land or ice to rest and breed. Pinniped diets are dominated by fishes and squids.

Most pinnipeds live at high latitudes.

It is thought that the extinction of most nautiloids starting in the Oligocene is due to the evolution of pinniped predators (Kiel et al., 2022). There remain to this date very few or no pinnipeds in the Indo-West Pacific.

11.6.2.1 Seals

There are about 19 species of seals, only one of which is freshwater. Seals propel themselves in the water with laterally undulations of their back flippers.

Seals can sense currents from camouflaged fish breathing and likely can sense water movements from cephalopod ventilations as well (Niesterok et al. 2017, JEB). They do this with their whiskers.

Weddell seals can contract their spleen during deep dives to excrete stored RBCs and transiently increase [RBC] by ~25-50% (Hurford et al. 1996, J Appl Physiol).

11.6.2.2 Sea lions and fur seals

There are 6 sea lion species and 9 fur seal species. Fur seals share morphological traits with sea lions such as external ears and flipper mobility. However, fur seals have an undercoat that makes them much furrier. Their hind flippers also have longer cartilage sticking off the ends, which helps them scratch their furry and itchy coat anywhere on their body.

Sea lions and fur seals can walk and run on land with all four flippers. They can also raise their neck and head up on land by moving their front flippers backwards to support their weight, something seals cannot do. Sea lions and fur seals propel themselves in the water with their front flippers.

Males are much larger than females.

Antarctic fur seals seem to prefer eating krill when abundant and eat less squid during these periods that when krill abundance is low and there are lots of beaks in their stomachs (Xavier's 2022 CIAC talk).

11.6.2.3 Walrus (*Odobenus rosmarus*)

There are two subspecies of walrus, one on the Russian / Alaskan coast in the Pacific and another on the Canadian / Greenland coast in the Atlantic.

Both sexes have tusks that are used for defense and holding onto ice.

While benthic invertebrates such as clams are their primary food, walruses do not use their tusks to dig, as once thought. Instead they feel around with their whiskers and then suck up their food.

11.6.3 Otters

11.6.3.1 Sea otter (*Enhydra lutris*)

Unlike other marine mammals, sea otters do not have any blubber, but instead insulate with air trapped in their thick fur coats. They have the densest fur of any animal.

There are three subspecies: the Asian, Alaskan, and California sea otter.

Sea otters breed and give birth in the water.

Sea otters feed on urchins (famously) but also bivalves and other invertebrates. They are well-known for laying a rock on their belly and smashing their prey against that rock to break it open.

11.6.3.2 Marine otter / sea cat (*Lontra felina*)

The marine otter inhabits mid-latitude regions of the eastern Pacific along the coast of South America. Unlike the sea otter, the marine otter forages in the ocean but spends much of its time on land.

11.6.4 Sirenians

Sirenians do not have any hind limbs and inside move by undulating their paddled tail up and down. They are large, blubbery and scantily haired herbivores that feed predominantly on seagrass beds.

A dugong's tail is shaped line a cetacean tail while the manatees' tails are rounded at the end.

11.6.4.1 Manatee

There are three species of manatees that all live in the Atlantic. Unlike dugongs, they also migrate up into freshwater environments.

11.6.4.2 Dugong (*Dugong dugon*)

The dugong is endemic to the Indian and western Pacific oceans.

11.6.5 Polar bears (*Ursus maritimus*)

Polar bears spend much of their lives on drifting sea ice, hunting for pinnipeds when they come to the surface to breathe.

Chapter 12

Humans

12.1 Oxygen sensing

Human cells sense oxygen in carotid bodies and neuroepithelial bodies (NEBs) (Baik and Jain, 2020).

12.1.1 Carotid body

The carotid body is a chemosensory organ at the split of the common carotid artery. It can sense P_{O_2}, P_{CO_2}, and pH. The carotid body is composed of glomus cells which contain O_2-sensitive K^+ channels (Baik and Jain, 2020). Under hypoxia, hypercapnia, or acidosis, the glomus cells trigger afferent nerves to activate respiratory centers in the brain.

12.2 Lungs

From the nose and mouth, both gas and food pass into the pharynx. From here, the pharynx splits into two paths. Either to the trachea through a flap known as epiglottis or down through the esophagus. Once into the cartilaginous rings of the trachea, there's a branch into the left and right bronchi, which enter the lungs.

Lung alveoli are lined with simple squamous epithelia.

The average adult alveolus is 200-300 μm in diameter. The cumulative surface area of all adult alveoli is ~70-100 m^2.

12.3 Metabolism and blood / O_2 delivery

Humans can tolerate P_{O_2} up to 300 kPa for at least a short amount of time for hyperbaric oxygen therapy.

Mammalian brain, heart, and kidney are capable of excellent cardiovascular autoregulation: where blood flow to an organ can be constant despite a range of blood pressures. This autoregulation is endothelium-dependent.

In response to cellular hypoxia, vertebrates (most well documented in mammals but also seen in fishes) upregulate blood levels of erythropoietin (EPO) by production from the kidneys (adults) or liver (fetus). This cytokine triggers RBC production in the bone marrow. Erythropoietin normally circulates in the blood at 10 mU/mL in humans, a sufficient level to compensate for RBC turnover, but can be upregulated 1000-fold.

Red blood cells have no organelles (no nucleus and no mitochondria). Therefore, they rely solely on anaerobic metabolism.

Humans have about 20 trillion RBCs, each with 270 million hemoglobin molecules in it! The body produces 2.5 million RBCs per second.

Table 12.1: Normal body P_{O_2} (Baik and Jain, 2020)

Tissue	mmHg	kPa
Arterial blood	100	13.3
Brain	34	4.5
Skeletal muscle	30	4

Table 2 Normal values of pO_2 in various human tissues, expressed in mmHg and in percentage of oxygen in the microenvironment

	pO_2		
	mmHg	%	References
Air	160	21.1	
Inspired air (in the tracheus)	150	19.7	
Air in the alveoli	110	14.5	
Arterial blood	100	13.2	
Venous blood	40	5.3	
Cell	9.9–19	1.3–2.5	[92]
Mitochondria	<9.9	<1.3	[92]
Brain	33.8 ± 2.6	4.4 ± 0.3	[53–56, 91]
Lung	42.8	5.6	[57]
Skin (sub-papillary plexus)	35.2 ± 8	4.6 ± 1.1	[58]
Skin (dermal papillae)	24 ± 6.4	3.2 ± 0.8	[58]
Skin (superficial region)	8 ± 3.2	1.1 ± 0.4	[58]
Intestinal tissue	57.6 ± 2.3	7.6 ± 0.3	[59–61]
Liver	40.6 ± 5.4	5.4 ± 0.7	[62–64]
Kidney	72 ± 20	9.5 ± 2.6	[66]
Muscle	29.2 ± 1.8	3.8 ± 0.2	[67–72]
Bone marrow	48.9 ± 4.5	6.4 ± 0.6	[73–75]

Figure 12.1: Human P_{O_2} values from (Carreau et al., 2011)

Oxygen consumption rates Typical basal human M_{O_2} is 0.3 LPM of O_2. Swimming values range from 0.5 to 2. A typical person's MMR is 3 LPM of O_2.

Average resting tidal volume is 0.5 L.

Hemoglobin Adult hemoglobin has two α subunits and two β subunits. The T-state has no oxygen bound, while the R-state is fully-oxygenated (4 O_2 molecules).

Hemoglobin and 2,3-BPG Human hemoglobins within RBCs naturally are surrounded by 2,3-BPG, a highly anionic sugar that raises P_{50} (MacDonald, 1977). It does so because pure Hb in the T-state has 6 positively charged residues at the junction between the two beta subunits. The positive charges repel and make the T-state unstable, causes the equilibrium to shift towards the R-state and have higher O_2 binding affinity (lower P_{50}). However, when 2,3-BPG is present, it can enter the highly positively charged space and stabilize it, thus stabilizing the T-state and favoring equilibrium away from the R-state and lowering O_2 binding affinity (raising P_{50}).

Chronic hypoxia in humans increases RBC 2,3-BPG levels.

Fetal hemoglobin is capable of having a lower P_{50} (so that the oxygen cascade continues from mother to fetus). It does so because it is composed of $\alpha_2\gamma_2$ and the gamma subunits have a serine that replaces one of the positively charged histidines (His143) in beta subunits. As a result, there are less positive charges in the central pocket (+4 rather than +6) and it has a lower binding-affinity to 2,3-BPG. By binding less 2,3-BPG, it favors the R-state more than the mother's blood, and thus, P_{50} is lower.

Responses to altitude (hypoxia)

Altitude (m)	Location	P_{O_2} (kPa)
2400	Aspen, CO	15
3400	Cusco, Peru	14
8848	Mt. Everest	7

Andeans, Ethiopians, and Tibetans all experience high-altitude adaptation.

Tibetans have SNPs in HIF2a that are key to their physiological adaption.

Immediately upon exposure to hypobaria, ventilation and heart rate both increase. Increase in ventilation rate is caused by carotid bodies detecting hypoxemia. This increase in ventilation rate not only increases O_2 flux to the alveoli, it also produces respiratory alkalosis, which increases Hb O_2 binding affinity (Piantadosi, 2003). While beneficial for O_2 loading, it can inhibit unloading at the tissues. Therefore, [2,3-BPG] also increases to help compensate the alkalosis by lowering Hb O_2 binding affinity.

Additionally, the kidneys begin excreting HCO_3^- to lower the alkalosis. Additionally, the kidneys lower blood volume to increase hematocrit. Furthermore, hemoglobin synthesis increases MCHC ([Hb] within RBCs) (Piantadosi, 2003).

In lowlanders, microcirculatory flow through a given capillary slows at altitude, though capillary density does increase. In Tibetans, however, no such slow in microcirculatory flow exists.

In humans, hypobaric hypoxia tolerance is not very well predicted by macrocirculation, but rather by microcirculation and mitochondrial performance (Xtreme Everest studies).

When lowlanders are brought to altitude, they exhibit a decrease in mitochondrial density in their skeletal muscles (Xtreme Everest studies).

At any given altitude, Sherpas have fewer RBCs than lowlanders (Xtreme Everest studies).

Sherpas have lower fatty acid oxidative potential than lowlanders (Xtreme Everest studies). This likely beneficial because fat may generate more ATP per gram than glucose, but fat also uses more oxygen. So under hypoxia, it could be beneficial to burn less fat.

Responses to breath-hold diving (hypoxia) Similar to Weddell seals, Korean diving women are able to contract their spleen during dives to excrete stored RBCs into circulation.

Responses to hyperbaric hyperoxia Hyperbaric hyperoxia causes Hb to be highly saturated in both arterial and venous blood because the O_2 flux in the capillaries is primarily dissolved O_2. This inactivity of Hb lowers its Haldane effect, which means more of the produced CO_2 remains dissolved in the blood rather than bound to Hb. As a result, the blood contains higher P_{CO_2}, which increases pulmonary ventilation rate.

12.4 Brain

The human brain has 100-200 billion neurons. Each neuron is synapsed to 5000-200,000 other neurons (O'Carroll and Schaefer, 2013).

Humans have five fast neurotransmitters (but these are not universally conserved or even do the same thing in all taxa):

- acetylcholine
- serotonin
- glutamate (excitatory)
- GABA
- glycine (inhibitory, vertebrate-specific)

12.4.0.1 Mammalian glia

Astrocytes are star-shaped glia (projections are not dendrites or axons, just projections) that support neurons through regulating chemical composition of ECF, neuronal waste removal, and repair. Some of their projections also wrap around capillaries, forming the blood-brain barrier.

Satellite cells cover PNS and have similar functions as astrocytes in the CNS. They cover PNS ganglia and regulate their microenvironment.

Oligodendrocytes insulate CNS axons with myelin. A single cell body has projections that can insulate multiple regions of multiple axons.

Schwann cells insulate PNS axons with myelin. A single cell body only wraps around a single region of a single axon.

Ependymal cells are found in the brain ventricles and filter blood to create cerebrospinal fluid for the CNS.

Radial glia support neurogenesis and regeneration by guiding axons to needed connections.

Microglia consume cells and pathogens in the CNS (like macrophages).

12.4.0.2 Altitude

Andean natives have lower glucose metabolism (lower metabolism) in their brains than lowlanders, especially in more "advanced" regions of the brain, indicative of hypoxia acclimation (Hochachka et al., 1994).

Cerebral blood flow increases at altitude by widening the middle cerebral artery 2x to increase flow 16x (Xtreme Everest studies).

12.4.0.3 Stroke physiology

Stroke is the fifth leading cause of death in Americans and the leading cause of long-term disability (Benjamin, 2017).

85% of strokes are ischemic strokes (blood flow blockage) while 15% are from bleeding.

The brainstem and cerebellum receive their primary blood supply through the vertebral arteries (posterior circulation), while the brain hemispheres receive their primary blood supply through the carotid arteries (anterior circulation). These contribute 30 and 70% of total cerebral blood flow, respectively. However, both kinds of arteries connect (anastomose) before reaching the brain at the circle of Willis, such that an arterial blockage in one artery can be compensated by any other arteries.

Causes of stroke (in order of frequency): atherosclerosis (plaque buildup), heart embolism (clot started in heart from atrial fibrillation that causes blood to swirl and coagulate and travels to brain supply)

Part III

Their phylogeny

Chapter 13

Diversity and history

13.1 Diversity

There are currently 49 families, nearly 180 genera, and nearly 800 species of extant cephalopods. There are also about 600 genera and 17,000 extinct species.

Over geologic time, cephalopod species appear and disappear very quickly compared to fish and other molluscs (Ritterbush's 2022 CIAC talk).

Among the decapodiforms, it is not clear which group branched the earliest, but idiosepiids and sepiolids seem to have separated after branching from sepiids and teuthoids. Similarly, teuthoids separated after branching from sepiids and the idiosepiid-sepiolid clade (Tanner et al. 2017 and Anderson's 2018 CIAC talk).

13.2 Timeline

Cephalopods likely diverged from other conchiferans in the Cambrian by leaving the benthos and inhabiting the pelagic and radiating in this newly explored niche (Young et al., 1998). They were likely some of the first animals to leave the benthos (Staaf, 2017). Packard (1972) proposed that from the Paleozoic through early Mesozoic, ectocochleates inhabited shallow waters. When fishes and marine reptiles radiated in the Mesozoic, however, they out competed the ectocochleates into deeper water. The strong selection for deeper habitat led to the removal of the depth limiting outer shell; its air spaces could not withstand the great pressure. With their shell removed, coleoids re-inhabited the shallow waters as competitors of fishes.

13.2.1 Hadean Eon (>4000 Ma)

The moon formed during the Hadean.

Earth's water likely accumulated during the Hadean.

13.2.2 Archean Eon (4000-2500 Ma)

Life seems to have first evolved about 3.8 Ba.

Initially, the ocean water was very reducing and full of dissolved iron. The atmosphere and water lacked any appreciable amount of oxygen. 2.8 Ba photosynthetic aerobic cyanobacteria first evolved and started emitting O_2 waste.

Kenorland was 2.7-2.5 Ba (first known supercontinent).

13.2.3 Proterozoic Eon (2500-541 Ma)

Nuna was the second known supercontinent (1.8-1.4 Ba). A supercontinent known as Rodinia existed from roughly 1100 to 750 Ma.

As seawater began being oxidized by the aerobic cyanobacteria that first evolved in the late Archean, iron oxide started forming, precipitating, and turning the ocean red (as can be seen in red bands on rocks today). In one of the worst extinction events known on Earth, this oxygen from these aerobes killed off the vast majority of anaerobic life in what is known as the Great Oxidation Event from 2.4-2.0 Ba.

GSA GEOLOGIC TIME SCALE v. 5.0

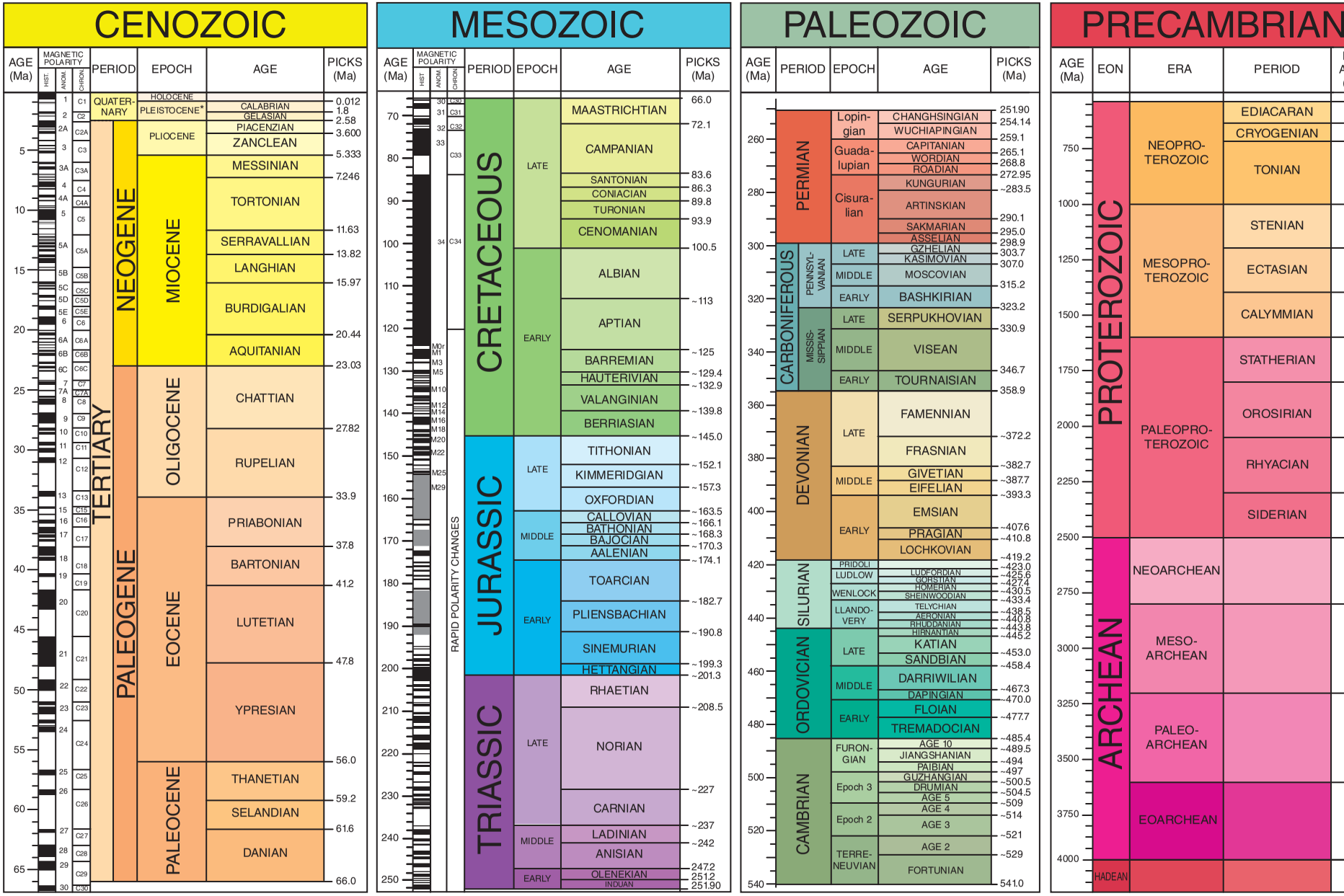

Walker, J.D., Geissman, J.W., Bowring, S.A., and Babcock, L.E., compilers, 2018, Geologic Time Scale v. 5.0: Geological Society of America, https://doi.org/10.1130/2018.CTS005R3C. ©2018 The Geological Society of America

*The Pleistocene is divided into four ages, but only two are shown here. What is shown as Calabrian is actually three ages—Calabrian from 1.80 to 0.781 Ma, Middle from 0.781 to 0.126 Ma, and Late from 0.126 to 0.0117 Ma.

The Cenozoic, Mesozoic, and Paleozoic are the Eras of the Phanerozoic Eon. Names of units and age boundaries usually follow the Gradstein et al. (2012), Cohen et al. (2012) , and Cohen et al. (2013, updated) compilations. Numerical age es and picks of boundaries usually follow the Cohen et al. (2013, updated) compilation. The numbered epochs and ages of the Cambrian are provisional. A "~" before a numerical age estimate typically indicates an associated error of ±0.4 to over

THE GEOLOGICAL SOCIETY OF AMERICA®

REFERENCES CITED

Cohen, K.M., Finney, S., and Gibbard, P.L., 2012, International Chronostratigraphic Chart: International Commission on Stratigraphy, www.stratigraphy.org (accessed May 2012). (Chart reproduced for the 34th International Geological Congress, B Australia, 5–10 August 2012.)
Cohen, K.M., Finney, S.C., Gibbard, P.L., and Fan, J.-X., 2013, The ICS International Chronostratigraphic Chart: Episodes v. 36, no. 3, p. 199–204 (updated 2017, v. 2, http://www.stratigraphy.org/index.php/ics-chart-timescale; accessed May 2018).
Gradstein, F.M, Ogg, J.G., Schmitz, M.D., et al., 2012, The Geologic Time Scale 2012: Boston, USA, Elsevier, https://doi.org/10.1016/B978-0-444-59425-9.00004-4.

Previous versions of the time scale and previously published papers about the time scale and its evolution are posted to http://www.geosociety.org/timescale.

Between 2.5 and 2.2 Ba, the Earth underwent the Huronian Glaciation (ice Earth) because of all the oxygen produced by the cyanobacteria. This oxygen left the ocean and oxidized methane in the atmosphere to CO_2, a less potent greenhouse gas. These photosynthesizers were also driving down P_{CO_2}. This sent the Earth into a global cold period.

Eukaryotes first evolved at least 2.4 Ba.

13.2.3.1 Ediacaran (635 - 541 Ma)

Environmental events A supercontinent known as Pannotia existed from roughly 600 to 540 Ma.

The sea floor in the Ediacaran was covered by a hard bacterial mat that nothing could dig through. As a result, most life forms lived on the surface of the seafloor. Then, in the Cambrian, worms would evolve and dig into the bacterial mats and brake them up into the soft sediment sea floor we know today.

Evolutionary events

13.2.4 Paleozoic Era (541 - 252 Ma)

The start of the Paleozoic era is marked by the appearance of something akin to priapulid burrows. This was the first time that animals burrowed into the benthos. Trilobites were abundant throughout the Paleozoic and died at the end-Permian extinction.

13.2.4.1 Cambrian (541 - 485 Ma)

Environmental events The "Cambrian explosion" occurred just after the oxidation of the atmosphere and ocean, as evidenced by iron rust bands in the geologic record. This was due at least in large part to photosynthetic oxygen production. Since the oxidation of the atmosphere, atmospheric P_{O_2} has remained relatively stable since (Pilson, 2013).

Most marine life lived on the benthos.

Evolutionary events The first unambiguously cephalopod species was *Plectronoceras cambria* found in the middle Late Cambrian. It likely diverged from benthic monoplacophorans with a high conical shell (Kröger et al., 2011; Wanninger and Wollesen, 2019). It likely swam with its shell upwards and arms downward. As in modern *Nautilus*, it had segmented chambers and a fleshy siphuncle running through them. It was likely one of the first nekton and thus had little predation and could eat easily and move easily from the benthos. Early cephalopods had straight shells.

Cephalopods split from gastropods ~520 Ma.

13.2.4.2 Ordovician (485 - 444 Ma)

Environmental events Vertebrates first evolved, but were still jawless and thus posed little threat to cephalopods. They were scavengers and developed good olfactory senses to find detritus.

First plants evolved on land 470 Ma.

Evolutionary events There were some big cephalopods here such as *Cameroceras* that grew up to 6 m long.

13.2.4.3 Silurian (444 - 419 Ma)

Environmental events Jawed fishes evolved during this time (420-410 MYA), creating the first pressure for high metabolism and likely were some of the first main predators to cephalopods in the water column.

Evolutionary events Due to high predation pressure from jawed fishes, some Silurian cephalopods evolved truncated shells, such that they could break off the end of their shell to make it easier to escape. This may have been possible by extending the mantle over the shell like a modern cowrie to dissolve the shell at the perforated point.

At the end of the Silurian, sea level decline led to the extinction of many cephalopod species.

13.2.4.4 Devonian (419 - 359 Ma)

Environmental events Fishes and cephalopods both diversified greatly in this period and both became more agile and faster swimmers. This is known as the Devonian Nekton Revolution (Tanner et al., 2017).

Trees evolved in the Devonian, creating a new nutrient flux into coastal waters and supporting high primary productivity along the coasts. This also led to coastal dead zones. Those dead zones put selective pressure on select fishes to breathe air instead of water and they formed the tetrapod lineage 365 Ma.

First insects evolved on land 400 Ma.

The Devonian ended with a large extinction event possibly due to coastal deadzones from the new nutrient fluxes.

Evolutionary events Due to selective pressure to be more agile and harder to eat, cephalopods began coiling their shells and moving away from the straight-shelled form.

The nautiloid divergence did not occur until the early Devonian (416 MYA) where they split from what would become the ammonoids (Kröger et al., 2011). The bactritoids (external, narrow pointy shell) diverged from the ammonoids very soon after the nautiloid-ammonoid divergence in the early Devonian (Kröger et al., 2011).

The beak first appears in the fossil record in the Devonian (Tanner et al., 2017) though it may have existed earlier.

Due to the increased coastal nutrients, cephalopods began to produce more, smaller eggs with smaller yolks unlike their ancestors which were primarily large-egged.

13.2.4.5 Carboniferous (359 - 299 Ma)

Environmental events Atmospheric P_{O_2} reached its peak here: ~35 kPa. This is mainly because decomposing bacteria had not yet evolved to decompose terrestrial plants and the associated respiration. As a result, the Mississippian and Pennsylvanian epochs were when a huge proportion of today's oil and coal, respectively were made from marine and swamp sources, respectively. The organic material was extremely abundant but would not decompose (or not very quickly at least).

The first amniotes (tetrapods not dependent on water to lay eggs) evolved 310 Ma.

Evolutionary events The earliest coleoid (internal shell) was *Hematites* which diverged from the bactritoids in the Early Carboniferous (Kröger et al., 2011). Coleoids would not become a large group until the belemnoids, however.

13.2.4.6 Permian (299 - 252 Ma)

Environmental events The end of the Permian was triggered by large volcanic activity in the Siberian Traps over about a million years which produced an oceanic anoxic event that caused anoxia in major ocean basins (Rabalais et al., 2010) and ocean acidification. 96% of all marine species went extinct (the most of any mass extinction) and 70% of terrestrial species as well. This is sometimes referred to as "The Great Dying". The trilobites, most crinoid echinoderms, and most brachiopods went extinct.

Pangaea formed during the Permian.

Evolutionary events Octopodiforms and decapodiforms diverged ~275 MYA (Albertin et al., 2015; Kröger et al., 2011). 38 and 78% of nautiloid and ammonoid species, respectively, went extinct at the end-Permian mass extinction (Knoll et al., 2007). The lesser impact on nautiloids than ammonoids may have been due to the former taxon's more K-selected life history strategy, allowing individuals to outlast poor environmental conditions.

13.2.5 Mesozoic Era (252 - 66 Ma)

13.2.5.1 Triassic (252 - 201 Ma)

Environmental events After the end-Permian extinction, there was lots of adaptive radiation amongst many groups of organisms. As an evolutionary generality, when competition is low in an ecosystem, there are many open niches that can be filled and so phenotypic evolution is fast. When competition is tight, there is no such room for mutational creativity and phenotypic evolution is slower. At the start of the Triassic, competition was low.

The early Triassic was extremely warm, with SST at the equator potentially near 40 °C and 20 °C at the poles and the ocean interior 25-35 °C (Kidder and Worsley, 2004). Pangea first formed at the start of the Triassic and first started falling apart at the end of the Triassic.

Ichthyosaurs first developed from terrestrial reptiles around the start of the Triassic and were dominant predators throughout the Triassic. Dinosaurs first evolved on land about 243 Ma, and flying reptiles first evolved in the late Triassic.

Diatoms first evolved.

The Triassic closed with the end-Triassic extinction event.

Evolutionary events Ammonoids radiated rapidly and became very abundant as well. At the end of the Triassic, all nautiloids except Nautilidae went extinct.

13.2.5.2 Jurassic (201 - 145 Ma)

Environmental events Pangea started coming apart around 201 Ma, defining the start of the Jurassic. This is also when the Atlantic first formed. Mammals first evolved on land during the Jurassic.

Plesiosaurs first developed around 200 Ma. Sea turtles first evolved in the late Jurassic.

Most ichthyosaur lineages went extinct by the end of the Triassic but some continued on into the Jurassic despite competition from the new plesiosaurs that had evolved during Jurassic, though the ichthyosaurs were never as dominant as during the Triassic.

Evolutionary events Belemnoids first evolved muscular mantles with longitudinal, radial, and circular muscles 185 MYA (Young et al., 1998) and diversified in the Mid-Jurassic before waning by the Jurassic-Cretaceous boundary (Tanner et al., 2017). In competition with belemnoids, modern teuthoids diverged and diversified about 150 MYA (O'Dor and Webber, 1991). Modern teuthoids may have had higher fitness than belemnoids because their mantle contractions (essential for jet propulsion) were more capable without the rigid phragmocone.

13.2.5.3 Cretaceous (145 - 66 Ma)

Environmental events Pangaea continued to break up. Angiosperms first evolved on land. The shallow water bridge connecting South America and Africa separated in the Late Cretaceous, thus prohibiting trans-Atlantic movement by warm, benthic cephalopods such as cuttlefishes and Sepiolinae (Young et al., 1998). The last major oceanic anoxic event occurred 93 Ma (Young et al., 1998). The end-Cretaceous meteor impact also likely triggered volcanism.

Modern teleosts radiated rapidly. The last remaining ichthyosaurs went extinct 91 Ma and plesiosaurs went extinct at the K-Pg boundary. Mosasaurs evolved in the Cretaceous and were important predators until the K-Pg extinction.

Evolutionary events Incirrates diverged from cirrates roughly 100 Ma year (Young et al., 1998; Tanner et al., 2017). Cuttlefishes evolved in the late Cretaceous (88 Ma; Tanner et al., 2017) sometime after the shallow waters connecting the New and Old Worlds disappeared. Sepiolids also radiated in the late Cretaceous (Sanchez et al., 2021). Ammonoids and belemnoids went extinct 66 Ma at the end of the Cretaceous (K-Pg boundary) (Arkhipkin and Laptikhovsky, 2012).

13.2.6 Cenozoic Era (66 Ma - present)

13.2.6.1 Paleocene (66 - 56 Ma)

Environmental events The Paleocene-Eocene Thermal Maximum (PETM) was an event of rapid climate warming (+5-8 °C) over the course of ~220 ky due to increased atmospheric CO_2. This also caused an ocean acidification event, as evidenced by a shoaling of the carbonate compensation depth (subsection 3.6.1).

Penguins first evolved.

Evolutionary events

13.2.6.2 Eocene (56 - 33.9 Ma)

Environmental events The PETM was occurring during this period (see subsubsection 13.2.6.1).

Cetaceans first evolved about 50 Ma.

Evolutionary events While teuthoids diverged from other decapods in the Mesozoic, some taxa, such as *Loligo*, only evolved much more recently (~44 MYA)(O'Dor and Webber, 1991).

The Sepiolidae subfamilies diverged from each other during the Eocene and Oligocene (Sanchez et al., 2021).

13.2.6.3 Oligocene (33.9 - 23.03 Ma)

Environmental events The Antarctic Circumpolar Current (ACC) likely formed during this time, isolating Antarctica and forming the modern Southern Ocean.

Evolutionary events The Sepiolidae subfamilies diverged from each other during the Eocene and Oligocene (Sanchez et al., 2021).

It is thought that the extinction of most nautiloids starting in the Oligocene is due to the evolution of pinniped predators (Kiel et al., 2022). There remain to this date very few or no pinnipeds in the Indo-West Pacific, the only place where nautiloids remain.

13.2.6.4 Miocene (23.03 - 5.333 Ma)

Environmental events

Evolutionary events

13.2.6.5 Pliocene (5.333 - 2.58 Ma)

Environmental events

Evolutionary events

13.2.6.6 Pleistocene (2.58 Ma - 12 ka)

Environmental events

Evolutionary events

13.2.6.7 Holocene (12 - 0 ka)

Environmental events

Evolutionary events

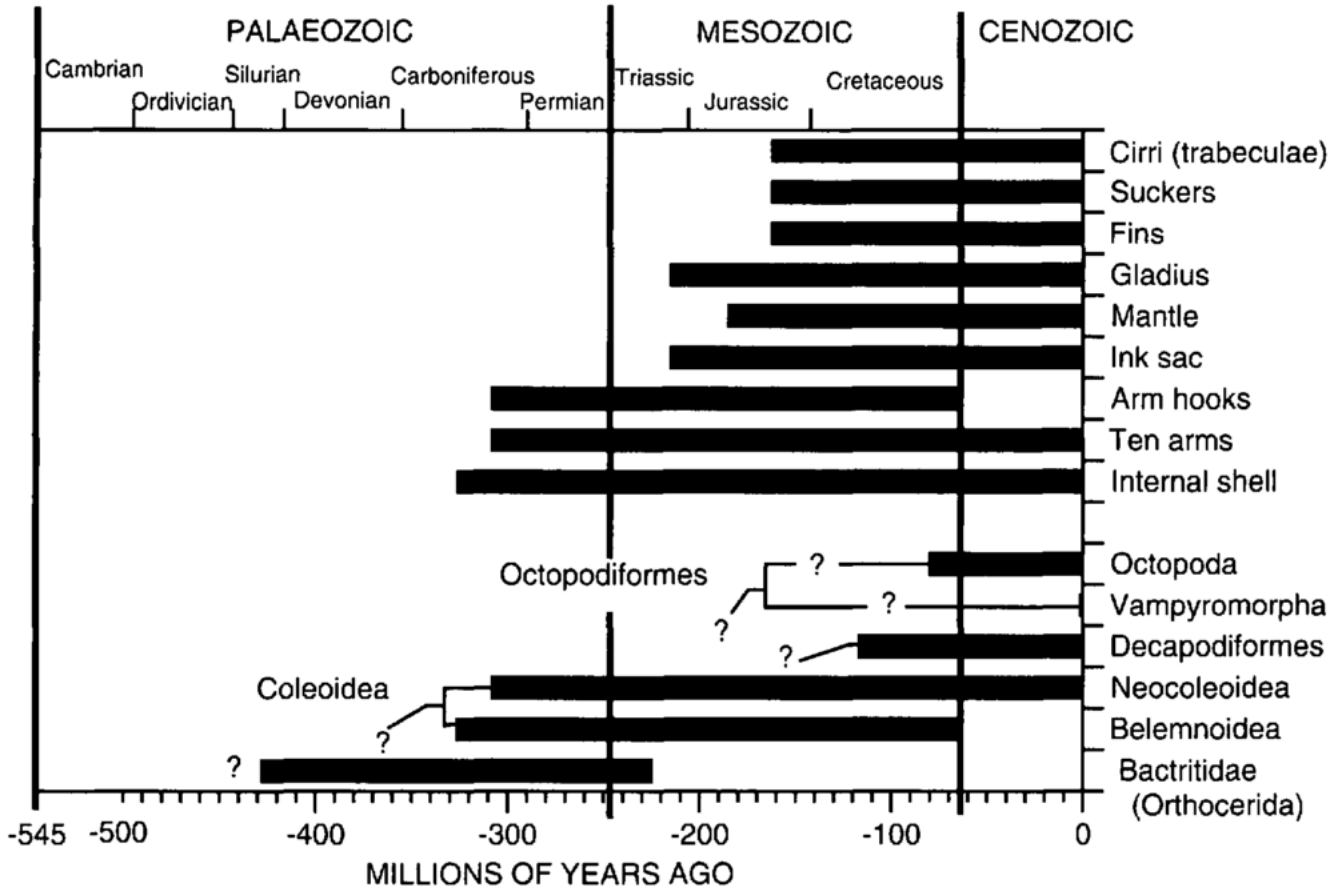

Fig. 2: Palaeochronology of the coleoid fossil record. The upper portion shows structures and the lower portion shows taxa. Solid bars indicate the time range over which a character or a taxon is known

Figure 13.2: Timeline of morphological adaptations. The lower half outlining taxa is outdated and much more clarification on phylogeny exists. Figure from (Young et al., 1998).

Chapter 14

The other molluscan classes

All four of the popular phylogenies for molluscan evolution support the monophylogeny of Conchifera, though Aculifera is not as unanimous (Wanninger and Wollesen, 2019). Within the Conchifera, the relationships among the classes are unclear, with cephalopods falling closest to either gastropods, scaphopods, or monoplacophorans (Wanninger and Wollesen, 2019).

Within the ocean, molluscs are more specious than any other phylum (Castro and Huber, 2019).

Molluscan shells are made of collagenous protein and $CaCO_3$. There are three layers with the outer layer with the highest protein composition. Their mantle is a thin layer of tissue that secretes the shell.

The radula is unique among molluscs compared to other phyla.

Most molluscs are dioecious (separate sexes). Bivalves, chitons, tusk shells, and some gastropods broadcast spawn, while most gastropods (and of course cephalopods) have internal fertilization. The larvae of clams, tusk shells, and some snails are veliger larvae.

Aculifera

- **Aplacophora**
  - **Caudofoveata**
  - **Solenogastres**
- **Polyplacophora**

Conchifera

- **Bivalvia**
- **Cephalopoda**
- **Gastropoda**
- **Monoplacophora**
- **Scaphopoda**

14.1 Bivalvia (a.k.a. Lamellibranchiata, Pelecypoda)

There are roughly 9,000 or so species of bivalves. Bivalves are laterally compressed (squeezed sideways) and their shell has two parts, or valves. Each valve grows from the hump near the hinge (known as the umbo) outwards.

Table 14.1: Oxygen transport traits among the molluscan classes

Trait	Bivalvia	Caudofoveata	Cephalopoda	Gastropoda	Monoplacophora	Polyplacophora	Scaphopo
Hemocyanin	No	Yes	Yes	Yes		Yes	
Tissue globin	Yes			Yes		Yes	Yes
Extracellular hemoglobin	Yes		No	Yes			
Hemocoelic erythrocyte	Yes		No				

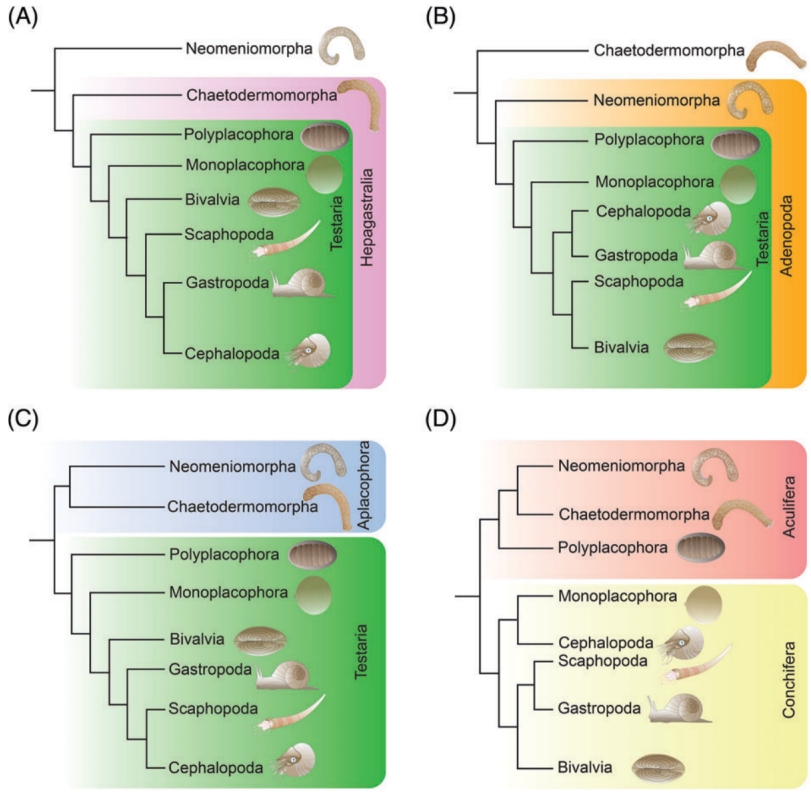

Figure 14.1: Four popular hypotheses for molluscan phylogeny. Figure from (Wanninger and Wollesen, 2019).

Bivalves have lost any sort of head, sensory structures, and also the radula. Their gills, however, have expanded in both size and function to not only provide gas exchange but also to filter food. Incurrent and excurrent siphons are both found on the same edge of the mantle (requiring a 180° turn of water flow within the mantle cavity). The siphons draw water through the mantle cavity. Developmentally, these siphons derive from the mantle.

As food particles are caught in the gill mucus, cilia transport the food-ladened mucus towards the labial palps, which push it all into the mouth. Inside the stomach, bivalves have another morphological novelty: a "style" or "crystalline style" is a protein rod that rotates around inside the stomach, mechanically breaking down food and also excreting enzymes.

Their mantle secretes the shell and thus the rest of the body is all within the mantle cavity. Bivalves grow their shell only along the mantle edge. The valves are kept shut with anterior and posterior adductor muscles. The anterior end is near the foot and the posterior end is near the siphons.

Bivalves broadcast spawn both their sperm and eggs for external fertilization.

Bivalves do not have a centralized "brain" but rather have multiple ganglia throughout their bodies.

Unlike any other known eukaryote, they inherit two mitochondrial genomes: one from the egg and one from the sperm (Ghiselli et al. 2021).

NOAA estimates that bivalve fishery and aquaculture together are about a 1 billion dollar annual industry in the USA.

14.1.1 Clams

Clams, by and large, burrow their bodies in the sediment. They use their foot to dig into the sediment. While all bivalves have siphons, the siphons of clams are extra long to accommodate their burrowing. Geoducks in particular have extreme siphons.

Just like some corals, giant clams can harbor symbiotic zooxanthellae that gives their mantles their bright colors (Castro and Huber, 2019).

Although most clams are filter feeders, a few species are deposit feeders.

14.1.1.1 Cockles

14.1.1.2 Shipworms

Shipworms are actually a kind of clam and they harbor bacteria in their gut that helps them digest the cellulose in wood (Castro and Huber, 2019). They eat mangrove roots and driftwood naturally, but also biofoul boats and pilings.

14.1.2 Mussels

Mussels don't burrow much but they attach themselves to solid surfaces by secreting byssal threads.

14.1.3 Oysters

Oysters don't burrow much but they attach their shells to other surfaces, especially other oysters, forming so-called "oyster reefs". When new oyster larvae attach to a hard surface, they are then known as "spat".

Pearls Oysters form pearls when they get an irritant between their mantle and shell. They cover this with iridescent material known as nacre or mother-of-pearl, as is the internal surface of their shells. Layers of this are added over time to make the pearl. Natural pearls are often oddly shaped but the round ones that are commercially valuable are "cultured" by injecting an irritant in specific places of the mantle of specific species of oysters to get the nice round shape.

14.1.4 Scallops

Unlike other bivalves, scallops can swim and are not at all sessile. They have up to 200 eyes along the edge of their mantle as well as many tentacles. The tentacles provide sensory input to the scallop and some even have eyes on them!

They have triangular extensions of their valves near the hinge known as "auricles".

14.2 Caudofoveata

The caudofoveates are small, worm-like molluscs. Rather than a shell, they have many aragonitic sclerites. They burrow in sediment and eat passing detritus. There are about 150 known species.

14.3 Gastropoda

There are thought to be 65,000 to 80,000 extant gastropod species. As such, gastropods are the most specious and abundant of the molluscan classes. Gastropod literally means "gut-foot".

All gastropods undergo torsion (where the viscera and mantle cavity rotate 180° such that the anus and gills are above the head) during their larval development, however some have secondarily undergone de-torsion. There is no clear evolutionary advantage to why this happened.

As a result of this torsion, the paired internal organs are asymmetrical with one side growing faster than the other.

Gastropods may be herbivores, deposit feeders, or carnivorous.

Gastropods do not have a centralized "brain" but rather have multiple ganglia throughout their bodies.

Some gastropods broadcast spawn both their sperm and eggs for external fertilization, but most internally fertilize females with a long flexible penis.

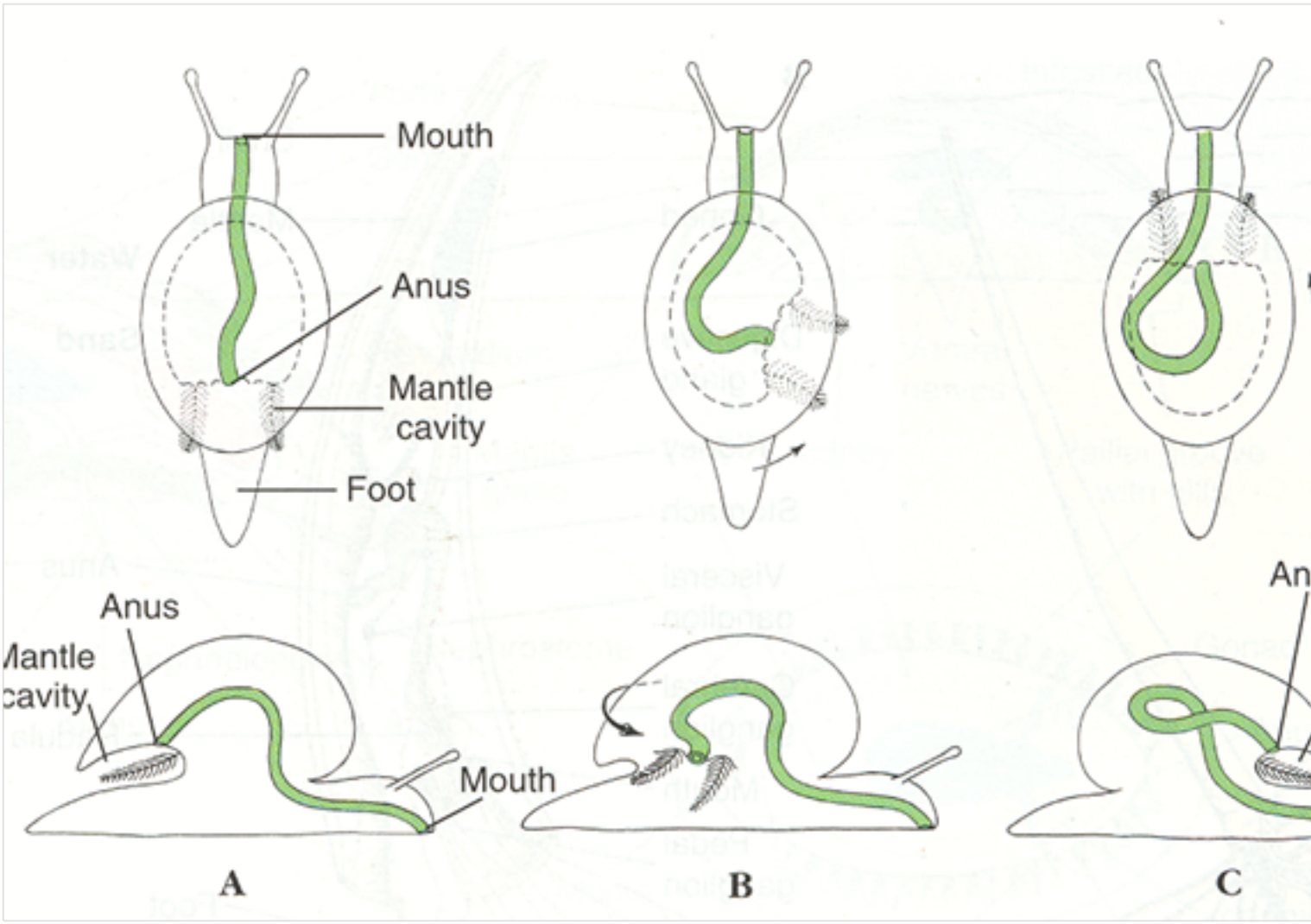

14.3.0.1 Limpets

Limpets are grazers, feeding on algae. The term is polyphyletic.

14.3.0.2 Abalones

The holes in abalone shells are known as respiratory pores.

14.3.0.3 Snails

14.3.0.4 Whelks

14.3.1 "Opisthobranchia"

Although not a monophyletic taxon, gastropods that have lost their shells and (typically) adopted chemical defenses are commonly referred to as opisthobranchs. They are hermaphroditic.

14.3.1.1 Pteropods

There are ~40 species of pteropods.

Their foot is split into two "wings".

Some pteropods have shells (Thecosomata) and others do not (Gymnosomata).

Thecosomata These pteropods form aragonitic shells (Pilson, 2013).
Their common name is "sea butterflies".

Gymnosomata These pteropods are shell-less and are known as "sea angels".

14.3.1.2 Nudibranchs

There are over 3000 species of nudibranchs that are found on nearly any available benthos in the ocean. They are all hermaphroditic. They eat a variety of sedentary benthic organisms such as sponges, corals, anemones, and bryozoans. Some, however, have symbiotic zooxanthellae that provide energy from photosynthesis. To avoid predation, they often utilize chemical deterrents and a fair proportion utilize nematocysts that they acquire from their cnidarian prey. Some species are extremely colorful. Some, such as the Spanish dancer, can swim!

All nudibranchs have olfactory tentacles known as rhinophores that are diverse in shape and are helpful for taxonomic identification.

There are two basic nudibranch body forms:

Dorid nudibranchs The mantle of dorid nudibranchs are rather smooth and flat except for prominent gills around the anus in some taxa.

Aeolid nudibranchs The mantle of aeolid nudibranchs are covered in finger-like projections called cerata. These cerata contain branches of the GI tract and also tipped with organs known as cnidosacs that are sacs of nematocysts obtained from their prey.

There's one species of neustonic aeolid known as a blue sea dragon that utilizes surface tension to stay on the surface and feed upon siphonophores.

14.3.1.3 Sea hares

Some sea hares live exclusively on sea grasses, eating off epiphytes and thus enhancing seagrass meadows.

14.4 Monoplacophora

Monoplacophorans are circular with a single shell (like a limpet). They were thought to be extinct until the 1950s when they were discovered on the benthic deep sea. There are only 30 recognized species today all still in the deep sea. Unlike other molluscs, the gills repeat down the length of the body like annelids.

14.5 Polyplacophora

Chitons are thought to be the closest morphologically to the ancestral mollusc. There are about 850 species of chitons and all are marine. They possess 8 overlapping plates (valves) to form their shells. These plates are surrounded by a tough fleshy structure that holds them together known as a girdle.

Most chitons live on rocky bottoms and scrape off algae with their radula. The teeth in their radula are the hardest known biomineral.

Interestingly, individuals seem to have a "home scar" that they consistently return to after feeding (Castro and Huber, 2019).

Polyplacophorans have visual sensory organs along the mantle edge known as aesthetes. They seem to function like a compound eye.

Chitons are dioecious and broadcast spawn both their sperm and eggs for external fertilization.

14.6 Scaphopoda

Scaphopods, or tusk shells, live exclusively within soft sediment within a hard elongated tapering shell, like an elephant tusk. They mainly live in the deep sea. Many species have thin adhesive tentacles that they use to capture prey in the sediment such as forams.

Scaphopods broadcast spawn both their sperm and eggs for external fertilization.

14.7 Solenogastres

The solenogasters are small, worm-like molluscs. Rather than a shell, they have many aragonitic sclerites.

Chapter 15

Orthoceratoidea

Chapter 16

Endoceratoidea

Chapter 17

Multiceratoidea

Chapter 18

Nautiloidea

The coiled shape of the nautiloid shell is convergent with ammonoid shells.

Unlike ammonoids, the nautiloid siphuncle runs through the middle of the whorl.

18.0.1 Nautilidae

Nautiloids are restricted to coastal shelf regions of the Indo-West Pacific, typically 150-300 m depth: the shallower surface waters are too warm and the deeper waters have too high of pressure for their gas-containing shells (Nixon and Young, 2003)(Barord's 2015 CIAC talk). They are diel vertical migrators within this range (Nixon and Young, 2003). It is thought that the extinction of most nautiloids starting in the Oligocene is due to the evolution of pinniped predators (Kiel et al., 2022). There remain to this date very few or no pinnipeds in the Indo-West Pacific.

Allonautilus are easily recognizable from *Nautilus* because they are "fuzzy".

Early nautiloid embryos have ten arms like other cephalopods unlike adults which possess 60 tentacles (Kröger et al., 2011). The tentacles do not possess suckers (Nixon and Young, 2003).

The protoconch is the first formed chamber of the shell, or phragmocone. The chambers are connected by a siphuncle which transfers fluids between compartments for buoyancy adjustment. They can develop 30-35 chambers over ontogeny (Tajika et al. 2020).

Nautiloids have two pairs of gills.

Nautilus don't reach maturity until they are ~15 years old, and they survive as mature adults for several more years (Nixon and Young, 2003).

The *Nautilus* nervous system is less expansive than in coleoids. They do not possess a giant fiber system or stellate ganglia (Budelmann, 1995).

18.0.1.1 *Nautilus pompilius*

This is the most abundant and well known nautiloid. It ranges from north Australia through the Indo-West Pacific (Jereb and Roper, 2005).

Chapter 19

Ammonoidea

Ammonoids first appeared in the Devonian around 390 Ma and went extinct at the end of the Cretaceous (66 Ma) (Arkhipkin and Laptikhovsky, 2012). During that time, their diversity and abundance were notable in the Paleozoic, but it was not until after the Permian extinction (into the Mesozoic) that they radiated widely and became extremely diverse and abundant.

Ecologically, they held a similar niche to modern-day *Argonauta*. They are an ancestor to all coleoids.

Ammonoids were extremely successful and are some of the most commonly found fossils. Certain species are used as age-markers for the rocks in which they are found (Staaf, 2017).

Ammonites are a sub-group of ammonoids.

Most ammonoids had a lifespan between 1 and 10 years.

Unlike nautiloids, the ammonoid siphuncle runs along the outer region of the whorl.

19.0.1 Shell morphology

The coiled shape of the ammonoid shell is convergent with nautiloid shells.

The shapes of ammonoid shells can fall along within the Westermann Morphospace between three extremes:

Oxycone slim disks (nekton?)

Serpenticone narrow coiled (plankton?)

Spherocone wide coiled (vertical migrators?)

also there are

Heteromorphs other strange shell shapes (e.g. "ice cream cone", "paper clip")

Baculites were straight-shelled heteromorphs while scaphites were "paper clip" heteromorphs.

The first chamber in an ammonoid shell was produced by the embryo and is known as the "ammonitella".

The largest ammonoid had a 2 m diameter shell (Staaf, 2017)!

Many species had suture lines that were quite elaborate. This may have been to strengthen the seals between the chambers to allow animals to go deeper. This would be less energetically costly than making a thicker shell and could be repaired faster. They may also have been selected to withstand predation. Finally, it is possible that the higher surface area of the suture lines would have allowed faster gas exchange to modulate buoyancy faster.

Ammonoids became progressively more coiled over the Devonian.

Many ammonoids developed "ornaments" (spines) in the Mesozoic for defense against the new reptilian predators, ichthyosaurs and plesiosaurs, as well as fishes, sharks, and crustaceans.

It is believed that females were larger than males and thus are referred to as macroconchs as opposed to the male microconch.

Chapter 20

Belemnoidea

Belemnoids were coleoids that had an internal calcareous shell. They first diverged in the early Jurassic (~200-175 Ma) and went extinct at the K-Pg boundary (66 Ma) (Arkhipkin and Laptikhovsky, 2012) though they seemed to be on their way out well before the K-Pg boundary. Their fossils are most often found on shelf faces, designating their primary habitat, rather than coastal or deep waters. Their fragile phragmocone prohibited them from inhabiting deeper water especially as paralarvae where it is estimated they could not descend deeper than 10 meters without implosion (Arkhipkin and Laptikhovsky, 2012).

Belemnoids were the first cephalopods to have mantle musculature similar to coleoids, with longitudinal, radial, and circular muscle groups (Young et al., 1998). They were also the first to have ten arms (*Jeletzkya* sp., Young et al., 1998). However, unlike most neocoleoids, their arms had hooks rather than suckers (Young et al., 1998).

Their relationship to extant coleoids is currently uncertain though they may be ancestral to squids with *Longibelus* as the "missing link".

Chapter 21

Octopoda

Octopods first evolved in at least the Late Cretaceous (Kröger et al., 2011). Arm pair II were lost in the Octopoda ancestor (Young et al., 1998).

21.1 Cirrata

There are about 40 species of cirrate octopods. They inhabit deep benthic habitats. They are the only benthic cephalopods in the deeper portions of the bathypelagic zone in the Atlantic (Rosa et al., 2008b). Most cirrates possess neither an ink sac nor radula (Young et al., 1998). Their mantle cavity is reduced and jet propulsion has been replaced by finning and medusoid locomotion (Young et al., 1998). The arms have one series of suckers with two cirri flanking each sucker. Cirrate spermatophores do not have ejaculatory apparatuses (Marian, 2015). Female cirroctopods are asynchronous spawners, spawning multiple times throughout their life (Rocha et al., 2001). They spawn large eggs with a hard coat secreted by the oviductal glands.

At least some cirrates do not have a paralarval stage, but hatch as juveniles (Shea et al., 2018). Hatchlings have disproportionately large fins (Shea et al., 2018).

21.1.1 Cirroctopodidae

This family contains a single genus, *Cirroctopus*, which is found exclusively in Antarctic and sub-Antarctic waters. They are much more muscular than most cirrates, have very large fins, a V-shaped shell, and arms attached directly to the primary web (Figure 50.3).

21.1.2 Cirroteuthidae

Cirroteuthids are very fragile, gelatinous cirrates. They have a saddle-shaped shell and secondary webs on the arms (Figure 50.3).

21.1.2.1 *Cirroteuthis muelleri*

This is the only species in the genus.

21.1.2.2 *Cirrothauma murrayi*

This is the only known "blind" cephalopod because the eye has no lens and a very reduced retina. It functions merely as a photoreceptor.

Family	Webbing	Shell shape
Cirroctopodidae	No secondary web	V-shaped
Cirroteuthidae	Secondary web	Saddle-shaped
Opisthoteuthidae	No secondary web	U- or W-shaped
Stauroteuthidae	Secondary web	U-shaped

Table 21.1: Cirrate morphological diagnostics

Family	Musculature	Armature	Ink sac	Adult habitat
Alloposidae	Gelatinous	Biserial	Present	Pelagic
Amphitretidae	Gelatinous	Uniserial	Present	Pelagic
Argonautidae	Muscular	Biserial	Present	Pelagic
Bathypolypodidae	Muscular	Biserial	Absent	Benthic
Eledonidae	Muscular	Uniserial	Present	Benthic
Enteroctopodidae	Muscular	Biserial	Mixed	Benthic
Megaleledonidae	Muscular	Uniserial	Mixed	Benthic
Octopodidae	Muscular	Biserial	Mixed	Benthic
Ocythoidae	Muscular	Biserial	Present	Pelagic
Tremoctopodidae	Muscular	Biserial	Present	Pelagic

Table 21.2: Incirrate morphological diagnostics

21.1.3 Opisthoteuthidae

Most opisthoteuthids are benthic or benthopelagic, swimming just above the benthos. Their anterior-posterior axis is highly compressed and they possess either a U- or W-shaped shell. Their arms attach directly to the primary web (Figure 50.3).

21.1.3.1 *Grimpoteuthis* sp.

Grimpoteuthis sp. is the deepest recorded cephalopod at nearly 7000 m deep (Jamieson and Vecchione, 2020).

21.1.4 Stauroteuthidae

This family contains a single genus, *Stauroteuthis*, which possesses a U-shaped shell. A unique characteristic of stauroteuthids is their small tubular mantle opening through which the funnel protrudes. They have a secondary web (Figure 50.3).

21.1.4.1 *Stauroteuthis syrtensis*

This species is one of the few octopods to possess photophores. They are found on the arms as modified suckers (Johnsen et al., 1999).

21.2 Incirrata

Within Incirrata, there are two well established superfamilies (Strugnell et al., 2014):

- Argonautoidea: males with a detachable hectocotylus
  - Alloposidae
  - Argonautidae
  - Ocythoidae
  - Tremoctopodidae
- Octopodoidea: males without a detachable hectocotylus
  - Amphitretidae
  - Bathypolypodidae
  - Eledonidae
  - Enteroctopodidae
  - Megaleledonidae
  - Octopodidae

Family	Radula pattern
Amphitretinae	Ctenoglossan
Bolitaeninae	Ctenoglossan
Vitreledonellinae	Not ctenoglossan

Table 21.3: Amphitretid morphological diagnostics

21.2.1 Alloposidae

The family Alloposidae contains a single species, *Haliphron atlanticus*. Alloposids brood their young (Young, 1972). To reproduce, they seem to stop eating (their digestive organs shrink) and their buccal mass swells to nearly cover the mouth (Young, 1972). Then, when eggs are released, they are brooded within the brachial web (Young, 1972).

21.2.1.1 *Haliphron atlanticus* (Seven-arm octopus)

H. atlanticus are known as seven-arm octopuses because the male hectocotylus is held coiled in a sac under the right eye. Males can also detach the hectocotylus during mating. Unlike in some other pelagic incirrate families, males are not dwarfs to the females (Young et al., 1998). In both sexes, maximal size can be very large (4 m total length), potentially the largest octopod known to date (O'Shea, 2004). These are a soft, gelatinous species.

Haliphron atlanticus are characterized by a deep arm web (40-60% arm length) connecting all arms except between arms IV (Young, 1972). Presumably, the lack of arm web between arms IV allows the funnel to deposit eggs and ventilate the brooding chamber.

They feed on jellyfish and siphonophores (Hoving and Haddock, 2017).

21.2.2 Amphitretidae

This family contains gelatinous, transparent, meso- and bathypelagic octopods that inhabit tropical or subtropical waters (Strugnell et al., 2014). Amphitretids are unique among incirrates in their rotated digestive system. When the animal is horizontal, the digestive gland, stomach, and caecum are oriented vertically, minimizing shadows from downwelling light (Young et al., 1998). They maintain neutral buoyancy by decreasing musculature and thus having a high water content.

Some amphitretids have photophores, the only incirrates to possess these organs (Young et al., 1998). *Amphitretus* spp. are the only octopods to have tubular eyes (Young et al., 1998).

Amphitretids are believed to have evolved via neoteny (retention of larval characteristics) from pelagic paralarvae of benthic octopods. This is due to their characteristics they share with paralarval octopods: transparency, small internal organs, large chromatophores, Kölliker's bristles, and teeth on their rostrum (Strugnell et al., 2004).

Bolitaenins Bolitaenins are sexually dimorphic, with the females developing a large yellow circumoral photophore (Robison and Young, 1981) as well as increasing chromatophore density especially around the arms and web (Young, 1978). To reproduce, they seem to stop eating (their digestive organs shrink) and their buccal mass swells to nearly cover the mouth. Then, when eggs are released, they are brooded within the brachial web.

The chromatophore patterning on the mantle is apparently unique in bolitaenins: with few chromatophores overlying the crop but many covering the stomach (Voight, 1995).

Japetella diaphana reach a larger size (80 mm DML) than *Bolitaena pygmaea* (50 mm DML) (Young, 1978).

21.2.2.1 *Bolitaena pygmaea*

Males larger than 20 mm DML have posterior salivary glands that are 2.5x larger than similar sized females (Voight, 1995) but it's unclear why.

21.2.2.2 *Japetella diaphana* (Hoyle, 1885)

Japetella diaphana are circumglobal in tropical and subtropical waters. They are ontogenetic vertical migrators, migrating to deeper water as they mature (Thore, 1949). They are known to eat euphausiids, fishes, chaetognaths, calanoids, decapod crustaceans, and other molluscs (Passarella and Hopkins, 1991). Mature males have greatly enlarged suckers on one of their arms (hectocotylus?). Females begin to develop their circumoral photophore between 40 and 50 mm DML (Herring et al., 1987).

Vitreledonellinae This subfamily contains a single species, *Vitreledonella richardi*.

21.2.2.3 *Vitreledonella richardi*

This species inhabits meso- and bathypelagic waters in tropical and subtropical regions worldwide. Females brood their eggs and paralarvae and apparently may hold them in their mantle cavity, as has been suggested by Young (1972) from an observation from Joubin (1929).

21.2.3 Argonautidae

Male argonautids have a detachable hectocotylus and are dwarfs (Young et al., 1998). Females form a magnesium-calcite shell (Young et al., 1998) from secretions that are arranged by a modified arm I pair. Based on genetic expression in these arms, their "shell" is a derived egg case (Hirota's 2022 CIAC talk).

Their funnel is not attached to the head (Jereb et al., 2013). *Argonauta* have some of the smallest paralarvae: < 0.4 mg at hatching.

At least in portions of the Brazilian coastline, *Argonauta* paralarvae could be found <100 km from shore and with bottom depths < 100 m (Araujo's 2022 CIAC talk).

21.2.3.1 *Argonauta nouryi*

Argonauta nouryi inhabit the eastern tropical Pacific in surface waters. Females are much larger than males (extreme sexual dimorphism) (Young et al., 1998), secrete $CaCO_3$ shells, and form chains at the surface by attaching to the female in front's shell (Rosa and Seibel, 2010c).

These pelagic octopods are very active, with $msMO_2$ similar to ommastrephids once adjusted for size and temperature (Rosa and Seibel, 2010c).

21.2.4 Bathypolypodidae

The family Bathypolypodidae contains a single genus, *Bathypolypus.* These are mid- to deep-water benthic octopuses which are cosmopolitan in the deep and high latitude oceans. They have a biserial armature(Nixon and Young, 2003).

21.2.5 Eledonidae

The family Eledonidae contains a single genus, *Eledone* (el-ED-o-knee). They are relatively shallow benthic octopuses, inhabiting depths from 10 m down to 800 m (Nixon and Young, 2003). They have a uniserial armature (Nixon and Young, 2003).

21.2.6 Enteroctopodidae

21.2.6.1 *Enteroctopus dofleini* (Giant pacific octopus)

GPO population abundance in Prince William Sound has been shown to be correlated with winter SST of the Alaska Current (Scheel's 2022 CIAC talk).

21.2.6.2 *Muusoctopus leioderma*

This species is typically found from 250-1400 m depth but with a peak abundance between 450 and 650 m (Trueblood's 2022 CIAC talk). However, a population was recently found at 20 m depth in the Salish Sea (Trueblood et al., 2022). They are distinct in having a ridge on their skin along their mantle at the margin between their dorsal and ventral sides (Trueblood's 2022 CIAC talk). They like to burrow in the sand (Trueblood's 2022 CIAC talk).

21.2.6.3 *Muusoctopus robustus*

A huge aggregation of brooding females of this species was found on Davidson Seamount off the coast of Monterey Bay, CA.

21.2.6.4 *Vulcanoctopus hydrothermalis*

This species lacks chromatophores (Strugnell et al., 2014).

21.2.7 Megaleledonidae

Many megaleledonids are endemic to the Southern Ocean or deep sea (Strugnell et al., 2014). All *Graneledone* species have "warty" mantles. Some *Graneledone* are often found on tubeworms near methane seeps (Levin's OSM talk).

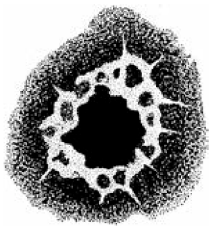

Figure 21.1: The ocellus of *O. bimaculatus* has spokes radiating outward from a broken chain link ring pattern.

21.2.7.1 *Graneledone boreopacifica*

Females of this species conduct the longest brooding of any known animal: 53 months (Robison et al., 2014).

21.2.8 Octopodidae

Octopodids lack a funnel-mantle locking apparatus.

21.2.8.1 *Abdopus aculeatus* (algae octopus)

This species of octopus seems to travel out of tide pools in search of food far and above any other known octopod species.

21.2.8.2 *Amphioctopus marginatus* (coconut octopus)

This octopus commonly uses bipedal walking and carries portable shelters such as coconuts or shells.

21.2.8.3 *Hapalochlaena fasciata*

H. fasciata inhabit the southern end of the east coast of Australia.

Unlike the other three species, *H. fasciata* have iridescent blue lines rather than rings on their dorsal mantle (Jereb et al., 2013).

21.2.8.4 *Hapalochlaena lunulata* (greater blue-ringed octopus)

H. lunulata inhabit Indonesia and nearby islands.

Blue-ringed octopuses possess tetrodotoxin (TTX)(Sheumack et al., 1978), a neurotoxin that blocks VGSCs and therefore incapacitates neuronal and muscle cells, throughout their bodies but especially in their posterior salivary glands. To avoid self-intoxication, *H. lunulata* have evolved a VGSC that is immune to TTX (Geffeney et al., 2019).

21.2.8.5 *Hapalochlaena maculosa*

H. maculosa inhabit Tasmania and the eastern end of the southern coast of Australia.

This species is nocturnal.

21.2.8.6 *Macrotritopus defilippi* (Atlantic long-arm octopus)

This species of octopus ranges from the Atlantic, Mediterranean, and Indian Oceans. It forms dens in sandy environments (Bennice et al., 2019).

21.2.8.7 *Octopus bimaculatus* (Verrill's two-spot octopus)

This species of *Octopus* inhabits the western north Pacific in subtropical regions such as in the Southern California Bight. Bigger individuals have a larger home range than smaller individuals (Hofmeister's 2015 CIAC talk). Unlike *O. bimaculoides,* this species has brown ink (Chuck Winkler, pers. comm.).

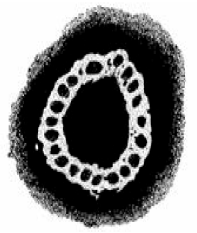

Figure 21.2: The ocellus of *O. bimaculoides* does not have spokes radiating outward from an intact chain link ring pattern.

21.2.8.8 *Octopus bimaculoides* (California two-spot octopus)(Pickford and McConnaughey, 1949)

Octopus bimaculoides are found in coastal waters from the intertidal down to at least 20 m along mid- and southern-California and the western side of the Baja peninsula.

Unlike *O. bimaculatus,* this species has black ink (Chuck Winkler, pers. comm.).

Hatchlings immediately become benthic.

This species matures after 7 months and lives up to 2 years (in captivity). During that time they attain a size of 18 cm DML (Grasse's 2022 CIAC talk).

21.2.8.9 *Octopus californicus*

This species is the most abundant deep water octopod off the coast of California (Hochberg 1997 cited in Seibel,Childress 2000).

21.2.8.10 *Octopus chierchiae* (Lesser Pacific striped octopus)

This species matures after 3.5 months and lives up to 2 years (in captivity). During that time they attain a size of 3 cm DML (Grasse's 2022 CIAC talk).

Octopus chierchiae is the only known incirrate that can spawn multiple times (Rodaniche 1984). In captivity they can spawn every 30-90 days (Grearson's 2022 CIAC talk). They lay large stalked eggs with direct development (Grearson's 2022 CIAC talk).

Males vigorously shake the tips of their arms to attract females (known as tasseling) (Grearson's 2022 CIAC talk).

21.2.8.11 *Octopus cyanea*

Unlike most other octopods studied to date, *O. cyanea* have 7 gyri on their vertical lobes unlike the "typical" 5 (Chung's 2022 CIAC talk).

21.2.8.12 *Octopus insularis*

This species can kind of reliably be distinguished from *O. vulgaris, americans,* or *sinensis* by its reticulate white patterning on the ventral side of its arms (rather than solid dark red) (Mather's 2022 CIAC talk).

21.2.8.13 *Octopus kaurna*

This species of *Octopus* inhabits sandy environments. It is the only known cephalopod to burrow deep into sandy sediment where it creates a "chimney" with its arms and secreted mucus to breathe (Montana et al., 2015).

21.2.8.14 *Octopus maya*

This species is endemic to the western Gulf of Mexico off the Yucatan peninsula (Vidal et al., 2014). It inhabits depths down to 50 m (Vidal et al., 2014). It has benthic hatchlings.

21.2.8.15 *Octopus micropyrsus*

This species is only found in 0-20 m depth from central California to Baja California. They are quite small and are often found in kelp holdfasts.

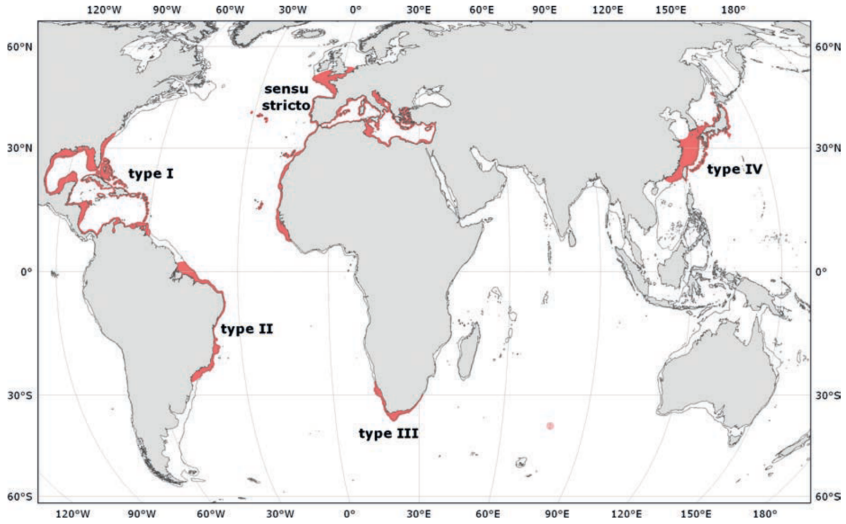

Figure 21.3: Distributions of the *vulgaris* species-complex. Figure from Jereb et al. (2013).

21.2.8.16 *Octopus rubescens*

This species inhabits the California Current System from the intertidal down to about 300 m. It inhabits the Puget Sound and San Juan Islands as well. It has an unusually long planktonic period during which individuals appear completely benthic morphologically, yet are found in pelagic environments.

21.2.8.17 *Octopus sinensis*

21.2.8.18 *Octopus tetricus*

21.2.8.19 *Octopus vulgaris*

This species is quite cosmopolitan and inhabits depth down to 200 m (Vidal et al., 2014). They commonly reach 3 kg in size (Vidal et al., 2014).

Newly settled juveniles on the Mediterranean coast of northern Spain settle year-round and amphipods are a huge proportion of their prey (Escolar's 2022 CIAC talk).

Octopus "vulgaris" Type I Alvaro Roura thinks that this doesn't really exist. No clear genetically distinct *Octopus* sp. here.

Octopus "vulgaris" Type II Now known as *Octopus americanus*.

Octopus "vulgaris" Type III

Octopus "vulgaris" Type IV Now known as *Octopus sinensis*.

21.2.8.20 *Thaumoctopus mimicus* (Norman and Hochberg, 2005)

This species was recently discovered (2020) in the Arabian Sea (Sajikumar et al. 2020).

21.2.8.21 *Wonderpus photogenicus* (Hochberg et al., 2006)

21.2.9 Ocythoidae

The family Ocythoidae contains a single species, *Ocythoe tuberculata*. Male ocythoids have a detachable hectocotylus and are dwarfs (Young et al., 1998).

21.2.9.1 *Ocythoe tuberculata*

This is the only species currently in the family Ocythoidae. Females brood their eggs in their oviducts, making them ovoviviparous (Naef 1923; (Young et al., 1998). These octopuses are epipelagic organisms inhabiting warm waters worldwide. Individuals have been observed to obtain and utilize *Physalia* tentacles possibly for defense or predation (Rosa's talk at CIAC 2015). The pygmy males also inhabit salp tests (Okutani and Osuga, 1986).

21.2.10 Tremoctopodidae

Tremoctopodids are pelagic. Male tremoctopodids have a detachable hectocotylus and are dwarfs (Young et al., 1998). Females have a large deep web between arms I and II. They brood their eggs on their dorsal arms which are much longer than the ventral arms.

Chapter 22

Sepiida

22.0.1 Sepiidae

Sepiids are at least from the Late Cretaceous if not earlier (Kröger et al., 2011). Cuttlefishes do not inhabit depths below 500-1000 m (Rosa et al., 2008b; Xavier et al., 2016). Cuttlefishes are the only decapodiforms which can completely retract their tentacles into their tentacle pockets (Young et al., 1998). Their species diversity is greatest in the Indian and western Pacific Oceans but there are also quite a few species in the eastern Atlantic (Jereb and Roper, 2005). No species range both basins. There are no sepiids in either the Arctic or Southern Ocean (Rosa's 2018 CIAC talk).

The *Sepia* genus needs to be revised and split into multiple genera.

22.0.1.1 *Metasepia pfefferi* (Flamboyant cuttlefish)

This species is only found in northern and western Australia north to New Guinea (Jereb and Roper, 2005).

This species matures after 3 months and lives up to 7 months (in captivity). During that time they attain a size of 4-6 cm DML (Grasse's 2022 CIAC talk).

22.0.1.2 *Sepia apama* (Giant Australian cuttlefish)

This species is well known for forming large breeding aggregations in Spencer Gulf in southern Australia. Here, they can reach abundances as high as 1 individual m^{-2} (Gillanders' 2015 CIAC talk) with up to 180,000 individuals! Its entire range spans the southern half of Australia (Jereb and Roper, 2005).

22.0.1.3 *Sepia bandensis* (Stumpy cuttlefish)

This species is only found in the Indo-Pacific (Jereb and Roper, 2005).

This species matures after 4 months and lives up to 9 months (in captivity). During that time they attain a size of 7 cm DML (Grasse's 2022 CIAC talk).

22.0.1.4 *Sepia elegans*

This species ranges from Angola on the west African coast up through the Mediterranean and around the western side of the UK (Jereb and Roper, 2005).

22.0.1.5 *Sepia officinalis*

S. officinalis is the most northerly distributed sepiid spanning from 62 °N in the Northern Sea throughout the Med and along the northwest coast of Africa (Jereb and Roper, 2005). Based on its metabolic rate, it can survive in temperatures ranging from 7 to 27 °C (Melzner et al., 2006a). It favors sandy environments down to 200 m (Vidal et al., 2014).

22.0.1.6 *Sepia pharaonis*

This species ranges all along the Indian Ocean, Indo-Pacific, northern Australia, north to the Yellow Sea (Jereb and Roper, 2005). This species has been observed to display "masquerading" behavior as crustaceans, moving their arms like the feeding appendages of crustaceans. They use this behavior to avoid predator recognition from their prey.

22.0.1.7 *Sepiella inermis*

This is a small cuttlefish species (up to 13 cm DML) that inhabits the Arabian Sea, Indo-Pacific, and South China Sea up to about 40 m depth.

The margin of their dorsal mantle just at the base of the fins sometimes expresses bright white dots, though these can apparently be masked by chromatophores.

There's a rather small commercial fishery for this species in India.

Chapter 23

Sepiolida

This group is colloquially known as bobtail and bottletail squids. The two families are distinguished by the morphology of their funnel-locking apparatus.

This whole clade's closest common ancestor are Idiosepiidae and after that are sepiids (Sanchez et al., 2021).

23.0.1 Sepiadariidae

This family is known as bottletail squids and includes the benthic brightly-colored bottletail squids of the Indo-Pacific. They are benthic and bury in the sand (Jereb and Roper, 2005).

23.0.1.1 *Sepioloidea lineolata* (Striped pyjama squid)

Sepioloidea lineolata are black and white striped bobtail squids that occur along the eastern, southern, and western coasts of Australia in the upper 20 m.

This species matures after 4 months and lives up to 10 months (in captivity). During that time they attain a size of 6 cm DML (Grasse's 2022 CIAC talk).

23.0.2 Sepiolidae

There are three subfamilies in Sepiolidae which each have different habitats:

- Rossinae are benthic cold-water taxa
- Sepiolinae are benthic and neritic in warm shallow water. The Indo-Pacific species are all more closely related to each other than the Atlantic/Mediterranean species are to each other (Sanchez et al., 2021).
- Heteroteuthinae are pelagic or benthopelagic (Young et al., 1998).

The Sepiolinae do not occur in the Americas but the other subfamilies do (Young et al., 1998). Due to their late evolution, they missed the last shallow bridge to the Americas and now are prohibited by cold and depth from reaching the Americas (Young et al., 1998).

Many sepiolid species are endemic because they are small, benthic, shallow species (Bello's 2015 CIAC talk).

Most but not all sepiolids possess photophores (Otjacques' 2022 CIAC poster).

23.0.2.1 *Eumandya parva*

23.0.2.2 *Euprymna berryi* (Hummingbird bobtail squid)

This species matures after 3 months and lives up to 6 months (in captivity). During that time they attain a size of 6 cm DML (Grasse's 2022 CIAC talk).

E. berryi are native to Japan and the surrounding region. Unlike *E. scolopes,* they have very little paralarval development and nearly go from eggs to benthic juveniles.

E. berryi have extremely small and abundant suckers on long stalks on their tentacular clubs.

23.0.2.3 *Euprymna morsei*

23.0.2.4 *Euprymna scolopes* (Hawaiian bobtail squid)

E. scolopes first evolved around 66 Ma (Lichilin's 2022 CIAC talk).

Euprymna scolopes are a sepiolin that inhabit shallow Hawaiian waters (Jereb and Roper, 2005). They form a symbiosis with the gram-negative bioluminescent bacteria *Vibrio fischeri* which inhabit *E. scolopes'* light organ. The bacteria are acquired soon after hatching. The bacterial colony in the light organ are flushed daily at dawn with only a small portion remaining to re-proliferate. This is because if not flushed, the *Vibrio* would multiply too quickly and begin dying, lessening the light. The light organ is on the center of the ventral mantle and disrupts the squid's shadow. They have been demonstrated to alter the light organ intensity to match ambient downwelling light.

E. scolopes also has symbionts in their accessory nidamental glands. These bacteria are added into the egg's jelly coat and provide anti-fungal protection (Kerwin et al., 2019).

E. scolopes have glands in their skin that produce a "glue" which helps them bind sand to their skin. When needed, they can secrete another substance to quickly shed the sand.

23.0.2.5 *Euprymna tasmanica*

23.0.2.6 *Rossia pacifica*

This species inhabits coastal waters around the north perimeter of the north Pacific from Japan to Baja California (Jereb and Roper, 2005).

23.0.2.7 *Sepiola affinis*

This species is distributed in the western Mediterranean basin as well as the Adriatic and Aegean Seas (Jereb and Roper, 2005).

23.0.2.8 *Sepiola atlantica*

This species is distributed in in the northeastern Atlantic including the North Sea and a portion of the western Mediterranean basin (Jereb and Roper, 2005).

Chapter 24

Teuthoidea

The teuthid squids are divided into myopsids and oegopsids based on the presence or absence of a cornea, respectively.

24.1 Myopsida

There are no myopsids in either the Arctic or Southern Ocean (Rosa's 2018 CIAC talk).

24.1.1 Australiteuthidae

This family contains a single species, *Australiteuthis aldrichi*. Australiteuthids differ from loliginids in their boomerang-shaped funnel-mantle locking apparatus. They also possess a large dumbbell-shaped photophore near the ink sac (Jereb and Roper, 2005).

24.1.1.1 *Australiteuthis aldrichi*

Australiteuthis aldrichi are very small squid inhabiting coastal north Australian waters and Papua New Guinea (Jereb and Roper, 2005).

24.1.2 Loliginidae

Loliginid diversity is greatest in the Indo-Pacific (Rosa's 2018 CIAC talk).

Loliginids all have a straight funnel-mantle locking apparatus.

Loligo first diverged 44-100 Ma . Males in this family implant spermatophores on the ventral buccal membrane of the female (Marian, 2015).

24.1.2.1 *Alloteuthis subulata*

This species inhabits coastal waters from the northwest coast of Africa, throughout the Mediterranean, and north throughout the North Sea (Jereb and Roper, 2010).

24.1.2.2 *Doryteuthis gahi* (Patagonian squid)

This species inhabits the Patagonian Shelf around the Falkland Islands and along the Pacific coast of South America (Jereb and Roper, 2010). Females lay eggs in shallow water where paralarvae hatch and grow. As juveniles they move into deeper water within the euphotic zone to feed and grow before returning to shallow regions to spawn (Arkhipkin, 2013). Typical female fecundity is in the range of 1000-5000 eggs.

24.1.2.3 *Doryteuthis opalescens* (Market squid)

This squid inhabits the California Current System, spanning from British Columbia south to the southern tip of Baja California (Jereb and Roper, 2010). During warm periods (e.g. El Ninos or 2015-at least 2019), they can be found as far north as the Gulf of Alaska (Navarro's 2018 CIAC talk). Reproducing adults form large aggregations and spawn terminally, dying quickly in a rather dramatic fashion. They lay eggs in consistent locations between 20 and 70 m depth where temperatures range from 10 to 15°C at the time of laying.

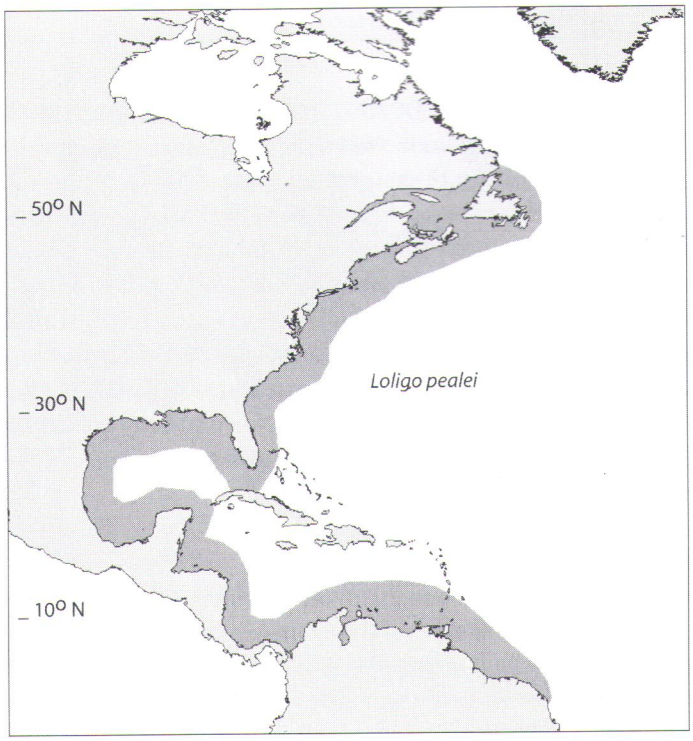

Fig. 17.14 The distribution of *Loligo pealei* in the western Atlantic Ocean (after Roper *et al.* 1984).

Figure 24.1: *Doryteuthis pealeii* distribution

There may be two populations: one in Monterey Bay area and the other in the Southern California Bight (Cheng's 2018 CIAC talk). The former spawns in the summer and the later in the winter (Cheng's 2018 CIAC talk). However, some microsatellite data suggest there is only one large population (Reichow and Smith, 2001).

They are the largest California fishery by volume and value since the 1990s.

24.1.2.4 *Doryteuthis pealeii* (Longfin inshore squid)(Lesueur, 1821)

Morphology *Doryteuthis pealeii* have wider gladius vanes (and thus whole gladius width) than *D. pleii*; the ratio of vane width (gladius width) (at its widest point) to rachis width is 2.4-3.7 (Cohen 1976 cited in Hixon 1980). In addition, the vane tapers away on its anterior end, whereas in *D. pleii* the vane sharply turns into the rachis on its anterior end (Hixon, 1980).

Life history Paralarvae inhabit surface water until they reach ~45 mm DML at which point they become juveniles. This transformation is associated with descent towards life near the bottom, countershading behavior, and tentacle use (Hanlon et al., 2013). Mating occurs year-round even in the northern migrating populations (Hanlon et al., 2013) but spawning in the north only occurs in spring and summer when the squid migrate inshore (Hanlon et al., 2013).

Distribution *Doryteuthis pealeii* were the first documented squid in the Americas. They inhabit the coastal shelf and upper slope of the western north Atlantic (Hixon, 1980). Although their range extends from Canada to the Amazon, they are certainly most abundant from Cape Cod to Cape Hatteras (Hixon, 1980). They are not found on Caribbean islands (Hixon, 1980).

In the northern part of their range, squids migrate seasonally, spending summer inshore to feed and spawn and migrating offshore to submarine canyons in fall and winter (Hanlon et al., 2013).

There is genetic differentiation indicating discrete populations even from George's Bank to Cape Hatteras (Garthwaite et al., 1989) and the Gulf of Mexico population is genetically distinct from the Atlantic coast of the US population (Herke and Foltz, 2002).

They only seem to inhabit depths <400 m (Hendrickson's 2022 CIAC talk).

24.1.2.5 *Doryteuthis pleii* (Tropical arrow squid)

Doryteuthis pleii typically live about 9 months (Perez et al. 2006).

Morphology *Doryteuthis pleii* are morphologically very similar to *Doryteuthis pealeii,* except that they have suckers on their ventral buccal lappets (TolWeb). In addition, *Doryteuthis pleii* have narrower gladius vanes (and thus whole gladius width) than *D. pealeii*; the ratio of vane width (gladius width) (at its widest point) to rachis width is 1.5-2.4 (Cohen 1976 cited in Hixon 1980). In addition, the vane sharply turns into the rachis on its anterior end, whereas in *D. pealeii* the vane tapers away on its anterior end (Hixon, 1980).

Distribution They inhabit coastal shelf and upper slope of the western north Atlantic from Cape Hatteras down to Brazil as well as Caribbean islands (Hixon, 1980).

24.1.2.6 *Heterololigo bleekeri*

This species inhabits the East China Sea, Yellow Sea, and waters around Japan (Jereb and Roper, 2010).

24.1.2.7 *Loligo forbesii*

This species inhabits coastal waters from the northwest coast of Africa, throughout the Mediterranean, and north throughout the North Sea (Jereb and Roper, 2010).

Because its range overlaps almost entirely with *L. vulgaris*, it is best differentiated by the presence of 4 rather than 2 sucker series on the tentacle club manus (Laptikhovsky's 2022 CIAC talk).

24.1.2.8 *Loligo reynaudii*

This species inhabits the southern tip of Africa (Jereb and Roper, 2010) and supports South Africa's 4th largest fishery.

24.1.2.9 *Loligo vulgaris*

Loligo vulgaris have two spawning periods: a major winter spawning (February) and smaller summer spawning (June) (Rosa et al., 2012b).

This species is distributed along the west coast of Africa, throughout the Mediterranean, and north around the U.K. including the North Sea and Baltic Sea (Jereb and Roper, 2010).

Because its range overlaps almost entirely with *L. forbesii*, it is best differentiated by the presence of 2 rather than 4 sucker series on the tentacle club manus (Laptikhovsky's 2022 CIAC talk).

24.1.2.10 *Lolliguncula brevis* (Atlantic brief squid)(Blainville, 1823)

Morphology *Lolliguncula brevis* rarely exceed 10 cm DML. They have rounded posterior mantles, more chromatophores on their ventral than dorsal mantle, and their gladius is visible through the anterior portion of their mantle (Hixon, 1980).

L. brevis lay egg masses with <30 eggs/mass (Bartol et al., 2002).

Distribution All *Lolliguncula* species are found in the Americas. *Lolliguncula brevis* can be found along the western Atlantic from Nova Scotia to southern Brazil (Rosa et al., 2013a). Although they are osmoconformers (Mangum, 1991), they are well adapted to survive in low-salinity and hypoxic estuaries where they take advantage of high prey abundance in warm months of the year. They have been found in brackish water as fresh as 8.5 psu (Laughlin and Livingston, 1982) at least for brief excursions and survive in the lab for long durations down to 17.5 psu (Mangum, 1991). Younger immature individuals seem to occupy brackish waters more than mature individuals that move out into more saline waters (Peyla's 2018 CIAC talk).

Individuals in the Gulf of Mexico may migrate seasonally, spending fall through spring along western Florida and migrating to the northern end of the Gulf during summer. They have been documented in estuaries along western Florida in the Gulf of Mexico, such as Tampa Bay, Charlotte Harbor, and Pine Island Sound particularly in the fall through spring (Dragovich and Kelly Jr., 1967).

Their preferred habitat seems to be soft bottom substrate of clay to silt (Dragovich and Kelly Jr., 1967) but can also be found in seagrass beds (Dragovich and Kelly Jr., 1964). They may prefer high-current velocity regions with salinity >20 psu (Laughlin and Livingston, 1982).

Their distribution seems to be controlled on a large spatiotemporal scale (e.g. monthly trends in and out of Tampa Bay) by environmental factors such as salinity and temperature and on a smaller spatiotemporal scale (e.g. daily movement within a bay) by food abundance (Laughlin and Livingston, 1982).

There are notable morphological differences between the North and South American forms of this species which will likely result in a new species designation for the southern form once genetic evidence is available to confirm the speciation (Rosa et al., 2013a).

24.1.2.11 *Lolliguncula panamensis*

This species is also highly tolerant of low salinity. In fact, it is almost always found between 15 and 23 psu (Jereb and Roper, 2010). They are found all along the coast from the west coast of Baja California Sur down to northern Peru (Jereb and Roper, 2010).

24.1.2.12 *Pickfordiateuthis pulchella*

This is the type species for the *Pickfordiateuthis* genus, which contains four known species of very small loliginids. They reach maximum DML of 2.2 cm and inhabit coastal waters, similar to other loliginids.

24.1.2.13 *Sepioteuthis lessoniana* species complex

This species complex is broadly distributed from Hawaii all along the west Pacific, Indo-Pacific, Indian Ocean, Red Sea, and even part of the Mediterranean (Jereb and Roper, 2010). It inhabits seagrass beds, coral reefs, and sandy environments down to 100 m (Vidal et al., 2014). *S. lessoniana* are demersal and will sometimes even hide inside of holes in the rock (Nakajima's 2022 CIAC talk).

The *Sepioteuthis* species are one of the few cephalopods that hatch as juveniles with no paralarval stage (Vidal et al., 2014).

Species 1: akaika (aka)

Species 2: shiroika (shiro)

Species 3: kuwaika (kuwa)

24.1.2.14 *Sepioteuthis sepioidea*

The fin runs the length of the mantle in this species.

This species ranges from southern Florida and the Yucatan Peninsula south throughout the Caribbean Sea and south along the northern half of South America (Jereb and Roper, 2010).

The *Sepioteuthis* species are one of the few cephalopods that hatch as juveniles with no paralarval stage (Vidal et al., 2014).

24.1.2.15 *Uroteuthis edulis* (Swordtip squid)

These squid inhabit the western Pacific around the East China Sea and Japan south to Australia and also throughout the Indian Ocean (Jereb and Roper, 2010). They migrate in and out of Japanese waters during winter (Pang's 2018 CIAC talk).

24.2 Oegopsida

The relative contributions of oegopsid families to pelagic cephalopod diversity are quite similar from the mesopelagic through upper bathypelagic zones (at least in the Atlantic)(Rosa et al., 2008b). The total cephalopod diversity in the pelagic Atlantic, however, drops from 80 species to less than 50 species at the bottom of the mesopelagic zone when all sunlight has been absorbed (Rosa et al., 2008b).

While oegopsids have no cornea covering their eyes, they are able to close their eyes into a slit (Young et al., 1998).

There are five family groupings within Oegopsida:

- Architeuthid families: oegopsids with fins attached to the dorsolateral mantle muscle rather than gladius
  - Architeuthidae
  - Neoteuthidae

- Chiroteuthid families: oegopsids without primary tentacular clubs
  - Batoteuthidae
  - Chiroteuthidae
  - Joubiniteuthidae
  - Magnapinnidae
  - Mastigoteuthidae
  - Promachoteuthidae
- Enoploteuthid families: small mesopelagic oegopsids with many photophores. Diagnosed by eight buccal supports (or remnants thereof).
  - Ancistrocheiridae
  - Enoploteuthidae
  - Lycoteuthidae
  - Pyroteuthidae
- Histioteuthid families: oegopsids with a histioteuthid tentacular club
  - Histioteuthidae
  - Psychroteuthidae
- Lepidoteuthid families
  - Lepidoteuthidae
  - Octopoteuthidae
  - Pholidoteuthidae

24.2.1 Ancistrocheiridae

This family contains a single species, *Ancistrocheirus lesueurii.*

24.2.1.1 *Ancistrocheirus lesueurii*

This mesopelagic species inhabits subtropical and tropical waters worldwide (Jereb and Roper, 2010).

24.2.2 Architeuthidae

24.2.2.1 *Architeuthis dux* (Giant squid)

Architeuthis is the 5th largest extant marine animal (by length) (Rosa et al., 2017).

This species is distributed world-wide (including the Mediterranean) at mesopelagic depths, but tends to avoid high latitudes where predatory male sperm whales are abundant. It is believed to be the only species in the Architeuthidae due to the very low genetic diversity amongst individuals worldwide (Winkelmann's 2018 CIAC talk). This is likely because their paralarvae drift around in geostrophic currents.

They are sexually dimorphic with mature females larger than males (Paxton, 2016). The largest individuals may be up to 10 m SL and 20 m TL based on extrapolations from the longest measured DML of 3 m and knowledge of the DML-to-SL and -TL relationships (Paxton, 2016).

A. dux are the only cephalopods to possess suckers and knobs along the length of the tentacular shaft (Kubodera and Mori, 2005) likely evolved to keep the extremely long tentacles coordinated.

At least from a single female that has been examined, she was covered in spermatangia all from the same male suggesting possible monoandry but it's too early still to tell (Murai et al., 2021).

Male *A. dux* do not have a hectocotylus and instead implant spermatophores directly with their terminal organ (putatively).

Family	Musculature	Arm armature	Buccal connective to arms IV	Funnel-locking appara
Ancistrocheiridae	(Weakly) muscular	Biserial	Dorsal	Straight
Architeuthidae	Muscular	Biserial	Dorsal	Straight
Batoteuthidae		Biserial	Ventral	Curved
Brachioteuthidae	Muscular	Biserial	Ventral	Straight
Chiroteuthidae	Gelatinous	Biserial	Ventral	Oval
Cranchiidae	Gelatinous	Biserial	Ventral	Fused
Cycloteuthidae		Biserial	Ventral	Triangular
Enoploteuthidae		Biserial	Dorsal	Straight
Gonatidae	Muscular	Tetraserial	Ventral	Straight
Histioteuthidae		Biserial	Dorsal	Straight
Joubiniteuthidae	Weakly muscular	Sexa- and tetraserial	Ventral	Oval
Lepidoteuthidae		Biserial	Ventral	Straight
Lycoteuthidae	Muscular	Biserial	Dorsal	Straight
Magnapinnidae		Bi- and tetraserial and irregular	Ventral	Oval
Mastigoteuthidae		Biserial	Ventral	Oval
Neoteuthidae	Weakly muscular	Biserial	Dorsal	Straight
Octopoteuthidae		Biserial	Ventral	Straight
Ommastrephidae	Muscular	Biserial	Dorsal	Inverted T
Onychoteuthidae		Biserial	Ventral	Straight
Pholidoteuthidae		Biserial	Ventral	Straight
Promachoteuthidae	Weakly muscular	Bi- and triserial	Ventral	Oval
Psychroteuthidae		Biserial	Dorsal	Straight
Pyroteuthidae	Muscular	Biserial	Dorsal	Straight
Thysanoteuthidae	Muscular	Biserial	Ventral	Lazy T

Table 24.1: Oegopsid morphological diagnostics

24.2.3 Batoteuthidae

This family contains a single species.

24.2.3.1 *Batoteuthis skolops*

B. skolops are Antarctic squids with a long tail and no tentacular club (Nixon and Young, 2003).

24.2.4 Brachioteuthidae

Brachioteuthids are oegopsids with irregular and small stalked suckers on the proximal region of the manus. Paralarvae have extremely elongate necks.

24.2.4.1 *Brachioteuthis picta*

This species inhabits oceanic subtropical and tropical waters (Jereb and Roper, 2010).

24.2.5 Chiroteuthidae

Chiroteuthids are gelatinous squids with ornate tails and ammonium chloride chambers in the mantle, head, and arms. Many species have extremely long tentacles. As paralarvae, they have long necks (Vidal's 2022 CIAC talk).

24.2.5.1 *Chiroteuthis calyx*

This species inhabits meso- and bathypelagic North Pacific waters (Jereb and Roper, 2010).

Table 24.2: Cranchiid genus key

Genus	Fin shape	...
Leachia	Large, round	
Taonius	Long, lance-shaped	
...		

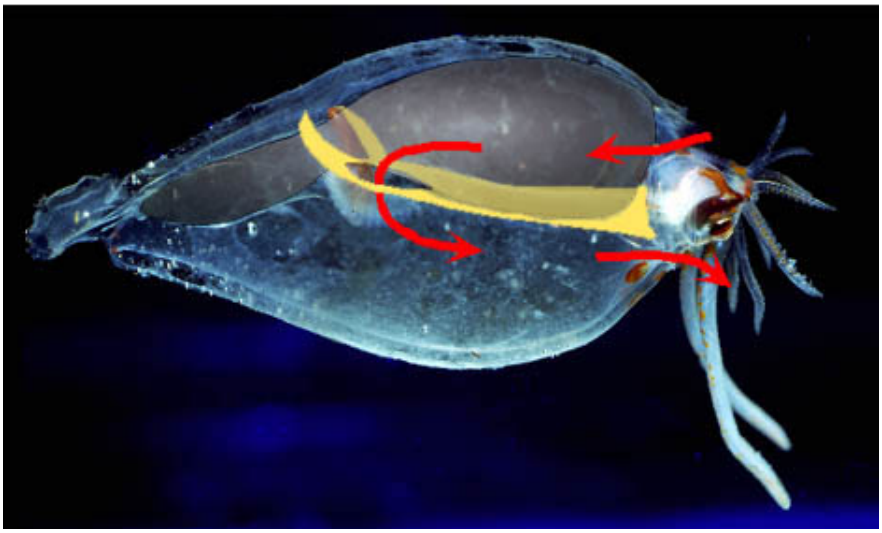

Figure 24.2: Cranchiid ventilation. Figure from ToLWeb.

24.2.5.2 *Chiroteuthis joubini*

24.2.5.3 *Grimalditeuthis bonplandii*

This species has a large tail with "tail fins". They live worldwide in tropical through temperate waters (Jereb and Roper, 2010). Unlike any other known cephalopod, this species has tentacle clubs with no suckers, hooks, or photophores. Based on limited *in situ* observations of waving the tentacles about, it seems that they may be used to lure prey towards the animal (Hoving et al., 2013).

24.2.6 Cranchiidae

It has been proposed that cranchiids may have evolved via neoteny from paralarvae due to their shared characteristics with paralarvae such as transparency, large chromatophores, stalked eyes, and small organs (Strugnell et al., 2004).

One unique characteristic of cranchiid squids is their storage of ammonium chloride in a large coelomic chamber (Denton et al., 1969). They can accumulate $[NH_4^+]$ higher than any other cephalopod: 300-600 mM (Seibel et al., 2004). They trap such high concentrations by keeping the coelomic pH ~5 and protonating all incoming NH_3 to NH_4^+ which cannot pass back out through the membrane.

The head and mantle are fused in three places in cranchiids.

Cranchiids are currently divided into two subfamilies: Cranchiinae and Taoniinae and can be distinguished based on the number of ocular photophores.

Ventilation behavior Cranchiids are unlike any other squids in that they ventilate their gills by using their enlarged coelom as a peristaltic pump rather than using their mantle. Their mantle cavity is divided by a horizontal septum (highlighted in yellow in Figure 24.2) into dorsal and ventral chambers. The septum has a gap where water can move past the gills into the ventral chamber. The coelom runs the length of the mantle cavity along the dorsal margin. At rest, the coelom can fill the entire dorsal chamber of the mantle cavity. To ventilate the gills, water is brought into the dorsal chamber through a one-way valve when the coelomic sac squeezes anteriorly to create a slight vacuum. Then, once water partially fills the dorsal chamber, the posterior portion of the coelom squeezes which enlarges the anterior portion again. This growing coelomic sac pushes water out of the dorsal chamber through the only opening: the hole in the septum near the gills. This means of ventilation allows the highly gelatinous cranchiids to maintain ventilation without requiring costly mantle musculature.

24.2.6.1 *Bathothauma lyromma*

B. lyromma have very large eye stalks when they are paralarvae.

They inhabit tropical through temperate waters worldwide (Jereb and Roper, 2010). Adults inhabit meso- and bathypelagic depths (Jereb and Roper, 2010).

24.2.6.2 *Cranchia scabra*

This species inhabits meso- and bathypelagic tropical through temperate waters worldwide (Jereb and Roper, 2010).

24.2.6.3 *Galiteuthis glacialis*

This species inhabits Antarctic waters and is one of the most abundant Antarctic squids (Jackson et al., 2002).

24.2.6.4 *Helicocranchia pfefferi*

This species inhabits tropical through temperate waters worldwide (Jereb and Roper, 2010).

24.2.6.5 *Leachia pacifica*

This species inhabits equatorial Pacific waters in the epi- and mesopelagic zones (Jereb and Roper, 2010).

24.2.6.6 *Mesonychoteuthis hamiltoni* (Colossal squid)

Not much is known about *M. hamiltoni*. At about 500 kg, it is the largest cephalopod (and largest invertebrate) by weight. It is the 11th largest extant marine animal (by weight) (Rosa et al., 2017). It is endemic to the Southern Ocean and preys upon Antarctic toothfishes (Jereb and Roper, 2010). Based on the $msMO_2$ of other cranchiids, when extrapolated out to the large body size of *M. hamiltoni* (circa 500 kg), it has a very low $msMO_2$ of 0.036 μmol O_2/g/h at 1.5 ^{o}C, and thus is likely not an active predator like teuthoids (Rosa and Seibel, 2010b). However, with a δ^{15}N of 16, it maintains a very high trophic position (Rosa et al., 2017). Thus, perhaps it is an ambush predator.

Unlike other cranchiids, *M. hamiltoni* musculature is much more dense and they possess swiveled hooks on their tentacular clubs (Rosa et al., 2017). They also possess two elongate large photophore on the ventral portion of their eyes (Rosa et al., 2017).

They seem to undergo an ontogenetic vertical migration at least from paralarvae into young juveniles (Rosa et al., 2017). Starting as juveniles through adulthood, they inhabit meso- and bathypelagic depths (Rosa et al., 2017). They do not reach sexual maturity until they are quite large, >30 kg and >1 m ML (Rosa et al., 2017).

24.2.6.7 *Taonius pavo*

This species inhabits temperate through tropical waters of the Atlantic (Jereb and Roper, 2010).

24.2.6.8 *Teuthowenia megalops*

This species inhabits North Atlantic waters (Jereb and Roper, 2010).

24.2.7 Cycloteuthidae

Cycloteuthids have large round fins (Nixon and Young, 2003). They are cosmopolitan in tropical and subtropical mesopelagic depths.

24.2.7.1 *Discoteuthis discus*

This species is short and squat and inhabits temperate through tropical waters worldwide (Jereb and Roper, 2010).

24.2.8 Enoploteuthidae

Enoploteuthids are some of the most abundant deep sea cephalopods (Judkins et al., 2017).

Enoploteuthids are small mesopelagic squids which typically have abundant ventral photophores. They are well known to undergo extensive diel vertical migrations. *Abraliopsis* spp. contain 2-3 large black photophores on the tips of arms IV.

24.2.8.1 *Abralia armata*

This species inhabits the Indo-Pacific (Jereb and Roper, 2010).

24.2.8.2 *Abraliopsis atlantica*

This species is documented to inhabit only the Atlantic (Jereb and Roper, 2010) but we have found it in the ETP as well.

24.2.8.3 *Watasenia scintillans* (Firefly squid)

This species inhabits Japanese waters in the lower epi- and mesopelagic (Jereb and Roper, 2010). It is the only known cephalopod that may be able to discriminate multiple wavelengths of light (Michinomae et al., 1994).

24.2.9 Gonatidae

Gonatid squids have a bipolar distribution, avoiding subtropical and tropical habitats .

24.2.9.1 *Berryteuthis magister*

This species lives in the subarctic north Pacific and supports and important Russian fishery.

24.2.9.2 *Gonatus fabricii*

This species is found in the Arctic and north Atlantic along Canada, Iceland, and Scandinavia. Only one spent females has ever been found to estimate fecundity. In this female, she had expelled about 25% of her ~10k eggs before dying (Golikov et al. 2021, Molluscan Research).

24.2.9.3 *Gonatus onyx*

Gonatus onyx are outliers among squids in that they brood and care for their eggs. This was first discovered off the coast of California in the bathypelagic zone where senescent females were found lacking tentacles, brooding their eggs, and apparently surviving on lipid reserves in the digestive gland (Seibel et al., 2000a). They hold their egg mass with their arm hooks and aerate the mass with arm movements (Seibel et al., 2005).

G. onyx are both diel and ontogenetic vertical migrators. In Monterey Bay, juveniles form shoals around 300-400 m during the day and some travel to shallower waters at night. Adults are solitary and deeper, spending the day near 700-800 m and coming up to 400-500 m at night (Hunt and Seibel, 2000). This adult daytime depth is in the peak of an OMZ. In fact, both juvenile and adult Pcrit are identical to the P_{O_2} of their most common habitat. It is curious why these animals would seek out their Pcrit P_{O_2} for their preferred habitat.

Metabolism Unlike the typical 3/4 power scaling "rule" of most animals, *Gonatus onyx* msMO_2 is size independent (Rosa et al., 2009). Its anaerobic potential also scales interestingly: there is a typical increase throughout ontogeny until individuals ontogenetically vertically migrate, at which point their anaerobic potential (i.e. ODH activity) decreases through the rest of their life (Rosa et al., 2009).

24.2.10 Histioteuthidae

Histioteuthids are sometimes known as "strawberry squids" because their red skin is covered in photophores that resemble a strawberry.

All histioteuthids have a much larger left eye than right eye. The left optic lobe is also 3x larger than the right optic lobe (Chung's 2018 CIAC talk).

Due to NH_4^+ being lighter than Na^+, histioteuthids can accumulate NH_4^+ in musculature vacuoles at high concentrations up to 300 mM, second only to cranchiids which store NH_4^+ in a coelomic chamber. They exchange Na^+ for NH_4^+ throughout ontogeny with [NH_4^+] increasing as an individual grows and vertically migrates deeper (Seibel et al., 2004). One tradeoff for the improved buoyancy associated with NH_4^+ is that musculature must be sacrificed to make room for NH_4^+ vacuoles. This is attainable though, because histioteuthids live in the mesopelagic around 300 m and rapid locomotion is not highly selected.

24.2.10.1 *Histioteuthis heteropsis*

This species inhabits the eastern Pacific from California to Chile. They are diel vertical migrators from a peak around 600 m during the day to above 400 m at night (Roper and Young, 1975).

24.2.10.2 *Stigmatoteuthis*

Male *Stigmatoteuthis* spp. have paired Needham sacs and penes.

24.2.11 Joubiniteuthidae

This family contains a single species.

24.2.11.1 *Joubiniteuthis portieri*

This species is the only species in the family Joubiniteuthidae. It is unique from other oegopsids in that its tentacles are quite short and arms I-III are greatly elongated to over 2x ML (Young et al., 1998). It also possesses a very long tail (> ML) with membranes. It is meso- to bathypelagic found in tropical and subtropical regions worldwide.

24.2.12 Lepidoteuthidae

This family contains a single species. Adult lepidoteuthids lack tentacles (Young et al., 1998).

24.2.12.1 *Lepidoteuthis grimaldii*

This is a rather large (1 m DML) squid that has scales covering its skin.

24.2.13 Lycoteuthidae

Lycoteuthids are small (sub)tropical squids with numerous large photophores, particularly around the eyes. They are DVMs nearly reaching the surface at night.

24.2.14 Magnapinnidae

This family contains a single genus, *Magnapinna*. These squids have extremely long narrow arms and tentacles and very large fins. The appendages are initially held at a right angle to the body axis but long slender portions trail behind the squid as it moves. A *Magnapinna* holds the current record for the deepest recorded squid, at 6212 m depth.

24.2.15 Mastigoteuthidae

Mastigoteuthids are squids with long whip-like tentacles (Young et al., 1998). The tentacular suckers are extremely small (c. 100 μm) and the tentacle length can be 3-4x ML (Young et al., 1998). Mastigoteuthids feed floating in the water column but with their tentacles dangling just above the benthos (Young et al., 1998).

24.2.16 Neoteuthidae

Neoteuthids are small weakly muscular oegopsids with peculiar fin attachments. Their posterior fin lobes are free and they do not possess anterior fin lobes.

24.2.17 Octopoteuthidae

Octopoteuthids are squids with broad, wide fins that span the length of the mantle to form a diamond shape. As adults, they also lack tentacles (Young et al., 1998).

Both males and females of the genus *Octopoteuthis* have been found to have spermatangia, suggesting possible indiscriminate mating to try to improve fitness.

24.2.17.1 *Taningia danae*

T. danae are very large squid with DML > 1 m. They have been filmed to be quite active. They have the largest photophores in the animal kingdom, the size of lemons (Kelly's 2015 CIAC talk).

Table 24.3: Ommastrephidae subfamilies

Subfamily	Photophores present	Dactylus sucker series	Carpal-locking apparatus (paired knobs and suckers)
Illicinae	No	8	No
Ommastrephinae	Yes	4	Yes
Todarodinae	No	4	No

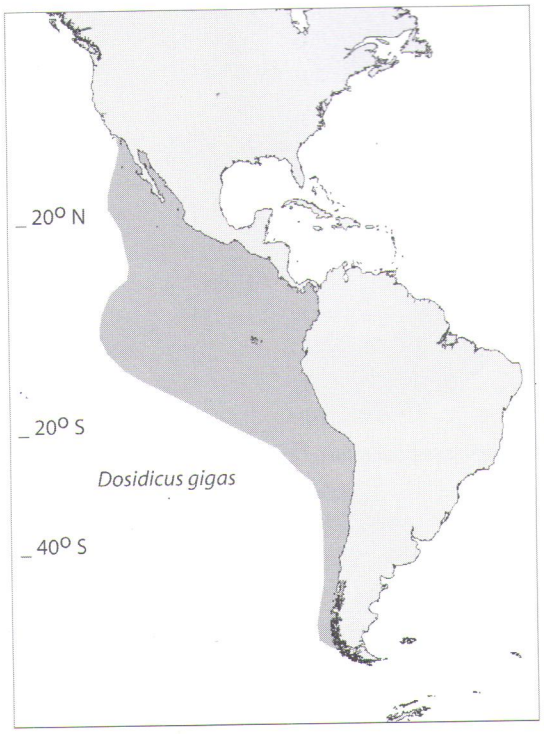

Fig. 17.11 The distribution of *Dosidicus gigas* in the western Pacific Ocean (after Roper *et al.* 1984).

Figure 24.3: *Dosidicus gigas* distribution (historically)

24.2.18 Ommastrephidae

Ommastrephids first diverged ~150 Ma .

Ommastrephids can be divided into three subfamilies:

24.2.18.1 *Dosidicus gigas* (Humboldt jumbo flying squid)(D'Orbigny, 1835)

Dosidicus gigas are the largest ommastrephids reaching up to 1.2 m DML and 65 kg (Rosa et al., 2013b). They are the largest invertebrate in the southeastern Pacific (Ibáñez et al., 2015).

This species inhabits the eastern tropical Pacific and can extend from Chile in the south to California and even Canada and Alaska in the north, at times (Zeidberg and Robison, 2007). Its presence in Chile seems to vary with ENSO (Ibáñez et al., 2015). Its range coincides with the productive regions of the temperate and tropical eastern Pacific (Nigmatullin et al., 2001), avoiding the subtropical gyres which are much less productive.

Schools tend to be rather small and individuals change locations every several days likely to follow available food (Gilly et al., 2006; Bazzino et al., 2010).

The size-at-maturity can vary widely, with corresponding changes in fecundity (Birk et al., 2017). Size-at-maturity correlates with ENSO patterns and this linkage seems to be through shifts in diet caused by changes in productivity (Portner et al., 2019).

OMZ physiology It undergoes diel vertical migrations throughout its range often inhabiting oxygen minimum zones (OMZs) (Gilly et al., 2006; Bazzino et al., 2010). Curiously, given their strong hypoxia tolerance, there is <1% of the ocean area where they have a P_{50} depth (subsubsection 53.6.8.2), and that is the exact habitat in which they thrive. Their P_{crit} depth is ~200 m

in the Gulf of California and ~600 m in the California Current System (due to differences in regional O_2-depth profiles) (Seibel, 2016).

Unlike most OMZ taxa (Childress and Seibel, 1998), *D. gigas* cannot maintain their metabolic rate in the hypoxic, hypercapnic environment: their basal MO_2 decreases by 80% due to hypoxia alone (Rosa and Seibel, 2008), their [octopine] increases, and ventilation rate decreases (Rosa and Seibel, 2010a). They get away with this by vertically migrating to shallow oxygenated waters at night. They return to the deep OMZ during the day where their predators (who have higher P_{crit} values and shallower P_{50} depths (Mislan et al., 2015)) are unable to hunt effectively for them. This diel migration brings the individuals through a 10-15 ºC temperature gradient twice a day. Temperatures above 20 ºC seem to be a stressor on *D. gigas* given that its inactive MR doubles from 20-25 ºC (Rosa and Seibel, 2008). Indeed, they have been documented to avoid surface temperatures $>$ 23 ºC (Gilly et al., 2006).

24.2.18.2 *Eucleoteuthis luminosa*

E. luminosa are small ommastrephids which inhabit subtropical latitudes in the northern Pacific and all around the southern hemisphere (Jereb and Roper, 2010). They have two long photophore stripes the length of their ventral mantle. They also have large white photophores on the ventral head and arms IV. Their posterior end is quite pointy compared to other ommastrephids such as *Dosidicus gigas* or *Sthenoteuthis oualaniensis*.

24.2.18.3 *Illex argentinus*

This species inhabits Patagonian Shelf waters of the southwest Atlantic (Arkhipkin, 2013). Over the course of their 1-year lifespan (Arkhipkin 1990), they migrate from spawning grounds in the north (~35 ºS) to feeding grounds near the Falkland Islands (~50 ºS) as juveniles. Then as maturing adults, they return northward to spawn and die (Arkhipkin, 2013). Typical female fecundity is 400,000 eggs (Laptikhovsky and Nigmatullin, 1993).

Generally, there are two cohorts: a large winter-spawning cohort (95% of the species) and a much smaller summer-spawning cohort (Hatanaka 1988).

24.2.18.4 *Illex coindetii*

This species inhabits the Mediterranean and the North Atlantic, on both coasts. Unlike other ommastrephids known to date, their egg masses frequently have a dark streak through the center (Ringvold).

24.2.18.5 *Illex illecebrosus*

This species inhabits the shelf and coastal waters of the northeastern Atlantic. Although it is not known entirely where all they spawn, there seems to be notable spawning activity on the continental slope near Cape Hatteras. From here, egg masses and paralarvae are advected northward in the Gulf Stream and are dispersed onto the shelf waters and coastal regions around New England and Canada. Many paralarvae arrive just as the spring bloom provides lots of food. In the coastal areas they feed, grow, and then migrate south again in the autumn to spawn in the south.

Females are smaller than males and often cannibalize them on their migration south when food is limiting.

24.2.18.6 *Martialia hyadesii*

This species inhabits epi- and mesopelagic waters in the Southern Ocean.

24.2.18.7 *Ommastrephes bartramii* (Neon flying squid)

Ommastrephes bartramii have been classically described as being distributed all across subtropical and temperate waters of the Atlantic, Indian, and Pacific Oceans. However, they likely make up 4 separate species (Fernandez-Alvarez's 2022 CIAC talk).

24.2.18.8 *Sthenoteuthis oualaniensis* (Purpleback squid)

Sthenoteuthis oualaniensis are large epipelagic ommastrephids. They are similar to *Dosidicus gigas* in physiology and life style but are notably different in that they possess a large aggregation of photophores on the anterior dorsal mantle which forms a large yellowish-white oval. They are found only in the (sub)tropical Pacific and Indian oceans and the Red Sea (Jereb and Roper, 2010).

Paralarvae and juveniles stay near the surface during the day and descend to ~50 m at night to avoid the predatory adults which spend the day in the mesopelagic and ascend to the surface at night (Jereb and Roper, 2010).

Sthenoteuthis oualaniensis are distinguished from *Sthenoteuthis pteropus* by their distribution but also that *S. oualaniensis* have a fused funnel-mantle locking apparatus where as *S. pteropus* do not.

24.2.18.9 *Sthenoteuthis pteropus* (Orangeback squid)

Sthenoteuthis pteropus are large epipelagic ommastrephids endemic to the (sub)tropical Atlantic. They possess a large aggregation of photophores on their anterior dorsal mantle that appear like a large yellowish-white oval. Unlike *S. oualaniensis*, they have a free funnel-mantle locking apparatus.

24.2.18.10 *Todarodes pacificus*

T. pacificus migrate annually around the islands of Japan, spawning in autumn and winter in the southern edge of their range near the East China Sea. Their single most important prey item is the Japanese anchovy, *Engraulis japonicas* (Sawamura's 2018 CIAC talk).

24.2.18.11 *Todarodes sagittatus*

24.2.19 Onychoteuthidae

24.2.19.1 *Kondakovia longimana*

This is a large squid that inhabits the Southern Ocean. It maintains a pale white coloration (Bolstad's 2018 CIAC talk).

24.2.19.2 *Onykia ingens*

This species inhabits sub-Antarctic waters in a circumpolar distribution and can reach 50 cm ML (cited from ToLWeb). As paralarvae and adults, they inhabit deep water in the meso- and bathypelagic, but they move into shallower (deep euphotic) waters as juveniles to feed (Arkhipkin, 2013).

Its lifespan is typically ~2 years. Unlike in most cephalopods, individuals of this species stop growing near the end of their life (Arkhipkin, 2013).

Females lay ~250,000 eggs (Laptikhovsky et al 2007).

It stores high concentrations of ammonium in its muscle tissues for buoyancy (Arkhipkin, 2013).

24.2.20 Pholidoteuthidae

This family contains a single genus, *Pholidoteuthis.*

24.2.21 Promachoteuthidae

This family contains a single genus, *Promachoteuthis.* These squids are unique among teuthids in their small eyes which are almost completely covered by gelatinous muscle.

24.2.22 Psychroteuthidae

This family contains a single species.

24.2.22.1 *Psychroteuthis glacialis*

This species in endemic to the Southern Ocean.

24.2.23 Pyroteuthidae

Pyroteuthids have a world-wide distribution and are all small pelagic squids which are epipelagic as paralarvae and juveniles and become DVMs down to mesopelagic depths as adults (Jereb and Roper, 2010). They are the smallest oceanic squids.

The family only contains two genera: *Pterygioteuthis* and *Pyroteuthis* which can be distinguished by the presence of a large lidded photophore on the anterior ventral rim of each eye in the former genus.

24.2.23.1 *Pterygioteuthis gemmata*

P. gemmata occur in the tropical and subtropical Atlantic as well as the temperate Pacific (e.g. southern California and New Zealand). They seem to be replaced by *P. microlampas* in the tropical Pacific.

24.2.23.2 *Pterygioteuthis giardi*

This is a tropical-subtropical species ranging from approximately 45 °N to 45 °S in both the Atlantic and Pacific(Jereb and Roper, 2010).

24.2.23.3 *Pterygioteuthis hoylei*

This species inhabits the ETP, maintaining high abundance in the Gulf of California. They are small squid, reaching only 40 mm ML (De Silva-Dávila et al., 2013). They are an important prey item for *Dosidicus gigas*. Their life cycle is short, 2-3 up to potentially 6 months (De Silva-Dávila et al., 2013).

24.2.23.4 *Pterygioteuthis microlampas*

P. microlampas range includes the central tropical Pacific Ocean. Most individuals have been found around Hawaii and north of New Zealand.

As an adult, *P. microlampas* spend the day near 300 m and migrate to 50 m at night (Seibel et al., 1997).

24.2.24 Thysanoteuthidae

24.2.24.1 *Thysanoteuthis rhombus*

T. rhombus is a large, warm water diamond-shaped squid. It can reach 1 m DML. This species is strange in that males and females pair for mating in a stable relationship throughout the reproductive period. Females spawn peculiar sausage-shaped egg masses with coiled filaments of eggs just below the surface (Biagi and Bello, 2009).

Chapter 25

Enigmatic and outlier taxa

25.1 *Vampyroteuthis infernalis* (Vampire squid)

The vampire squid, *Vampyroteuthis infernalis,* shares characteristics with both octopods and decapodiforms, but was placed in its own order, Vampyromorpha, due to its modified arm pair II as sensory filaments. It inhabits OMZs worldwide in the tropical to temperate range in the 600-800 m range, but is most commonly found in the California Current System OMZ (Seibel, 2016).

Female *V. infernalis* store spermatangia in a spermatheca in front of each eye (Marian, 2015).

Unlike in Monterey Bay, *V. infernalis* in the Gulf of Mexico eat deep sea fishes and have a high δ^{15}N, suggesting they are predatory (Judkins' 2022 CIAC talk). It is possible that they are detritovores in OMZs and predators elsewhere.

As a juvenile, its high mantle citrate synthase (CS) activity indicates that jet propulsion from mantle contractions is likely the primary means of locomotion. It undergoes a metamorphosis during its juvenile stage (near 23 mm ML, 8 g) where its small posterior fins are replaced by larger, more active anterior fins. Once fully developed, the anterior fins result in higher Reynolds numbers for locomotion than posterior fins and thus are more efficient. As a result, their use is increased after metamorphosis, an ontogenetic gait-transition. Unlike the rest of the body, these anterior fins increase in CS activity throughout ontogeny indicating their increased importance for locomotion especially as adults. Octopine dehydrogenase (ODH) activity also increases throughout ontogeny not only in anterior fins, but mantle and arms as well demonstrating the use of all these body parts for burst escape swimming (Seibel et al., 1998).

Because this species inhabits the OMZ, it has the lowest mass-specific metabolic rate (0.07 μmol/g/h) (Seibel et al., 1997) and the lowest P_{50} (0.47 kPa) and P_{crit} measured in any cephalopod (Seibel et al., 1999; Seibel, 2016).

25.2 Spirulida (*Spirula spirula*)

Spirulids seem to be most closely related to oegopsids and bathyteuthoids (Lindgren's 2022 CIAC talk).

Spirulids first appear in the fossil record in the Late Jurassic (Kröger et al., 2011).

There is only a single extant species in this order: *Spirula spirula.* They possess an aragonitic phragmocone, a large luminous organ between their fins, and males have two hectocotylzed arms.

S. spirula are mesopelagic and vertically migrating from 500-1000 m during the day to 100-300 m at night (Young et al., 1998; Nixon and Young, 2003). They are subtropical, ranging from 40 °N to 40 °S (Nixon and Young, 2003) but are only found relatively near landmasses.

They possess a large yellow-green photophore between their fins.

The single observation of a live animal *in situ* demonstrates that they swim with their heads up and phragmocone down and frequently beat their fins (Lindsay et al., 2020).

25.3 Idiosepiidae

Idiosepiids are decapodiforms with a single extant genus, *Idiosepius.* Characteristically, idiosepiids have an adhesive organ on their dorsal mantle that they use to attach to seagrass blades (Young et al., 1998). These are the smallest decapodiforms, with some species reaching maturity at only 8 mm DML and 50 days old (Young et al., 1998) and reaching a maximum DML of 16-20 mm (Renard's 2018 CIAC talk). Curiously, they do not possess tentacles at hatching (Young et al., 1998).

Table 25.1: Bathyteuthoid morphological diagnostics

Family	Buccal connectives on arms IV
Bathyteuthidae	Dorsal
Chenopterygidae	Ventral

25.4 Bathyteuthoidea

Squids in this groups are somewhat like myopsids and somewhat like oegopsids. They lack a cornea and have paired oviducts as in oegopsids, but possess tentacle pockets and suckers on their buccal supports as in myopsids. However, based on molecular data, they are sister to oegopsids (Lindgren's 2022 CIAC talk).

25.4.1 Bathyteuthidae

Bathyteuthids inhabit the lower mesopelagic and upper bathypelagic zones worldwide (Roper, 1969). They are small squids, < 80 mm DML (Jereb and Roper, 2010). There is a single genus: *Bathyteuthis*. They have a very large photosensitive vesicle just posteriorly to their eyes, which may possibly be used for detecting small bioluminescent organisms stirred up in their mantle cavity.

25.4.1.1 *Bathyteuthis abyssicola*

This species is most abundant in the Southern Ocean (Roper, 1969) but also inhabits continental slope waters worldwide (Jereb and Roper, 2010). They mainly inhabit lower mesopelagic waters and deeper, undergoing diel vertical migrations (Jereb and Roper, 2010).

25.4.1.2 *Bathyteuthis bacidifera*

This species inhabits the eastern tropical Pacific and equatorial Indian (Roper, 1969). It has larger gills than *B. abyssicola* (Roper, 1969), which may enable it to outcompete its congener in hypoxic regions.

25.4.1.3 *Bathyteuthis berryi*

This species is only known off the coast of California. Females of this species are known to brood their eggs in their arms (Bush et al., 2012).

25.4.2 Chenopterygidae

This family possesses very long fins with large ribs that run the length of the mantle as in *Sepia*. It is a monogeneric family containing *Chtenopteryx* spp. They are deep-sea squids. There may be seven species, though they are not yet all currently recognized (Braid's 2018 CIAC talk).

25.4.2.1 *Chtenopteryx sicula*

This species inhabits meso- and bathypelagic tropical through temperate waters (Jereb and Roper, 2010).

Part IV

Their universal biological principles

Homeostasis is the maintenance of identical physiological conditions in the face of environmental change. Enantiostasis is the maintenance of physiological function in the face of environmental change.

Chapter 26

Questions about fundamental biochemistry

26.1 Why H, C, N, O, P, and S?

Of all the elements on the Earth, these six are the primary elements utilized in biology. This is because they form covalent bonds which can form and break much easier than ionic bonds. But why are all of these frequently used rather than just a few? Each element shares a different number of electrons: H=1, O=2, N=3, C=4, P=5, and S=6.

26.2 Why is ATP the "energy currency" of life?

The three phosphate groups on ATP have very high energy bonds. When these bonds are broken, they release a lot of energy that can be used in unfavorable reactions (see section 27.1). The phosphate group cleaved from the ATP must be bound to the substrate that the cell is trying to convert to product for its cleavage to be energetically effective. Once the substrate has been phosphorylated, the phosphate (which is an excellent leaving group) can be replaced by the desired compound to form the product.

ATP hydrolysis releases about 30.5 kJ/mol.

The phosphate bonds are high energy for a number of reasons: 1. their highly negative charges create lots of repulsion, 2. ADP is *so much* more stable, 3. its hydrolysis increases entropy, 4. the reaction produces $[H^+]$ which is in very low intracellular concentrations, and 5. ADP and P_i are both better solvated than ATP.

There are other high-energy compounds as well (e.g. Arg-P) but ATP can be hydrolyzed multiple times (into ADP then AMP) and ATP is easier for many enzymes to bind than other high-energy compounds.

Chapter 27

Energetics of chemical reactions

Given the chemical equilibrium $aA + bB \rightleftharpoons cC + dD$, the equilibrium constant, K_{eq}, is

$$K_{eq} = \frac{k_{for}}{k_{rev}} = \frac{[C]^c \times [D]^d}{[A]^a \times [B]^b}.$$

For multi-step reactions, the equilibrium constant for the whole system is the product of each individual equilibrium constant ($K_{eq} = K_1 + K_2$).

Bimolecular reactions (e.g. protein-ligand binding)

$$K_a = \frac{[AB]}{[A][B]} = \frac{k_{association}}{k_{dissociation}} (\text{e.g. } \mu M^{-1})$$

$$K_d = \frac{[A][B]}{[AB]} = \frac{k_{dissociation}}{k_{association}} (\text{e.g. } \mu M)$$

In the common situation where the coefficients in a bimolecular reaction are all 1, the dissociation constant (K_d) can be interpreted as the ligand concentration ([A]) at which 50% of the protein (B) is bound to the ligand (A).

$[ligand] = K_d/9$ protein is 10% bound

$[ligand] = K_d$ protein is 50% bound

$[ligand] = 9K_d$ protein is 90% bound

27.1 Enzyme bioenergetics

$$\Delta G^\circ = -RT \ln(K_{eq})$$

$$\Delta G^\circ = \Delta H^\circ - T\Delta S^\circ$$

At equilibrium, $\Delta G^\circ = 0$. The more negative the ΔG^o from the reactant(s) to the product(s), the higher the ratio of forward reaction rate to backwards reaction rate, and thus the further a reaction goes to the right. Although enzymes do not change the ΔG^o from reactant(s) to product(s), they do lower the ΔG^o from reactant(s) to transition state (aka activation energy, E_a) and thus increase the reaction rate. They do this by binding substrates, destabilizing them, and holding their reactive sites close together.

$$\Delta H^\circ = E_a - RT$$

Different isozymes can favor the forward or backward reaction and animals can maintain concentrations of various isozymes in tissues appropriate for where those reaction directions are needed.

Complex, multi-step reactions like glycolysis must have a net $\Delta G^{\circ o} < 0$. There are a variety of ways that cells achieve this. 1. they increase the mass action ratio (increase [substrate] and/or decrease [product]). 2. they connect an unfavorable reaction with a favorable one to "pull" or "push" the unfavorable reaction forward. 3. they connect an unfavorable reaction with ATP hydrolysis.

ΔH	binding will	as temperature increases, binding becomes
+	absorb energy	more likely
−	release energy	less likely

27.2 Influence of temperature on equilibria (Van't Hoff equation)

As temperature changes, the concentrations of the reactants and products shift according to the Van't Hoff equation:

$$\ln \frac{K_{eq_2}}{K_{eq_1}} = \frac{-\Delta H^{\ominus}}{R} \times \left(\frac{1}{T_2} - \frac{1}{T_1} \right) \tag{27.1}$$

Given K_{eq} at any two temperatures, $\Delta H^{\ominus}$ can be calculated and then K_{eq} at any temperature can be predicted.

27.3 Redox potential

The redox potential difference (ΔE, expressed in mV) can be determined as:

$$\Delta G = nF\Delta E$$

where n is the number of electrons transferred in the reaction.

27.4 Protein cooperativity

Cooperativity of ligand binding by multi-subunit enzymes can be explained by two different models. Both describe a "relaxed" R-state and a "tense" T-state with higher and lower ligand-binding affinity, respectively.

27.4.1 MWC "symmetry" / "concerted" model

According to this model, the entire polymeric enzyme converts between the T- and R-state with no intermediates. The binding of each ligand shifts the equilibrium between T- and R- towards the relaxed state, thus lowering population ligand-binding affinity.

According to this model, R-state subunit can exist without a ligand bound.

27.4.2 KNF "sequential" model

According to this model, the polymeric enzyme can be in the T- or R-state or intermediates in between. The binding of each ligand alters the conformation of the subunit from T to R and tweaks the neighboring subunits to have higher ligand-binding affinity (closer to the R conformation).

According to this model, R-state subunit cannot exist without a ligand bound.

27.5 How long does it take for something to diffuse?

The mean distance travelled by a population of molecules diffusing in 3 dimensions can be calculated as:

$$x = \sqrt{6Dt}$$

where x is the distance, D is the diffusion coefficient ($cm^2 \cdot s^{-1}$), and t is time.

Generally, for small molecules, the diffusion coefficient in cytoplasm is 25% that in water. For most sized proteins, it is <5% and for nucleic acids longer than a few 100 bp, it is <10%.

Chapter 28

Macromolecule structure

28.1 Nucleic acids

Nucleic acids are composed of three key parts:

1. pentose sugar (five carbon sugar ring)
2. phosphate group
3. nucleobase
    - pyrimidine (one ring)
        - cytosine (C)
        - thymine (T)
        - uracil (U)
    - purine (two rings)
        - adenine (A)
        - guanine (G)

Once the three parts are combined, the entire entity is known as:

- adenosine (A)
- cytidine (C)
- guanosine (G)
- thymidine (T)
- uridine (U)

Nucleoside A pentose sugar and nucleobase

Nucleotide A pentose sugar, nucleobase, and one or more phosphate groups

Nucleic acids are arranged with the pentoses and phosphates alternating to form the "backbone" and the nucleobases bonded to the pentoses. The 5' end of the nucleic acid strand has a hanging phosphate while the 3' end has a bare pentose sugar. The pentose sugars are synthesized by the pentose phosphate pathway section 34.6.

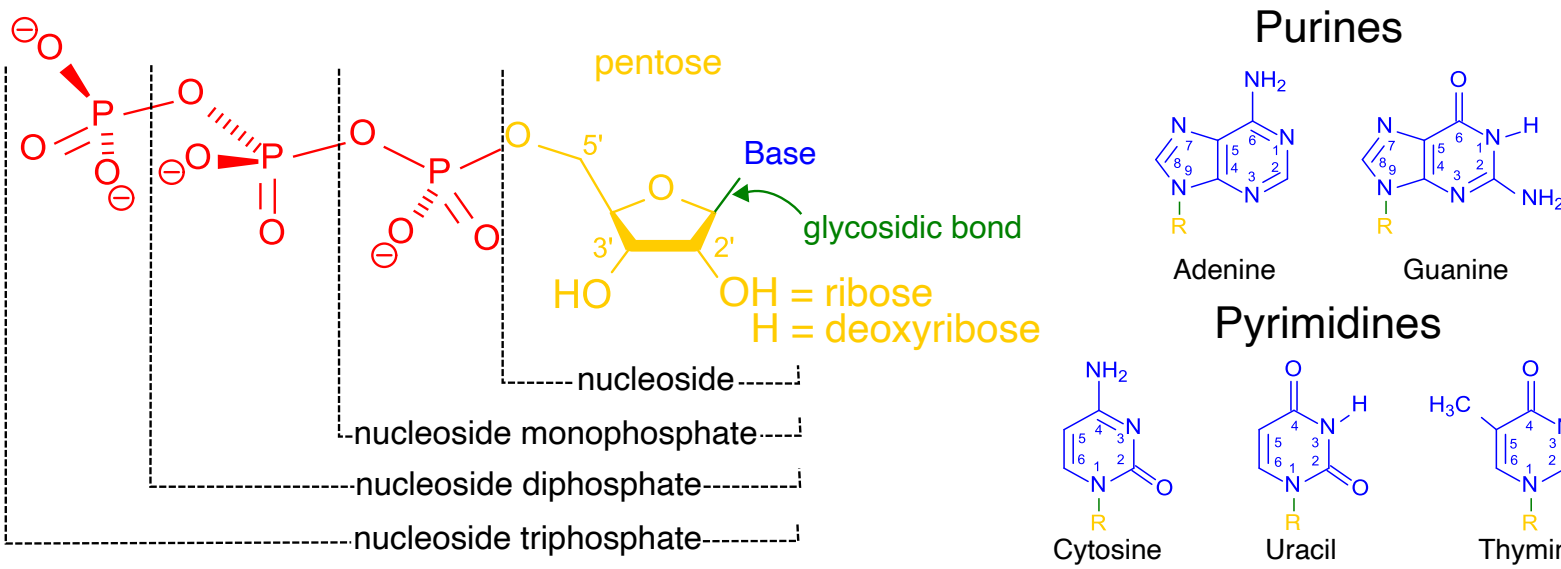

Figure 28.1: Nucleotide structure.

28.1.1 DNA

DNA is composed of four nucleobases: A, G, C, and T. Adenine pairs with thymine via two hydrogen bonds while cytosine pairs with guanine via three hydrogen bonds. In addition to the interstrand hydrogen bonds, there are also base stacking interactions between base pairs both on the same strand and the complementary strand. Both base pairing and base stacking interactions help maintain the double-stranded structure (Watson and Crick, 1953).

There are three common forms of DNA:

A-DNA Shorter and more compact helix than B-DNA. When RNA is double-stranded, it forms in the A-form.

B-DNA Most common.

Z-DNA Left-handed turn, unlike in A- and B-DNA.

28.1.1.1 Double-helix structure

The two sugar-phosphate backbones of dsDNA protrude out the most in the double helix. In B-DNA, the base pairs are nearly perfectly perpendicular to the helical axis.

Double-stranded nucleic acids form a major and minor groove. These form as a result of the orientation in which the nucleobases pair. When a pyrimidine and purine pair, they are arranged in such a way that the carbon atoms on which both bases bind to their respective sugar riboses are on the same side. Therefore, the backbones are scrunched closer together on one side than the other, resulting in a minor groove (on the side where the bases bind their backbones), and a major groove on the opposite side. In B-DNA, the major groove is 22 Å wide, while the minor groove is only 12 Å wide. As a result, most nucleic-acid binding proteins tend to interact with bases from the major groove because it is wider and more accessible.

Each nucleotide in B-DNA contributes ~340 pm to its length, such that a 1 kb nucleic acid is ~340 nm long.

28.1.1.2 Chromosomes and copy number

In eukaryotes, the naked DNA strand is wrapped around histone proteins to form nucleosomes. These nucleosomes, in turn are bundled into chromatin. Finally, these chromatin strands are interconnected into chromosomes.

As like all metazoans, cephalopods are diploid, they possess two copies of each gene.

28.1.2 RNA

RNA is composed of four nucleobases: A, G, C, and U. Adenine pairs with uracil via two hydrogen bonds while cytosine pairs with guanine via three hydrogen bonds, at least normally. RNA allows many more variations than DNA, such as a G-U "wobble" pairing.

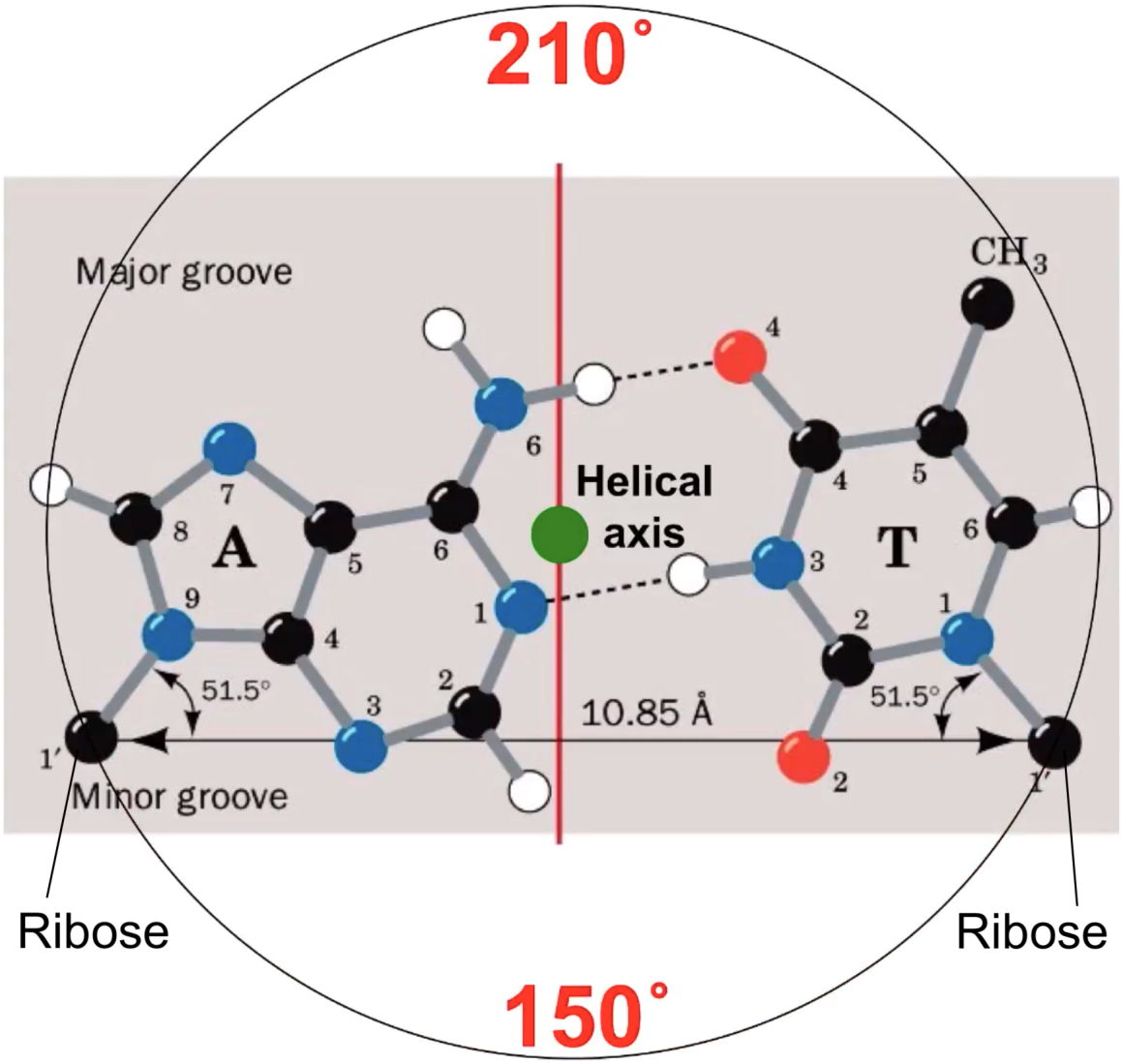

Figure 28.2: DNA-B grooves. The carbon atoms (black) that connect with the ribose backbones on each nucleobase are on the same side, thus causing the backbones to scrunch together (150°) on one side and be far apart on the opposite side (210°).

There is a free hydroxyl group on the 2' carbon of the pentose sugar that can form H bonds, making RNA "sticky". This, in part, allows RNA to form secondary and tertiary structures. Freely dissolved monovalent ions (e.g. K^+) interact with the RNA to form secondary structures and divalent ions (e.g. Mg^{2+}) interact to form tertiary structures.

Small RNAs are noncoding RNAs that are < 200 nt (nucleotides) and include tRNA, rRNA, miRNA, and a diversity of other uncommon forms.

The total RNA pool in the cell is ~90% rRNA and 1-2% mRNA (Conesa et al., 2016).

28.1.2.1 messenger RNA (mRNA)

Mature eukaryotic mRNA has a 5' cap and a poly-A tail on the 3' end. mRNA are often not uniformly distributed throughout the cell, but rather are localized to specific regions where their protein product is needed. They are often moved by motor proteins along actin filaments to their destination. While being transported, they are bound to prohibit translation.

28.1.2.2 transfer RNA (tRNA)

tRNAs are the adapter between the nucleotide-based code of the mRNA and the amino acid-based code of the protein. Their nucleotide sequence (76-90 bp) is clover-shaped with four distinct regions. The anticodon loop has the anticodon. The 3' CCA tail is where the amino acid binds. The T- and D-loop are involved in regulating amino acid binding.

There are 30-40 different kinds of tRNAs in the cytoplasm. In order for the 30-40 tRNAs to pair with the 64 (61 without stop codons) codon options, some allow a "wobble" on the third pairing. There are also 22 separate mitochondrial tRNAs.

28.1.2.3 ribosomal RNA (rRNA)

rRNA is the RNA component of ribosomes (which are predominantly RNA but also contain proteins). rRNA is synthesized within the nucleolus of a cell nucleus. rRNA is by far the most abundant type of RNA in the cell.

28.1.2.4 microRNA (miRNA)

miRNA molecules are universal molecules that conduct post-transcriptional modification to mRNA molecules. They can do this either by destroying mRNAs or binding to them to make them inactive. Both of which are forms of RNA interference (see subsection 32.3.4).

28.2 Proteins

Proteins have many functions in cells: regulation of processes, forming cellular structure, facilitating movement, catalysis of reactions, transport of substances, and signaling.

Most eukaryotic proteins vary in size from 50 to 1000 amino acids ($\approx 5-100$ kDa) with the median size around 300-400 amino acids ($\approx 30-40$ kDa).

28.2.1 Primary structure

Proteins are composed of amino acids, each of which are composed of a central alpha carbon ($C\alpha$), an amino and carboxylic acid group, a hydrogen, and R group. While D-amino acids exist, all proteins are composed of solely L-amino acids. Amino acids are connected by peptide bonds: a single covalent bond between the N of the amino group from one amino acid and the C from the carboxylic acid group from another amino acid. Although the peptide bond is a single bond, it has many properties of a double bond, including the limitation on bond rotation.

Table 28.1: Intrinsic pK values of amino acid side chains when flanked by alanines (Pace et al., 2009).

Amino acid	Reaction	Charge shift with rising pH	pK (probably at 37°C)	When internally, pK will be...	W
Asp (D)	$-COOH \rightleftharpoons -COO^- + H^+$	$0 \rightarrow -$	3.9	↑	
Glu (E)	$-COOH \rightleftharpoons -COO^- + H^+$	$0 \rightarrow -$	4.3	↑	
His (H)	$-NH^+ \rightleftharpoons -N + H^+$	$+ \rightarrow 0$	6.5	↓	
Cys (C)	$-SH \rightleftharpoons -S^- + H^+$	$0 \rightarrow -$	8.6	↑	
Tyr (Y)	$-OH \rightleftharpoons -O^- + H^+$	$0 \rightarrow -$	9.8	↑	
Lys (K)	$-NH_3^+ \rightleftharpoons -NH_2 + H^+$	$+ \rightarrow 0$	10.4	↓	
Arg (R)	$-NH_2^+ \rightleftharpoons -NH + H^+$	$+ \rightarrow 0$	12.3	↓	

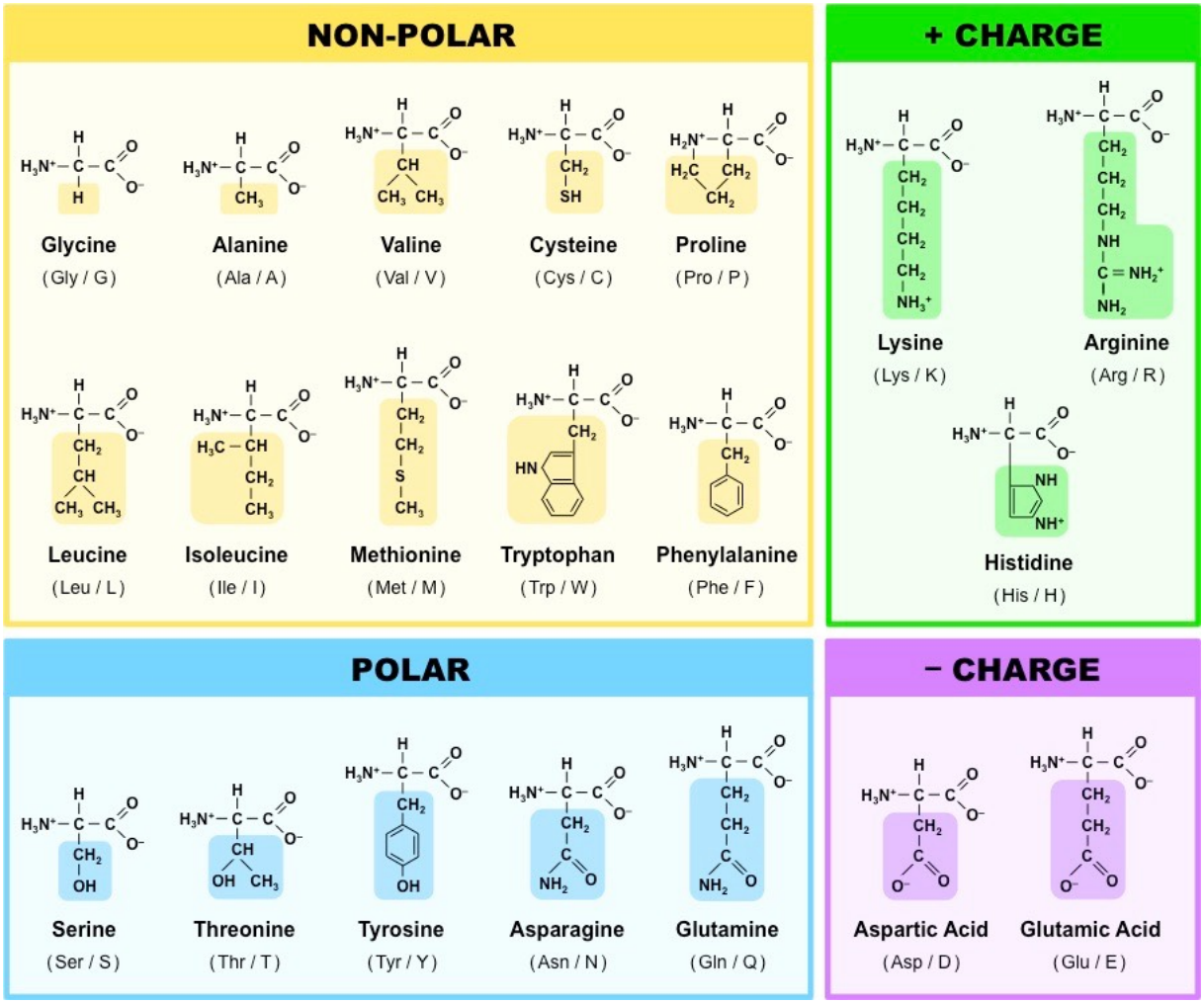

28.2.1.1 Side chain pK values

Intrinsic pK values of amino acid residues are shown in Table 28.1. However, the environment around the side chain can change these values dramatically. When the residue is within the hydrophobic core of the protein, pK values of all residues shift toward values that favor neutrality (Pace et al., 2009). When charged residues are close to other charged residues, the propensity of the charged residues to hold its H^+ will move in favor of an arrangement that avoid like-like charges (e.g. if near a positive charge, it will favor dropping its H^+ (lowering pK)) (Pace et al., 2009). The shorter the distance between residues, the stronger the effect. Furthermore, hydrogen bonding to nearby polar residues can alter pK in such a way as to favor hydrogen bonding (Pace et al., 2009).

28.2.1.2 R group modifications

The R groups of amino acids can be modified through a number of additions (section 32.5).

- Acetylation
- Phosphorylation
- Hydroxylation
- Methylation
- Carboxylation
- Glycosylation
- Ubiquitylation

These additions can diversify amino acid variety from the 20 common ones to >100.

28.2.2 Secondary structure

28.2.2.1 Alpha helix

Polypeptide chains often form α-helices and β-sheets. α-helices are stabilized by hydrogen bonds between the H from an amino group from one amino acid and the O from a carboxylic group from another amino acid 4 amino acids down the line. The most common alpha helix has 3.6 residues per turn.

28.2.2.2 Beta sheet

In β-sheets, the same hydrogen bonds are formed between an amino group from one amino acid and the carboxylic group of another, but the two bonded amino acids are not a set distance away.

28.2.3 Tertiary structure

Many proteins are folded into multiple domains, or portions of the protein that function independently of the others.

Tertiary structure is maintained by ionic bonds, disulfide bonds, hydrophobic interactions, and hydrogen bonding between the R groups.

Some amino acids provide more stability to the protein's tertiary and quaternary structure than others. Small amino acids such as glycine do not provide much stability. Large and polarized amino acids, in contrast, can build salt bridges which increase stability. Nonpolar amino acids can form hydrophobic pockets and are important for membrane-bound proteins to stay embedded in the hydrophobic inner membrane.

Disulfide bridges, when present in a protein, are important stabilizers of proper structure and are important to prevent misfolding and subsequent aggregation (Diaz et al., 2010). Because they are so stabilizing they are rather rare in intracellular proteins that have very stable microenvironments but are more common in extracellular proteins that have to maintain stability in more variable conditions (Hochachka and Somero, 2002).

Overall, most globular proteins have a net tertiary stability of only 8-40 kJ/mol (Pace et al., 2009) (compared to ATP hydrolysis = 30.5 kJ/mol). However, hydrophobicity and protein net charge neutrality help stabilize conformation.

Ankyrin repeat domain Ankyrin repeat domains are very common and facilitate protein-protein interactions. They are formed from multiple HTH motifs.

bHLH (basic helix-loop-helix) domain This domain is common in transcription factors. It is formed of two α helices connected by a loop.

Helix-turn-helix (HTH) This motif can bind DNA and is common in proteins involved in gene regulation. It is formed of two α helices connected by a β turn.

Leucine zipper Leucine zippers can bind DNA and are formed of an αhelix with leucine residues in periodic repetition. Two leucine zippers can interdigitate and bind to each other.

Nest and niche A nest and niche are each 3-4 consecutive amino acid residues that form an anion and cation binding site, respectively.

PAS domain PAS domains are common sites where the protein binds to other proteins or molecules. It is named after the first three proteins it was found in (though it is now known to be found in many proteins).

Zinc finger A zinc finger is a motif for binding to DNA.

28.2.4 Quaternary structure

Multiple polypeptide subunits are held together using the same kinds of bonds as hold together tertiary structure.

28.3 Carbohydrates

28.4 Lipids

28.4.1 Phospholipids

Phospholipids are composed of a hydrophilic head group and two hydrophobic hydrocarbon tails. Often one of the tails is fully saturated and straight, while the 2nd often has a double-bond which "kinks" the tail. In animals, the head group is composed of a 3-carbon glycerol, a phosphate group, and a variable group.

28.4.2 Cholesterol

Cholesterol molecules are formed by 1) a hydroxyl group, 2) a complex of hydrocarbon rings, and 3) a short hydrocarbon tail.

Chapter 29

Small organic compounds

29.1 ATP system

ATP is a good energy storage system because the hydrolytic cleavage of an inorganic phosphate group has a very large and negative ΔG (at least when there is lots of ATP and not a lot of ADP, as during normal metabolic state).

ATP concentration varies between tissues. [ATP] is highest in mantle muscle ($\approx$5 μmol/g) (Häfker, 2012), but is about 1 μmol/g in axoplasm (Lasek and Brady, 1985).

Most ADP and AMP in muscle cells at rest is bound to proteins. In *Sepia,* 70% and 85%, respectively, are bound (Häfker, 2012). In contrast, because [ADP] and [AMP] increase during metabolic stress, most of these species are free (not bound to proteins). Cephalopods do not seem to break down AMP into anything else (Pörtner et al., 1993). [ADP] is the most important activator of the phosphoarginine system (Pörtner et al., 1993).

ATP is only biologically active when bound to a Mg.

The synthesis of ATP from ADP and P_i by ATP synthase in the mitochondrial matrix (oxidative phosphorylation) consumes about 0.56 mol H^+ per mole ATP created (depending on pH_i) (Vaghy, 1979). This is due to the differing pK values of ATP vs. ADP at the same pH; ATP has a higher pK value than ADP and thus dissociates H less than ADP.

29.2 Phosphoarginine system

Since phosphoarginine is more abundant and diffuses faster than ATP, phosphoarginine is the dominant phosphagen storage system in tissues; it transports more energy than ATP (Kinsey et al., 2007).

The phosphoarginine system is an energy storage system that is utilized for anaerobic metabolism. In the cephalopod body, the highest quantities of Arg-P (or phospho-L-arginine (PLA)) are in the mantle muscle (˜10-40 μmol/g)(Häfker, 2012; Storey and Storey, 1978; Seibel et al., 2014) with much lower concentrations in other more aerobic tissues such as the systemic heart (˜ 0.5 μmol/g) (Häfker, 2012).

At normal resting conditions in many animals (including cephalopods), Arg-P comprises ˜60-70% of the phosphoarginine system (Arg-P and Arg) (Pörtner et al., 1993). Similar results have been demonstrated with *Sepia officinalis* maintaining a nearly 1:1 ratio of Arg-P and Arg (Häfker, 2012).

$$\text{L-arginine} + \text{ATP} \overset{\text{arginine kinase}}{\rightleftharpoons} \text{phospho-L-arginine} + \text{ADP}$$

29.3 Taurine

Taurine is a molecule derived from the amino acid cysteine. It is highly water-soluble, making it unable to pass through membranes (Huxtable, 1992). However, it interacts with membranes as well as cations such as Ca^{2+} (Huxtable, 1992).

29.4 Trimethylamine oxide (TMAO)

Chapter 30

Cell membranes

In eukaryotic cells, the plasma membrane is only a small proportion of total cellular membrane (measured by mass or surface area), the majority being intracellular membranes (Alberts et al., 2008). The relative proportions of membrane allocated to each organelle varies by species and tissue.

30.1 Membrane composition and structure

Cell membranes (plasmalemmas) are phospholipid bilayers roughly 5 nm thick (Alberts et al., 2008). A single μm^2 contains $\approx 5 \times 10^6$ lipid molecules (Alberts et al., 2008). By mass, cell membranes are often 50% lipid and 50% protein; due to the much smaller size of lipids, they are 50x as abundant in a 50:50 membrane. Individual phosphoglycerides rarely flip-flop between surfaces of the bilayer, but cholesterol flip flops much more rapidly. The compositions of the extracellular monolayer and the cytosolic monolayer can vary drastically (Alberts et al., 2008).

30.1.1 Phosphoglyceride composition

The fluidity of the membrane is determined in large part by the composition of the phosphoglycerides. Saturated fatty acids are straight and can pack together tightly while unsaturated fatty acids are bent and cause the membrane to be less dense and more fluid.

The composition of a membrane is determined by the length and saturation of the fatty acid tails and the composition of the head group.

30.1.2 Cholesterol composition

Eukaryotic membranes may contain large quantities of cholesterol, even up to an even proportion with phosphoglycerides (Alberts et al., 2008). These cholesterol molecules stabilize neighboring phosphoglyceride tails and thus make the entire phospholipid bilayer more impermeable to small water-soluble molecules slipping through (Alberts et al., 2008). Cholesterol also lowers the fluidity of the membrane (Bastiaanse et al., 1997) and can increase or decrease enzymatic activity of membrane bound proteins depending on the protein and cell type (Bastiaanse et al., 1997).

Cephalopod membranes are high in cholesterol (Rosenthal, pers. comm.).

30.1.3 Lipid rafts

Patches of membrane bilayer with distinct composition (often rich in cholesterol) can form "lipid rafts" in which proteins may be found. This may stabilize groups of proteins that interact in protein complexes.

30.1.4 Membrane proteins

Membrane-associated proteins can be transmembrane or peripheral. Transmembrane proteins typically form alpha helices or beta barrels in their transmembrane domains since this is the most stable conformation for the polar peptide bonds to pass through the nonpolar inner portion of the membrane (Alberts et al., 2008). When a protein possesses multiple transmembrane alpha helices, the alpha helices often interact and can even exclude contact of an alpha helix with many or any phosphoglycerides (Alberts et al., 2008).

30.1.5 Glycocalyx

Almost all membrane proteins that are in contact with non-cytosol (organelle lumen or extracellular) sides of the bilayer are glycosylated (have a saccharide added). Therefore, the extracellular side of all eukaryotic cells are rich in various carbohydrates, giving rise to the term "cell coat" or glycocalyx (Alberts et al., 2008). There is a huge diversity of possible saccharide combinations and this diversity is what permits cell-specific recognition and characteristics.

30.1.6 Gap junctions

Gap junctions are intercellular connections that directly connect the cytoplasms of two adjacent cells. In invertebrates, gap junctions are formed by innexin proteins.

30.2 Transmembrane transport of substances

Substances can move across cell membranes by 1. simple diffusion, 2. vesicular transport, or 3. membrane proteins.

30.2.1 Vesicular transport

Vesicular transport is the engulfing of substances by a phospholipid sphere and subsequent integration of that phospholipid sphere with the membrane. This is less selective but faster than membrane proteins. Vesicular transport is the mechanism for neurotransmitter release into the synapse in neurons.

30.2.2 Membrane proteins

Membrane proteins are always gated. The gates can be activated by a variety of stimuli such as voltage, ligands or light. Some membrane proteins are channels (they are open to both sides simultaneously and can only move substances down their electrochemical gradient) while others are transporters (they are open to one side at a time and can move substances up their electrochemical gradient). Transporters allow orders of magnitude slower flow rates of ions than channels due to the time for binding substrate, moving, and releasing (Holmgren and Rosenthal, 2015). The physiological traits of a given membrane protein can include:

- opening rate
- closing rate
- stimulus sensitivity: required level of voltage perturbation or ligand concentration before opening the gate
- ion selectivity: the selectivity of a membrane protein to the ions that pass through it
- inactivation/desensitization: the tendency of a channel to spontaneously close despite the continued stimulus to stay open. Voltage-gated channels are "inactivated" and ligand-gated channels are "desensitized".

30.2.2.1 NKA

The main purpose of Na^+/K^+ ATPase (NKA) is not the transportation of these ions, but rather the maintenance of an electrical gradient (membrane potential) across the membrane. This potential allows other ions to be transported passively across the membrane.

NKA is a quaternary structure, composed of an α and β subunit. The α subunit contains all the key functional components: ATP binding site, ion binding sites, gate, etc. The α subunit is composed of 10 transmembrane segments.

NKA pumps 3 Na^+ out for every 2 K^+ it brings in, thus creating a negative charge inside the cell. The pump has a maximal cycling rate of around 30 Hz, or 90 Na^+/s and 60 K^+/s (Colina et al., 2010). Its continuous functioning costs most animals 10-40% of their entire ATP demand (Colina et al., 2010).

During its cycle, it alternates back and forth between an intracellular facing (E1) conformation that binds 3 Na^+ and an extracellular facing (E2) conformation that binds 2 K^+. The same ion binding residues are utilized to bind 2 Na^+ and 2 K^+, while the 3rd Na^+ is bound by a third ion-binding group of residues. This cycling is powered by dephosphorylating ATP.

The ion turnover rate is related to the membrane potential by a sigmoid relationship. The less negative the cell's membrane potential (as during an action potential), the higher the activity of the NKA enzymes; at resting potential NKAs in many animals run at $\approx$50% their maximal rate (Colina et al., 2010). This is because at a highly negative membrane potential, the

high extracellular concentration of Na^+ and relative positive charge outside the cell both resist the unbinding of three Na^+ ions and release outside the cell (Colina et al., 2010).

NKA activity is suppressed by heightened cholesterol content in the membrane (Bastiaanse et al., 1997).

RNA editing is known to occur in NKA mRNA transcripts in squid (Colina et al., 2010). Here, editing increases pumping rate at resting membrane potential (Colina et al., 2010).

30.2.2.2 Na^+/Ca^{2+} exchanger (NCX)

Sodium-calcium exchangers are ubiquitous on the plasma, mitochondrial, ER membranes of excitable cells (neurons and muscles). It is an antiporter that exports 1 Ca^{2+} ion up-gradient at the cost of importing 3 Na^+ ions down-gradient. Unlike PMCA (below), NCX has a low affinity for Ca^{2+} but is fast, and thus is best suited for removing Ca^{2+} after an excitation event, unlike PMCA, which mainly functions to maintain chronically low $[Ca^{2+}]_i$ when cells are not excited.

30.2.2.3 Plasma membrane Ca^{2+} ATPase (PMCA)

Plasma membrane calcium ATPases export one Ca^{2+} from the cytoplasm out of the cell for one ATP hydrolysis. Unlike NCX (above), PMCA has a high affinity for Ca^{2+} ($K_m = 100-200\,nM$) but is slow, and thus is best suited for maintaining chronically low $[Ca^{2+}]_i$ when cells are not excited, unlike NCX, which mainly functions to remove Ca^{2+} after an excitation event.

PMCA activity is suppressed by heightened cholesterol content in the membrane (Bastiaanse et al., 1997).

30.2.2.4 Solute carrier proteins (SLCs)

Solute carrier proteins are a diverse family of membrane transport proteins.

30.2.2.5 NCCK

NCCK cotransports 1 Na^+, 2 Cl^-, and a K^+ in the same direction across a membrane.

30.2.2.6 ATP-sensitive K^+ channels (K_{ATP} channels)

K_{ATP} channels open when intracellular [ATP] falls. This hyperpolarizes the cell which limits ATP-consuming action potentials and NKA activity (Shimoda and Polak, 2011).

30.2.2.7 Aquaporins

Aquaporins transfer water molecules across the membrane but can also transport dissolved gases (Zwiazek et al., 2017).

30.2.2.8 Lipid-gated ion channels

These are ion channels that are gated by either specific kinds of lipids (e.g. PIP_2) or by changes in the lipid tension or thickness.

TREK-1 TREK-1 is a mechanosensitive potassium channel that is chiefly responsible for anesthesia (at least in mammals).

30.3 Membrane-extracellular interactions

30.3.0.1 G protein-coupled receptors

Cephalopods possess a much higher diversity of G-protein coupled receptors than other bilaterians (Albertin et al., 2015). *Octopus bimaculoides* have >300 G-protein coupled receptors.

Chapter 31

Organelles

31.1 Endoplasmic reticulum

The ER functions as a protein trafficker and Ca^{2+} storage and regulator.

31.1.1 Rough ER

Rough endoplasmic reticula are covered with ribosomes, thus functioning in protein synthesis especially of membrane-bound proteins or those to be excreted from the cell (cytosolic proteins are translated by free-floating ribosomes independently of the ER). For this reason, rough ER surround the nucleus so that mRNA exported from the nucleoplasm can efficiently reach ribosomes for translation. Once proteins are synthesized, they are enclosed in a vesicle which is sent to the Golgi apparatus.

Membrane-bound proteins are incorporated into phospholipid bilayer in the ER then packaged in the Golgi and added to the destination membrane intact (Alberts et al., 2008). Nascent membrane-destined polypeptides contain a 15-30 residue "signal peptide" that is rather hydrophobic and leucine-rich in many cases. This signal is detected by a signal recognition particle (SRP) that brings the ribosome and nascent polypeptide to the ER membrane. At the ER, the polypeptide is shuttled through a translocon by its N-terminal signal peptide. Once inside the ER lumen, the signal peptide is cleaved, and the polypeptide folds into a protein.

31.1.1.1 Ribosomes

Eukaryotic ribosomes are 80S ("S" being an archaic unit of sedimentation measurement, which is a proxy for size). They are composed of two subunits: a large 60S subunit and a small 40S subunit. In total, ribosomes are 60% rRNA and 40% protein.

Large (60S) subunit The 60S subunit is composed of 28S rRNA, 5.8S rRNA, 5S rRNA, and 46 proteins.

Small (40S) subunit The 40S subunit is composed of 18S rRNA and 33 proteins.

31.1.2 Smooth ER

Smooth endoplasmic reticula function in lipid and steroid synthesis as well as the breakdown of glycogen into glucose and the storage and release of calcium. Smooth ER in muscle cells are known as sarcoplasmic reticula.

31.2 Golgi apparatus

The Golgi apparatus receives vesicles containing proteins produced in the ER and repackages, concentrates, modifies, and releases them into vesicles for extracellular excretion or incorporation into the cell membrane. The Golgi has a *cis* side for receiving vesicles from the ER and a *trans* side for releasing vesicles.

31.3 Mitochondrion

Because mitochondria evolved from symbiotic bacteria, they produce their own DNA, RNA, and ribosomes. The mitochondrial DNA contains the genes for all the proteins in the electron transport chain as well as all the tRNAs and both the large and small subunits of ribosomes (subsection 41.1.1).

The inner membrane is rather permeable to protons such that there is a chronic proton leak that lowers the efficiency of ATP production from respiration (Divakaruni and Brand, 2011).

The high membrane potential across the inner membrane leads to the aggregation of Ca^{2+} in the matrix.

In humans at least, typical mitochondrial $[O_2]$ = 1.5-3 μM.

Mitochondria can undergo fission and fusion (Heine and Hood, 2020). Fission is beneficial when a part of the mitochondrion is damaged and needs to be destroyed but the functioning portion can remain.

Density At least in mammals, mitochondrial density is regulated by peroxisome proliferator-activated receptor γ coactivator 1α (PGC-1α), a coactivator that binds to nuclear hormone receptor heterodimers and facilitates transcription (Moyes, 2003). This has not been found in an invertebrate except *Drosophila*, however.

At least among mammals, the mitochondrial density within a cell is proportional to an animal's MMR (as opposed to variation in mitochondrial-volume-specific M_{O_2}) (Weibel et al., 1991). Therefore, changes in oxygen demand due to allometry or adaptation are induced primarily by changes in mitochondrial quantity rather than quality. As an example, typical mammalian skeletal muscle has $1x10^{10} - 1x10^{11}$ $\mu m^3 \cdot g^{-1}$ of mitochondrial volume (Weibel et al., 1991). However, mitochondrial quality and location can also influence ATP production in important ways.

Mitochondrial abundance and membrane composition can be altered in a tissue in response to chronic changes in activity level (Moyes, 2003).

31.3.1 Structure

Mitochondria are typically about 0.75 to 3 μm in diameter and (at least in mammals) can vary in abundance from 0 to over 2000 per cell.

31.3.1.1 Outer membrane

The outer membrane is rich in porin proteins such as the voltage-dependent anion channel (VDAC) which allows exchange of small hydrophilic molecules ($<$ 5 kDa) between the cytosol and intermembrane space. Proteins that are too large to fit through VDACs must be shuttled through translocase of the outer membrane (TOM). The outer membrane also contains MIRO, an adapter protein for binding mitochondria to motor protein complexes.

The outer membrane also contains a diversity of proteins from the Bcl-2 family (named after B cell lymphoma cell line from which they were first discovered). Under normal conditions, the majority of these Bcl-2 proteins are anti-apoptotic, but when the majority shifts to pro-apoptotic, apoptosis is induced (subsection 39.10.1).

31.3.1.2 Intermembrane space

The intermembrane (perimitochondrial) space has the same composition of small molecules as the cytosol (because of the porins on the outer membrane) but has different proteins.

31.3.1.3 Inner membrane

The inner membrane has many folds or "cristae", the exact number being correlated with the aerobic demand of the cell (Heine and Hood, 2020). It is extremely dense with membrane-bound proteins (much more so than the outer membrane or cell membrane). In addition to the normal phospholipids, the inner membrane is also composed of cardiolipin, a phospholipid containing four fatty acyl chains rather than the normal two, which is believed to help make the inner membrane less permeable to small molecules (e.g. H^+). All molecules must pass through transport proteins such as translocase of the inner membrane (TIM). There is a steep membrane potential across the inner membrane due to the electron transport chain. Most of the proteins involved in the electron transport chain, as well as ATP synthase, are imbedded in the inner membrane.

The enzyme complex involved in processing branched α-keto acids (in amino acid catabolism) is embedded in the inner membrane (subsubsection 34.2.2.3).

Adenine nucleotide translocators (ANTs) are transport proteins that move ADP from the cytoplasm into the matrix and ATP from the matrix into the cytoplasm.

Among mitochondria in mammalian skeletal muscle (at least), inner membrane surface area stays nearly constant at 35 μm^2 per μm^3 of mitochondrion (Weibel et al., 1991).

31.3.1.4 Matrix

The matrix is the region within the inner membrane and is rich in proteins, mtDNA, tRNA, and ribosomes. Also, because of the O_2 conversion to H_2O and occassional H_2O_2, the matrix is rich in antioxidant enzymes.

31.3.2 Localization and interactions

Mitochondria are moved around the cell by motor proteins on microtubule tracks (Hirokawa, 1998). These motor proteins can include kinesin and dynein, but also a mitochondrial-specific myosin: myosin 19 (Quintero's MBL talk). Myosin 19 binds to the outer mitochondrial membrane both directly through a polarized alpha helix into the membrane, and indirectly through a MIRO protein embedded in the membrane (Quintero's MBL talk).

Under higher energetic demand, mitochondrial can form inter-mitochondrial junctions (IMJs), which seems to allow "communication" and resource exchange between mitochondria (Heine and Hood, 2020).

31.4 Nucleus

The nucleus is enclosed by a nuclear envelope, a double phospholipid bilayer composed of the inner and outer nuclear membranes. Between these membranes is the perinuclear space, which is 20-40 nm wide. This envelope is studded with nuclear pores which regulate transport of substances into and out of the nucleus. The nucleoplasm within is full of chromatin. Within the core of the nucleus is the nucleolus where rRNA is synthesized for ribosome biogenesis.

There are ~3000 nuclear pores in a nuclear envelope (Robert Singer's iBio talk).

31.4.1 Histones

In eukaryotes, histones are positively-charged proteins (rich in Lys and Arg residues) which spool negatively-charged DNA into nucleosomes. They protect the DNA from being tangled and damaged and also are key regulators in replication and transcription.

There are five families of histones, H1 (linkers), and H2A, H2B, H3, and H4 (all core histones). The nucleosome is an octamer formed from two H2A-H2B dimers and an H3-H4 tetramer.

31.4.1.1 Post translational modifications

These histones can be methylated or acetylated which can alter how they hold the DNA and thus modify the rate of transcription of a gene. When acetyl groups bind to histones, the DNA is uncurled and upregulated. When deacetylated, the histone respools the DNA and downregulates transcription. This is conducted by histone acetyltransferase and histone deacetylase transcription factors, respectively.

These (de)acetylating enzymes can be regulated by cellular signals such as TCA cycle intermediates.

31.5 Lysosome

Lysosomes breakdown cellular waste and "debris" including nonfunctional proteins and organelles, bacteria, viruses. They do this by concentrating digestive enzymes such as acid hydrolases. Within the cytosol these enzymes would be detrimental, but contained within lysosomes they can function as selected degradation sites.

The lysosomal environment is more acidic than the cytosol. Cathepsins are a highly conserved family of proteases, most of which are only active at lysosomal pH, a mechanism of regulation and prevention of non-intended degradation.

31.6 Peroxisome

Peroxisomes detoxify free radicals with oxidases and catalases. They are also a site of fatty acid synthesis and degradation.

31.7 Cytoskeleton

The eukaryotic cytoskeleton is composed of microfilaments (actin, 5-9 nm diameter), intermediate filaments (~10 nm diameter), and microtubules (α, β-tubulin heterodimers, 25 nm diameter). Prokaryotes lack intermediate filaments. All three are very dense within the cytoplasm, though actin tends to be more peripheral and microtubules more central within the cytoplasm, as a generality. All three are formed from many subunits that are non-covalently bound to each other (Alberts et al., 2008). This

enables quick and cheap disassembly and reassembly as needed. All three cytoskeletal filaments are primarily regulated by a plethora of accessory binding proteins (Alberts et al., 2008).

31.7.1 Microfilaments (actin)

Microfilaments determine the shape of the cell surface and cellular locomotion (Alberts et al., 2008). Microfilaments are dimer helices of globular actin proteins (Alberts et al., 2008). Microfilaments are most dense just underneath the plasma membrane (Alberts et al., 2008). Microfilaments can bend under a gradual force but will snap if a force is applied quickly.

Microfilaments are highly dynamic, constantly being formed and reformed.

31.7.1.1 Filamin

Filamin proteins hold actin filaments together at high angles to maintain cytoskeletal organization.

31.7.2 Intermediate filaments

Intermediate filaments are only found in eukaryotes and provide mechanical structure to the cell (Alberts et al., 2008). They are formed from elongated subunits (Alberts et al., 2008).

31.7.3 Microtubules

31.7.3.1 Structure

Microtubules are hollow tubes formed from $\alpha$and β heterodimers of 55 kDa globular tubulin proteins (Alberts et al., 2008). Each μm of microtubule is formed from 1650 heterodimers. Heterodimers first form end-to-end connections to form a protofilament. 13 protofilaments then fuse in parallel to form the final cylindrical shape (so the cylinder circumference is composed of 13 heterodimers). Their protein sequence is highly conserved amongst eukaryotes, which is what makes their dimensions so universal.

31.7.3.2 Nucleation and polymerization

Microtubules can polymerize spontaneously but the rate is too slow for *in vivo* function. Therefore, they are nucleated by γ-tubulin ring complex ($\gamma-$TuRC), a complex of gamma tubulins and other proteins that form a cone with a 13-fold symmetry on which the alpha and beta tubulins can bind. This complex protects the minus end from degradation. The $\gamma-$TuRC is the main functional component of the microtubule-organizing center (MTOC) such as a centrosome.

They are constantly polymerizing and depolymerizing. The rate of polymerization is dependent on cellular mileu, tubulin concentration, and temperature. The polymerization dynamics are regulated by microtubule-associated proteins (MAPs). Polymerization utilizes GTP.

The microtubules are sided, with a plus end and minus end (Hirokawa, 1998). The plus end polymerizes faster than the minus end. In neurons, the plus end runs away from the cell body; in epithelial cells, the plus end runs towards the basement membrane; and in nonpolarized cells, the plus end runs towards the cell periphery (Hirokawa, 1998).

31.7.3.3 Function

Microtubules determine intracellular organelle locations and direct intracellular transport (Alberts et al., 2008). Most of the microtubules radiate from a centralized centrosome. Other organelles are embedded within the microtubule web to keep them in place. Microtubules also act as tracks along which motor proteins can transport substances (e.g. vesicles, proteins).

Cargo being transported along MTs can move at a rate of 5-40 cm/day (Prahlad et al., 2000).

31.7.4 Motor proteins

Most kinesins move along microtubules in an anterograde motion (plus-end directed) (moving cargo from the interior to exterior of the cell)(Vale et al., 1985) while dyneins move in a retrograde motion (minus-end direction) (from exterior to interior of cell). Their cargo can include organelles, protein complexes, and endosomes (Hirokawa, 1998). Myosin moves along actin filaments. In each motor protein, the head determines the filament track and the tail determines the cargo (Alberts et al., 2008). Kinesins and myosins are closely related, but dyneins are much more distantly related (Kull et al. 1996, Nature).

Motor proteins can exert a force of 1-7 pN (Vale's iBio talk).

Mitochondria are moved by various motor proteins, commonly through a MIRO protein embedded in the mitochondrial outer membrane and acting as a binding point.

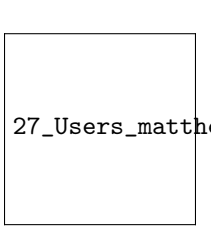

Figure 31.1: Kinesin motility cycle from (Vale and Milligan, 2000)

31.7.4.1 Kinesin

There are 14 kinesin families (Lawrence et al., 2004). In humans, there are 45 kinesin genes (Vale's iBio talk). A conventional kinesin molecule is composed of two kinesin heavy chains (KHCs) and two light chains (KLCs) (Hirokawa, 1998)(except in fungi, which do not have light chains). The KHCs form globular heads that bind the microtubule, while the KLCs form a fan-like end that binds the cargo (Hirokawa, 1998). Different light chain isoforms convey differences in cargo binding affinity (Wozniak and Allan, 2006). Conventional kinesins can move from 0.02 to 2-3 μm/s (Alberts et al., 2008) by "walking" along the microtubule alternating heads. Each step is roughly 8 nm, utilizing one ATP per step (Coy et al., 1999b).

Each kinesin paralog has very similar motor domains, but very divergent coiled-coil and tail domains, which provide the functional diversity (Vale's iBio talk).

Three kinesins assessed in budding yeast had a protein half-life of 12-27 hours (Belle et al., 2006) while kinesins have a half-life of 12-72 hours in mouse neurons, depending on the specific gene (Mathieson et al., 2018).

Kinesin-1 KIF5, conventional kinesin, intracellular organelle transport

Kinesin-2 KIF3, (heterotrimers with kinesin associated protein (KAP)), cilia and flagella axoneme assembly/maintenance

Kinesin-3 KIF1, (often monomers) synaptic vesicle movement in axons, mitochondrial and Golgi movement

Kinesin-4 KIF4, chromosome-associated kinesin involved in DNA repair, replication, chromosome condensation

Kinesin-5 KIF11, (tetrameter) forms cross-bridges that create the mitotic spindle during mitosis

Kinesin-14 KIFC, unlike most kinesins, kinesin-14 is a (-) end motor. involved in mitotic spindle formation

Kinesin structure The motor domain is on the N-terminus of most KHCs (Hirokawa, 1998) and contains both the ATP and microtubule binding sites (Atherton et al., 2014). It is ~10 nm in diameter (Vale's iBio talk). This domain is composed of a highly conserved "catalytic core" and a ~15-40 residue "neck linker" that is on the carboxyl end of the catalytic core that undergoes the conformational change with each swing of the head up the microtubule (Vale and Fletterick, 1997). The helix-α4 domain is the contact point with microtubules (Atherton et al., 2014).

On the C-terminal end of each motor domain, the neck linker from the motor domains lead to the stalk to form the functional dimer complex (Atherton et al., 2014). The "stalk" is formed of a coiled-coil domain (Vale and Fletterick, 1997) formed by a heptad repeat of amino acids. The long coiled-coil buffers the a natural "limping" behavior exhibited by the heads when the coiled-coil domain is truncated (Asbury et al., 2003). Along this coiled-coil, there are one or more hinges that provide flexibility (Vale's iBio talk).

On the C-terminal end of the stalk, there is a globular "tail" domain on some kinesins (Vale and Fletterick, 1997). When not bound to cargo, this tail can bend around and interrupt the motor domain, thus inhibiting kinesin movement when not transporting cargo (Friedman and Vale, 1999; Coy et al., 1999a).

Motor domain catalysis When the motor domain binds to the microtubule, it triggers ADP release and primes the nucleotide binding site for ATP binding (Atherton et al., 2014). When the ATP binds, it causes the neck linker to zipper to the motor domain, restricting motion and swinging the partner head forward. Each head moves forward 16 nm each cycle, but since there are two steps per cycle, each step is 8 nm.

Kinesin motility cycle (Vale and Milligan, 2000):

bind MT $\rightarrow$ release ADP $\rightarrow$ bind ATP $\rightarrow$ swing partner head forward (zipper neck) $\rightarrow$ hydrolyze ATP $\rightarrow$ release MT $\rightarrow$ release P_i $\rightarrow$ unzi

The hydrolysis of ATP alters the conformation of the central core, which in turn slides a "relay helix" to, in turn, push around some mechanical elements of the structure (Vale's iBio talk).

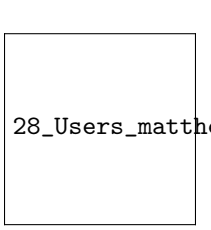

Figure 31.2: Myosin motility cycle from (Vale and Milligan, 2000)

31.7.4.2 Dynein

In humans, there are 15 dynein genes (Vale's iBio talk).

A dynein molecule is composed of two heavy chains (DHCs), three intermediate chains (DICs), and four light intermediate chains (DLICs) (Hirokawa, 1998). The DHCs have globular heads that bind to the microtubules. Unlike kinesins that are diverse, with many paralogs, there are far fewer dyneins within a given species (Alberts et al., 2008). Dyneins are the fastest motor proteins, moving up to 14 μm/s (Alberts et al., 2008), though at least in squid giant axons they seem to be slightly slower than kinesin at around 1-1.5 μm/s (Song et al., 2016).

31.7.4.3 Myosin

In humans, there are 40 myosin genes (Vale's iBio talk).

Myosin motility cycle (Vale and Milligan, 2000):

bind actin $\rightarrow$ release P_i $\rightarrow$ lean forward $\rightarrow$ release ADP $\rightarrow$ bind ATP $\rightarrow$ release actin $\rightarrow$ hydrolyze ATP $\rightarrow$ swing loose head forward

Myosin motor domains are ~2x larger than kinesin motor domains (Vale's iBio talk).

Each "push" displaces the actin 10 nm (Vale's iBio talk).

Myosins can move 0.2 to 60 μm/s (Alberts et al., 2008).

The hydrolysis of ATP alters the conformation of the central core, which in turn slides a "relay helix" to, in turn, push around some mechanical elements of the structure (Vale's iBio talk).

Myosin-19 is specific to localizing mitochondria (Quintero's MBL talk).

Myosin structure Muscle myosin heads are dimers on a coiled-coil attached to a thick filament.

31.7.5 Flagellum

Bacterial and eukaryotic flagella have the same name but are very different structures! Only bacteria flagella can rotate 360°.

Chapter 32

"Central dogma of molecular biology"

The "central dogma of molecular biology" is the conversion of information from DNA through RNA to protein. Protein is expensive to produce; in animals it costs 70-100 mmol ATP per gram, requiring 10-40% of total M_{O_2} (Fraser and Rogers, 2007).

32.1 Replication

1. **Topoisomerase** introduces temporary single-stranded breaks to prevent over- or under-winding of DNA.
2. **Helicase** unwinds the double-stranded DNA strand to create a replication fork
3. **Single-stranded binding (SSB) protein** binds open nucleobases to prevent "rezipping"
4. **RNA primase** binds an RNA primer for the starting region for replication
5. **DNA polymerase III** makes a complementary strand from the primer towards the 5' end (new strand is formed in the 5' to 3' direction)
6. **DNA polymerase I** replaces the RNA primers with DNA
7. **DNA ligase** seals the Okazaki fragments between the polymerase III and polymerase I DNA
8. Daughter DNA strand is complete

As the replication fork spreads down the DNA strand, the **leading strand**'s complement is formed simply (DNA polymerase III runs down the length of the open strand). The **lagging strand**'s complement, however, requires many primers because the DNA polymerase IIIs run in the opposite direction to the direction the replication fork is moving.

32.1.1 Regulation of replication

Replication can be "universally" regulated by high-mobility group (HMG) proteins, which bend DNA.

32.2 Transcription

RNA polymerase I transcribes rRNA (everything except 5S rRNA), while RNA polymerase II transcribes mRNA and miRNA, while RNA polymerase III transcribes 5S rRNA and tRNA. The promoter determines which polymerase binds.

1. **RNA polymerase** binds to a gene's promoter region
2. A "transcription bubble" forms which splits the DNA to expose the bare nucleobases from one of the strands
3. RNA polymerase runs down the parent DNA to create a complementary pre-mRNA molecule (elongation)
4. **Topoisomerase** introduces temporary single-stranded breaks to prevent over- or under-winding of DNA as the transcription bubble moves.
5. The pre-mRNA molecule is capped, polyadenylated, and spliced (see section 32.3)

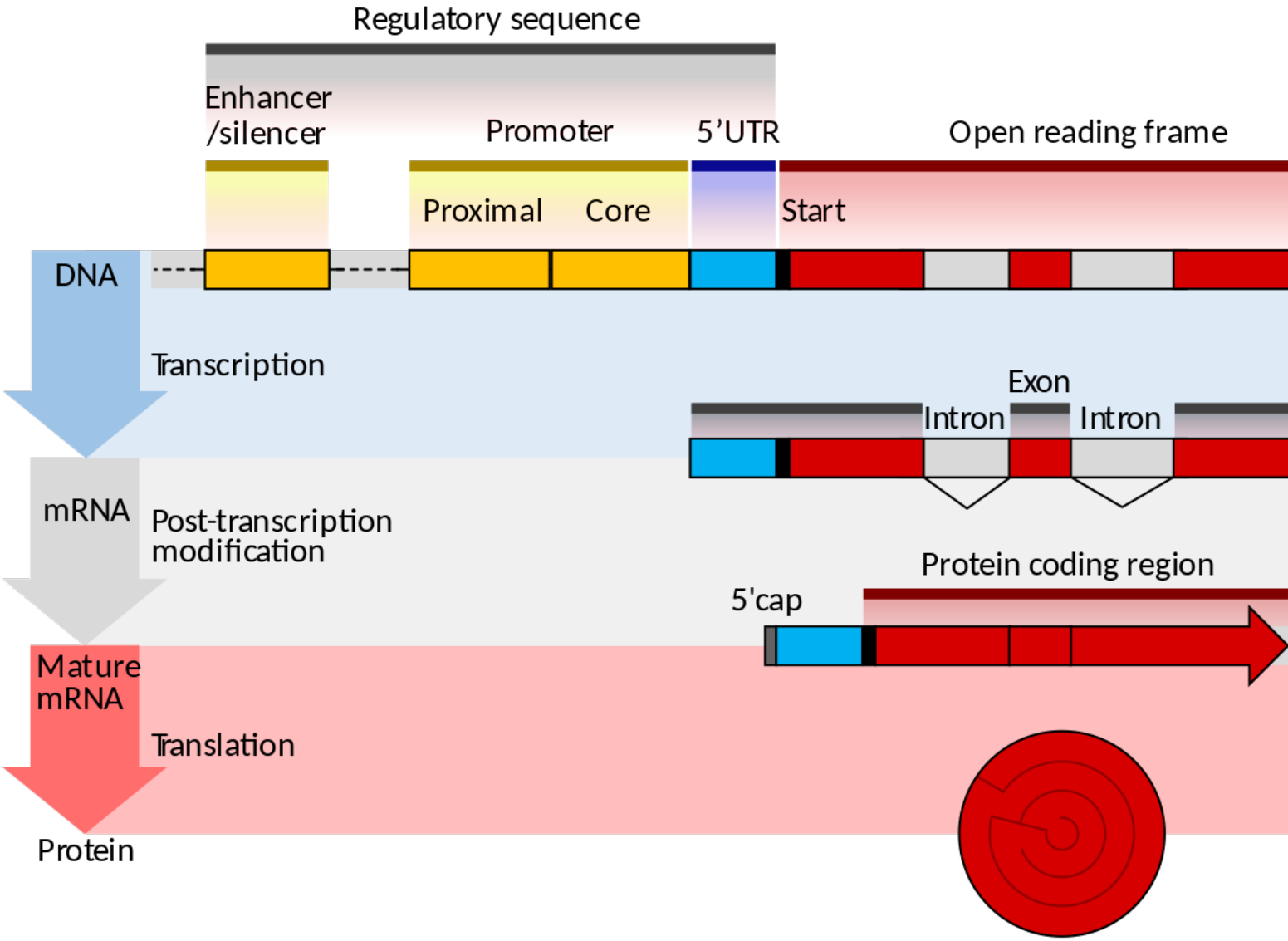

Figure 32.1: Central dogma in eukaryotes

6. The pre-mRNA is now a mature mRNA molecule

Sometimes, multiple genes are found in the same pre-mRNA. In those cases, the individual genes are known as polycistronic genes.

In eukaryotes, transcription elongation occurs at ≈5-100 nucleotides per second (at 37°C) (Singh and Padgett, 2009). At least in yeast, histone genes are the most highly transcribed genes in the transcriptome (though they're only transcribed during the S phase of the cell cycle) (Pelechano et al., 2010). Furthermore, only 14% of yeast genes have an RNA polymerase on them at any given time (Pelechano et al., 2010). In the yeast transcriptome, transcription rates follow a log-normal distribution with most rates falling between 1 and 100 molecules transcribed per hour, with a median of 10 molecules per hour (Pelechano et al., 2010).

32.2.1 Promoter regions

See section 41.3.3.1.

32.2.2 Regulation of transcription

Regulation of gene transcription can be broadly categorized into cis- and trans-regulatory elements. Cis-regulatory elements (CREs) are neighboring genetic sequences that influence the expression of a nearby gene (e.g. promoters, enhancers, silencers, and operators). In contrast, trans-regulatory elements (TREs) are genetic sequences far away or on different chromosomes that influence a gene (e.g. transcription factors). (subsection 41.3.3).

Transcription can be "universally" regulated by high-mobility group (HMG) proteins, which bend DNA.

In mammals, there are about 8000 genes that are ubiquitously expressed in all cell types.

At least in vertebrates, ubiquitously expressed genes tend to have CpG islands on their promoters (section 43.1) and are hypomethylated, while tissue-specific genes have promoters with low CpG abundance and hypermethylation. It should be noted, however, that invertebrates have less DNA methylation globally than vertebrates, and thus this signal may not be as strong in invertebrates as has been characterized in vertebrates.

In a single cell, the total # of mRNA molecules can range from $10^5 - 10^6$ or even more depending on cell type and conditions. In general, mRNA synthesis rates are larger in larger cells so that transcript concentration stays constant across various cell sizes (Berry and Pelkmans, 2022).

32.2.2.1 RNA polymerase II regulation

RNA polymerase II activity and concentration is regulated to control global mRNA synthesis rates in cells (Berry and Pelkmans, 2022).

32.2.2.2 Histone modifications

See subsection 31.4.1.

32.2.2.3 Transcription factors

All transcription factors have one or more of the following motifs: zinc fingers, HTH, leucine zippers, or bHLH (subsection 28.2.3). The C2H2 zinc-finger protein gene family is greatly diversified in cephalopods (Albertin et al., 2015). In general and very broadly, transcription factors are under stronger positive selection than other gene families.

32.3 Post-transcriptional modification

There are over 150 different mechanisms of RNA modification known across domains of life.

32.3.1 Splicing

Splicing removes introns and can rearrange large sections of RNA. The average cephalopod gene is spliced into ~4 exons of ~150 bp while the remaining introns are ~1500 bp, though of course great variation exists between genes (*O. bimaculoides*; Albertin et al., 2015). In particular, as a generalization, the larger the gene, the more alternative splicing exists (Matthew McCoy's MBL talk). In addition, there is a strong negative relationship between intron size and gene expression, presumably because it is energetically wasteful to transcribe huge introns in highly expressed genes (Castillo-Davis et al., 2002).

Splicing typically takes ≈5-10 minutes (37°C) (Singh and Padgett, 2009).

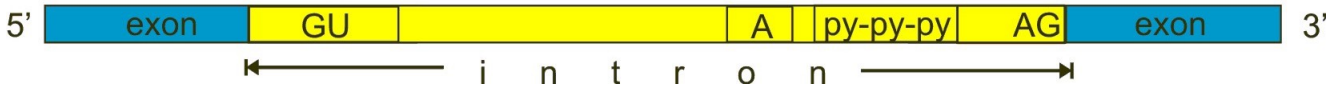

Figure 32.2: Intron structure

Alternative splicing is much more common in neuronal tissue than other cell types (Matthew McCoy's MBL talk).

32.3.1.1 Intron structure

Introns can occur between two codons (phase 0 introns), between the 1st and 2nd base pair of a codon (phase 1 introns) or between the 2nd and 3rd base pair of a codon (phase 2 introns).

Introns generally have a consistent structure. They are formed of:

- a donor sequence on the 5' end of the intron. This often contains a GU in the sequence.
- a branch point. This often contains an A.
- a polypyrimidine tract. This is a sequence rich in pyrimidines (C and U).
- an acceptor sequence on the 3' end of the intron. This often ends with an AG sequence.

32.3.1.2 Spliceosomal splicing

Splicing is often (99% of the time) conducted by an RNA-protein complex known as a spliceosome that is composed of five small nuclear ribonucleoproteins (snRNPs) known as U1, U2, U4, U5, and U6, as well as some other accessory proteins. Through a series of steps, the spliceosome binds all four components of the intron structure (see above) as well as the exons, pulls the exons together (causing the intron to bow out like a lariat), then cuts the intron and splices the exons together.

32.3.2 Capping with a 5' cap

Nuclear mRNA is capped but mitochondrial mRNAs are not capped.

The cap is a 7-methylguanosine bound on its 5' end to the 5' end of the mRNA via a triphosphate bridge. Various other modifications (e.g. hydroxylated ribose sugar carbons) can occur to the 7-methylguanosine as well.

32.3.3 Polyadenylation

Eukaryotic nuclear mRNAs are cleaved near their 3' end and then ~250 adenosine bases are added so that exonucleases can have something to chew on before they get to the coding region of the transcript. Poly-A tail binding proteins also bind here and are important for initiating translation.

Mitochondrial and chloroplast transcripts are also polyadenylated at least sometimes but the tails may also contain other bases mixed in amongst the adenosines and it is unclear what function these tails have on RNA stability or translatability.

32.3.4 RNA interference (RNAi)

Mature mRNAs can be silenced and/or degraded by micro RNA and small interfering RNA. Both miRNA and siRNA are short (18-25 nucleotides) single-stranded RNA strands that are formed from longer double-stranded RNA segments. The difference between them is that miRNAs are encoded in the genome while siRNAs are made from either normally transcribed RNA that has hairpin structures, two RNA strands transcribed from the sense and anti-sense strands of a given genomic locus, viral RNA, or artificially injected strands. Also, siRNAs do not need to be spliced by the Pasha/Drosha complex.

The siRNA pathway is conserved across all eukaryotes. miRNAs have convergently evolved out from the siRNA pathway in both plants and animals but not fungi (Ameres and Zamore, 2013).

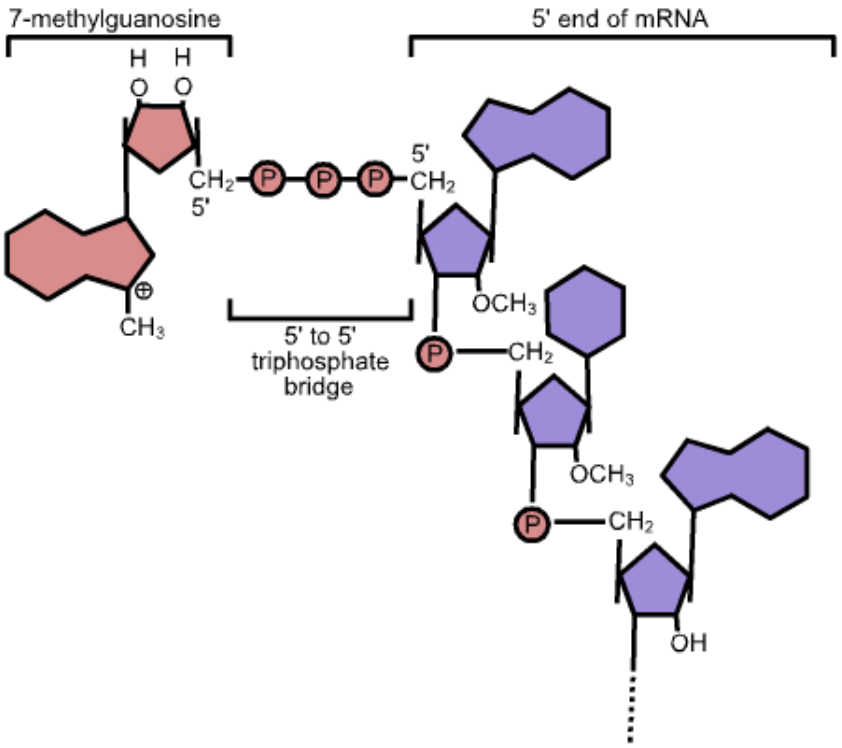

Figure 32.3: 5' cap (specifically, the cap-2 variety)

32.3.4.1 miRNA nomenclature for e.g. dgi-miR-252a-2-5p

dgi from *Dosidicus gigas*

miR mature miRNA. "mir" refers to pri- and pre-miRNAs.

252 miRNA #

a (optional) there are multiple dgi-miR-252 miRNAs with very similar sequences. Just off by a few nt. This is "a"

2 (optional) there are two dgi-miR-252a miRNAs with 100% identical sequences in the genome. This one is from locus 2.

5p (optional) came from the 5' arm of the pre-miRNA but the 3' arm is also a mature miRNA, not just a passenger strand.

Note that even if there are 3 mature miRNAs on a single primary-miRNA, they are still considered separate miRNA genes. Families of miRNA genes are defined based on sequence homology of nt 2-8.

32.3.4.2 miRNA biogenesis

Outlined by O'Carroll and Schaefer (2013), the below sequence is the canonical pathway of miRNA synthesis:

1. miRNA gene is transcribed by RNA polymerase II to form pri-miRNA (long (i.e. 1000s of bp) hair-pin shaped dsRNA)
2. 5' cap and poly-A tail added to pri-miRNA
3. The Pasha protein (aka DGCR8 in vertebrates) binds to the hairpin's stem region and stabilizes the pri-miRNA
4. The Drosha protein (bound to Pasha) is a ribonuclease III (RNase III) enzyme that cleaves off the 5' and 3' ends of the pri-miRNA with its RNase domain, producing a much shorter (60-70 bp) pre-miRNA. Note that several pre-miRNAs (known as polycistronic miRNAs) can be cut from a single pri-miRNA.
5. pre-miRNA is exported from the nucleus into the cytoplasm by the nuclear membrane protein Exportin-5 (requires GTP)
6. Once in the cytoplasm, Dicer (a second RNase III enzyme)(along with TRBP in mammals) cleaves a single bulging loop (~22 bp) off the pre-miRNA to form a miRNA duplex (i.e. miRNA/miRNA*, where miRNA* is the passenger strand) with 5' and 3' overhangs that are 2 nt long, each.
7. The miRNA duplex binds to an Argonaute protein (Ago2 most commonly) which is a subunit of the RISC-loading complex (RLC) along with Dicer and TRBP.
8. The miRNA duplex is then unwound by Ago such that the guide strand remains bound to the Ago protein and the passenger strand is degraded
9. Other proteins join the RLC to form the complete RNA-induced silencing complex (RISC). The identity of these proteins are not well characterized.
10. The guide strand bound to RISC is now a mature miRNA and can target mRNAs that align with the guide strand sequence

While this is the canonical pathway, there is an alternative pathway conserved across animals (found in mammals and *Drosophila,* at least) that makes pre-miRNA independently of Pasha/Drosha processing (O'Carroll and Schaefer, 2013). This pathway is only available to miRNA genes within mRNA introns because they are transcribed within the mRNA and then spliced out into the pre-miRNA. miRNAs produced in such a pathway are called "mirtrons". There's also a third pathway that needs Pasha/Drosha but not Dicer, but it has only been found for a single miRNA (miR-451) and no other known miRNAs, so maybe it's just a weird anomaly... (O'Carroll and Schaefer, 2013)

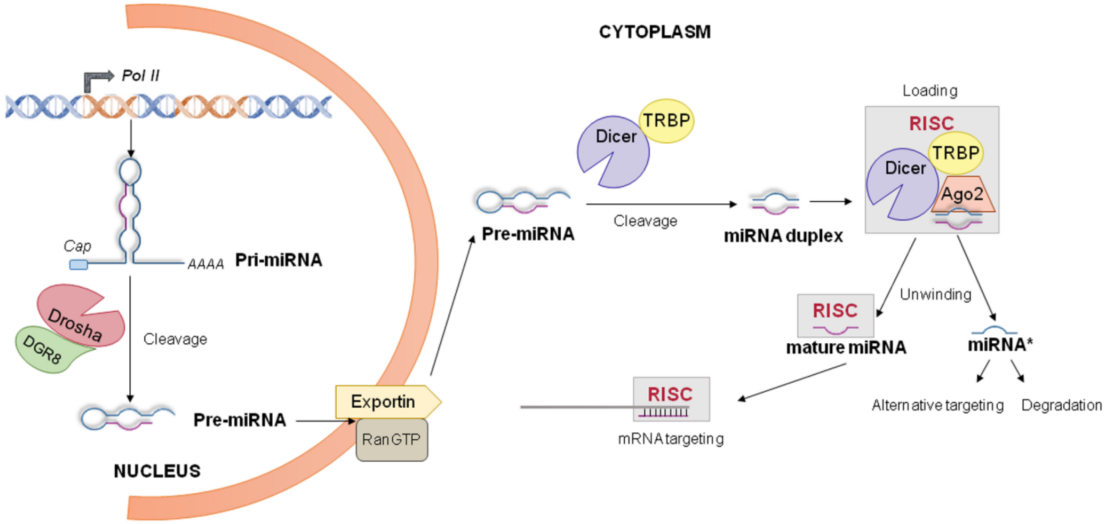

32.3.4.3 Mechanism of mRNA silencing

The mechanics of the silencing all occurs within P-bodies (subsection 32.3.10).

1. When the miRNA guide strand matches the mRNA target strand perfectly, then the Ago2 within the RISC can slice the mRNA. This happens almost exclusively in plants. Much more commonly in animals, when the two strands are not a perfect match, and the 3' end does not pair with the target, the Ago cleavage domain cannot reach the target mRNA and the RISC stays bound.
2. RISC recruits GW182 (in flies, TNRC6 in mammals) which in turn recruits two more proteins:
   (a) a poly-A binding protein that binds to the poly-A tail. This prevents a key eIF from binding the poly-A tail for translation initiation (O'Carroll and Schaefer, 2013).
   (b) a deadenylase complex (e.g. Ccr4-Not) containing deadenylase proteins that cut the mRNA's poly-A tail short
3. Once the poly-A tail is shortened, the 5' end of the mRNA is decapped and the mRNA is degraded.
4. These protein complexes also prevent eIFs and ribosomal subunits from binding, thus inhibiting translation (O'Carroll and Schaefer, 2013).

32.3.4.4 Regulation of miRNA transcription

~50% of mammalian miRNAs are transcribed independently with their own enhancers and promoters (O'Carroll and Schaefer, 2013).

~40% of mammalian miRNAs are transcribed within a protein-coding gene's intron (O'Carroll and Schaefer, 2013). The miRNA may likely be transcribed at a different time from its host mRNA gene, since transcription of the intronic miRNA may interfere with mRNA transcription (O'Carroll and Schaefer, 2013).

~10% of mammalian miRNAs are transcribed within a protein-coding gene's exon (O'Carroll and Schaefer, 2013). If the miRNA is on the sense strand with the exon, the transcription pattern tends to follow the mRNA transcription (O'Carroll and Schaefer, 2013).

miRNA genes that are clustered within 100-50,000 bp from each other tend to have similar expression patterns, while those >50kb apart are not coordinated (O'Carroll and Schaefer, 2013).

32.3.4.5 Targeting

siRNAs bind perfectly to mRNA targets and thus are very specific gene silencers. siRNAs often target their host locus, but not always.

In contrast, miRNAs do not bind perfectly (in animals) and can target more diverse mRNA targets. In animals, the 5' end of the miRNA (nt 2-7) is a perfect match to the target sequence (this is the "seed region"), while the 3' end is almost always less specific (<5% of the time in mammals does the 3' end match)(Doench and Sharp, 2004). In addition to nt 2-7, often either nt

8 is a match, or there is an adenosine across from nt1 on the miRNA side of the duplex (Bartel's iBio talk). miRNAs typically target the 3' UTR of a transcript, but 5' UTR and CDS have also been demonstrated (Tomaselli et al., 2013; O'Carroll and Schaefer, 2013).

A single miRNA sequence might have hundreds of targets and a single target may be regulated by multiple miRNAs. In humans, 60% of mRNAs have conserved regions that match with at least one miRNA (Friedman et al., 2009). Additionally, it is likely that some miRNAs are nascently evolved and have no target. If so, they will soon evolve out of existence.

In general, the more miRNA targets exist on an mRNA, the more repressed it will be, though the targets seem to operate independently (i.e. no synergy) (Bartel's iBio talk).

Once bound, the miRNA can inhibit translation, facilitate mRNA degradation through deadenylation of the polyA tail (Wu et al., 2006), or sequester the mRNA in P-bodies. Experiments across numerous cell types have demonstrated that 70-90% of the suppression at the protein level can be explained by mRNA degradation, while only 10-30% of the change in protein level is left to be explained by inhibition of translation (Bartel's iBio talk).

Very broadly speaking, more generalized genes that are universal across animals have fewer miRNA targets than specialized genes.

miRNAs that are located within mRNA genes have been demonstrated to complement their host gene's function in some cases (e.g. an apoptotic mRNA gene has a miRNA gene that suppresses translation of anti-apoptotic proteins) and in other cases can suppress expression of their host gene (O'Carroll and Schaefer, 2013).

Factors that influence efficiency of target suppression

- The more highly conserved the target sequence in the mRNA, the more likely it is to be repressed by the miRNA (Bartel's iBio talk)
- Target sequences in the 3' UTR are more likely to be repressed by the miRNA than target sequences in the CDS (Bartel's iBio talk)
- Target sequences surrounded by low %GC are more likely to be repressed by the miRNA, likely because they're more accessible (Bartel's iBio talk)

ADARs can alter miRNAs ADARs have been demonstrated to edit adenosines on the stem-loops of pri-miRNAs (Blow et al., 2006; Kawahara et al., 2007). In so doing, all subsequent steps of biogenesis may be altered (Kawahara et al., 2008). This has also been demonstrated to alter the target of the miRNA, when it occurs in the seed region (Kawahara et al., 2007).

In mice, ADAR1 can form a dimer with Dicer to accelerate pre-miRNA cleavage and loading of the miRNA onto RISC (Ota et al., 2013). It also has the potential to alter the complementary sequence and change the target or the efficiency of target binding.

32.3.5 RNA editing by pseudouridylation

Uridine can be exchanged for pseudouridine which pairs tighter to adenine (Somero, 2018).

32.3.6 C-to-U RNA editing

Cytidine deaminases deaminate cytidine to uridine. This is conserved throughout eukaryotes (at least).

32.3.7 RNA Editing by ADARs

RNA molecules can be edited before being translated. This is typically (90+% of editing sites in most taxa; Porath et al., 2017) the conversion of adenosine to inosine which is translated as guanosine (Basilio et al., 1962). A to I editing is mediated through an Adenosine Deaminase that Acts on RNA enzyme (ADAR) (Bass, 2002). Inosines can be found in the tRNA of all domains of life but are only found in mRNAs in eukaryotes, and especially in metazoans. While some metazoans have lost one of the ADAR paralogs, all known metazoans express at least one if not two or three ADAR paralogs (Thomas and Beal, 2017).

RNA editing (especially by ADAR2, at least in humans) is much more common in nervous tissue than any other tissue (Bass, 2002). Its activity was originally discovered in *Xenopus* oocytes as an "unwinding" enzyme.

32.3.7.1 Editing statistics

- Number of unique mRNAs with 1+ editing sites
- Number of unique mRNAs with 1+ editing sites in ORF
- Number of unique mRNAs with 1+ recoding editing sites in ORF
- Editing levels (proportion of transcripts for a given gene with an edit): $G/(A + G)$
- Editing index (average editing level over all adenosines, rather than a particular site): $n_G/(n_A + n_G)$
- Number of editing sites within a unique mRNA
- Number of editing sites within a unique mRNA ORF
- Number of recoding editing sites within a unique mRNA ORF

Cephalopods differ from everything else we know In humans, there are many (~80k, Porath et al., 2017; >1 million, Jantsch MBL talk) A-to-I editing sites but most (92%) occur in the *Alu* regions (SINES) of UTRs and only 31 are in coding regions (Porath et al., 2017). In mice there are 100,000 known sites (Jantsch MBL talk). This is typical among metazoans, where there is often 10ks to 100ks of hyper editing sites (median among 19 metazoans = 76k hyper-edited sites), but often 40-95% of those sites are in repeat regions and rarely many more than 1000 editing sites (or 0-6% of all sites) are in coding regions (Porath et al., 2017). Humans only have >50 recoding editing sites (Jantsch MBL talk).

In contrast, in *O. bimaculoides,* there are ~800k edits in the entire transcriptome of nervous tissues and ~900k edits in the entire transcriptome from various tissues combined (Liscovitch-Brauer et al., 2017). Now, over a million editing sites have been found in octopus CNS (Porath et al., 2017). One third of these edits occur in repeat regions, but unlike in other taxa, many of these edits occur in the coding sequences (CDS) of cephalopod neural tissues: from 80k-130k editing sites across the CDS of all coleoids (Liscovitch-Brauer et al., 2017). 65% of these sites are recoding across all coleoids (Liscovitch-Brauer et al., 2017).

Humans and mice have ~70 recoding sites (Rosenthal, 2015).

In *D. pealeii*, there are over 87,000 A-to-I editing sites within the ORFs (start to stop codons which may contain introns and exons) of mRNAs in nervous tissue (Alon et al., 2015). From these 87,000 sites, over 57,000 recoding events (codon changes) result (compared to 645 in *Drosophila* and 115 in humans) (Alon et al., 2015). In other cephalopods, there are 54k-86k recoding events in nervous tissues (Liscovitch-Brauer et al., 2017). As a result, nearly 60% of all mRNAs in nervous tissue are recoded by editing in *D. pealeii* (Alon et al., 2015) and nearly 25% in *O. bimaculoides* (compared to 1-4% in *Drosophila* and 0.5-3% in humans). There are 7k-8k recoded proteins in the neural tissues of all coleoids (Liscovitch-Brauer et al., 2017). In addition, about 75% of recoded proteins are not just recoded once but are recoded in multiple sites (Alon et al., 2015). About 1 in 3 of all mRNAs in *D. pealeii* nervous tissue are recoded 3+ times and ~10% are recoded 10+ times (Alon et al., 2015).

Unlike in other taxa where most recoding editing sites are species-specific (Xu and Zhang, 2014), recoding editing is often conserved among closely related taxa in cephalopods, suggesting positive natural selection for the recoding events (Liscovitch-Brauer et al., 2017). There are 887 recoding sites that are shared by all coleoids examined to date and the editing levels of these sites are also conserved between taxa (Liscovitch-Brauer et al., 2017). In contrast, humans and mice only share 36 recoding sites and two *Drosophila* species only share 57 recoding sites. Pairwise comparisons (one species from each) of decapodiforms and octopodiforms share 2k-3k recoding sites (Liscovitch-Brauer et al., 2017).

Also unlike in other taxa, those sites with high editing levels in coleoids are much more likely to be recoding than synonymous (in most species, 90% of sites with editing levels = 90-100% are recoding, rather than the expected 65% of sites) (Liscovitch-Brauer et al., 2017). Highly edited sites are also more likely to be conserved across taxa (Liscovitch-Brauer et al., 2017).

The reason why cephalopods have such elevated rates of editing is unclear, but mechanistically, it may be at least in part due to their relative abundance (compared to other metazoans) of genomic sequences that, if expressed, would be capable of forming dsRNA (Porath et al., 2017).

Unlike in any other organism we know, cephalopods exhibit RNA editing outside the nucleus on mature mRNAs (Vallecillo-Viejo et al., 2020).

32.3.7.2 Mechanism

ADAR RNA editing is thought to occur in the nucleus during transcription (Garrett and Rosenthal, 2012b), however cytosolic editing does occur as well, at least in cephalopods (Vallecillo-Viejo et al., 2020).

ADAR morphology

Diversity and distribution Cephalopods possess two ADAR proteins: ADAR1 and ADAR2 (Albertin et al., 2015), although the second protein can be alternatively spliced to form two isoforms: ADAR2a and ADAR2b with 3 and 2 dsRBDs, respectively (Palavicini et al., 2009; Yablonovitch et al., 2017). ADAR1 has Z-DNA binding domains, unlike ADAR2. In cephalopods, ADAR2a is only expressed in the nucleus, whereas ADAR2b is expressed in both the nucleus and the cytoplasm.

Mammals can alternatively splice ADAR1 to form ADAR1 p150 or p110, which have 2 or 1 Z-DNA binding domains, respectively. The former occurs mainly in the cytoplasm while the later occurs mainly in the nucleus, though both can shuttle back and forth to some extent; ADAR2 is only in the nucleus (again, in mammals) (Janetsch MBL talk).

Humans, at least, also express a catalytically-inactive ADAR3.

Domains All ADARs have at least one double-stranded RNA binding domain (dsRBD) on the N-terminus and a deaminase domain on the C-terminus (Bass, 2002; Deffit and Hundley, 2016). ADAR1 has a single dsRBD(?) while ADAR2 may have 2 or 3 dsRBDs depending on the splice isoform (Palavicini et al., 2009). In *D. pealeii*, the third domain increases the activity of ADAR2 (Palavicini et al., 2009). Each dsRBD is formed of ~65 residues composing two alpha helices surrounding three beta-sheets (Tomaselli et al., 2013). The deaminase domain contains a highly-conserved "TWD" residue sequence that is critical for ADAR homodimerization (Thuy-Boun et al., 2020). Two ADARs can form homodimers on the dsRNA, which increases editing efficiency at that site (Deffit and Hundley, 2016).

The ADATs from which ADARs evolved do not have dsRBDs but can bind and edit tRNA (Bass, 2002). rRNA and miRNA can also be edited.

In human ADAR2, the primary sequence is ~65 residues of dsRBD1, 93 residues of gap, ~65 residues of dsRBD2, 22 residues of gap, and the deaminase domain (Thomas and Beal, 2017).

Process of binding and deamination When the amino group is removed from the nucleobase, it is replaced with an oxygen atom pulled from water (Bass, 2002). The water is activated by a zinc atom which is bound to three residues in the deaminase domain (Bass, 2002).

ADARs do not seem to run down the length of an mRNA, deaminating as they go. Rather, they seem to release after only one or two deamination events at a time, needing to rebind again to deaminate more sites (Bass, 2002). The target site selection seems to be influenced by both the deaminase domain and the dsRBDs, since alteration of these domains changes editing (Deffit and Hundley, 2016; Matthews et al., 2016).

The dsRBD binds to a single side of an RNA double helix: binding down the length of the RNA in contact with a minor groove, a major groove, and a 2nd minor groove (cited by (Thomas and Beal, 2017).

The target adenosine is flipped out and the gap in the double helix structure is filled and stabilized by ADAR's helix penetrating loop (human ADAR2: residues 487-489) (Matthews et al., 2016). Specifically, E488 (in hADAR2) or E1008 (in hADAR1) hydrogen bonds with the orphan nucleotide, stabilizing the flipped-out conformation (Matthews et al., 2016; Thuy-Boun et al., 2020; Malik et al., 2021).

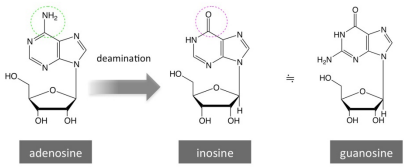

Target site morphology Target site recognition seems to be highly conserved based on the fact that human ADAR2 expressed in *Drosophila* will correctly edit hundreds of *Drosophila* transcripts (reviewed in Khan et al. 2020).

Secondary structure ADARs require at least a 100 bp dsRNA stretch to edit effectively (Nishikura et al., 1991) and can target long helical or hairpin turns of double-stranded sections of RNAs (both mRNAs, small RNAs, and viral RNAs) (Bass, 2002; Deffit and Hundley, 2016; Porath et al., 2017). This preference for dsRNA is due not only to the dsRBDs but also to the deaminase domain itself, which can recognize dsRNA (Phelps et al. 2015).

Up to 100 bp away from the editing site, there is a higher GC content than in the genome generally, which should support double-stranded structure since CG bonds have 3 hydrogen bonds while AU bonds only have 2 (Liscovitch-Brauer et al., 2017). ADAR specificity is more strongly influenced by secondary than primary structure of the RNA molecule because the nitrogenous bases are tucked into the deep and narrow major groove of the dsRNA helix, which makes them less influential in determining specificity (Bass, 2002). The more loops and mismatches around the target site, the lower binding affinity ADARs have for the

site (Bass, 2002). For example, perfectly double-stranded sequences that are >50 bp long have ≈50% of the adenosines converted to inosines (EI = 50%) whereas sequences with mismatches or bulges are targeted with far more selectivity (Bass, 2002). This is because bulges and loops make the substrate less double-stranded. Therefore, the more adenosines an ADAR converts to inosine, the more mismatches it makes which makes the substrate less double-stranded and thus, lowers the ADAR binding affinity for subsequent deaminations.

Neighbors Across metazoans, the 5' neighbor of hyper edited sites is enriched in A and depleted in G (Porath et al., 2017). In other studies, ADAR editing sites have an enrichment of U 5' neighbors and G 3' neighbors (Liscovitch-Brauer et al., 2017; Buchumenski et al., 2017; Deffit and Hundley, 2016). The 5' preference is because a C-G or G-C pair on the 5' neighbor position would have guanine's 2-position amino group sticking out into the minor groove and this amino group interferes with G489 (in human ADAR2) in the helix penetrating loop (Matthews et al., 2016). This loop already twists the RNA helix out of the A-form quite a bit and the addition of this amino group makes it even worse. Thus, A or U 5' neighbors are preferred.

The 3' G preference is for the same reason: the 2-position amino group on the guanine. This amino group is a hydrogen donor that can hydrogen bond with the backbone carbonyl of S486 (in human ADAR2) and thus improve stability (Matthews et al., 2016).

The neighbor preference varies somewhat based on the deaminase domain of the specific ADAR isoform, which can lead to isoform-specific editing site preference (Deffit and Hundley, 2016). Since different deaminase domain isoforms have different base-flipping capability, each will respond to a different extent to such changes neighboring sequence (Deffit and Hundley, 2016).

Opposing bases A mis-match opposite the target adenosine can alter the likelihood of editing. A-C mismatches enhance editing the most, while A-U matches are also quite selective (Thomas and Beal, 2017). A-A and A-G mismatches make a given adenosine less likely to be edited (Thomas and Beal, 2017). This preference is because once the target adenosine is flipped out, a helix penetrating loop fills the gap in the dsRNA helix. E488 (in human ADAR2) on this loop can hydrogen bond with the 2-position carbonyl on a pyrimidine (C or U) nucleobase and thus stabilize the structure (Matthews et al., 2016). The purines (A and G) do not have this carbonyl and thus cannot stabilize the structure. Furthermore, C is likely more selective than U because the A-C mismatch makes flipping out the adenosine easier(?)

32.3.7.3 Function

Influence on mRNA Editing can alter codons, splice-sites, miRNA binding sites, pri-miRNA processing, mRNA stability, cellular localization, or translatability (Bass, 2002; Yablonovitch et al., 2017; Yang et al., 2006; Ben-Zvi et al., 2013; Deffit and Hundley, 2016). Especially in non-coleoid metazoans, editing often occurs in 5' and 3' UTRs and introns, which is often how it affects splicing, stability, localization, and translatability (Deffit and Hundley, 2016).

RNA editing can cause recoding (non-synonymous change)(65% of edits due to chance) or be non-recoding (synonymous change)(35% of edits due to chance). The editing levels in mRNA transcripts are correlated with editing levels in proteins (Liscovitch-Brauer et al., 2017). Because inosine can Watson-Crick base pair with cytosine in the anti-codon of tRNAs, it is interpreted by the tRNA as a guanosine.

Some edits alter the kinetics of the resulting proteins and thus may be a mechanism for acclimation, especially to low temperature (Garrett and Rosenthal, 2012b). Temperature-related adaptive editing has been demonstrated in cephalopods and *Drosophila* (Yablonovitch et al., 2017). The most common edits replace lysines (K) with arginines (R), isoleucines (I) with valines (V), and glutamates (E) with glycines (G) (Garrett and Rosenthal, 2012b). Each of these edits can destabilize the protein since each of the AAs removed are stabilizers and each of the AAs added are destabilizers (Garrett and Rosenthal, 2012b). This can be beneficial for cold acclimation.

In both cephalopods (Liscovitch-Brauer et al., 2017) and *Drosophila* (Khan et al., 2020) as well as mammals (I believe), editing activity is highest by far in the nervous system.

mRNA targets Recoding in all animals occurs most frequently in transcripts for neuronal and cytoskeletal function (Yablonovitch et al., 2017; Alon et al., 2015) especially for ion channels (but less so for ion pumps) (Holmgren and Rosenthal, 2015). Housekeeping genes (e.g. tubulin, kinases) are also targeted in cephalopods (Albertin et al., 2015).

In humans, ADAR2 is the primary paralog involved in editing non-repetitive sites, while ADAR1 primarily edits repetitive sites (Tan et al., 2017).

Summing across the entire mammalian body, filamin A is mRNA target with the most editing events. This is due to its high EL, abundance in the cell, and large percentage of the body composed of tissue-types that at express it (Jantsch MBL talk).

ADARs can also support immune function by targeting viral genomic dsRNA (Rosenthal, 2015).

Cellular / organismal influence At least in mice, ADAR2 knock-outs die before birth because an AMPA subunit 2 glutamate receptor (*gria2*) is *not* edited, which is lethal (Higuchi et al. 2000). Similarly, ADAR1 knock-outs die because of a resulting interferon signaling issue. Thus, both ADAR genes are required for survival in mammals.

ADAR null mutant *Drosophila* are less viable, can't move, and have neurodegeneration compared to wild-type *Drosophila* (Khan et al., 2020).

32.3.7.4 Regulation

The activity of ADARs can also be controlled by alternative splicing of the enzyme (sometimes by itself) or altering its location within the cell (Garrett and Rosenthal, 2012b).

RNA editing can vary across ontogeny (Bass, 2002). In coleoids, ADARs are expressed from the start of embryogenesis (Pierce, 2017). In *Drosophila*, editing is low in larval brains but becomes much more abundant in adult brains, correlating with nervous system complexity.

Studies on mammals have demonstrated that for those ES that form dsRNA structures between intron and exon, the EL correlates with the ratio of intron reads to exon reads (a proxy for splicing velocity). It is inferred therefore, that the longer the mRNA is in the nucleus, the more opportunities for editing and the higher the EL. For those ES that form dsRNA structures between two exons or within an exon, no splicing correlation was found, showing that the duration of the dsRNA structure is important (Janetsch MBL talk).

Intrinsic activity of ADAR The protonation of the orphan-binding residue (E488 in hADAR2 or E1008 in hADAR1) is known to modify editing activity (Malik et al., 2021). Having this residue protonated allows it to hydrogen bond to the orphan base and increase stability. This is at least part of the reason why intracellular acidosis raises editing and why E488Q increases editing efficiency (Q is always protonated).

[ADAR] The half-life of ADAR (in humans) is ~2 hours, so [ADAR] can change quickly when downregulation is needed (Li et al., 2016). At least in humans, ADAR1 p150 is only expressed in response to inflammation, while ADAR1 p110 is constitutively expressed (Janetsch MBL talk).

However, numerous studies have demonstrated that [ADAR] is not a good predictor of *in cellula* editing activity.

Even so, changes in ADAR activity may or may not affect editing levels for a particular site, depending on the binding affinity of ADAR for that site. High affinity sites will likely have high editing levels regardless of ADAR concentration or activity, while the editing levels of low affinity sites will be much more ADAR-dependent (Deffit and Hundley, 2016).

ADAR localization Editing is also tissue-specific, with recoding editing events most frequently in the giant fiber lobe and stellate ganglia even among other nervous tissues (Alon et al., 2015). Different neuronal populations in *Drosophila* have also been shown to have characteristic editing. These spatiotemporal regulations may be enacted by other RNA binding proteins and/or small RNAs (Deffit and Hundley, 2016). In *D. pealeii*, it is demonstrated that ADARs are localized not just in the stellate ganglia but also the giant axoplasm (Vallecillo-Viejo et al., 2020).

At least in mouse embryonic fibroblasts, ADAR nuclear localization is dependent on *Pin1* (Marcucci et al. 2011, EMBO J.).

Autoregulation Both ADAR1 and ADAR2 are edited in cephalopods (ADAR1 much more so) which could have a feedback response (Albertin et al., 2015). *Drosophila* ADAR is also self-edited. The edited form of dADAR has lower editing activity, thus acting as a negative feedback loop (Savva et al., 2012). Furthermore, this ES is temperature-sensitive such that it is more highly edited at cold temperatures (Savva et al., 2012).

32.3.8 Nuclear export

RNA molecules transcribed in the nucleus have been demonstrated to diffuse passively within the nucleus for about 30-60 seconds on average until they run into a nuclear pore, as opposed to any sort of cytoskeletal-driven direction (Robert Singer's iBio talk). At the nuclear pore, they are stripped of proteins that mark them as a nuclear RNA, pass through the pore, then are equipped (or stripped?) of further proteins that mark them as cytoplasmic, thus preventing immediate re-entry into the nucleus (Robert Singer's iBio talk).

Rates of nuclear export are synchronized with mRNA synthesis rates to maintain homeostasis (Berry and Pelkmans, 2022).

32.3.9 Cellular localization

mRNAs are not uniformly floating throughout the cytoplasm. Instead, they are often highly localized to their location of need. This is thought to be achieved through zipcode binding proteins (ZBPs), which bind to the 3' UTR of an mRNA and direct the localization of that mRNA within the cytoplasm. In addition to cellular localization, it also prohibits ribosomal binding until it is phosphorylated and detaches (Hüttelmaier et al., 2005).

Cellular localization of mRNAs occurs through motor proteins operating on the cytoskeletal tracts (Vale's iBio talk).

In neuronal dendrites, manipulative experiments in mice neurons have demonstrated that mRNAs show up to a site of post-synaptic stimulation within ~10 minutes of stimulation (Robert Singer's iBio talk). This is thought to be the primary means of subsequent protein translation and enforcement of that stimulated synapse.

32.3.10 Sequestration in RNA granules

RNA granules are non-membrane bound compartments within the cytoplasm. They can merge together and flow rather than break when a shear stress is applied. The contents within these granules are fluid and can freely move within the bounds of the compartment.

RNA granules can be categorized based on their cell type and function as 1) processing bodies (P-bodies), 2) stress granules, 3) neuronal granules, or 4) germ cell granules (Anderson and Kedersha, 2006).

Type	mRNA specificity	Function
Processing body	Low	Primarily to degrade mRNAs
Stress granule	Low	Primarily to store mRNAs so they cannot be translated during stress
Neuronal granule	High	Primarily to store mRNAs during transport from the cell body to the synapse
Germ cell granule	High	Primarily to store maternal mRNA until needed in embryonic development

Within P-bodies, mRNA can be decapped, poly-A truncated, nonsense-mediated decayed, and silenced by RNAi. Within stress granules, mRNA can be stored to stop translation during stress.

32.3.11 mRNA degradation

The average mammalian mRNA half life is 5-10 hours (cited by (Rädle et al., 2013)), while in organisms generally, half life can range from minutes to days.

Poly-A tails shorten over a mRNA molecule's lifetime and in general the shorter the poly-A tail, the sooner it's degraded and the less it is translated.

In general, the longer the CDS and the longer the 3' UTR of a transcript, the faster it is degraded (Yang et al. 2003, Genome Research).

32.4 Translation

In humans, the average rate of translation is 6 amino acids per second.

In most cell types, the vast majority of translation occurs on the rough ER. In neurons, however, (in mammals at least), much translation occurs via free ribosomes in the dendrites and axons (O'Carroll and Schaefer, 2013).

Typically, once the mRNA molecule has been formed, it is shuttled out of the nucleus into the cytosol. From here, it is translated into a protein:

32.4.1 Initiation

1. The 5' end of the **mRNA** binds to the small subunit of a **ribosome** at the ribosome binding site (RBS)
   (a) ribosomes have three sites (EPA): exit site (E), peptidyl site (P), and aminoacyl site (A)
2. The mRNA slides through the ribosome until the **Kozak consensus sequence** (in eukaryotes only) which contains the **AUG start codon**, which enters the P site
3. The large subunit of the ribosome binds the small subunit

Table 32.1: Standard genetic code

	U		C		A		
U	UUU	Phe - F (phenylalanine)	UCU	Ser - S (serine)	UAU	Tyr - Y (tyrosine)	UGU
	UUC		UCC		UAC		UGC
	UUA	Leu - L (leucine)	UCA		UAA	STOP ("ochre")	UGA
	UUG		UCG		UAG	STOP ("amber")	UGG
C	CUU		CCU	Pro - P (proline)	CAU	His - H (histidine)	CGU
	CUC		CCC		CAC		CGC
	CUA		CCA		CAA	Gln - Q (glutamine)	CGA
	CUG		CCG		CAG		CGG
A	AUU	Ile - I (isoleucine)	ACU	Thr - T (threonine)	AAU	Asn - N (asparagine)	AGU
	AUC		ACC		AAC		AGC
	AUA		ACA		AAA	Lys - K (lysine)	AGA
	AUG	Met - M (methionine) / START	ACG		AAG		AGG
G	GUU	Val - V (valine)	GCU	Ala - A (alanine)	GAU	Asp - D (aspartic acid / aspartate)	GGU
	GUC		GCC		GAC		GGC
	GUA		GCA		GAA	Glu - E (glutamic acid / glutamate)	GGA
	GUG		GCG		GAG		GGG

Table 32.2: Invertebrate mitochondrial genetic code. Differs from the standard code in that: AGA -> S, AGG -> S, AUA -> M, UGA -> W.

	U		C		A		
U	UUU	Phe - F (phenylalanine)	UCU	Ser - S (serine)	UAU	Tyr - Y (tyrosine)	UGU
	UUC		UCC		UAC		UGC
	UUA	Leu - L (leucine)	UCA		UAA	STOP ("ochre")	UGA
	UUG		UCG		UAG	STOP ("amber")	UGG
C	CUU		CCU	Pro - P (proline)	CAU	His - H (histidine)	CGU
	CUC		CCC		CAC		CGC
	CUA		CCA		CAA	Gln - Q (glutamine)	CGA
	CUG		CCG		CAG		CGG
A	AUU	Ile - I (isoleucine)	ACU	Thr - T (threonine)	AAU	Asn - N (asparagine)	AGU
	AUC		ACC		AAC		AGC
	AUA	Met - M (methionine) / START	ACA		AAA	Lys - K (lysine)	AGA
	AUG		ACG		AAG		AGG
G	GUU	Val - V (valine)	GCU	Ala - A (alanine)	GAU	Asp - D (aspartic acid / aspartate)	GGU
	GUC		GCC		GAC		GGC
	GUA		GCA		GAA	Glu - E (glutamic acid / glutamate)	GGA
	GUG		GCG		GAG		GGG

32.4.2 Elongation

1. A tRNA binds an amino acid to form aminoacyl-tRNA
2. An **aminoacyl-tRNA** with a complementary anticodon to the AUG codon in the P site binds to an **elongation factor**
3. The tRNA-EF complex binds the mRNA
4. Another aminoacyl-tRNA-EF complex complementary to the codon in the **A site** binds the mRNA
5. The **amino acid chain** attached to the tRNA in the P site are transferred to the amino acid on the tRNA in the A site. The amino acids bind with a peptide bond.
6. The ribosome **shifts** down the mRNA strand by three nucleotides (one codon) due to an elongation factor
7. The empty tRNA and EF in the **E site** leaves
8. Steps 4-7 are repeated until the A site reaches a **stop codon** (UGA, UAA, or UAG)

- Elongation occurs at ≈6 amino acids per second (37°C) (Ingolia et al., 2011).

32.4.3 Termination

1. The tRNA molecules with stop anticodons do not possess amino acids. Instead of the P site tRNA transfering the amino acid chain, the chain is hydrolyzed and released.
2. The ribosome subunits dissociate from each other and the mRNA via eRFs, or eukaryotic release factors.
3. After translation, the amino acid chain is folded into a functional protein inside chaperone proteins

32.4.4 Ribosome recycling

Ribosomes are primarily RNA (exclusively in prokaryotes) but also contain some proteins. There is both a small and large subunit that come together to form a functional molecule for translation.

32.4.5 Regulation of translation

Under stress, cells form stress granules that sequester mRNA, eIFs, and 40S rRNA (Liz Alexander's talk). miRNAs can also bind mRNAs to suppress translation.

32.4.5.1 Translation factors

Translation factors allow translation to occur faster or more efficiently. These include eukaryotic initiation factors (eIFs), elongation factors (eEFs), and release factors (eRFs).

Some eIFs effectively block the A and E sites on the ribosome so that the first tRNA can only bind to the P site. Other eIFs bind to the 5' cap and poly-A tail. Still others facilitate the binding of the small and large subunits of the ribosome once the start codon has been found.

Some eEFs bind aminoacyl-tRNAs and arrange them into the A site in the ribosome.

32.5 Post-translational modification (PTM)

After being translated, proteins must be folded and are often modified before becoming functional. Modifications can occur on the C-terminus, N-terminus, or in the middle of the peptide.

32.5.1 Phosphorylation

Phosphorylation is the most common PTM. In eukaryotes, it occurs on Ser, Thr, and Tyr residues since they have hydroxyl groups.

32.5.2 Acetylation

Acetylation, or the addition of an acetyl group, can occur on the N-terminus of a protein or on a Lys residue.

32.5.3 Amidation

Amidation, or the addition of an amide group, can occur on the C-terminus of a protein.

32.5.4 Glycosylation

Eukaryotic cells often glycosylate (attach a carbohydrate) their proteins. Asparagine (N) is most often glycosylated on its side chain nitrogen when it is two residues upstream of serine (S) or threonine (T) (i.e. N-X-(S/T)). Serine and threonine can also be glycosylated on their side chain oxygen.

32.5.5 Lipidation

Lipidation is the attachment of a lipid to a peptide. This often occurs to facilitate membrane-binding of proteins.

32.5.6 SUMOylation

32.5.7 Folding

Protein folding is facilitated by chaperone proteins such as heat shock proteins and chaperonins. In eukaryotes, Hsp60 and Hsp10 are the structural and functional equivalents to the classical *E. coli* GroEL and GroES. However, Hsp70 is the most abundant.

32.5.8 Protein degradation

See subsection 39.8.3.

Chapter 33

Tissue morphology

The entire body is composed of:

1. epithelial tissue
2. connective tissue
3. muscle tissue
4. nervous tissue

and these tissues in turn are composed of:

1. cells
2. extracellular matrix
3. body fluids

Parenchymal cells are those cells that perform the function of their organ, as opposed to "secondary" tissues such as structural tissues. This term seems quite overly simplistic, but still occurs in the literature.

In general, molluscan cells are 10-20 up to 50 μm in diameter, though, of course, wide variations exist.

33.1 Epithelial tissue

Epithelia are the cells that line the entire body (and GI tract) and compose the secretory cells in glands. They are polarized, with a basolateral side facing the basement membrane (a thin sheet of extracellular matrix) upon which the tissue attaches and an apical side facing the external environment. There is little connective material between cells (i.e. they are tightly packed together) and no vascularization. Oxygen is supplied by diffusion.

33.1.1 Covering epithelia

Covering epithelia support diffusion into/out of the body, absorb or secrete substances, and physically protect underlying tissue.

Covering epithelial cells can be either squamous, cuboidal, or columnar and these can be singular (simple), stacked (stratified), or appear to be stacked but actually singular (pseudostratified).

Simple squamous epithelia are rather metabolically inactive and serve as a minimal diffusion boundary to the outside.

Stratified epithelia are often stacked with squamous cells on top, cuboidal cells in the middle, and columnar cells on the basement membrane.

33.1.2 Glandular epithelia

During development, epithelia sometimes proliferate and project into the underlying tissue. When they retain a duct to the outside surface, they are exocrine glands (e.g. sweat glands) but when the duct to the outside is closed, they are endocrine glands, excreting substances into the blood.

33.2 Connective tissue

Connective tissue is composed of a mixture of cells and extracellular matrix. The extracellular matrix is composed of protein fibers and polysaccharide matrix. Often, the dominant volume of connective tissue is ECM rather than cells.

Connective tissues each have a distinctive cell type that synthesizes both the extracellular matrix and collagen around it. These may be called fibroblasts (fibrous tissue), chondroblasts (cartilage), or osteoblasts (bone).

33.2.1 Fibrous connective tissues

Fibrous (or proper) connective tissues are quite fibrous, in general.

Different kinds of proper connective tissues are distinguished by the composition of their ECM fibers and ground substance.

33.2.1.1 Loose connective tissues

Loose connective tissue is characterized by cells that are sparsely spread throughout a special kind of ECM containing fibrous proteins and an amorphous mass of proteins known as "ground substance". Blood vessels run through loose connective tissue to provide nutrients and gas exchange to surrounding tissues.

Macrophages are considered loose connective tissue.

Adipose tissues are considered loose connective tissue and appear empty in H&E staining because the cells are full of triglyceride droplets and the nuclei are pushed close to the cell membrane. At least in humans, during fat gain the number of cells does not increase, just the size of them.

33.2.1.2 Dense connective tissues

Dense connective tissues (e.g. tendons, ligaments) have lots of collagen fibers in their ECM, which makes them very stiff.

33.2.2 Special connective tissues

Each of the special connective tissues have unique composition of their extracellular matrices.

33.2.2.1 Blood

The ECM of blood is plasma.

33.2.2.2 Cartilage

Cartilage is composed of a single cell type, chondrocytes, which produce their ECM mainly of collagen and proteoglycans such as chondrin. Cartilage can resist compression so well because it has a high water content in its ECM and water is incompressible. Cartilage lacks blood vessels in the main bulk of the tissue (at least in vertebrates).

33.2.2.3 Bone

Bone is composed of osteocytes that produce their ECM mainly of collagen and calcium salts.

33.3 Muscle tissue

Muscle tissue is unique in that it can contract. Actin and myosin are found in other tissues but are not as abundant or consistently arranged as in muscle.

Multipotent muscle cells are known as myosatellite cells.

Free-floating molecules diffuse 2x slower radially (across the width of myocytes) than axially (across the length of myocytes) because they are running into all the axially-oriented filaments (Kinsey et al., 2007).

33.3.1 Transparency

Transparent muscle tissue has larger myofibrils than opaque tissue.

33.4 Nervous tissue

Multipotent nervous cells are known as neural stem cells.

33.4.1 Neurons

See subsection 51.5.4.

33.4.2 Neuroglia

See subsection 51.5.4.

33.5 Extracellular matrix

33.5.1 Fibrous proteins

Extracellular matrix contains a combination of polysaccharides and proteins. Among those proteins are fibrous proteins, chiefly collagen and elastin. Both are created by cells known as fibroblasts. The functional difference between collagen and elastin is that collagen makes things stiff while elastin is stretchy.

33.5.1.1 Collagen

Collagen is by far, the most abundant protein in at least the human body.

Collagen can be slack, but when put under stretching force will straighten out but not stretch much at all beyond their straight length.

33.5.1.2 Elastin

Unlike collagen, elastin can be slack, but when put under stretching force, will stretch and recoil back to its original length after the stretching force is removed.

33.5.1.3 Reticulin

Reticulin does not provide a lot of mechanical strength like collagen and elastin do. Tissues with lots of reticulin probably do not undergo much mechanical forces.

33.5.2 Microcirculation

The composition of the interstitial fluid surrounding tissue cells is influenced by both the cells and the blood. The high pressure blood entering the capillary at the arteriole pushes water and small molecules through gaps in the endothelial lining of the capillary. This adds new material to the interstitial fluid. However, this removal also increases the osmolarity of the remaining blood in the capillary, and thus, by the time the blood reaches the venuole end of the capillary and its blood pressure is lower, then osmotic pressure will return water and small molecules back into the blood. This creates a “microcirculation” and gradual turnover of interstitial fluid.

Chapter 34

Metabolism

All animals (except a cnidarian parasite of fishes; Yahalomi et al., 2020) utilize aerobic respiration and consume oxygen. There are other anaerobic eukaryotes, but they are all single cellular.

Generally, 1 μmol O_2 generates 0.5 J of energy (Wells and Clarke, 1996). In aerobic metabolism, generally each O_2 molecule produces 5-6 ATP.

Fishes turnover their ATP supply approximately once a minute. Therefore, if ATP supply is depressed, [ATP] drops rapidly if ATP demand is not immediately depressed as well (Nilsson and Östlund-Nilsson, 2008).

34.1 Microcirculation

At least in humans, non-pulmonary cells typically have $[O_2]$ = 20-120 μM, while the mitochondrial $[O_2]$ = 1.5-3 μM.

34.1.1 Krogh cylinder model

The Krogh-Erlang cylinder model is based on vertebrate red muscle, where capillaries are unbranched and equidistant supplying the muscle. It assumes tissue M_{O_2} is constant and uniform, capillary P_{O_2} is constant and uniform, there is no longitudinal O_2 diffusion, and no globin-facilitated diffusion. Given those assumptions:

$$P(r) = P_{O_{2cap}} - \frac{M_{O_2}}{2K}\left(R_t^2 \times \ln\frac{r}{R_{cap}} - \frac{r^2 - R_{cap}^2}{2}\right)$$

P(r) P_{O_2} in tissue that is at r(kPa)

r distance from center of capillary (μm)

$P_{O_{2cap}}$ capillary P_{O_2} (kPa)

M_{O_2} tissue metabolic rate (μmol $O_2 \cdot \mu m^{-3} \cdot hr^{-1}$)

K Krogh diffusion coefficient (μmol $O_2 \cdot \mu m^{-2} \cdot \mu m \cdot kPa^{-1} \cdot hr^{-1}$)

R_t tissue radius (μm)

R_{cap} capillary radius (μm)

When the above assumptions are not acceptable, there are a number of modifications that can be made to recalculate with fewer assumptions. Some of these calculations can be found at (Goldman, 2008).

34.1.2 Globins

Most animals possess some sort of globin for oxygen storage and transport in tissue. The globins may be monomers (as in myoglobin), dimers (as in some insects), tetramers (as in vertebrate RBC hemoglobin), or polymers (as in some invertebrate intracellular globins) (Bashford et al., 1987). Molluscan tissue globins are generally monomeric, though there are exceptions such as dimeric globins in some gastropods (Bonaventura and Bonaventura, 1983).

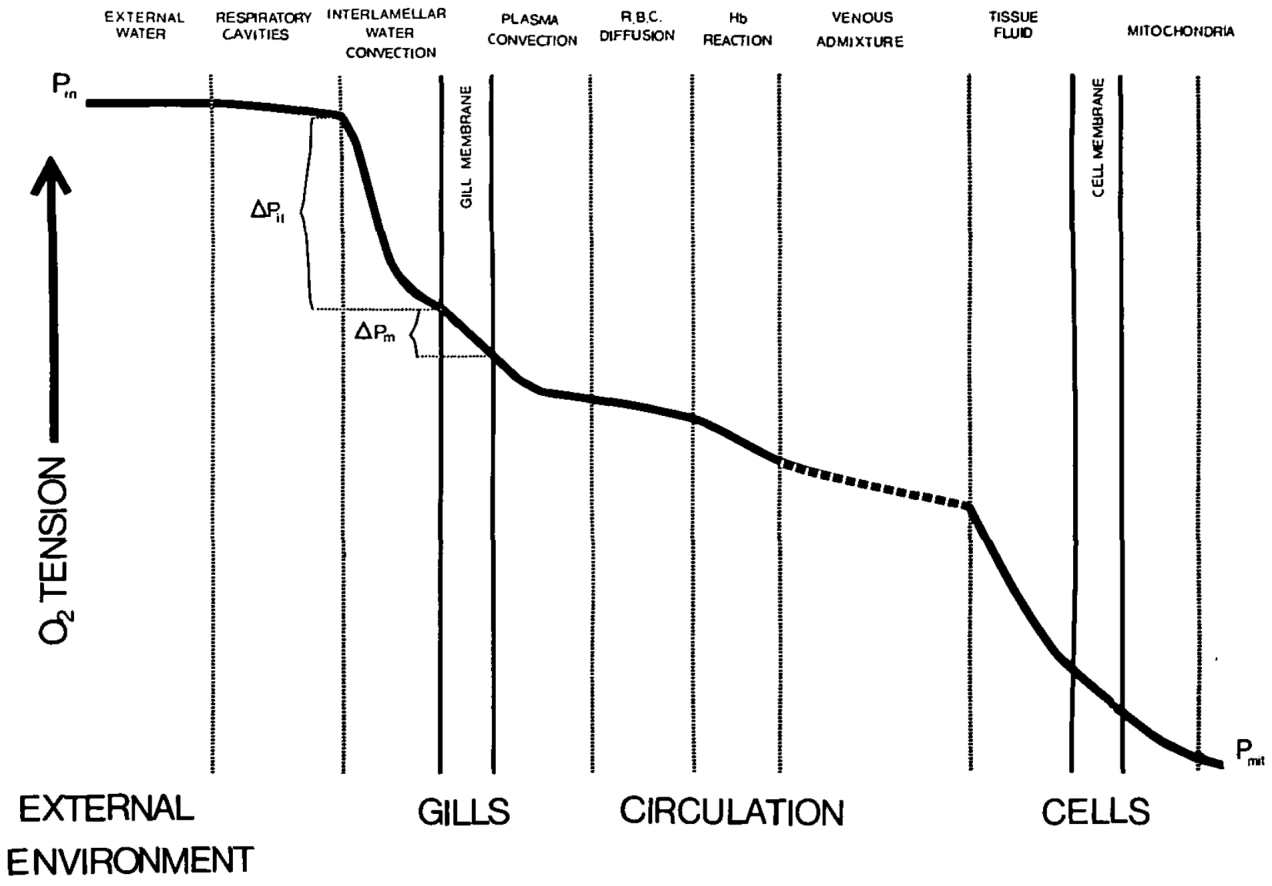

Figure 34.1: Generalized oxygen cascade. Model intended for fishes (RBCs, hemoglobin) but general idea is applicable for cephalopods as well. Figure from Hughes 1973.

Table 34.1: Krogh cylinder radii (μm)

Tissue	Radius (μm)	Reference
Sepia vertical lobe	28	(Abbott and Miyan, 1995)
Sepia optic lobe	20	(Abbott and Miyan, 1995)
Rat brain cortex	20	(Abbott and Miyan, 1995)
Sepia funnel muscle	32	(Abbott and Miyan, 1995)
Sepia tentacle muscle	61	(Abbott and Miyan, 1995)
Rat red muscle	9	(Abbott and Miyan, 1995)
Rat white muscle	41	(Abbott and Miyan, 1995)

In addition to storing oxygen, globins also help regulate O_2 flux rate from the blood into the cell by regulating the intracellular P_{O_2}, and thus, the ΔP_{O_2} between blood and cytoplasm.

In vertebrates, both red skeletal and cardiac muscle are rich in myoglobin. Gastropods are known to have globins in their radular muscle, heart, and nerves (Bonaventura and Bonaventura, 1983).

Although neuroglobins (Burmester et al., 2000) seem to be exclusive to vertebrates, molluscs (as well as arthropods, nemerteans, and nematodes) are known to possess nerve hemoglobins in high concentrations (mM) that store and transport oxygen (Dewilde et al., 2006). Mouse total brain extract has a neuroglobin concentration of ~2 μM, while retinal [neuroglobin] is 100-200 μM (Schmidt et al., 2003). Neuroglobins differ from hemoglobins in that the neuroglobins diverged from the myo/hemoglobin line early on (Burmester et al., 2000). Additionally, it seems to have a very low P_{50} (0.25 kPa in bivalve, 0.5 kPa in *Aplysia*; Wittenberg et al., 1965; Dewilde et al., 2006), on par with vertebrate myoglobin.

As an apparent adaption to hypoxic environments, cyprinid fishes (e.g. carp and goldfish) have duplicated their myoglobin gene to have two paralogs (Roesner et al., 2008).

In bivalves, nerve hemoglobin has been demonstrated to maintain neuronal excitability under anoxia for up to 30 minutes compared to only a few minutes without (Kraus and Colacino, 1986). In some molluscs, this nerve hemoglobin is only expressed in the glial cells, while in other molluscs, it also is expressed in the neurons themselves (cited in (Dewilde et al., 2006)).

At least in some diving animals (i.e. pinnipeds and birds but not cetaceans), the myoglobin P_{50} is highly correlated with diving duration (Wright and Davis, 2015), suggesting a functional benefit to hypoxia tolerance through lower P_{50}.

Globins have been shown to protect cells from reactive oxygen species (Nayak et al., 2009).

Monomeric globins have the following O_2 saturation:

$$\%\,\text{saturation} = \frac{P_{O_2}}{P_{O_2} + P_{50}}$$

34.1.2.1 Structure

Globins are globular proteins (132-157 residues) that possess 8 alpha helices (A through H, defined by Bashford et al., 1987) that compose a "globin fold" in which, the iron of a heme group covalently binds (Weber and Vinogradov, 2001) on the "proximal" F8 histidine. There is also a "distal" E7 histidine that interacts with the heme from the other side, stabilizing the oxygen-heme bond. The heme lies within a hydrophobic pocket and interacts with numerous nonpolar residues in the pocket. The so called "distal pocket" is an opening through which oxygen (or other ligands) can enter and exit the protein. At least in myoglobin, the distal pocket is closed off in low energy states and, thus, the fluctuations of the side chains (especially the distal histidine) gates the availability of the oxygen to enter the protein and bind to the heme (Tomita et al., 2010; Wright and Davis, 2015). There are also four so-called "Xe pockets" through which oxygen may also be able to reach the heme (Tomita et al., 2010).

All globins tend to be highly conserved in their tertiary structure but primary sequence can vary widely depending on the functional need of the protein (Naylor and Gerstein, 2000).

34.1.2.2 Globins can facilitate O_2 diffusion

Without globin-facilitated diffusion, the flux of oxygen through tissue can be described by:

$$\text{flux} = D_{O_2}\alpha_{O_2}\nabla P_{O_2}$$

whereas, when globin facilitated-diffusion is incorporated, the flux rate becomes:

$$\text{flux} = D_{O_2}\alpha_{O_2}\left(1 + \frac{D_{\text{globin}}C_{\text{globin}}}{D_{O_2}\alpha_{O_2}}\frac{P_{50}}{(P_{O_2} + P_{50})^2}\right)\nabla P_{O_2}$$

D_{O_2} O_2 diffusion coefficient ($K = D_{O_2}\alpha_{O_2}$)

α_{O_2} O_2 solubility coefficient ($K = D_{O_2}\alpha_{O_2}$)

D_{globin} globin diffusion coefficient

C_{globin} oxygen binding capacity of the globin

∇P_{O_2} gradient (partial derivatives in x, y, and z) of P_{O_2}

34.1.2.3 Neuroglobin adaptation to hypoxia

Hypoxia-tolerant subterranean mole rats have 3x as much neuroglobin protein and 2x as much cytoglobin protein in their CNS neurons than hypoxia-sensitive rats (Avivi et al., 2010). Goldfish have 5x as much neuroglobin protein in their brains as zebrafish (Roesner et al., 2008). However, seal neurons have just as much neuroglobin protein as mouse and rat (Mitz et al., 2009), suggesting that adaptive up-regulation is not a universal adaptation. Although the concentration in neurons may or may not increase in hypoxia-tolerant taxa, neuroglobin expression has spread from just neurons (in most mammals) to both neurons and glia in mole rats (Avivi et al., 2010) and seals (Mitz et al., 2009; Schneuer et al., 2012), suggesting globins provide hypoxia-protective benefits. Cetaceans, however, maintain neuroglobin protein expression in just the neurons, not the glia, suggesting that different strategies evolve differently for each hypoxia-tolerant taxon (Schneuer et al., 2012).

34.1.2.4 Human globin diversity

- Cytoglobin (CYGB, human chromosome 17, Burmester et al. 2002) (fibroblasts, neurons OR ubiquitous)
- Neuroglobin (NGB, human chromosome 14, Burmester et al. 2000) (neurons, endocrine)
- Myoglobin/hemoglobin
  - Myoglobin (MB, human chromosome 22) (striated and cardiac muscle)
  - Hemoglobin
    - Alpha globin gene cluster in order from 5' to 3' (human chromosome 16)
      - zeta (HBZ) (some embryonic yolk sac Hb is $\zeta_2\epsilon_2$ = hemoglobin E Gower-1)
      - pseudozeta (HBZP1)
      - mu (HBM) (transcribed in RBCs at 0.1% the expression of α, but no protein has ever been detected)
      - pseudoalpha-1 (HBAP1)
      - alpha-2 (HBA2) (CDS identical to alpha-1. Mainly differs in 3' UTR.)
      - alpha-1 (HBA1) (CDS identical to alpha-2. Mainly differs in 3' UTR.)
      - theta-1 (HBQ1) (expressed in fetal RBCs)
    - Beta globin gene cluster in order from 5' to 3' (human chromosome 11)
      - epsilon (HBE1) (embryonic yolk sac Hb is $\zeta_2\epsilon_2$ = hemoglobin E Gower-1 or $\alpha_2\epsilon_2$ = hemoglobin E Gower-2)
      - gamma-G (HBG2) (residue 136 = G) (most of fetal blood Hb is $\alpha_2\gamma_2$ = hemoglobin F (HbF)
      - gamma-A (HBG1) (residue 136 = A) (most of fetal blood Hb is $\alpha_2\gamma_2$ = hemoglobin F (HbF)
      - delta (HBD) (1-3% of adult blood Hb is $\alpha_2\delta_2$ = HbA_2)
      - beta (HBB) (~97% of adult blood Hb is $\alpha_2\beta_2$ = HbA_1)
- Androglobin

34.1.2.5 Teleost globin diversity

- Hemoglobin
  - alpha
  - beta
- Myoglobin (striated and cardiac muscle)
  - in cyprinids, there are two genes: Mb1, Mb2 (brain only) (Fraser et al., 2006; Roesner et al., 2008)
- Neuroglobin
- Cytoglobin
  - 1
  - 2
- Globin X (membrane-bound)
- Androglobin

Table 34.2: Amino acids, metabolites, and NH_3

metabolite $+NH_3 \rightleftharpoons$ AA
α-ketoglutarate $+2NH_3 \rightleftharpoons$ glutamate (Glu)$+NH_3 \rightleftharpoons$ glutamine (Gln)
pyruvate $+NH_3 \rightleftharpoons$ alanine (Ala)
oxaloacetate $+2NH_3 \rightleftharpoons$ aspartic acid (Asp) $+NH_3 \rightleftharpoons$ asparagine (Asn)

34.2 Amino acid oxidation

Proteins are the main source of energy and fuel for cephalopods (Lee, 1995; Speers-Roesch et al., 2016) (although some specific tissues like the brain rely much more heavily on glucose). Thus, amino acid oxidation is the most heavily utilized catabolic process (compared to glycolysis and fatty acid oxidation). This is demonstrated by atomic O:N ratios in the range of 4-20 rather than higher values such as 20-140 in carbohydrate and lipid oxidizing crustaceans (Hoeger et al., 1987) and also by much higher enzymatic activities of AA catabolic enzymes than lipid or glycolysis enzymes in muscle such as mantle and heart (Speers-Roesch et al., 2016). Cephalopods have a typical O:N ratio of 11-17 (Ikeda, 2016). Oxidized proteins can come from 3 sources: diet, typical cellular proteolysis, and starvation.

34.2.1 Ammonia removal

The first step in AA oxidation is the removal of the NH_3 group by an aminotransferase: α-ketoglutarate takes the NH_3 to become glutamate. The resulting deaminated AA is now an α-keto acid.

$$\alpha \text{ ketoglutarate} + \text{AA} \rightarrow \text{glutamate} + \alpha \text{ keto acid}$$

Glutamate's NH_3 is later removed by glutamate dehydrogenase to reform α-ketoglutarate (Wright, 1995). Because α-ketoglutarate is a metabolite in the Kreb's cycle, glutamate dehydrogenase is very important for co-regulating carbohydrate and protein metabolism.

Cephalopods excrete most of this NH_3 in its fully reduced form (rather wasteful) through the gills. The NH_3 ion is excreted through the Rhesus protein (RhP) in the gills and once it passes through the gill membrane, it binds to a H^+ excreted from the NH_3 protein which is also in the gill (the H^+ excreted comes from carbonic anhydrase in the gill membrane cells) (Hu et al., 2015).

Why is NH_3 so toxic? Buildup of NH_3 pushes the α-KG - Glu - Gln reaction towards glutamine which decreases [α-KG] and [Glu]. This in turn impairs the Kreb's cycle (due to decreased [α-KG]) and impairs neural transmission (Glu is easily converted to GABA, an important neurotransmitter). NH_4^+ also has a similar ionic radius to K^+ and thus can take potassium's place in transporters such as NKA (Na^+-K^+ ATPase) (Wright, 1995).

Table 34.2 shows some important metabolite-amino acid relationships that involve exchange of NH_3.

Some of the nitrogen that is excreted is urea as well, comprising 5-40% of N excretion in some species (Hoeger et al., 1987; Boucher-Rodoni and Mangold, 1989). But it is not closely correlated to changes in MO_2 suggesting that it is not mechanistically connected. The enzyme arginase converts arginine to urea which may be a source (Hoeger et al., 1987).

34.2.2 α-keto acid processing

The remaining AA carbon skeleton after deamination (α-keto acid) can be either converted to acetyl-CoA or one of the Kreb's cycle metabolites for further metabolism in the Kreb's cycle (ketogenic AAs), or it can be converted to pyruvate then to glucose through gluconeogenesis (glucogenic AAs). Under normal conditions, the α-keto acids are predominantly sent into the Kreb's cycle to generate NADH and $FADH_2$ for oxidative phosphorylation. Figure 34.3 shows the pathways through which each AA enters the Kreb's cycle or gluconeogenesis.

The composition of AAs that are utilized during metabolism can be species-specific (Pörtner et al., 1993) but proline is generally important.

34.2.2.1 Ketogenic amino acids

Ketogenic amino acids can be degraded into acetyl-CoA

34.2.2.2 Glucogenic amino acids

Glucogenic amino acids are converted into glucose

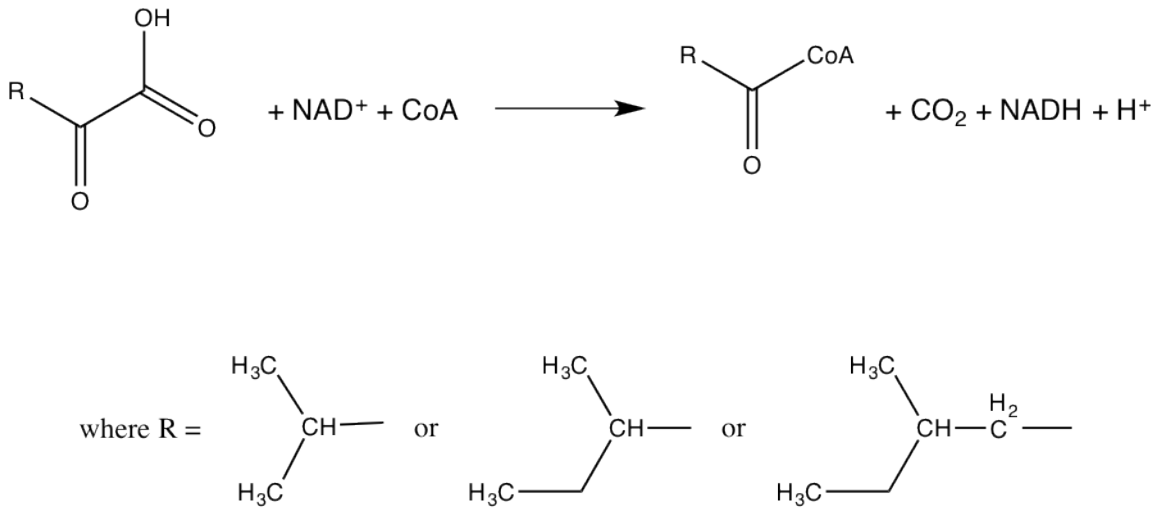

Figure 34.2: BCKDC reaction

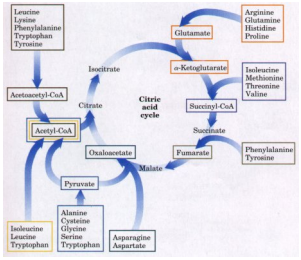

Figure 34.3: Catabolic pathways of different amino acids

34.2.2.3 Branched chain processing

Amino acids with branched side chains (Iso, Leu, Val) are processed by the branched-chain α-ketoacid dehydrogenase complex (BCKDC) which is an enzyme complex on the mitochondrial inner membrane.

34.3 Glycolysis

Input 1 glucose, 2 ADP, 2 NAD^+

Output 2 pyruvate, 2 ATP, 2 NADH

Conversion of glucose to CO_2 is favorable in the first place because the bonds holding glucose together are weaker than the bonds holding CO_2 together.

The energetic state of any carbon-containing compound can be determined from its e^- : C ratio. The more electrons the compound has, the more redox reactions it can go through, and the more energy it can create. Lipids have a higher e-/C ratio which is why they are better energy storage molecules than carbohydrates. Conversion of glucose to CO_2 through glycolysis and the Kreb's cycle removes 24 electrons. Thus, glucose starts with an e^- : C ratio of 4 and CO_2 ends with 0.

Although cephalopods do not utilize glycolysis and carbohydrate metabolism much under aerobic metabolism (at least in muscle) (Lee, 1995), the process is used extensively for anaerobic conversion of glycogen stores to octopine (Seibel et al., 2014). Based on hexokinase activity, brain tissue utilizes glycolysis much more than muscle (Abbott and Miyan, 1995).

34.3.1 Glycogen

Carbohydrate stores are not maintained as glucose because this would result in an extremely high [glucose]. Instead, the glucose molecules are chained together as glycogen. When needed, glycogen can be broken down one glucose at a time by the smooth ER. Unlike in mammals, cephalopod glycogen is stored primarily in the muscle cells for immediate use, rather than having main stores in the digestive gland.

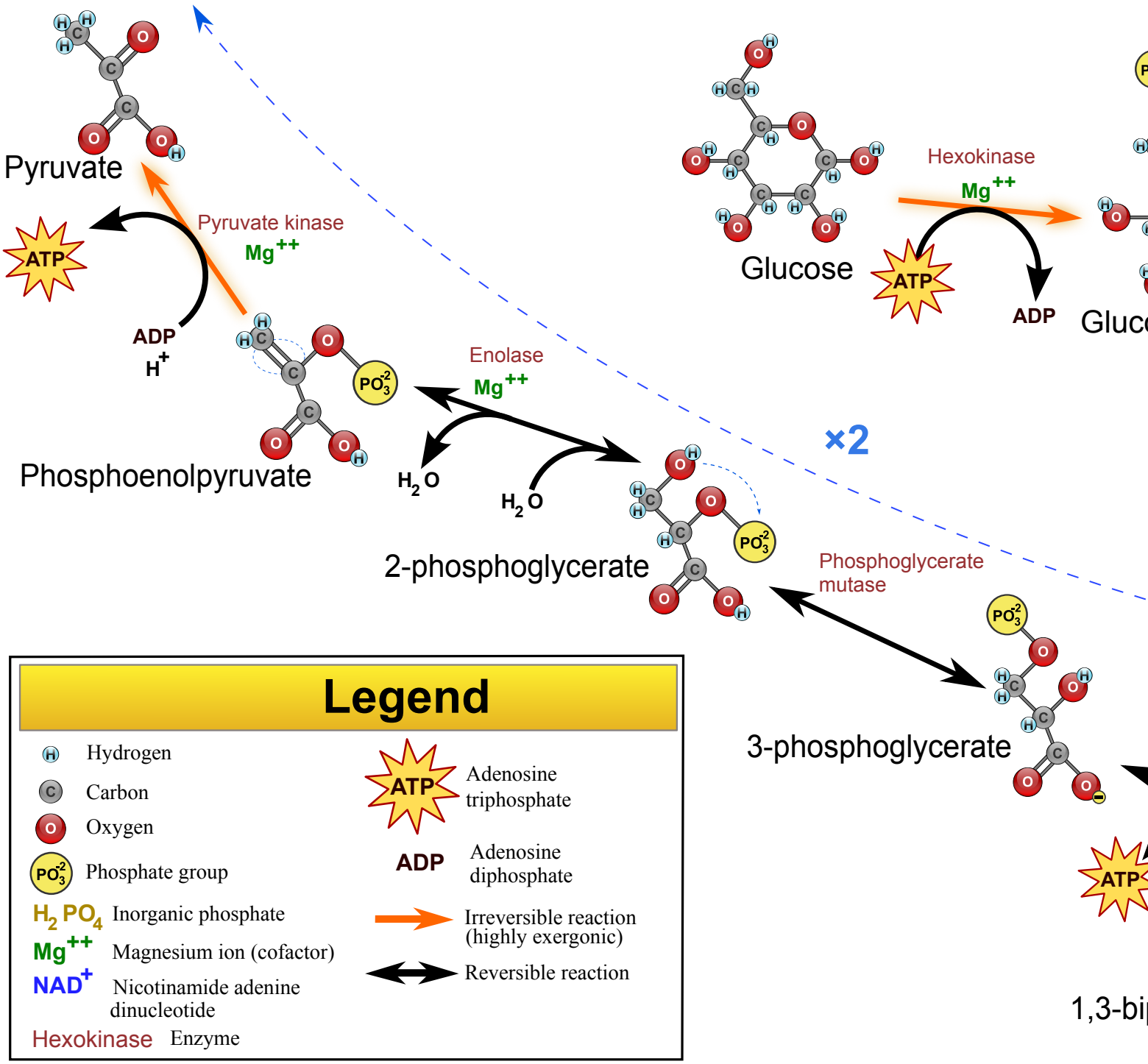

Figure 34.4: Glycolysis

34.3.2 Regulation

Hexokinase, the first enzyme in glycolysis, has a K_m that is 2-3 orders of magnitude lower than typical intracellular glucose concentration of ~10 mM. This results in any hexokinase in the cell always initiating glycolysis.

Glycolysis is regulated primarily by the enzyme-limiting reactions: while hexokinase is not regulated very much in muscle cells (at least in mammals?), it does regulate glycolysis in the mammalian liver. Note that since cephalopods do not store much glycogen in their digestive gland, hexokinase regulation may not be an important process in cephalopods. Glucose upregulates expression of hexokinase, while glucose-6-phosphate downregulates hexokinase.

PFK-1 is likely the most dominant regulator of glycolysis. ATP and citrate both allosterically bind to PFK-1 increasing its K_m and thus slowing glycolysis. Fructose-2,6-bisphosphate is an important metabolite that also can allosterically bind to this enzyme to change reactions from glycolysis to gluconeogenesis.

Finally, pyruvate kinase is the 3rd and final enzyme in glycolysis that is regulated. Similarly to PFK-1, it is also inhibited by its products: ATP and acetyl-CoA.

Additionally, although not technically part of glycolysis, pyruvate dehydrogenase complex (PDH) converts pyruvate to acetyl-CoA and is strongly regulated by its substrates and products.

Gluconeogenesis is opposite of glycolysis except it by-passes the enzyme limiting steps (pyruvate kinase, PFK-1, and hexokinase) because they would be so energetically unfavorable.

34.4 Lipid oxidation

Fatty acids are transported into the mitochondria with coenzyme A attached (known as fatty acyl-CoAs) and oxidized via β-oxidation: in this four-step process, the fatty acid is 1. dehydrogenated (remove 2 Hs to form double bond), 2. hydrated (add H_2O), 3. dehydrogenated again (remove the Hs to leave only O remaining), and 4. an acetyl-CoA is broken off (remove 2 carbons) to go into the Kreb's cycle. This process is repeated the entire length of the fatty acid until all its carbons are oxidized and broken apart. If a fatty acid is unsaturated or odd-numbered, there are a few more steps involved.

The fatty acid oxidation process is only regulated by the gate allowing fatty acyl-CoAs into the mitochondria. The opposing process of lipid synthesis is conducted outside the mitochondria in the cytosol.

34.5 NADH-proxy (reducing equivalent) shuttles

NADH that are produced in the cytosol (such as those by glycolysis) are unable to enter the inner mitochondrial membrane for oxidative phosphorylation directly. Instead, they must transfer their electrons to proxies which can cross the mitochondrial membrane, release their electrons inside the mitochondria, and be returned again to the cytosol. There are two primary reducing-equivalent shuttles:

34.5.1 Malate-aspartate shuttle

This shuttle converts an NADH from the cytosol to an equivalent NADH within the mitochondrial matrix.

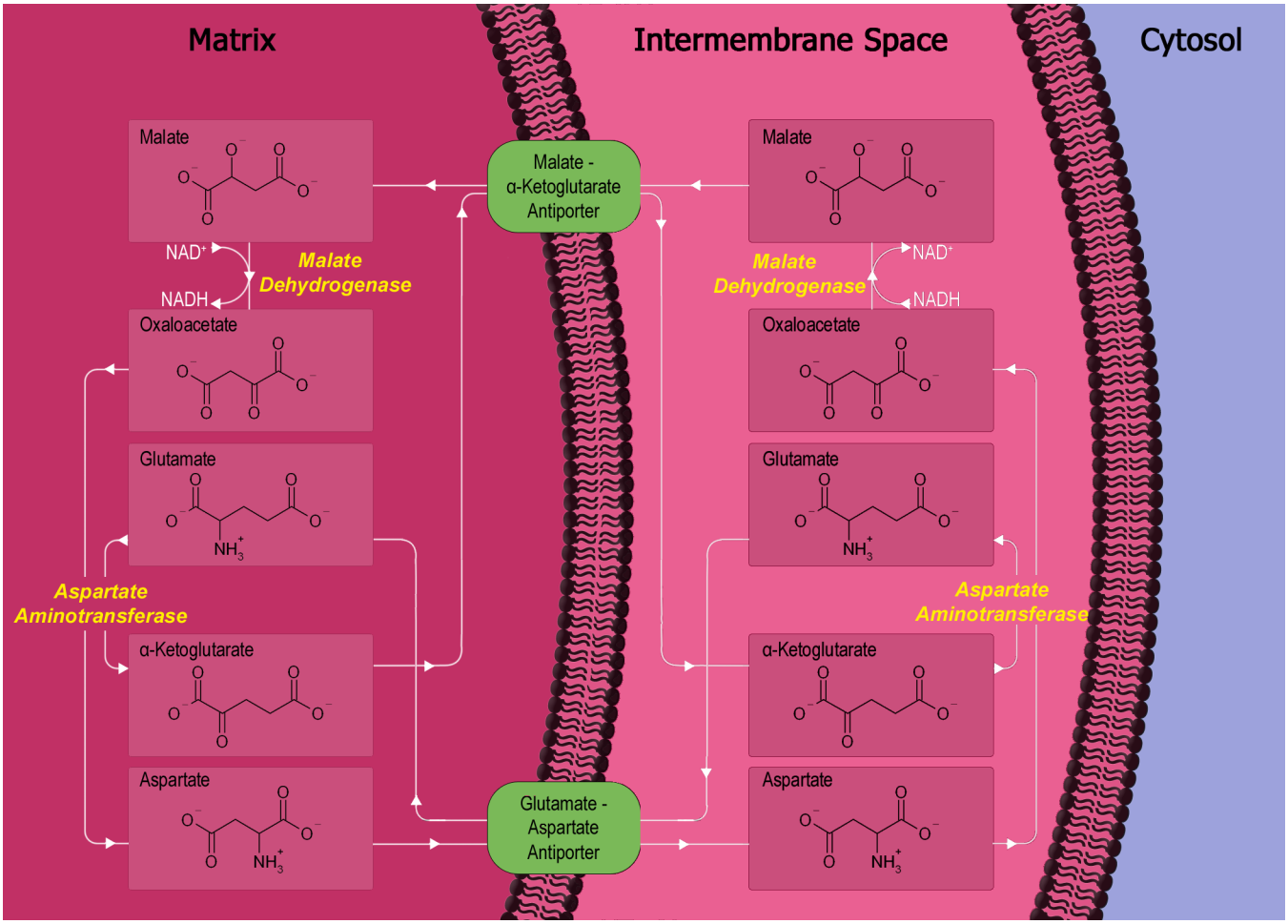

34.5.2 Glycerol-phosphate shuttle

This shuttle converts an NADH from the cytosol to an equivalent $FADH_2$ within the mitochondrial matrix.

It does so by a rather simple loop:

1. Dihydroxyacetone phosphate (DHAP) oxidizes NADH (to NAD^+) to form glycerol-3-phosphate. This is done via the enzyme known as cytoplasmic glycerol-3-phosphate dehydrogenase (GPDH-C / GPD1).
2. Glycerol-3-phosphate crosses the mitochondrial inner membrane to enter the matrix.
3. Glycerol-3-phosphate reduces FAD (to $FADH_2$) to form dihydroxyacetone phosphate (DHAP). This is done via the enzyme known as mitochondrial glycerol-3-phosphate dehydrogenase (GPDH-M / GPD2).
4. Dihydroxyacetone phosphate (DHAP) crosses the mitochondrial inner membrane to enter the cytosol.

34.6 Pentose phosphate pathway

The pentose phosphate pathway starts with glucose-6-phosphate and reduces 2 $NADP^+$ to form 2 NADPH while also forming either an intermediate product in glycolysis or ribose-5-phosphate, which is used in nucleic acid synthesis. The pathway can work in reverse as well. This is useful, for example, when glycolysis is needed and free nucleic acids can be broken down and through this pathway, added to the glycolysis pathway. The production of NADPH is an important antioxidant section 39.2. This pathway runs in the cytosol.

34.7 TCA cycle

Input 1 pyruvate, 4 NAD^+, 1 GDP

Table 34.3: Oxygen-energy conversions for ammonotelic animals in general. Data from Elliott and Davison 1975.

Substrate	J/μmol O_2	cal/μmol O_2
Protein	0.4284	0.1024
Carbohydrate	0.4726	0.1130
Lipid	0.4391	0.1050

Output 1 CO_2, 4 NADH, 1 GTP

While there are many steps in the Kreb's cycle, the important ones for ATP production are the redox reactions. Below are some highlights of the cycle:

- Citrate synthase is the first enzyme in the cycle and is an important metric for overall aerobic metabolic rate.
- The conversion of isocitrate to ∝-ketoglutarate is the CO_2 producing step (and also creates an NADH).
- The removal of coenzyme A from succinyl-CoA to form succinate is the GTP producing step.
- Conversion of succinate to fumarate produces an $FADH_2$.
- Conversion of malate to oxaloacetate produces an NADH.

Amino acids also feed into the Kreb's cycle as metabolites.

Citrate synthase (CS) activity is correlated to mass-specific O_2 consumption rate in cephalopods such that it is a good metric for RMR (Seibel and Childress, 2000; Seibel et al., 2000b). This is true both interspecifically, and intraspecifically throughout ontogeny (assuming the tissue in which CS activity is measured does not change in relative important through ontogeny; see Seibel et al. 1998).

34.8 Oxidative phosphorylation (OP)

The proton gradient between the intermembrane space and matrix of the mitochondria creates a ΔpH near 0.75. A common metric for the efficiency of O_2 utilization is the P:O ratio, or the moles of ATP generated per mole O_2. This varies based on the electron transporter (e.g. NADH, $FADH_2$, etc.) and on the proton leak through the mitochondrial inner membrane. A typical P:O ratio is 2.5-3 (5-6 ATP per O_2). Each NADH produces 3 ATP and each $FADH_2$ produces 2 ATP.

The majority of O_2 consumed by an organism is utilized during oxidative phosphorylation (OP) in the cellular mitochondria. The rate of OP (and hence the rate of O_2 consumption) is controlled by the availability of its substrates: NADH, $FADH_2$, O_2, ADP, and P_i. These [substrates] are not equally influential on OP, however. Often, one or a few of these substrates are the limiting reactants while the others are available in excess. Animals that are oxyconformers are those in which OP is limited by O_2 availability. In contrast, oxyregulators are those in which OP is limited by either redox state ([NADH], [$FADH_2$]) or phosphorylation state ([ADP], [P_i])(Connett et al., 1990). An organism reaches its P_{crit} when environmental P_{O_2} is low enough to cause intracellular [O_2] to be the limiting substrate to OP (subsection 53.6.3).

34.8.1 Proton leakage

The mitochondrial inner membrane contains uncoupling proteins (UCPs) which allow protons to bypass ATP synthase and return to the matrix without producing any ATP. In endotherms, this is beneficial since it produces heat. In eukaryotes generally, it may be beneficial because overly high [H^+] in the intermembrane space (for example, when [ADP] is low and ATP synthase cannot turn) can lead to production of superoxide (Divakaruni and Brand, 2011). Proton leakage scales with body size such that smaller individuals have leakier membranes, thus lower P:O ratios, and thus higher mass-specific oxygen-consumption rates (Porter and Brand, 1993). For more information on scaling, see subsection 51.9.2.

34.9 Anaerobic pathways

Under anaerobiosis, glycogen stores are utilized extensively in cephalopods, much more than under aerobic conditions. Glycogen concentration in *Dosidicus gigas* mantle muscle is ≈ 300 μmol glucosyl units g^{-1} (Seibel et al., 2014). This may be higher than most cephalopods given this species' hypoxia-prone lifestyle. It is certainly much higher than average whole-body glycogen concentration in fishes of 5-20 μmol glucosyl units g^{-1} (Nilsson and Östlund-Nilsson, 2008).

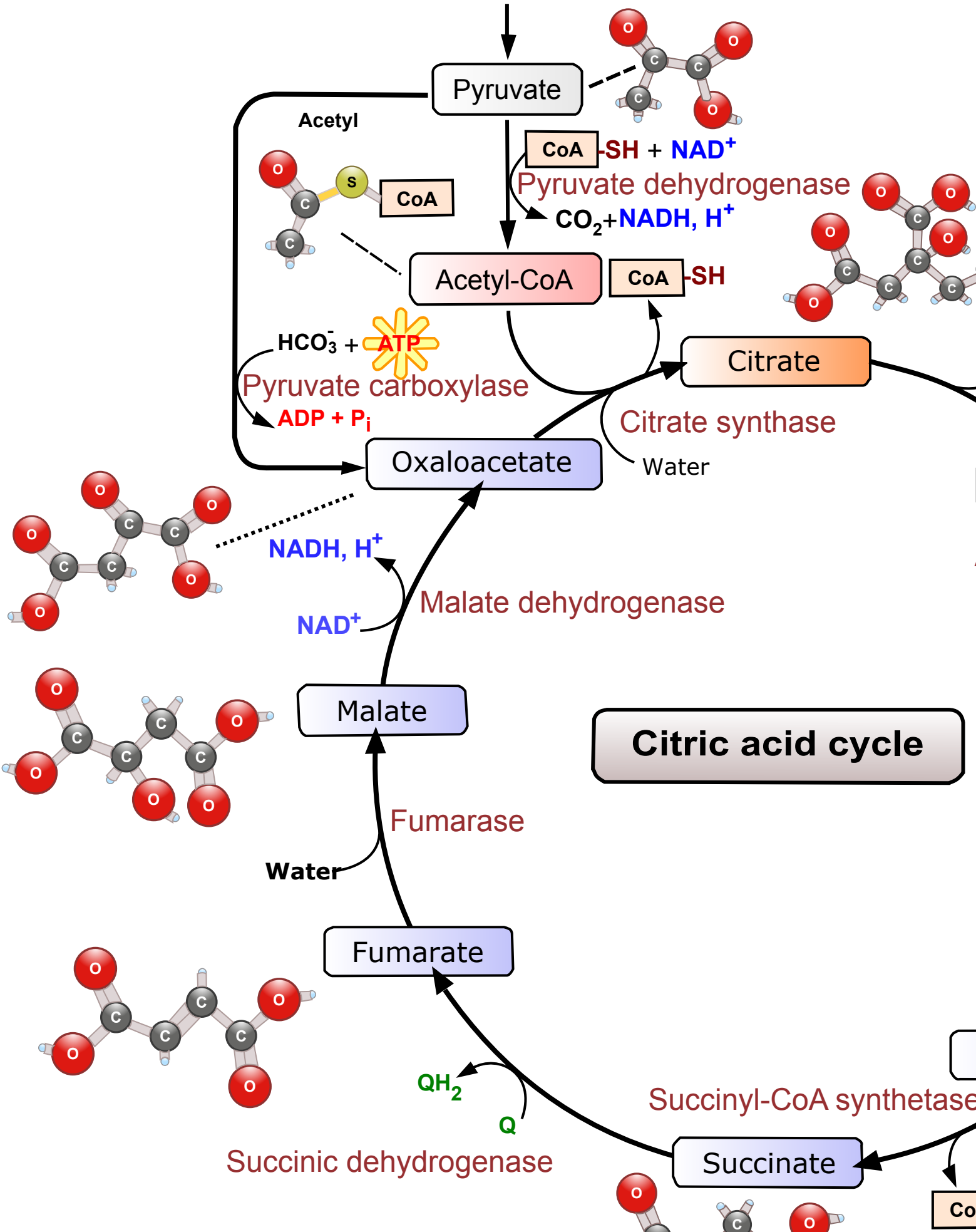
Pyruvate
Acetyl
CoA
-SH + NAD+
Pyruvate dehydrogenase
CO2+NADH, H+
Acetyl-CoA
CoA
-SH
HCO3- + ATP
Pyruvate carboxylase
ADP + Pi
Citrate
Citrate synthase
Water
Oxaloacetate
NADH, H+
NAD+
Malate dehydrogenase
Malate
Citric acid cycle
Fumarase
Water
Fumarate
QH2
Q
Succinic dehydrogenase
Succinyl-CoA synthetase
Succinate

Table 34.4: Enzymatic indicators of metabolic ability in cephalopods

Indicator	Enzyme	"Typical" maximal activity (μmol/min/g)	Re
Overall metabolic rate	Citrate synthase	Systemic heart = 8	Speers-Ro
		Mantle = 0.6	Speers-Ro
		Gill = 0.3	Speers-Ro
Catabolism			
Amino acid oxidation	Aspartate aminotransferase (AspAT)	Systemic heart = 50	Speers-Ro
		Mantle = 15	Speers-Ro
		Gill = 10	Speers-Ro
Glycolysis	Hexokinase		
Glycolysis	Glycerol-3-phosphate dehydrogenase (GPDH)		
Lipid oxidation	Carnitine palmitoyltransferase (CPT)	Systemic heart = 0	Speers-Ro
		Mantle = 0.01	Speers-Ro
		Gill = 0.04	Speers-Ro
Anaerobic glycolysis	Octopine dehydrogenase	Systemic heart = 20	Speers-Ro
		Mantle = 35	Speers-Ro
		Gill = 2	Speers-Ro
Anabolism			
Lipid synthesis	Glycerol 3-phosphate dehydrogenase (G3PDH)	Systemic heart = 1	Speers-Ro
		Mantle = 1.5	Speers-Ro
		Gill = 0.3	Speers-Ro

Cephalopods utilize octopine dehydrogenase (ODH) rather than lactate dehydrogenase (LDH) to convert pyruvate to octopine (Hochachka et al., 1975).

The efficiency of anaerobic pathways (i.e. mole ATP per mole glucose) is about 3-10% of aerobic metabolism (Nilsson and Östlund-Nilsson, 2008; Richards, 2009) since anaerobic pathways do not decrease the $e^- : C$ ratio as fully as the Kreb's cycle.

In mammals, lactate is transported out of the cell, through the blood to the liver, converted back to glucose via gluconeogenesis, then available again for the cells. This process is the Cori Cycle. A similar phenomenon may occur in cephalopods with octopine and the digestive gland (Storey and Storey, 1979; Storey et al., 1979).

34.10 Enzyme indicators of metabolic capacity

34.11 Anabolism

34.11.1 Nucleic acid synthesis

34.11.2 Glycogen synthesis

In animals, glycogen costs about 10-12 mmol ATP per gram to synthesize (Fraser and Rogers, 2007).

34.11.3 Lipid synthesis

In animals, lipid costs about 15-25 mmol ATP per gram to synthesize (Fraser and Rogers, 2007).

34.11.4 Protein synthesis

In animals, protein costs about 70-100 mmol ATP per gram to synthesize (Fraser and Rogers, 2007).

34.12 Photosynthesis

The objective of photosynthesis is to generate NADPH, and the production of O_2 is a side effect of oxidizing H_2O.

34.13 Calvin (CBB) cycle

The CBB cycle uses the RuBisCO enzyme to capture and reduce CO_2.

Chapter 35

Acid-base balance

Living organisms maintain their intra- and extra-cellular compartments within a pH range of 6.5 and 8.3 (Heisler, 1986).

Animals have very little net production of protons other than that associated with CO_2. Since CO_2 is released in its gaseous form, there is no net flux of H^+ out of animals in most situations. Some H^+ is produced from the incomplete oxidation of substrates but not much (Heisler, 1986). Protons produced by glucose oxidation (coming off the glucose) are consumed by oxidative phosphorylation (ATP synthesis absorbs H^+, reducing O_2 to H_2O, reducing cytochromes and coenzyme Q with each iteration) (Vaghy, 1979).

35.0.0.1 pH regulation mechanisms

Intracellular pH is regulated by 3 primary mechanisms: 1. use of acids/bases in metabolic reactions, 2. buffering by weak acids and bases, and 3. acid-base transport across membranes (Seibel and Walsh, 2001).

Use of acids/bases in metabolic reactions As a metabolic substrate (e.g. glucose) enters a cell, its metabolism produces H^+ through removal of hydrogens from the substrate as well as the conversion of ATP to the stronger acid ADP (section 29.1). Oxidative phosphorylation, however, compensates by converting ADP back to ATP and thus absorbing H^+ from solution (Vaghy, 1979).

In the blood, deoxygenation of hemocyanin results in the uptake of H^+ (Haldane effect).

In a hypoxic cell, the dephosphorylation of phosphoarginine absorbs H^+ and is coupled with ATP formation which also absorbs H^+. Thus, the utilization of this compound helps buffer the cell as well as provide ATP. The production of octopine also affects the H^+ pool.

Buffering The buffer value, β, can be quantified as the amount of H^+ bound to proton-acceptors per unit change in pH per liter (Heisler, 1986). This is equivalent to the increase in conjugate acid or decrease in conjugate base per unit change pH per liter.

The pK_a of a chemical is a measure of how easily it removes its proton (i.e. how strong of an acid it is) such that the smaller the pK_a, the more acidic the chemical. This influences the pH of a system or how a weak acid equilibrates in a given pH according to the Henderson-Hasselbalch equation:

$$\mathrm{pH} = \mathrm{pK_a} + \log_{10}\left(\frac{[\mathrm{A^-}]}{[\mathrm{HA}]}\right)$$

For a weak acid, its effective buffer range is $\mathrm{pK_a} \pm 1$ (conjugate base-acid ratio of 10:1 or 1:10) (Heisler, 1986). Proteins need to remain within a small pH window near their pK_a, therefore, in order to be able to (de)protonate in their reactions.

Physiologically relevant buffers are (Heisler, 1986):

Table 35.1: Comparisons of acid-base parameters in intracellular vs. extracellular compartments. Since cephalopods have extracellular respiratory proteins, the differences are not as large as in most other animals (Pörtner and Reipschläger, 1996).

Compartment	pH	$[HCO_3^-]$	β
Extracellular	↑	↑	↓
Intracellular	↓	↓	↑

Table 35.2: Weak acids relevant as acid-base buffers in cephalopods

Buffer	Reaction	pK_a at T=25 ºC, S=35 psu	pK_a at T=10 ºC, S=35 psu
H_2CO_3	$H_2CO_3 \rightleftharpoons HCO_3^- + H^+$	5.85	5.99
HCO_3^-	$HCO_3^- \rightleftharpoons CO_3^{2-} + H^+$	8.97	9.21
$H_2PO_4^-$	$H_2PO_4^- \rightleftharpoons HPO_4^{2-} + H^+$	5.97	6.09
NH_4^+	$NH_4^+ + OH^- \rightleftharpoons NH_3 + H_2O$	9.27	9.80
Imidazole		6-7.5	
Cysteine		7-8.3	
Terminal NH_2 groups		7.4-8.5	

- Polypeptide residues: histidine (imidazole group specifically), cysteine, and terminal NH_2 groups
- Phosphates: ATP and constituents, dissolved inorganic phosphate (DIP)(subsection 3.3.1), and organic phosphates
- Dissolved inorganic carbon

Buffering capacity of a physiological fluid is constant over physiological pH spectrum even though the buffering capacity of the individual component buffers are each highly pH sensitive. But with all components present, the overall capacity remains quite constant.

Buffers are divided into bicarbonate buffering ($\beta_{\text{Bic}} = -\Delta[HCO_3^-]/-\Delta\text{pH}$) and non-bicarbonate buffering ($\beta_{\text{NB}} = \frac{-(\Delta B_1^- + \Delta B_2^- + ... + \Delta B_n^-}{-\Delta\text{pH}}$ where B_i^- represent the conjugate bases of the buffers above. Bicarbonate buffering has higher capacity because it is an open system (CO_2 can leave) compared to the other closed system buffers (Heisler, 1986). Over short timeframes non-bicarbonate buffer concentration remains constant while DIC concentration can vary quickly (Heisler, 1986).

The bicarbonate and non-bicarbonate buffer systems share a common H^+ pool. Therefore, when non-bicarbonate buffers absorb H^+ they push the following reaction forward: $CO_2 + H_2O \rightleftharpoons HCO_3^- + H^+$ which results in non-bicarbonate buffers increasing the concentration of HCO_3^- (Heisler, 1986).

In cephalopods, there are a few primary weak acids that are important in acid-base balance. These are shown in Table 35.2. Because the pK values vary so much, all the non-bicarbonate buffers together provide a rather continuous β_{NB} over a broad pH range (Heisler, 1986).

Octopine dehydrogenase (ODH) activity is strongly correlated with buffering capacity in cephalopods (Seibel et al., 2000b) such that it is a good metric for buffering capacity. As one would expect, highly active taxa have higher buffering capacity than more sedentary taxa because they need to be able to buffer muscle-induced acidosis.

Transmembrane acid-base transport Often either H^+ or HCO_3^- are transferred across membranes to control acid-base balance (Heisler, 1986). At equilibrium (i.e. if carbonic anhydrase is present), removing a H^+ is equivalent to adding a OH^- or HCO_3^- (Heisler, 1986).

35.0.0.2 Alpha-stat hypothesis

In order to protect enzymatic function, physiological pH decreases with increasing temperature by roughly 0.02 pH units per ºC (Hochachka and Somero, 2002; Howell and Gilbert, 1976). According to the alpha-stat hypothesis (Reeves, 1977), this correlated change maintains the fractional dissociation (α) of the imidazole side-chain of histidine residues near 0.5 so that those residues can continue to respond appropriately under the new temperature (**??**). Increased temperature would cause more hydrogens to disassociate from the imidazole but this is countered by the lower pH which favors hydrogen to stay on the imidazole. Unintuitively, although the pH decreases, the tissues do not become more "acidic". This is because the decrease in pH is caused by increased temperature dissociating water molecules. While this reaction produces H+, it also produces OH- in equal amounts, thus maintaining the system's acidity.

35.0.0.3 Carbonic anhydrase

Carbonic anhydrase is a ubiquitous enzyme found in all animals. It accelerates the conversion between CO_2 and HCO_3^- which, uncatalyzed, has a half-reaction rate of 30 seconds to 5 minutes (Kern, 1960)! There are many different isoforms of CA. Cytosolic CA (cCA) is often found in the cytosol of gill epithelia but CA_{IV} has also been found on the membrane of pillar cells in the gills which converts the HCO_3^- in the blood.

35.0.0.4 Effect of pH on cells

The protonation of protein residues is directly affected by pH such that enzymes (and thus metabolic processes) can be turned on or off directly by pH.

One example of the effect of pH on enzyme function is for lactate dehydrogenase, an enzyme functionally equivalent to octopine dehydrogenase that is found in mammals. In this enzyme, one of the key residues for binding to pyruvate has a pK near intracellular pH. Therefore, when pH drops in the cell under hypoxia, the residue is protonated which makes pyruvate binding amenable. Conversely, lactate can only bind to be converted back to pyruvate under high pHi conditions when the residue is unprotonated. In this way, enzymes can be controlled directly by pH.

Chapter 36

Neurobiology

36.1 Electrical principles

A single monovalent ion has a charge of 1.602×10^{-19} coulombs.

Potential volts (V)

Current amperes (A) = 1 coulombs per sec

Resistance ohms (Ω)

Conductance siemens (S)

Capacitance farads (F) = 1 coulombs per volt

Power watts (W) = 1 J/s

Ohm's law states that:

$$V = IR = \frac{I}{G} \tag{36.1}$$

where V is voltage, I is amperage, R is resistance, and G is conductance.

36.2 Neuroanatomy

Nervous tissue is composed of neurons (transmits information) and neuroglia (wrap around neurons).

Dendrite structures attached to the soma which receive incoming neurotransmitters

Soma the main neuron cell body. Also known as the perikaryon.

Axon structure which transmits outgoing action potentials

Collateral a branch of the axon. Axons can branch multiple times to form many connections.

Most neurons produce and release only one neurotransmitter but can receive many via different receptors on the dendrites.

Neurons can be unipolar, bipolar, or multipolar, based on the number of projections from the cell body (e.g. dendrites or axons). Most cephalopod neurons are unipolar (Budelmann, 1995). A single projection proceeds from the cell body and splits, with one direction being the upstream equivalent of dendrites and the other direction functioning as the downstream axon (Brown and Piscopo, 2013).

Because axons can be very long, substances do not diffuse passively between the synapse and soma. Rather, they are moved by motor proteins on microtubule networks. Kinesin motor proteins move substances from the soma to the synapse and dynein motor proteins move substances from the synapse back to the soma often for degradation. These are the only means of delivery to the axon since all proteins are synthesized in the cell body (Hirokawa, 1998).

In most cell types, the vast majority of translation occurs on the rough ER. In neurons, however, (in mammals at least), much translation occurs via free ribosomes in the dendrites and axons (O'Carroll and Schaefer, 2013).

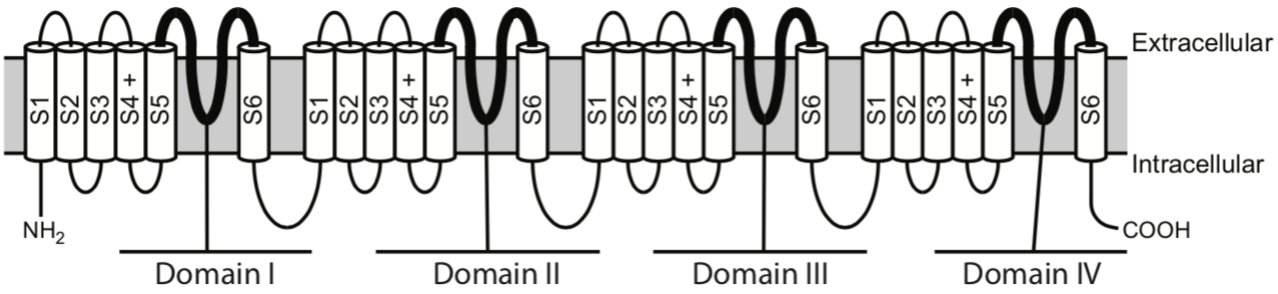

Figure 36.1: VGSC α subunit.

36.3 Ion channels and pumps

It is believed that the first voltage-gated ion channels to evolve were the single domain K_v channels from which evolved the four domain Ca_v channels from which evolved the four domain Na_v channels (Zhou et al., 2004; Zakon, 2012).

36.3.1 Na^+/K^+-ATPase (NKA)

See subsubsection 30.2.2.1.

36.3.2 Voltage-gated Na^+ channels (Na_v channels; VGSCs)

All invertebrates possess two VGSC orthologs: Na_v1 and Na_v2. The first is orthologous to the vertebrate VGSC family and responds to the voltage membrane potential. The second is selective for both Na^+ and Ca^{2+} but much more so to Ca^{2+} (Zhou et al., 2004). It is still considered a Na_v because it evolved from other Na_v channels even though the selectivity filter has changed its function (Zakon, 2012).

VGSCs evolved from VGCC and thus share highly similar structure (Zakon, 2012). Na_v channels are composed of α and β subunits, though only the former is needed for basic functions. The α subunit has four repeated domains each with six transmembrane segments (S1-S6) (Figure 36.1). In each domain, S4 has many positively charged residues which allows it to sense voltage. The S4 motifs in domains I through III trigger activation, while domain IV S4 triggers inactivation (Zakon, 2012). The loop between S5 and S6 in each domain contain a key residue that controls selectivity for Na^+. In the four domains, the key residues are D-E-K-A, respectively for Na_v1 and D-E-E-A for Na_v2. The latter may make Na_v2 permeable to both Na^+ and Ca^{2+} (Zakon, 2012). The intracellular loop between Domain III S6 and Domain IV S1 is the gate that causes inactivation (Zakon, 2012).

36.3.3 Voltage-gated K^+ channels (K_v channels, VGKCs)

K_v channels are quaternary structures, composed of four αsubunits. Each αsubunit has six transmembrane segments (S1-S6): the first four are voltage-sensing (S1-S4) and the last two form the pore (S5-S6) (Holmgren and Rosenthal, 2015). Cephalopods possess K_v1 and K_v2 family channels (Holmgren and Rosenthal, 2015).

36.3.3.1 mRNA editing

Cephalopod K_v channels are highly edited by ADARs (subsection 32.3.7). For example, the K_v1 mRNA has 14 non-synonymous edits in *Doryteuthis* and 19 in *Octopus.* These editing sites occur in the tetramerization domain, S1, S3, and S5 segments that affect the mutual affinities of subunits to form the quaternary structure, voltage threshold of activation, and closing kinetics (Rosenthal and Bezanilla, 2002; Holmgren and Rosenthal, 2015). The K_v2 mRNA has over 12 editing sites in *Doryteuthis* including non-synonymous edits in S4 and the pore (Patton et al., 1997). Edits around the pore alter channel closing and inactivation rates. Among all coleoids examined, there are 34-55 editing sites on K_v2 transcripts, with 5 sites shared by all coleoids (Liscovitch-Brauer et al., 2017).

36.3.4 Voltage-gated Ca^{2+} channels (Ca_v channels, VGCCs)

Ca_v channels are quaternary structures composed of a variety of subunits. The main subunit, α_1, is composed of four identical domains, each with six transmembrane segments. Together this subunit has voltage-sensitivity function and forms the pore

through which Ca^{2+} travel. Ca_v channels spontaneously inactivate (like K_v channels) but the inactivation only occurs after closing and is influenced by $[Ca^{2+}]$ (Holmgren and Rosenthal, 2015).

Homologous to the VGSC D-E-K-A, VGCCs have E-E-E-E residues that control Ca^{2+} specificity.

The α_2 and δ subunits have a modifying role on activation and inactivation kinetics as well as altering maximum current.

The β subunit is on the intracellular side of the protein and has a modifying role on activation and inactivation kinetics as well as altering maximum current.

VGCCs are not solely expressed in excitable (AP causing) cells. They are also expressed in nonexcitable cells but their function is not well understood (Pitt et al. 2021).

36.3.5 Na^+/Ca^{2+} exchanger (NCX)

See subsubsection 30.2.2.2.

36.3.6 Ionotropic glutamate receptors (iGluRs)

36.3.6.1 Structure

Cephalopods possess three kinds of ionotropic (i.e. ligand-gated) glutamate receptors (Di Cosmo et al., 2006):

- AMPA receptors (GluA) (13 genes in *O. bimaculoides* (Albertin et al., 2015))
- kainate receptors (GluK) (3 genes in *O. bimaculoides* (Albertin et al., 2015))
- NMDA receptors (GluN) (4 genes in *O. bimaculoides* (Albertin et al., 2015))

All glutamate receptors are tetrameters, with four similar subunits (Holmgren and Rosenthal, 2015). Each subunit has four transmembrane segments, or secondary structures than span across the plasmalemma (Holmgren and Rosenthal, 2015). At least among AMPA receptors (maybe all ionotropic glutamate receptors?), the quaternary structure can be composed of any combination of subunits, and the composition varies by tissue type (Holmgren and Rosenthal, 2015).

36.3.6.2 Function

iGluRs are glutamate-gated cation channels. Thus, once opened, Na^+, K^+, and Ca^{2+} can all pass across the membrane, depending on which receptor is open (NMDA is the only to allow Ca^{2+} in). Due to the influx of Na^+ and Ca^{2+}, the opening of iGluRs create EPSPs (even though K^+ can still pass out). The NMDA receptors can allow Ca^{2+} ions in, which act as secondary messengers to allow further NMDA receptor production, thus contributing to LTP.

36.3.7 Nicotinic acetylcholine receptors (nAChRs)

There are two kinds of acetylcholine receptors. The nicotinic kind are the receptors involved in neurotransmitter uptake and post-synaptic response in neurons.

nAChRs are composed of five similar but not identical subunits that form a pore. Each subunit has four trans-membrane domains. There are various forms of both α and β subunits.

36.3.8 ATP-sensitive K^+ channels (K_{ATP} channels)

See subsubsection 30.2.2.6.

36.4 Resting potential

Resting neuron membrane potential (resting E_m) is typically around -70 mV but can vary between -40 and -90 mV. This is maintained by the leakage of K^+ ions out of the neuron into the extracellular space down their concentration gradient via leakage K^+ channels. Na-K-ATPase (NKA) returns K^+ back into the cell to maintain the slow outward flux via K^+ leak channels. As a result of the NKA activity, Na^+ concentration is much higher outside the cell than inside, which creates a very strong electrochemical potential for Na^+ to flux into the cell. In fact, there are also leakage Na^+ channels but they are not as fast as the leakage K^+ channels.

The membrane potential for each ion can be quantified by the **Nernst equation**:

$$E = \frac{RT}{zF} \ln\left(\frac{[\text{ion outside cell}]}{[\text{ion inside cell}]}\right) \tag{36.2}$$

Table 36.1: Squid giant axon ion concentrations and permeabilities at rest from Hodgkin 1958. Values can vary widely so this is just an example.

Ion	Intracellular concentration (mM)	Extracellular concentration (mM)	Permeability ratio
K^+	400	20	100
Na^+	50	440	1
Ca^{2+}			
Cl^-	40	560	10

E membrane potential (V)

z ionic charge

The Nernst equation, however, does not account for the variable permeability of different ions through the membrane. If more than one ion is permeable, then all relevant ions must be considered together to calculate the net membrane potential. More permeable ions have larger influences on the total membrane potential. The **Goldman equation** accounts for such permeabilities factors:

$$E = \frac{RT}{F} \ln \left(\frac{P_K[K_{out}] + P_{Na}[Na_{out}] + P_{Cl}[Cl_{in}]}{P_K[K_{in}] + P_{Na}[Na_{in}] + P_{Cl}[Cl_{out}]} \right) \tag{36.3}$$

P_x permeability ratio of ion x. This varies by the number of activated ion-channels (see section 36.6).

Since P_K is much higher than P_{Na}, P_{Ca}, P_{Cl}, a typical neuron at rest has a membrane potential near that predicted by the Nernst equation for potassium.

36.5 Graded potentials

Graded potentials are the changes in the dendrite or soma membrane potential due to alterations from resting potential from changes in ion flux due to opening or closing ion channels. Graded potentials can vary in intensity, duration, and direction and can be summed. The larger the incoming stimulus, the stronger the graded potential. They dissipate quickly, losing strength with distance.

36.5.1 Excitatory postsynaptic potentials (EPSPs)

EPSPs are graded potentials that make the membrane potential less negative. These are typically caused by the influx of cations such as Na^+ or Ca^{2+}.

36.5.2 Inhibitory postsynaptic potentials (IPSPs)

IPSPs are graded potentials that make the membrane potential more negative. These are typically caused by the influx of Cl^- or efflux of K^+.

36.6 Action potentials

Action potentials are large, brief (5-10 ms) depolarizations of membrane potential that travel down the axon. They are triggered when the membrane potential around the axon hillock ("spike-initiation zone") increases above a given threshold value, typically somewhere around -55 to -40 mV. Once triggered, action potentials are "all or none" in strength and the intensity does not dissipate with distance. Information is transmitted by the frequency of axon potentials.

The action potential sequence is rest → depolarization → repolarization → hyperpolarization → rest.

36.6.1 Depolarization

When the membrane potential rises above the activation threshold, voltage-gated Na^+ channels open, allowing Na^+ to flux into the cell down its electrical and concentration gradient, thus depolarizing the membrane. This depolarization triggers even more voltage-gated Na^+ channels to open, creating a positive-feedback loop known as the Hodgkin cycle. As the membrane potential

approaches (but never reaches) the equilibrium potential for Na^+ ($\approx$ +50 mV), the voltage-gated Na^+ channels spontaneously inactivate due to a portion of the channel protein which blocks the pore opening like a ball and chain. Their spontaneous inactivation stops the influx of Na^+.

36.6.2 Repolarization

The membrane also contains voltage-gated K^+ channels (aka delayed rectifiers) which were also activated by the initial activation potential, but they open much slower than the Na^+ channels. However, after their delay, they open to allow K^+ to efflux down its concentration gradient, thus repolarizing the cell.

36.6.3 Hyperpolarization

In addition to opening slowly, the voltage-gated K^+ channels also close slowly after the membrane potential becomes more negative than the original threshold potential. This delay allows more K^+ out of the cell than when at rest. This causes a temporary hyperpolarization before the K^+ channels finally close and the NKA return the cell to resting potential.

36.6.4 Conduction down the axon

Action potentials progress down the length of the axon in one direction. This is possible due to the inactivation of voltage-gated Na^+ channels by their "ball and chain" mechanism. Once the channels open and are inactivated, they cannot be reopened for a time which prevents the action potential from being re-triggered back up the axon towards the soma.

The larger the axon diameter, the faster the action potentials conduct because there is less resistance. Altering axon diameter is commonly used in invertebrates to vary conduction velocity. Vertebrates, however, vary myelin sheathing. Cuttlefish giant axons are 200 μm in diameter and conduct APs at 7 m/s while squid giant axons are 700-1000 μm and can conduct APs at 20-30 m/s (Budelmann, 1994).

36.7 Synapses

Synapses are the connections between the axon terminal of one neuron and another neuron. The post-synaptic connection may be on the post-synaptic neuron's dendrites, soma, or axon. The small space between the neurons is the synaptic cleft. Synapses may be chemical (commonly) or electrical (rarely).

36.7.1 Chemical synapses

Chemical synaptic transmission takes 0.3-5 ms.

Synapses form through interactions of proteins on the synaptic membranes. One common interaction is the "handshake" interaction between neurexin on the presynaptic membrane and neuroligin on the postsynaptic membrane that maintains synapse structure.

When an action potential reaches the end of an axon, voltage-gated Ca^{2+} channels open, allowing an influx of Ca^{2+} into the terminus.

Through some sort of cellular signaling, cAMP dependent protein kinase (protein kinase A, PKA) is activated, which in turn, phosphorylates synapsin. Synapsin is a protein that connects vesicles to the cytoskeleton. While dephosphorylated, they keep vesicles stuck to the cytoskeleton and prevent them from approaching the pre-synaptic membrane (McGuinness et al., 1989). Once phosphorylated, however, they allow movement and subsequent docking.

36.7.1.1 Synaptotagmin

Two to three of the cytosolic Ca^{2+} ions bind with each of the Ca^{2+}-sensing C_2 domains on synaptotagmin (Ubach et al., 1998), which is located on the membranes of neurotransmitter-containing vesicles (Davletov and Sudhof, 1993). According to the "electrostatic switch" hypothesis, the Ca^{2+} binding region of the C_2 domains are full of highly negatively charged residues that repel the negatively charged phospholipids. However, once at least two of the Ca^{2+} ions bind per C_2 domain, the negatively charged region is now positively charged and has a high affinity for the negatively charged phospholipids (Zhang et al., 1998). Both the C_2A and C_2B domains must bind phospholipids to allow successful docking of the vesicle. The C_2A domain binds the presynaptic membrane, while the C_2B domain binds the vesicle membrane (Bryan Sutton pers. comm.). The synaptotagmins trigger the vesicles to dock on the cell membrane (line up adjacent to the membrane). Then SNARE proteins fuse the vesicle to the membrane, which exocytoses neurotransmitters into the synaptic cleft.

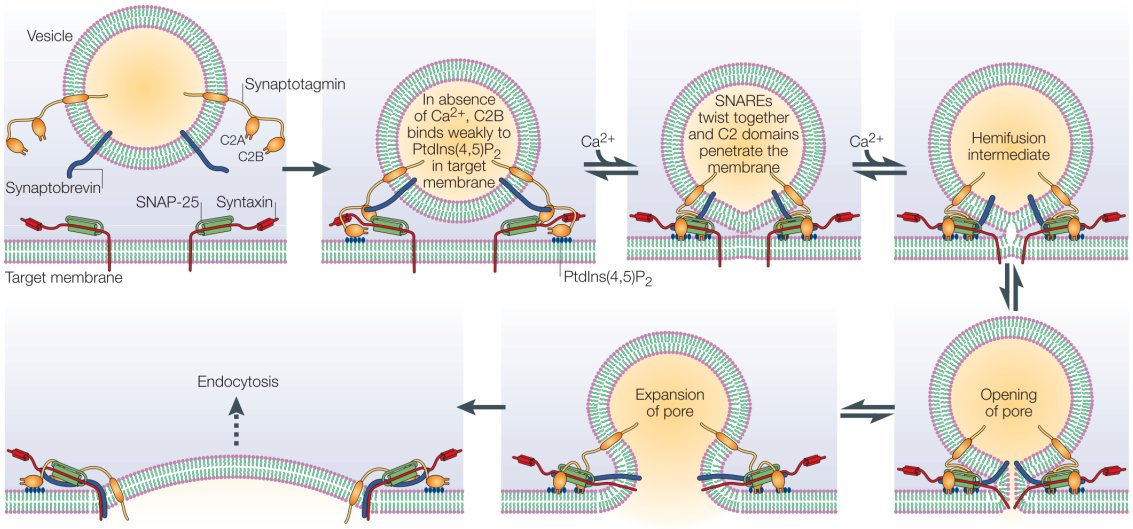

Figure 36.2: Vesicle fusion to the synapse. Figure from Chapman (2002).

Neurotransmitters (either excitatory or inhibitory) are released into the synaptic cleft and connect with neurotransmitter receptors (ligand-gated ion channels) on the postsynaptic neuron. Most neurons release only one neurotransmitter into the synapse but they can receive many neurotransmitters through their receptors.

After neurotransmitters are released, they are "cleaned up" by either reuptake, degradation, or diffusion away from the synaptic cleft. Degradation is facilitated by post-synaptic membrane-bound acetylcholinesterases (AChE) that hydrolyze acetylcholine. Synaptotagmin C2B domain is involved in vesicular endocytosis (Fukuda et al., 1995; Llinas et al., 2004). Intracellular Ca^{2+} is removed by NCX (subsubsection 30.2.2.2).

36.7.2 Electrical synapses

Electrical synapses are far less common than chemical synapses and are less regulated. Pre- and post-synaptic cells are connected by gap-junctions in electrical synapses. Therefore, the two cells share cytoplasm which allows for rapid and simple and bidirectional transmission of potentials. In invertebrates, gap junctions are formed by innexin proteins.

36.8 Neurotransmitters, neuromodulators, and neurohormones

Neurotransmitter A chemical compound released from the axonal terminal to one neighboring neuron across a synapse

Neuromodulator A chemical compound released from a neuron to multiple neighboring neurons within the neuronal tissue which have receptors

Neurohormone A chemical compound released from a neuron into the plasma to reach multiple distant neurons with have receptors

In nearly all animals, glutamate is a key excitatory neurotransmitter and GABA is a key inhibitory transmitter (Gou et al., 2012). Glutamate is a key cephalopod excitatory neurotransmitter (Messenger, 1996).

Neurotransmitters are released from the axon terminal of the pre-synaptic neuron into the synapse and are received by receptors on the dendrites of the downstream neuron.

36.8.1 Acetylcholine

Octopuses have been shown to have acetylcholine-gated channels that may be either excitatory or inhibitory (Courtney's 2022 CIAC talk).

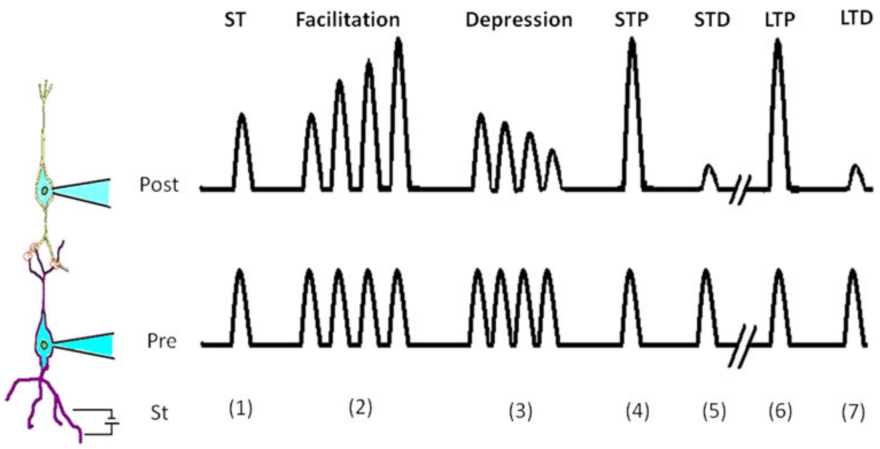

Figure 36.3: Neuronal plasticities. STP = short-term potentiation. LTD = long-term depression. All have been observed in cephalopods. Figure from Brown and Piscopo 2013.

36.8.2 Dopamine

Dopamine is typically found as a slow neurotransmitter (not in the synapse). The dopamine channels are typically expressed in extra-synaptic sites, but in octopus they are in the synapse (Courtney's 2022 CIAC talk).

36.8.3 GABA

GABA is a common inhibitory transmitter. Its inhibitory nature is due to the function of the $GABA_A$ receptor. The receptor is an ion-channel that allows Cl^- and HCO_3^- to enter neuronal somas down their electrochemical gradients, thus hyperpolarizing the cell, making it less prone to activate. Generally, Cl^- is 2-5x more permeable than HCO_3^- (Heuer and Grosell, 2014). GABA is present in cephalopods, but not nearly as abundant as in vertebrates (Conti et al., 2013).

Due to blood buffering under OA, blood $[HCO_3^-]$ increases which can cause depolarization and neuronal excitation.

36.9 Neuronal plasticity

36.9.1 Synaptic plasticity

Synapses can be plastic (Brown and Piscopo, 2013; Mitchell and Johnson, 2003). Repeated stimulation may build on the post-synaptic response (facilitation) or lessen the post-synaptic response (depression) (Brown and Piscopo, 2013). This is thought to be due to build-up of cytosolic $[Ca^{2+}]$ in the pre-synaptic axon terminal either increasing or decreasing neurotransmitter release (Brown and Piscopo, 2013). Frequent stimulation can also increase isolated post-synaptic responses (potentiation) or decrease it (depression) (Brown and Piscopo, 2013). This can be maintained on a short-term basis (STP and STD) or long-term (LTP and LTD) (Brown and Piscopo, 2013). Long-term potentiation (LTP) is the underpinnings of learning and memory (Brown and Piscopo, 2013).

36.9.2 Mechanisms of plasticity

Neuronal activity can be plastic through differential expression of ion-channels and therefore membrane potential, action potential dynamics, etc. Neurons can also change the size of the somas, dendrites, and axons.

On a molecular level, potentiation is thought to be driven by localized protein translation at the site of stimulation. In neuronal dendrites, manipulative experiments in mice neurons have demonstrated that mRNAs show up to a site of post-synaptic stimulation within ~10 minutes of stimulation (Robert Singer's iBio talk). This is thought to be the primary means of subsequent protein translation and enforcement of that stimulated synapse.

Neuromodulators can also modulate neuronal activity. The concentration of neuromodulators in neuronal tissue is determined by the the activity of neuromodulatory neurons, the size and quantity of neuromodulatory terminals on those neurons, the rate of reuptake after being released, and the rates of synthesis and degradation within the neuromodulatory neurons (Mitchell and Johnson, 2003). In addition to changes in neuromodulator concentration, changes in neuromodulator receptor density, and intracellular signaling pathways also influence the impact of neuromodulators on plasticity (Mitchell and Johnson, 2003).

36.9.2.1 RNAi regulation

At least in mammalian brains, 50% of identified miRNAs in the genome are expressed in the brain, suggesting that they are commonly used in cellular acclimation within the brain (O'Carroll and Schaefer, 2013). Furthermore, these miRNAs are localized subcellularly (some concentrated in dendrites and axons), in different cell types, and also in different brain regions (O'Carroll and Schaefer, 2013). The localization of some miRNAs near pre- and post-synaptic regions is suggestive that they are involved in neuronal potentiation.

Chapter 37

Cell signaling and signal transduction

Signal transduction often has so many steps because each step amplifies the response. Therefore, a few primary messengers can activate orders of magnitude larger cellular responses.

37.1 Primary messengers

Primary messengers are extracellular molecules such as hormones and neurotransmitters. Many bind to a form of G protein-coupled receptor (GPCR). The GPCR gene family in cephalopods is much more diverse than in other bilaterians (Albertin et al., 2015).

37.2 Secondary messengers

37.2.1 cAMP

cAMP is derived from ATP and is produced by adenylyl cyclase.

A common mechanism is: Primary messenger → G protein-coupled receptor → G protein → Adenylyl cyclase → cAMP → some sort of protein kinase

37.2.2 Phospholipase C

37.2.3 Diacylglycerol

37.2.4 Ca^{2+}

Intracellular [Ca^{2+}] is kept low. Therefore, Ca^{2+} can act as a secondary messenger. It is stored in the smooth endoplasmic reticula and extracellularly. For example, in the skeletal muscle cell, when a neurotransmitter reaches the membrane-protein, a series of signal transductions steps leads to Ca^{2+} being released from the sarcoplasmic reticula so they can allow the binding of actin and myosin for muscle contraction.

Ca^{2+} binding is primarily done by proteins containing C_2 domains (Rizo and Sudhof, 1998).

37.3 MAPK pathways

Mitogen-activated protein kinases are serine/threonine kinases (phosphorylate the serine or threonine on proteins). They are poorly named since they are activated by many cellular stimuli, not just mitogens. There are three main MAPK pathways (ERK, JNK, p38) that have the following hierarchial structure:

$$\text{stimulus} \rightarrow \text{transducer} \rightarrow \text{MAP3K (MAPK kinase kinase)} \rightarrow \text{MAP2K (MAPK kinase)} \rightarrow \text{MAPK} \rightarrow \text{effectors} \rightarrow \text{cellular responses}$$

The transducer (often but not always a GPCR) transduces the stimulus from outside the cell to inside. Many of the MAP2Ks are various MEKs or MAPK/ERK kinases (aka MKKs). The MAPK effectors are primarily transcription factors, leading to alterations in gene expression. Among these three pathways there are over 200 intermediates either upstream or downstream of the MAPK. These abundant intermediates allow the pathways to be tightly regulated.

37.3.1 ERK signaling pathway

MAP2K MEK1 or MEK2 (MKK1 or 2)

37.3.2 JNK signaling pathway

MAP2K MEK4 or MEK7 (MKK4 or 7)

c-Jun NH_2-terminal kinase (JNK) can be activated by a number of cellular stimuli such as UV radiation, oxidative stress, osmotic stress, cytokines, and growth factors, among others. JNK phosphorylates a number of downstream targets including Heat Shock Factor 1 (subsection 39.8.2) and c-Jun. At least in vertebrates, c-Jun and c-Fos form a heterodimer known as Activator Protein 1 (AP-1) which is a transcription factor. The downstream effects of JNK activation ultimately include inflammatory response, apoptosis, and altered cell growth among others.

37.3.3 p38 signaling pathway

MAP2K MEK3 or MEK6 (MKK3 or 6)

p38 MAPKs are activated by a number of cellular stimuli such as radiation, oxidative stress, osmotic stress, cytokines, and growth factors, among others. p38 MAPK phosphorylates a number of downstream targets that ultimately activate inflammatory response (subsection 51.8.3), apoptosis (subsection 39.10.1), among others.

37.4 Phosphate regulation

Phosphates are important compounds which are commonly added to enzymes (by kinases) or removed from enzymes (by phosphatases) to alter their function.

In eukaryotes, kinases either add phosphates to tyrosine (Y) or to serine/threonine (S/T). These residues are the only ones with a free hydroxyl group to which the phosphate is bound.

Chapter 38

The cell cycle

Multipotent cells are the only cells that undergo division in adult animals.

During mitosis, cytoskeletal filaments and associated motor proteins are highly involved in moving the organelles, chromosomes, and cell membrane during mitosis and cytokinesis (Alberts et al., 2008).

38.1 Gap 0 (resting)

The cell is stable.

38.2 Gap 1

38.3 Synthesis

DNA replication occurs. Each chromosome replicates into two sister chromatids connected by cohesion protein complexes that run along the length of the chromatids.

38.4 Gap 2

38.5 Mitosis

During mitosis, you are separating sister chromatids from each duplicated chromosome, but retaining homologous chromosomes.

38.5.1 Prophase

Chromatin condense into duplicated chromosomes (dyads of sister chromatids). The sister chromatids adhere to each other through cohesion protein complexes.

Centrosomes migrate to poles and spindle starts to form.

38.5.2 Prometaphase

Nuclear envelope dissociates. On each duplicated chromosome, a protein complex known as the kinetochore assembles around a special region of DNA sequence known as the centromere. Spindle microtubules attach to kinetochore on each sister chromatid.

38.5.3 Metaphase

Duplicated chromosomes line up along middle line of dividing cell. This movement and localization is facilitated by the organization of microtubules into a mitotic spindle. Motor proteins localize the chromosomes and also maintain the mitotic spindle structure.

38.5.4 Anaphase

The sister chromatids split and move towards ends of cell. The splitting is induced by the degradation of the cohesion, a protein complex that maintains bonding of sister chromatids. The chromatids are moved along microtubules by chromokinesins, members of the kinesin family with DNA-binding domains.

38.5.5 Telophase

Chromatids (i.e. chromosomes) reach ends of cells. Nuclear membranes reform around both sets of chromosomes and the chromosomes uncoil into chromatin. The spindle fibers also dissociate leaving just the centrosomes.

38.6 Cytokinesis

The cell splits into two daughter cells.

38.7 Meiosis

During meiosis I, you are separating homologous chromosomes, but retaining sister chromatids from each duplicated chromosome.

Meiosis entails one DNA replication, and two cellular divisions, resulting in 4 haploid cells from one diploid cell.

Before meiosis begins, the gametogonium (a kind of stem cell) must replicate its DNA and undergo mitosis to produce two diploid daughter cells known as primary gametocytes. This happens during embryogenesis such that even paralarvae have primary gametocytes.

$$\text{gametogonium} \overset{\text{gametocytogenesis (mitosis)}}{\rightarrow} \text{primary gametocyte}$$

38.7.1 Meiosis I

Each primary gametocyte begins the S (synthesis) phase of the cell cycle resulting in DNA replication, such that each gene (which has two alleles each with one copy during interphase) is copied so there are now 4 copies of each gene: the two copies of the maternal allele on sister chromatids of the duplicated maternal chromosome, and two copies of the paternal allele on sister chromatids of the duplicated paternal chromosome. The two duplicated chromosomes are "homologous chromosomes" and are held together in a tetrad known as a bivalent. It is at this time that recombination can occur between homologous chromosomes, thus leading to genetic diversity in the eventual gametes.

During meiosis I, the primary gametocyte divides, separating the maternal and paternal "homologous" chromosomes. The resulting secondary gametocytes are haploid since they only contain an allele from one parent, but the two identical sister chromatids (same alleles from the same parent) are still bound together forming the "X" duplicated chromosome shape.

38.7.1.1 Prophase I

In addition to cohesion protein complexes forming to adhere sister chromatids, synaptonemal protein complexes also form, adhering homologous chromosomes together. It is this time when the homologous proteins are bound together that crossing over can occur.

38.7.1.2 Prometaphase I

38.7.1.3 Metaphase I

38.7.1.4 Anaphase I

Unlike in mitosis, when cohesion protein complexes holding the sister chromatids together disassociate leading to splitting of the chromatids, in meiosis I, the synaptonemal complex holding homologous proteins together disassociates, leading to splitting of the homologous proteins. The cohesion protein complexes holding the sister chromatids together holds fast.

38.7.1.5 Telophase I

$$\text{primary gametocyte} \overset{\text{Meiosis I}}{\rightarrow} \text{secondary gametocytes}$$

38.7.2 Meiosis II

During meiosis II, the secondary gametocytes divide, separating the sister chromatids. The resulting gamete cells are still haploid since they only contain an allele from one parent.

38.7.2.1 Prophase II

38.7.2.2 Prometaphase II

38.7.2.3 Metaphase II

38.7.2.4 Anaphase II

38.7.2.5 Telophase II

$$\text{secondary gametocyte} \overset{\text{Meiosis II}}{\rightarrow} \text{gamete}$$

38.7.3 Sperm vs. egg formation

In males, four sperm cells (spermatids) are formed from one germ cell (primary spermatocyte). However, in females, typically only one egg (ovum) is formed from one germ cell (primary oocyte). The egg cell gets the vast majority of the cytoplasm during cytokinesis and the remaining three haploid cells become polar bodies that are tiny and often undergo apoptosis soon after forming. The first polar body forms during meiosis I and the second polar body during meiosis II.

38.8 Cell cycle regulation and checkpoints

Checkpoints exist at every transition in the cell cycle (Kültz, 2005).

Cyclins regulate the phases of the cell cycle. They do so by binding with cyclin-dependent kinases (Cdks) that in turn, phosphorylate molecular targets. The cyclin identity determines the Cdk target preference. There are four cyclins: G_1, G_1/S, S, and M cyclins, each of which varies in concentration throughout the cell cycle, peaking when appropriate.

DNA damage can cause checkpoints to fail (for more information, see subsection 39.6.3).

38.8.1 G_1 checkpoint

38.8.2 G_2 checkpoint

The G_2 checkpoint is passed when DNA is completely copied without damage.

38.8.3 M (spindle) checkpoint

The M checkpoint is passed when all the sister chromatids are bound to spindle microtubules (i.e. not free floating in the cytoplasm).

Chapter 39

Cellular stress and responses

Cells respond to stressors with both a multi-stressor response pathway (the cellular stress response) and a stressor-specific response pathway known as the cellular homeostasis response (Kültz, 2005). The core triggers of the cellular stress response is denatured proteins, DNA, or membrane lipids and/or ROS (Kültz, 2005). It doesn't matter whether this is caused by oxidative stress, temperature shock, or artificial injection of denatured proteins. In contrast, the cellular homeostasis response relies on stressor-specific sensors to activate (Kültz, 2005). However, both pathways are interconnected and use some of the same elements.

External stressors often affect cells through the MAPK pathways (section 37.3).

The stress response is composed of (Kültz, 2005):

1. halting of the cell cycle
2. decreased anabolism
3. increased macromolecule repair
4. apoptosis

All organisms (eukaryotes, bacteria, and archaea) share about 300 universally conserved stress response proteins (44 of which we know the function of) (Kültz, 2005).

39.1 Triggers of cellular stress response

39.1.1 Lipid membrane damage

The phospholipid membrane can be damaged by a variety of stressors. This damage can alter membrane fluidity, permeability, composition, membrane protein properties, and transmembrane potential (Kültz, 2005).

One common mechanism of damage is lipid peroxidation: where free radicals steal hydrogens from fatty acids (especially PUFAs) and thus alter membrane composition and its properties.

39.1.2 DNA damage

39.1.2.1 Double-stranded break

39.1.2.2 Single-stranded break

39.1.2.3 Base-pairing mismatch

One of the most common forms of DNA damage is the ROS formation of 8-oxoguanine from guanine (Kültz, 2005) due to guanine's low redox potential relative to the other bases. 8-oxoguanine functionally mimics thymine and thus can result in a C:G to A:T mutation once the affected strand undergoes replication.

39.1.2.4 Base modification

39.1.3 Protein damage

Proteins are most typically damaged by either oxidation or un- / misfolding (Kültz, 2005). The most common kinds of oxidative damage are cysteine and methionine oxidation. The former causes disulfide bridges to form in the protein while the later adds an oxygen to the sulfur atom which can lead to protein misfolding.

39.2 Oxidative stress

39.2.1 ROS production

Reactive oxygen species (ROS) are produced in a variety of subcellular compartments including the mitochondria, peroxisomes, endoplasmic reticula, and plasma membrane (Zhang and Wong 2021, JEB). The single most dominant source of ROS is not the mitochondria, but rather NADPH oxidases, which are transmembrane electron transporters abundant in the plasma membrane and ER (Zhang and Wong 2021, JEB).

Many ROS are produced at the inner mitochondrial membrane. During normal O_2 reduction in the mitochondria, about 0.1-2.0% of O_2 reduced forms ROS. Much more ROS is formed when local [O_2] goes above or below normal. ROS species, such as hydrogen peroxide (H_2O_2), superoxide ($^{\bullet}O_2^-$), hydroxyl radicals ($^{\bullet}OH$) and peroxynitrite (ONO_2^-), can cause cellular and tissue damage by interacting with macromolecules.

ROS target proteins with -SH groups, membrane lipids (especially the PUFAs), and nucleic acids.

The abundance of carbonyl groups on proteins can be an indicator of oxidative damage (Loughland's SEB talk). The abundance of 8-oxoguanine in DNA is also a common oxidative stress metric.

H_2O_2 is nonpolar and can pass through membranes easily, thus quickly reaching DNA, for example.

39.2.2 Antioxidants

To prevent oxidative damage, cells support an antioxidant system composed of both molecules and enzymes. Reduced glutathione (GSH) is a "buffer" molecule that reacts with ROS to neutralize them. In so doing it is converted to its oxidized form, GSSG (Kültz, 2005). Three enzymes are also important antioxidants: 1. superoxide dismutase (SOD) converts O_2^- to H_2O_2, 2. catalase (CAT) converts H_2O_2 to O_2 and H_2O, and 3. glutathione reductase (GR) creates GSH (Kültz, 2005). The glutathione reductase reaction consumes NADPH, thus making this reducing equivalent critical for antioxidant activity.

ROS formation increases with increased MO_2 which is commonly induced by increased temperature or emergence from hypoxia. Some organisms that are well adapted to chronic hypoxia will upregulate antioxidant enzyme formation during hypoxia in anticipation of the ROS increase upon emergence but this is not always the case. In fact, hypoxia exposed *Dosidicus gigas* decrease rather than increase antioxidant enzymes relative to normoxic levels (Trübenbach et al., 2013).

Molecular antioxidants

- Reduced glutathione (GSH)
- Vitamin A
- Vitamin C (ascorbic acid, ascorbate)
- Vitamin E

Enzymatic antioxidants

- Superoxide dismutase (SOD)
- Catalase (CAT)
- Glutathione reductase (GR)
- Glutathione peroxidase (GPX)
- Glutathione S-transferase (GST)
- Peroxiredoxin (PRDX)
- Thioredoxin (TXN, TRX)

39.3 Immediate early genes

Immediate early genes (IEGs) are ~40 genes (identified so far) that are activated within minutes of cellular stress. Most of these genes encode transcription factors but some structural proteins are included as well. These differ from "late genes" in that the altered transcription of "late genes" does not occur until the protein products of IEGs are complete. A variety of upstream signals can initiate IEG transcription including the MAPK pathways (section 37.3). The ultimate outcomes of IEG activation include antioxidant production (Kassahn et al., 2009).

39.4 Stress-induced transcription factors

39.4.1 HIF

It is well known that hypoxia inducible factor (HIF) is an extremely important player in acclimation to hypoxia but it is also induced in response to temperature stress (Kassahn et al., 2009). HIF is composed of two subunits, α and β (Wang et al., 1995; Jiang et al., 1996). In some mammalian cell types, both subunits are constantly transcribed and translated at an O_2-independent rate, but in fishes and other mammalian cell types, the α subunit is transcribed to a greater extent under hypoxia (Richards, 2009). Amazingly, a number of crustaceans have lost their HIF1a genes and sometimes PHD or VHL genes as well (Graham and Barreto, 2019).

Invertebrates only have one HIFα and one HIFβ, while it was duplicated as part of the two whole-genome duplication events in vertebrates to give rise to HIF1-3 (Graham and Presnell, 2017).

HIF-1β ARNT (Aryl hydrocarbon receptor nuclear translocator)

HIF-2α EPAS1 (Endothelial PAS domain-containing protein 1)

39.4.1.1 PHD-HIF-pVHL pathway

Once the αsubunit is formed, it is quickly degraded under normoxia due to O_2-dependent degradation domains (ODD; (Masson et al., 2001)) that contains two prolines (P402 and P564 in human HIF-1α; (Jaakkola et al., 2001) and P405 and P531 in human HIF-2α) that can be hydroxylated by the oxygen-sensitive protein PHD (prolyl hydroxylase domain-containing protein). This hydroxylation also is dependent on Fe^{2+}, ascorbate, α – ketoglutarate (aka oxoglutarate) and forms succinate and CO_2. Ascorbate's role is to maintain Fe^{2+} in the reduced state (prevent Fe^{3+} formation). PHD1-3 exist in humans and 2 is most important in humans (aka HIF-PH or EGLN), which tags the HIF-1α for recognition by pVHL (Hon et al., 2002; Min et al., 2002) and subsequent ubiquitination and degradation by the proteasome (Baik and Jain, 2020).

The N-terminal ODD (NODD containing P402) is more sensitive to hypoxia than the CODD (containing P564). In humans, NODD is hydroxylated above ~2% O_2 while CODD is hydroxylated until ~0.5% O_2 (Chowdhury et al., 2016).

Factor inhibiting HIF (FIH-1; aka HIF1N) can also inactivate HIF-1α by hydroxylating the asparagine-803 on the C-terminal transactivation domain (CTAD) (Mahon et al., 2001), which prevents HIF1a from binding with p300/CBP and thus being able to bind to HREs. In the absence of oxygen, this hydroxylation does not occur. Importantly, this hydroxylation inactivates the protein but does not degrade it.

Both PHD and FIH require O_2 as a substrate for enzymatic activity, but between the two PHD has a much higher K_m than FIH and thus is triggered first by progressive hypoxia (Brahimi-Horn and Pouysségur, 2009).

In a normoxic mammalian cell, HIF-1αhas a half-life of 5-10 minutes (Richards, 2009). More details about the pathway of degradation are reviewed by Richards (2009).

When the cell O_2 falls, however, PHD and FIH are inactivated and thus HIF-1α abundance increases and the HIF-1 dimer can form (Richards, 2009). The HIF-1 dimer first binds to the p300/CBP coactivator and then together they bind to hypoxia response elements (HREs) in the promotor regions of target genes to up- or down-regulate a number of pathways to optimize the cell to survive hypoxia (Richards, 2009).

39.4.1.2 HIF targets

HIF-1 and HIF-2 targets generally have a hypoxia response element (HRE) defined as RCGTG (Mole et al., 2009) in their promoter, enhancer, or intronic regions.

HIF-1 alters glucose transport gene expression and suppresses TCA cycle and oxidative phosphorylation pathways to minimize ROS production from inefficient respiration.

One such gene with an HRE promoter is miR-210. When expressed, it helps stabilize HIF-1α, thus serving as a positive feedback for the HIF pathway.

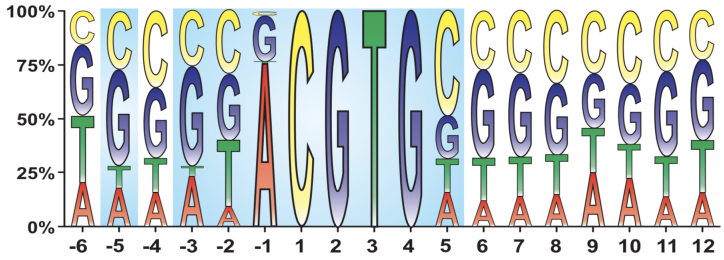

Figure 39.1: Hypoxia response element (HRE) nucleotide sequence frequencies mainly from mammals but also a few invertebrates. Note that CGTG is always conserved. Figure from Wenger et al. (2005).

In vertebrates, HIF-1 also upregulates genes for erythropoiesis (RBC production) and is critical for proper development of the heart. At least in zebrafish, HIF expression during embryogenesis can result in improved hypoxia tolerance later in life (Robertson et al., 2014).

39.4.2 NF-κB

Nuclear factor-κB is a transcription factor family that is triggered by a variety of cellular stress stimuli such as cytokines, ROS, heavy metals, radiation, among others.

39.5 Stress granules

Under stress, cells produce phase-separated liquid granules that are a mix of RNA and proteins. It is unclear whether this is just a side effect of the cell's "attention" elsewhere under stress or whether it is functionally adaptive. It can be viewed as functionally adaptive to consider that mRNA molecules are sequestered along with translation initiation factors, and 40S (but not 60S) rRNA (Liz Alexander's talk). By sequestering these molecules, translation will be downregulated, saving energy, but keeping these components around for post-stress activity (since they were expensive to make and should not be degraded).

Along with the RNAs are DNA and RNA binding proteins.

39.6 DNA repair

Many forms of DNA repair utilize at some point the BRCA-1-associated genome surveillance supercomplex (BASC) (Kültz, 2005).

39.6.1 Double-stranded break repair

If a double-stranded break occurs, either HDR or NHEJ can be employed depending on the cell cycle state. If replication has occurred but cell division has not yet occurred, HDR is an option since a homologous region to the broken region may be nearby. If the cell is in any other cell cycle state, however, then NHEJ is the only option for repair (Thurtle-Schmidt and Lo, 2018).

39.6.1.1 Homology directed repair (HDR)

Rad51 (homologous to RecA in prokaryotes) is an important protein in this process.

Homologous recombination Homologous recombination is the most common form of HDR.

39.6.1.2 Nonhomologous end-joining (NHEJ)

NHEJ ligates blunt ends together and is quite likely to introduce indels (Thurtle-Schmidt and Lo, 2018).

39.6.2 Excision repair

39.6.2.1 Base excision repair (BER)

Base excision repair fixes small issues through a relatively simple pathway.

1. DNA glycosylase removes the damaged base, thus forming an AP site (i.e. abasic, apurinic, apyrimadinic site)
2. AP endonuclease nicks the phosphodiester backbone of the DNA at the AP site, creating a single-stranded break
3. DNA polymerase fills in the gap
4. DNA ligase binds the phosphodiester backbone break

39.6.2.2 Nucleotide excision repair (NER)

Nucleotide excision repair fixes large issues through a relatively complex pathway.

39.6.2.3 DNA mismatch repair (MMR)

DNA mismatch repair is facilitated by two proteins: MSH (MutS homolog) and MLH (MutL homolog). MSH finds mismatch sites and then MLH binds to it and starts assembly of the entire MMR complex (Kültz, 2005). These genes are upregulated under stress (Kültz, 2005).

39.6.3 Damage-induced regulation of the cell cycle

p53 has been considered the "guardian of the genome" since it does a number of things when damaged DNA is detected:

- produces Cdk inhibitors that bind to Cdk and thus prevent the G_1 checkpoint from being passed in the cell cycle.
- activates DNA repair enzymes
- triggers apoptosis

39.7 RNA protection

Under stress, RNA can be protected. For example, cold-inducible RNA-binding protein (CIRBP) is known to be produced under not just cold-stress but also UV and hypoxia. CIRBP binds to the 3' UTR of mRNAs to regulate their stability (Zhong and Huang, 2017).

39.8 Protein repair

39.8.1 Repair of oxidized proteins

Protein oxidative damage typically occurs by oxidation of the sulfur on either Cys or Met residues. These are reduced (repaired) by glutathione (GSH/GSSG) and thioredoxin systems (Kültz, 2005).

39.8.2 Heat shock proteins

Heat shock proteins (HSPs) are synthesized in response to a variety of physiological stressors to try to acclimate. They refold damage proteins, prevent protein aggregates from forming, among other actions. The intensity of response to a stressor depends on stressor intensity, duration, and previous exposure, making the heat shock response challenging to predict (Kassahn et al., 2009). Comparisons of the hsp responses of congeneric (of the same genus) intertidal snails demonstrated that species that are used to heat stress induce hsp production faster than more stenothermal or cool adapted species (Hochachka and Somero, 2002).

Heat shock protein transcription is regulated by Heat Shock Factor 1 (HSF-1) in eukaryotes, a transcription factor that binds to the Heat Shock Element on HSP genes (among others). In unstressed conditions, HSF-1 is bound to HSPs. However, when denatured protein levels rise, HSPs bind to target proteins and remove HSF-1 which is then free to enter the nucleus and upregulate HSP transcription.

HSP production generally follows the following pattern with variation based on taxon and stressor (Gunderson et al., 2016):

- 0.5 to 6 hours after stressor begins, HSP upregulates

- 15 hours after stressor begins, HSP reaches peak expression
- By 24 hours after stressor, HSP typically returns to basal levels.

HSPs are highly conserved across eukaryotes and bacteria and fall into 3 major groups: HSP90, HSP70, and small HSPs (Bols et al., 1992).

Hsp70/Hsc70 is a common indicator of HSP expression. Hsc70 is constitutively expressed at a stable level under most conditions, but Hsp70 increases in response to stressors.

39.8.3 Protein degradation

HeLa cell line (cervical cancer) protein half-lives typically range from 15 to 70 hours (Cambridge et al., 2011). Rat primary hippocampal neuron culture proteins have a median half life of 5 days (ranging from 2 to 14 days, excluding outliers) (Dörrbaum et al., 2018). Mouse brain cortex proteins have a median half-life of 8 days with a range from 1 to 30 days (Fornasiero et al., 2018).

Different subunits in a protein complex tend to have similar half-lives (Mathieson et al., 2018).

Proteins with large (>30-40 residues) intrinsically disordered regions have shorter half lives than those without (van der Lee et al., 2014).

Lysosomes are nonselective degraders while proteasomes select only ubiquitin-tagged proteins.

39.8.3.1 Degradation in lysosomes

See section 31.5.

39.8.3.2 Ubiquitination

Damaged or misfolded proteins are tagged with a ubiquitin molecule by ubiquitin ligases. Once a single ubiquitin is tagged onto a lysine residue, many other ubiquitins are also added until the protein has a polyubiquitin chain. This polyubiquitin chain is a signal to proteasomes to degrade the protein.

Activation, conjugation, and ligation of ubiquitin are facilitated by E1s, E2s, and E3s, respectively.

Activation Activation is facilitated by ubiquitin-activating enzymes (E1s) that adenylate ubiquitin and pass them on to E2 for conjugation.

Conjugation Conjugation is facilitated by ubiquitin-conjugating enzymes (E2s) that pass the ubiquitin on to E3 for ligation.

Ligation Ligation is facilitated by ubiquitin ligase enzymes (E3s) that identifies the target protein and adds the ubiquitin.

39.8.3.3 Proteasomes and proteolysis

26S proteasome is a huge (2 MDa) multi-subunit complex that degrades polyubiquitinated proteins (at least 4 ubiquitins) in the cytosol and nucleus (Bard et al., 2018). It utilizes ATP to break apart the structure of the protein and then degrades the unfolded polypeptide. The proteasome is composed of a large 20S degradation chamber where proteolysis occurs that is gated on one or two ends by 19S regulatory particles that contain small pores such that only completely unfolded polypeptides can enter the 20S chamber (Bard et al., 2018). The 19S regulatory particles detect target the polyubiquitin tag on proteins. Once inside the core, the peptide bonds are broken and the polypeptide is broken into 7-8 amino acid chain oligopeptides.

Eukaryotic cells contain ubiquilin, an apparent adapter protein with a ubiquitin-binding domain on one end and a "pseudo-ubiquitin" domain on the other end, so that it can link ubiquitins to the proteasome (Liz Alexander's talk). Although not necessary for proteolysis, it may regulate the process somehow.

39.9 Metabolic regulation

The cellular stress response can heavily modulate the flow of metabolic pathways such as glycolysis, the Kreb's cycle, and the pentose phosphate pathway by targeting key enzymes. Upregulation of these pathways does two things that helps mitigate stress:

1. produces more reducing equivalents (NADH, NADPH) which is necessary for the oxidative stress response.
2. produces more ATP which is consumed by macromolecular repair pathways.

39.10 Cell death

Cells can die through either apoptosis or necrosis. Apoptosis may be a naturally occurring programmed death, but necrosis only occurs due to external factors. While apoptosis does not induce inflammation, necrosis does.

39.10.1 Apoptosis

When a threshold quantity of DNA or proteins are damaged, apoptosis is triggered. It can also be triggered by development, viral infection, or various signs of stress.

Apoptosis is orderly and controlled to minimize stress signaling to nearby cells or inflammation as would occur by simple release of cytoplasmic contents.

Apoptosis can be triggered through two mechanisms: intrinsic and extrinsic pathways.

39.10.1.1 Intrinsic pathway

The intrinsic pathway outlined below was developed in mammalian cell lines but it has also been demonstrated in molluscs (Kiss, 2010).

Releasing cytochrome c The intrinsic pathway occurs by the mitochondrial outer membrane releasing proteins (e.g. cytochrome c) from the intermembrane space into the cytosol. The mitochondrial outer membrane releases these proteins because the Bcl2 family of proteins present in the membrane shift in abundance from an anti-apoptotic majority to a pro-apoptotic majority. Since the anti- and pro-apoptotic Bcl2 proteins form heterodimers and inhibit each other, whichever is more abundant dominates the phenotype. All Bcl2 proteins contain at least one Bcl2 homology (BH) domain. Anti-apoptotic Bcl2 orthologs contain 4 BH domains (BH1-4) while pro-apoptotic Bcl2 orthologs contain either 3 (BH123) or just 1 BH domains (BH3-only) (Alberts et al., 2008). If the pro-apoptotic orthologs are sufficiently abundant, they can oligomerize and form a pore in the outer mitochondrial membrane, thus allowing the release of cytochrome c (Alberts et al., 2008).

	Bcl2 orthologs
Pro-apoptotic	Bax, Bad
Anti-apoptotic	Bcl2 (especially with Ser70 phosphorylation (Ruvolo et al., 2001)), Bcl-X_L

One of the pathways for Bcl2 shift is through the transcription factor p53 (subsection 39.6.3). p53 is inactivated until it is phosphorylated at Ser46 by a phosphorylated p38 (subsection 37.3.3). Once p53 has been phosphorylated at this residue, it induces expression of pro-apoptotic Bcl2 proteins.

Activating caspases When cytochrome c is in the cytosol, it can bind to Apaf1. Seven of these dimers can oligomerize to form a wheel-like structure known as an apoptosome. The Apaf1 contains a death fold and the congregation of these death folds attract the death folds of initiator procaspases (such as procaspase 9) and thus activate the initiator caspases.

Thus, initiator caspases are auto-activated when brought together in a large protein complex and effector caspases are activated by initiator caspases.

A procaspase is activated when it is cleaved at two sites: 1) the N-terminal prodomain is removed, and 2) the rest of the procaspase is cut in two. The prodomain is discarded and the two remaining pieces of the original polypeptide bind together to form a heterodimer. Two of these heterodimers often pair to form an active heterotetramer caspase.

39.10.1.2 Extrinsic pathway

The extrinsic pathway occurs by cell surface receptors receiving ligands and triggering the caspase pathway. Caspase 8 and 10 are involved in the extrinsic pathway (Alberts et al., 2008).

39.10.1.3 Caspases

Caspases are proteases that use a cysteine in their active site to break proteins after the aspartate residue (hence "c***asp***ase") (Alberts et al., 2008). Inactivated caspases (known as procaspases) must be activated before functioning.

At least in mammals, caspases have the following functions:

Initiators Caspase 2, 8, 9, 10. Have a >90 residue N-terminal prodomain.

Executioners/effectors Caspase 3, 6, 7. Have a 20-30 residue N-terminal prodomain.

Inflammatory Caspase 1 (aka ICE), 4, 5, and 11.

Caspase 3 is the most commonly tracked apoptosis metric because it is an executioner caspase that is activated by both the intrinsic and extrinsic pathways.

Caspase inhibition by IAPs Even once activated, caspases can be inhibited by inhibitors of apooptosis (IAPs). IAPs bind to activated caspases and either inactivate them or polyubiquitinate them (Alberts et al., 2008).

39.10.1.4 Features of apoptosis

The cytoskeleton shrinks the cell down, the membrane removes cell-cell adhesion proteins, the membrane also shifts the phospholipid phosphatidylserine from exclusively on the inner side of the phospholipid bilayer to also the outer side where it signals phagocytosis. The nucleus is also degraded and chromosomes degraded and cellular contents are packaged into vesicles known as "apoptotic bodies".

39.10.2 Necrosis

Necrosis caused by the destruction of the cell membrane and subsequent loss of cytoplasm into the extracellular fluid.

Unlike apoptosis, the organelles themselves may not degrade, but they do lose their function.

39.10.3 Hypoxic death

See subsection 53.6.5.

Chapter 40

Biomechanics

40.1 Reynolds number

$$\mathrm{Re} = \frac{\text{inertial forces}}{\text{viscous forces}} = \frac{\rho \mathrm{uL}}{\mu} = \frac{\text{density}_{\text{fluid}} \times \text{velocity}_{\text{fluid}} \times \text{characteristic linear dim.}}{\text{dynamic viscosity}_{\text{fluid}}}$$

Table 40.1: Physical characteristics of fluids relevant for Reynolds numbers calculations

Fluid	Density (ρ)	Velocity (u)	Dynamic viscosity (μ)
Seawater	1020-1050 $\mathrm{kg \cdot m^{-3}}$	Varies	$1 - 2 \times 10^{-3}\,\mathrm{kg \cdot m^{-1} \cdot s^{-1}}$
Blood			

Part V

Their genetics

Chapter 41

Genomics

41.1 Genome size and chromosomes

1 pg DNA $\approx$ 1 Gb.

Coleoid cephalopod genomes span in size from 2.1 to 5.1 Gb ((Albertin et al., 2015; Belcaid et al., 2019); Simakov's 2018 CIAC talk) compared to a human genome of 3 Gb. This is 5-10x the average molluscan genome (Ritschard's 2018 CIAC talk). Snail and oyster genomes are both ~500 Mb (Albertin's MBL journal club talk) and *Nautilus pompilius* genome is ~785 Mb (Huang et al., 2022).

Haploid chromosome number is often in the 20s (Vitturi et al., 1982; Hixon, 1980) though a haploid number of 30 occurs in *Octopus bimaculoides* and 42-46 is typically found in loliginids (Albertin's 2022 CIAC talk) and a haploid number of 52 has been found in *Sepia officinalis* (Vitturi et al., 1982). *Euprymna scolopes* has 46 chromosomes (Simakov's 2018 CIAC talk). *Nautilus pompilius* has 26 chromosomes (Huang et al., 2022).

Individual chromosomes in *D. pealeii* range in size from 40 to 158 Mb (MBL Loligo genome seminar).

Cephalopods do not seem to have a duplicated genome, at least based on current evidence (Albertin et al., 2015; Belcaid et al., 2019).

41.1.1 Mitochondrial genome

Mitochondrial genomes are circular dsDNA as in most multicellular organisms. Across all animals, they range in size from 4-48 kb and, unlike the nuclear genome, do not contain introns. The *Octopus* mitochondrial genome is ~16kb (which is very typical) and encodes 13 proteins (along with 92% of animals) as well as some rRNAs and 22 tRNAs (Yan et al., 2018).

These 13 genes in order around the plasmid are:

- COX1
- COX2
- ATP8
- ATP6
- ND5
- ND4
- ND4L
- CYTB
- ND6
- ND1
- COX3
- ND3

- ND2

The COX genes encode subunits for cytochrome c oxidase, the ATP genes encode subunits for ATP synthase, and the ND genes encode subunits for NADH dehydrogenase.

In addition, the 12S and 16S rRNA genes are also here.

The oegopsids seem to have a partially duplicated mitochondrial genome, including duplication of COI (Winkelmann's 2018 CIAC talk). The genetic code is different in the mitochondria from the nuclear genome (Table 32.2).

41.2 Coding sequences

A gene is composed of exons and introns. Exons are composed of CDS and UTRs. The CDS is only the protein coding portion (i.e. gene - introns - UTRs).

~10% of the *O. bimaculoides* genome codes for structural proteins (Simakov, pers. comm.). *Octopus bimaculoides* has ~34k protein coding genes in its genome (Albertin et al., 2015), *D. pealeii* has ~25k genes (Albertin's 2018 CIAC talk), and *E. scolopes* has ~29k genes (Belcaid et al., 2019), compared to the human 20-25k.

Paralog Two similar genes in the same species (e.g. $K_v1.1$ and $K_v1.2$ ion channels both in *D. pealeii*)

Ortholog Two similar genes in different species (e.g. $K_v1.1$ in *D. pealeii* and $K_v1.1$ in *O. bimaculoides*)

Homolog A paralog or ortholog

Cephalopods possess ~125 gene families for which we know of no non-cephalopod ortholog (Albertin et al., 2015).

Cephalopods have some of the largest genes among all living things thanks to very large introns (especially on the 5' end) (McCoy's 2022 CIAC talk). In contrast, most human genes are ~30 kb including introns and *C. elegans* (along with many other inverts) only have median gene sizes of ~3 kb (McCoy's 2022 CIAC talk). Most of the very large genes are expressed in the nervous system and because of nervous tissue's inherent complexity, it is thought that these large genes with large introns have lots of room for gene regulatory elements to form the complexity present in their nervous tissue (McCoy's 2022 CIAC talk).

41.2.1 Gene family expansions in cephalopods

Relative to other bilaterians, cephalopod genomes have much more diverse protocadherin, C2H2 zinc-finger protein, interleukin-17-like, G-protein coupled receptor, chitinase, and sialin gene families (Albertin et al., 2015; Belcaid et al., 2019).

41.3 Noncoding sequences

41.3.1 RNA genes

RNA genes are DNA sequences that produce functional RNA products such as tRNA, rRNA, and miRNA.

There are ~2000 tRNA genes and ~1000 rRNA genes in the *Octopus* genome (Albertin et al., 2015).

41.3.2 Introns and untranslated regions (UTRs)

The introns and UTRs of an mRNA can influence the splicing, stability, cellular localization, and translatability of the mRNA (Deffit and Hundley, 2016).

As a generalization, the larger the gene, the more alternative splicing exists (Matthew McCoy's MBL talk).

In addition, there is a strong negative relationship between intron size and gene expression, presumably because it is energetically wasteful to transcribe huge introns in highly expressed genes (Castillo-Davis et al., 2002).

However, cephalopods have humongous introns leading to huge gene sizes (especially in neural-expressed genes). In general, the intron size declines along a gene from the 5' to 3' end (McCoy's 2022 CIAC talk).

41.3.3 Cis- and trans-regulatory elements

41.3.3.1 Cis-regulatory elements (CREs)

CREs regulate nearby genes and often occur within introns and UTRs of the regulated gene.

Promoters Promoter regions in eukaryotes often (10-25% of genes in mammals) contain a **TATA box**, or a region with many adenines and thymines. Because A and T have less hydrogen bonds than C and G (subsection 28.1.1), the TATA box opens easier to allow the RNA polymerase to attach and begin transcribing.

Enhancers Enhancers are DNA sequences that are rather far away from the promoter, yet through looping chromatin (such as within topologically associating domains) they can bind to the promoter, along with transcription factors, to enhance transcription.

Silencers Silencers are DNA sequences that are rather far away from the promoter, yet through looping chromatin (such as within topologically associating domains) they can bind to the promoter, along with transcription factors, to suppress transcription.

41.3.3.2 Trans-regulatory elements (TREs)

TREs regulate distant genes by coding for transcription factors. Transcription factors tend to remain conserved in the active domains but can radiate rapidly outside of the functional domains.

Cephalopods have many more C_2H_2 Zinc finger protein factor genes than other lophotrochozoans (1800 in *O. bimaculoides* and 3000 in *D. pealeii*) (Albertin et al., 2015).

In the human genome, ~5-10% of genes are TREs (transcription factors).

41.3.4 Repetitive elements (repeated sequences, repeats)

Repetitive elements compose ~45% of the *O. bimaculoides* genome (Albertin et al., 2015) and 61% of the *D. pealeii* genome (Albertin's 2018 CIAC talk); this is much higher than in most lophotrochozoan genomes (Simakov's 2015 CIAC talk).

41.3.4.1 Long terminal repeats (LTRs)

41.3.4.2 Variable number tandem repeats (VNTRs, tandem repeats)

Tandem repeats are adjacent repeated sequences often repeated 5-50x.

Satellites Satellite DNA forms the centromere, where two sister chromatids pair to form the chromosome.

Satellites compose <0.1% of the *Octopus* genome (Albertin et al., 2015).

Minisatellites Minisatellites are repeated units 10-60 bp in length.

Microsatellites Microsatellites are repeated units <10 bp in length.

See subsection 42.3.1.

41.3.4.3 Transposable elements (TEs, transposons)

Transposons are repeated sequences arranged far away from each other in the genome. They can move around by cut-paste or copy-paste mechanisms.

The *Octopus* genome is ~7% transposons (Albertin et al., 2015). By contrast, the human genome is ~50-66% transposons (Deschamps-Francoeur et al., 2020).

Retrotransposons (Class I TEs) Retrotransposons copy-and-paste via an RNA intermediate.

Retrotransposons compose ~6.5% of the *Octopus* genome (Albertin et al., 2015).

Short interspersed nuclear elements (SINEs) SINEs compose ~3.5% of the *Octopus* genome (Albertin et al., 2015).

Long interspersed nuclear elements (LINEs) LINEs compose ~3% of the *Octopus* genome (Albertin et al., 2015). However, they are much more abundant in the *Euprymna scolopes* genome (Belcaid et al., 2019).

DNA transposons (Class II TEs) DNA transposons copy-and-paste via a DNA intermediate.

DNA transposons compose ~0.5% of the *Octopus* genome (Albertin et al., 2015).

41.3.4.4 Telomeres

Telomeres are repetitive sequences on the ends of chromosomes that protect the chromosome from deterioration of functional sequences.

41.3.5 Pseudogenes

Pseudogenes were once functional genes but accumulated mutations in the regulatory elements or coding sequences that made them either not expressible as RNA or unable to code for a protein. The older the pseudogene, the more mutations it accumulates.

Chapter 42

Evolution of the genome

42.1 Whole-genome duplication

Taxa that have recently had a genome duplication may be more likely to utilize different paralogs for different tissues or environmental conditions than taxa that do not have a free copy available for manipulation (Schulte, 2004). Cephalopods, however, do not seem to have a duplicated genome, at least based on current evidence (Albertin et al., 2015; Belcaid et al., 2019). In this way, they differ from vertebrates that have had two rounds of genome duplication (4x genes) and teleosts that have had three rounds (8x genes).

42.2 Point mutations

Within the genomic CDS of cephalopods, roughly 1 in 4 of inter-species mutations are non-synonymous (change amino acid), 1 in 10 are deletions, and the rest are synonymous changes in DNA sequence (Liscovitch-Brauer et al., 2017).

Across the all the ORF of the genome, orthologs of octopodiforms and decapodiforms on average differ in 15 of every 100 bp, teuthoids and sepioids differ in 6 of every 100 bp, and congeneric *Octopus* species differ in only 1 in every 100 bp (Liscovitch-Brauer et al., 2017).

42.2.1 CpG islands and C-to-T mutations

The most common cause of point mutations in eukaryotes in general are C $\rightarrow$ T conversions caused by the spontaneous deamination of 5-methylcytosine to thymine. If not corrected by a DNA glycosylase, the point mutation stays. Because cytosines with a guanosine as its 3' neighbor are more likely to be methylated than other cytosines, this dinucleotide (known as a CpG site) is much rarer than expected by chance in genomes, because it has been mutated away over time. Genomic regions that are not able to be methylated, however, do not undergo this selection, and thus form "CpG islands" in the genome.

Note that DNA methylation is less frequent in invertebrates than vertebrates, and thus the CpG island phenomenon may be less notable in cephalopods than vertebrates.

42.2.2 RNA editing lowers mutation rates around editing sites

RNA editing by ADARs is positively selected for in many mRNA transcripts. These edits conserve not only the editing site itself but also lower mutation rates up to 100 bp away from the editing site so that dsRNA structure is maintained (Liscovitch-Brauer et al., 2017). The base pairs immediately adjacent to conserved editing sites have 1/3 the mutation rate of the mRNA transcripts generally (Liscovitch-Brauer et al., 2017). Because of the abundance of editing sites in neural transcriptomes, the cumulative portion of base pairs that have a suppressed mutation rate is 20-40% of the entire CDS (Liscovitch-Brauer et al., 2017).

42.3 Intraspecific genetic diversity and populations

Cephalopods, as with most marine invertebrates, have a higher variation in their genomic sequence within a population (~1% difference between individuals in a population) than mammals such as humans (0.1% difference between individuals). The *D. pealeii* genome is 1.2% heterozygous (Albertin's 2018 CIAC talk).

Genes that are closer together on a chromosome are more likely to be co-inherited because they are less likely to be split during meiosis than genes that are further apart from each other or on different chromosomes.

Table 42.1: Phylogenetically tractable genes

Gene	Evolutionary rate	Reference
COI		
18S rRNA		

42.3.1 Microsatellites

Microsatellites are also known as simple sequence repeats (SSR), short tandem repeats (STR), or simple sequence length polymorphisms (SSLP) depending on the scientific community.

Microsatellites are 1-10 nt long sequences of DNA that are tandemly repeated (adjacent to each other) 5-50x and are found throughout the genome of just about all eukaryotes. They are key intraspecific markers because they mutate up to 10 orders of magnitude more frequently than point mutations.

The *Octopus* genome is ~9% microsatellites (Albertin et al., 2015).

Microsatellite markers can reveal whether a species distribution has expanded or contracted recently (Pecl's 2018 CIAC talk).

42.3.2 Single-nucleotide polymorphism (SNP)

SNPs are variations in a single nucleotide within a population. This most commonly occurs from the spontaneous deamination of 5-methylcytosine to create thymine. If not repaired by a G/T mismatch-specific thymine DNA glycosylase, then that cell and its progeny will carry this SNP. Alleles can be defined by SNPs. Across the entire ORF of the genome, SNPs occur roughly 200-700 times per 1 million bp (Liscovitch-Brauer et al., 2017).

SNPs are far less likely to occur near RNA editing sites than in the genome generally as part of a general conservation of dsRNA structure around editing sites (Liscovitch-Brauer et al., 2017).

42.4 Interspecific genetic diversity

While individuals within a population are ~1% different, different species vary more. For example, *Doryteuthis pealeii* and *D. opalescens* are 4-5% divergent even though they only diverged a few million years ago (MBL Loligo genome seminar).

Synteny (preservation of the spatial relationships of genes to each other on the chromosomes) between cephalopods and other bilaterians is almost completely absent, but is high between *Octopus* and *Euprymna* (Belcaid et al., 2019). This is because coleoids seem to have broken up their chromosomes and then fused them together at some point early in their evolution (Simakov's 2022 CIAC talk). Novel gene linkages in cephalopods are more often than by chance associated with neuronally-expressed genes (Simakov's 2022 CIAC talk).

Transcription factors tend to remain conserved in the active domains but can radiate rapidly outside of the functional domains, more so than most genes.

Chapter 43

Epigenetics and transgenerational effects

43.1 DNA methylation

Unlike prokaryotes, which are typically methylated on adenines, animals, such as cephalopods, are predominantly methylated on cytosines, especially CG dinucleotides (known as CpG sites). Although all animals favor methylation on cytosines, invertebrates methylate less frequently than vertebrates (broadly speaking) and some invertebrates such as *Drosophila* and *C. elegans* barely methylate their DNA at all. Though, some data suggest that molluscs methylate more than insects, for example.

Methylated cytosines in CpG sites have a tendency to spontaneously deaminate leading indirectly to a C $\rightarrow$ T mutation (subsection 42.2.1). Thus, highly methylated genomic regions are likely to be CpG-poor while poorly methylated genomic regions are likely to be CpG-rich (i.e. "CpG islands").

43.2 Epigenetic effects on development

Temperature exposure condition in an embryo has been shown to cause DNA methylation that lasts the animal's entire life (Schulte's SEB talk). This is likely the case for cephalopods as well. Thus, variation in embryonic conditions (e.g. temperature) can be a source of individual variation in traits throughout a cephalopod's life.

43.3 Transgenerational effects on development

It has been well demonstrated in a variety of marine taxa (and thus likely in cephalopods too) that a stressful event in an individual's life can effect the traits of their offspring (Munday's SEB talk). For example, a stressor in a female cephalopod can cause her to allocate nutrients to her egg yolks in a different manner and thus effect yolk volume in the offspring. This can be either beneficial or not depending on the situation. It is well established that during early embryogenesis (pre-organogenesis), developmental regulation is conducted by maternal genes rather than the embryonic genome (Lee et al., 2014).

In a variety of fishes, if a parent is raised in a stressful environment then their offspring can be pre-acclimated to that stressor (Munday's SEB talk).

Part VI

Their development

Cephalopods have up to five phases in their life cycle (Vidal's 2022 CIAC talk):

Embryonic Fertilization through hatching: the individual is inside an egg

Paralarval Hatching through loss of transitory morphology: the individual retains transitory morphological structures from its embryonic phase such as an internal yolk sac, Hoyle's organ, etc.

Juvenile Loss of transitory morphology through adult morphology (other than size and sex)

Sub-adult Adult morphology (other than size and sex) through onset of gonadal maturation: the individual has all morphological characters used to describe the species (other than sex)

Adult Onset of gonadal maturation through death

Note that each phase may have several stages, such as the stages of embryonic development or maturation.

Chapter 44

Embryonic development

44.1 Egg casings and perivitelline fluid

Octopus vulgaris eggs are on stalks.

The jelly secreted by the oviductal gland is critical for chorion expansion in the developing embryo.

The jelly secreted by the accessory nidamental gland (when present) is rich in symbiotic bacteria that prevent fungal fowling (Kerwin et al., 2019).

Egg volume decreases at first but then increases until hatching as the egg wall thins (Zatylny-Gaudin's 2018 CIAC talk).

The PVF is more viscous than seawater which may help prevent the embryos from becoming too active and hatching early (Marthy, 1976), however there seems to be some sort of protein in PVF which also contributes to tranquilization (Weischer and Marthy 1983).

At least in *Loligo vulgaris* PVF volume increases by 300x over the course of embryogenesis (Marthy, 1976).

44.1.1 O_2, CO_2, pH, and NH_4^+ conditions

Cephalopod egg casing are beneficial in that they provide protection from predators and rapid environmental changes, but they are also barriers to gaseous exchange. Thus, the perivitelline fluid (PVF) inside eggs is often hypercapnic, hypoxic, and high in NH_4^+ relative to seawater (Hu et al., 2011; Hu and Tseng, 2017). PVF P_{CO_2} is often 100-400 Pa (pH 7.2-7.7) (Gutowska and Melzner, 2009; Long et al., 2016), P_{O_2} can fall to 0.2 kPa in late-stage embryos (Long et al., 2016), and $[NH_4^+]$ reaches 3 mM even under ideal abiotic conditions (Hu and Tseng, 2017; Gutowska and Melzner, 2009). As the embryo grows, its metabolic rate increases which causes these environmental conditions to get progressively more extreme. To alleviate some of this, the eggs swell as development progresses so that the egg casing membrane has an increasing surface area and decreasing thickness (Hu and Tseng, 2017), both of which increase diffusive flux (subsection 51.1.2). Additionally, worsening environmental conditions can also facilitate swelling to increase diffusion. This has been demonstrated in squid eggs under hypercapnia (Hu and Tseng, 2017). The mechanism for this swelling is thought to be increasing protein concentration (on the order of 50 mM) (Hu and Tseng, 2017) facilitating osmosis into the egg and thus increasing hydrostatic pressure. Embryos also upregulate hemocyanin and ODH expression as well as several other established hypoxia-responsive genes late in embryogenesis as metabolism is highest and aerobic conditions are worst (Pierce, 2017). At the same time, NKA, Rhesus protein, and proton pump expression levels are highest just before hatching (Pierce, 2017). Hemocyanin expression is even more highly upregulated under hypoxic and hypercapnic environmental conditions (Pierce, 2017).

44.2 Fertilization through gastrulation

Polar body

Table 44.1: Useful keys for embryonic developmental staging

Taxon	Key
Loliginidae	Arnold, 1965
Ommastrephidae	Watanabe et al., 1996
Sepia bandensis	Dwarf_cuttlefish_development_poster.pdf

Table 44.2: Egg size

Taxon	Diameter (mm)	
Loliginids	1-1.5	
Incirrate octopods	2-20	(Schwarz et al., 2018)
Mesonychoteuthis hamiltoni	3	Remeslo et al 2019 (DSRI)

Table 44.3: Hatchling size

Taxon	DML (mm)	
Incirrate octopods	2-10	(Schwarz et al., 2018)
Graneledone boreopacifica	28	(Schwarz et al., 2018)

Zygote a single fertilized cell

Morula a multicellular solid ball of cells known as blastomeres. Each blastomere is determinate (its fate is determined upon formation and, if separated, cannot form its own separate embryo).

Blastula a hollow sphere composed of a single-cell layer of blastomeres with the hollow center filled with blastocoel

Gastrula a cup-shaped structure composed of a multicellular layer of blastomeres differentiated into 3 germ layers: endoderm, mesoderm, and ectoderm. The first opening to form (blastopore) will become the mouth (molluscs are protostomes).

Epiboly the spreading of cells down the yolk until the entire yolk is surrounded by cells

Eggs (ova) have a pore known as a micropyle through which the sperm (spermatid) enters.

During early embryogenesis (blastulation and gastrulation) in all animals, including cephalopods, the genetic control of development is run by maternally-contributed factors. It is not until the maternal-to-zygotic transition that the embryonic genome begins to exhibit control of its own development (Lee et al., 2014).

Unlike other molluscs, cephalopods (or at least coleoids) do not undergo holoblastic spiral cleavage but instead have superficial (meroblastic) cell cleavage that grows on top of a large yolk that takes up most of the cell and sits on one end of the egg (a telolecithal yolk) (Albertin's 2015 CIAC talk).

44.3 Organogenesis through hatching

Organogenesis after gastrulation, the germ layers further differentiate and develop into the organs

Hatching

In adult cephalopods, the arms are anterior and the mantle is posterior, the funnel and arm pair V are ventral and arm pair I is dorsal. In the embryonic cephalopod, however, the nomenclature is rotated 90°. The arms are ventral and the mantle is dorsal, the funnel and arm pair V are posterior and arm pair I is anterior (Albertin's MBL journal club talk).

As embryos, the adult circulatory system is poorly developed. Instead, the yolk sac pulsates which drives blood through the body (von Boletzky, 1987). Additionally, the yolk epithelium, not the gills, is the primary site of ion-exchange (e.g. NH_3 excretion and acid-base balance) as evidenced by many ion channels and mitochondria-rich cells (Hu and Tseng, 2017).

Sepia officinalis express an embryonic hemocyanin isoform that is exclusively expressed until organogenesis and is still dominant until hatching when the adult isoforms dominate (Thonig et al., 2014).

Due to the high PVF P_{CO_2}, embryonic blood P_{CO_2} should be even higher to maintain flux, possibly as high as 600-700 Pa (Melzner et al., 2009).

44.3.1 Hox genes and developments

Hox genes code for transcription factors that regulate the body plan of the developing embryo along the anterior-posterior axis. Note that embryonic orientation notation is rotated 90° from adult notation. So in this context, the anterior-posterior axis is from arm pair I to arm pair V. Hox gene expression has been confirmed to roughly follow anterior-posterior axis in cephalopods (Albertin's 2022 CIAC talk). The Hox genes in cephalopods are not in tight clusters within the genome (as in most other bilaterians) but are all *much* further separated (at least 50kb to 1.5-2 Mb away) from all other Hox genes (Albertin et al., 2015;

Table 44.4: Rough estimates of embryonic development durations. High variation due to abiotic conditions (notably temperature).

Taxa	Embryonic duration (days)	Temperature (°C)	Degree-days	Reference
Loliginids	10-27			(Hanlon et al., 2013)
Ommastrephids	5			
Illex illecebrosus	16	13	200	Jereb and Roper 2010
Cuttlefishes	65-70	16	1000	Sigwart et al. (2015)
Sepia apama	90-150			Cronin and Seymour 2000
Graneledone boreopacifica	53 months	3	4770	(Robison et al., 2014)
Octopus vulgaris	40			Elagoz's 2022 CIAC talk

Belcaid et al., 2019) and the whole cluster spanning 5.5-20 Mb as opposed to *Lottia*'s 470 Kb span (Albertin's MBL journal club talk). The Hox genes are most expressed between stages 7 and 10 in *O. bimaculoides* (Albertin's 2015 CIAC talk) but are still active in some adult tissues (particularly nervous tissue) (Albertin et al., 2015).

Unlike limpets that have 11 HOX genes, *D. pealeii* has 10 and *O. bimaculoides* only has 8 (Albertin's 2022 CIAC talk). The loss of HOX3 in *Octopus* correlates with the loss of arm pair 2 in Octopoda (Albertin's 2022 CIAC talk).

44.3.2 Morphological differentiation

In loliginids, rings in the statoliths begin forming during late embryogenesis (Arkhipkin et al., 2018).

Eye pigmentation begins late in embryogenesis. In *Sepia*, pigmentation does not begin until Stage 24 of 30 and light stimulus response begins at Stage 25 (Bonade's 2018 CIAC talk).

44.3.2.1 Hoyle's organ

Hoyle's organ is a structure on the posterior dorsal mantle which uses both mechanical and chemical mechanisms to hatch from the egg (Cyran et al., 2013). Once hatched, the Hoyle's organ tissue is autophagosed within a few days.

44.4 Timing

Cephalopods have rather long developmental times compared to most other invertebrates. They have similar developmental periods as fishes and crabs, which may be related to the acid-base regulatory abilities of all three groups. They can develop to advanced stages within the egg because they are able to cope with the worsening PVF conditions (Melzner et al., 2009).

Developmental timing can be measured in degree-days: duration times ambient temperature. For example, an embryo that takes 120 hours to develop at 25 °C develops in 3000 degree-days.

In species that do not have maternal care, hatching is often synchronized by photoperiod, with hatching occurring at night (Vidal et al., 2014).

Chapter 45

Paralarval development

All known cephalopods are direct developers; they do not have a true larval stage with subsequent metamorphosis. Thus, their young are known as "paralarvae" rather than true "larvae" (Vidal's 2022 CIAC talk).

At least some cirrates and large-egged octopodids do not have a paralarval stage, but hatch as juveniles (Shea et al., 2018).

msMO$_2$ of paralarvae and hatchlings can often be 3x as high as late-stage embryos (Sigwart et al., 2015).

Developing cephalopods require high concentrations of copper due to its importance in synthesizing hemocyanin. It is likely that they acquire most of their Cu through their diet. Crustaceans are the preferred prey of many young cephalopods likely (in part) because crustaceans also have hemocyanin respiratory pigment which makes them a high-Cu containing food source (Villanueva and Bustamante, 2006). Other essential elements acquired through diet in paralarvae are Fe, Mn, P, and Zn (Villanueva and Bustamante, 2006); these are all in low concentration in natural seawater.

The statoliths can record past stress history such as starvation. In ommastrephids, rings in the statoliths begin forming early in the paralarval stage; in loliginids they already started forming during late embryogenesis (Arkhipkin et al., 2018).

Paralarval *Octopus vulgaris* brains have ~200,000 cells (Styfhals' 2022 CIAC talk).

Paralarval ommastrephids often have their tentacles fused together as a proboscis.

Often immediately after hatching, paralarvae ascend towards the surface (Zakroff et al., 2017) and spend the first part of their lives in shallow surface water.

Lab-raised *Octopus vulgaris* are paralarval for 50-60 days before settling (Roura's 2022 CIAC talk). During that time, they grow roughly 500x larger than hatchlings before settling (Roura's 2022 CIAC talk).

Often, all the arms are not developed in squid hatchlings.

Rhynchoteuthion paralarvae (ommastrephid squids) have large quantities of mucus covering their mantle which collect microbes and plankton. While their arms and proboscis are still developing, they are not able to actively capture prey. Once their yolk is depleted, mortality risk increases. To counteract this, small rhynchoteuthions ($<$ 3 mm DML) consume their mucus to digest the microbes and plankton (Vidal and Haimovici, 1998). As they develop, mucus consumption decreases until no mucus is consumed at ~5 mm DML.

O. vulgaris paralarvae start with 3 suckers on each arm when born and attain 22-25 per arm by the time they settle (Roura's 2022 CIAC talk).

Table 45.1: Paralarval life history?

Taxon	Paralarval life history?	Reference
Grimpoteuthis (cirrate)	No, hatch as juveniles	(Shea et al., 2018)
Euprymna berryi	No	
Octopus vulgaris	50-60 day planktonic stage	Roura's 2022 CIAC talk
Chiroteuthids	No	Vidal's 2022 CIAC talk

Chapter 46

Juvenile and sub-adult development

46.1 Paralarval-settlement transition

O. vulgaris's pupil starts to change from round to horizontal shortly after beginning the settlement phase (Roura's 2022 CIAC talk).

46.2 Growth rates

Juvenile cephalopod growth rates are often exponential, growing with the same principle are compound interest. Therefore the starting size at hatching is highly influential in the size-at-age (Pecl and Jackson, 2007). Since embryos raised at warmer temperatures tend to hatch at smaller sizes (), the faster growth rates in juveniles at warmer temperatures will only result in a larger size-at-age after growth has exceeded the smaller starting size. Statoliths form new rings daily in most cephalopods, thus providing a size-at-age marker.

Growth rates in the laboratory fed ad libitum can be very high, as much as 5-10% ww per day in coastal species (or even a case of 20% per day, Sykes et al. 2006) when animals are young (Wells and Clarke, 1996) . With unlimited food, individuals of all coastal cephalopods examined grow exponentially at first and logarithmically as they reach maturity. Based on mark-recapture studies, wild octopuses tend to actually grow closer to 1-3% ww per day on average throughout their lives (Wells and Clarke, 1996). Incirrate octopods broadly can grow from nearly zero up to 6% body weight per day with interspecific differences driven mainly by habitat temperature (Schwarz et al., 2018). Octopuses, cuttlefishes, and squids all seem to be capable of reaching growth rates in the wild indistinguishable of ad libitum fed laboratory animals, though sometimes squids in particular have slower growth rates (Wells and Clarke, 1996).

Whole-animal growth rates are determined by factors at lower levels of biological organization (Moltschaniwskyj, 2004). For example, mantle muscle in cephalopods grows through both hypertrophy (increased fiber size) and hyperplasia (increased fiber number) (Moltschaniwskyj, 2004). Muscle fibers have a physiological limit to their maximum size, thus hypertrophy alone (as in adult fishes) can limit growth. Since cephalopods also utilize hyperplasia they can continue to grow quickly.

Growth rates are also determined by the relative rates of protein synthesis and degradation. Apparently, *O. vulgaris* retains about 80-90% of the protein it synthesizes (Houlihan et al., 1990). This is similar to other molluscs but double that of cod (Moltschaniwskyj, 2004).

Cephalopod growth across their whole lifespan seems to follow the pattern that juvenile molluscs follow, suggesting that coleoids may have evolved a progenesis growth strategy (Rodhouse, 1998).

As a very rough rule of thumb for organisms in general: 1 g C = 13 g wet weight.

O. vulgaris grow 500x larger from hatchling to juvenile and up to 65,000x larger from settler to death (in lab raised animals) (Roura's 2022 CIAC talk).

46.2.1 von Bertalanffy growth function (VBGF)

The von Bertalanffy growth function (VBGF) is a very popular model of animal growth in fisheries with an asymptotic growth curve. While very good for fishes, individual cephalopods do not often demonstrate asymptotic growth very well (Semmens et al., 2004; Arkhipkin and Roa-Ureta, 2005; Moltschaniwskyj, 2004; Wells and Clarke, 1996; Rodhouse, 1998). Pauly (1981) proposed that gill size is the ultimate limiting mechanism behind growth, but this is not true for squids (O'Dor and Hoar, 2000) or even for fishes (Lefevre et al., 2017).

$$L_t = L_\infty - (L_\infty - L_0)e^{-Kt}$$

where:

L_t is the length at time t

L_∞ is the average maximal length

L_0 is the average length at birth

K is the Brody growth rate coefficient

46.3 Morphometric scaling

If an organism grows isometrically, then surface area (SA) grows to the square of its linear dimensions (i.e. SA $\propto l^2$) and its mass/volume grows to the 3rd power of its linear dimensions (i.e. V $\propto l^3$) (Kardong, 2012).

In paralarvae and juveniles, most organs grow with positive allometry until adulthood when all but the reproductive organs grow isometrically (Moltschaniwskyj, 2004).

As cephalopods grow, jet propulsion becomes increasingly inefficient. To alleviate this issue, loliginids' body plan scales allometrically to improve locomotory efficiency. They do this by elongating mantle length for streamlining, and increasing fin length, width, and area for stronger fin locomotion (O'Dor and Hoar, 2000). In most sized squid, however, mantle diameter and thickness and funnel orifice area (important for jet propulsion) scale isometrically (O'Dor and Hoar, 2000).

Overall, the surface area-to-volume ratio of the squid body plan stays relatively constant with growth, unlike fishes and most other animals (O'Dor and Hoar, 2000).

Many of the brain lobes are still developing during the paralarval stage, but the eyes and optic lobes are fully developed so they can hunt in the plankton (Borgo De la Rosa's 2018 CIAC talk).

46.4 Mortality

There are four main sources of mortality in paralarvae: 1. first feeding, 2. starvation, 3. predation, and 4. advection (Vidal's 2015 CIAC talk).

Chapter 47

Maturation and reproduction

It is possible that there is a sex-determining gene on *E. scolopes* chromosome #43 (Lichilin's 2022 CIAC talk).

Maturation seems to be facilitated by the optic glands (Minakata, 2006).

Unlike in fishes where the production of gonadal tissue is supported by stored energy reserves, cephalopods grow their gonadal tissue directly from their consumed food (Moltschaniwskyj, 2004).

Age-at-maturity is almost always <500 days in temperate and tropical incirrates but polar and deep incirrates can have much longer juvenile stages, reaching up to nearly 11 years (???) (Schwarz et al., 2018).

47.1 Maturity scales

47.1.1 Lipiński and Underhill 1995

47.1.2 Macy III 1982a

This maturity scale was originally developed for *Doryteuthis pealeii* but has been widely used in various loliginids species.

47.2 Maturation-induced physiological changes

Sexual behavior is driven by underlying sexual dimorphism in neuronal circuitry. This dimorphism does not develop until maturation (in *C. elegans*).

47.3 Fecundity

Female fecundity can be expressed as potential fecundity (# of eggs in ovary) or actual fecundity (# of eggs laid).

Loliginids have a potential fecundity of 1000s to 10,000s of eggs (Hixon, 1980). Octopuses vary in their fecundity whether they are a small- or large-egged species. *Octopus vulgaris* produces 100k - 600k small-sized eggs (Vidal et al., 2014). Gonatid squids have a potential fecundity of 8k-16k eggs (Golikov et al. 2019).

Ovulation patterns (Rocha et al., 2001):

Synchronous All oocytes grow and ovulate (leave the ovary) in unison

Group-synchronous The ovary contains "populations" of oocytes in distinct developmental groups

Asynchronous Oocytes of all stages are present at once with no notable grouping

These definitions are merely "nodes" on a continuous scale of ovulation patterns.

Most cephalopods are oviparous, but at least one incirrate, *Ocythoe*, is ovoviviparous (Young et al., 1998). Cephalopod fecundity is size-dependent (Birk et al., 2017).

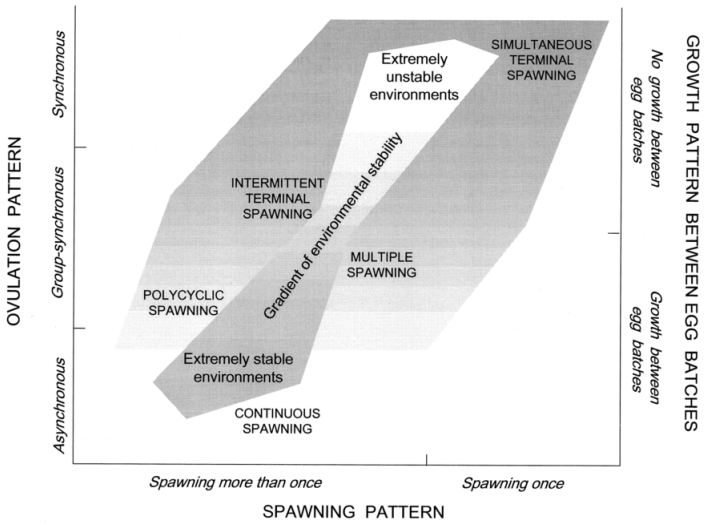

Fig. 1. Diagram illustrating the five cephalopod reproductive strategies in relation to the type of ovulation, the spawning pattern and whether or not somatic growth between egg batches occurs. These strategies are adapted to a given degree of environmental stability, as successful adaptations of each species to the different environmental and demographic pressures faced during evolutionary processes.

Figure 47.1: Reproductive strategies as a function of environmental stability. Original figure from Rocha et al. (2001).

47.4 Egg laying

The female's choice of where she deposits her eggs can be very important for the survival of the young. Many species of decapodiforms lay their eggs nearby existing egg masses. This has been seen in loliginids(Arnold, 1962; Larcombe and Russell, 1971), sepiolids (Deickert and Bello, 2005; Laptikhovsky et al., 2008), cuttlefishes (Hall and Hanlon, 2002), and potentially ommastrephids (Birk et al., 2017). In *Doryteuthis pealeii* it has been demonstrated that they are actively choosing to deposit eggs near other masses, not merely wanting the same habitat directly (Arnold, 1962).

Fertilization is typically believed to occur when the female is holding the egg near the buccal mass (Puneeta et al., 2015; Iwata's 2018 CIAC talk).

47.4.1 Incirrates

All known incirrates (except *Octopus chierchiae*) have terminal reproduction (Wang's 2022 CIAC talk).

Benthic incirrate octopods lay eggs with the chorion stretched to form a stalk for attachment to a surface (Young et al., 1998). Unlike other cephalopods, they do not deposit any jelly on their eggs. They typically attach their eggs to the undersides of ledges but they seem to favor any hard substrate they can find including sponges growing off of manganese nodules in the deep sediment-ladened benthos (Purser et al., 2016).

All known pelagic incirrates brood their eggs within their arms (Nixon and Young, 2003; Young, 1972).

Ocythoe tuberculata is a notable exception to all cephalopods; it is ovoviviparous (Young et al., 1998).

47.4.2 Cirrates

Cirrates typically lay a single large egg on the benthos with a tough coating formed by the oviductal gland. Cirrates have been known to lay their eggs on chrysogorgiid corals; they seem to prefer long branching corals putatively because this may keep the eggs up off the seafloor where convection is higher for gas exchange (Pratt's 2022 CIAC talk). No cirrates are known to exhibit any sort of maternal care.

47.4.3 Sepiids

Some species of cuttlefish (e.g. *Sepia officinalis*) add ink to the egg casings but other *Sepia* do not.

47.4.4 Idiosepiids

Idiosepius spawns continuously (Wang's 2022 CIAC talk).

47.4.5 Myopsids

Most loliginids in temperate regions migrate inshore to shallow waters to spawn and lay their eggs (Hixon, 1980). Myopsids lay egg masses typically on hard substrates or plant matter but sometimes also merely sediment (Hanlon et al., 2013). Their egg masses are composed of 10s of "fingers" each with 10s to 100s of eggs (Hixon, 1980) forming a "mop".

47.4.6 Oegopsids

Oegopsids display a diversity of egg laying behaviors. Ommastrephids lay pelagic gelatinous egg masses (Staaf et al., 2008; Birk et al., 2017) while gonatids and bathyteuthids brood their eggs (Seibel et al., 2005; Bush et al., 2012).

47.5 Death

In a number of female incirrate octopods, while eggs are brooded, the female stops eating and the digestive organs begin to deteriorate (Young, 1972). This behavior is driven by the optic glands (Wang and Ragsdale, 2018).

Most cephalopods have a lifespan of around a year. The short lifespan of cephalopods has been proposed to be due at least in part to their low antioxidant capacity (Trübenbach et al., 2013) relative to their high metabolic rates. This may lead to frequent cellular oxidative damage which may lead to shorter lifespan.

In *Octopus vulgaris*, white spots on the skin are a sign of the beginning of senescence. Small purple spots show up just a few days before death (Roura's 2022 CIAC talk). The arm tips also start to decay and get eaten away during senescence by the animal (Roura's 2022 CIAC talk).

Chapter 48

Regeneration

Cephalopods are able to regenerate their arms. Regeneration begins with a mass of dividing cells known as the blastema that will produce all the cell types necessary for regeneration. In *O. bimaculoides*, the blastema forms 7 days after arm amputation and by day 21, a miniature arm has grown with suckers, chromatophores, and locomotory ability (Schulz's 2022 CIAC talk).

Regeneration requires the suppression of "mature" genes and the upregulation of "develop" genes (Escheverri's MBL talk; Callaghan et al. 2019, JEZ-B) as well as germline genes at least in some non-cephalopod organisms.

Chapter 49

Rhythmicity

An organism's circadian clock is composed of a variety of genes that are cyclical. The foundation of the clock is a transcription factor heterodimer of CLOCK and BMAL (ARNTL). These are modulated by other positive or negative elements such as CRY and TIMELESS.

Part VII

Their morphology and physiology

Chapter 50

External morphology and physiology

50.1 Mantle

50.1.1 Morphology

Octopods and sepiolids (at least, maybe more) have a band of muscle that runs anterior-posteriorly the length of the mantle cavity along the ventral margin. This separates the mantle into left and right sides.

50.1.1.1 Muscle fibers

Arrangement The mantle is composed of 2-3 mutually perpendicular muscles (Kier and Thompson, 2003). Most coleoid mantle is mainly (by volume) composed of circular muscle which runs around the circumference of the mantle. Interspersed between circular muscle fibers are radial muscle fibers which run from the inner tunic (mantle cavity) to the outer tunic (outer mantle surface). In loliginids, at least, radial muscles compose about 10% of the total mantle muscle volume (Bone et al., 1981). In octopods and sepioids and some deep-water teuthoids, there is also longitudinal muscle which runs anterior-posteriorly along the most superficial margins of the mantle cross-section (Kier and Thompson, 2003).

Gelatinous cephalopods contain a gelatinous layer between the circular muscles (Kier and Thompson, 2003).

Myocyte ultrastructure Mantle muscle, as well as most of coleoid muscle, is obliquely striated: the myofilaments and Z-disc line are staggered down the length of the muscle fiber cell rather than in distinct bands when viewed longitudinally (Kier, 2016). It is also uninucleate (Kier and Thompson, 2003). Aerobic circular muscle fibers are fusiform and are 4-8 μm (up to 10 μm) in diameter and 1-2 mm long (Bone et al., 1981; Kier and Thompson, 2003). Anaerobic circular muscle fibers are smaller, up to 5 μm in diameter (Bone et al., 1981) which is surprising given that in vertebrates, anaerobic fibers are typically larger than aerobic fibers. Radial muscles can be up to 5 μm wide (Kier and Thompson, 2003). These are all smaller than most fish, crustacean, and mammalian myocytes which are often 10-1000 μm wide (Kinsey et al., 2007).

Since cephalopods grow by increasing myocyte size (hypertrophy) and also number (hyperplasia) (Moltschaniwskyj, 2004), the sizes of muscle fibers will vary, as observed by Bone et al. (1981). The proportion of mitochondria vs myofibril scales isometrically with increasing myocyte size (Bone et al., 1981). The mitochondria within each myocyte are congregated in the core of the cell with the myofibrils surrounding them, rather than being uniformly distributed amongst the myofibrils (Hochachka et al., 1978; Mommsen et al., 1981; Bone et al., 1981).

Aerobic fibers can attain 50% mitochondria by volume (Mommsen et al., 1981) which is higher even than hummingbird wing skeletal muscle (Suarez et al., 1991).

"Sandwich" pattern The circular musculature is arranged in a "sandwich", at least in shallow-water species, where the outer layers of muscle cells (both on the outside of the animal and the inner mantle cavity) are mitochondria-rich aerobic fibers with large mitochondrial cores in the center of the myofilaments (approx. 50% mitochondria)(Mommsen et al., 1981) and have relatively high capillary density (Bone et al., 1981). The inner layer is mitochondria-poor anaerobic fibers with small mitochondrial cores (approx. 5% mitochondria)(Mommsen et al., 1981) and lower capillary density (Bone et al., 1981). Of the entire mantle musculature of *Illex illecebrosus*, for example, 80% is anaerobic inner layer and 20% is the aerobic outer layers, with the anaerobic layer growing allometrically as squids grow (Kier and Thompson, 2003; Thompson and Kier, 2006).

The radial muscles are also mitochondria-poor ($\approx 5\%$) (Bone et al., 1981).

50.1.1.2 Connective tissue

Most (if not all) connective tissue in the mantle is collagenous (Kier and Thompson, 2003).

There is a layer of connective tissue just underneath the skin. In squids, each layer is known as a tunic. Tunics are composed of parallel helical fibers (Kier and Thompson, 2003). In *Octopus*, the superficial connective tissue is more randomly arranged (Kier and Thompson, 2003).

In addition, in most (but not some deep-water) squids, intramuscular connective tissue fibers run diagonally through the cross-section of mantle connecting to the inner and outer tunics (Bone et al., 1981; Kier and Thompson, 2003). Some are found in the circular muscle fibers and others are oriented and located with the radial muscle fibers (Kier and Thompson, 2003). Finally, in all coleoids, there is also coiled connective tissue that runs in parallel with the circular muscles (Bone et al., 1981; Kier and Thompson, 2003). In *Octopus,* there is also connective fibers found within and parallel to the longitudinal muscle (Kier and Thompson, 2003). The intramuscular connective tissue fibers are on the order of 1-5 μm diameter (Kier and Thompson, 2003).

In gelatinous species, there is a 3D meshwork of collagen that supports a matrix of ammoniacal capsules (Kier and Thompson, 2003).

50.1.1.3 Vasculature

Unlike fish muscle fibers which have 3-7 capillaries around each muscle fiber, squid muscle fibers are much more sparsely supplied. In the outer aerobic layers of circular tissue, capillaries are found every 5-8 muscle fibers and in the central anaerobic layers, capillaries are found 20+ muscle fibers apart (Bone et al., 1981). It should be kept in mind, however, that cephalopod myocytes may easily be an order of magnitude smaller than fish myocytes (Kinsey et al., 2007) so the O_2 and CO_2 diffusion distances may be similar.

50.1.1.4 Innervation

Nerves radiate from the stellate ganglia to innervate the mantle muscle. The axons branch extensively (Bone et al., 1981).

50.1.2 Cellular composition

Sepia officinalis mantle muscle at rest maintains ≈3 $\mu\text{mol} \cdot \text{g}^{-1}$ of glucose (Sykes et al., in review). Mantle muscle is ≈15% protein by mass (≈15 mg/g) (Sykes et al., in review).

50.1.2.1 Anaerobic potential

Due to the disproportionate width of anaerobic fibers in the mantle cross-section, mantle muscle as a whole is better equipped for rapid-contraction anaerobic glycolysis than aerobic catabolism as demonstrated by both the highest levels of ODH anywhere in the body (high anaerobic capacity) and CS and AspAT levels dwarfed (low aerobic capacity) by the other major muscle, the systemic heart which is highly aerobic section 34.10.

In addition, mantle muscle has high enzymatic activity for PEPCK, the first enzyme in gluconeogenesis, but not for enzymes later in gluconeogenesis (Speers-Roesch et al., 2016). Thus, it may be that when glycogen stores are low in mantle muscle (just after anaerobic exercise), gluconeogenesis begins directly in the mantle muscle and intermediate product(s) are sent to the digestive gland (where the remaining enzyme activities are high) to complete gluconeogenesis before returning the final glycogen product to the mantle tissues.

Glycogen concentration in *Dosidicus gigas* mantle muscle is ≈ 300 $\mu\text{mol glucosyl units g}^{-1}$ (Seibel et al., 2014). This may be higher than most cephalopods given this species' hypoxia-prone lifestyle. It is certainly much higher than average whole-body glycogen concentration in fishes of 5-20 $\mu\text{mol glucosyl units g}^{-1}$ (Nilsson and Östlund-Nilsson, 2008). Additionally, the concentrations of phosphoarginine, an energy reserve utilized during anaerobic metabolism, is 10x higher in mantle muscle than other major tissues like systemic or branchial hearts, or funnel (Häfker, 2012).

50.1.3 Biomechanics

The mantle functions as a muscular hydrostat. Since the muscle is nearly completely incompressible (Kier and Thompson, 2003), the total muscle volume always remains constant. Therefore, as one dimension shortens, another must lengthen.

Mantle contraction can create pressure in the mantle cavity up to 100 kPa (*Dosidicus gigas,* O'Dor, 2013).

50.1.3.1 Hyperinflation

Before a jet (and sometimes during normal breathing), the radial muscles contract to inflate the mantle cavity larger than a normal resting size (Kier and Thompson, 2003).

Table 50.1: Contractile properties of mantle circular muscle

Taxon	Maximum force ($mN \cdot mm^{-2}$)	Delay from stimulation to maximum force (ms)	Reference
Loliginid	260	90	(Milligan et al., 1997)
Sepiid	230	200	(Milligan et al., 1997)

50.1.3.2 Exhalation

The mantle is contracted by contraction of circular muscle fibers which are oriented parallel to the mantle circumference (Bone et al., 1981). During this mantle contraction, radial muscle fibers that are oriented perpendicularly to the circumference of the mantle expand as the mantle thickens. The diagonal collagen fibers also stretch. Either longitudinal muscles or the tunic (depending on taxon) prevents elongation along the long-axis of the animal (Kier and Thompson, 2003).

As mentioned above (subsection 50.1.1), the circular muscle is composed of a "sandwich" of aerobic fibers on the outside and anaerobic on the inside. Mommsen et al. (1981) proposed that when only a small portion of circular muscles are being utilized, as during breathing or routine swimming contractions (Bone et al., 1981), this arrangement allows the passive central mantle muscle to be pressurized as a hydrostatic working fluid. As in all hydrostatic skeletons, the pressurizing muscle must surround the working fluid.

50.1.3.3 Refilling

During the refilling stage, the diagonal connective fibers recoil back to their normal length and the radial fibers contract. These forces cause the mantle cross section to thin and the circumference increases along with the expansion of the circular muscle fibers (Kurth et al., 2014). The majority of the force comes from the recoiling connective fibers rather than the radial muscle (Kier and Thompson, 2003). This produces a pressure depression within the mantle cavity, thus drawing water in across the gills.

50.2 Fins

Loliginid fins connect to the mantle on the side of the mantle, while in ommastrephids, the fins connect on top of the mantle (O'Dor and Hoar, 2000).

50.2.1 Morphology

The fin is separated dorsoventrally by a median connective tissue fascia (Kier and Thompson, 2003). The dorsal and ventral regions are mirrored in their muscular and collagenous arrangements. There are three fin muscles arranged in mutually perpendicular directions (Kier and Thompson, 2003). The transverse muscle runs from the fin cartilage in the mantle to the outer edge of the fin, the dorsoventral muscle runs vertically from the median fascia to either the dorsal or ventral fascia just underneath the dermis, and the longitudinal muscle runs in parallel with the long axis of the animal (Kier and Thompson, 2003).

Fin transverse muscles are arranged in a similar "sandwich" pattern as the mantle, with mitochondria-rich muscle fibers superficially next to the dorsal and ventral fasciae and mitochondria-poor fibers in the center of the fin (Kier and Thompson, 2003). The dorsoventral and longitudinal muscles are mitochondria-poor (Kier and Thompson, 2003). Fin muscles are innervated directly from the fin lobes in the brain (section 51.5.2.4). The larger the fins, the larger the fin lobes (Budelmann, 1995).

50.2.2 Biomechanics

In order to bend the fin, the transverse muscles on either the dorsal or ventral portion of the fin must contract to shorten the fin width while the opposite portion of the fin must resist increasing in thickness (Kier and Thompson, 2003). During resting (e.g. hovering) fin movements, the aerobic transverse fibers contract on one side, and the collagen on the other side provides enough resistance to thickening (Kier and Thompson, 2003). During rapid swimming undulations, however, the entire transverse muscle (both aerobic and anaerobic fibers) contracts and the dorsoventral (and longitudinal muscles to some extent) contract to resist thickening or lengthening of the other side of the fin (Kier and Thompson, 2003).

50.3 Funnel

The funnel orifice area scales isometrically in loliginid squids (O'Dor and Hoar, 2000).

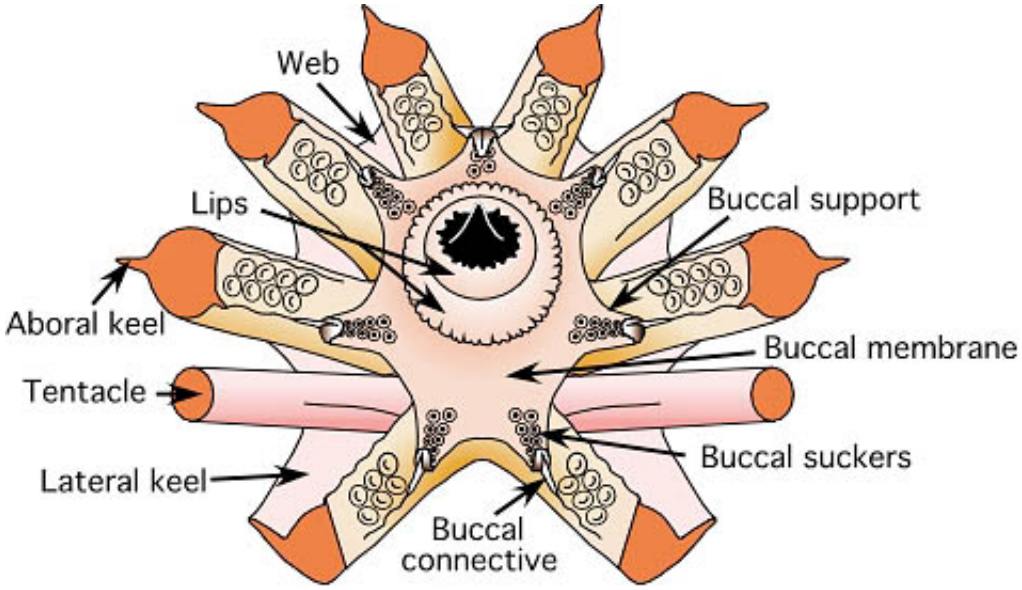

Figure 50.1: Buccal membrane. Figure from TolWeb.

50.3.1 Morphology

Loliginids have funnel retractor muscles that connect from the gladius to the funnel (Kier and Thompson, 2003).

As in the mantle, the muscle is obliquely striated and arranged in three mutually perpendicular muscles with longitudinal muscles superficially, circular muscle centrally, and radial muscle interspersed (Kier and Thompson, 2003). There are also connective fibers more superficial than the longitudinal muscles (Kier and Thompson, 2003).

Sepia funnel muscle is vascularized to yield 32 μm radius Krogh cylinders, 3x as large as rat red muscle (Abbott and Miyan, 1995).

50.3.2 Biomechanics

The funnel, or siphon, is very flexible and can be pointed in almost any direction. Contraction of the circular fibers narrows the diameter and extends the length of the funnel (Kier and Thompson, 2003). Contraction of the longitudinal muscles shortens the length and widens the diameter (Kier and Thompson, 2003). Contracting the radial muscles also widens the orifice diameter (Kier and Thompson, 2003). The funnel is bent by simultaneously contracting the radial muscles as well as the longitudinal muscles on only the inner bending side (Kier and Thompson, 2003). By contracting both, the longitudinal muscle pressure shortens the length rather than just widens diameter (Kier and Thompson, 2003).

50.4 Head

The posterior region of the head is the occipital region. More specifically, the dorsal posterior region has historically been known as the nuchal region. The head is connected to the gladius in decapodiforms by the cephalic and nuchal retractor muscles (Kier and Thompson, 2003). These muscles control how far into the mantle cavity the head is positioned (Kier and Thompson, 2003). The occipital crest is the posterior edge of the head, typically furthest back on the sides of the head.

The brain (but not optic lobes) is enclosed by a cartilaginous casing.

The head possesses a rhinophore in nautiloids and olfactory pits in coleoids.

50.5 Arms and tentacles

Ancestors to coleoid cephalopods (e.g. belemnoids) had ten arms. However, a pair have been lost or modified in both octopods and decapods. Octopods have lost arm pair II resulting in the current eight-arm state (Young et al., 1998). This is based on phylogeny regarding *Vampyroteuthis'* arm pair II feeding tentacles as well as HOX gene expression patterning: *Octopus* lost the HOX3 gene and their arm pair II have HOX expression like *Doryteuthis* arm pair III, suggesting *Octopus* arm pair II are

equivalent to the ancestral pair III) (Albertin's 2022 CIAC talk). Decapods, however, retain arm pair II but pair IV were modified into tentacles.

The appendages are muscular hydrostats, creating movement by antagonistic contraction and elongation of muscle groups. Sepioids and myopsids have tentacle pockets in which their tentacles can be at least partially retracted. Only sepiids can fully retract their tentacles (Young et al., 1998).

The arms and tentacles are innervated by brachial and tentacle nerves, respectively which originate in the brachial lobe of the brain (Nixon and Young, 2003).

50.5.1 Muscular morphology

All coleoid appendages are composed of three main muscle groups: transverse muscles, longitudinal muscles, and oblique/circular muscles Figure 50.2. Octopodid arms have three different layers of oblique muscles. A single nerve and artery run down the center of each appendage. In addition, the appendages are covered by dermal connective tissue which contains chromatophores, blood vessels, and nerves (Kier, 2016). Octopodid arms have fibrous connective tissue known as trabeculae that run in between many of the longitudinal muscle bundles (Kier, 2016).

The tentacles and octopodid arms can expand in length by over 80% while decapodid arms do not notably change length (Kier, 2016).

50.5.1.1 Myocyte ultrastructure

Within each muscle group, the individual muscle cell fibers are obliquely striated: the myofilaments and Z-disc line are staggered down the length of the muscle fiber cell rather than in distinct bands when viewed longitudinally (Kier, 2016). Within the center of the myofilaments are the mitochondrial cores. Relative to other tissues, coleoid appendages are rather poor in mitochondria (Kier, 2016).

Unique tentacles Unusually for cephalopods, the transverse and circular muscles in tentacles are cross-striated, as in vertebrates, rather than obliquely striated like the rest of the appendages and body (Kier, 2016). Also, the individual thick filaments (myosin) are 10x shorter than in arm transverse muscle. This provides faster contraction performance (10x faster contraction than the arms) which would be beneficial since the transverse muscles are the active muscle group involved in the tentacle strike subsubsection 50.5.3.1(Kier, 2016). The mitochondria are not in the muscle fiber core, as in obliquely striated muscle, but instead are peripheral to the cells (Kier, 2016).

Sepia tentacular muscle is vascularized to yield 61 μm radius Krogh cylinders, 50% larger than rat white muscle (Abbott and Miyan, 1995).

When squids first hatch, their tentacles are obliquely striated like the arms; the cross-striation does not appear until a few weeks later (Kier and Thompson, 2003). In parallel, hatchlings lunge at their prey with splayed arms rather than use tentacle strikes (Kier and Thompson, 2003).

Interestingly, cephalopods seem to adjust muscle performance by changes in ultrastructure with unchanged biochemistry (i.e. protein isoforms), which is the opposite of vertebrates which have unchanged ultrastructure but modify biochemistry (Kier and Thompson, 2003).

Interestingly, tentacles possess Na_v channels unlike the arms or vertebrate muscle. This is thought to facilitate rapid, simultaneous burst contraction (Rosenthal, pers. comm.).

50.5.2 Tentacular club morphology

The tentacular club and stalk is composed of three main regions: the carpus, manus, and dactylus. The carpus is the most distal region of the stalk. It has a carpal locking apparatus, composed of carpal suckers and knobs, which adhere to their counterparts on the opposite tentacle. *Architeuthis* also possess suckers and knobs running the length of the shaft (Kubodera and Mori, 2005).

The manus is the proximal region of the club which is wider than the rest and typically contains the largest suckers.

Finally, the dactylus is the most distal portion of the club. It often has irregularly arranged suckers and is narrower than the manus. In some squids, there is a circular ring of small suckers distally to the dactylus known as the terminal pad. The suckers can bind to their pair on the opposing tentacle to keep the clubs attached. Finally, some species possess a keel which is found on the dorsal side of the dactylus.

The boundary between the manus and dactylus varies in its prominence in different species.

In some species, hooks have replaced suckers on the tentacular club.

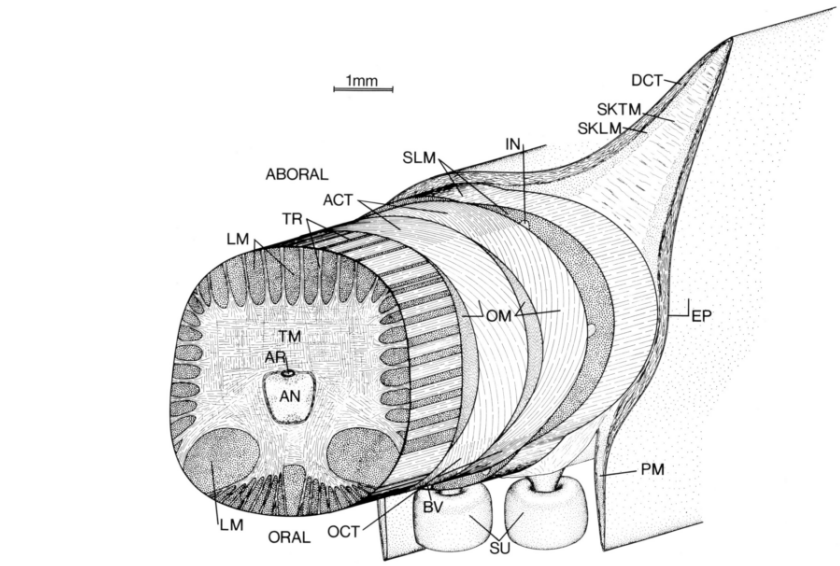

FIGURE 4 | Schematic diagram of left arm of a loliginid squid. AN, axial nerve cord; ACT, aboral connective tissue (fibrous); AR, artery; BV, superficial brachial vein; DCT, dermal connective tissue; EP, epithelium; IN, intramuscular nerve cord; LM, longitudinal muscle; OCT, oral connective tissue (fibrous); OM, oblique muscle; PM, protective membrane; SKLM, swimming keel longitudinal muscle; SKTM, swimming keel transverse muscle; SLM, superficial longitudinal muscle; SU suckers; TM, transverse muscle; TR, trabeculae of transverse muscle. From Kier (1982).

(a) Decapod arm

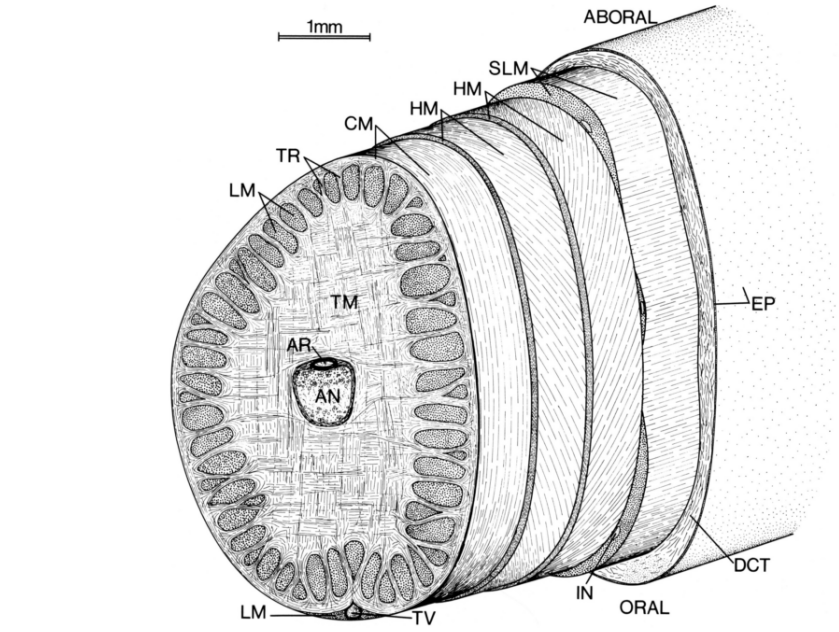

FIGURE 1 | Schematic diagram of left tentacular stalk of a loliginid squid. AN, Axial nerve cord; AR, artery; CM, circular muscle; DCT, dermal connective tissue; EP, epithelium; HM, helical muscle; IN, intramuscular nerve cord; LM, longitudinal muscle; SLM, superficial longitudinal muscle; TR, trabeculae of transverse muscle; TM, transverse muscle; TV, superficial tentacular vein. From Kier (1982).

(b) Decapod tentacle

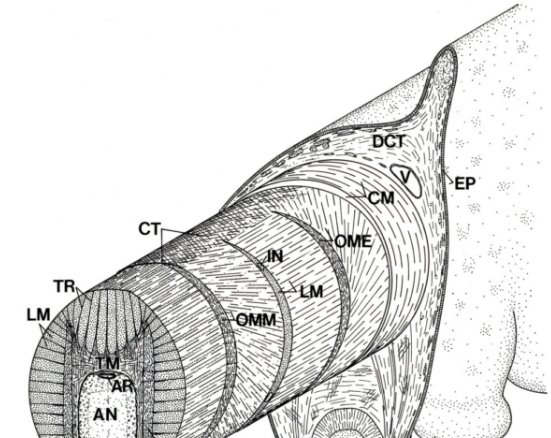

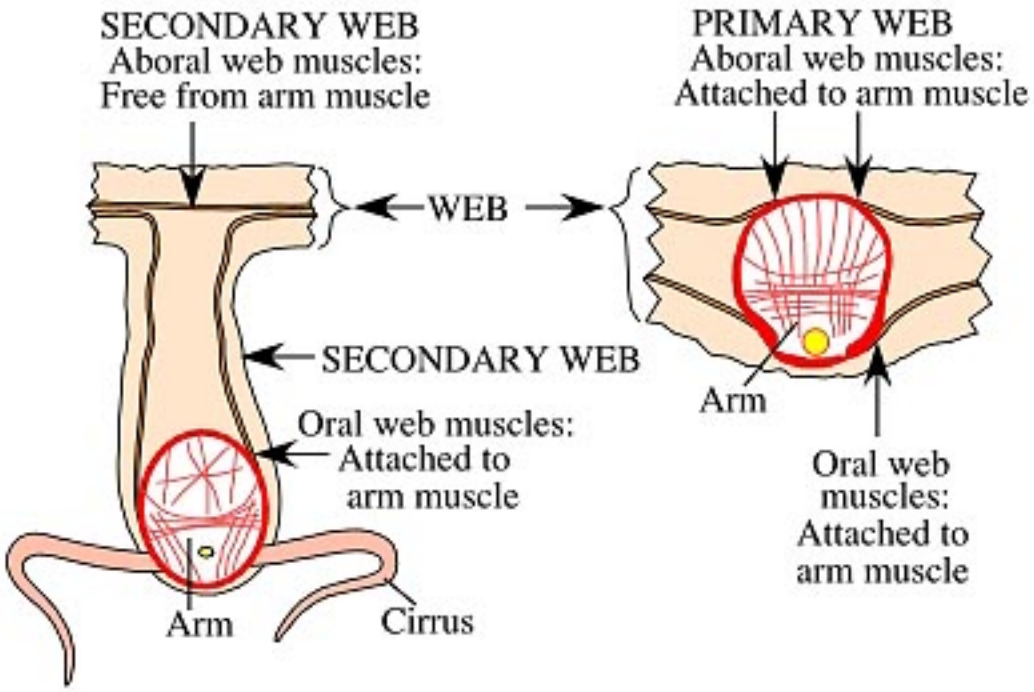

Figure 50.3: Cirrate octopod webbing. Figure from ToLWeb.

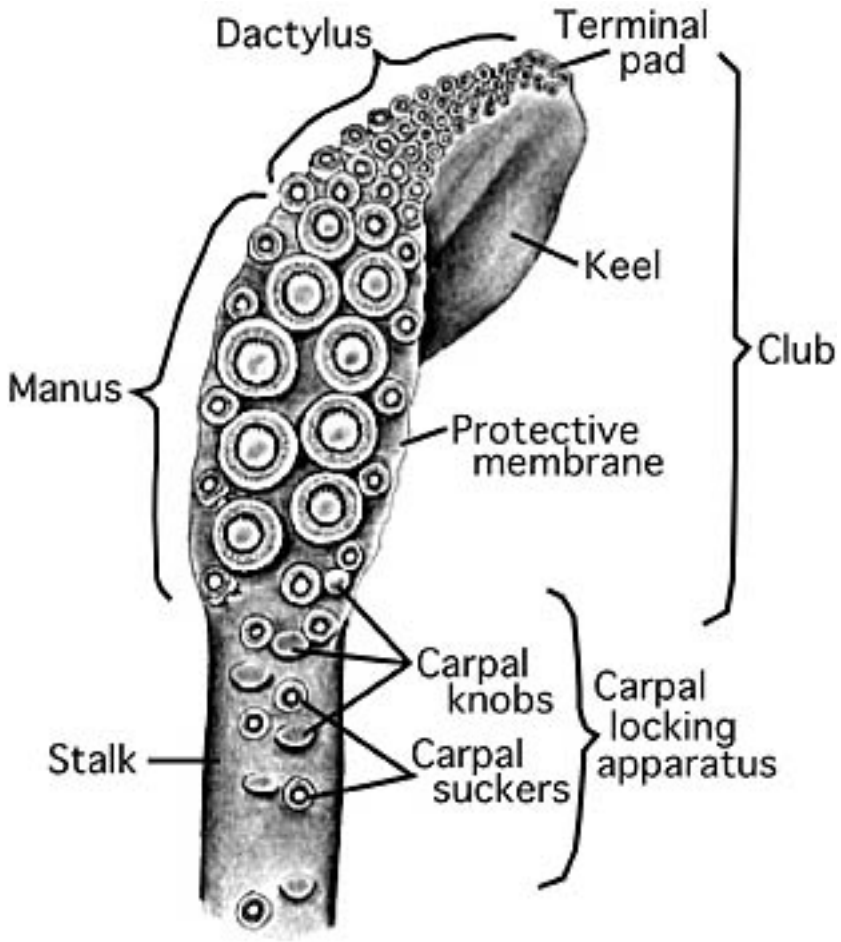

Figure 50.4: Tentacular club morphology. Figure from ToLWeb.

50.5.3 Biomechanics

50.5.3.1 Tentacle strike

Since the total volume of the tentacles must remain constant, contraction of the transverse and circular muscles decrease the tentacle stalk diameter which leads to expansion of the tentacle length by expansion of the longitudinal muscles 50.2b. To return the tentacles to their original contracted length, the longitudinal muscles are then contracted (Kier, 2016). Tentacles must also be able to twist to align the clubs with the prey. Twisting is possible through both left- and right-handed helical muscles which have greater torque being on the periphery of the stalk (Kier, 2016).

The same principles are applicable for elongating and contracting octopod arms (Kier, 2016).

In *Doryteuthis pealeii*, tentacle strikes have been documented to reach 2 m/s, accelerating at 250 m/s^2 (Kier and Thompson, 2003).

50.5.3.2 Arm bending

In order to bend the arm, longitudinal muscles on one side of the arm must contract while the transverse muscles resist diameter increase or, alternatively, the transverse muscles must contract and the longitudinal muscles on the bend-ward side of the arm must resist length increase 50.2a. Because bending is often towards the mouth to move prey towards the beak, the longitudinal muscles on the oral side of the arms in squids and cuttlefishes are larger than on the aboral side (Kier, 2016). Both longitudinal and oblique muscles are on the peripheral of the arms which provide good leverage for bending and resisting twisting, respectively (Kier, 2016). When prey are trying to escape the arms, the oblique muscles must contract to prevent twisting the arms (Kier, 2016).

50.5.4 Autonomy and regeneration

Both arms and tentacles can be regenerated to be indistinguishable from the original appendages. In *Octopus* spp., over half of individuals found have at least one truncated arm and that arm was missing on average about 25-33% of its length (Voss and Mehta 2021, Zoology). Often there is a bias towards losing the left arms (L1 and L2) relative to the right but the anterior/posterior bias is species-specific (Voss and Mehta 2021, Zoology).

50.5.5 Suckers

50.5.5.1 Morphology

The suckers attach to the arm's connective tissue by extrinsic muscles (Kier and Thompson, 2003). Octopod suckers are sessile while decapod suckers are raised on a stalk. The stalk can elongate, shorten, and bend (Kier and Thompson, 2003).

The suckers are composed of an outer disc-like infundibulum and an inner spherical cavity known as the acetabulum (Kier and Thompson, 2003).

Sucker muscles are oriented in three mutually-perpendicular directions. The radial muscles are perpendicular to the outer surface of the sucker, the circular muscles run around the circumference of the sucker, and meridional muscles run the length of the sucker. There are also sphincter muscles that regulate the size of the opening between the infundibulum and acetabulum (Kier and Thompson, 2003).

Some decapodiform suckers possess sucker teeth, chitinous nodules within the sucker ring. These sucker ring teeth are regulated by suckerins, a cephalopod-specific gene family.

50.5.5.2 Biomechanics

To stay attached to an object, the pressure inside the acetabulum must be lower than ambient pressure. To achieve this, the radial muscles contract to decrease the thickness of the acetabular wall. Since the volume of the acetabular muscle is constant, decreasing thickness increases surface area of the acetabular cavity, thus increasing volume and decreasing pressure according to Boyle's law (Kier and Thompson, 2003). This mechanism requires constant muscular contraction, however. Long-term attachment to objects can be attained by first contracting the circular and meridional muscles before reaching an object. These thicken the acetabular wall which stores energy into collagen fibers. Then, when the infundibulum seals on the object, the circular and meridional muscles can relax and the collagen fibers can thin the wall, increasing acetabular cavity volume and creating suction (Kier and Thompson, 2003).

The infundibulum creates good seals on objects by its radial, circular, and meridional muscles as well.

Forces which seek to pull the sucker away from an object actually make the suction stronger (Packard, 1988).

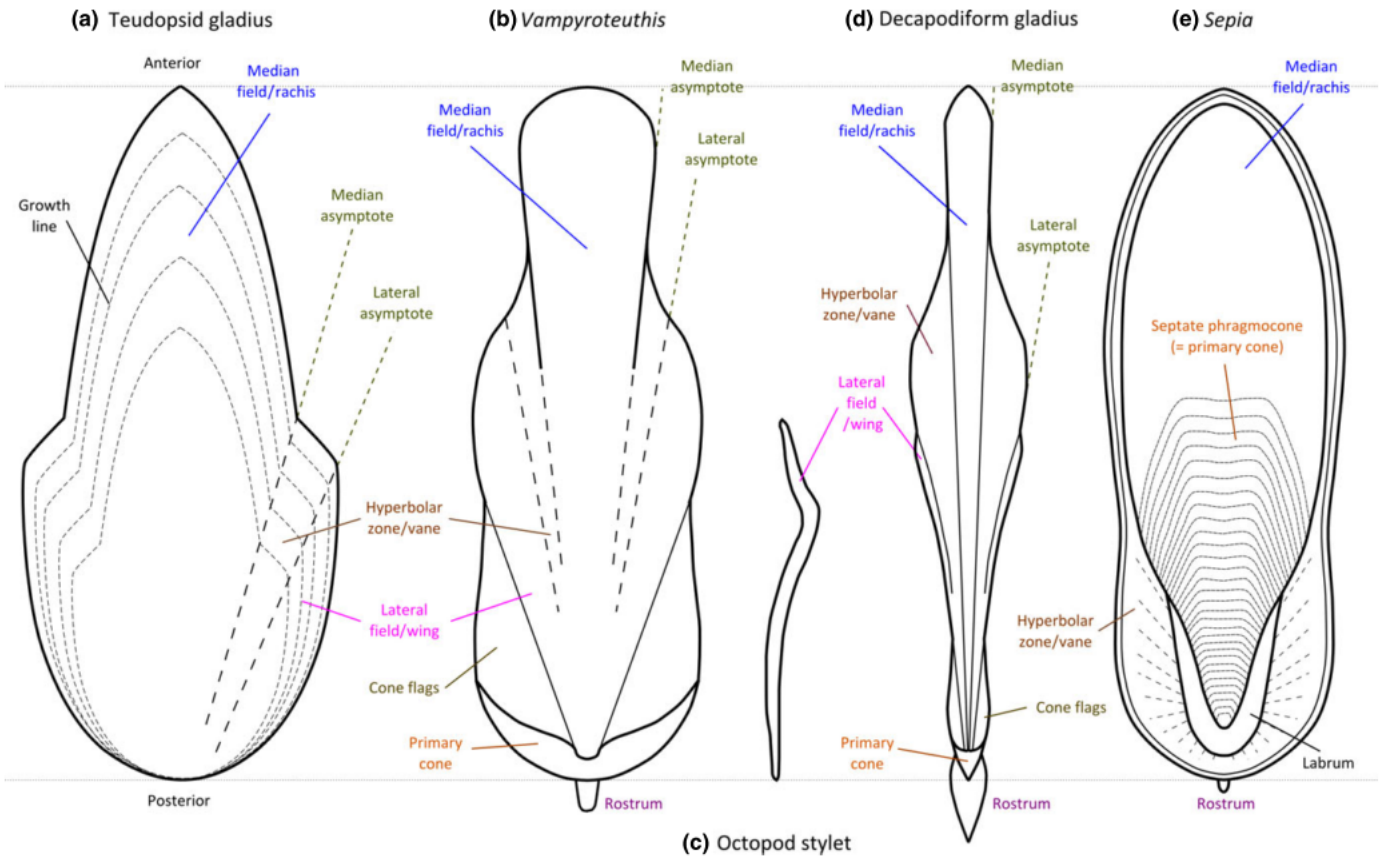

Fig. 1. Homologies for the neocoleoid gladius. Median field, hyperbolar zone, lateral field and phragmocone are treated here as homologous to rachis, vane, wing and primary cone of living Neocoleoidea. Idealised representations of (a) fossil and (b-e) extant gladii.

Figure 50.5: Morphology of coleoid cephalopod shell remnants. Figure originally from (Sutton et al., 2015).

50.5.5.3 Sensation

Octopus vulgaris has 10,000 chemosensory cells per sucker compared to only 100 in cuttlefish (Morse's 2022 CIAC talk).

In octopuses (at least), rhodopsin kinase (GRK1), a key canonical component of a rhodopsin-based visual system, is expressed not only in the retina but also the skin and suckers (de Zoysa's 2022 CIAC talk).

50.5.5.4 Chitinase activity

The suckers express much more chitinase than most other tissues (Albertin et al., 2015), suggesting that it may be functional for handling chitinous prey.

50.5.6 Hectocotylus

See subsubsection 51.7.1.1.

50.6 Shell (remnants)

The loss of the shell in coleoids may have been driven, at least in part, by the echolocation of cetaceans. Shells are a strong signal, and selective pressures to reduce or remove shells would have been strong.

50.6.1 Cuttlebone

The cuttlebone is formed of aragonitic $CaCO_3$ and thus is rich in both Ca and Sr (Villanueva and Bustamante, 2006). As the individual ages, its shell thickens with new layers secreted on the ventral side of the cuttlebone (Sigwart et al., 2015). The

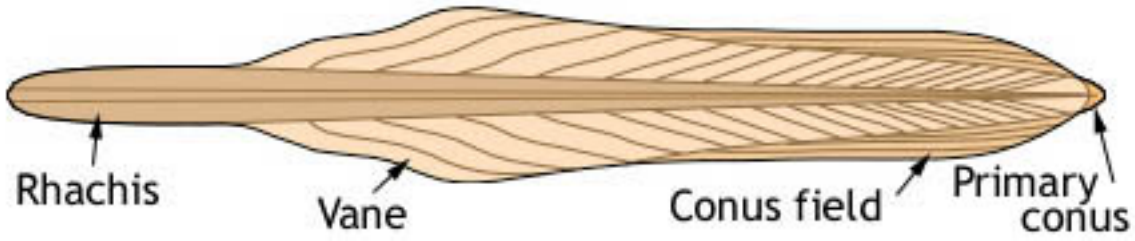

Figure 50.6: Gladius morphology.

individual chambers in the cuttlebone are ~1 mm wide (Peyla's 2022 CIAC talk).

50.6.2 Gladius

The gladius is the demineralized form of a belemnoid phragmocone (Fuchs' 2015 CIAC talk). Gladii are chitinous in sepiolids, teuthids, and vampyromorphs (Arkhipkin et al., 2018). They possess periodic increments (Naef 1922). Cirrate vestigial shells are also known as gladii but are different (see below).

The gladius is divided into three main sections by two asymptotes: the rachis, vanes, and wings are demarcated by the median and lateral asymptotes (Sutton et al., 2015). The gladius grows anteriorly as the individual grows, resulting in the posterior end being the oldest portion of the structure. The posterior end has less well defined increments than the anterior end, making absolute aging from the gladius impossible (Arkhipkin et al., 2018). The periodicity of increment formation is less conserved than the daily increment growth in statoliths (Arkhipkin et al., 2018).

In loliginids, the gladius is an anchor point for the funnel retractor muscles (Kier and Thompson, 2003). The cephalic and nuchal retractor muscles also anchor to the gladius (Kier and Thompson, 2003).

The gladius is surrounded by the shell sac that contains roughly double the $[Ca^{2+}]$, half the $[Na^{+}]$, and 33% less $[Mg^{2+}]$ and $[Cl^{-}]$ than blood (Messerli et al., 2019).

50.6.3 Stylet

The stylet is considered homogenous to the gladius wing (Sutton et al., 2015) and is found in three families of incirrate octopods: Alloposidae, Octopodidae, and Tremoctopodidae (Young et al., 1998) on the dorsolateral side of the mantle. They can be used for aging, which is useful since octopodiform statoliths do not form increments (Arkhipkin et al., 2018). Concentric rings grow daily on stylets in many commonly studied species (Arkhipkin et al., 2018).

50.6.4 Cirrate shell

Shells in cirrates can be diagnostic at the family level. They vary in shape from U-, V-, W-, or saddle-shaped.

50.7 Beak

The cephalopod beak is composed of a chitin-protein complex in coleoids and is tipped with $CaCO_3$ in nautiloids (Arkhipkin et al., 2018). In coleoids, it is produced by beccublast cells (Arkhipkin et al., 2018). Many shallow-water coleoids form daily growth rings on both the lateral wall and tip of the rostrum (Arkhipkin et al., 2018). However, a number of cold-water and deep-sea species have increments laid on longer timescales. Moving anteriorly along the beak (towards the tip), the proportion of chitin decreases and the other protein composition rises, resulting in greater stiffness and pigmentation (Arkhipkin et al., 2018). In fact, the tip of the beak is one of the hardest and stiffest entirely organic materials known (Miserez et al., 2008). The strength in the beak corresponds with the pigmentation with the tip strongest and gradually getting weaker towards the wings (Miserez et al., 2008).

Octopod-like beaks tend to be better for crushing while squid-like beaks are better for piercing (though there's a broad continuum between these extremes in any given species) (Roscian's 2022 CIAC talk). As a reflection of this, squid upper beaks have a bigger pointier hood than octopod beaks, while the octopod rostrum is duller than the squid rostrum (Roscian's 2022 CIAC talk).

The feeding mechanics are controlled by the superior basal lobe in the brain and by the inferior buccal ganglion in the PNS (Budelmann, 1995) that control the mandibular muscles. Nautiloids have a unique buccal musculature compared to coleoids (Rouget's 2022 CIAC talk).

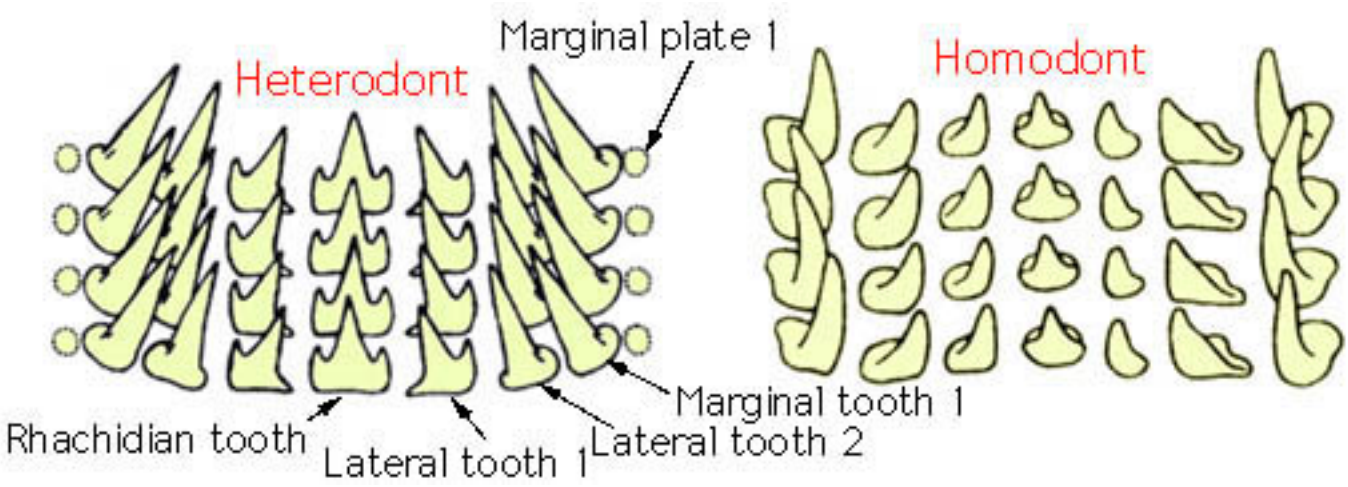

Figure 50.7: Neocoleoid radula morphology. Figure from ToLWeb.

50.8 Radula

The radula is a toothed tongue possessed by most but not all cephalopods (cirrates do not have radulae). In extant coleoids, there are no more than nine elements (teeth) in each row. In *Nautilus*, by contrast, there are 13 elements: possessing two pairs of marginal teeth and two pairs of marginal plates.

Heterodont radulae are distinguished from homodont radulae by their multicusped rhachidian teeth and first lateral teeth. Some of the incirrate amphitretids have a "ctenoglossan" radula in which both the lateral teeth are multicusped.

The radula is controlled by the subradula ganglion (Budelmann, 1995).

50.9 Skin

Octopod and sepioid skin are vascularized, but teuthid skin lacks blood vessels (Madan and Wells, 1997). Additionally, teuthid skin (100-400 μm) is much thinner and more delicate than octopod or sepioid skin (1300-1600 μm) (Madan and Wells, 1997).

When injured, cephalopod skin heals much slower than fishes, probably because the iso-osmotic cephalopod tissues are not selected to seal off as strongly as hypo-osmotic fish tissue and blood (Polglase et al., 1983).

In octopuses (at least), rhodopsin kinase (GRK1), a key canonical component of a rhodopsin-based visual system, is expressed not only in the retina but also the skin and suckers (de Zoysa's 2022 CIAC talk).

50.9.1 Skin layers

The epidermis is very thin (sometimes a single cell layer thick) composed mainly of columnar cells but also some secretory goblet cells and sensory cells (especially on the suckers) (Packard, 1988). Below the epidermal cells is the basal lamina, an extracellular matrix of fibers that the epidermis creates for attachment. Below the epidermis and its basal lamina is the dermis. The dermis contains the chromatophores, iridophores, and leucophores . Beneath these cells is a deep layer of connective tissue which contains the blood vessels and capillaries, some nerve fibers and muscle tissue (Packard, 1988).

50.9.2 Chromatophores

Nearly all coleoid cephalopods have many small pigment organs in their skin known as chromatophores that are used for camouflage and communication (Hanlon and Messenger, 1996). The incirrate *Vulcanoctopus hydrothermalis* lacks chromatophores entirely (Strugnell et al., 2014).

In addition to the pigments, chromatophores also possess structural coloration through crystallins (Williams et al., 2019).

50.9.2.1 Chromatophore control

Except for in the cirrate octopods (Collins and Villanueva, 2006), they are innervated with axons stemming from the chromatophore lobes (lower motor centers) in the brain (Williamson and Chrachri, 2004). The higher motor center which exerts the highest level of control, however, is the lateral basal lobe (Budelmann, 1995).

Each chromatophore is composed of a sacculus of pigment (ommochrome) granules that is elastic and stretched by 4-24 radial muscle fibers that surround it. The ratio of motor neurons in the posterior chromatophore lobe to chromatophores in the body varies from 1:0.8 in *Sepia officinalis* (more neurons than there are chromatophores) to 1:7 in *Euprymna* (1 motor neuron controls 7 chromatophores) (Liang's 2022 CIAC talk).

When an action potential is sent from the chromatophore lobes, the excitatory transmitter, glutamate, triggers contraction of the muscle fibers and, therefore, expansion of the pigment-containing sacculus (Cloney and Florey, 1968). In *Octopus vulgaris*, chromatophores can expand at up to 12 Hz (Messenger, 2001). Because cephalopod chromatophores are directly innervated, an individual can change its body pattern via chromatophore expansion/contraction in 100-300 milliseconds (Hanlon, 2007). There are small muscle-muscle electrical connections such that chromatophore muscle activation can contribute towards activating their neighbors, which may be a possible mechanism of the passing cloud (Senft et al. 2021, J. of Morphology).

Skin color change control in non-cephalopod taxa This is in contrast to fish or amphibian skin color change which works by hormonal driven activation of kinesin or dynein motors that expand or contract, respectively, melanosome organelles within melanocyte skin cells (Vale's iBio talk). Most non-cephalopod taxa that can change their color do so by one of two mechanisms: morphological changes are common in mammals and bird melanophores, where new melanophores are synthesized in the skin to change coloration. This results in a color change on the order of days to months. The second mechanism is the use of physiological changes such as endocrine systems or the sympathetic nervous system. Elasmobranchs and crustaceans control their coloration through endocrine systems while bony fishes predominantly use sympathetic neural systems (Fujii, 2000; Thurman, 1988). These changes in coloration occur on the scale of minutes to hours.

50.9.2.2 Chromatophore abundance, types, and density

Many cephalopods possess chromatophores that are brown (melanophores), red (erythrophores), and yellow (xanthphores), though some oceanic species (e.g. *Dosidicus gigas*) have only one chromatophore color. In decapodiforms, the yellow chromatophores are the most superficial while in octopodiforms the brown chromatophores are most superficial (Packard, 1988).

Chromatophores from different species have different sizes, densities, distributions, and functions. The chromatophore structure and patterns have been best studied in benthic cephalopods such as *Sepia officinalis* (Hanlon and Messenger, 1988) and *Octopus vulgaris*, but some neritic species have also been well studied (e.g. *Doryteuthis pealeii*, (Hanlon et al., 1999). Many benthic cephalopods, being almost exclusively octopuses and cuttlefishes, have very small, densely distributed chromatophores. For example, *Sepia officinalis* and *Octopus vulgaris* both have chromatophores with a maximum diameter of only 300 μm and a density of up to 200-500 chromatophores mm^{-2} (Messenger, 2001). For comparison, loliginid and ommastrephid squids such as *Doryteuthis pleii, Alloteuthis subulata, Lolliguncula brevis*, and *Dosidicus gigas* have much larger chromatophore diameters up to 1300-1500 μm and much less density (3-14 chromatophores mm^{-2})(Messenger, 2001; Rosen et al., 2015). A 10 cm DML *Lolliguncula brevis* individual was estimated to have 27,000 chromatophores total (Dubas et al., 1986), ,while *Sepia officinalis* have 2-3 million chromatophores (Chiao et al., 2015). Chromatophores are denser on dorsal than ventral surfaces for both pelagic and benthic taxa (Ferguson and Messenger, 1991).

50.9.2.3 Photoreceptors

Squids and cuttlefishes have been shown to possess rhodopsin and retinochrome in their chromatophores (Kingston et al., 2015).

50.9.2.4 Development

In embryos and paralarvae, chromatophores are created in "generations". New generations form between existing chromatophores (Packard, 1988). Also as chromatophores age they become darker and larger (Packard, 1988).

50.9.3 Iridophores

Iridophores are platelets slightly deeper in the skin than the chromatophores that reflect ambient light. They provide the animal's iridescent appearance under white light. *Doryteuthis* are capable of actively controlling their iridophores unlike most other cephalopods.

Iridophore platelets are composed of reflectin proteins, an entirely cephalopod-specific gene family (Albertin et al., 2015). Correspondingly, *Doryteuthis* has 2x more reflectin paralogs (n=17) than other cephalopods examined to date (MBL Loligo genome seminar).

50.9.4 Leucophores

Leucophores are structures deeper than the iridophores that also reflect ambient light levels. They are only found in some cuttlefishes, some octopuses, and the squid *Sepioteuthis* (Hanlon and Messenger, 1996).

50.9.5 Photophores

Many deepwater cephalopods possess photophores, though they are possessed by decapodiforms much more than octopodiforms (Otjacques' 2022 CIAC poster). Photophores have evolved multiple times and different kinds have different morphologies. Some photophores are surrounded by chromatophores which allows them to be concealed by the animal. Photophores in squids have been demonstrated to change the color of light emitted in a temperature dependent manner, presumably to match downwelling light throughout DVM across a temperature gradient (Young and Mencher, 1980).

In most mesopelagic animals studied, bioluminescent light emission peaks between 440 and 515 nm (Widder 2002), which is similar to downwelling light (section 53.1).

50.9.6 Papillae

Some octopuses and cuttlefishes can contort the surface of their skin to form papillae. In octopods with planktonic paralarvae, these papillae do not develop until settlement on the substrate (Villanueva's 2018 CIAC talk).

The lateral basal lobe is the higher motor center for papillae expression (Budelmann, 1995) (?). Papillae on the mantle are innervated by the stellate ganglion (Gonzalez-Bellido et al., 2018).

50.9.7 Kölliker's bristles

Planktonic paralarval and juvenile incirrate octopods possess spiny protrusions on their skin called Kölliker's bristles that are presumably used for protection (Packard, 1988) and/or to lessen sinking rates. Across many species and sizes, rodlet length is 50 μm (Villanueva's 2018 CIAC talk). Bristle density is highest on the head and arms (900 mm^{-2}) and about half that on the mantle (Villanueva's 2018 CIAC talk). Furthermore, density is highest in the smallest animals and decline with ontogeny (Villanueva's 2018 CIAC talk).

50.9.8 Cutaneous respiration

The expectation that cephalopods gain oxygen through their skin is supported by blood acid-base calculations (Pörtner, 1990).

In vitro measurements of cutaneous respiration on extracted skin in a variety of coleoids have all had a similar O_2 consumption rates, ~0.1 $\mu molO_2/cm^2/hr$ (Madan and Wells, 1996). *In vivo* consumption may be 2-3x higher, however (as in *Octopus vulgaris*), due to cutaneously-derived O_2 entering the blood vessels in the skin. Squids do not have cutaneous blood vessels but they have thinner skin which may diffuse O_2 directing into underlying tissues. Additionally, cutaneous respiration likely increases with increased water flow over the skin's surface, to diminish the formation of boundary layers. Some loliginids and octopuses (if not others) twitch their skin, potentially to disrupt boundary layer formation (A. Packard's hypothesis). For octopuses and sepioids that hide in dens or bury themselves in the substrate, cutaneous respiration must necessarily be much lower since the skin is not in contact with oxygenated seawater.

Live *Octopus vulgaris* have been demonstrated to consume from 13% up to 82% of their whole animal M_{O_2} through their skin (Madan and Wells, 1996; Wells and Wells, 1983). Some authors have predicted that cutaneous respiration may be as much as 20% of whole animal O_2 consumption (*Lolliguncula brevis*; Wells et al., 1988) or even as much as 73% in actively swimming squids (Pörtner, 1994), but this is unlikely in adult squids (Birk et al., 2018).

50.10 Light organ

Light organs that harbor bacteria are only present in sepiolids and loliginids (Belcaid et al., 2019). Light organs in all *Euprymna* spp. and most other sepiolids harbor *Vibrio fischeri* bacteria to produce their light. The only known exception is a *Sepiola* that inhabits the Meditteranean and has either *V. fischeri* or *V. logei* depending on temperature (Nishiguchi 2000). This is impressive because *V. fischeri* are only ~0.1% of the bacterioplankton but must be selected by the light organ to make a pure culture (McFall-Ngai's 2022 CIAC talk). Each morning 95% of the bacteria are expelled and the remaining stock recolonize. The bacteria avoid overpopulating by quorum sensing.

The light organ possesses tissue-specific expression of genes that seem to have paralogously evolved from gene duplication for host-specific needs (Belcaid et al., 2019). The light organ is made of crystallins for transparent structure and is rich in reflectins (Belcaid et al., 2019). 40% of the mRNA transcripts in the light organ on *Euprymna* are reflectins (Belcaid et al., 2019). In

order to maintain specificity to *V. fischeri* only, the light organ produces hypohalous acid as an anti-microbial agent (Belcaid et al., 2019). There are also a number of immune responses that maintain specificity.

The light organ is photosensitive; you get ERG signals when exposing it to light (Heath-Heckman's 2022 CIAC talk).

50.10.1 Mechanism of colonization

In order for hatchlings to acquire *V. fischeri*, the bacteria have to pass through:

1. ciliated appendages
2. pores (3)
3. ducts
4. antechamber
5. bottleneck
6. crypts (3)

This whole path is about 100 μm long (McFall-Ngai's 2022 CIAC talk). In *Euprymna* hatchlings, the light organ possesses ciliated appendages at the entrance to their pores. When the base of these appendages sense peptidoglycan (a signal of bacteria being present), mucus containing nitric oxide is released (McFall-Ngai's 2022 CIAC talk). This nitric oxide causes the cilia on the appendages to start beating faster to encourage bacterial contact with the pores (McFall-Ngai's 2022 CIAC talk). Within a few hours of hatching, 5-10 *V. fischeri* cells typically land on the cilia and they trigger production of anti-microbial agents within the antechamber (McFall-Ngai's 2022 CIAC talk). The bacteria also upregulate their own resistance to the squid's anti-microbial agents so that only *V. fischeri* will be selected within the antechamber (McFall-Ngai's 2022 CIAC talk). Once the *Vibrio* make it inside the crypts, the grow extracellularly on epithelial cells and start bioluminescing, which triggers lots of differential expression in the light organ (McFall-Ngai's 2022 CIAC talk). After 3 days post-hatching, the ciliated appendages have done their job and apoptose away (Heath-Heckman's 2022 CIAC talk).

50.11 Measurements

50.11.1 Length

DML Dorsal mantle length. The distance from the posterior tip of the mantle dorsally to the anterior tip (including gladius)

SL Standard length. The distance from the posterior tip of the mantle to the furthest tip of the arms (not including tentacles, if present)

TL Total length. The distance from the posterior tip of the mantle to the furthest tip of the tentacles (without stretching)

TL is often 1.5x DML (O'Dor and Hoar, 2000; Fields, 1965). Mantle diameter in active squids is 1/8th of TL (Packard, 1972).

Chapter 51

Internal morphology and physiology

51.1 Respiratory system

51.1.1 Gill morphology

Cephalopod gills are located in the mantle cavity. Nautiloids possess two pairs of gills while coleoids possess only one pair (Eno, 1994). In nautiloids, the inner pair are slightly smaller than the outer pair (Eno, 1994). The gills are positioned in the mantle cavity such that incoming water must pass through the gill lamellae (counter-current to blood flow) in order to reach the posterior end of the mantle cavity (Wells and Wells, 1982). When the mantle contracts, the lamellae collapse together forcing water to move through the center of the mantle cavity and out through the funnel (Wells and Wells, 1982).

Teuthid, incirrate, and *Vampyroteuthis* gills all contain a branchial canal, or a canal through the middle of the gill (Eno, 1994). In contrast, nautiloid and sepioid gills do not possess a branchial canal.

The branchial gland runs the length of each gill (Eno, 1994)(light brown oval in 51.2a) and is the site of hemocyanin production (Messenger et al., 1974). Histologically, the glands are filled with rough ER and vacuoles, producing hemocyanin molecules (Messenger et al., 1974). Cephalopods possess tertiary lamellae unlike fishes which only have secondary lamellae.

Blood runs through the gill lamellae, being driven primarily by the branchial hearts (Schipp, 1987; Eno, 1994) counter-current to seawater flow (Eno, 1994; Wells and Wells, 1982).

The gills can contract in length by roughly 33% (pers. obs. in *D. pealeii*) similarly to the extensively-studied *Aplysia* gill withdrawal reflex.

Other animal gills Fishes have neuroepithelial cells on their gills which, depending on location, can detect P_{O_2} levels in the water or the arterial blood (Zachar and Jonz, 2012). They are the phylogenetic precursors to the mammalian carotid body found in the carotid artery which is the main blood P_{O_2} and P_{CO_2} sensor (Zachar and Jonz, 2012).

At least in fish gills, the pavement cells are squamous or columnar epithelia that cover most of the surface area and thus are responsible for most of the gas exchange, which mitochondrion-rich cells (or chloride cells) are responsible for most of the salt balance and ammonia excretion (Evans et al. 1999).

51.1.1.1 Decapodiform lamellae

The 1°, 2°, and 3° vessels are clearly annotated in 51.2a. The 1° and 2° efferent vessels run along the outside margin of the gill whereas the 1° and 2° afferent vessels run along the gill interior (Eno, 1994). The 1°, 2°, and 3° lamellae are folded like a wave (or oriental hand fan, or roadmap), with the amplitude oscillating along the x, y, and z axes, respectively (51.2b shows this well). The 2° vessels run the length of the 1° lamellae and the 3° vessels run the length of the 2° lamellae.

51.1.1.2 Octopodiform lamellae

The octopodiform gill differs in two key ways from the decapodiform gills: 1. the mid-sections of the 2° and 3° lamellae are fused, and 2. the tertiary lamellae do not fold like a map or fan, but rather are branching. In incirrates, the secondary efferent vessels run through the center of the 1° lamellae along the fused axis, unlike in decapodiforms where it runs along the outer margin (Eno, 1994).

Vampyroteuthis are different from all other octopodiforms in that the proximal 2/3rds of the gill lack efferent 2° vessels. I wonder if this is adaptive for their extremely low Pcrit...

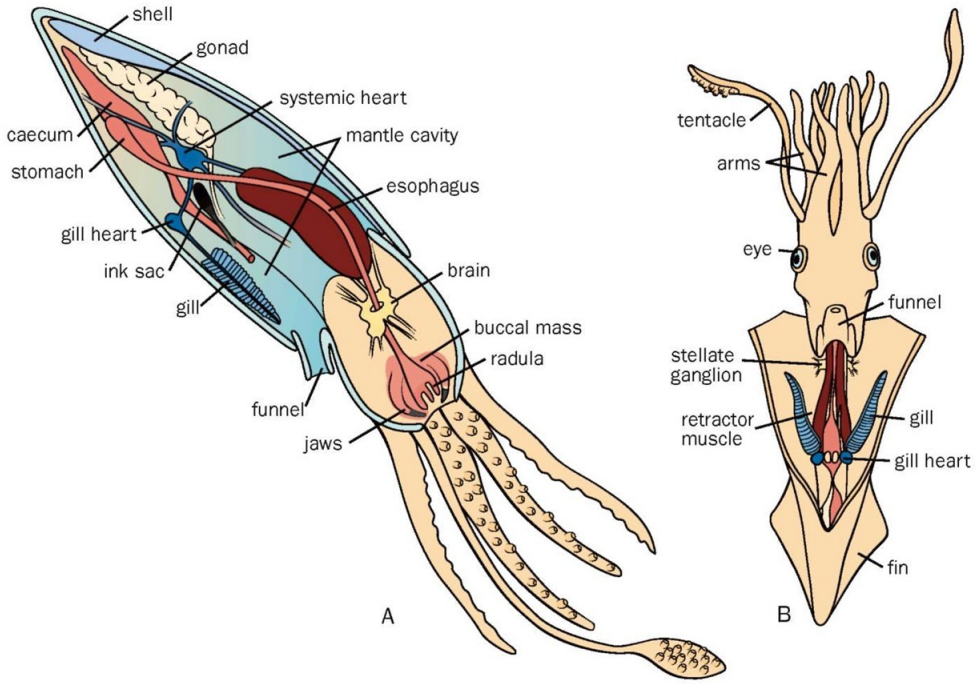

Figure 51.1: General squid anatomy. Figure from what-when-how.com

Table 51.1: Gill morphometrics. Data from Eno 1994.

Taxon	Respiratory surface area (mm^2 **per g animal mass**)	Tissue thic
Nautilus spp.	491	15
Octopus vulgaris	293	10
Sepia officinalis (hatchlings; thus adult values would be lower)	1334	4
Alloteuthis subulata	1063	6

51.1.2 O_2 diffusion (Fick's law)

The diffusion rate of oxygen from seawater to the gills (umol O_2 min^{-1}) is a function of gill respiratory surface area, tissue thickness, the difference in P_{O_2} between seawater and blood, and Krogh's diffusion coefficient according to Fick's law:

$$\text{Diffusion rate} = \text{K} \cdot \frac{\text{surface area}}{\text{tissue thickness}} \cdot \left(\text{P}_{\text{O}_{2_{\text{seawater}}}} - \text{P}_{\text{O}_{2_{\text{blood}}}}\right)$$

where K is Krogh's diffusion coefficient (a quantity of $\mu\text{mol}\,O_2 \cdot \text{mm}^{-2} \cdot \mu\text{m} \cdot \text{kPa}^{-1} \cdot \text{hr}^{-1}$; Krogh, 1919; Table 51.2). Some typical surface area and tissue thickness values are shown in Table 51.1 and are generally similar to fish gills (Gray, 1954).

Branchial surface area and thickness can be modulated by blood pressure, with higher pressure increasing perfusion and decreasing thickness (Melzner et al., 2009).

51.1.2.1 Allometric scaling

As an individual grows, its mass-specific gill surface area decreases (Eno, 1994). This is likely because as the gills and mantle cavity grow, the Reynolds number of water flowing through them increases, thus having a shorter boundary layer of seawater on top of the tissue thickness.

At least in mammals, however, the overall mass-specific diffusion capacity (K, surface area, and tissue thickness) increases in larger species relative to smaller ones (even though $msMO_2$ decreases) (Weibel et al., 1991). Therefore, in order to supply MMR, larger species that have higher mass-specific diffusion capacity should have a smaller ΔP_{O_2} than smaller species that have lower mass-specific diffusion capacity. It is unclear whether this difference is due to a similar response to surface area but changes in tissue thickness between cephalopods and mammals, or whether it is due to the very different Reynold numbers of water versus air that in turn drive differences in allometric scaling.

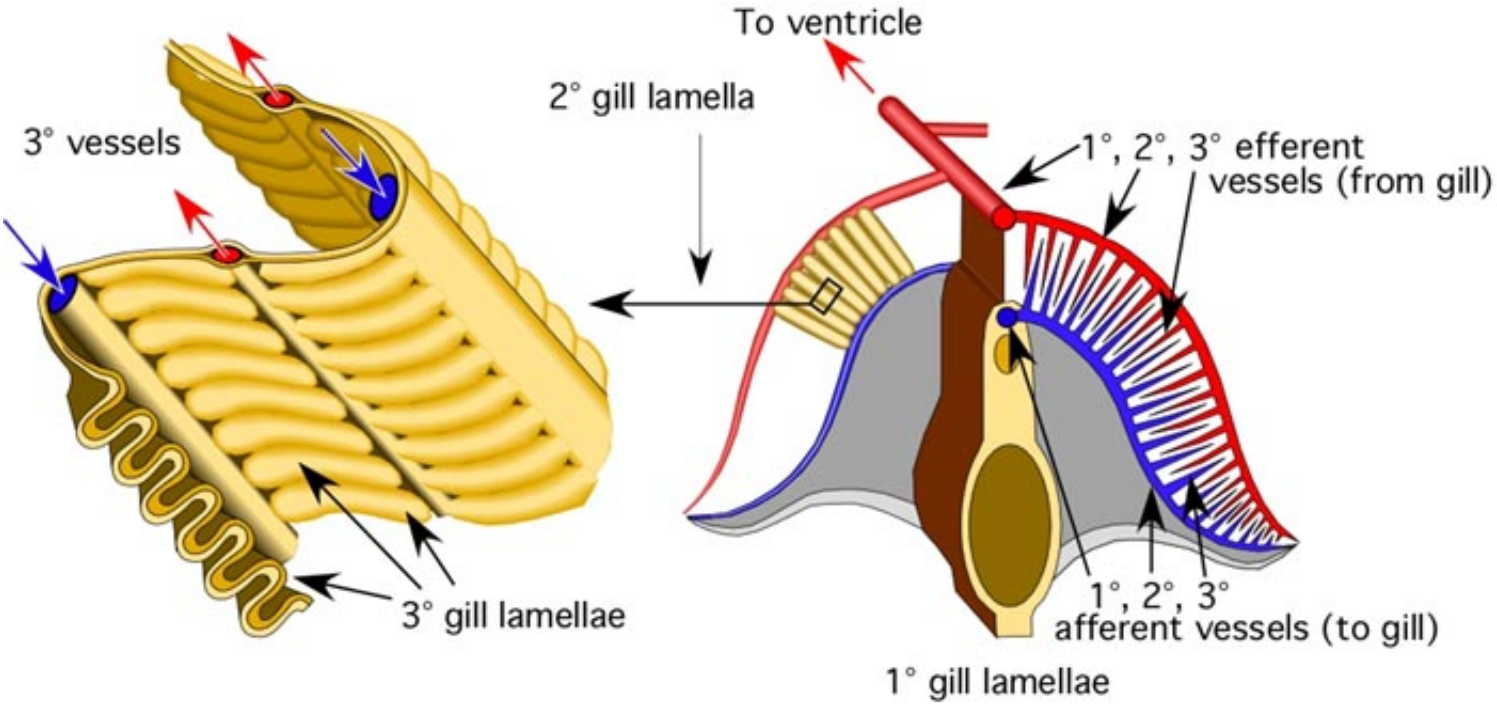

(a) Model from *Sepia officinalis* but representative of all decapodiforms.

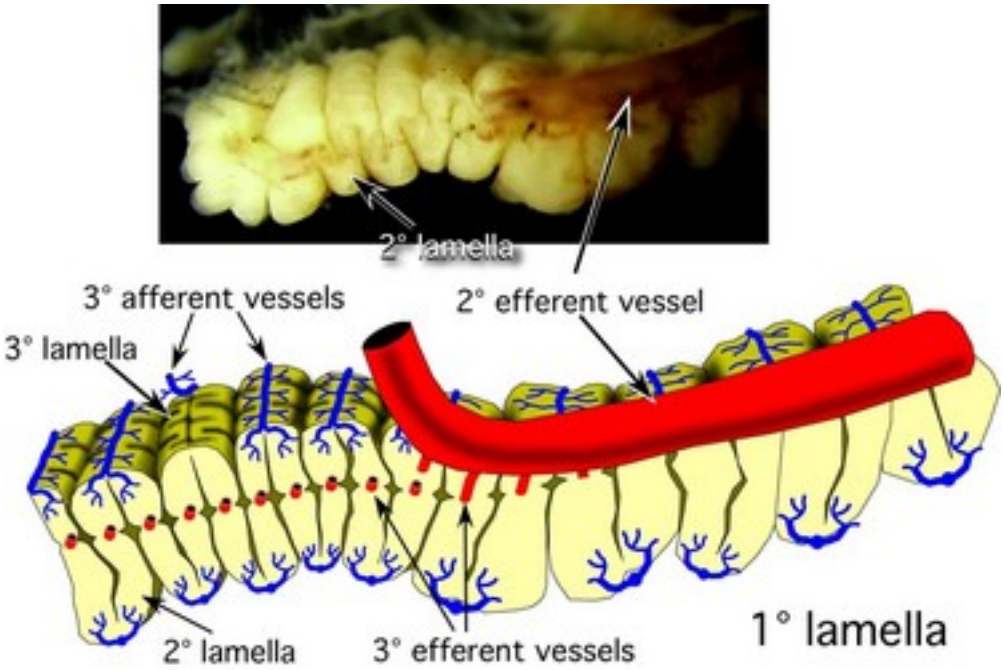

(b) Model and image from *Histioteuthis* gill.

Figure 51.2: Decapodiform gill morphology. Figures are from ToLWeb.

Table 51.2: Reasonable Krogh's coefficients ($\mu\text{mol}\,O_2 \cdot \text{mm}^{-2} \cdot \mu\text{m} \cdot \text{kPa}^{-1} \cdot \text{hr}^{-1}$) at 20 °C. Values change $1\% \cdot {}^\circ\text{C}^{-1}$ (Krogh, 1919).

Tissue	O_2	CO_2
Muscle	0.0369	1.3185
Connective tissue	0.0303	1.0831

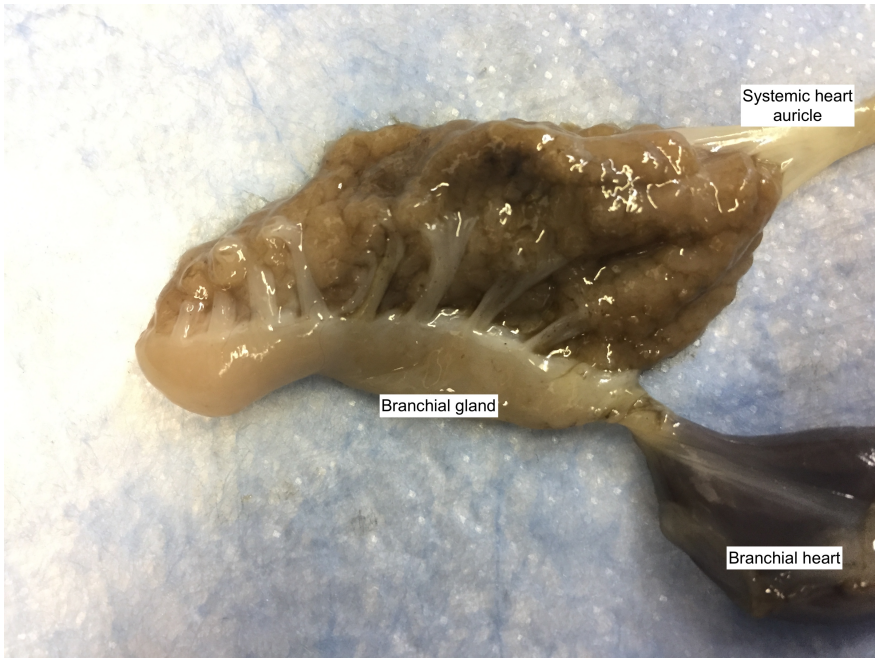

Figure 51.3: *Octopus vulgaris* gill

51.1.3 Ventilatory dynamics

The dynamics of respiration can measured by the following parameters:

- Ventilation rate (VR)
- Mantle cavity pressure amplitude
- O_2 extraction (EO_2)
- Ventilatory stroke volume (VSV) = $MO_2 \div VR \div EO_2 \div [O_2]_{seawater}$
- Ventilatory flow rate = VR × VSV

For all these parameters, there is a deep phylogenetic trend such that ventilatory dynamics are least in cuttlefishes, intermediate in neritic octopods, and most in shallow squids.

51.1.3.1 Ventilation rate (VR)

Loliginids at rest have a ventilatory rate half as fast as their heart rate (Shadwick et al., 1990; Wells et al., 1988). At ~15 °C, both loliginids and sepiids have a ventilatory rate at rest of 30-40 strokes per minute (Shadwick et al., 1990; Melzner et al., 2006b), but it varies with temperature (subsubsection 53.2.7.1). Similarly, *Octopus* have ventilatory rates in the 20s-30s per minute at 20-25 °C (Wells and Wells, 1985, 1995). However, the ventilatory and cardiovascular frequencies do not seem to be coordinated either at rest or during exercise (Shadwick et al., 1990).

VR is controlled by the central nervous system sending impulses to the mantle musculature through the stellate ganglia. The CNS receives information about environmental P_{O_2} from the branchial ganglia in the gills via the visceral nerves (Wells and Wells, 1995).

51.1.3.2 Mantle cavity pressure amplitude

Resting ventilatory mantle contractions have a pressure amplitude of ~25-100 Pa in *Sepia* (Melzner et al., 2006b), around 40-200 Pa in neritic octopods (Wells and Smith, 1985; Wells, 1990; Wells and Wells, 1995), 300 Pa in loliginids (Wells, 1990; Wells et al., 1988), and 750 Pa in ommastrephids (Wells, 1990), increasing with temperature.

Mantle cavity pressure amplitude is controlled by the central nervous system sending impulses to the mantle musculature through the stellate ganglia. The CNS receives information about environmental P_{O_2} from the branchial ganglia in the gills via the visceral nerves (Wells and Wells, 1995).

51.1.3.3 O_2 extraction (EO_2)

The percentage of O_2 extracted from the water with each ventilation varies greatly among cephalopods. Extraction efficiency is especially low in squids. *Lolliguncula brevis*, for example, extracts ~7% of O_2 from the water when at rest (Wells et al., 1988). *Sepia officinalis*, however, can achieve anywhere from 30-100% extraction efficiency depending on temperature (Melzner et al., 2006b) and *Octopus* can achieve 30-70% extraction (Wells and Wells, 1982, 1985). In fishes, hyperventilation increases O_2 extraction (Perry's SEB talk) and this may be similar in cephalopods.

51.1.3.4 Ventilatory stroke volume (VSV)

At rest and a moderate temperature, *Sepia* pump 1% of their body weight in seawater past their gills with each ventilation, while *Octopus* pump 5% (Wells and Wells, 1985) and *Lolliguncula* pump 10% of their body weight (Melzner et al., 2006b).

51.1.3.5 Ventilatory flow rate

Cephalopods must pump seawater past their gills to sustain their high metabolism. The quantity of seawater required correlates with total metabolic rate. A relatively inactive cephalopod like *Sepia* only needs ~30% of its body weight in seawater flow per minute (Melzner et al., 2006b) while an *Octopus* requires 100-200% of its body weight (Wells and Wells, 1985) and a neritic squid at the same temperature requires 900% of its body weight in seawater to flow past its gills just to sustain resting metabolism (*Lolliguncula*; Wells et al., 1988). The range in ventilatory flow rate is reflected in the proportion of total metabolism required to fuel ventilatory muscles. Ventilation can cost as little as ~1% for an inactive, efficient extractor like *Sepia* or can cost ~20% of total metabolism in an active squid like *Lolliguncula* (Melzner et al., 2006b).

51.1.4 Control of breathing

Respiration is ultimately controlled by the median basal lobe in the supra-esophageal mass of the brain (Budelmann, 1995) and this signal is passed down the pallial nerves to the stellate ganglia (Imperadore et al., 2019). Respiration is driven primarily by the mantle muscles (subsection 50.1.3), but water expulsion can also be forced out by the collar flaps (Bone et al 1994 cited in (Kier and Thompson, 2003).

Breathing is controlled by a central pattern generator (CPG) neural circuit.

51.1.5 Ammonia excretion

See subsection 51.4.1.

51.1.6 Acid-base balance

Metabolically produced CO_2 passively diffuses down its partial pressure gradient across the thin gill membrane on the outside folds of the 3rd order lamellae. However, carbonic anhydrase (CA) is required to accelerate the conversion of HCO_3^- to CO_2. At a pH_e of 7.8 (sepiids) or 7.4 (teuthids), 95-98% of the CO_2 species are HCO_3^- (according to the CO_2 dissociation constant, K_1). Thus, CA in the thin outer gill membrane facilitates the conversion to CO_2 and thus the diffusion into seawater. In loliginids and ommastrephids, CA produces 8000 μmol CO_2/g/min (Nyack et al.).

51.1.6.1 Acidosis compensation

In the context of acidosis compensation due either to exercise or to environmental hypercapnia, blood acquires high concentration of DIC. When this is due to exercise, increased metabolism increases the flux of CO_2 into the blood from the tissues. When this is due to environmental hypercapnia, the lower P_{CO_2} gradient between blood and seawater causes less CO_2 to diffuse with each pass through the gills and thus the DIC accumulates in the blood. In exercise, it is likely that ventilatory adaptations are the primary solution. This will enable faster fluxes of CO_2 from the blood to the seawater.

In environmental hypercapnia (and maybe somewhat in exercise as well), the situation is notably more complex: as this high-DIC blood reaches the ion-regulating epithelia on the inner folds of the 3rd order gill lamellae, CO_2 transfers through the basolateral membrane of the respiratory cell. CO_2 transfers passively down its partial pressure gradient into the epithelium directly through the membrane since CO_2 is nonpolar. Inside the epithelium, cytosolic carbonic anhydrase (CA_c) catalyzes the following reaction:

$$CO_2 + H_2O \overset{CA}{\rightleftharpoons} HCO_3^- + H^+$$

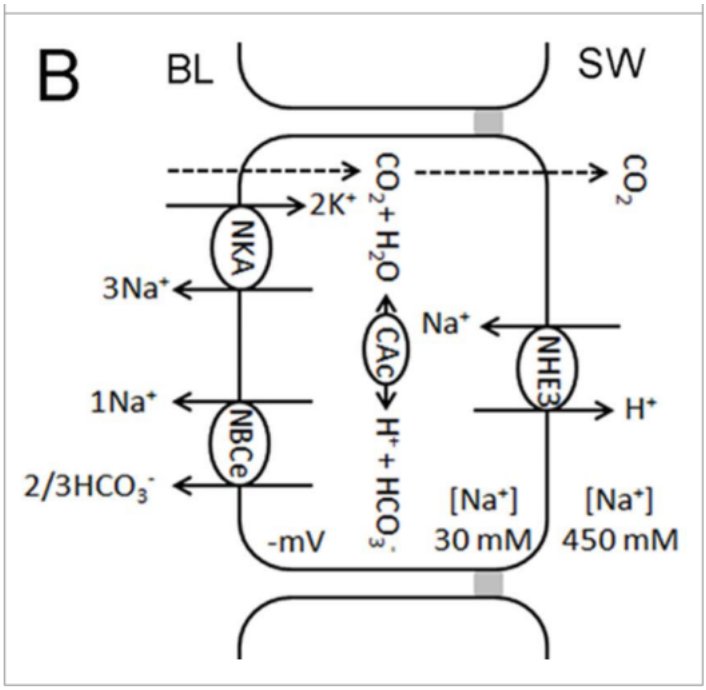

Figure 5. The branchial acid-base regulatory machinery. Immunohistochemical localization of NHE3 in apical membranes of the cephalopod (*Sepioteuthis lessoniana*) gill facing the semi-tubular space of the 3rd order gill lamellae (**A**). Hypothetical model for acid-base relevant ion transport in the cephalopod gill, including apical proton secretion and basolateral HCO_3^- import (**B**).

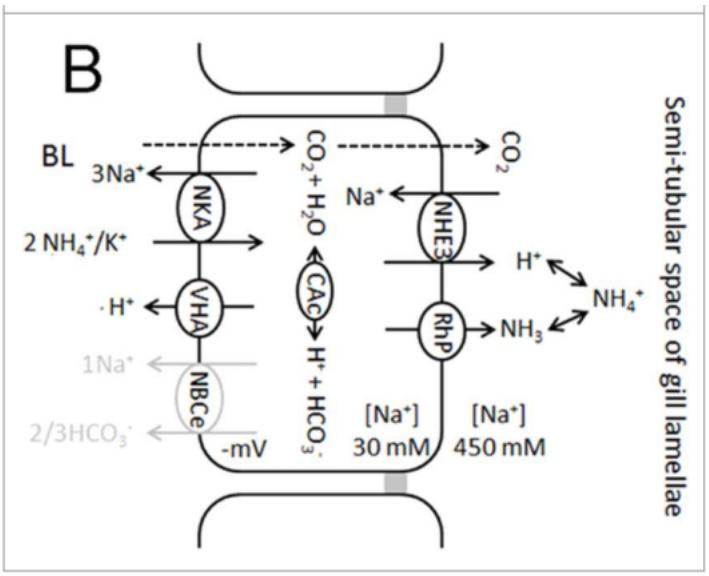

Figure 6. Identification of NH_4^+ transport pathways in cephalopod branchial epithelia. Immunohistochemical analyses demonstrate the presence of RhP in apical membranes of the inner epithelium of the third order gill lamellae (**A**). Hypothetical model for the transport of NH_4^+ across the branchial epithelium (**B**). At the basolateral membrane NH_4^+ is imported into the cell by the NKA. At the apical membrane NH_4^+ is deprotonated and NH_3 and H^+ are separately transported into the semi-tubular space where a trapping of NH_4^+ is proposed.

Figure 51.4: Enzymes relevant in the acid-base balance machinery of gills. Figures from Hu et al. (2015).

The resulting H^+ is transferred through the apical membrane into the seawater via a Na^+/H^+-exchanger 3 (NHE3). This exchanger is thermodynamically enabled by the high Na^+ gradient between the gill epithelium and seawater and thus H^+ should be able to be excreted at quite high rates without cost. The bicarbonate from the CA reaction is turned around and shuttled back into the blood with a sodium-bicarbonate cotransporter (NBC). When this happens, most of the HCO_3^- remains as this species (~95% at pH = 7.4, P_{CO_2} = 30 Pa, T = 25 °C). Among the ~5% of HCO_3^- molecules that do not remain as HCO_3^-, a little over half (at this pH) absorb a H^+ to become CO_2 and a little less than half release a H^+ and become CO_3^{2-}. Thus, there's a slight net removal of H^+ from blood solution by pumping HCO_3^- back into the blood. However, the primary reason that this mechanism can increase blood pH is not because of this small removal of H^+ when the HCO_3^- re-enters the blood, but rather is because of the CA reaction and removal of H^+ in the epithelium. By removing H^+ but returning HCO_3^- to the blood, the total blood DIC is maintained high which keeps P_{CO_2} high but blood alkalinity has also increased ($\uparrow [HCO_3^-]$) which allows blood pH to remain high even at a high P_{CO_2}.

This process accelerates upon minutes to hours of hypercapnic exposure (Melzner et al., 2009).

There is a possibility that cephalopods may be like fishes in that they possess chloride cells which can be covered up or exposed as a function of acidosis (Goss et al. 1994).

51.2 Circulatory system

Circulatory systems are conserved amongst all bilaterians and thus appeared roughly 600-700 Ma. The earliest documented circulatory system and heart was in the arthropod *Fuxianhuia protensa*, 520 Ma. Heart-like structures occur in arthropods, molluscs, and vertebrates.

Almost all circulatory systems have four primary tasks:

1. transport respiratory gases
2. deliver nutrients

Table 51.3: Differences in cardiovascular morphology and physiology between cephalopods and other taxa

Taxon	Heart chambers	Flow	
Cephalopods	1 ventricle	↪ Branchial hearts → Gill → Systemic heart → Tissues	
Fishes	1 artrium, 1 ventricle	↪ Atrium → Ventricle → Gill → Tissues	M
Mammals	2 atria, 2 ventricles	↪ Right atrium → Right ventricle → Lungs → Left atrium → Left ventricle → Tissues	

Note: The heart in most inactive fishes have only the spongy layer, while active fishes like tuna and trout have 60% spongy, 40% compact layer (Driedzic, 1988).

3. remove waste
4. deliver hormones / messengers

Insects do not utilize their circulatory system to transport respiratory gases, but all other animals I know of do.

Octopus vulgaris have been shown to circulate blood throughout their body every 1-2 minutes (O'Dor and Wells, 1984). Neritic squids, which have 2x the heart rate, may have faster circulation time if their blood volume and cardiac stroke volume are similar. Circulation time is likely inversely correlated with metabolic rate since higher metabolic rate requires more blood-borne O_2 delivery. The total volume of blood is 5-7% of total body weight (Wells, 1983).

Differences from vertebrates The cephalopod heart size (just systemic heart; 0.1-0.3% of body weight) is 2-6x smaller relative to body weight than mammals (which consistently have hearts that are 0.58% of body weight) (Shadwick, 1994) but similar in size to fish ventricles (Wells and Smith, 1987). Also each ml of blood holds much less O_2 at saturation (1/3rd at best). Cephalopod capillaries have much more variable diameters than vertebrates and vasculature is completely covered in pericytes, unlike vertebrates (Wells, 1983). Both of these are due to the lack of RBCs.

Vertebrate (or just human?) hematocrit (RBC volume as a percentage of total blood volume) is optimal between 30 and 50% (Crowell and Smith, 1967). Furthermore, typical human [Hb] within RBCs (known as mean corpuscular hemoglobin concentration (MCHC)) is 4.8-5.6 mM.

In a human at rest, venous hemoglobin is still 70-80% saturated, far higher than in squid venous hemocyanin.

Cephalopod blood also does not clot.

Despite these differences, the circulatory system of cephalopods can compete with that of mammals in its performance.

When humans increase stroke volume, they do so by decreasing end-systolic ventricle volume, while *Octopus* (at least) do so by increasing end-diastolic ventricle volume (Wells and Smith, 1987).

51.2.1 Gross morphology of circulation

Unlike their molluscan ancestors, cephalopods have a closed circulatory system with distinct arteries and veins (Williams, 1902). Many other molluscs have large venous sinuses that also double as a hydrostatic skeleton (like muscle in cephalopods) (Wells and Smith, 1987).

The gross morphology of the arterial system is rather conserved in all cephalopods, but more variability exists in the venous system (Wells, 1983). Coleoids have three hearts: a systemic heart and two branchial (gill) hearts while nautiloids only have a single systemic heart (Wells and Wells, 1982; Wells, 1983). The mantle musculature could also be considered a fourth "functional heart" in jet-swimming cephalopods since its rhythmic contractions can greatly improve blood circulation (Shadwick, 1994) or it may hinder venous return (Wells, 1992).

Octopus have large sinuses behind the eyes and around the gut (O'Dor and Wells, 1984; Wells, 1983). The sinuses in cephalopod vasculature are all venous and do not mix arterial and venous blood (Williams, 1902).

In *Octopus,* $\approx$ 70% of blood goes to the dorsal aorta while $\approx$ 30% goes to the posterior aorta (Wells and Wells, 1986). The dorsal aorta is generally largest with the posterior aorta being smaller or equally sized (in teuthoids and cirrates due to the blood supply necessary for mantle and fin locomotion) (Wells, 1983). Squids, however, have a much higher proportion delivered to the mantle.

The hearts and blood vessels are innervated by the vasomotor lobes in the suboesophageal brain (Nixon and Young, 2003).

51.2.1.1 Cerebrovascular morphology

Supra-esophageal lobes are vascularized from the cephalic aorta and venous output predominantly runs along the superficial outer surface of the lobes (Abbott and Miyan, 1995).

The optic lobes have venous output that forms centralized channels through the center of the lobe (Abbott and Miyan, 1995).

Cephalopods maintain a blood-brain barrier through perivascular glial cells in capillaries and venules (Abbott and Miyan, 1995), unlike other molluscs (Budelmann, 1995).

Sepia cerebrovascularization is sufficient to minimize Krogh cylinder radii down to 28 μm in the vertical lobe and 20 μm in the optic lobe, comparable to rat cortex (20 μm) (Abbott and Miyan, 1995).

51.2.2 Systemic heart

The systemic heart is a single-chambered organ (Williams, 1902) which pumps O_2 rich blood from the gills to the rest of the body (Schipp, 1987). There are two input vessels (two efferent branchial veins) and three output vessels (anterior (aka dorsal) and posterior and genital aortae) (Williams, 1909). Valve flaps exist on the branchial vein ports as well as the anterior and posterior aortae to prevent blood from flowing in the wrong direction (Williams, 1909). It is composed of striated muscle (Wells, 1983).

The heart receives blood directly from the lumen in all cephalopods, though *Octopus* (unlike loliginids and sepiids) have a thick ventricular wall that requires additional coronary arteries for blood supply (Driedzic, 1988). Although the heart requires a fair amount of O_2 to operate, it does not lower blood O_2 content (C_{O_2}) for the tissues "downstream". Instead, the blood that enters the heart tissue leaves directly to the nephridial sinus rather than entering the aortae (Williams, 1902).

Since it is always surrounded by O_2 rich blood, it would be expected to be highly aerobic and have little to no anaerobic capacity. Indeed, the systemic heart has a high mitochondrial density and also has much lower concentrations of ATP or Arg-P, two energy rich stores utilized for anaerobiosis but not aerobiosis, than anaerobiosis-equipped tissues like mantle (Häfker, 2012). The systemic heart also has a higher metabolic capacity (enzyme activities) for both aerobic glycolysis and amino acid catabolism than any other cephalopod tissue (at least in cuttlefish; squids may have higher rates in mantle than cuttlefish due to locomotory differences) (Speers-Roesch et al., 2016)section 34.10. Across temperate cephalopod species, there is a tight correlation between heart maximal ATPase activity (a metric of energy demand) and heart hexokinase activity (a metric of energy supply through glycolysis) (Driedzic, 1988). This is a good demonstration of how energy supply and demand in biological systems are tightly regulated.

The size of the systemic heart is taxon-dependent. Most benthic octopod hearts are 0.1-0.15% of total body mass. Cuttlefish have smaller hearts, at 0.07-0.08%, loliginids and sepiolids at 0.16-0.18%, and ommastrephids at 0.3%. For reference, salmon hearts are 0.22% of body mass, while cod and hake ventricles are ~0.04%.

51.2.2.1 Innervation

The heart contractions are myogenic (originated directly by the myocytes rather than nerve cells) (Wells, 1980, 1983). However, heart contractions are dependent on the filling of the chamber, not solely a fixed rate (Wells, 1980). Therefore, systemic heart dynamics are heavily dependent on the dynamics of the branchial hearts. In *Octopus* (at least), there is also innervation between the systemic heart and the lateral vena cavae (Wells and Smith, 1987).

External input can modulate cardiac dynamics, however. The systemic heart is innervated by the visceral nerve which is connected to the vasomotor lobes in the suboesophageal brain (Nixon and Young, 2003). The visceral nerve can provide inhibitory and excitatory neurotransmitters via acetylcholine and serotonin (5-HT)/glutamate, respectively.

51.2.3 Branchial hearts

Coleoids possess two branchial hearts, one for each gill (Shadwick, 1994). They are necessary for circulation because the hydrostatic skeleton of coleoids hinders venous return such that by the time it reaches the gills, blood pressure is too low to push blood through the branchial capillaries and accessory pumps are necessary (Wells, 1992). The veins just before the branchial hearts are also rather large, also lowering blood pressure. The branchial hearts are composed of striated muscles (Williams, 1902; Wells, 1983) and pump venous blood from the nephridial sinus to the gills (Schipp, 1987; Williams, 1909). The heart intake is guarded by two semi-lunar valves that prevent backwards flow, while the outtake is closed by an enlarged artery enriched in circular muscle that can clamp the artery closed (Williams, 1909). Although they pump O_2 poor blood, they do not depend on this venous blood for O_2 but rather they receive arterial blood from the posterior aorta (Williams, 1902).

In addition to circulatory function, they are also a key part of the excretory system and urine production (subsection 51.4.2).

The branchial hearts in octopods are rich in adenochrome which makes them purple-red in appearance compared to the cream or yellow appearance of decapod branchial hearts (Fox and Updegraff, 1943).

In incirrates, each branchial heart is roughly the same mass as the systemic heart, while in decapodiforms, they tend to be smaller than the systemic heart, due to enlargement of the later, rather than much decline in the former (Wells and Smith, 1987).

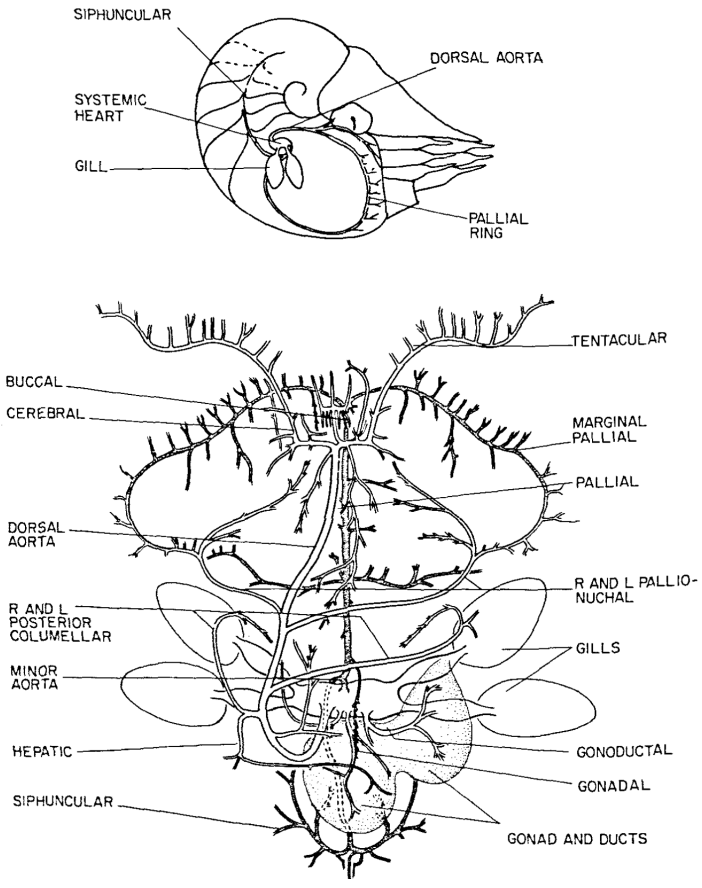
SIPHUNCULAR
DORSAL AORTA
SYSTEMIC HEART
GILL
PALLIAL RING
TENTACULAR
BUCCAL
CEREBRAL
MARGINAL PALLIAL
PALLIAL
DORSAL AORTA
R AND L PALLIO-NUCHAL
R AND L POSTERIOR COLUMELLAR
GILLS
MINOR AORTA
HEPATIC
GONODUCTAL
GONADAL
SIPHUNCULAR
GONAD AND DUCTS

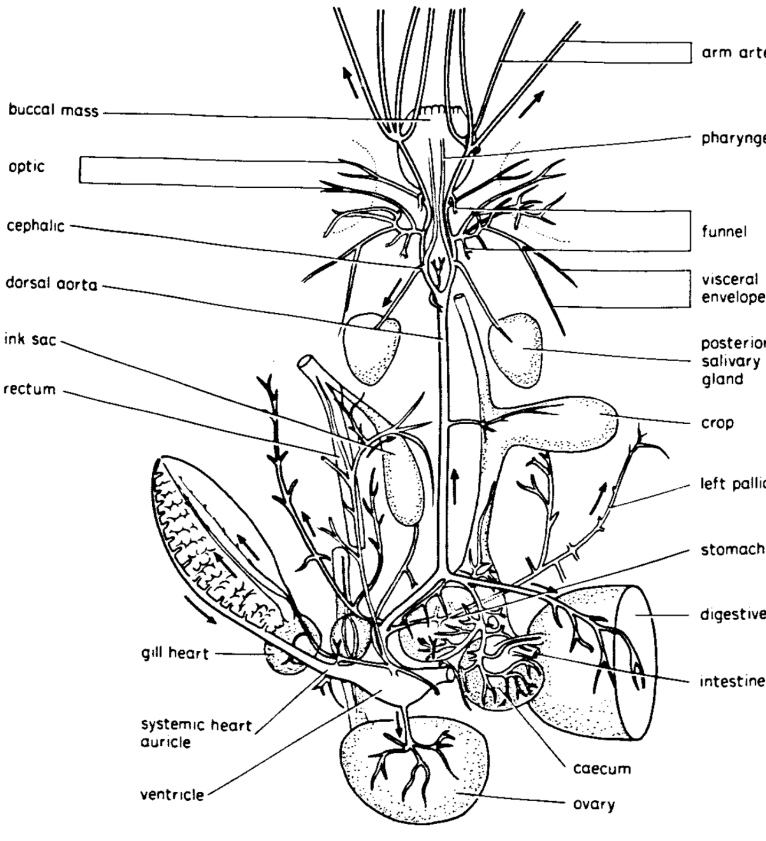
buccal mass
optic
cephalic
dorsal aorta
ink sac
rectum
gill heart
systemic heart auricle
ventricle
caecum
ovary
crop
stomach
digestive
intestine

(a


A

51.2.3.1 Innervation

The branchial hearts are innervated directly by the cardiac ganglia (Alexandrowicz, 1963; Wells, 1980) and ultimately by the vasomotor lobes in the suboesophageal brain (Nixon and Young, 2003). The cardiac ganglia (in octopodiforms only) actively pulsate due to the "intraganglionar (IG) body" (Alexandrowicz, 1963) and are pacemakers for the branchial hearts (Wells, 1980) and, in turn, the systemic heart; the fusiform ganglia provide a nervous connection between the hearts to keep them synchronized (Wells, 1980). The branchial hearts contract slightly before each systemic heart contraction (Wells, 1980). If the principle is similar to the mammalian heart, then the cells have leakage pumps that allow Na^+ and Ca^{2+} to leak in a bit faster than K^+ can leak out. Over time, this gradually depolarizes the cell until reaching the threshold of the voltage-gated Na^+ channels which trigger the action potential that stimulates contraction.

51.2.4 Gills

Unlike in fishes, cephalopod gills do not allow blood to by-pass the narrow, high-pressure capillaries when oxygen demand is low (Wells and Smith, 1987).

51.2.5 Arteries, veins, capillaries, and sinuses

Artery carries blood away from the heart

Vein carries blood towards the heart

Arteriole transition pipe from artery to capillary

Venule transition pipe from capillary to vein

The arteries and veins are formed by circular and longitudinal muscular tissue "sandwiched" by connective tissue (Williams, 1902; Wells, 1983). Veins have much thinner musculature than arteries (Williams, 1902) (just like in mammals). The inner lining of intermediate-sized vasculature is composed of endothelial cells, but the large vessels (e.g. dorsal aorta) and smallest vessels have incomplete endothelial linings (Barber and Graziadei, 1967; Gray, 1969). Despite an incomplete endothelial lining, vessels seem to be completely coated in basement membrane and pericytes (smooth muscle) (Barber and Graziadei, 1967). The muscular linings of both arteries and veins are innervated and controlled by the vasomotor lobes in the suboesophageal brain (Wells, 1983). The arteries and veins are elastic (just like in mammals) and thus can buffer systolic pressure spikes when the systemic heart contracts, a phenomenon known as the Windkessel effect, named after 18th century fire trucks that used air tanks in the fire lines to maintain smooth hose flow (Shadwick, 1994; Wells and Smith, 1987). The elastic recoil can also help keep blood moving through the artery (Shadwick, 1994). In coleoids, the arteries and veins use peristaltic contractions to assist the heart (Williams, 1902) (in mammals, arteries are contractile but veins are not). This is particularly important since movement in a hydrostatic skeleton inhibits rather than promotes blood flow. Localized sources of flow are useful. The teuthoids have the smallest veins although even in teuthoids the veins are rather large before reaching the branchial hearts (Wells, 1983).

I do not know if cephalopod arteries or veins have valves like mammalian veins (especially those to the extremities, but not mammalian arteries).

Capillaries deliver blood supplies to the destination tissues. The individual capillaries are composed of endothelial cells (just like in mammals) and have very small diameters (7-9 μm; Browning, 1982) to support diffusion and transport across the tissue boundary (Williams, 1902). Technically the term "capillary" is questionable since the size of the vessels is not as regimented as the vertebrate capillaries. This is because cephalopod blood does not contains RBCs which, in vertebrates, are most efficient when squeezed through exchange vessels, thus constraining the acceptable exchange vessel diameters.

To avoid the leakage of extracellular hemocyanin, cephalopod vasculature has a complete layer of pericyte cells covering the endothelial cells (unlike vertebrates in which there are many uncovered regions) (Wells, 1983). The gaps between pericyte cells are about 12 nm wide, which is too small for hemocyanin to leak (Wells, 1983).

The lateral vena cavae are innervated with the systemic heart directly, such that even if the cardiac ganglia on the branchial hearts are experimentally removed, some level of synchronicity can remain (Wells and Smith, 1987).

Developing squid express a vascular endothelial growth factor (VEGF) receptor in their systemic and branchial hearts, similar to the mammalian pathway of development (Yoshida et al., 2010).

51.2.5.1 Capillary density

At least in mammalian skeletal muscle, capillary density scales proportionately with mass-specific M_{O_2} both as an animal grows larger and in more active species compared to sedentary ones (Weibel et al., 1991).

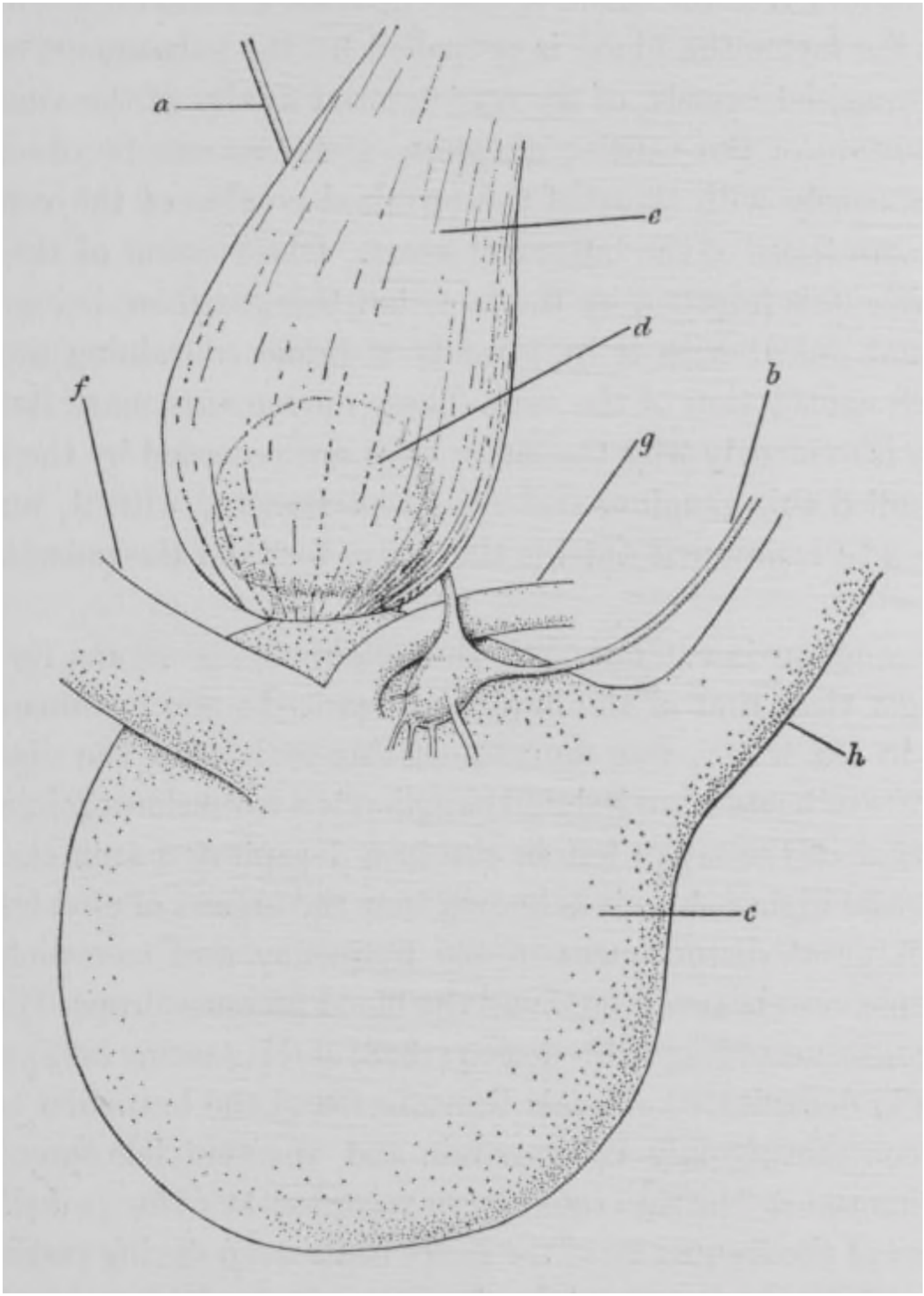
a
c
d
f
b
g
h
c

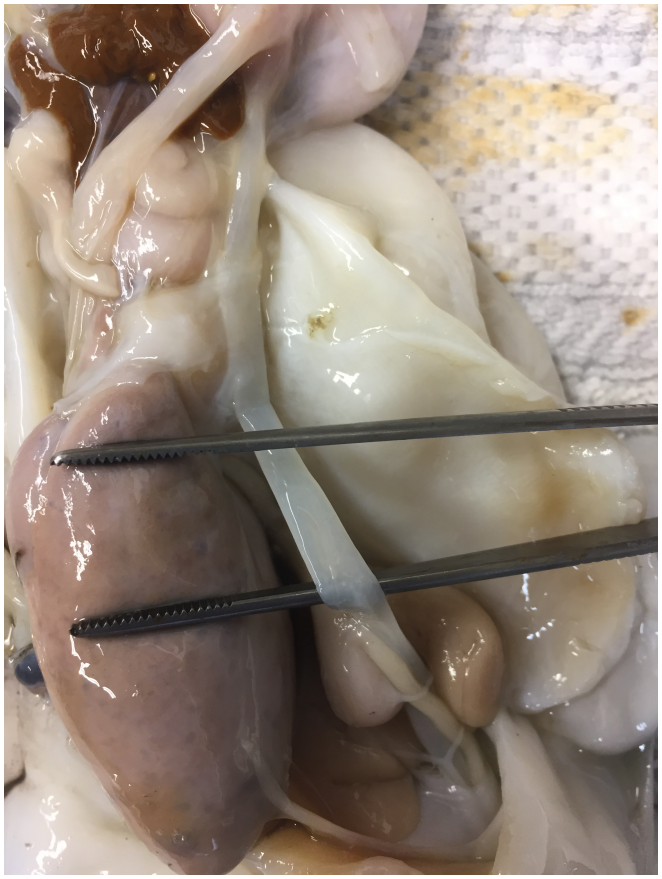

Figure 51.7: *Octopus vulgaris* dorsal aorta

Table 51.4: Concentrations of ions in blood vs. other fluids

Ion	Cephalopod blood (mM) (Seibel, 2013; Häfker, 2012; Oellermann et al., 2015a; Shoukimas et al., 1977; Brix e
Cl^-	495 - 506
Na^+	373 - 471
SO_4^{2-}	1.6
Mg^{2+}	45-50
K^+	8 - 15
NH_4^+	2 - 8?; or 0.25-0.3 in *O. vulgaris* and 0.02-0.03 in *S. lessoniana*
PO_4^{3-}	
Ca^{2+}	7 - 10.5
Taurine	100-200 (should be μM?) or 4.6 (Deffner, 1961)
Glucose	0.3-4 (10-70 mg/dL) (Goddard, 1968; Storey et al., 1979; Deffner, 1961)
Fructose	0.5 (Deffner, 1961)
Sucrose	
Mannose	
Betaine	4.3 (Deffner, 1961)
Osmolarity (mOsm)	963

Unlike fish muscle fibers which have 3-7 capillaries around each muscle fiber, squid muscle fibers are much more sparsely supplied. In the outer aerobic layers of circular tissue, capillaries are found every 5-8 muscle fibers and in the central anaerobic layers, capillaries are found 20+ muscle fibers apart (Bone et al., 1981).

51.2.6 Blood composition

Cephalopod blood is about as viscous as human plasma (however, it is unclear from what species or temperature this claim comes from) (Wells, 1983). Human whole blood viscosity at 37°C is 3-4 mPa · s, while plasma viscosity is 1.3-1.7 mPa · s.

51.2.6.1 Small molecules

Enteroctopus dofleini blood glucose levels range from 0.5-4 mM (Goddard, 1968) and *Sepia officinalis* blood has been measured at 1.2 mM (Storey et al., 1979). Blood glucose levels seem to have a seasonal periodicity as seen in other molluscs where sugar levels are highest in the summer and lowest in winter (Goddard, 1968). It is likely that they have insulin-like proteins that function in a feedback cycle with glucose.

Octopus blood seems to have an order of magnitude more NH_4^+ than squid blood (Tseng's 2018 CIAC talk). Due to this higher level, the proportion of glutamine relative to glutamate is also higher in octopus than squid.

Cephalopod blood possesses >200x more taurine than vertebrate blood (MacCormack's 2018 CIAC talk).

51.2.6.2 Protein, hemocyanin, and oxygen

By volume, the blood is ≈ 9% hemocyanin, 1-2% hemocytes, and the rest is plasma (Wells, 1983). This stands in stark contrast to human blood, which ranges from 37-52% hematocrit. There are ~5000 hemocytes / μL blood (Collins et al., 2012).

Cephalopod blood is high in protein, with ~100-150 g/L protein content (Schipp, 1987) (vertebrate plasma protein conc. is 60-80 g/L; Heisler 1986). Much of this is hemocyanin; cephalopods have the highest hemocyanin concentration in the animal kingdom (Pörtner and Reipschläger, 1996). Pörtner (1990) reported quantities of O_2 bound to squid hemocyanin equivalent to 70-80 g/L Hc (17.5 μM Hc). Unlike other molluscs, cephalopods do not have any blood-bourne hemoglobin (Wells and Smith, 1987).

Cephalopod blood also contains hemocytes which are part of the immune system (subsection 51.8.1).

Cephalopod blood is limited in its O_2 transport ability compared to fishes and other vertebrates due to its freely dissolved hemocyanin (Shadwick et al., 1990). Putatively, hemocyanin concentrations cannot become excessive without increasing blood viscosity and osmolarity, however cephalopod blood is about as viscous as human plasma (though I do not know for what species or temperature this is true) (Wells, 1983). Between the hemocyanin and freely dissolved oxygen, squid blood can hold as much as 2 mmol $O_2 \cdot L^{-1}$ (Redfield and Goodkind, 1929), *Octopus vulgaris* 1.4 mmol $O_2 \cdot L^{-1}$ (Houlihan et al., 1986), though in *Nautilus* it may reach only 1 mmol $O_2 \cdot L^{-1}$ (Wells, 1983). In *O. vulgaris* at rest, venous return only contains 250 μmol $O_2 \cdot L^{-1}$, resulting in ~80% of oxygen content consumed even at rest (Houlihan et al., 1986). Humans, in contrast can hold ≈ 8 mmol $O_2 \cdot L^{-1}$ and active fishes ≈ 7 mmol $O_2 \cdot L^{-1}$ (Root, 1931).

Table 51.5: Typical blood P_{O_2} in cephalopods at rest and normoxia

Species	Location	P_{O_2} (kPa)	Reference
Octopus vulgaris	Arterial	10.4	Houlihan et al. 1982
	Venous	4.0	Houlihan et al. 1982
Sepia officinalis	Arterial	13.3	Johansen et al. 1982
	Mixed venous	2.3-5.3	Johansen et al. 1982
	Venous	2-3	(Häfker, 2012; Gutowska et al., 2010)
Squid	Arterial	16	(Redfield and Goodkind, 1929)
	Venous	5.8	(Pörtner et al., 1991)
Trout / cod	Arterial		
	Venous	4.4-5.5	(Driedzic, 1988)
Nautilus pompilius	Arterial	13.2	(Mangum, 1990) citing Johansen et al 1978
	Venous	2.7	(Mangum, 1990) citing Johansen et al 1978

Oxygenated blood is blue and deoxygenated blood is clear (Redfield et al., 1926). Arterial P_{O_2} may be far from environmental P_{O_2} (and hemocyanin may not be fully saturated) because the cost of a high ventilation rate is not worth the very high arterial P_{O_2}. A lower value may suffice for O_2 transport with lower ventilatory cost.

51.2.7 Hemocyanin

Molluscan hemocyanins were first described from *Octopus vulgaris* by Frederico (1878). They evolved from a class of tyrosinase, a Cu-containing enzyme in the melanin synthesis pathway, about 740 Ma (Lieb and Markl, 2004; Markl, 2013).

Hemocyanin molecules are synthesized in the branchial glands: structures than run the length of the gills, in coleoids. In nautiloids (and other molluscs), they are synthesized in the midgut gland (Thonig et al., 2014). In fact, even in coleoids, until the branchial glands are fully formed in the embryo, the midgut gland is the source of hemocyanin (Thonig et al., 2014). They are catabolized in the ovoid cells of the branchial hearts (Beuerlein et al., 1998).

Their blood concentration is typically ~15-25 μM (60-100 mg/ml)(Pörtner, 1990; Markl, 2013; Redfield and Goodkind, 1929; Miller and Mangum, 1988).

Paralogs Nautiloids have one gene (NpH) while coleoids have two to three paralogs (*Sepia officinalis,* at least, has a third that is only expressed in embryos (Thonig et al., 2014) and *D. opalescens* has three, the third is most highly expressed prior to hatching (Pierce, 2017)). *Enteroctopus dofleini* and *O. bimaculoides* have A-type and G-type paralogs (Lang and van Holde, 1991) while *Sepia officinalis* has SoH1 through SoH3 (Sepia officinalis Hemocyanin 1-3). One paralog has also been sequenced from *Sepiella maindroni* (Li et al., 2017).

It seems that the duplication of the hemocyanin gene into two isoforms occurred independently at least between octopods and decapods (Warnke et al., 2011), suggesting that selection for multiple isoforms is strong. *Sepia officinalis* isoforms differ in their isoelectric point (Melzner et al., 2007), suggesting functional differences exist.

Cephalopod hemocyanin genes have 9-11 introns.

51.2.7.1 Molecular structure

Cephalopod hemocyanins are multi-subunit proteins, or oligomers. Each hemocyanin quaternary structure is composed of ten 350-450 kDa subunits, each of which with 7-8 functional units (FU) that are ~50 kDa (≈ 400 amino acids) each (Markl, 2013; Thonig et al., 2014). Thus, in total, a single hemocyanin molecule is 3.5-4.5 MDa (Mg/mol), ≈ 33,000 amino acids, and can transport up to 70 (*Nautilus* and octopods) to 80 (decapods) O_2 molecules. The entire molecule is cylindrical with inner collar domains on the inside of the cylinder wall (Kato et al., 2018).

Gastropod hemocyanins are formed into di-decamers, with the decamer rings stacked on top of each other (with the collars on the periphery of the cylinder hole), while polyplacophoran hemocyanins are mono-decamers like cephalopods (Kato et al., 2018). In all molluscan hemocyanins, the wall FUs seem to be stable while the number and type of collar FUs varies among taxa (Kato et al., 2018). Cerithioid snails are unique in having a tri-decamer "mega-hemocyanin" composed of two typical gastropod Hc rings (FU-a through FU-h) sandwiching a "mega-subunit" with six additional FUs: FU-f1 through FU-f6 that form a huge inner domain (Kato et al., 2018).

Cylinder wall The cylinder wall has a five-pointed (D_5) symmetry (51.8c). Each of the 5 equivalent sections is composed of a subunit (protomer) dimer (Kato et al., 2018). Within these subunit dimers, the functional units themselves also form dimers:

FU-(a-b) forms between FU-a and -b from the same subunit, however, FU-(d-e), and FU-(c-f) forms between FUs from different subunits, thus holding the subunit (protomer) dimer together (Kato et al., 2018). Therefore, the entire subunit (protomer) dimer is composed of three layers of two FU dimers (see Fig. 4 in Kato et al., 2018).

The cylinder wall also contains carbohydrate clusters at five sites that help hold the protomer dimers together (Gai et al., 2015). All coleoid hemocyanins examined contain these five potential glycosylation sites while *Nautilus* have four and gastropods only have two. It is thought that the addition of stabilizing glycosylation sites may help compensate for the lack of stabilizing FU-h in cephalopod hemocyanins (Gai et al., 2015).

Collar domains The five collar domains in *Nautilus* / octopodiform hemocyanins occur on only one side of the cylinder and are composed of an FU-g homodimer (FU-g from two subunits), and thus reinforce subunit (protomer) dimers (Kato et al., 2018). Decapodiform hemocyanins also possess additional collar domains on the opposite side of the cylinder from the FU-g collar domains composed of FU-d* monomers, the only FUs in any known hemocyanin that is not a dimer (Kato et al., 2018).

Subunit structure All molluscan hemocyanins contain FU-a through FU-g, but decapodiforms have duplicated FU-d (known as FU-d*) and non-cephalopod molluscs (nearly all gastropods, polyplacophorans, all?) possess an additional FU-h that forms another collar domain that is not found in the cephalopods (Kato et al., 2018). Nautilus and octopods have 7 FUs while decapods have 8 FUs (Miller, 1995; Markl, 2013) due to the duplication of FU-d (Thonig et al., 2014).

The cylinder wall is composed of FU-a through FU-f and the inner collar domains are composed of FU-g and FU-d* (when present) (Kato et al., 2018).

Functional unit (FU) structure All cephalopod FUs are composed of two domains: an N-terminal α-helix rich core domain (NTD) and a C-terminal β-sheet rich sandwich domain (CTD) (Kato et al., 2018). FU-h (which is found in gastropods and polyplacophorans but not cephalopods) also has a C-terminal cupredoxin (type-1 copper center) domain (Kato et al., 2018).

Molluscan hemocyanin active sites are found in the NTD and are composed of six histidine residues that bind two copper atoms (which makes it a type-3 copper center) which in turn bind a single O_2 molecule (Terwilliger, 1998). These six histidine residues (His41, 60, 69, 179, 183, and 210 (numbers from squid FU-a) as well as a thioether bridge between His60 and nearby Cys58 are conserved among all FUs of all known molluscs, highlighting their critical function (Kato et al., 2018).

The tendency of an O_2 molecule to enter the active site is modulated by a hinge connecting the α-helical core domain to the β-sandwich domain (Markl, 2013). There is, of course, variation between species and among isoforms within an individual species (Thonig et al., 2014). Furthermore, 4 FUs in each subunit are arranged to permit cooperativity between O_2-binding sites (section 51.2.7.2)(Zhang et al., 2013).

Based on crystal structure, there are two allosteric modifiers that occur on asparagine residues, both carbohydrates: mannose and glucosamine (Gai et al., 2015). In squid hemocyanin, four of these glycosylation sites occur at identical residues on FU-a, -b, -d, and -e CTDs while a fifth occurs on the FU-d NTD (Kato et al., 2018). Without these sugars attached, the subunits cannot form (Gai et al., 2015).

51.2.7.2 O_2-binding function

Fully saturated hemocyanin holds much more oxygen than is freely dissolved in the blood fluid. While dissolved blood [O_2] likely never exceeds ~0.25 mmol $\cdot$ L^{-1}, fully saturated squid hemocyanin has been shown to hold 1.5-2 mmol $O_2 \cdot L^{-1}$ (Redfield and Goodkind, 1929; Pörtner, 1990) and *Octopus* blood can hold 0.8-2 mmol $O_2 \cdot L^{-1}$ (Wells and Wells, 1995). Of course, this will vary based on [Hc], but at all times, hemocyanin should carry more O_2 molecules than are freely dissolved in the blood. Hemocyanin functions as a blood P_{O_2} buffer, releasing O_2 to replenish blood P_{O_2} as O_2 is transferred to the tissues along the circulatory path. The dumping of O_2 along the circulatory path is facilitated by dropping P_{O_2} and dropping pH (due to CO_2 fluxing into the blood) (Pörtner, 1990).

The oxygen affinity of a hemocyanin (Hc) isoform is a function of temperature, pH, and allosteric modifiers, and is typically expressed as P_{50}, the P_{O_2} required for 50% of the Hc to be oxygenated. There is more variation in P_{50} between species of cephalopods than in most any other group of animals (Lykkeboe and Johansen, 1982). Increased temperature decreases oxygen affinity (increases P_{50}) in most cephalopods (Seibel, 2013; Mislan et al., 2015) (but maybe not in *Octopus dofleini*; Miller, 1985). Lower ionic strength blood increases P_{50} (Miller, 1985).

For blood pH = 7.4, P_{100} is about 10-13 kPa for both loliginids and ommastrephids (Pörtner, 1990; Seibel, 2013). As a general rule in organisms, short-term environmental perturbations that require modification of blood respiratory pigments are modulated by allosteric modifiers, while long-term perturbations are compensated by increased respiratory pigment synthesis (Terwilliger, 1998). The latter mechanism, however, is limited in cephalopods due to their respiratory pigments being freely dissolved.

Hemocyanin saturation is a function of blood P_{O_2}, affinity (P_{50}), and cooperativity (n):

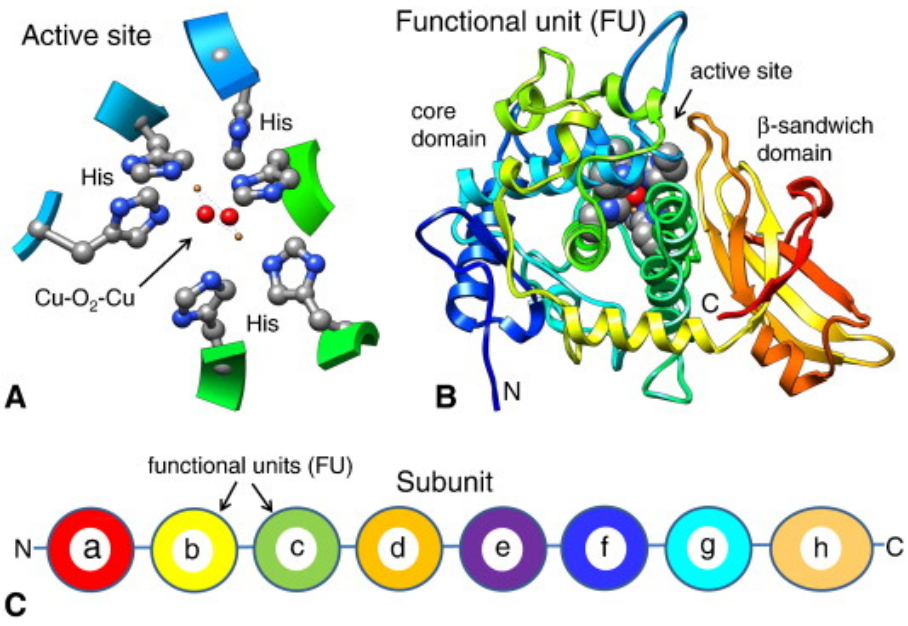

(a) A. O_2-binding active site. Small orange sphere are Cu and are bound by six His residues. B. Entire functional unit. α-helical core domain hinges with β-sandwich domain. C. Subunit h is present in gastropods but not cephalopods (see panel b) Decapods have an additional d functional unit.

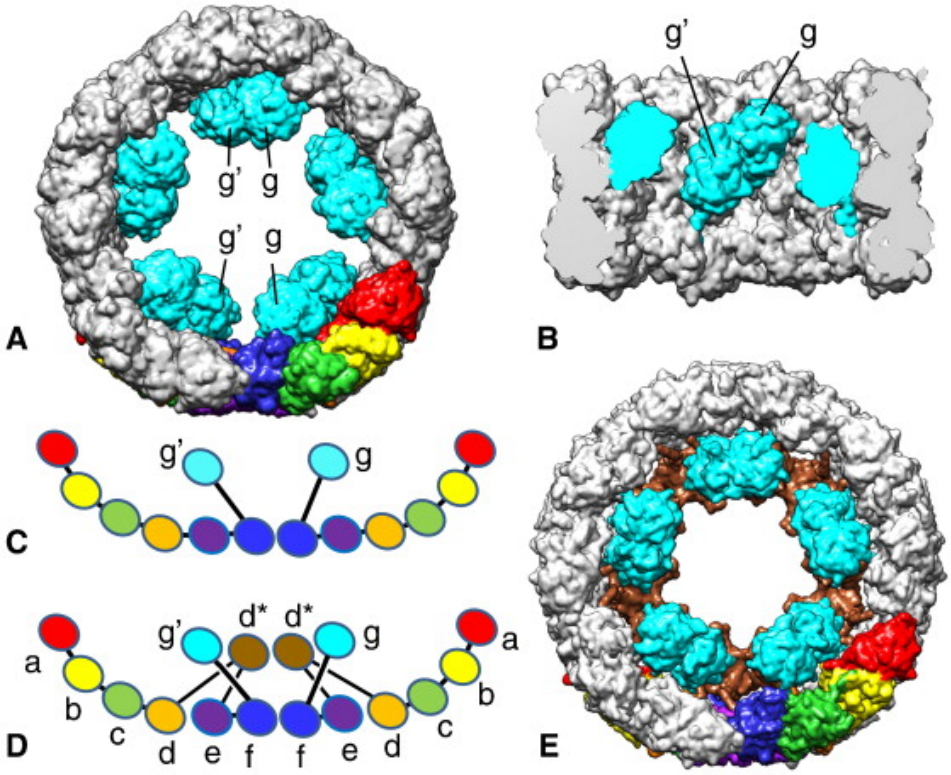

(b) Quaternary structure highlighting a single subunit and all the collar functional units. A, C. *Nautilus*/*Octopus* hemocyanin. D, E. Decapod hemocyanin with the extra d* FU.

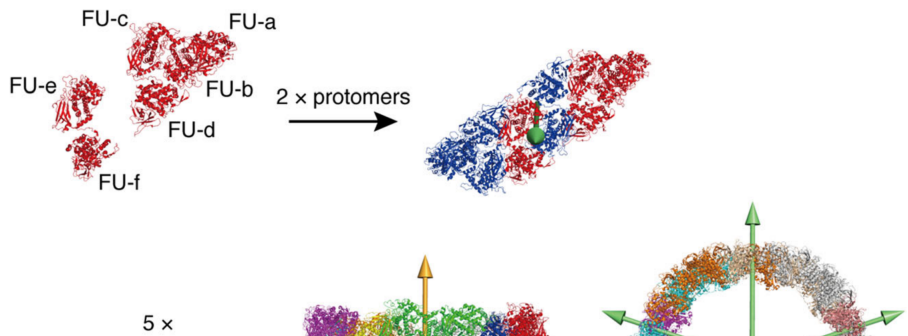

Table 51.6: Cooperativity pro/con list

Cooperativity (n)	Pro	Con
High	Full saturation at wide range of arterial P_{O_2}	Does not maintain stable decline in
Low	Buffers a gradual, even decline in P_{O_2} through the circulatory path	Arterial saturation can fall even at interm

$$\%\,\text{saturation} = \frac{(P_{O_2})^n}{(P_{50})^n + (P_{O_2})^n} \times 100$$

O_2 affinity (P_{50}), in turn, is influenced by:

- temperature
- pH
- inorganic ions
  - Mg^{2+} is most influential (it stabilizes the protein and decreases P_{50}) (Miller, 1985; Van Holde and Cohen, 1965).
- blood sugars? (Gai et al., 2015)(see section 51.2.7.2). Sugar-binding strongly affects mammalian Hb P_{50} (De Rosa et al., 1998).
- but not organic phosphates as in vertebrate RBC Hb (Mangum, 1997).

Exactly how much saturation is necessary to support aerobic metabolism is not well known. Redfield and Goodkind (1929) estimated saturation to be 10-40% before *Doryteuthis* died of hypoxia. Similarly, elasmobranchs have been estimated to reach P_{crit} at 35% saturation (Speers-Roesch et al., 2012).

Among various taxa, those with high metabolic rates and active lifestyles tend to have high O_2 carrying capacity and high P_{50}, both of which support O_2 delivery to tissues (Johansen and Weber, 1976).

Intracellular hemoglobin, as found in the red blood cells of vertebrates, is highly influenced by ATP and GTP as allosteric modifiers. Higher concentrations of the phosphates increases P_{50} (Mandic et al., 2009).

Cooperativity Hc subunits are cooperative when binding O_2 molecules, such that one functional unit binding O_2 molecules makes other functional units even more prone to binding O_2 molecules in the future. This cooperativity (expressed as a Hill coefficient, n) gives the Hc-P_{O_2} relationship a sigmoidal curve shape (when $n > 1$) rather than a typical Michaelis-Menten type logarithmic shape when there is no cooperativity ($n = 1$; e.g. mammalian myoglobin). A typical cephalopod Hill coefficient is 3-10 (Pörtner, 1990; Seibel, 2013), where:

$$n_{50} = \frac{\log(\frac{S}{1-S})}{\log P_{O_2} - \log P_{50}}$$

when S is the fraction of all available Hc binding sites bound to O_2 (ranges from 0 to 1; $S = 0.5$ at P_{50}). The larger the Hill coefficient, the steeper the slope of the PO_2 vs. S relationship. The Hill coefficient itself is pH dependent and is largest at *in vivo* pH conditions (Pörtner, 1990). Cooperativity seems to be unaffected by temperature, however, at least in *Dosidicus gigas* (Seibel, 2013). The more cooperative binding sites are, the more they will add or drop O_2 with a small change in P_{O_2}. So if sites are highly cooperative then saturation will change greatly for a given change P_{O_2}, and thus the numerical n value is great. If cooperativity is not as extreme, however, then the change in the numerator is smaller for a given change in denominator and the resulting Hill coefficient is smaller. Physiologically, there are benefits to both high and low cooperativity:

Typically, species with high cooperativity have lower O_2 affinity (higher P_{50}) and are more active (Brix et al., 1989).

Mechanism of cooperativity Cooperativity in molluscan hemocyanins is proposed to emerge from "communication clusters" between functional units that interact at the intersection between protomer dimers (Zhang et al., 2013). In each of these intersections, there are interacting loops between the CTD of one FU and the NTD of another. Importantly, the loop in the NTD contains a cysteine that forms a thioether bond with one of the histidine residues that holds the copper ion. Thus, the movement of these loops can directly affect the O_2-binding site.

At each of the 5 intersections between different protomer dimers, FU-a and FU-b from subunit 2 in protomer dimer X have loops that interact with loops on FU-e and FU-d respectively from subunits 2 and 1 respectively in the neighboring protomer dimer Y. Just below this as you follow the protomer dimer intersection down, FU-e and FU-d from subunits 1 and 2 in protomer

dimer X have loops that interact with loops on FU-a and FU-b respectively from subunit 1 in the neighboring protomer dimer Y. Therefore, among the 70 total FUs that compose the cylinder wall, 40 of them (FU-a, -b, -d, and -e) are arranged in such a way that their loops can interact and result in allosteric modification and cooperativity (Zhang et al., 2013). This seems to support the sequential model of enzyme-ligand binding cooperativity for hemocyanin (subsection 27.4.2).

Additionally, glycosylation sites occur on the FU-a and FU-d interacting loops in all hemocyanins, suggesting that the sugars bound to these sites have an effect on O_2-binding cooperativity (Gai et al., 2015).

Bohr and Haldane effects Cephalopod hemocyanins have a very extreme Bohr coefficient often < -1 (Redfield and Goodkind, 1929; Houlihan et al., 1982; Pörtner, 1990; Brix et al., 1989). The Bohr coefficient is:

$$\text{Bohr coefficient} = \frac{\log_{10}(P_{50_b}) - \log_{10}(P_{50_a})}{\Delta pH}$$

$$\text{Haldane coefficient} = \frac{\Delta HcH^+}{\Delta HcO_2}$$

where a and b are two different pH conditions.

This is in contrast to an optimal Bohr coefficient (for O_2 transport) of -0.35 to -0.5 (Lapennas, 1983). The optimal Bohr coefficient is half the value of the respiratory quotient (RQ). Smaller Bohr coefficients result in smaller Bohr shift even though ΔpH is greater (smaller Bohr coef. = smaller Haldane coef. thus more CO_2 remains free). Larger Bohr coefficients result in small ΔpH (thus small Bohr shift) because the Haldane coefficient is then large and much of the CO_2 produced is absorbed by hemocyanin. Therefore, the Bohr and Haldane effects in cephalopods may be less important in their traditional function of O_2 unloading at the tissues and instead be more important for blood pH stabilization and O_2 loading at the gills (Lykkeboe and Johansen, 1982).

As a general trend from fishes, respiratory proteins with high affinity (low P_{50}) tend to have smaller Bohr coefficients (Johansen and Weber, 1976). Though some crustaceans with low P_{50} have large Bohr coefficients.

The cephalopod extreme Bohr effect exists not just for the whole molecule, but for each subunit and O_2-binding domain (Miller, 1995). The Bohr coefficient is also temperature dependent such that increased temperature increases the Bohr coefficient (less extreme) (Seibel, 2013).

The Bohr effect is directly equivalent to the Haldane effect but from different perspectives (Wyman, 1964). The Bohr effect is caused by the dissociation constant (K_a) of histidine. When blood pH decreases, $[H^+]$ increases and binds more histidine residues in the active sites of the Hc molecule, thus limiting their O_2-binding ability and causing the Bohr effect. The Haldane effect derives from this same histidine K_a mechanism. At the tissues where $[H^+]$ is high, when O_2 is unbound and sent to the tissues, protons are transferred from a dissolved state in the blood to binding to Hc His residues. This decrease in dissolved H^+ drives $CO_2 + H_2O \rightleftharpoons HCO_3^- + H^+$ forward, thus decreasing dissolved P_{CO_2} in the blood. This draws even more CO_2 out from the tissues and into the blood than would occur solely due to the tissue-blood P_{CO_2} gradient which supports CO_2 transport out of the body.

In mammalian hemoglobin (Hb), the Bohr effect results from the following reaction: at low pH, a key His+ residue binds to an Asp- residue which conforms Hb into its tense state. When pH increases above the His+ residue's pK_a, the His+ deprotonates, breaking the bond and conforming Hb to its relaxed state which has a much higher O2 affinity (lower P_{50}).

51.2.8 Acid-base balance

Cephalopods must maintain very tight control over blood pH because their respiratory pigment, hemocyanin (Hc) is very sensitive to pH. Tissue-produced CO_2 in the blood must leave the circulatory system if its buildup and resulting acidosis is to be avoided. The majority of CO_2 produced by the tissues are released through the gills (subsection 51.1.6).

Typical blood pH is about 7.4-7.5 units in squids (Pörtner et al., 1991) and 7.7 in cuttlefishes (Gutowska et al., 2010). Typical $[HCO_3^-]_e$ is 2-3 mM in both squids and cuttlefishes (Pörtner et al., 1991; Gutowska et al., 2010). Thus typical cuttlefish blood P_{CO_2} is ~200 Pa (Gutowska et al., 2010) while squid blood is ~300 Pa (Redfield and Goodkind, 1929; Hu et al., 2014).

The conversion of CO_2 to H_2CO_3 is a rather slow process. The half-life of the reaction ranges from 30 seconds to 5 minutes as the temperature falls from 25 to 0 °C (Kern, 1960). Given that squid circulation can be as fast as 30 second circulation time (Shadwick et al., 1990) even at rest, it is likely that the CO_2 system in cephalopod blood is in disequilibrium, with more CO_2 and less HCO_3^- than expected at equilibrium. Importantly, there is no detectable carbonic anhydrase activity in cephalopod blood so there is no biological acceleration of this slow CO_2 hydrating step.

Cephalopod blood is buffered by both bicarbonate and non-bicarbonate buffering capacities. A typical non-bicarbonate buffer value (section 35.0.0.1) is ~10 mM pH^{-1} for cuttlefishes (*Sepia officinalis,* Gutowska et al., 2010) and ~5-6 mM pH^{-1} for squids (Pörtner, 1990). In comparison, intracellular β_{NB} is often 40-70 mM pH^{-1} in animals in general (Heisler, 1989). The buffering capacity is independent of pH even though the buffering capacity of the individual buffers is highly pH dependent because they

Table 51.7: Typical cephalopod blood acid-base parameter values

Taxon	Location	P_{CO_2} (Pa)	pH (free)
Octopus	Arterial		
	Venous		
Cuttlefish	Arterial		
	Venous	200 (Gutowska et al., 2010)	7.7 (Gutowska et al., 2010)
Squid	Arterial	290-300 (Redfield and Goodkind, 1929; Hu et al., 2014)	7.35 (Redfield and Goodkind, 1929)
	Venous	300-800 (Hu et al., 2014; Redfield and Goodkind, 1929)	7.2-7.35 (Hu et al., 2014; Redfield and Goodkind,

all average out across the physiological pH spectrum. The vast majority of this buffering capacity is due to titratable groups on hemocyanin (Miller and Mangum, 1988).

Climbers experience high altitude sickness because they increase their respiration rate to attain adequate O2. This off-gasses CO2 which increases blood pH (respiratory alkalosis). This is one of the primary causes of high altitude sickness.

51.2.9 Circulatory dynamics

The hearts and blood vessels are innervated by the vasomotor lobes in the suboesophageal brain (Nixon and Young, 2003). This may be a central pattern generator (CPG) neural circuit. The anterior vena cava also secretes hormones that that affect cardiovascular dynamics (Martin and Voigt, 1987) when stimulated by the visceral nerve (Fiedler, 1992). Neurotransmitters injected straight into the heart alter dynamics (Wells, 1980). FMRFamide is a peptide hormone released from the vena cava which increases heart rate and heart contraction pressure amplitude (Minakata, 2006). Other excitatory neuropeptides known as Ocp-1 through Ocp-3 are found in *Octopus* systemic heart (Minakata, 2006).

The dynamics of circulation can measured by the following parameters:

- Heart rate (HR)
- Heart contraction pressure amplitude
- Cardiac stroke volume (CSV)
- Cardiac output = HR × CSV

Squid have been reported to have 30 second circulation at rest (Shadwick et al., 1990), while *Octopus* is closer to 60 seconds (O'Dor and Wells, 1984).

Taurine Cephalopods possess blood taurine levels >200x higher than vertebrates (MacCormack's 2018 CIAC talk). Increased blood taurine reduces cardiac stroke volume but has no effect on heart rate (MacCormack's 2018 CIAC talk).

51.2.9.1 Heart rate (HR)

The heart contractions are myogenic (originated directly by the myocytes rather than nerve cells) (Wells, 1983). However, there is external input from the visceral nerve (subsubsection 51.5.3.10). FMRFamide and other FaRPs are known to increase heart rate in *Octopus* (Minakata, 2006).

The branchial hearts contract slightly before the systemic heart and seem to be the main pacemakers for the circulatory system (Wells, 1980).

Heart rate is rather stable in octopods, varying only with temperature and environmental hypoxia (Wells, 1980). *Octopus vulgaris* HR is 0.5-0.8 Hz (Wells and Wells, 1986).

At least in mammals, resting heart rate slows as an individual grows and SMR lowers (Weibel et al., 1991). In mammals again, however, maximal heart rate (at MMR) is consistent in various species regardless of how active or sedentary they are, suggesting that active lifestyles in mammals are supported by changes in CSV and blood $[O_2]$ rather than HR (Weibel et al., 1991).

51.2.9.2 Heart contraction pressure amplitude

The systemic heart produces pressure amplitudes around 1-2.5 kPa in *Octopus* (Wells, 1980, 1983). Branchial hearts produce pressure amplitudes of 0.5-1 kPa in *Nautilus* and *Loligo* and 0.25-0.5 kPa in *Octopus* (Wells, 1992).

FMRFamide and other FaRPs are known to increase heart contraction pressure amplitude in *Octopus* (Minakata, 2006).

Table 51.8: Typical systemic heart rate. Generalizations from (Schipp, 1987).

Taxon	BPM at ~20 °C
Nautiloids	25
Benthic octopuses	30-50 (Wells and Wells, 1986)
Cuttlefishes	35-50
Neritic squids	100
Cods and cypriniforms	50-60 (Rinne et al., 2001)
Rainbow trout	40 (Priede and Tytler, 1977)

51.2.9.3 Cardiac stroke volume (CSV)

CSV will vary based on heart (animal) size and O_2 demand (Weibel et al., 1991). At least among mammals, CSV is proportional to a species activity in its normal life history, such that more athletic species have higher CSV (Weibel et al., 1991). In a 1 kg *Eledone*, maximum CSV has been measured at 0.5 to 0.8 mL (Wells, 1983). *Sepia officinalis* has a CSV of 0.8 mL (MacCormack's 2018 CIAC talk). The higher the efferent branchial artery (input) pressure the larger the stroke volume (Wells, 1983).

Increased blood taurine reduces cardiac stroke volume (MacCormack's 2018 CIAC talk).

51.2.9.4 Cardiac output

Cardiac output ($L \cdot min^{-1}$) can be calculated from the Fick principle if M_{O_2} and arterial and venous O_2 content ($\mu mol\, O_2 \cdot L^{-1}$) are known:

$$\text{Cardiac output} = \frac{M_{O_2}}{C_{O_2a} - C_{O_2v}}$$

or it can also be calculated if heart dynamics are known:

$$\text{Cardiac output} = HR \times CSV$$

It is often mass-specific: $mL \cdot kg^{-1} \cdot min^{-1}$. Cardiac output is about 5-10x higher in *Loligo* (100-250 $mL \cdot kg^{-1} \cdot min^{-1}$) than *Octopus* (20-30 $mL \cdot kg^{-1} \cdot min^{-1}$) and roughly 50x higher than *Nautilus* (5 $mL \cdot kg^{-1} \cdot min^{-1}$)(Bourne, 1987). Cephalopod cardiac output (at least in squids) is more comparable with mammals than other invertebrates or fishes (Wells, 1992).

At least based on studies using invasive flow probes in the dorsal aorta, *Octopus* at rest send about 2/3 of the total cardiac output to the head and arms (Wells and Smith, 1987).

51.2.9.5 Blood pressure

Blood pressure in cephalopods must be rather high in order for blood to remain flowing during movement, when their hydrostatic skeleton creates great localized pressures (Wells and Smith, 1987). Blood pressure also affects branchial diffusion capacity, with higher pressure increasing gill perfusion and decreasing thickness (Melzner et al., 2009).

Blood pressure obviously oscillates with heart contractions but also is affected by the elasticity of the vasculature. In *Octopus*, for example, the pressure in the dorsal aorta spikes with the systemic heart contraction, falls rapidly as the valve in the systemic heart closes, and then falls slowly as the aorta relaxes (after being stretched by the pressure) (Wells, 1983).

Vasodilators and vasoconstrictors Acetylcholine (ACh) is a vasodilator (lowers blood pressure) whereas serotonin (5-HT) is a vasoconstrictor (raises blood pressure) (Wells, 1983). At least in mammals, acetylcholine vasodilates in an endothelium-dependent manner, by binding to receptors on the vascular endothelia and triggering the production of nitric oxide (NO) (see below).

At least in mammals, nitric oxide (NO) is also an important vasodilator produced by the vascular endothelial cells and acting on the vascular smooth muscle. The mechanism of action is as follows:

1. Vascular endothelia release NO that are taken up by neighboring vascular smooth muscle
2. Within the smooth muscle, NO binds to guanylate cyclase, activating it to cleave two P_i groups from GTP to form cGMP
3. cGMP phosphorylates myosin, which inactivates it and relaxes the muscle

Table 51.9: Blood pressures throughout the body (kPa). (s) = systolic and (d) = diastolic.

Taxon	Dorsal aorta	Vena cava	Afferent branchial veins	Efferent
Nautiloid	2-6 (Gosline and Shadwick, 1982); 3.5 (s) and 1.5 (d)			0.1-0.2
Octopod	3-6.9 (s) and 1.5-4.4 (d) (Wells, 1980, 1983)	0.2-0.4 (Wells, 1983)	0.2-5 (s) and 1.5 (d)	0.1-0.2
Cuttlefish	2.75 (MacCormack's 2018 CIAC talk)			
Loliginid	7 (s) and 2.7 (d); 4-11		0.9 (s) and 0.04 (d)	0.1-0.2
Ommastrephid	10-20 (Gosline and Shadwick, 1982)			
Trout / cod	4-5 (Driedzic, 1988)			
Humans	16 (s) and 10 (d)	0.25-0.8	3.3 (s) and 1.6 (d)	

51.2.9.6 Blood flow

Blood flow to a given organ is determined by $F = \frac{\Delta P}{R}$, where F is flow, ΔP is the arteriovenous pressure difference, and R is the resistance (determined by vessel diameter and blood viscosity). At least in mammals, some organs such as brain, heart, and kidney are highly capable of autoregulating blood flow over a rather wide range of pressures (e.g. 70-175 mmHg) by changing blood vessel diameter, while other organs such as skin have little or no autoregulation.

Control of these dynamics is important for regulating oxygen delivery to the tissues. The systemic and branchial hearts do not receive environmental P_{O_2} information from the branchial ganglia in order to modulate their dynamics accordingly, and yet heart rate and contraction amplitude respond to changes in environmental P_{O_2} within seconds of exposure (Wells and Wells, 1995). Thus, the key regulatory response from the systemic heart may be blood P_{O_2} directly (Wells and Wells, 1995).

51.2.10 Parameters affecting blood O_2 transport

The following cardiovascular parameters are the minimum variables to influence the rate of blood O_2 transport to tissues:

- arterial P_{O_2}
- P_{50}
- n_{50}
- arterial pH
- [hemocyanin]
- cardiac output
- arteriovenous ΔpH
- Bohr coefficient

51.3 Digestive system

The primary diet and fuel of all cephalopods is protein. In the digestive tract, HCl denatures proteins and proteases break the AA chains. The AAs are absorbed in the digestive gland and/or caecum, and transported in the blood to the rest of the body as fuel.

The digestive tract is U-shaped and contains the following organs: buccal mass, esophagus, digestive gland, crop (in nautiloids and octopods), stomach, caecum, intestine, ink sac, and anus.

The crop (when present), stomach, caecum, and intestine are all innervated by the gastric ganglion (Budelmann, 1995).

Cephalopod digestive systems are rich with *Mycoplasma* spp. and *Photobacterium* spp. bacteria (Kang et al., in prep 2021).

51.3.1 Organs

51.3.1.1 Salivary glands

All cephalopods possess a pair of anterior salivary glands (ASGs) that are attached to the buccal mass and all except cirrates possess a single posterior salivary gland (PSG) that may be branched or unbranched. The PSG connects to the esophagus near

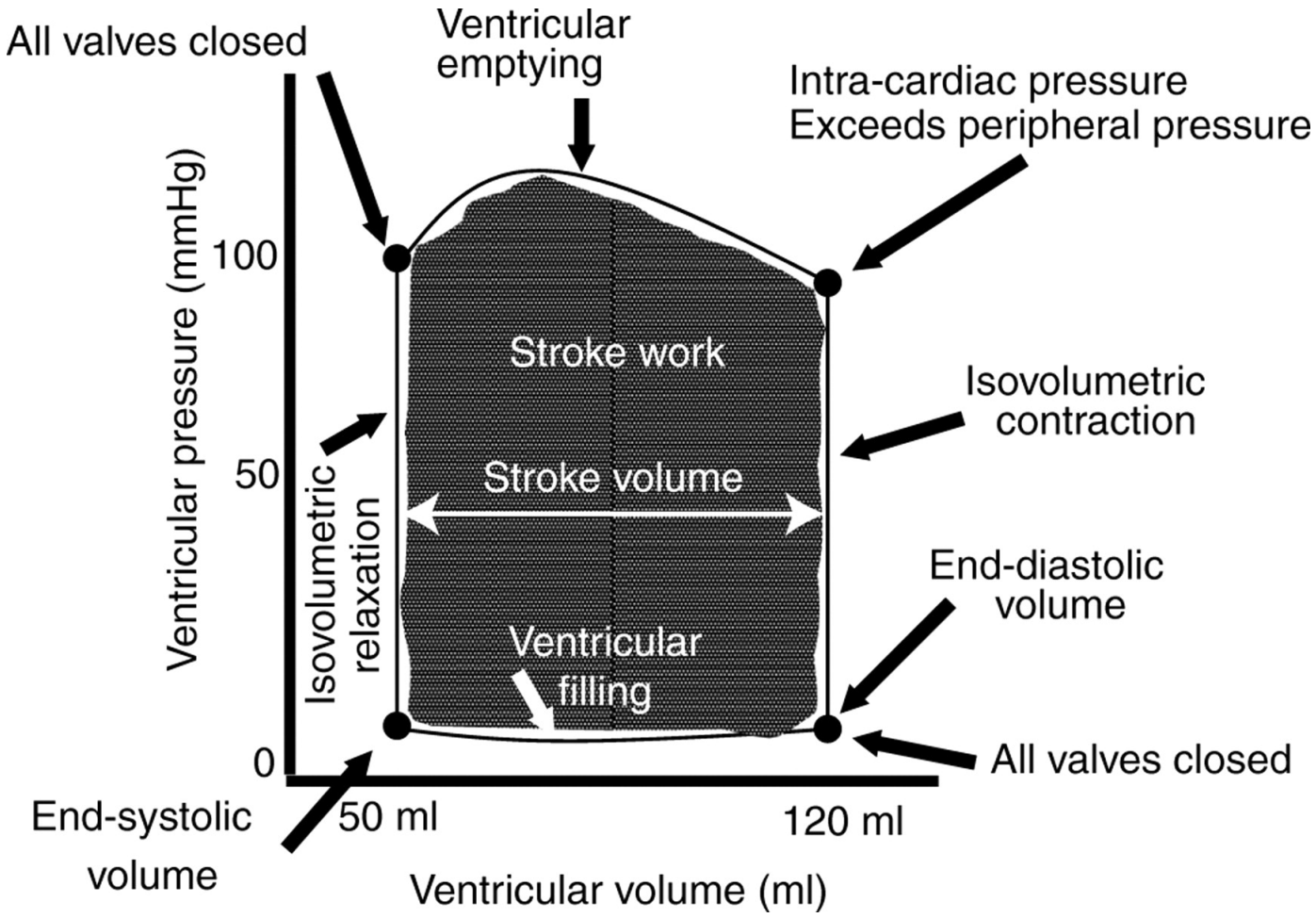

Figure 51.9: Theoretical pressure-volume (PV) loop

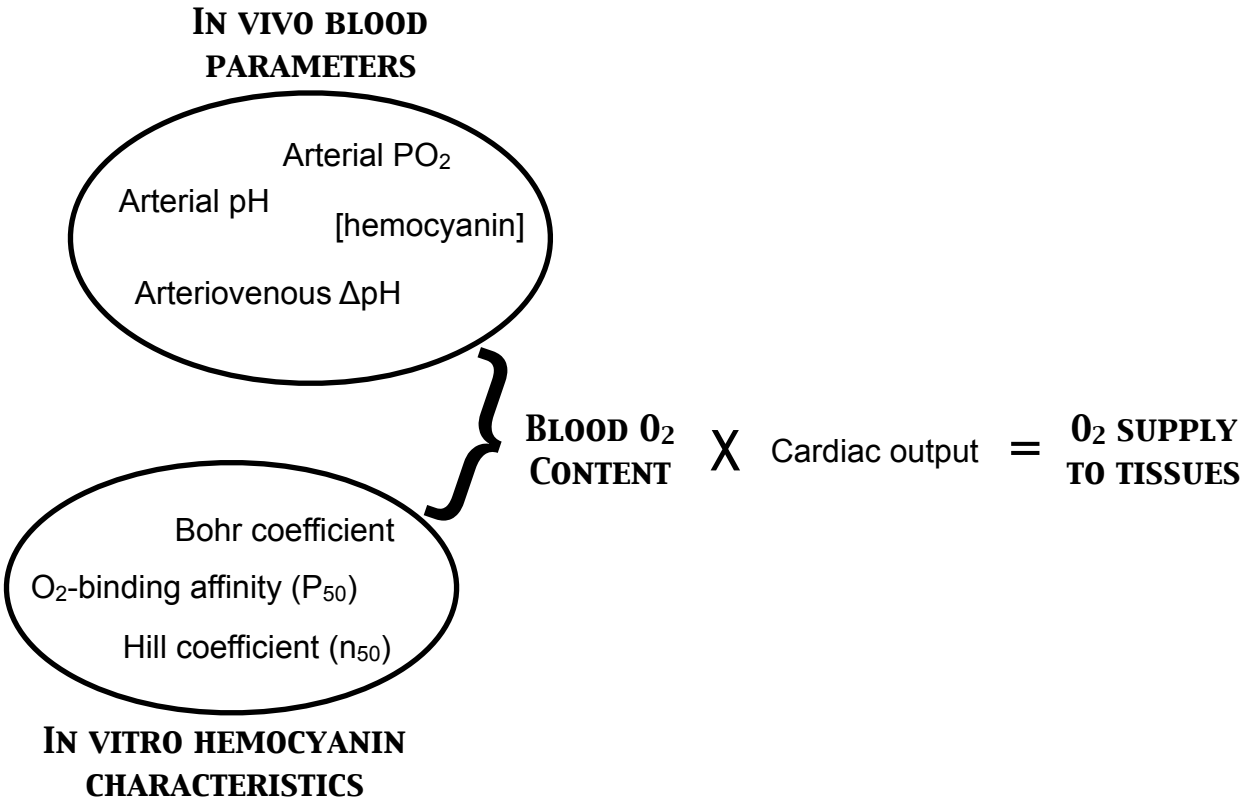

Figure 51.10: Parameters affecting blood O_2 transport

the buccal mass via a long anteriorly directed duct (Figure 51.11). In *Hapalochlaena* spp., high concentrations of tetrodotoxin is stored in the PSG. In more common octopodids, the PSG harbors cephalotoxin, a glycoprotein toxin extremely potent for paralyzing crustacean prey.

51.3.1.2 Digestive gland (DG) (hepatopancreas, liver)

The digestive gland is the primary source of digestive enzymes (Boucaud-Camou and Boucher-Rodoni, 1983). The DG stores large quantities of lipids in many cephalopods, which are utilized during starvation (Speers-Roesch et al., 2016). For reference, well-fed *Sepia officinalis* DG has 15 mg/g triacylglycerol (TAG) (Speers-Roesch et al., 2016). In addition, enzyme activities of two late-step gluconeogenesis enzymes (FBPase and G6Pase) are much higher in the DG than anywhere else in the body (Speers-Roesch et al., 2016). This suggests that glucose synthesis via gluconeogenesis is completed in the digestive gland. Since glycogen stores are not abundant in the DG, however, most glycogen must be sent back to the tissues, primarily mantle muscle.

The DG may be a notable site of hemocyanin storage(?).

51.3.1.3 Crop

The crop exists in octopodiforms and nautiloids only and stores food.

51.3.1.4 Stomach

The stomach is a muscular organ that grinds down food.

51.3.1.5 Caecum

The caecum is an important absorptive region in the digestive tract. Especially in teuthoids where food does not pass to the digestive gland, the caecum is the dominant site of absorption (Boucaud-Camou and Boucher-Rodoni, 1983). Digestive enzymes enter the caecum from the digestive gland ducts. Caeca can frequently be infected by *Aggregata* protozoans, which impair absorption (Castellanos-Martínez and Gestal, 2013).

51.3.1.6 Ink sac

The ink sac connects to the digestive tract at the intestine just prior to the anus (Boucaud-Camou and Boucher-Rodoni, 1983). Ink release is controlled by a pair of sphincters (Derby, 2014). The ink is produced by the ink gland and is composed primarily of melanin but can be mixed with mucous produced by the funnel gland (Derby, 2014). It also contains L-dopa and dopamine (precursors to melanin) which conspecifics can detect chemically as well as visually (Lucero et al., 1994).

The ink sac is rich in reflectin proteins which give it its iridescent appearance (MBL Loligo genome seminar).

51.3.1.7 Anus

Expulsion of feces is under CNS control (Ponte et al., 2017). Both *Octopus* and *Sepia* produce "fecal ropes". Feces is often coated in mucus and contains undigested food, enzymes from the DG, dead cells, digestive tract microbes, and parasites (Ponte et al., 2017).

51.3.2 Process of digestion

Among commonly studied shallow water cephalopods at moderate temperatures (10-30°C), the oro-anal transit time is 2-12 hours in teuthoid squids and 8-30 hours in octopus, *Sepia*, and *Nautilus* (Ponte et al., 2017).

The esophagus brings food from the buccal mass via peristalsis to the U-turn where a vestibule splits to the stomach and caecum. Both stomach and caecum are gated by sphincters allowing each organ to be isolated from the rest of the tract. In nautiloids and octopods the food may also be stored temporarily in a crop before reaching the stomach. Otherwise, the food reaches the stomach where it is digested with the digestive enzymes secreted by the digestive gland. After much digestion, the digestive fluid is sent to the caecum and (in octopods and sepioids) it also travels through the digestive ducts' appendages to the digestive gland. Nutrients are then absorbed in the digestive gland and caecum. Finally, the remaining digestive fluid is sent through the intestine where some final absorption occurs before being excreted through the anus (Boucaud-Camou and Boucher-Rodoni, 1983).

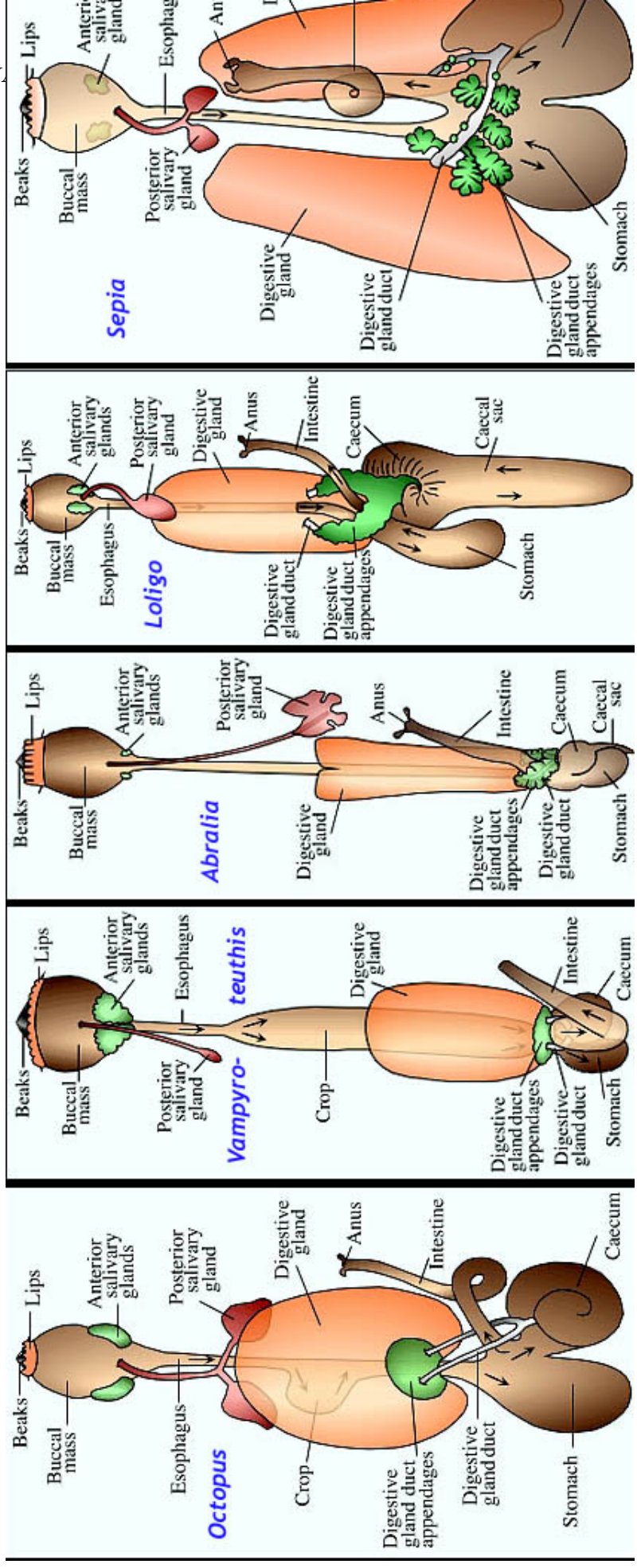

Figure 51.11: Digestive organs of cephalopods.

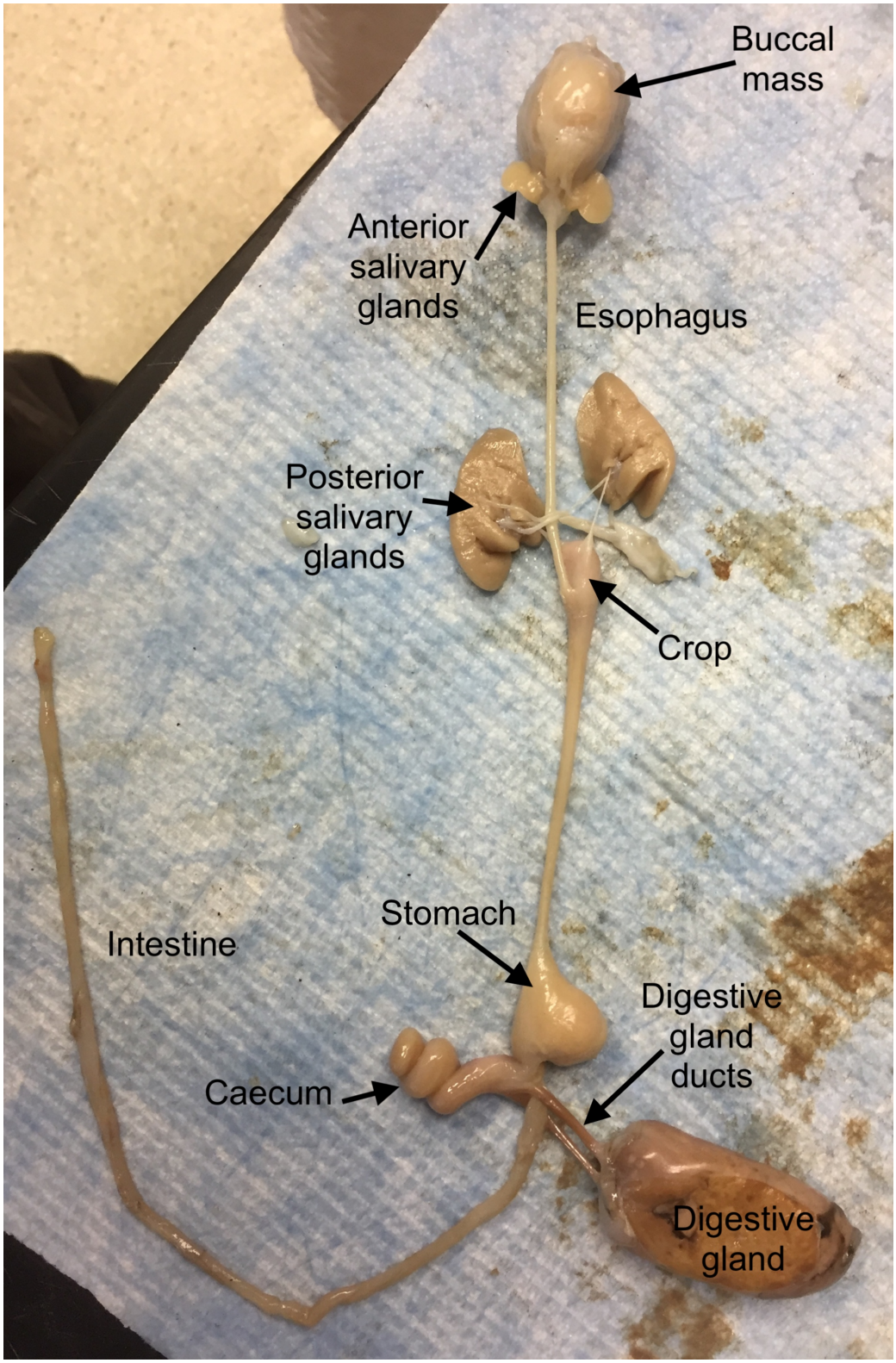

Figure 51.12: *Octopus vulgaris* digestive tract

51.3.3 Microbiome

As in vertebrates and other invertebrates, cephalopods have microbiomes within their gut cavities. The most abundant genera are *Photobacterium* and *Mycoplasma* (Kang et al., 2022).

51.3.4 Digestive shutdown during senescence

When female incirrate octopods brood their young, they cease eating. At least in alloposids, the crop and stomach become infested with ciliates and the posterior salivary and digestive glands shrink (Young, 1972).

51.4 Excretory system

The excretory system functions to remove byproducts of metabolism and broken-down pieces of the body from the blood. These functions are performed by the gills, branchial heart appendages, renal appendages and sac, the digestive gland, and the renopericardial canals (Boucher-Rodoni and Mangold, 1994). *Octopus* are known to excrete 10-15% of their body mass in urine per day (Wells and Clarke, 1996).

Cephalopod urine is acidic (pH = 5-6) and high in ammonium (3 mM) (Hu and Tseng, 2017; Hu et al., 2017). The majority of NH_3 produced in the body is excreted through the gills; the renal sac only excretes ~1% of NH_3 (Hu et al., 2017).

51.4.1 Gills

Cephalopod gills possess a variety of proteins for ion exchange. Both ammonia and acid-base equivalent ions are important for homeostasis. Rhesus protein (RhP) is utilized primarily for ammonia excretion but may also be important for acid-base balance (Hu et al., 2013). RhP transports ammonia across the gill membrane in the gaseous form (NH_3) despite ammonium's very high pK_a. At least in fish gills, RhP forms a metabolon with NHE3 so that the ammonia excreted by RhP binds to the the H^+ excreted by the NHE3 rather than taking a H^+ from the ambient seawater. The resulting NH_4^+ only very weakly dissociates (pK_a = 9-10) so ammonia excretion by cephalopods has nearly no effect on the ambient seawater pH.

Cephalopods have a typical O:N atomic ratio of 11-17 (Ikeda, 2016).

It has been proposed that due to the presence of receptors for the peptide hormone cephalotocin in the gills, that cephalotocin may be involved in ammonia excretion (Minakata, 2006).

51.4.2 Branchial heart appendages

The branchial heart appendages (BHA) are attached to the branchial hearts. The later creates the pressure required for ultrafiltration of the blood in the BHA (Wells, 1983).

BHAs possess epithelial cells (podocytes) that surround capillaries. There is lots of hemocyanin found within these podocytes, suggesting they recycle hemocyanin subunits that were lost during ultrafiltration, reassemble them, and return functional hemocyanin molecules to the blood (Beuerlein et al., 2000).

51.4.3 Renal appendages

The renal appendages conduct ultrafiltration of the blood, similar to the mammalian kidney.

Renal appendages possess epithelial cells (podocytes) that surround capillaries. There is lots of hemocyanin found within these podocytes, suggesting they recycle hemocyanin subunits that were lost during ultrafiltration, reassemble them, and return functional hemocyanin molecules to the blood (Beuerlein et al., 2000).

The renal appendages are often infested with dicyemid parasites.

51.4.4 Renal sac

The renal sac excretes urine into the mantle cavity via the nephridial pore.

51.5 Nervous system

51.5.1 Evolution of the nervous system from other molluscs

All molluscs have 5-6 pairs of ganglia: cerebral, buccal, pedal, pleural, parietal, and visceral ganglia (Budelmann, 1995). Each pair of ganglia are connected by a commissure and each ganglion pair is connected to other pairs in other parts of the body

by connectives (Budelmann, 1995). Due to shortening of the connectives between ganglia, the cephalopod nervous system is more centralized than any other mollusc nervous system and is tied with insects for the most centralized in any invertebrate (Budelmann, 1995). The shorter connectives are particularly advantageous given the unmyelinated form of the neurons; shorter connections result in faster propagation of signals (Budelmann, 1995).

Based on transcriptome data, it is suspected that coleoids at least may have a vertebrate-like blood brain barrier (Zhang et al., 2012). Cephalopods are the only molluscs to have a blood-brain barrier (Budelmann, 1995).

Within the cephalopods, neuroanatomy varies by the position, fusion, addition or removal, and the relative sizes of ganglia (Budelmann, 1995).

Unlike vertebrates and insects, there does not seem to be somatotopy in cephalopod brains; there is no correspondence of a particular area of the body with a specific point in the CNS (Budelmann, 1995).

CNS neuronal soma are 5-20 μm in diameter, which is similar to mammalian CNS neurons but much smaller than other molluscs (e.g. *Aplysia* and gastropod: 20-150 μm).

Octopus have 500 million neurons (Young, 1963), which is similar to many birds and small mammals, while the next invertebrate that I know of is the cockroach with 1 million neurons.

51.5.1.1 Expansion of neuronal gene diversity

Cephalopods have diversified a number of gene families compared to other bilaterians. Notably, the protocadherin (cell adhesion proteins), G-protein coupled receptors, and C2H2 zinc-finger proteins (transcription factors) are all greatly diversified and are most strongly expressed in nervous tissue (Albertin et al., 2015), thus correlating with the higher complexity of cephalopod brains.

Cephalopods (and vertebrates) have expanded the intron size of their neuronal genes, possibly to allow for expansion of regulatory mechanisms such as miRNAs in their increasingly complex nervous systems (McCoy and Fire, 2020).

Protocadherin gene diversity The protocadherin gene family codes for a family of cell-adhesion molecules. These genes are required for neuronal development by promoting dendritic self-avoidance and regulating the formation of neural circuits. Knockout neurons have dendrites that collapse and touch each other. They are almost exclusively expressed within the CNS (Albertin's 2018 CIAC talk). *Octopus* have an order of magnitude greater protocadherin gene diversity compared to other molluscs (168 vs 17) (Albertin et al., 2015) and *Doryteuthis pealeii* has almost twice as many as *Octopus* (315; Albertin's 2018 CIAC talk). *Doryteuthis opalescens* also have many (Pierce, 2017). They occur in tight clusters on the same chromosome (Albertin's 2018 CIAC talk).

All protocadherins are composed of intra- and extracellular domains as well as a transmembrane domain. Since protocadherins can form quaternary structures, the potential diversity of quaternary proteins is an order of magnitude greater even than that of humans (Albertin et al., 2015). In addition to the diversity of genes, protocadherin transcripts are disproportionately highly edited (Liscovitch-Brauer et al., 2017) which further enhances protein diversity. Vertebrates also independently diversified their protocadherin genes, suggesting that their diversification is important for advanced neuronal morphology.

While the diversification events seemed to have happened after the octopodiform-decapodiform divergence, the radiation of this gene family occurred independently in both taxa. In *Octopus*, radiation occurred ~135 MYA (Albertin et al., 2015).

51.5.2 Central nervous system (CNS)

Brain size The brain-to-body mass ratio of shallow-water coleoids (at least *O. vulgaris*) is larger than any other invertebrate and is roughly equivalent to or even exceeds that of fishes and reptiles (Packard, 1972). Thus, it is likely that the cephalopod brain requires 5-10% of SMR (Nilsson 1996) (compare to 20% in humans). I am not sure how deep-water coleoids compare... In fact, *Octopus* has 500 million neurons (5x that of a mouse brain)(Young, 1963) though the majority are in the PNS. Generally, octopodiform brains are more compact than decapodiform brains which in turn are more compact than nautiloid brains (Nixon and Young, 2003).

Paralarval *Octopus vulgaris* brains have ~200,000 cells (Styfhals' 2022 CIAC talk).

Brain anatomy For a very nice visualization of a *Sepia bandensis* brain, go to `https://www.cuttlebase.org/3d-brain-histology` or open the cuttlefish_brain.glb file.

Coleoid brains are divided into supra- and sub-esophageal masses with the former being much more complex (Nixon and Young, 2003). These divisions are connected by the magnocellular lobes. In total, the CNS is composed of 25 (26 in decapodiforms) lobes described below (Budelmann, 1995). There are many nerves interconnecting the lobes which makes it likely that any given lobe has many interconnected functions and does not have a single hierarchical main function (Budelmann, 1995). Furthermore, functions are likely spread across multiple lobes.

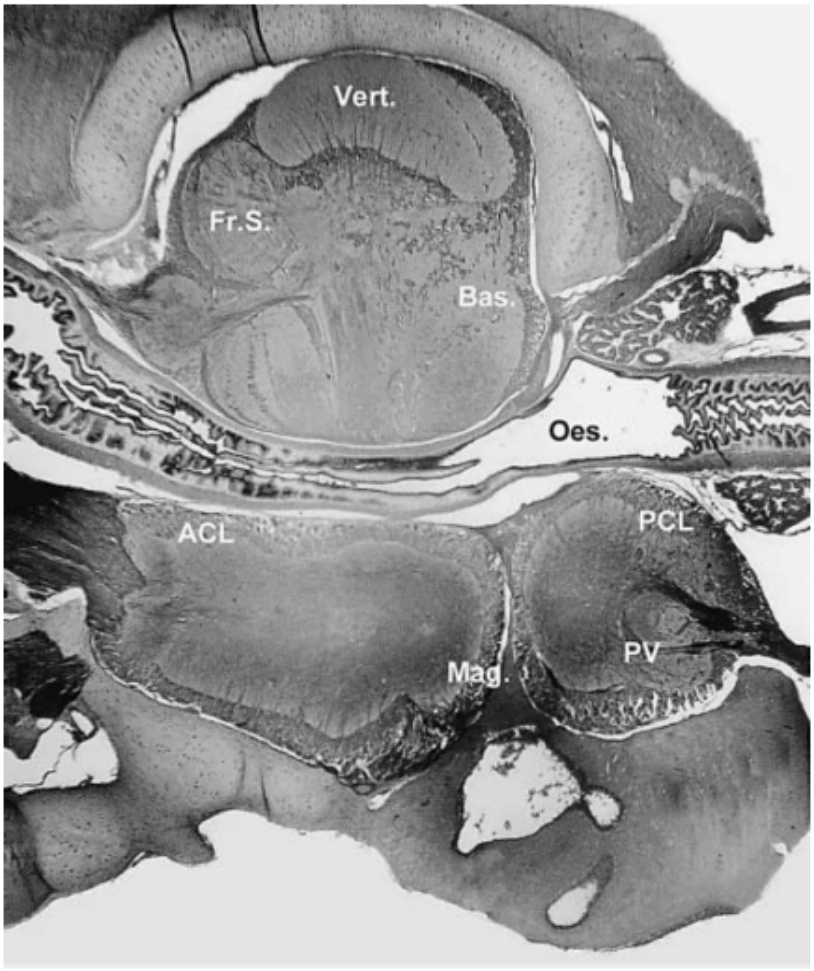

Fig. 1. Sagittal histological section through the brain of the squid, *Alloteuthis subulata*, showing some of the major lobes within the brain. Anterior chromatophore lobe (ACL), basal lobe (Bas.), superior frontal lobe (Fr.S.), magnocellular lobe (Mag.), oesophagus (Oes.), posterior chromatophore lobe (PCL), palliovisceral lobe (PV), and vertical lobe (Vert.).

Figure 51.13: Brain morphology of *Alloteuthis subulata*

Nautiloid brains are divided into the supra-esophageal cerebral cord, and the anterior and posterior sub-esophageal cords. These divisions are subdivided into 12 lobes (Budelmann, 1995).

51.5.2.1 Optic lobes

The optic lobes are the largest lobes in the CNS in all species examined (Budelmann, 1995). They are especially large in decapodiforms relative to octopodiforms (Budelmann, 1995). Furthermore, the optic lobes compose 45% of the CNS in shallow-water taxa and 85% in deep-water taxa (Chung's 2018 CIAC talk). Most cephalopod optic lobes are bean-shaped but diurnal shallow-water octopods have croissant-shaped optic lobes (Chung's 2022 CIAC talk). They are connected to the eye by multiple optic nerves and to the brain by a single optic tract. The optic lobes process visual information to determine the appropriate body pattern for camouflage (subsubsection 52.1.3.1). They are also involved in visual discrimination learning and memory (Budelmann, 1995).

Each optic lobe is well-organized, containing a distinct thin outer cortex and thick central medulla (Budelmann, 1995). The outer cortex has three layers: inner and outer granule layers that sandwich a plexiform layer (Nixon and Young, 2003). The central medulla is further divided into a radial column zone on the outside and a tangential zone on the inside. The medulla is filled with a tree-like structure that appears like "cell islands" in cross sections (Liu et al., 2017). Signals reach the optic lobe on the superficial surface, then are processed as the signal travels inwards through the medulla before going to the brain (Niell's 2018 CIAC talk).

Sepia optic lobe is vascularized to yield 20 μm radius Krogh cylinders, comparable to rat brain cortex (Abbott and Miyan, 1995).

51.5.2.2 Supra-esophageal mass

The basal lobes are important for choosing the chromatophore body pattern expressed based on input from the optic lobes (Williamson and Chrachri, 2004). Most learning and memory is thought to occur in the supra-esophageal mass (Brown and Piscopo, 2013).

Basal anterior lobe This is a higher motor center (Budelmann, 1995). It is also part of the statocyst / oculomotor system (Budelmann, 1995).

Basal dorsal lobe This is a higher motor center (Budelmann, 1995).

Basal inter lobe This is a higher motor center (Budelmann, 1995).

Basal lateral lobe This is a higher motor center (Budelmann, 1995). It is also involved in control of chromatophores and skin muscles (Budelmann, 1995).

Basal median lobe This is a higher motor center (Budelmann, 1995). It is also involved in motor control of swimming and respiration (Budelmann, 1995).

Buccal superior lobe This lobe controls feeding motor activity (Budelmann, 1995).

Buccal posterior lobe This lobe is involved in analyzing sensory input, learning, and memory (Budelmann, 1995).

Frontal superior lobes Further divided into medial and lateral.

This lobe is involved in analyzing sensory input, learning, and memory (Budelmann, 1995).

This lobe possesses soma whose axons extend posteriorly into the vertical lobe (Winters, pers. comm.).

Frontal inferior lobes Further divided into medial and lateral.

This lobe is involved in analyzing sensory input, learning, and memory (Budelmann, 1995). The inferior frontal lobes are larger in octopodiforms than decapodiforms (Budelmann, 1995).

Olfactory lobe The olfactory lobe in *Nautilus* is much larger than in coleoids (Basil et al., 2005).

Peduncle lobe The peduncle lobe is connected to the optic lobe right where the optic nerves connect (Wardill's 2022 CIAC talk).

This is a higher motor center (Budelmann, 1995). It is also part of the statocyst / oculomotor system (Budelmann, 1995). It is the functional equivalent of the cerebellum (Shigeno et al., 2018).

Precommissural lobe This lobe is involved in analyzing sensory input, learning, and memory (Budelmann, 1995).

Subfrontal lobe This lobe is involved in analyzing sensory input, learning, and memory (Budelmann, 1995).

Subpedunculate lobe This lobe is involved in analyzing sensory input, learning, and memory (Budelmann, 1995). It also innervates the optic glands.

Subvertical lobe This lobe is involved in analyzing sensory input, learning, and memory (Budelmann, 1995).

Vertical lobe The vertical lobe is utilized during learning and memory and as such is the functional equivalent of the vertebrate hippocampus (Alves et al., 2008). However, it is also involved in sensory input analysis (Budelmann, 1995).

The vertical lobes of octopodiforms and decapodiforms are quite different (Albertin et al., 2015). Decapodiform vertical lobes (at least squids) have 2 gyri ("sublobes") unlike the vertical lobes in octopodiforms (at least most *Octopus*) that have 5 gyri (Winters pers. comm.). However, *Abdopus capricornicus* and *Octopus cyanea* both have 7 gyri in their vertical lobes (Chung's 2022 CIAC talk) and *V. infernalis* does not have any (Chung's 2022 CIAC talk). Each one has different neurochemical identities suggesting differentiated function (Winters, pers. comm.). Generally, shallow-water species (of both decapodiforms and octopodiforms) have larger vertical lobes than deep-water species (Budelmann, 1995). *Octopus* vertical lobes possess 25 million neurons compared to 2 million in the mouse hippocampus (Winters pers. comm.). Unlike in most other lobes, 99% of vertical lobe neurons are actually very small interneurons (Budelmann, 1995).

Sepia optic lobe is vascularized to yield 28 μm radius Krogh cylinders, ~50% larger than rat brain cortex (Abbott and Miyan, 1995).

51.5.2.3 Peri-esophageal mass

Magnocellular lobes Further divided into dorsal, ventral, and posterior.

The magnocellular lobes span around the sides of the brain partially above and below the oesophagus (Nixon and Young, 2003).

Generally, the magnocellular lobes are intermediate motor centers bridging connections between the higher motor centers in the subra-esophageal lobes and the lower motor centers in the sub-esophageal lobes (Budelmann, 1995). The giant fiber escape jetting first order neuron somas are in the magnocellular lobes (Williamson and Chrachri, 2004).

51.5.2.4 Sub-esophageal mass

The sub-esophageal lobes are all motor lobes (Budelmann, 1995).

The following muscles are directly innervated by motoneurons from the sub-esophageal mass: head retractor muscles, chromatophores, funnel, fins, and eyes (Nixon and Young, 2003).

Brachial lobes Further divided into pre and post.

The brachial lobe is the anterior-most portion of the suboesophageal mass (Nixon and Young, 2003). Brachial and tentacle nerves extend from the brachial lobe to innervate the arms and tentacles. All of the brachial nerves are connected by an interbrachial commissure (Nixon and Young, 2003). The brachial lobes are larger in octopodiforms than decapodiforms due to their increased arm use (Budelmann, 1995).

Chromatophore lobes Further divided into anterior and posterior.

The chromatophore lobes possess neurons whose axons directly extend to chromatophores (i.e. they are lower motor centers) (Chiao et al., 2015). The ratio of motor neurons in the PCL to chromatophores in the body varies from 1:0.8 in *Sepia officinalis* (more neurons than there are chromatophores) to 1:7 in *Euprymna* (1 motor neuron controls 7 chromatophores) (Liang's 2022 CIAC talk).

Information from the optic and basal lobes are sent to the chromatophore lobes which function as lower motor centers (Williamson and Chrachri, 2004; Chiao et al., 2015).

Fin lobes Only decapodiforms and cirrates have fin lobes (Budelmann, 1995). The size of the fin lobe parallels the size of the fins (Budelmann, 1995).

Funnel lobes Further divided into anterior and posterior.

The funnel lobes are lower motor centers, directly innervating the funnel (Budelmann, 1995).

Palliovisceral lobe The palliovisceral lobe has some role in innervating the circulatory system (Smith and Boyle, 1983).

Pedal lobes Further divided into anterior and posterior.

The pedal lobes are the motor centers for a variety of muscle groups. They are involved either directly or indirectly with the head retractor muscle, eye muscle, fin, and arm movement (Nixon and Young, 2003). The pedal lobes are larger in octopodiforms than decapodiforms (Budelmann, 1995).

Pedal lateral lobes Further divided into anterior and posterior.

Vasomotor lobes Further divided into two lateral and two medial.

The vasomotor lobes are lower motor controls of the hearts and blood vessels. In *Octopus,* the vasomotor lobes are composed of 1.3 million neurons (Nixon and Young, 2003), making it the largest lobe in the sub-esophageal mass. These neurons connect to the visceral nerve in the PNS (I think).

51.5.3 Peripheral nervous system (PNS)

At least in *Octopus*, the PNS contains twice as many neurons as the CNS (Budelmann, 1995). All peripheral ganglia are lower motor centers (Budelmann, 1995).

51.5.3.1 Brachial nerves (axial nerve cords)

The brachial nerves transport sensory information between the brain and arms (Gutnick et al. 2020, Current Biology).

All of the brachial nerves are connected by an interbrachial commissure (Nixon and Young, 2003). The brachial nerves run the length of the arms. They have brachial ganglia for each sucker and additional smaller sucker ganglia (Budelmann, 1995). They transmit motor control to the arms but also send back chemo- and mechano-sensory information (Budelmann, 1995).

51.5.3.2 Branchial ganglia

The branchial ganglia innervate the gill lamellae (Budelmann, 1995). They are small and form chains along the length of the gill (Wells, 1980). They connect to the cardiac ganglion on each branchial heart (Wells, 1980).

51.5.3.3 Cardiac ganglia

There is one cardiac ganglion near each branchial heart. The cardiac ganglia are innervated directly by the visceral nerve in decapodiforms and from the fusiform ganglia in octopodiforms (Wells, 1980). Each cardiac ganglion functions as a pacemaker for branchial heart contraction (Wells, 1980). The cardiac ganglion is also the connection for the branchial ganglia on each gill (Wells, 1980). For more information, see subsubsection 51.2.3.1.

51.5.3.4 Fusiform ganglia

Fusiform ganglia only occur in octopodiforms (Wells, 1980). In decapodiforms, the function of the fusiform ganglia are fulfilled by the cardiac ganglia. Fusiform ganglia are intermediate ganglia between the visceral nerves and cardiac ganglia (Wells, 1980) which is why they have also been described as "first cardiac ganglia". The two fusiform ganglia are linked by a commissure (Wells, 1980). This linkage provides a nervous connection between the cardiac ganglia and, in turn, the branchial hearts to keep the hearts synchronized even in the artificial experimental situation where only one heart receives hormones (Wells, 1980).

51.5.3.5 Gastric ganglion

The gastric ganglion innervates the entire digestive system (Budelmann, 1995).

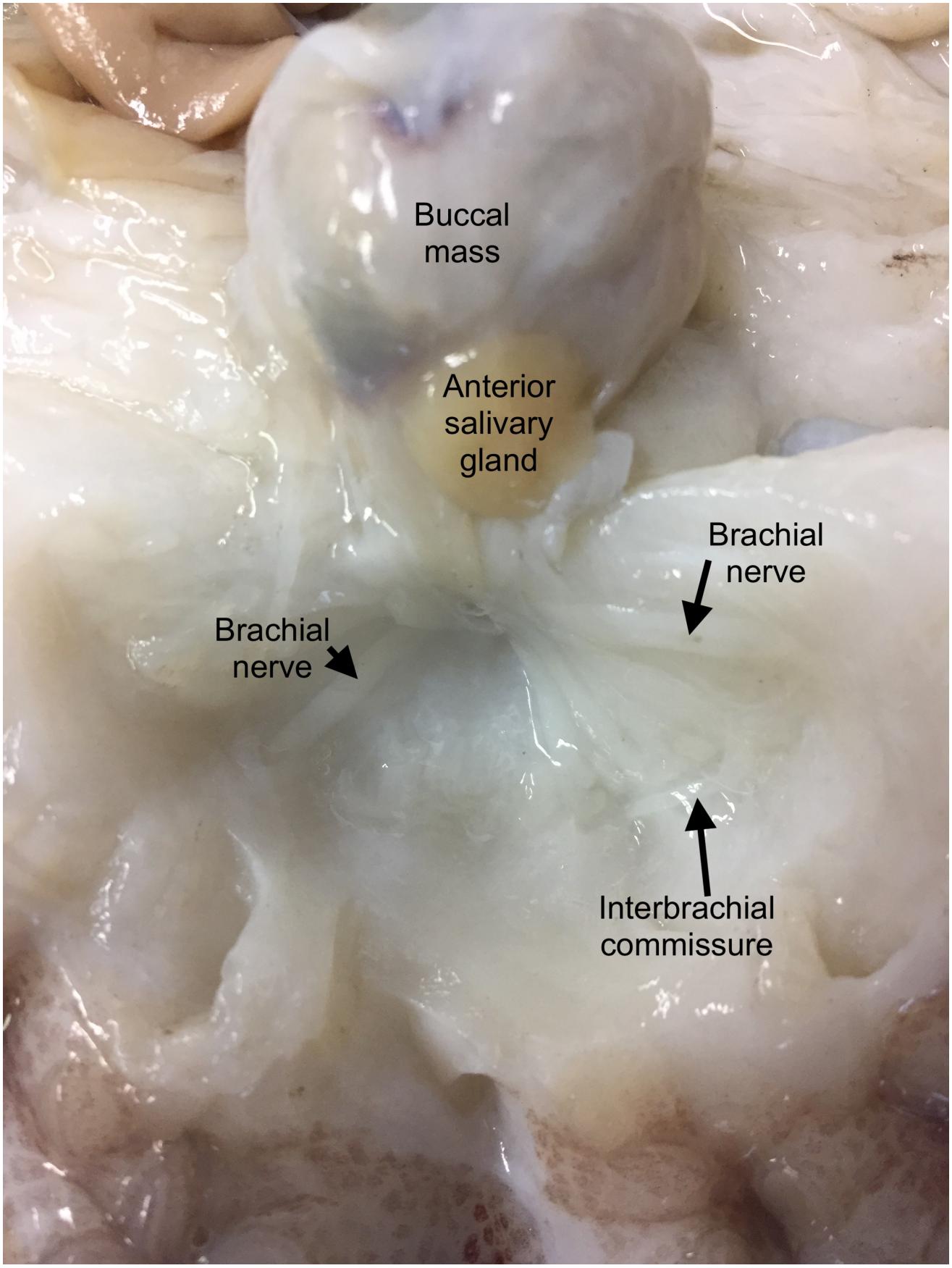

Figure 51.14: *Octopus vulgaris* brachial nerves and interbrachial commissure

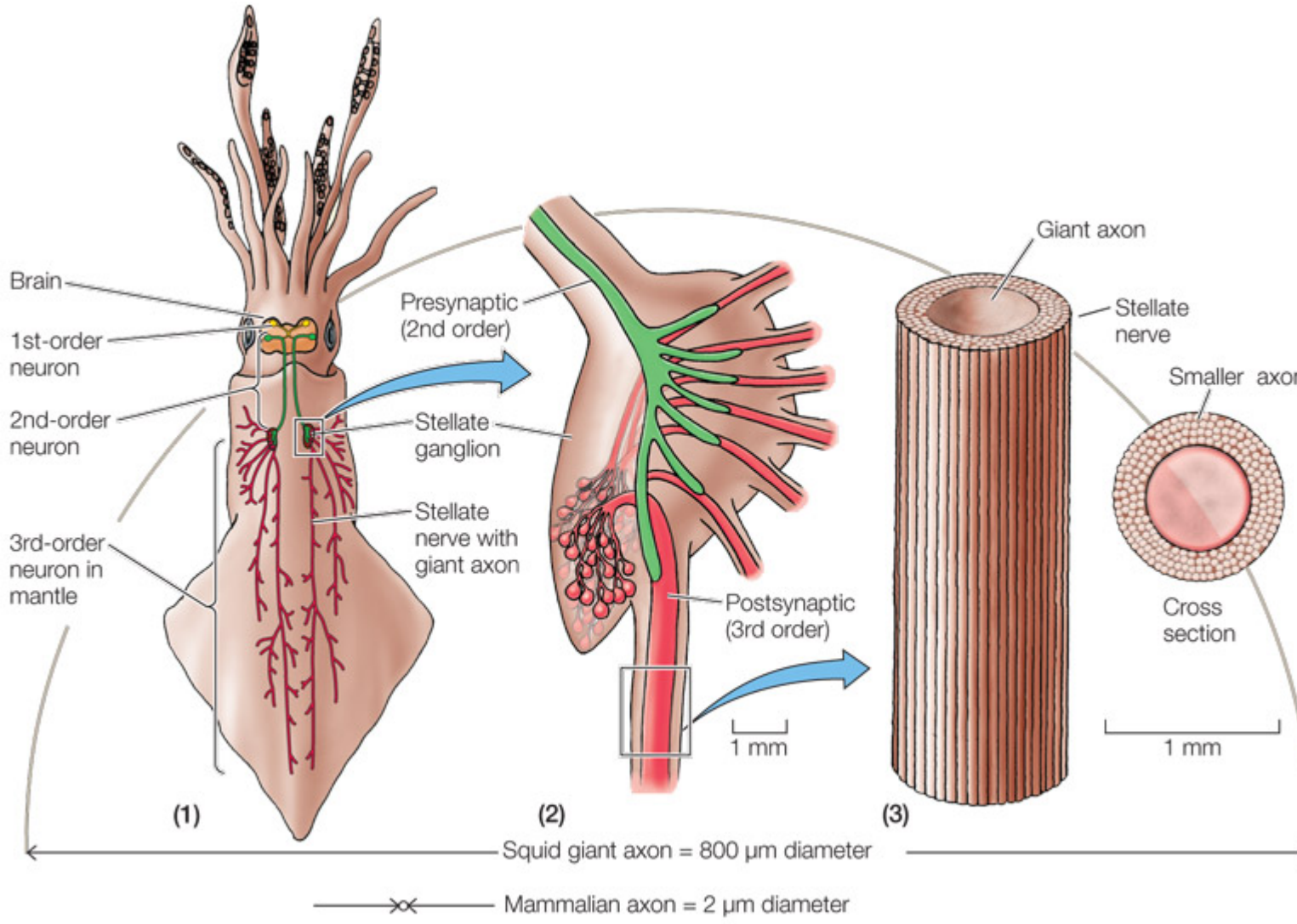

Figure 51.15: Stellate ganglion anatomy.

51.5.3.6 Inferior buccal ganglion

The inferior buccal ganglion controls the buccal mass (Budelmann, 1995).

51.5.3.7 Pallial nerve

A pair of pallial nerves run from the posterior supra-esophageal mass to the stellate ganglia (Imperadore et al., 2019).

51.5.3.8 Stellate ganglia

The stellate ganglion is connected to the brain by the pallial nerve (Gonzalez-Bellido et al. 2014). These ganglia are lower motor centers for the mantle muscle (Budelmann, 1995). In *Octopus,* each of the stellate ganglia are composed of roughly 100,000 neurons. Within the ganglion is "the giant synapse", which is where the second-order neuron from the palliovisceral lobe makes ~15,000 synaptic connections to the 12-13 third-order axons (the largest of which is the stellate nerve), which in turn emerge from each stellate ganglion to innervate the mantle muscle (Wang and Ragsdale, 2019). These nerves are graded to control AP velocity such that the short ones are narrower and the longer ones are wider (Wang and Ragsdale, 2019). "The giant axon" is the longest and thus widest.

According to Josh, the stellate ganglion has mostly neural bodies on the surface and the middle is composed of neuropil.

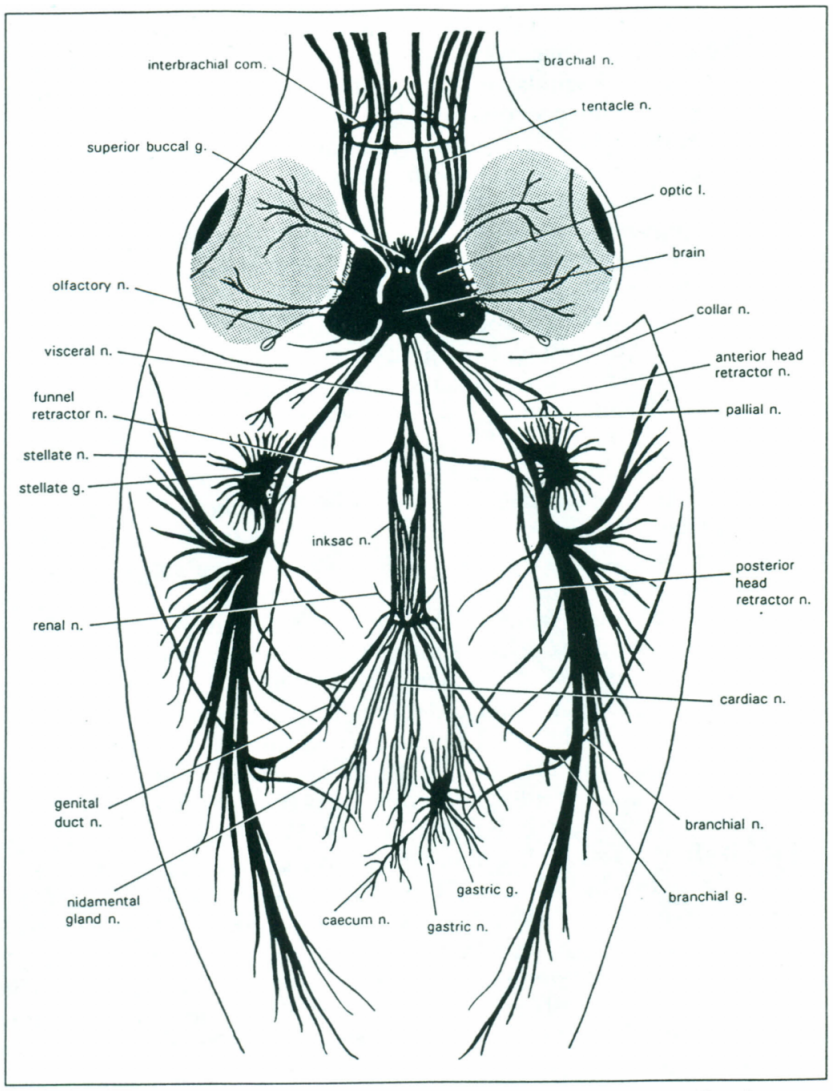

Figure 1. The central and peripheral nervous system of the cuttlefish *Sepia officinalis*. com., commissure; g., ganglion; l., lobe; n., nerve. (Modified from Hillig, 1912.)

Figure 51.16: Peripheral nervous system of a cuttlefish.

51.5.3.9 Subradula ganglion

The subradula ganglion controls the radula (Budelmann, 1995).

51.5.3.10 Visceral nerves

The visceral nerves connect the brain with the cardiac and branchial ganglia and straight to the systemic heart (Wells and Wells, 1995; Wells, 1983). They also connect the brain to the neurosecretory vena cava. The visceral nerves seem to be the means of behaviorally-induced cardiac alterations (e.g. exercise, cardiac arrest when startled in *Octopus*) (Wells, 1980).

51.5.4 Microanatomy and neurophysiology

Nervous systems are composed of two types of cells: neurons and glia. Neurons create synapses while glia support neurons through regulating neuronal communication, osmoregulation, neurogenesis, neuroregeneration, blood-brain barrier formation, and neuroprotection (Ortega and Olivares-Bañuelos, 2020).

Cephalopod neurons are unmyelinated as in all invertebrates (Budelmann, 1995). Most neurons in the CNS and peripheral ganglia are unipolar, possessing no dendrites (Budelmann, 1995). The neurons in the lobes and ganglia are arranged such that the somas (perikarya) form an outer perikaryal layer and all their axons extend inwards to form an inner neuropil mass

Table 51.10: Neurotransmitters and their corresponding receptors in cephalopods

Neurotransmitter	Effect	Receptor
L-glutamate	Excitatory	AMPA receptors, kainate receptors, NMDA receptors
Serotonin (5-HT)	Excitatory	5-HT receptors, serotonin receptors
Octopamine	Excitatory	
Noradrenaline (norepinephrine)	Excitatory	
Dopamine	Excitatory	
Acetylcholine	Either	
GABA	Inhibitory	

(Budelmann, 1995). The perikaryal layer is even further arranged such that the largest soma are on the outside and the smallest soma are on the inside of the perikaryal layer, adjacent to the neuropil (Budelmann, 1995). The neuropil composition varies by lobe/ganglion. Lower motor centers have rather tangled convoluted neuropils while the sensory and memory centers are more orderly (Budelmann, 1995).

Glial cells in the CNS provide a blood-brain barrier (Budelmann, 1995).

Based on hexokinase and triosephosphate isomerase activities, brain tissue utilizes glycolysis far more than muscle (Abbott and Miyan, 1995; Ballantyne et al., 1981).

51.5.5 Neurotransmitters and receptors

51.5.6 Cerebrovascular morphology

See subsubsection 51.2.1.1.

51.5.7 Giant axon escape jetting

The giant fiber system is only in decapodiforms (Budelmann, 1995). The first order giant axons somas are in the magnocellular lobes (one on each side of the brain) where they are triggered by either visual input or the statocysts detecting water movement. They cross to the opposite side of the brain (connecting in the middle to synchronize responses) and synapse with seven pairs of second-order giant neurons in the palliovisceral lobes. Six of the second-order neurons are motorneurons and their axons terminate at the head retractor muscles but one large axon (in squids) leaves the brain through the pallial nerves to connect with the stellate ganglia (Williamson and Chrachri, 2004). At the stellate ganglia the second-order axons synapse with the third-order axons which innervate mantle circular muscle to trigger rapid contraction (Nixon and Young, 2003). The third-order giant neurons are actually ˜100 soma with a huge fused axon reaching up to 1.5 mm in diameter (Williamson and Chrachri, 2004). The third-order giant axons radiate from the stellate ganglia to innervate various regions of the mantle. The longer axons are also larger in diameter such that contractions all along the mantle are synchronized. Cuttlefish giant axons are 200 μm in diameter and conduct APs at 7 m/s while squid giant axons are 700-1000 μm and can conduct APs at 20-30 m/s (Budelmann, 1994).

Decapodiforms also have giant axons that are synaptically linked to the first order axons that run anteriorly to coordinate the arms during jetting behavior (Nixon and Young, 2003).

51.5.8 Chromatophore neurobiology

The chromatophores on the skin of cephalopods are controlled directly by the brain. The processing of visual information and translation to appropriate chromatophore pattern is conducted in the brain in a hierarchical flow. First, visual information is acquired at the eyes and sent to the optic lobes. From the optic lobes, information travels to the lateral basal lobes where it is suspected that the choosing of chromatophore pattern takes place. This information is then sent to the anterior (ACLs) and posterior chromatophore lobes (PCLs). Generally, the ACLs innervate the chromatophores on the arms and head while the PCLs innervate the chromatophores of the mantle. Axons are sent from these chromatophore lobes to the chromatophores across the skin (Williamson and Chrachri, 2004). Interestingly, there does not seem to be any neural feedback from the chromatophores back to the brain.

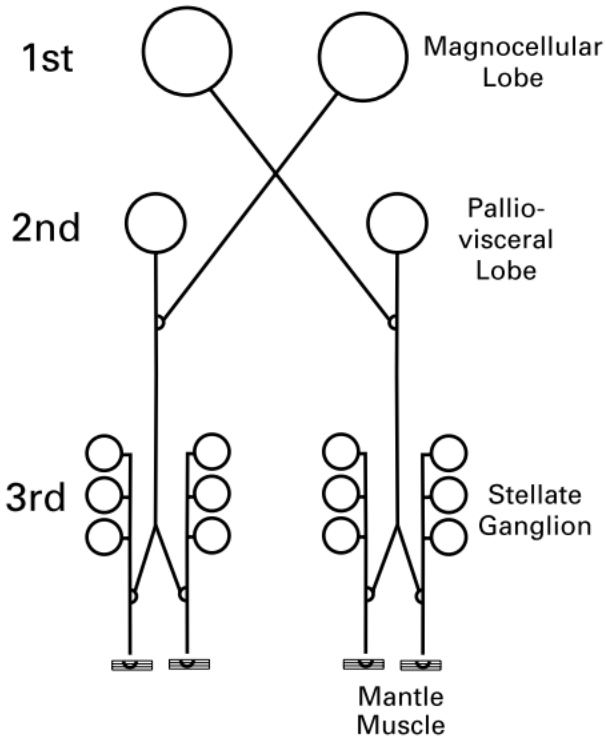

Figure 51.17: Decapodiform giant axon system neuroanatomy.

51.6 Endocrine system

The endocrine system produces hormones in glands that are released into the blood to reach distal target organs. The identities of those target organs are demonstrated by responses to the hormone and presence of hormone-specific receptors. A series of glands with downstream effects on each other are known as an axis. In addition to dedicated endocrine glands, many other organs can have secondary endocrine functions.

The endocrine system also produces cytokines. These differ from hormones in that they are not produced by discrete glands.

51.6.1 Glands

51.6.1.1 Anterior vena cava

The anterior vena cava is a part of the venous system, but also an important part of the endocrine system (Martin and Voigt, 1987), functioning as the equivalent of the vertebrate pituitary gland. There is a large mass of neurons (neuropil) in the vena cava that secretes peptide hormones into the blood (Minakata, 2006). They are connected to the brain by the visceral nerve.

51.6.1.2 Branchial glands

Each branchial gland runs the length of each gill (Eno, 1994) and is the site of hemocyanin production (Dilly and Messenger, 1972; Messenger et al., 1974; Muzii, 1981). Histologically, the glands are filled with rough ER and vacuoles, producing hemocyanin molecules (Messenger et al., 1974; Muzii, 1981).

51.6.1.3 Optic glands

Optic glands are heavily-vascularized, orange structures on the dorsal side of the optic tracts of *Octopus* (Minakata, 2006). They seem to produce a hormone that facilitates gonad growth (Minakata, 2006). Growth of the optic glands are inhibited by input from the subpedunculate lobe in the brain (Minakata, 2006). When this inhibitory signal stops, the optic glands grow, and the gonads grow as well (Minakata, 2006).

The optic gland has been described as the equivalent of the vertebrate pituitary gland.

The optic glands trigger female senescence and death through a variety of pathways including upregulation of certain steroids and insulin-like growth factor binding proteins (IGFBPs) and downregulation of catecholamines (Wang and Ragsdale, 2018; Wang et al., 2022).

51.6.2 Hormones

Hormones are molecules secreted by one organ and transported through the circulatory system to reach a distant organ.

There are three kinds of hormones: amines, peptides, and steroids.

Most hormones are in the nanomolar concentration range in animal blood and typically vary in concentration less than one order of magnitude.

Tropic hormones act upon other glands to influence the release of other hormones.

51.6.2.1 Amines

Catecholamines and relatives Catecholamines are organic compounds composed of a benzene ring with two hydroxyls and a side chain containing an amine. The various kinds of catecholamines (e.g. epinephrine, norepinephrine, dopamine) differ only in the other parts of the side chain. Octopamine, although not technically a catecholamine, is the protostome functional equivalent of the vertebrate norepinephrine.

Catecholamines trigger the "fight-or-flight" response in all animals including molluscs (Lacoste et al., 2001).

51.6.2.2 Peptides

Cephalotocin and octopressin Cephalotocin and octopressin are peptide hormones in the oxytocin/vasopressin superfamily that are released by the vena cava into the blood (Minakata, 2006). Cephalopods are the only known invertebrate to have two-members of this superfamily, as in vertebrates (Minakata, 2006). Based on the locations of cephalotocin receptors in the gills, vans deferens, and testis, cephalotocin likely is involved in ammonia excretion and regulating steroid hormone production (Minakata, 2006). Both of these roles are known to be played by other oxytocin/vasopressin superfamily members in vertebrates (Minakata, 2006). Octopressin is known to stimulate contractions in oviduct, vascular, and rectal smooth muscle in *Octopus* (Minakata, 2006).

FMRFamide and FaRPs FMRFamide (Phe-Met-Arg-Phe) is a neuropeptide and peptide hormone. FaRPs (FMRFamide-related peptides) are similar peptides which also have an RFamide on their C-terminus. Both FMRFamide and other FaRPs are released into the blood by the anterior vena cava. FMRFamide is a cardioexcitatory hormone in a number of invertebrate phyla.

51.6.2.3 Steroids

Cholesterol Cholesterol biosynthesis has two canonical pathways and both are known to occur in cephalopods (Wang et al., 2022). It has important roles in membrane composition subsection 30.1.2.

Cortisol Cortisol is a stress-induced steroid hormone. It upregulates heat shock protein and ubiquitin transcription (Kassahn et al., 2009) thus having a wide-reaching cellular protection effect. At least in vertebrates, cortisol stimulates gluconeogenesis in the liver and suppresses systemic growth, reproduction, and immune system function (Kassahn et al., 2009). Again in vertebrates at least, cortisol levels are regulated by a number of upstream tropic hormones, as well as neuronal and immune inputs (Kassahn et al., 2009).

51.6.3 Growth factors and cytokines

Based on the response of octopus neurons to fetal bovine serum, it seems that growth factor receptors are highly conserved between cephalopods and mammals (Maselli et al., 2018).

51.7 Reproductive system

All coleoid cephalopods are semelparous: they have only one cycle of development, maturation, and spawning.

Germline cells in animals can be identified by *vasa* gene expression.

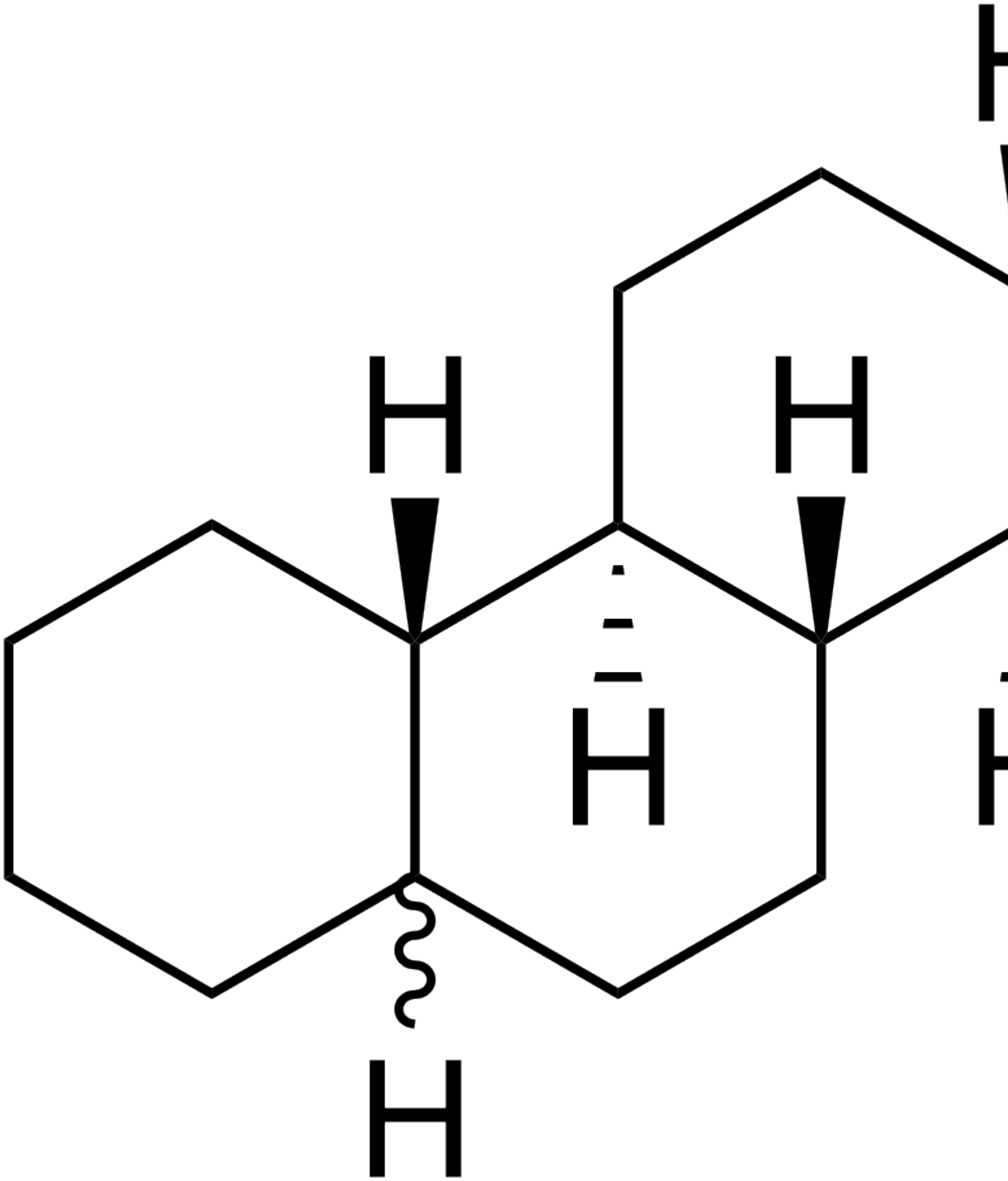

Figure 51.18: The core of all steroids.

51.7.1 Males

Male sperm in all cephalopods pass through the following route: testis, spermatophoric organ or gland, Needham's/spermatophoric sac, terminal organ (penis) (Arkhipkin, 1992). In many cephalopods (especially shallow water species (Arkhipkin and Laptikhovsky, 2010)), sperm are passed to the hectocotylus (Marian, 2015). At least in loliginids (not sure about other cephalopods) the vans deferens connects the testis to the spermatophoric organ.

At least in loliginids, the entire male anatomy except the testis is on the left side. In species of *Stigmatoteuthis* (Histioteuthidae), males have two spermatophoric organs, Needham's sacs, and penes.

Vans deferens long skinny, opaque white structure with many "switchbacks"

Spermatophoric organ/gland round spiral, translucent structure

Needham′s/spermatophic sac large translucent structure full of spermatophores

51.7.1.1 Hectocotylus

Incirrates have either LIII or RIII hectocotylized, however, cirrates do not have a hectocotylus. Most decapodiforms have an arm IV hectocotylized. Species without hectocotyli typically have longer terminal organs (penes) than species with hectocotyli (Arkhipkin and Laptikhovsky, 2010). In fact, in at least some deep species (e.g. *Onykia ingens*), the penis can become erect, lengthen to greater than total body length, and attach spermatophores directly onto the female's body (Arkhipkin and Laptikhovsky, 2010).

The "hectocotylus" name derives from *Hectocotyle octopodis,* the name of a "parasitic worm" found within female argonauts before it was realized that this was a disembodied male arm.

51.7.1.2 Spermatophores

Coleoid spermatophores are some of the most complex sperm transfer structures in the animal kingdom(Marian, 2015). Briefly and generally (Marian, 2015):

1. Spermatophores are taken from the terminal organ by the hectocotylus.
2. The male places the spermatophore on the female body.
3. The elastic tunic, osmotic pressure, ejaculatory apparatus, and spiral filament propel the spermatangium into the female (perforating (in decapodiforms) and penetrating).
4. The cement body ensures attachment.
5. The sperm mass travels from the spermatophore into the forming spermatangium.
6. The empty spermatophore case detaches.

Aspects of spermatophore size, morphology, and physiology are different between consort and sneaker males (subsubsection 59.3.1.1).

51.7.2 Females

Female eggs in all cephalopods pass through the following route: ovary, oviducts, oviductal glands, and egg mass. In decapodiforms, they pass by nidamental glands as well between the oviductal glands and egg mass. Cuttlefishes, myopsid squids, and sepiolids also have accessory nidamental glands (mottled red when mature due to bacterial populations). In octopods, the oviductal gland is in the middle of the oviduct such that the oviduct spans both "upstream" and "downstream" of the oviductal gland. In octopuses and cuttlefishes, mature eggs are stored in the ovary until spawning, while in teuthids, mature eggs are stored in the oviducts until spawning (Arkhipkin, 1992).

Generally, larger females produce larger eggs among conspecifics and cold-water species produce larger eggs than warm-water species (Laptikhovsky's 2018 CIAC talk).

Males implant spermatangia into females at taxon-specific locations. Most female octopods have spermathecae (seminal storage structures) in their oviductal glands. Thus male octopods implant their spermatophores directly into the oviducts. In contrast, sepiids, loliginids, and some oegopsids have seminal storage structures in the buccal membrane. Loliginids, idiosepiids, and bathyteuthids have a single seminal receptacle while sepiadariids and sepiids have a pair of receptacles. Ommastrephids can vary widely in the number of receptacles, up to 30! (Sato's 2018 CIAC talk). Other oegopsids merely implant the spermatangia on the mantle, arms, or head (Marian, 2015).

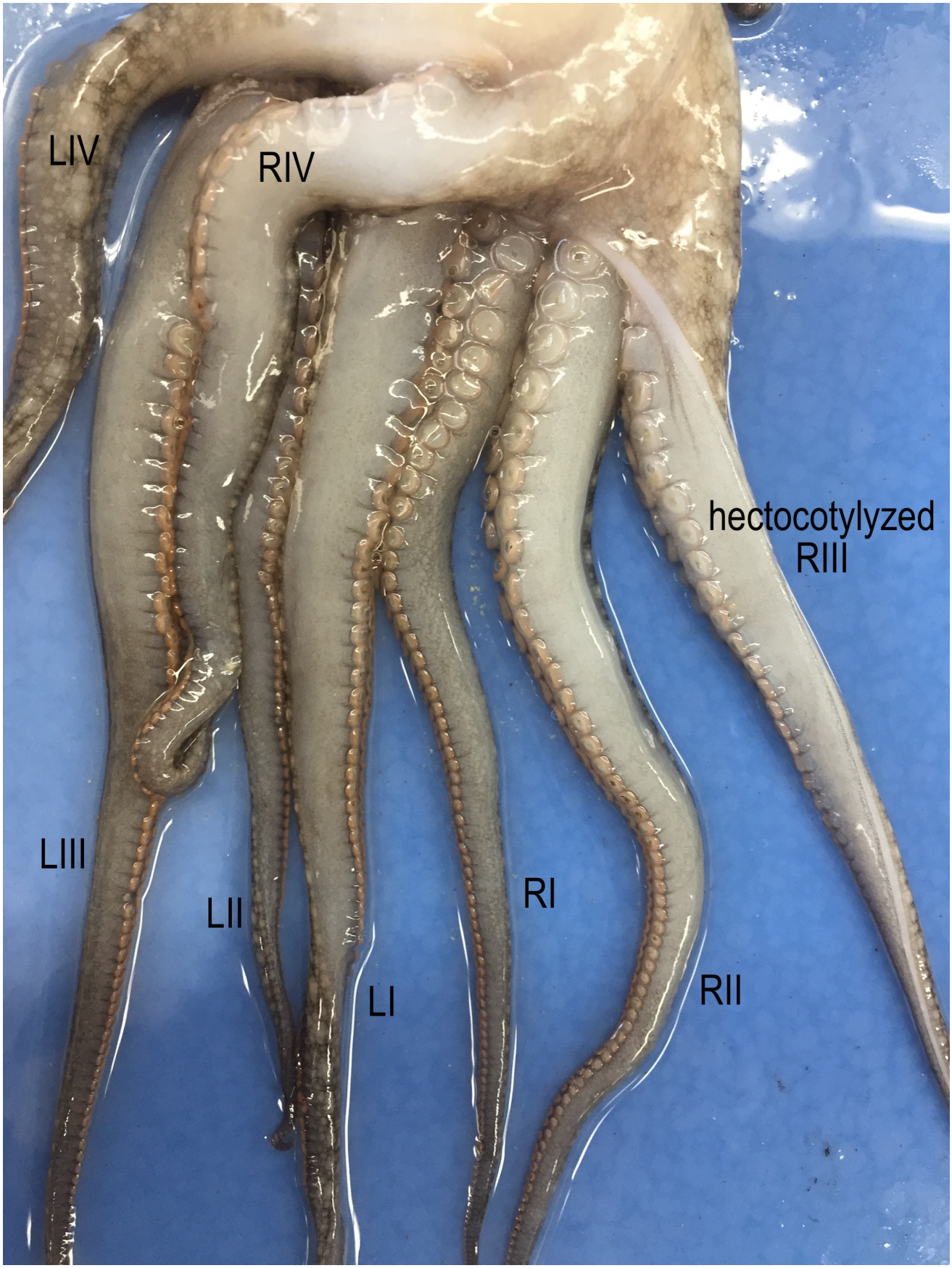

Figure 51.19: *Octopus bimaculoides* hectocotylus (RIII). A pale white tract runs the length of the arm and the arm tip is white and transparent unlike the pigmented arm tips of the other arms.

51.7.2.1 Oviducts

Cuttlefishes, myopsids, and cirrates only have a single left oviduct, rather than a pair as in most oegopsids and incirrates (Nixon and Young, 2003).

51.7.2.2 Accessory nidamental gland

Accessory nidamental glands (ANGs) are present in sepiids, myopsids, idiosepiids, spirulids, and sepiolids. They are formed of many tubules.

The ANG is rich in symbiotic bacteria ($\approx 6 \times 10^{10}$ bacteria / ANG) that are deposited into the jelly coating of eggs for anti-fungal function (Belcaid et al., 2019; Kerwin et al., 2019). Although a diversity of bacteria exist, *Roseobacter* is most common in the *E. scolopes* ANG (Collins et al., 2015). More broadly, all species with ANGs (for which we have data) have alphaproteobacteria, gammaproteobacteria, and flavobacteria in their ANGs (Vijayan's 2022 CIAC talk). In fact, the ANG seems so tied to the bacterial symbionts that a female animal raised in a sterile environment does not even develop an ANG.

51.8 Immune system

Cephalopod immune systems are not adaptive at least in the classical sense of antibody production (Castellanos-Martínez and Gestal, 2013) but they do have a variety of innate defenses (Castillo et al., 2015). Innate immune functions can recognize "non-self" and "missing-self". Most immune cells are either in the skin or circulating through the blood. A common immune response to a pathogen is the production of reactive oxygen species (ROS) which not only damage the pathogen, but facilitates further immune response (Castillo et al., 2015).

51.8.1 Cellular defenses

Hemocytes are the cephalopod equivalent of vertebrates' phagocytes (Castillo et al., 2015). They are nucleated cells that circulate in the blood that will phagocytose foreign particles such as bacteria (Heming et al., 1990). They identify bacteria based on the properties of its surface (McAnulty's 2018 CIAC talk). They can also break down old cells for normal cytolytic reactions (Castillo et al., 2015). When a wound is inflicted, hemocytes can aggregate and multiply around the wound which both plugs and begins to heal the wound (Castillo et al., 2015).

Hemocytes are synthesized by tissue around the optics nerves known as white bodies (Johnson 1987; (Castillo et al., 2015)).

51.8.2 Humoral defenses

Humoral defenses are immune functions performed by molecules and enzymes circulating in the blood. Molecules bind to foreign particles thus tagging the particles for digestion by hemocytes. Proteases circulate in the blood as well, digesting foreign proteins. In addition, protease inhibitors block the proteases of invading biota.

Interleukins are signaling proteins that play key roles in an immune response. Cephalopods have a much greater diversity of interleukin-17-like genes than other bilaterians and these are most strongly expressed in tissues that are in contact with the external environment (Albertin et al., 2015).

ADARs can defend a cell against viral RNAs by editing double-stranded viral RNA genome to disrupt their proteins and decrease virulence (Deffit and Hundley, 2016).

Hemocyanin plays some role in the immune system (Castillo et al., 2015). Portions of their subunits been documented to have anti-viral properties via their glycans (Dolashka et al., 2020).

51.8.3 Inflammation response

Cephalopods have an inflammatory response. In mammals it is as follows:

1. Damaged cells release cellular stress signals (i.e. chemokines)
2. Nearby mast cells in the connective tissue respond by releasing histamine
3. Histamine reaches vascular endothelial cells which vasodilate arterioles and vasoconstrict venules, thus increasing localized blood flow and capillary pressure (thus the redness and heat)
4. The pressurized capillaries leak platelets and white blood cells (WBCs) to the site of injury which supports pathogen destruction, wound healing, and stops damaged blood vessels

51.8.4 The Complement System

Invertebrates use the Alternative and Lectin pathways to produce C3(?).

51.9 Integrative physiology

51.9.1 Respiratory quotients

$$\mathrm{RQ} = \frac{\mathrm{CO_{2released}}}{\mathrm{O_{2consumed}}}$$

An organism's respiratory quotient varies based on its diet. An RQ of 1 is typical of carbohydrate consumption, while protein consumption leads to an RQ value from 0.8 to 0.9 and lipid consumption resulting in RQ $\approx$ 0.7.

Excretory atomic O:N ratios also indicate metabolic substrate with ratios from 4 to 12 indicative of protein catabolism and higher ratios up to even 140 indicative of carbohydrates and lipids. *Illex illecebrosus* and *Octopus vulgaris* have both been examined to have O:N near 15 indicative of a primarily protein composed diet (Hoeger et al., 1987).

51.9.2 Scaling with body size

51.9.2.1 Aerobic metabolism

Aerobic metabolism ($\mathrm{M_{O_2}}$) scales remarkably similarly with body size in a great diversity of taxa. Specifically, Kleiber's law states that:

$$\mathrm{M_{O_{2_{whole\,animal}}}} = \mathrm{aM^{b=0.75}}$$

$$\mathrm{M_{O_{2_{mass-specific}}}} = \mathrm{aM^{b=-0.25}}$$

There are a diversity of arguments and evidence to explain these allometric changes:

- Larger animals can save energy by having a smaller SA:V and thus less expensive temperature or osmotic regulation (Childress and Somero, 1990).
- Cell and organelle membranes of larger animals are more highly saturated (i.e. less polyunsaturated phospholipids) and therefore better "packed". As a result, they have less proton (and other ion) leakage. Specifically, $\mathrm{H^+}$ leakage across the mitochondrial inner membrane scales with body size across mammals (Porter and Brand, 1993). This decreases expensive ion-exchange costs and, importantly, increases the P/O ratio of the mitochondria. More ATP per $\mathrm{O_2}$ molecule results in less $\mathrm{O_2}$ needed and therefore lower mass-specific $\mathrm{M_{O_2}}$ (Hochachka and Somero, 2002).

A variety of hypotheses have been set forth claiming that aerobic metabolic rates of all organisms are essentially the same once mass, temperature, and other factors are accounted for. Cephalopods are a dramatic demonstration of the error of this idea because they possess a 200-fold range in $\mathrm{M_{O_2}}$ even after adjusting for mass and temperature (Seibel, 2007). Differences in selection for locomotory ability nullify any universal $\mathrm{M_{O_2}}$ (Seibel and Drazen, 2007).

Active squids break the "-0.25 rule" for mass-specific $\mathrm{M_{O_2}}$ scaling. They possess scaling coefficients closer to -0.07-0.09 (Seibel, 2007; Seibel et al., 2014), or even 0 in *Gonatus onyx* (Rosa et al., 2009) though some fall right in line (b = -0.24, *Lolliguncula brevis*, (Bartol et al., 2001)). Seibel (2007) proposes that this is due to the unique shape of squids (hollow tubes) and their presumed cutaneous respiration. As these squids grow, their body surface area-to-volume ratio stays constant rather than decreases with increasing size (O'Dor and Hoar, 2000). Additionally, these squids are believed to utilize cutaneous respiration which greatly increases respiratory exchange surface compared to most other animals. For more information on cutaneous respiration, see subsection 50.9.8. Deep sea squids as wells as octopods follow the "-0.25 rule" rather closely (Seibel, 2007).

Cephalopods are likely similar to fishes in that individual variation in SMR can vary 2-3 fold with increased variation under stress (Tommy Norin's SEB talk).

Oxygen demand drives supply rather than the other way around (Weibel and Hoppeler, 2005).

Maximum metabolic rate (MMR) In teleosts (and likely cephalopods too) it has been demonstrated that MMR has a larger scaling coefficient than the resting metabolic rate described above. MMR in teleosts is typically larger in the 0.8-1.0 range (Norin and Clark, 2016). This is likely because as fishes or cephalopods grow, their muscle mass grows allometrically compared to their other organs and thus a larger proportion of their mass is muscle.

51.9.2.2 Anaerobic metabolism

As an individual grows, it becomes more easily detectable from a distance. Additionally, its predators become bigger and thus faster. In order to continue to avoid predation as an individual increases in size, escape acceleration (anaerobically fueled) must increase as well. Prey-capture acceleration must increase too as its prey become bigger and faster. This is one idea put forth by Childress and Somero (1990) as to why anaerobic potential (i.e. ODH activity) increases with body size, all else being similar.

Of course, this relationship can change if other factors change. For example, taxa such as *Gonatus onyx* or *Chiroteuthis calyx* that undergo ontogenetic vertical migration have decreased predatory pressure in dark depths that dominate the change of predation pressure and thus leads to decreased anaerobic capacity with ontogeny (Seibel et al., 2000b; Hunt and Seibel, 2000; Rosa et al., 2009).

51.9.3 Metabolic rate

Cephalopod metabolic rate varies broadly based on species, size, temperature, and O_2. The lowest M_{O_2} ever recorded to date was for a 1050 g *Vampyroteuthis infernalis* at 5 ºC which consumed 0.02 μmol O_2 $g^{-1}h^{-1}$ (Seibel et al., 1997). In total, RMR ranges from 0.025 μmol O_2 $g^{-1}h^{-1}$ in *Vampyroteuthis infernalis* to 15.26 μmol O_2 $g^{-1}h^{-1}$ in *Loligo forbesii* (adjusted to 5 ºC) (Seibel, 2007). Once adjusted for mass and temperature, active squids have a higher mass-specific M_{O_2} (msM_{O_2}) than some mammals and many fishes (Seibel, 2007)! As an example, a very active squid species, *Dosidicus gigas,* has a inactive msMR higher than many sharks and tunas once adjusted for size and temperature (Rosa and Seibel, 2008). For perspective, a human size and temperature *Dosidicus gigas* would require over 4000 Calories per day while a *Vampyroteuthis* would require a mere 20 Calories per day! See Table 34.3 for O_2-energy conversion rates.

Octopuses and squids can be generally categorized into four groups based on their metabolic rates (which are a function of their environments) (Rosa et al., 2009). From highest to lowest msM_{O_2}, these groups are 1. neritic and oceanic muscular squids, 2. neritic/demersal benthic octopods, 3. oceanic ammoniacal squids, and 4. deep-sea gelatinous octopods.

$$\frac{\mathrm{MMR}}{\mathrm{SMR}} = \frac{\mathrm{P_{crit_{max}}}}{\mathrm{P_{crit}}}$$

51.9.4 Energy budget

A balanced energy equation for any animal is:

$$\mathrm{C} = \mathrm{R_{m+d+a+s+g}} + \mathrm{S} + \mathrm{G} + \mathrm{F} + \mathrm{U}$$

Generally, 1 μmol O_2 generates 0.5 J of energy (Elliott and Davison, 1975) (but see Table 34.3 for details) and 1 J $\cdot$ sec^{-1} = 1 watt (Wells and Clarke, 1996).

51.9.4.1 C (energy ingested)

51.9.4.2 R (energy used in "respiration")

R_m **(energy used for maintenance (e.g. protein/DNA/membrane turnover, osmosis, circulation, muscle tonus, nervous function))** This would be a true standard metabolic rate (SMR).

The ventilatory cost of *Sepia officinalis* can range from a negligible ~1% at low temperature up to almost 10% of total metabolic energy budget at extremely warm temperatures (Melzner et al., 2006b).

R_d **(energy used for consuming, digesting, and absorption)** This is only considering the costs of catabolism. Anabolic costs are accounted for in R_s and R_g. Since SDA is R_{d+s+g}, much of the cost of SDA is accounted for here. In octopus consuming a crab, $R_{d+s+g} = 0.04 \times C$ (Wells and Clarke, 1996).

R_a **(energy used for activity/locomotion)**

R_s **(energy used to produce somatic tissue)** Typically 20-30% of the energy stored in the tissue (S) was spent through inefficiencies in forming the tissue.

R_g **(energy used to produce reproductive tissue)** Typically 20-30% of the energy stored in the tissue (G) was spent through inefficiencies in forming the tissue.

51.9.4.3 S (energy invested into somatic tissue)

Somatic tissue typically contains 3-4 $kJ \cdot g^{-1}$ wet mass of energy stored within its molecules (Wells and Clarke, 1996) at least in shallow-water muscular cephalopods.

51.9.4.4 G (energy invested into reproductive tissue)

Reproductive tissue typically contains a higher energy density than somatic tissue. In one study from a single female *Octopus cyanea*, her eggs were ≈ 12 $kJ \cdot g^{-1}$ wet mass. In a large-egged octopus, I am not sure how different the energy density would be of the eggs.

51.9.4.5 F (energy excreted in feces, egestion)

Cephalopod feces contains about 7-8 $kJ \cdot g^{-1}$ (Wells and Clarke, 1996). At least in one study, *Octopus* produce 0.2% of their body weight in feces per day. Octopuses also shed their suckers which is loss of somatic tissue.

51.9.4.6 U (energy excreted in urine, excretion)

Octopus are known to excrete 10-15% of their body mass in urine per day. This results in 1-3 $J \cdot g^{-1} \cdot day^{-1}$ lost through urine. Much of this is protein.

51.9.4.7 Conversion efficiency

The gross conversion efficiency is $\frac{S+G}{C}$, or the amount of energy added to the animal's body per energy consumed in prey tissue. This is an important metric for both aquaculture efficiency and biogeochemical models. Conversion efficiency will decrease as respiratory and excretory factors increase. Broadly, gross conversion efficiency is 40-50% in octopuses and sepioids and 15-30% in squids (likely because of their higher R_a) (Wells and Clarke, 1996).

The net conversion efficiency is $\frac{S+G}{C-R}$, or the amount of energy added to the animal's body per energy available from food after basal needs.

Chapter 52

Sensory morphology and physiology

While the sensory systems are part of the nervous system, they are separated in their own chapter due to the fact that they have been studied extensively and therefore merit their own discussion. Cephalopods have an unusual number of neurons that originate in the brain and send signals back to the sense organs (Budelmann, 1995). Most of these neurons are inhibitory (Budelmann, 1995). Sensory neurons have dendrites that are in contact with the environment.

52.1 Vision

Cephalopods can view polarized light (Budelmann, 1994).

Squids and cuttlefishes have been shown to possess the photosensitive molecules rhodopsin and retinochrome in their chromatophores (Kingston et al., 2015).

Cephalopod skin has light-activated chromatophore expansion (LACE).

Octopus arms have reflexive phototaxis, curling the arm away from the light, putatively to keep appendages out of view from predators (Katz et al. 2021, JEB).

Octopuses will bob their heads to judge distance with monocular parallax (Hanlon and Messenger, 1996).

52.1.1 Optics

Two objects can be distinguished from each other only if they are ≥ 1 Airy radius away from each other, where
$\mathrm{r_{airy}} = \frac{0.61\lambda}{\mathrm{NA}}$

λ wavelength of light (nm)

NA numerical aperture: $\mathrm{NA} = \mathrm{n} \times \sin\theta$, where n is the index of refraction and θ is the angle of a right triangle between the focal point and the eye radius.

52.1.2 Eyes

The eyes are large in coleoids relative to body size compared to other animals but they can be especially large in some deep sea squids, where they can reach 1/3rd of the body mass in some species (Sweeney's 2018 CIAC talk).

Coleoid eyes are rich in reflectin proteins which make them very iridescent (MBL Loligo genome seminar).

Squids will contract and dilate their pupils in response to light stimuli (McCormick and Cohen, 2012).

Cuttlefish (at least) can move their eyes independently, like a chameleon (Wardill's 2022 CIAC talk).

52.1.2.1 Morphology

While oegopsids have no cornea covering their eyes, they are able to close their eyes into a T-shaped slit (Young et al., 1998). Other coleoids possess a cornea. Under the cornea, the iris regulates pupil size. The pupil dilates and contracts in response to light (Budelmann, 1994). *O. vulgaris's* pupil starts to change from round to horizontal shortly after beginning the settlement phase (Roura's 2022 CIAC talk). Behind the iris is the lens. Behind the lens, the retina contains receptor cells and efferent neurons (Budelmann, 1994).

The eyes are surrounded by extraocular muscles that control eye movement. There are two extraocular muscles in nautiloids, seven in octopodiforms, and 13-14 in decapodiforms. The increase in eye muscle number in decapodiforms allows them to orient

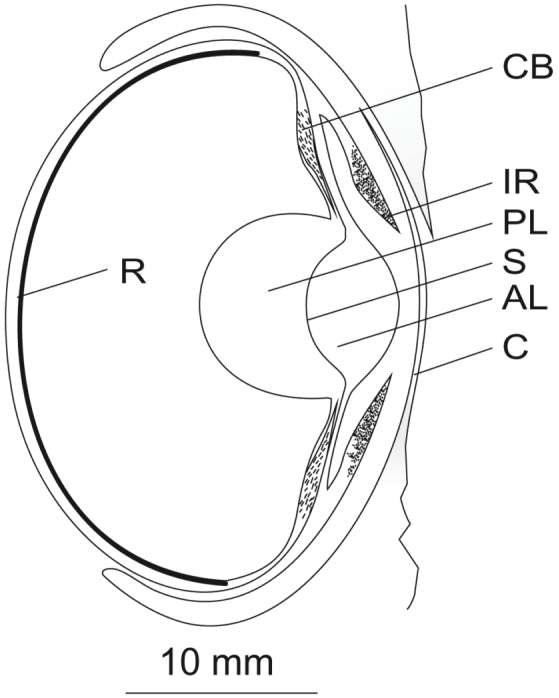

Figure 52.1: *Octopus vulgaris* eye schematic from (Hanke and Kelber, 2020). AL = anterior lens, C = cornea, CB = ciliary body, IR = iris, PL = posterior lens, R = retina, S = septum

their eyes forward and produce binocular vision (Budelmann, 1994). All coleoids possess extraocular muscles that rotate the eye within the head, allowing for counter-rolling (Budelmann, 1994).

Lenses The lens is composed of two hemispherical halves (the anterior and posterior lenses separated by a septum) and layered like an onion and is held in place by ciliary muscles (Budelmann, 1994). Its spherical shape provides a high refraction within a short distance, which is especially beneficial for oegopsids without corneas to refract any light (Sweeney's 2018 CIAC talk). Furthermore, the round shape inverts incoming light just like vertebrate eyes such that the dorsal region of the retina detects light from below while the ventral region of the retina detects light from above. The refractive index of the lens proteins fall along a gradient (low on the periphery, high in the center) so that all the light focuses on a single focal point on the retina (Sweeney's 2018 CIAC talk). The lens proteins in the center evolved first and peripheral proteins evolved from later gene duplication events and adapted to have lower refractivity (Sweeney's 2018 CIAC talk).

Cephalopod lenses (as well as vertebrate ones) are made of crystallin proteins, which increase the lens' refractive index while maintaining its transparency.

Terrestrial and shallow-water animals (cephalopods included) have lenses that absorb ultraviolet light. However, deep-sea cephalopod and fish lenses do not absorb UV light since there is nearly none that reaches depth. Uniquely, the large eye on histioteuthids absorb UV light while the small eye does not (Denton and Warren, 1968).

Retinal receptor cells (photoreceptors) Unlike in vertebrates, the receptor cells face towards the lens and are not specialized into rods and cones (Budelmann, 1994). The photoreceptor cells, like vertebrate rods, have an outer (distal) segment that is photosensitive (contains photopigment(s)) and an inner (proximal) segment that creates the electrical stimulus. Each photoreceptor (green) has two rhabdomeres (red) with one on each side of a pigmented separating line. Four rhabdomeres facing each other from four neighboring photoreceptors form a square rhabdome (blue).The darkly pigmented "screening layer" between the two rhabdomeres of each photoreceptor prevents overstimulation. To improve visual sensitivity the screening layer can be moved towards the inner segment (proximally), and to reduce sensitivity it can be moved further up the outer segment (distally) (Daw and Pearlman 1974).

The receptor cells of shallow-water species that have been examined contain a single pigment: rhodopsin, which has an absorbance peak between 470 and 500 nm (Budelmann, 1994). The only known case (to my knowledge) of an exception to this trait is the enoploteuthid *Watasenia scintillans* which may be able to discriminate multiple wavelengths (Michinomae et al., 1994).

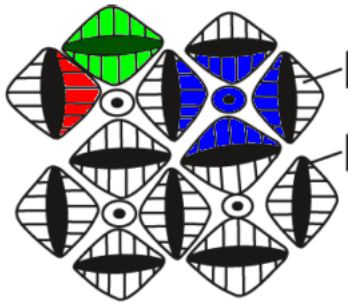

Figure 52.2: Photoreceptor arrangement into rhabdomes. Figure modified from (Hanke and Kelber, 2020). Cross section of the distal (outer segment) retina (view from the incoming light). Each photoreceptor (green) has two rhabdomeres (red) with one on each side of a pigmented separating line. The rhabdomeres are full of the rhodopsin photopigments. Four rhabdomeres facing each other from four neighboring photoreceptors form a square rhabdome (blue).

Receptor cell density is 20k-100k / mm^2 in shallow water coleoids, but can reach 250k / mm^2 in deep sea taxa (Budelmann, 1994). At least in *Octopus* and *Sepia,* higher density exists along a line in the center of the retina, likely functioning as a fovea, or region of extra-high resolution (Budelmann, 1994). In *Octopus*, receptor cells have an angular resolution of 1.3 min (0.022°) (Budelmann, 1994). This leads to a visual acuity of 5-10 min (Budelmann, 1994). The microvilli on the surface of the receptor cells are arranged orthogonally which allows cephalopods to view polarized light (Budelmann, 1994). Polarization vision is useful for detecting transparent prey and also recognizing visual contrast in turbid waters. It may also be useful in navigation.

The total combined length of the outer and inner segments also influences light sensitivity. As such, in deep-sea squids that have been examined, the ventral retina has longer cells than the dorsal retina to improve sensitivity to downwelling light (Matsui et al. 1988).

At least in fishes and mammals, the retina is one of the highest oxygen demanding tissues in the body (cited by (Schmidt et al., 2003; McCormick and Levin, 2017); Waser and Heisler 2005), and as such, has a rather high amount of neuroglobin (˜100-200 μM, compared to ˜2 μM in total brain) (Schmidt et al., 2003).

52.1.3 CNS processing

In rhabdomeric phototransduction, light opens ion channels, which depolarizes the membrane potential and sends the AP stimulus towards the brain (Pinto and Brown, 1977). This is opposite of the ciliary (rod and cone) phototransduction pathway utilized by vertebrates through which light closes ion channels and causes hyperpolarization.

All of the visual information is processed in the optic lobes (subsubsection 51.5.2.1) (Chiao et al., 2015) and also some other lobes in the supra-esophageal mass (Budelmann, 1995). The axons from the retinal receptor cells (photoreceptors) form the optic nerve and terminate at the plexiform layer of the outer cortex of the optic lobes (Nahmad-Rohen and Vorobyev, 2019).

When an octopus senses a stimulus, the chromatophores around the eye reflexively expand briefly (Nahmad-Rohen's 2018 CIAC talk).

52.1.3.1 Psychophysics of camouflage pattern selection

Most knowledge of cephalopod camouflage psychophysics derives from studies on *Sepia officinalis.* In this species, the animal incorporates visual information from both the bottom substrate and vertical features in its environment (to protect from predators above and beside). The disruptive body pattern is shown when light and dark substrate patches are 40-120% the size of the white square light skin component (Barbosa et al., 2007, 2008; Chiao et al., 2009). The darker and more contrasted the substrate overall, the stronger the disruptive pattern (Chiao et al., 2015). Small scale, high contrast substrates elicit mottle patterns (Barbosa et al., 2008).

In addition to the characteristics of the bottom substrate, objects provide important visual information for pattern choice. Discrete light objects on dark backgrounds strongly elicit a disruptive pattern (Chiao and Hanlon, 2001a) though not as much as dark objects (Chubb et al., 2018). To some extent, the light skin components are differentially sensitive to light objects while the dark components are more sensitive to dark objects (Chiao et al., 2015). The contrast within an object determines its influence on the cuttlefish. High contrast objects in the visual field elicit disruptive patterning while low contrast objects are apparently ignored (Chiao et al., 2015).

Effective camouflage involves more than just chromatophore expression. Skin papillae expression also can match the environments texture to aid in crypsis. Papillae expression is also visually, rather than tactilly, determined (Allen et al., 2009). Arm

posturing to match nearby objects (e.g. branches of coral or algae) also aids in crypsis (Barbosa et al., 2012).

52.1.4 Non-ocular vision

In octopuses (at least), rhodopsin kinase (GRK1), a key canonical component of a rhodopsin-based visual system, is expressed not only in the retina but also the skin and suckers (de Zoysa's 2022 CIAC talk).

52.2 Vestibular / audition

52.2.1 Statocysts

Statocysts are sensory organs in the head which are sensitive to acceleration and also likely sound detection (Samson et al., 2016). There are two statocysts in the head, each with a mineral statolith which presses against sensory "hairs", triggering neurons which provide sensory information to the brain. Within the brain, the anterior basal and peduncle lobes of the supra-esophageal masses are important in processing signals (Budelmann, 1995).

Nautiloid statocysts are simple ovals, while octopodiform statocysts are more complex and decapodiform statocysts are most complex (Budelmann, 1994). All coleoid statocysts possess a macula system of gravity detection, but decapodiform statocysts possess 3 mutually perpendicular ones. Here, the statolith rests on top of the macula and pushes on the hairs when accelerating linearly. Additionally, coleoid statocysts can detect angular acceleration with multiple crista/cupula systems (Budelmann, 1994). Here, the gelatinous cupula is flexible and shifts as fluid moves. This shift in the cupula gel against cristae sensors triggers detection of angular acceleration.

There are three mutually perpendicular planes to detect acceleration in any direction.

Most cephalopods seem to be able to hear in the 10-1000 Hz range (Samson et al., 2016). By comparison, fishes also hear in the 1-5000 Hz range and I hear in the 200-15,000 Hz range.

52.2.1.1 Statolith

Statoliths are aragonitic $CaCO_3$ structures (Hu's 2018 CIAC talk).

The statolith grows a ring daily in most decapodiforms examined to date (Loliginidae, Ommastrephidae, Chiroteuthidae, Octopoteuthidae)(Hoving and Robison, 2017), but maybe not the cranchiid *Galiteuthis* sp. (Hoving and Robison, 2017). Octopodiform statoliths do not form discrete rings (Clarke, 1978). The rings are composed of alternating layers of transparent aragonite and opaque organic matrix (Arkhipkin et al., 2018). Rings begin forming either during late embryogenesis or as hatchlings (Arkhipkin et al., 2018).

52.2.2 Neck proprioceptors

Decapodiforms have epidermal hair cells on the dorsal head near the nuchal crest that may be used for sensing head position relative to the body (Budelmann, 1994).

52.3 Mechanoreception

The sucker and brachial ganglia in the arms send mechanosensory information from the suckers through the brachial nerve and into the brain (Budelmann, 1995).

52.3.1 Lateral line

Octopodiforms do not seem to possess a lateral line (Villanueva's 2018 CIAC talk). Squids and cuttlefishes, however, possess rows of polarized epidermal hair cells on their head and arms that are just as sensitive to water movements as the fish lateral line (Budelmann, 1994). These cells are so sensitive they can detect a water velocity of 0.2 mm per second and a 1 m long fish swimming from 30 m away (Budelmann, 1994)!

52.4 Olfaction

Odorants disperse much slower in water than in air, making olfactory tracking much easier in water than air.

Cephalopods are thought to utilize trace amine-associated receptors (TAARs), a kind of GPCR, for olfaction.

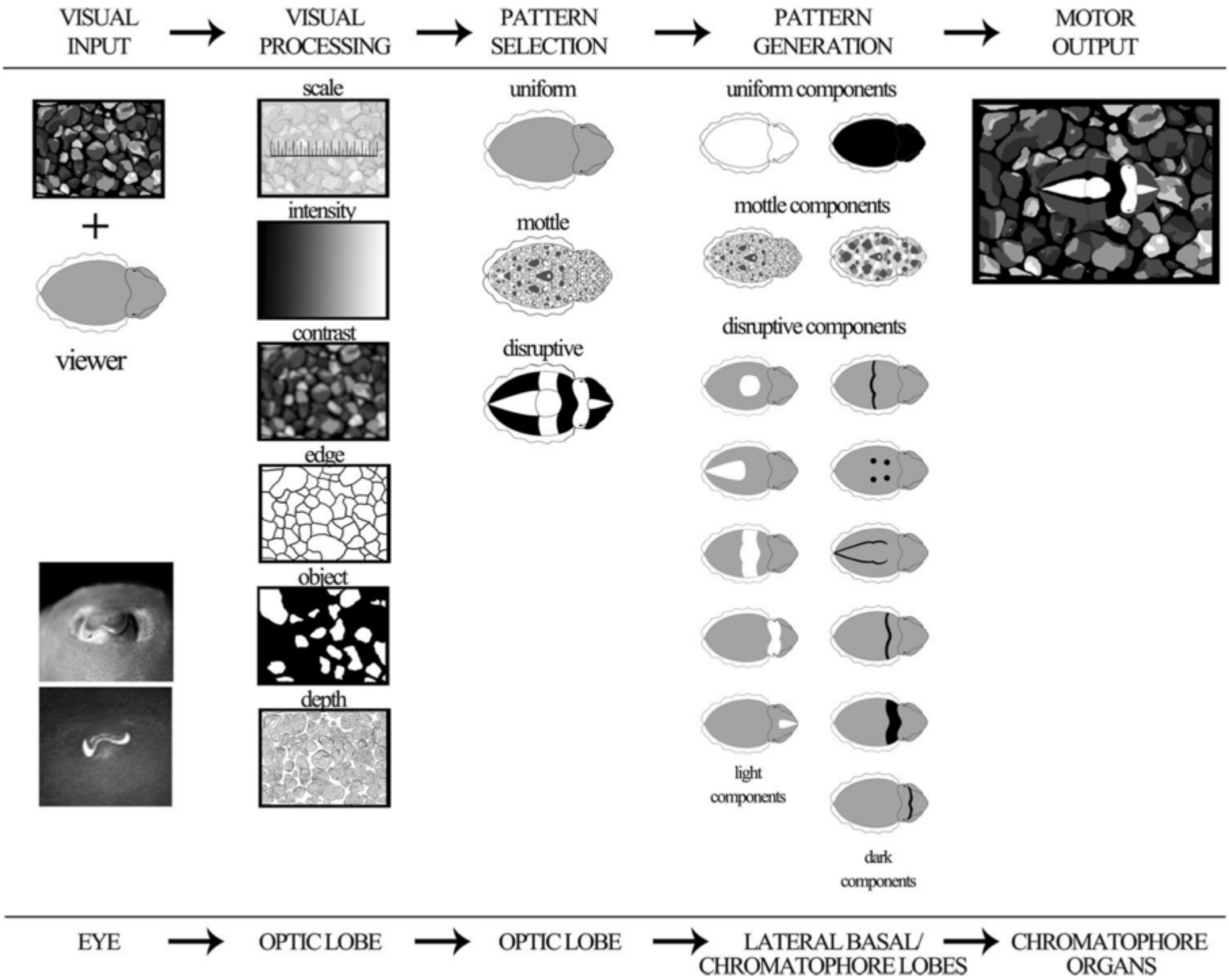

Figure 52.3: Workflow of camouflage pattern psychophysics. Figure from Chiao et al., 2015.

Deep sea benthic octopuses have been observed congregated around whale falls and baited traps, suggesting they can follow odor plumes to search for food (Weertman's 2022 CIAC talk). In experimental setups, *O. rubescens* has been shown to follow odor plumes to find prey and because it doesn't rotate its head towards the source in any way, it seems more likely to be using brachial chemosensation rather than the olfactory pits (Weertman's 2022 CIAC talk).

52.4.1 Olfactory pits / rhinophore

Squids and octopods have chemoreceptor organs in olfactory pits below and behind their eyes (Gilly and Lucero, 1992). In Octopoda (at least), they are white (lacking chromatophore) spots near the junction between the head and the dorsal margin of the mantle (Polese et al., 2016). These pits are lined with folds of odorant-sensitive cells that connect to olfactory receptor neurons (Campinho et al., 2018). These epithelial cells can be erected to protrude out of skin folds and be exposed to odorants (Polese et al., 2016).

Similarly, *Nautilus* possess a rhinophore organ below each eye that is larger than coleoid olfactory pits and functions as an olfactory organ (Basil et al., 2005).

52.4.2 Brachial senses

There are chemosensitive cells in the suckers of all coleoids, however there are many more in octopods than decapodiforms. For example, there are 10,000 cells per sucker in octopods and there are only 100 per sucker in *Sepia* (Graziadei 1964a,b). At least in octopods, there are chemosensitive-gated ion channels expressed in these cells that can be triggered when making physical contact with an odorant (van Giesen et al., 2020).

As a result, octopods can detect odorants as dilute as 10 μM (Budelmann, 1994). In Octopoda (at least), the chemosensitivity is highest in arms I and decreases towards arms IV.

Male octopods can detect past mates and avoid them based on physically touching them (Morse and Huffard, 2022).

The sucker and brachial ganglia in the arms send chemosensory information from the suckers through the brachial nerve and into the brain (Budelmann, 1995).

52.5 Gustation

52.6 Electrosensing

We are not currently aware of any electrosensation in any cephalopods.

Part VIII

Their environmental physiology

A cephalopod's physiology is not isolated from its external environment. Rather, its activity and behavior is regulated by its physiology which in turn is influenced by the environment (Fry, 1947). Environmental factors influence cephalopod physiology in five unique ways as defined by Fry (1947). A physical parameter may function as a:

1. controlling factor: sets the rate of a physiological process (e.g. temperature sets metabolic rate)
2. lethal factor: prohibits a physiological process (e.g. carbon monoxide prohibits oxygen from binding to hemoglobin in mammals)
3. limiting factor: restrains a physiological process (e.g. low P_{O_2} impairs oxygen uptake)
4. masking factor: loads a physiological process with added homeostatic challenges (e.g. salinity increases ion-pumping cost)
5. directive factor: directs an organism's physiology and behavior in response to changes

Physical parameters typically do not function on physiology independently. Rather, combinations of factor levels can cause additive, synergistic, or antagonistic effects section 53.8.

The mechanism of how an environmental parameter affects physiology is best understood using a deductive analysis beginning on an organismic scale (e.g. behavior) to progressively smaller spatial scales (Fry, 1947). This is due to emergent properties that are seen at higher dimensions, but cannot be predicted at low dimensions.

$$\text{Organism} \rightarrow \text{Organ system} \rightarrow \text{Organ} \rightarrow \text{Tissue} \rightarrow \text{Cellular} \rightarrow \text{Organelle} \rightarrow \text{Molecular} \rightarrow \text{Physical}$$

Many different stressors such as environmental conditions, starvation, exercise, or captivity trigger a universal molecular stress response. The animal's cells switch from cellular growth to cellular repair (Kassahn et al., 2009).

Chapter 53

Responses to physical parameters

All acclimatory responses are ultimately due, at least in part, to changes in gene expression (Schulte, 2004).

53.1 Light

The optic lobes compose 45% of the CNS in shallow-water taxa and 85% in deep-water taxa (Chung's 2018 CIAC talk).

Squids will contract and dilate their pupils in response to light stimuli (McCormick and Cohen, 2012).

53.1.1 Minimum depth of occurrence (MDO)

For pelagic cephalopods (both squids and octopods), metabolic rate decreases with increasing minimum depth of occurrence (MDO) (Seibel et al., 1997; Seibel and Carlini, 2001). In other words, the shallower a cephalopod ever has to go, the higher its metabolic rate must be. This is because inhabiting shallow waters requires locomotory ability to evade visually-hunting predators and function well as a visual predator on one's own prey. This decline in MO_2 with deeper MDO is observed in fishes and crustaceans too (Childress and Seibel, 1998), but not to the same extent as in cephalopods (Seibel et al., 1997) because cephalopods have a very large shift from highly inefficient locomotion at the surface (i.e. jet-propulsion) to much more efficient fin and medusoid swimming in dark, deep water where predatory risk does not require fast swimming (Seibel et al., 2000b). Cranchiids seem to be an exception to this trend: they have low MO_2 at all MDOs likely because their transparency alleviates their predatory risk even at shallow depths (Seibel et al., 1997). Similarly, pelagic taxa without image forming eyes such as chaetognaths or jellies have no relationship between MO2 and MDO (Seibel and Drazen, 2007).

Unlike their pelagic cousins, for benthic cephalopods such as most octopods, aerobic MO_2 does not scale with MDO (Seibel and Childress, 2000). This is likely because in the light epipelagic, these taxa depend upon hiding and camouflage much more than aerobic swimming and thus have less need for high MO_2 in shallow waters.

For both pelagic and benthic cephalopods, anaerobic potential (ODH) decreases with increasing MDO (Seibel and Childress, 2000; Seibel et al., 2000b). While hiding and camouflage are good primary defenses, if these fail, the taxa still need to be able to quickly escape from a predator. Thus, anaerobic potential must stay high in the high predatory-risk epipelagic, but can drop off in the less risky darker depths.

It is important to recognize that this decrease in MO_2 with increasing depth is due to light levels rather than other factors such as food availability, P_{O_2}, temperature, or pressure. Seibel and Drazen (2007) assessed the merits of these factors on impacting MO_2 and found decreasing light to be the dominating factor. Their evidence were as follows:

- MO_2 is only related to habitat depth in visually orienting animals where light impacts their responses to prey and predators.
- Food availability 1000 m below eutrophic surface waters can be similar to food availability in surface oligotrophic waters. Despite similar food supply, MO_2 is still lower at depth. Also, decreasing MO_2 with depth often tapers off near the bathypelagic zone (1000 m) but food availability continues to decrease an order of magnitude with each kilometer of depth .
- Oxygen does not decline uniformly with depth. There are normoxic and deep habitats where taxa still have low MO_2.
- Temperature does not decrease with depth in Antarctica, but MO_2 of Antarctic organisms still decrease with depth.
- Pressure gradients with depth do not affect gelatinous and benthic taxa.

Many deep-sea cephalopods have lost their ink sac presumably due to lack of necessity in the aphotic deep sea.

Table 53.1: Influence of minimum depth of occurrence (MDO) on metabolism. As taxa MDO increases...

Group	Aerobic potential (MO_2)	Anaerobic potential (ODH)	Locomotion
Pelagic	Decreases	Decreases	Mantle → Fins / medusoid
Benthic	No change	Decreases	

53.1.2 UV-B radiation

UV-B radiation is quickly absorbed by seawater, but for those cephalopods inhabiting the upper meter or so of the surface (e.g. *Argonauta*), UV-B can affect DNA, proteins, lipids, or can produce reactive oxygen species (ROS) (Franklin's SEB talk). When UV-B reaches DNA, it can cause adjacent bases on a nucleic acid chain to bind to each other rather than merely their pair on the complementary chain. These can only be fixed by photolyase repair enzymes which themselves require light to function (Franklin's SEB talk).

Terrestrial and shallow-water animals (cephalopods included) have lenses that absorb ultraviolet light. However, deep-sea cephalopod and fish lenses do not absorb UV light.

53.1.3 Camouflage in the deep pelagic

In animals generally, transparency is most highly selected in the mesopelagic while black or red pigmentation is selected in the bathypelagic (Zylinski and Johnsen, 2011).

In the deep pelagic, ambient light from above is best avoided by being transparent. However, predators with searchlight photophores can easily detect transparent animals and thus being red or black provides better camouflage. Therefore, meso- and bathypelagic cephalopods (e.g. *Japetella* and *Onychoteuthis*) have been demonstrated to maintain transparency under ambient light but to expand chromatophores to turn red under directed blue light (Zylinski and Johnsen, 2011) thus maintaining camouflage under both conditions.

53.2 Temperature

There are two main viewpoints on how temperature limits systems at the organismal level: 1. temperature directly affects molecules and 2. mismatches in oxygen supply-demand.

Temperature shifts the concentrations of chemicals in equilibrium according to the Van't Hoff equation (section 27.2).

The more complex an organism is (i.e. prokaryote vs animals) the lower its thermal tolerance often is. For example, archaeans can tolerate 120 °C, while animals can only tolerate 40 °C in general (Pörtner's 2022 CIAC talk).

53.2.1 Enzymatic and metabolic rates

53.2.1.1 Arrhenius equation

Temperature is a ubiquitous influence on all levels of organismal physiology from molecular kinetics to whole-animal thermal tolerance. At the molecular scale, temperature increases the kinetic energy of the molecules involved in biological reactions. At biologically-relevant temperatures, a small proportion of the molecule population has kinetic energy greater than the activation energy (E_a) required to begin the reaction. When temperature is increased 10 ^{o}C, for example, this only increases the highest frequency kinetic energy of the molecule population by ≈3% ($\frac{10K}{298K+10K} \approx 3\%$), but, it doubles the number of molecules that have kinetic energy above the activation energy (E_a), and thus doubles the number of molecules capable of biological reactions (Hochachka and Somero, 2002). This is described by the Arrhenius equation:

$$k = A \cdot \exp\left(-\frac{E_a}{RT}\right)$$

where k is the reaction rate (# of molecular collisions that result in reaction), A is the number of collisions regardless of whether they result in a reaction, and the exponential term is the probability of the reaction per collision.

The Arrhenius equation is useful in describing temperature-induced alterations in properties of a given enzyme *in vitro* or animal under acute temperature exposure. Acclimation or adaptation, however, modify enzymatic and metabolic rates away from the relationship predicted by the Arrhenius equation (subsection 53.2.3).

Arrhenius breakpoint temperature (ABT) The Arrhenius breakpoint temperature (ABT) is the breakpoint at which a reaction (or M_{O_2} as a whole) no longer increases according to the Arrhenius equation but increases slower or even decreases with increasing temperature (Schulte, 2015). There are four theories explaining why enzymatic rates do not exhibit Arrhenius behavior with infinitely increasing temperature but rather reach a plateau then decrease (Schulte, 2015):

Classical model The decrease in enzymatic rate with high temperature is due to irreversible enzyme denaturation.

Equilibrium model The decrease is because enzymes undergo a reversible conformational change to an inactivated form before denaturing. As temperature increases, an increasing proportion of the molecule population inactivates. This explains why some enzymatic rates begin decreasing below the enzyme's denaturation temperature.

Sharpe-Schoolfield model Similar to the equilibrium model except that inactivated conformations can occur at extremely high or low temperatures.

Macromolecular rate model The heat released during the reaction changes the energy of the transition state somehow?

53.2.1.2 Temperature dependency of whole-animal metabolic rate

At higher levels of biological organization such as organelles and cells, the effect of temperature must be considered not only for enzymes but also for other rate-determining variables such as [substrate], [product], or [allosteric modifiers] (Schulte, 2015). Since unicellular organisms have higher thermal tolerances than metazoans, it seems likely that whole-animal cephalopod thermal limits are imposed not by single enzymes, but rather by higher-level organization failures, such as the nervous system (subsubsection 53.2.7.5)(Schulte, 2015). Surprisingly, however, a similar temperature-activity relationship seems to scale up from enzyme activity to whole-organism response, following an Arrhenius response (despite the theoretical enigma of why this relationship would hold for such a more complex system than single enzyme reactions) (Schulte, 2015). The influence of temperature on metabolic rates in a diversity of organisms has shown to be roughly doubled by a 10 ^{o}C increase in temperature within their normal temperature range. This can be expressed as

$$Q_{10} = (k_2/k_1)^{10/(T_2-T_1)}$$

or

$$k_2 = k_1 \times Q_{10}^{(T_2-T_1)/10}$$

where k represents reaction rates and T represents temperatures. Q_{10} is often around 2-3 at temperatures to which the species is adapted (Scholander et al., 1953). When temperature is higher than an organism's thermal tolerance, increases in temperature result in $Q_{10} < 1$ (Melzner et al., 2006b). This impairment of aerobic metabolism could be caused by a failure anywhere in either the oxygen supply or demand processes (Schulte, 2015). Additionally, a mismatch in the temperature sensitivity of oxygen supply and demand processes within or between resting and active behavioral states will result in change in the organism's aerobic scope (Schulte, 2015).

Decreasing temperatures below tolerable ranges has an impact greater than merely decreasing the proportion of molecules with sufficient kinetic energy. Below tolerable temperatures, Q_{10} can be much greater than 2 (Hochachka and Somero, 2002; Melzner et al., 2006b).

The warmer temperature to which an organism is adapted, the narrower the range between its "normal" temperature and its ABT (Hochachka and Somero, 2002). Thus, cold-adapted organisms have a larger temperature range they can increase before reaching ABT.

Due to temperature's effect on MO_2, increased temperature increases oxidative stress section 39.2.

53.2.2 Temperature impacts on RNA secondary and tertiary structures

The secondary and tertiary structures of RNA are temperature-sensitive and can affect the interactions of RNAs with other molecules (including ribosomes (i.e. translation)) (Somero, 2018; Chursov et al., 2013). Some RNAs function as "thermometers" with translation initiation sequences only functional under elevated temperature when the 5' UTR structure melts (Somero, 2018; Chursov et al., 2013). The expression of these "thermometers" can function as signals for other cellular acclimations to temperature changes.

RNAs can also be edited by pseudouridylation (U $\rightarrow$ pseudo-U) which forms a tighter base-pair bond with adenine, thus strengthening double-stranded RNA (dsRNA) structure under high temperatures (Somero, 2018).

53.2.3 Enzymatic acclimations and adaptations to temperature

Peter Hochachka established a paradigm explaining the biochemical adaptations of enzymes to temperature. These alterations allow enzymes to deviate from an Arrhenius relationship and in some cases even come close to fully compensating to temperature (temperature independence). Organisms acclimate or adapt to temperature by changing their enzyme properties, concentrations, and milieu (Somero, 2004). These changes allow similar enzyme activities to occur in tissues of animals from two very different temperatures. In the few cases that have been closely examined, changes in the properties of enzymes seem to be the dominant influence in evolutionary adaptations, rather than concentration or milieu (Somero, 2004). During acclimation, changes in concentration may be a more dominant influence (Somero, 2004).

Residue-specific influences on protein thermostability Thermophilic bacteria have more aliphatic residues in their proteins (Ala, Val, Ile, Leu) than are found in the orthologs of normal proteins, suggesting that aliphatic residues support thermostability (Ikai, 1980). Lysine residues and β-sheet structures also support thermostability in proteins, while aspartic acid is more abundant in proteins with low thermostability (Leuenberger et al., 2017).

In general, shorter proteins are more thermostable than long ones (Leuenberger et al., 2017).

As temperature rises, the relative contribution of hydrophobic interactions to protein stability increases and hydrogen bonding decreases (Hochachka and Somero, 2002). Correspondingly, extremophile microbes tend to replace polar residues (good for hydrogen bonding) with hydrophobic residues (Hochachka and Somero, 2002).

Based on a molluscan model protein, polar residues, along with proline and glycine enhance thermostability, especially on the protein surface, while charged residues on the surface lower thermostability (Liao et al., 2019).

53.2.3.1 Enzyme properties (k_{cat} and K_m)

Overall, global enzyme stability is positively related to the adapted temperature of its organism. That is to say, warm-adapted orthologs are more stable globally than cold-adapted orthologs when brought to the same temperature.

The rate-determining step in enzyme function is often not converting substrate(s) to product(s), which happens rapidly, but the conformational change of the enzyme to establish the catalytic vacuole (Hochachka and Somero, 2002). In interspecific comparisons of enzyme orthologs, the AA sequence of the residues directly involved in catalysis is almost always conserved. Because the conformational change of the enzyme is the rate-limiting step, it is the AA sequence affecting the conformational change that adapts and can influence k_{cat}. k_{cat}, the rate of conversions per enzyme given unlimited [substrate], is inversely related to the temperature a species is adapted to (when being measured at the same temperature). This helps cold-adapted organisms maintain sufficient enzyme activity without the expensive prospect of increasing enzyme concentration.

k_{cat} and K_m have tradeoffs in interspecific comparisons. The more flexible an enzyme, the faster its conformational change (higher k_{cat}) but the smaller proportion of enzymes in a cell are in a conformational state (microstate) amenable to binding substrate (higher K_m). Thus cold-adapted species, which have more flexible enzymes, have higher k_{cat} and higher K_m. Similarly, warm-adapted species have enzymes which are relatively rigid compared to cold-adapted species. This decreases their k_{cat} but decreases their K_m relative to colder species. Studies with a few groups of fishes have shown that only a few degrees change in temperature is sufficient to favor AA substitutions and change in the kinetic properties of an enzyme (Hochachka and Somero, 2002).

When considering a temperature change intraspecifically, higher temperatures increase the rate of substrate-enzyme interaction due to more molecular motion (increase k_{cat}), but temperature also increases the rotation of enzyme bonds which leads to less binding affinity or higher K_m. This has important implications for changes in an individual's environment. Individuals that are exposed to high temperature will have to deal with the degraded binding affinity of their enzymes for substrate.

Which parameter is favored (k_{cat} or K_m), then depends upon the availability of the substrate(s) in the cell. For example, if the enzyme being considered is cytochrome c oxidase, the terminal protein in the electron transport chain, then its adaptation may depend upon intracellular $[O_2]$. If $[O_2]_i$ is stable and high during most of an organism's existence (i.e. anaerobiosis from either high activity or environmental hypoxia is rare), then $[O_2]$ is often above K_m. Therefore, it would be favorable, all else being equal, to increase k_{cat} even though doing so would increase K_m. On the other hand, if substrate concentration is frequently near or below K_m (as I would expect in organisms that frequently undergo hypoxia or high activity), then decreasing K_m at the cost of decreasing k_{cat} may be favorable. I chose cytochrome c oxidase as an example relevant to my research, however, I would expect that environmental hypoxia would have other effects on hemocyanin and cytochrome c oxidase gene expression that may make this example unrealistic, but the principle should hold.

RNA editing often replaces stabilizing amino acids with destabilizing ones, thus destabilizing enzymes which should be beneficial for cold acclimation (Garrett and Rosenthal, 2012b).

Changes in enzyme properties may explain acclimation of metabolic rate to temperature For many animals, when first exposed to a new higher temperature that stresses them, their metabolic rate is higher than after a few hours or days of

acclimation (Lefevre, 2016). A potential mechanism to explain MO_2 decreasing after acclimation to a higher temperature is that initially when an animal is placed at higher temperature its tissues contain lots of isozymes intended for low temperatures which are "loose" and react quickly subsubsection 53.2.3.1. Over acclimation time, however, higher-temperature isozymes fill out the enzyme population and they react at a more appropriate slower rate. This may be true if substrate concentrations are saturating and there are no other feedback regulators restricting high enzymatic activity. If this is true, then a quick change to cooler temperatures should result in initial drop then MO_2 rising throughout acclimation.

53.2.3.2 Enzyme concentration

Differential expression of various isoforms of an enzyme can occur under different temperatures such that isoform concentrations alter with temperature (Somero, 2004).

In general, the more abundant a protein within the proteome, the more thermostable it is (Leuenberger et al., 2017). According to the “translational robustness” theory, more abundantly expressed proteins will, by probability, have more occurences of mis-translations floating around in the cell. If those mis-translations cause a toxic misfolding, then the cell will be harmed. Therefore, abundant proteins have evolved robustness to mis-translations so that their structures are more stable even if a single residue changes. The thermostability of abundant proteins is, therefore, an exaptation according to this theory.

53.2.3.3 Enzyme milieu

Since intracellular (and extracellular) pH varies with temperature (often following the alpha-stat hypothesis), the pH of the surrounding medium of enzymes changes along with the enzyme itself. For example, lowering of pH with increasing temperature maintains sustainable proton activity for enzymes to function (Somero, 2004).

53.2.4 Temperature impacts on membranes

Membrane fluidity must be conserved under all environmental temperatures an organism inhabits. To acclimate and adapt to this change, the membrane composition is adjusted to maintain proper fluidity (Cossins and Prosser, 1978; Hochachka and Somero, 2002). At least in fishes, adjustment takes 2 days to 2 weeks depending on temperature . This fluidity compensation occurs both by modulation of the saturation of the phosphoglycerides and adding cholesterol to decrease fluidity. As temperature warms, the phosphoglycerides become increasingly saturated and the proportion of unsaturated phosphoglycerides declines (Cossins and Prosser, 1978). This increase in saturation allows the phosphoglycerides to be packed more tightly. Because lipids are not genetically determined, but rather are constructed by a wide diversity of potential enzymes, they have high acclimation potential compared to genetically restricted proteins (Hochachka and Somero, 2002).

Proteins that are embedded in the membrane bilayer have decreased activity at cooler temperatures not just because of the protein kinetics by itself, but also because it’s lipid environment is more viscous (Hochachka and Somero, 2002). It should be kept in mind that many of the key enzymes in aerobic metabolism are membrane-bound (Schulte, 2015).

As temperature increases, mitochondrial proton leak increases as well, resulting in a lower P/O ratio, and thus O_2 consumption increase in excess of that required by the increase in ATP demand due to temperature (Schulte, 2015).

53.2.5 Cellular temperature stress responses

Heat-shock proteins (HSP) are chaperonin molecules that protect proteins from denaturing at high temperatures (as well as other stressors). Heat stress is a function of the change in temperature (ΔT), the heating rate, and the duration of exposure.

Heat stress has great implications on metabolism. In addition to the regular increase in reaction rates with temperature, if temperature is great enough to denature proteins, then a metabolically expensive system goes into gear: HSPs must be synthesized to refold reversibly denatured proteins. Ubiquitin must also be produced to tag irreversibly damaged proteins for proteolysis. Finally those destroyed proteins must be replaced via protein synthesis to return to their normal concentrations. The energetic costs associated with these responses can be considerable, especially if the individual has stopped feeding in the hot environment.

A species’ ability to induce such a heat-shock response correlates well with whether it is stenothermal or eurythermal (Logan and Buckley, 2015).

High mobility group (HMG) proteins are DNA-binding proteins that seem to be highly responsive to temperature and regulate cellular transcription (Logan and Buckley, 2015).

53.2.5.1 Temperature-induced protein denaturation

Proteins are held together by a number of bonds and forces such as ionic bonds, H bonds, hydrophobic interactions, and van der Waals forces. As temperature changes, the ability of these bonds to maintain the protein’s conformation changes, but not in a

consistent manner. Hydrophobic interactions become relatively stronger at high temperatures while ionic and H bonds become relatively stronger at lower temperatures (Hochachka and Somero, 2002). Thus, at extreme low temperatures, proteins denature due to loss of hydrophobic interactions; at extreme high temperatures, proteins denature due to loss of hydrogen bonds.

53.2.6 Temperature impact on mitochondria

Cold-adapted demersal fish species have more mitochondria by muscle volume than warm-adapted, all else the same ($R^2 = 0.4$) but active pelagic taxa do not seem to have much relationship and cold-acclimated fishes may or may not raise mitochondrial volume depending on the species (Guderley, 2004).

53.2.7 Impact on specific body systems

53.2.7.1 Temperature's effect on respiratory system

The diffusivity of O_2 dissolved in seawater is temperature dependent. Increasing temperature decreases water viscosity and increases diffusivity, both of which supporting higher oxygen diffusion rates at higher temperatures.

Ventilation rate can increase logarithmically (*Lolliguncula*; Wells et al., 1988) or exponentially (*Sepia*; Melzner et al., 2006b) with temperature, ranging from 20 up to 90 ventilations per minute (covering 8-26 °C, most temperatures encountered by cephalopods)(Melzner et al., 2006b). Ventilatory stroke volume, however, is constant at all reasonable temperatures in *Lolliguncula brevis* (Wells et al., 1988), but in *Sepia officinalis* ventilatory stroke volume and mantle cavity pressure amplitude increase with temperature (Melzner et al., 2006b). Stroke pressure amplitude increases from 25 to 100 Pa with increasing temperature. I would expect that ventilatory stroke volume would increase with temperature to compensate for the increased metabolic rate and decreased extraction (Melzner et al., 2006b). In *Sepia*, ventilatory flow increases disproportionately more than metabolic rate with temperature. This disproportionate increase is due to the extraction decrease which fills the unexplained gap in O_2 supply-demand balance.

In total, the ventilatory flow (volume of water run through the mantle cavity per minute) increases greatly with increasing temperature in an animal's upper temperature range. Ventilatory flow can increase from a mere 10% body weight of seawater per minute up to 150% body weight per minute at maximal temperatures (*Sepia*; Melzner et al., 2006b). This can be at a great energetic cost to the animal. For example, *Sepia officinalis* ventilatory cost increases from a negligible ~1% at low temperature up to almost 10% of total metabolic energy budget at extremely warm temperatures (Melzner et al., 2006b).

53.2.7.2 Temperature's effect on cardiovascular system

Heartbeat rate increases exponentially with temperature (Wells et al., 1988). *Octopus* heart rate has a Q_{10} of 3 (Wells, 1980, 1983). Cardiac stroke volume, however, decreases with increasing temperature at least for *Lolliguncula brevis* (Wells et al., 1988), although the increasing frequency overcompensates for this decline leading to the net increase in blood flow with temperature. This temperature-response in cardiac dynamics seems be locally controlled within the hearts and PNS (Wells, 1980).

In vitro squid and octopod blood decreases 0.015 - 0.02 pH units per °C (Howell and Gilbert, 1976; Oellermann et al., 2015a), following the alpha-stat hypothesis (subsubsection 35.0.0.2).

In theory, as temperature warms the blood becomes less viscous and a higher [Hc] could be sustained which would be helpful to support the higher M_{O_2} and impaired affinity (subsubsection 53.2.7.3). This occurs in fishes (Johansen and Weber, 1976).

53.2.7.3 Temperature's effect on hemocyanin

Since energy is released during Hc-O_2-binding in all cephalopods ($\Delta H < 0$) (Mislan et al., 2015) and most fishes too (Johansen and Weber, 1976), increased temperature increases P_{50} ~0.25 kPa / °C (Seibel, 2013; Mislan et al., 2015; Brix et al., 1989). This can be modelled with the Vant-Hoff equation, with P_{50} replacing K_{eq} (Equation 27.1). Increased temperature also increases the Bohr coefficient (less negative) (Seibel, 2013). These effects work together to benefit the animal with an increasing metabolic rate with increasing temperature in the following way: at higher temperature, oxygen loading at the gills should be impaired by higher P_{50} and lower pH, but it is protected somewhat by the smaller Bohr coefficient, so that at least the effect from the temperature-induced drop in pH is somewhat minimized. Meanwhile, at the tissue capillaries, the higher temperature raises P_{50}, which encourages oxygen unloading. At least in *Todarodes sagittatus,* this results in temperature having a large effect on the lower end of the O_2-binding curve (T-state), while there is little temperature effect on the higher end (R-state) (Brix et al., 1995). Temperature has also been shown to influence hemoglobin P_{50} in fishes not through changes in hemoglobin itself but through changes in allosteric modifiers (Johansen and Weber, 1976)(subsubsection 51.2.7.2).

It is expected that cephalopod hemocyanin will have similar selective pressures as fish hemoglobin such that eurythermal species will have hemocyanin with less sensitivity to temperature than stenothermal species (Johansen and Weber, 1976).

Temperature has also lead to adaptation in hemocyanin O_2 affinity. When two *Octopus* species Hc P_{50} are compared at the same temperature, the Hc from the cold-water species has a higher P_{50} than the warm-water species. This is to compensate (partially) for the temperatures experienced *in situ* such that in their natural environment, the P_{50} values are similar (subsubsection 53.2.3.1).

Hemocyanin of cold-adapted octopod species generally has a more positive net charge among surface residues than warm or temperate species (Oellermann et al., 2015b). This is thought to raise residue pK values to compensate for the higher blood pH at cold temperatures, though it is unclear to me why α-stat compensation (which is present) is not sufficient alone to maintain enantiostasis.

53.2.7.4 Temperature's impact on muscle

Based on crustacean preps, the resting membrane potential of muscle at neuromuscular junctions is more hyperpolarized at higher acclimation temperatures (Stephens and Atwood, 1982; Zhu and Cooper, 2018).

53.2.7.5 Influential impact on neurons

One recently proposed concept for how neurons manage to balance all the various processes' Q_{10}s as described below, is that given a fixed Q_{10} of each protein involved in a process, the expression of that protein can be regulated by a feedback mechanism such as a Ca^{2+}-dependent transcription factor (O'Leary and Marder, 2016).

In general, ion channel conductance has a Q_{10} = 1.2-1.5 (Hodgkin and Keynes, 1955; O'Leary and Marder, 2016).

In general, ion channel gating has a Q_{10} = 2-4 (O'Leary and Marder, 2016).

Ion permeabilities also differ: in cuttlefish giant axon, P_{Na^+} (Q_{10} = 1.4) is more temperature-sensitive than P_{K^+} (Q_{10} = 1.1) (Hodgkin and Keynes, 1955).

Active ion transport is more temperature-sensitive than passive ion conductance (Carpenter, 1981).

Sudden warming tends to cause neurons to slow and sudden cooling causes them to accelerate (Carpenter, 1981).

Acute temperature changes One of the primary issues of thermal perturbation in animals is due to the effects on neuronal membranes (Schulte, 2015). Temperature perturbations primarily affect synapses but also conduction down the axon (Hochachka and Somero, 2002; Schulte, 2015). This can lead to issues in neuronal regulation of ventilation and circulation, muscle membrane potential, or cardiac failure (Schulte, 2015). Due to the myriad of steps in neuronal transmission (see below), the overall effect of temperature on neuronal function is hard to predict and is likely species-specific (Montgomery and MacDonald, 1990).

Acute temperature effects on resting membrane potentials Generally, resting membrane potential (E_m) hyperpolarizes with increasing temperature due largely to the higher rate of NKA activity (Montgomery and MacDonald, 1990). Though, increased ionic permeabilities may counter this effect in some cases documented in other animals (Montgomery and MacDonald, 1990). Particularly, if Na^+ leak channels are more temperature sensitive than K^+ leak channels then the resting potential can depolarize in some cases.

Acute temperature effects on action potentials A given neuron will have longer duration and lower amplitude action potentials and the conduction velocity will be slower at colder acute temperatures (Kukita, 1982; Weight and Erulkar, 1976; Joyner, 1981). Though in squid giant synapse preps, presynaptic action potentials had not only longer duration but also higher amplitude as well and colder temperatures (Charlton and Atwood, 1979). In most animals, conduction velocity is linearly related to temperature (Montgomery and MacDonald, 1990; Kukita, 1982). Voltage-gated K^+ channels (responsible for repolarization) are more temperature-sensitive than voltage-gated Na^+ channels (responsible for depolarization) (Kukita, 1982) and this corresponds to a higher acute temperature sensitivity of repolarization than depolarization, though both exhibit Q_{10} values from 1-4 (Rosenthal and Bezanilla, 2000). The slower action potentials also increase the duration of the refractory period, thus lowering the maximal firing rate of neurons (Montgomery and MacDonald, 1990).

Acute temperature effects on presynaptic transmission Cooler temperatures cause action potentials to be longer (see above). This lengthens the amount of time that voltage-gated calcium channels are open (Montgomery and MacDonald, 1990). However, the cooler temperatures also slow the flow (lowers current) of Ca^{2+} through the open channels (Charlton and Atwood, 1979). Altogether, a chilled squid giant synapse prep demonstrated that the delayed onset of Ca^{2+} current only explained 1.5 ms of the 6 ms synaptic delay (time to first neurotransmitter release) (Charlton and Atwood, 1979). Therefore, the majority of the temperature-sensitivity of synaptic delay occurs in the steps after Ca_v channels opening (e.g. vesicle docking and exocytosis).

Squid giant synapse preps demonstrate that neurotransmitter release is lesser at acute colder temperatures even if the incoming action potential characteristics were the same (Weight and Erulkar, 1976; Charlton and Atwood, 1979), though they

tend to be higher (see above). This lower quantity and delayed release (synaptic delay) are common pre-synaptic responses to cold temperature (Charlton and Atwood, 1979).

The warmer the temperature, the shorter the synaptic delay (Katz and Miledi, 1965; Weight and Erulkar, 1976) due to an acceleration of all the following: neurotransmitter discharge, diffusion rate of neurotransmitter molecules across the synapse, neurotransmitter receptor binding, conformational change (channel opening), and diffusion rate of ions across post-synaptic membrane (Montgomery and MacDonald, 1990).

Acute temperature effects on postsynaptic transmission Cold temperatures cause postsynaptic potential to be less responsive (smaller ΔV for a given frequency and intensity of synaptic transmission) and longer in duration than at warmer temperatures (Montgomery and MacDonald, 1990). For example, cooling squid giant synapses from 10 to 6 °C causes a 5x smaller ΔV in response to synaptic signals (Weight and Erulkar, 1976). However, this is not always the case. For example, some crustacean neuromuscular junctions become more responsive (larger ΔV) yet remain slower at colder temperatures, causing summation that makes them much more responsive overall at cold temperatures than warm (Montgomery and MacDonald, 1990). In addition, warm temperatures above the animal's native tolerance can lower postsynaptic potential responses rather than continuing to increase indefinitely (Montgomery and MacDonald, 1990).

It is important to keep in mind that the temperature-dependence of postsynaptic responses to signals may be different for excitatory and inhibitory signals. Differential temperature-response relationships will influence the overall effect of temperature on the activity of neuronal transmission globally (Montgomery and MacDonald, 1990).

Seasonal acclimation In animals generally, cold acclimation causes action potentials to progress faster than warm-acclimated neurons when measured at the same temperature (cited in (Rosenthal and Bezanilla, 2000)). However, *D. pealeii* giant axons from spring and summer seasons (10 °C apart) have identical AP properties (AP duration, conduction velocity, de- and repolarization rates) when measured at the same temperature (Rosenthal and Bezanilla, 2000), a curious lack of compensation. Although AP properties are identical, cooler acclimated animals (spring) maintained ~3 mV less negative resting potentials in the giant axons than warm acclimated animals (summer) when measured at the same temperature (Rosenthal and Bezanilla, 2000). In addition, spring-time animals had 30% larger giant axon diameters than summer-time animals (possibly because they're older individuals that migrated inshore earlier). Since conduction velocity should normally be faster with larger axon diameter, the fact that conduction velocity between the two seasons of squid was the same means that the spring-time animals had slower conduction velocities for a given size and temperature axon than summer-time animals, a counter-compensatory effect (Rosenthal and Bezanilla, 2000). It is possible that compensated temperature-dependence of synaptic transmission compensates for the lack of compensation in action potential propagation (Rosenthal and Bezanilla, 2000).

RNA editing helps *Doryteuthis* have been shown to utilize RNA editing to alter the isoform of the voltage-gated K^+ channel to maintain proper neuronal function under temperature stress (Colina et al., 2010). In addition, cold-adapted octopus species have adapted to increase editing levels at a key site of a voltage-gated K^+ channel which increases the rate of repolarization compared to warm species (Garrett and Rosenthal, 2012a).

RNA editing in general is likely to be less prevalent at warm temperatures (all else the same) since ADARs only bind to double-stranded RNA, which is less stable at warm temperature (Yablonovitch et al., 2017).

53.2.8 Organismal temperature acclimation

Whole-animal metabolic rate and activity of ectotherms can acclimate and temperature compensate to deviate from an Arrhenius relationship (Bullock, 1955).

53.2.9 Impact on behavior

Squid giant-axon mediated escape jetting behavior is just a tad bit slower at colder temperatures, which *could* lower the success rate for predator escape (Neumeister et al., 2000).

Cephalopods (and ectotherms generally) are less active at colder temperatures.

Photophores in squids have been demonstrated to change the color of light emitted in a temperature dependent manner, presumably to match downwelling light throughout DVM across a temperature gradient (Young and Mencher, 1980).

53.2.10 Oxygen and capacity limited thermal tolerance (OCLTT)

Hypoxia tolerance is often strongly influenced by temperature due to temperature's effect on metabolic rate. As metabolic rate increases with increasing temperature, the flux of O_2 into the body must increase as well to meet demand. This increased

flux must occur either by increased gill diffusion or perfusion (subsection 51.1.3). In normoxic conditions, oxyregulators like cephalopods may be limited by diffusion (ventilation rate) or perfusion (cardiac output). Under low O_2 conditions, diffusion is limited so much that SMR cannot be sustained (P_{crit}). When temperature is higher, SMR is higher and thus the diffusion limitation occurs at a higher P_{O_2}.

53.2.11 Biogeographic boundaries set by temperature

Temperature is an important boundary for biogeography (Bartol et al., 2002). This is likely in part due to its effects on proteins: K_m is increased, k_{cat} is increased, and protein damage is very costly. The thermal windows for reproduction and development are often narrower than for survival, suggesting that the distribution of stable populations are constrained by reproduction and development rather than adult survival (Schulte, 2015).

A species' tolerable temperature range (how steno- or eurythermal it is) seems to be highly correlated with its cells' ability to induce a cellular heat-shock response (Logan and Buckley, 2015). In very broad terms, species at higher latitudes (excluding the poles) tend to be more eurythermal than low latitude taxa (Sunday et al., 2011).

Cuttlefishes do not occur in polar regions presumably due to temperature. I am not aware of what adaptive restraint impairs their adapting to these cold waters. *Sepia officinalis* is the most northward reaching cuttlefish, reaching up to 62 °N off Europe and sepiids in general reach as far south as 42 °S off Australia (Xavier et al., 2016).

53.2.11.1 Habitat choice behavior influenced by temperature

In ectotherms generally, there is seasonal variation in preferred temperature following the temperatures to which an animal is acclimated. In the winter, animals prefer cooler temperatures than they prefer in summer.

53.3 Salinity

All cephalopods are strictly marine osmoconformers. Almost all cephalopods are stenohaline, with *Lolliguncula* being an exception (*L. brevis* can invade habitat as low as 8.5 psu at least for a short duration). There are a few cases of high salinity tolerance as well. *Sepia apama,* for example, spawns its benthic egg masses in water up to 44 psu in the furthest regions of Spencer Gulf, Australia (Gillanders' 2015 CIAC talk).

Deviations from an animal's tolerable salinity range can affect blood ion balance (Table 51.4) because they are osmoconformers.

53.3.1 Impact on specific body systems

53.3.1.1 Hemocyanin function

Stenohaline cephalopods have impaired Hc-O_2 binding affinity under exposure to low salinity. For example, 11 psu seawater-exposed *D. pealeii* blood raised P_{50} by 2.5 kPa and completely lost its Bohr effect (Mangum, 1991). This is because lower ionic strength blood increases P_{50} (Miller, 1985). Specifically, Mg^{2+} seems to be the most important ion influencing Hc (Mangum, 1997; Miller, 1985).

53.3.2 Impact on behavior

53.3.3 Biogeographic boundaries set by salinity

Salinity is an important boundary for biogeography (Bartol et al., 2002). The mouth of the Amazon river, for example with a salinity ~25 psu, has been suggested to be a barrier between south Atlantic and north Atlantic / Gulf of Mexico coastal cephalopod taxa. Broadly, in coastal and estuarine habitats, salinity is likely a more important driver of cephalopod distribution than temperature or oxygen (Bartol et al., 2002).

53.3.3.1 Habitat choice behavior influenced by salinity

53.4 Density

Many deep sea cephalopods adjust their internal density to match seawater density and thus achieve neutral buoyancy (Clarke et al., 1979). However, shallow-water cephalopods (with the exception of sepiids and nautiluses) are more dense than seawater. Typical shallow water species of squids and octopods are ~2-4% more dense than seawater (Packard, 1972; Bartol et al., 2001), or about 1.05 $g \cdot cm^{-3}$.

53.4.1 Impact on specific body systems

53.4.1.1 Ectocochleate buoyancy

Ectocochleates can alter blood osmolarity in their siphuncle to utilize osmosis to keep water out of chambers. Then dissolved gas from the blood can fill the vacuum. This gas counteracts the weight of the shell and allows neutral buoyancy.

53.4.2 Impact on behavior

53.4.3 Biogeographic boundaries set by density

53.4.3.1 Habitat choice behavior influenced by density

53.5 Pressure

Organisms adapted to high pressure have adaptations that stabilize their proteins relative to shallow-water forms. Organic molecules like TMAO, for example, help stabilize proteins.

The metabolic rates of mesopelagic vertically-migrating cephalopods seem to be pressure-insensitive at least between the surface and 1300 m (the range tested) (Belman, 1978). This is similar to other gelatinous zooplankton, with pressure-insensitive M_{O_2} at least to 1000 m (Childress and Thuesen, 1993). Though some pressure-related changes in M_{O_2} have been documented in animals (reviewed by Robison, 2004).

53.5.1 Impact on specific body systems

53.5.2 Impact on behavior

53.5.3 Biogeographic boundaries set by pressure

Nautiloids and cuttlefishes are highly depth limited due to pressure. *Sepia officinalis* cannot survive deeper than 150-200 m, and other sepiids 1000 m, before the gas-filled cuttlebone implodes (Xavier et al., 2016). Nautiloids are typically found no deeper than 300 m but have been seen as deep as 650 m (Nixon and Young, 2003). Any deeper and their shells would likely implode. Deep bottom depth (combined with the low temperature) is the likely factor limiting cuttlefishes and Sepiolinae bobtail squids from migrating to the Americas (Young et al., 1998).

Cirrates are the deepest found cephalopods, with maximum depths of occurrence at nearly 7 km (Jamieson and Vecchione, 2020). Incirrates can be found rather deep as well, with the deepest observations to date over 4000 m (Purser et al., 2016). A *Magnapinna* holds the current record for the deepest recorded squid, at 6212 m depth.

53.5.3.1 Habitat choice behavior influenced by pressure

53.6 Oxygen

Childress and Seibel (1998) have put forth the idea that the adaptations of cephalopods to environmental oxygen can be roughly predicted by the consistency of their exposure to hypoxia. Generally, chronic hypoxic environments encourage adaptations to maintain RMR through increased aerobic efficiency (i.e. blood-O_2 affinity, gill surface area, etc.) whereas ephemeral hypoxic environments encourage adaptations to increase anaerobic potential or suppress metabolism.

1. Initially O_2 is sufficiently high.
2. Then, ventilatory and cardiovascular responses maintain stable O_2 supply to tissues despite lower environmental P_{O_2}.
3. Then, the animal reaches P_{crit}.
4. Then, the animal has to suppress metabolism (in hypoxia-tolerant species) and utilize fermentable substrates to maintain metabolic balance.
5. Then, the cells run out of ATP and they die.

53.6.1 O_2 sensing

Fishes have neuroepithelial cells (NECs) on and in their gills. There is an unidentified molecule within the cells that senses a decrease in P_{O_2}. This unknown molecule lowers the activity of background K^+ channels which depolarizes the cell, triggering voltage-gated Ca^{2+} channels to open, influx Ca^{2+}, and release serotonin (neurotransmitter) from storage vesicles to signal hypoxia to the brain (Zachar and Jonz, 2012). Adding cyanide to the incurrent water also triggers this response in fishes. In *Octopus*, however, adding cyanide has no impact on cardiorespiratory dynamics, suggesting that cephalopods may sense O_2 using a different mechanism (Wells and Wells, 1995).

53.6.2 P_{crit}

P_{crit} is a metric of hypoxia tolerance that has been assessed since the 1920s (Keys, 1930). It is quantified either as the environmental P_{O_2} below which an individual can no longer maintain its SMR or below which anaerobiosis increases. Theoretically, (and experimentally in other taxa) the value is identical in both metrics (Pörtner and Grieshaber, 1993). P_{crit} is the threshold at which O_2 transitions from a limiting factor to a lethal factor (Claireaux and Chabot, 2016). Individual organ and cell metabolisms have a P_{crit} as well as the whole animal (Pörtner and Grieshaber, 1993). Thus the phenomenon of a P_{crit} threshold is a direct result of cellular responses (subsubsection 53.6.3.1, Stage 3) rather than an emergent property of the whole animal. P_{crit} increases with increasing organism complexity (Ekau et al., 2010). In a cell, O_2 diffusion across the membrane and cytosol are limiting. In a tissue, capillary P_{O_2} is limiting. In an organism, branchial and cardiovascular dynamics are limiting.

Humans are hypoxic at 16 kPa and lose consciousness below 10 kPa.

53.6.2.1 Influence of adaptation to environment

P_{crit} is influenced strongly by the environment a species is adapted to inhabit (Mandic et al., 2009). For example, pelagic cephalopods off California (low P_{O_2} in OMZ) were found to have lower P_{crit}s than similar species off Hawaii (high P_{O_2}) (Seibel et al., 1997). *Gonatus onyx* P_{crit} matches exactly the lowest P_{O_2} at which the animals typically inhabit in Monterey Bay (Hunt and Seibel, 2000). In high O_2 environments, however, organisms do not necessarily have very high P_{crit}s. For most organisms (including cephalopods), if in a suitable temperature range, P_{crit} is often no higher than about 5 kPa (Seibel, 2011; Rogers et al., 2016) though exceptions certainly exist (e.g. *Lolliguncula brevis* (T = 20 °C, P_{crit} = 7.9 - 9.4 kPa O_2, Zielinski et al., 2000). On the other hand, there seems to be a lower threshold at which organisms are unable to adapt any further to hypoxia: ~0.8 kPa (Seibel, 2011).

Most organisms that inhabit OMZs have a variety of adaptations to maintain aerobic metabolism at very low environmental P_{O_2} (Childress and Seibel, 1998). This is in contrast to organisms adapted to ephemeral hypoxia as found in intertidal zones or estuaries which typically either utilize anaerobiosis and/or depress metabolism. Many cephalopods, as well as fishes and crustaceans, in OMZs and other hypoxic regions have some of the following adaptations to maintain aerobic metabolism at low P_{O_2} (Childress and Seibel, 1998; Mandic et al., 2009):

1. enhanced ventilatory ability
2. enhanced O_2 extraction from seawater
3. large gill surface area
4. short diffusion distance between seawater and blood
5. **Hc with low P_{50} (high affinity)**(e.g. *Vampyroteuthis infernalis;* Seibel et al., 1999)
6. low mass-specific metabolic rate
7. cytochrome c oxidase P_{50} (Lau et al., 2017)

If the physiological parameters driving P_{crit} in cephalopods are the same as in sculpins, then P_{50} is a stronger determinate of P_{crit} than msMO_2 or gill surface area (Mandic et al., 2009).

Childress and Seibel (1998) examined OMZ inhabiting crustaceans and found that their Pcrit often closely matched the lowest pO2 to which they are normally exposed. In a mysid shrimp species for which good data existed, they found that MO2 was the same, but Pcrit varied by location between the well oxygenated Hawaiian waters and the OMZ off California.

Very broadly, benthic octopod P_{crit}s are around 2-4 kPa at "normal" temperatures (Seibel and Childress, 2000) though there is, of course, lots of variation depending on environment and life history.

53.6.2.2 Scaling

In fishes, P_{crit} does not scale with body size (Nilsson and Östlund-Nilsson, 2008) because the gill surface area scales evenly with whole-animal M_{O_2} and thus provides a stable relative quantity of oxygen. This scaling trend is true both intra- and interspecifically. It also does not seem to scale with body size in cephalopods.

53.6.3 Cellular responses to decreasing oxygen

At least in mammalian cell culture, hypoxia raises RNA editing activity likely mediated through intracellular acidosis (Malik et al., 2021).

53.6.3.1 The four ranges of intracellular [O_2]

Connett et al. (1990) introduced a scheme of understanding cellular responses to oxygen levels that is relevant for hypoxia-sensitive cells (e.g. mammalian cells). Hypoxia-tolerant cells (e.g. turtle, *Dosidicus*) complicate matters due to metabolic suppression that combines levels 3 and 4. Regardless, for hypoxia-sensitive cells there are four [O_2] ranges:

1. Saturation: at high [O_2] the rate of oxidative phosphorylation (OP), and thus ATP formation, is not limited by [O_2]. In this range, a decrease in [O_2] will have:

   (a) no effect on metabolic state (i.e. AEC, redox state).

   (b) no effect on MO_2.

   (c) no effect on ATP turnover rate.

   Indicators(s): Everything at normal levels

2. OP compensation: at this range decreases in [O_2] must be compensated by changes in metabolic state in order to maintain the same ATP production. This range is characterized by:

   (a) decreased AEC and a more reduced redox state (i.e. NADH:NAD^+ increases).

   (b) no effect on MO_2.

   (c) no effect on ATP turnover rate.

   Indicators(s): decreased AEC, decreased Arg-P:Arg, but normal MO_2 and [octopine]

3. Anaerobic compensation: at this range [O_2] is so low that oxidative phosphorylation (OP) cannot maintain normal ATP production rate. Therefore, in order to maintain stable ATP supply, anaerobic pathways must compensate for the impaired OP pathway. This is known as the Pasteur effect and is characterized by:

   (a) decreased AEC and a reduced redox state.

   (b) decreased MO_2.

   (c) no effect on ATP turnover rate.

   Indicators(s): decreased MO_2, increased [octopine], but normal indicators of protein synthesis

4. Metabolic depression: at this lowest range the combination of aerobic and anaerobic pathways are unable to sustain enough ATP supply to match ATP demand. Therefore, the only way to maintain supply-demand balance is to decrease ATP demand (i.e. metabolic depression). At this range, there is:

   (a) decreased AEC and a reduced redox state.

   (b) decreased MO_2.

   (c) decreased ATP turnover rate.

   Indicators(s): decreased indicators of protein synthesis

Unlike cephalopods, oxyconformers do not utilize these four stages because mitochondrial [O_2] is the limiting substrate at all environmental P_{O_2} exposures (Pörtner and Grieshaber, 1993).

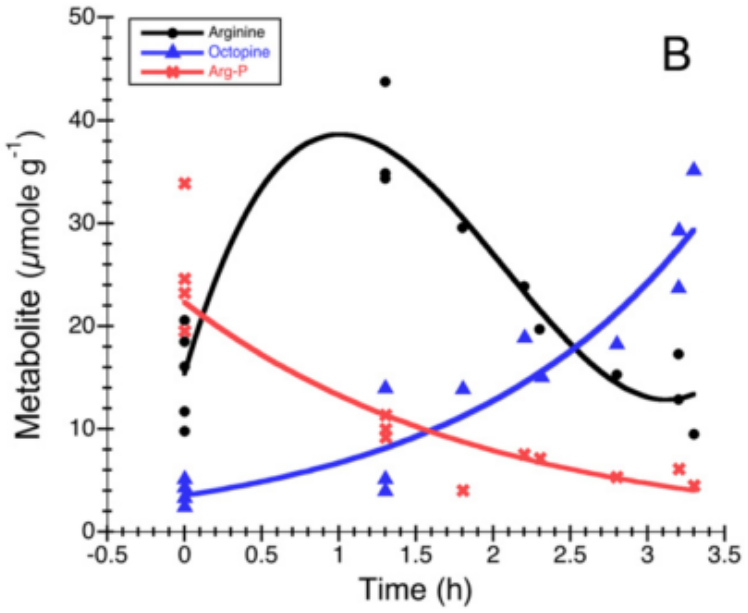

Figure 53.1: Cellular response to environmental hypoxia in *Dosidicus gigas* at P_{O_2} = 1.0 kPa; T = 10 ^{o}C.

53.6.3.2 Metabolites accumulate

Cytosol The metabolite levels of *Dosidicus gigas* under hypoxia at 10 ^{o}C have been well studied (Seibel et al., 2014; Seibel, 2015). While the timescale will scale with temperature, the trends discussed below are applicable to all cephalopods under environmental hypoxia (Figure 53.1): Initially, Arg-P levels start high, but decreased ATP synthesis from functional hypoxia is counterbalanced by ATP synthesis from the dephosphorylation of Arg-P to arginine. In one to a few hours, Arg-P reserves are spent (Seibel et al., 2014; Zielinski et al., 2000). Arginine begins to build in the cell until it reaches high concentrations where the rate of octopine synthesis (from arginine + pyruvate) increases (Rosa and Seibel, 2008; Seibel et al., 2014). Thus, octopine is a good indicator of cytosolic hypoxia (at least after a few hours of exposure) (Grieshaber et al., 1994). For every mole of octopine created, a mole of protons is also created. Importantly, octopine synthesis is a byproduct of glycolysis, not amino acid catabolism. Thus, octopine comes primarily from glycogen stores rather than "normal" AA metabolism. As stated above, the rate of these changes can vary. For *Lolliguncula brevis* under extreme hypoxia (2.8 kPa O_2) at 20 °C, the following intracellular changes occurred within 15 minutes of exposure: ↓ [ATP], ↑ [AMP], ↓ [Arg-P], ↑ [octopine], ↓ [HCO_3^-], and ↓ pH_i (Zielinski et al., 2000).

$$\text{pyruvate} + \text{arginine} + \text{NADH} + \text{H}^+ \overset{\text{ODH}}{\rightleftharpoons} \text{octopine} + \text{NAD}^+ + \text{H}_2\text{O}$$

While it is unclear whether octopine synthesized in hypoxic tissues leaves the tissues to be oxidized in another tissue at another time (), the decrease in all arginine-containing metabolites (Arg-P, Arg, octopine) in *Lolliguncula brevis* after 15 minutes at 2.8 kPa O_2 (T = 20 °C) suggests that octopine may be leaving the mantle tissues (Zielinski et al., 2000). Apparently ODH isoforms differ by tissue as well (as in vertebrate LDH; (Schulte, 2004)), with octopine-producing isoforms in anaerobic tissues and octopine-consuming isoforms in aerobic tissues . This also supports octopine leaving the tissues.

Mitochondria ATP are still produced in the mitochondria even under hypoxia when oxidative phosphorylation has shut down. Rather than the typical TCA cycle, however, malate is imported from the cytosol, and ultimately from glycogen stores. In the mitochondria, malate produces an ATP in its conversion to succinate. [succinate] increases and thus is a good indicator of mitochondrial anaerobiosis (Pörtner and Grieshaber, 1993). This also leads to the production of propionate.

53.6.3.3 Free energy of ATP hydrolysis falls

ATP is only a high energy molecule (highly negative ΔG) as long as there is lots of ATP and not much ADP. As ATP and ADP approach equilibrium, the ΔG approaches zero. Thus, when ATP levels are low, not only is there less ATP available, but each molecule also has less energy! At some threshold ΔG, ATP is no longer energetic enough to power enzymes and the cell dies. Some studies have shown that -52 kJ/mol is that threshold for ion pumping (e.g. NKA) (Richards, 2009).

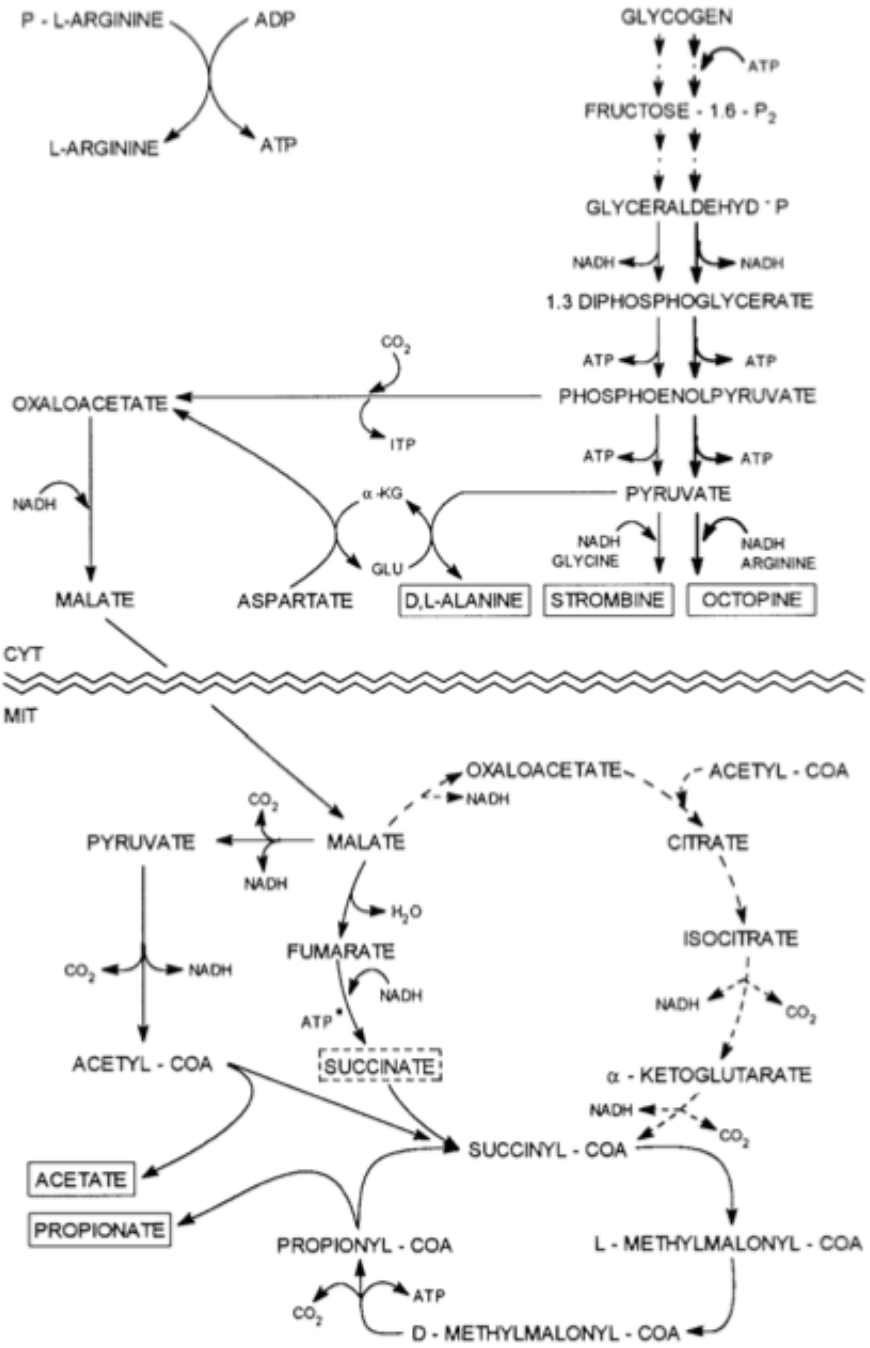

Figure 53.2: Anaerobic metabolite pathways. Figure from Grieshaber et al., 1994.

53.6.3.4 Intracellular acid-base balance

Under weak environmental hypoxia, many organisms induce respiratory alkalosis (see subsubsection 53.6.6.3). This draws CO_2 out of the tissues, thus decreasing intracellular P_{CO_2} and $[HCO_3^-]$ (as seen in *Lolliguncula brevis*, Zielinski et al., 2000). This mechanism also increases pH_i, but this increase may be masked by a larger decrease in pH driven by proton-producing anaerobic pathways leading to a net decrease in pH_i under hypoxia.

When environmental hypoxia is more severe, however, intracellular P_{CO_2} may increase relative to baseline due not to an increase in T_{CO_2}, but rather the decrease in pH_i driven by anaerobic mechanisms (increased $[H^+]$ increases P_{CO_2} at the expense of $[CO_3^{2-}]$).

When [ATP] falls, this results in the net production of H^+ (for an explanation, see section 29.1).

53.6.3.5 Reversal of ATP synthase activity

ATP synthase in mitochondria normally utilizes the H^+ gradient from the intermembrane space into the matrix to convert ADP to ATP. However, under extreme hypoxia or anoxia when the mitochondria are anoxic, the proton leakage out of the intermembrane space reverses the H^+ gradient and drives ATP synthase in the opposite direction, consuming ATP rather than producing it (Boutilier, 2001). Although no animals are known to be able to lower H^+ permeability and thus slow the proton leak, anoxia-tolerant animals are able to slow ATP synthase through a pH-dependent inhibitor, such that inhibition only occurs when the matrix becomes too acidic (Boutilier, 2001). This inhibition slows the wasteful ATP consumption.

53.6.3.6 Alteration of cellular membrane fluidity

Alteration in membrane cholesterol content can have strong impacts on membrane-bound proteins such as NKA and other ATP-demanding proteins.

It has been demonstrated at least in goldfish that super-P_{crit} hypoxia acclimation can result in enhancement of membrane cholesterol and slight increase in phospholipid saturation (Farhat et al., 2019).

53.6.3.7 Hypoxic hypoxanthine accumulation

During hypoxia, ATP levels fall and AMP accumulates. The accumulation of AMP pushes forward the first three steps of the following reaction series, resulting in accumulation of hypoxanthine during hypoxia (Saugstad, 1975).

$$\textbf{AMP} \overset{\text{nucleotidase}}{\rightleftharpoons} \textbf{adenosine} + P_i$$

$$\textbf{adenosine} \overset{\text{adenosine deaminase}}{\rightleftharpoons} \textbf{inosine} + NH_3$$

$$\textbf{inosine} + P_i \overset{\text{nucleoside phosphorylase}}{\rightleftharpoons} \textbf{hypoxanthine} + \text{ribose} - 1\,\text{phosphate}$$

Once oxygen returns, the accumulation of hypoxanthine can then lead to the production of lots of ROS.

$$\textbf{hypoxanthine} + O_2 \overset{\text{xanthine oxidase}}{\rightleftharpoons} \textbf{xanthine} + H_2O_2$$

$$\textbf{xanthine} + O_2 \overset{\text{xanthine oxidase}}{\rightleftharpoons} \textbf{uric acid} + H_2O_2$$

53.6.4 Metabolic suppression

Metabolic suppression in cephalopods has been best studied in *Dosidicus gigas* and thus, much of the knowledge and generalizations in this area have been shaped by this species. However, *Gonatus* have also been suggested to suppress metabolism under hypoxia (Seibel et al., 2000a). *Octopus bimaculatus* and *bimaculoides* also can suppress metabolism when they encounter hypoxia in intertidal or subtidal burrows (Seibel, pers. comm.).

When cells are unable to maintain aerobic metabolism (functional hypoxia), and anaerobic metabolism is unable to supplement the decrease in aerobic metabolism, the cephalopod suppresses its whole body metabolism in an effort to maintain ATP concentrations. In *D. gigas,* this is accompanied by decreased ventilation rate and lethargy (Rosa and Seibel, 2010a). Neural tissue has a much higher ATP demand than most other tissues and thus, will be heavily impacted by metabolic suppression (Nilsson and Östlund-Nilsson, 2008; Seibel et al., 2014).

53.6.4.1 Targets of suppression

Metabolic suppression tends to occur by suppression of the same kinds of processes in many different taxa (Richards, 2009). In hypoxia-tolerant cells, the two most dominant sources of energetic savings are suppression of protein synthesis and downregulation of NKA activity (Hochachka et al., 1996).

Membrane ion transport ATP-sensitive K^+ channels (K_{ATP} channels) open when intracellular [ATP] falls. This hyperpolarizes the cell which limits ATP-consuming action potentials and NKA activity (Shimoda and Polak, 2011). Downregulation of NKA activity has been reported in several tissues of several vertebrate species (Richards, 2009). Downregulation of brain NKA activity is correlated with activity: turtles (which hibernate) downregulate brain NKA while carp (which remain active) do not (Richards, 2009).

Alternatively, hypoxia tolerant cells (such as turtle hepatocytes) are able to both decrease NKA activity and yet maintain electrochemical gradients by decreasing membrane permeability to Na^+ and K^+ (known as channel arrest) (Hochachka et al., 1996). Channel arrest may be facilitated by increases in adenosine concentration since adenosine is an end product of ATP degradation and has been demonstrated to reduce cell excitability (Boutilier, 2001).

Transcription

Protein synthesis microRNAs, an important component of RNA interference (gene silencing), are upregulated in brain, muscle, and heart tissue during metabolic suppression in *Dosidicus* (Hadj-Moussa et al., 2018).

In some fishes, transcripts for proteins involved in protein synthesis (e.g. ribosomal protein transcripts) are downregulated (Richards, 2009). This saves a lot of energy since protein synthesis is a notable portion of total energy budget (subsection 51.9.4).

In eukaryotes generally, suppression of protein synthesis occurs most frequently through blocking the function of initiation or elongation factors (Hochachka et al., 1996).

Neuronal firing activity In turtle brain cells, synaptic rates lower under hypoxia to save energy (Hochachka et al., 1996).

Movement proteins In some fishes, transcripts for proteins involved in movement (e.g. actin and myosin) are downregulated (Richards, 2009). I expect this is especially pronounced in muscle tissue.

Gluconeogenesis

Cell growth / division In some fishes, transcripts for proteins involved in stimulating cell growth and division are downregulated and some involved in suppressing it are upregulated (Richards, 2009).

Other anabolic pathways

Upregulation of glucose transporters Fishes are known to upregulate glucose transporters to sustain glucose supply (Richards, 2009).

Upregulation of amino acid catabolism Apparently, amino acid catabolism is coupled with gluconeogenesis (Richards, 2009) at least in a fish species in which this has been examined. Thus, enzymes for amino acid catabolism are upregulated to result in glucose production and maintenance of fermentable substrates to sustain energy balance under hypoxia.

Upregulation of anaerobic enzymes Some fishes are known to upregulate LDH under hypoxia (Richards, 2009).

Altered regulation of metabolite transporters Fishes have been shown to increase transcript abundance of lactate and pyruvate transporters, increasing the tissue's ability to remove wastes (Richards, 2009).

Upregulation of vascular endothelial growth factors (VEGF) This at least occurs in mammals. I am not sure whether this occurs in cephalopods since they do not have consistent endothelial lining throughout their vascularization but they do have a VEGF receptor that is expressed during development (Yoshida et al., 2010).

Downregulation of protein degradation Under OMZ hypoxia, *Dosidicus gigas* increase Hsp70/Hsc70 but decrease antioxidant enzyme activities (Trübenbach et al., 2013). HSP activity likely increases in anticipation of high ROS production upon the individual's return towards the warm oxygenated surface waters.

53.6.4.2 Mechanisms of regulation

The mechanisms of suppression are protein kinases (e.g. AMPK) that add phosphate groups to enzymes (Richards, 2009) and miRNAs that turn off or down gene expression via chromatin condensation (Seibel et al., 2014) and commit post-transcriptional modifications (Ken Storey's talk). HIF is also activated and regulates gene expression.

HIF See subsection 39.4.1.

AMPK and other protein kinases AMP-activated protein kinase (AMPK) is known in mammals to lower anabolic rates such as glycogen, fatty acid, and protein synthesis (Richards, 2009).

Other In *D. gigas*, the regulatory enzyme 4EBP (eukaryotic translation initiation factor 4E binding protein) has been shown to suppress mRNA translation in the brain, heart, and gills (Seibel et al., 2014).

To help the animal during recovery from suppression, miRNAs modify mRNAs and quarantine them within protein granules. When environmental oxygen later rises, the mRNAs are released and can quickly begin normal protein synthesis rather than having to begin at transcription again (Ken Storey's talk).

Because protein synthesis is depressed under metabolic suppression, more un-utilized ammonia is released, increasing ammonia excretion and decreasing the O:N ratio.

53.6.5 Oxygen debt and cell death

Oxygen debt can be quantified mechanistically through, for example, cellular metabolites such as octopine or succinate or can be estimated externally through a proportional index such as oxygen deficit (DO_2) (Claireaux and Chabot, 2016):

$$DO_2 = \sum_{t=0}^{t=end} P_{crit} - P_{O_2\ env}$$

with a time increment (e.g. 5 minutes). When an individual reaches a critical temperature-dependent DO_2, death occurs.

Time-to-death The time-to-death is dependent on 1. the animal's ability to suppress metabolism and 2. the quantity of fermentable substrate reserves (e.g. glycogen) (Richards, 2009). Hypoxia intolerant species suppress metabolism little below P_{crit} and thus run out of fermentable substrates and die quickly. Hypoxia tolerant species, however, suppress metabolism greatly and thus can survive longer because the rate of utilization of the fermentable substrates is much lower (Boutilier, 2001). Due to the lower msM_{O_2} of larger cephalopods, all else being equal, large cephalopods can maintain Connett et al. (1990)'s third P_{O_2} range: anaerobic compensation (subsection 53.6.3) for a longer duration than smaller cephalopods (Nilsson and Östlund-Nilsson, 2008). This is because they require a lower anaerobic glycolytic rate to reach their basal ATP synthesis rate, and because they have larger glycogen stores than smaller cephalopods.

Death is triggered when fermentable substrates are unavailable and ATP supply limits essential ATP consuming processes (Richards, 2009). NKA activity is arguably the most relevant ATP consuming process that fails; after all, NKA alone consumes ~30% of normal metabolic ATP production. When NKA shut down, the cell depolarizes which allows the invasion of Ca^{2+} into the cytosol from organelles and extracellular fluid. This, in turn, triggers phospholipases (phospholipid hydrolyzers) and Ca^{2+}-dependent proteases (protein degraders). Once these are active, the cell membrane and proteins quickly are destroyed and the cell is no more.

53.6.6 Impact on specific body systems

53.6.6.1 Ventilation and respiratory rate

In squids, ventilation rate and ventilatory stroke volume have been found to remain constant at all P_{O_2} (until metabolic suppression) (*Lolliguncula brevis*; Wells et al., 1988) in some cases, but in others, ventilation rate and stroke volume both increase with progressive hypoxia (Birk, 2018). O_2 extraction efficiency increases with decreasing P_{O_2}, however so that enough O_2 is reaching the blood.

In octopuses and cuttlefishes, by contrast, O_2 extraction efficiency remains stable under hypoxia (Wells and Wells, 1982, 1985), and both ventilation rate and ventilatory stroke volume increase to compensate for decreased seawater P_{O_2} (Wells and Wells, 1995, 1985). Houlihan et al. (1982) found *Octopus vulgaris* to decrease ventilation rate rather than increase. Increasing stroke volume seems to lower P_{crit} more than increasing ventilation rate (Wells and Wells, 1985). Below P_{crit}, however, *Octopus* ventilation rate and stroke volume have been shown to decrease as metabolic rate drops (Wells and Wells, 1995). This makes energetic sense since ventilation is costly with little benefit in extreme hypoxia.

In comparison, fish and crustaceans typically increase ventilation rate under hypoxia (Perry and Gilmour, 2002; McMahon, 2001).

Changes in seawater P_{O_2} are detected by the branchial ganglia and that information is transferred to the central nervous system which tells the mantle musculature to modify ventilation (Wells and Wells, 1995). Cephalopods may be similar to fishes which have neuroepithelial cells which detect O_2 and also CO_2 (Perry and Gilmour, 2002). Because the ventilatory dynamics are neurally controlled, the dynamics change within a couple ventilations of encountering water with a new P_{O_2} (Wells and Wells, 1995).

53.6.6.2 Gill lamellae

Many fishes have been shown to increase their "functional respiratory surface area" under hypoxia by increasing blood pressure in the gills and altering lamellar vasoconstriction to enhance blood flow through optimal channels for O_2 uptake as well as contracting pillar cells on the outer surfaces of the lamellae (decreasing tissue thickness; see subsection 51.1.2)(Nilsson, 2007). These alterations to the gills are induced by neurotransmitters and hormones (Nilsson, 2007). Similar mechanisms in cephalopods may be present, but there is some evidence to suggest otherwise. *Octopus vulgaris* have been found to maintain similar P_{crit} despite a surgical 50+% reduction in gill surface area, suggesting that gill surface area is not limiting hypoxia tolerance (Wells and Wells, 1984). Thus, altered gill perfusion is not necessary under hypoxia.

In addition, cephalopods may respond similarly to shrimps which have been demonstrated to lengthen their gill lamellae by 10% after hypoxia exposure (Peruzza's SEB talk). Stingrays, similarly have exhibited a 70% increase in gill surface area after chronic hypoxia (~6 kPa) exposure (Dabruzzi and Bennett, 2014).

Bathyteuthis bacidifera are endemic to the ETP and equatorial Indian Ocean (both contain OMZs) and have notably larger gills than the cosmopolitan *Bathyteuthis abyssicola* (Roper, 1969). Furthermore, gill size within populations of *B. abyssicola* covaried with ambient P_{O_2} between specimens captured in the Southern Ocean, vs. Atlantic, vs. the ETP (Roper, 1969).

53.6.6.3 Circulatory and blood responses to decreasing oxygen

Cardiovascular dynamics Cephalopod systemic hearts are bathed in oxygenated blood from the gills (subsection 51.2.2) and thus may be limited when environmental hypoxia becomes too low to provide enough oxygen for heart muscle metabolism.

In squids, heartbeat frequency is stable throughout a range of hypoxia levels except under very high temperatures where (presumably) metabolic suppression slows heartbeat until death (*Lolliguncula brevis*; Wells et al., 1988). In *Octopus*, however, the systemic and branchial hearts decrease heart rate (bradycardia), pulse pressure amplitude, and stroke volume within seconds upon exposure to hypoxia (Wells, 1980; Wells and Wells, 1983, 1986). Bradycardia is also a common response to hypoxia in fishes (Perry and Gilmour, 2002), though in humans heart rate increases at altitude. This seems to be due to a drop in blood P_{O_2} directly, rather than a nervous control from the CNS or branchial ganglia (Wells and Wells, 1995; Wells, 1980). This causes a decrease in blood flow (Wells and Wells, 1986). This response, combined with increased blood pH under hypoxia may allow the circulatory costs to drop while maintaining at least some O_2 delivery.

In the bathypelagic shrimp, *Gnathophausia ingens*, hypoxia has no effect on blood pressure ().

Blood composition Blood sugar levels lower at least within 15 minutes of severe hypoxia, if not sooner (Storey et al., 1979).

Hemocyanin It is common in most organisms with circulatory systems to increase respiratory pigment concentration in response to prolonged hypoxia (Burnett and Stickle, 2001; Head, 2010; Tommerdahl et al., 2015; DeFur et al., 1990). In vertebrates, this is stimulated by hypoxia-induced production of erythropoietin (EPO), a protein that causes increased production of RBCs (Richards, 2009). In crabs (and others, I'm sure), upregulation of [Hc] is due to HIF-1 (Head, 2010). Increase of blood pigment concentration is likely in cephalopods as well, at least to a moderate extent as permitted by blood viscosity and osmolarity. Embryonic *Doryteuthis opalescens* under combined OA and hypoxia more than doubled hemocyanin mRNA expression levels compared to control animals (Pierce, 2017). Li et al. (2017) found that hemocyanin gene expression was initially downregulated, then upregulated, then downregulated again during progressive hypoxia to 6 kPa, a curious result.

As a general rule in organisms, short-term hypoxia elicits allosteric modifiers to modulate the affinity of Hc to O_2, while long-term hypoxia promotes increased Hc synthesis and blood [Hc] (Terwilliger, 1998). Cephalopods are not known to have as

many allosteric modifiers as vertebrates with RBCs though. Though they do have glycosylation sites that strongly influence quaternary structure (Thonig et al., 2014).

Differences in P_{50} are also possible (Snyder, 1985; Winslow, 2007). Mandic et al. (2009) found that P_{50} explained much variation in sculpin P_{crit}. Midwater crustaceans in the relatively hypoxic waters off California have higher hemocyanin-O_2 binding affinity than species off Hawaii where P_{O_2} is higher (Childress, 1995). Crabs exposed to chronic hypoxia could alter hemocyanin subunit isoform abundance to produce hemocyanins with lower P_{50}s (DeFur et al., 1990). Similarly, cod populations in the North Atlantic are known to have polymorphic hemoglobin variants that vary based on ambient O_2 levels (Andersen et al., 2009) and the same molecular principle occurs in high altitude birds. In humans, RBC intracellular pH alters the [2,3-DPG], which in turn allosterically bind to hemoglobin and alter P_{50} (Winslow, 2007), and such a phenomenon may likely be convergently evolved in cephalopod hemocyanins (Gai et al., 2015).

Crustacean hemocyanin isoforms have been shown to be changed by hypoxia and these isoforms have different allosteric sensitivities (Kölsch et al., 2013).

Cavefishes that inhabit hypoxic caves have been shown to increase RBC size and maintain [Hb] within the RBCs, thus increasing total [Hb] in the blood relative to surface-dwelling conspecifics (Boggs et al., 2022).

pH A number of cephalopod species have been shown to increase pH_e under hypoxia (*Octopus vulgaris,* Houlihan et al. 1982; *Sepia officinalis*, Johansen et al. 1982; *Dosidicus gigas* and for a review Seibel et al. 2014). This alkalosis facilitates Hc-O_2 binding at the gills despite the low environmental P_{O_2}. This is caused potentially by the Haldane effect: O_2 deprived Hc entering the tissues pick up and draw away metabolically produced CO_2 (Häfker, 2012). This blood alkalosis may at least sometimes be induced by increased ventilation rate which not only increases CO_2 offgassing (to increase pH_e) but also increases the water flux past the gills (Seibel et al., 2014). It can also occur by sacrificing intracellular pH (Seibel et al., 2014).

Hypoxia can also lead to decreased pH_e. In a variety of organisms (though maybe documented in cephalopods to date), hypoxia-induced cellular acidosis acidifies the blood which results in decreased O_2-binding affinity (Pörtner and Grieshaber, 1993). Thus arterial O_2 content in the blood may decrease under hypoxia not only due to environmental decrease in P_{O_2} but also due to decrease Hc-O_2 binding affinity.

Vascular endothelial cells At least in mammals, endothelial cells lining blood vessels of organs are the most sensitive cells in the organs to ischemia and reperfusion (I/R) (Carden and Granger, 2000). Mammalian blood vessels trigger an acute inflammatory response (subsection 51.8.3) and the endothelial cells undergo numerous changes after I/R such as changes in membrane potential and fluidity, differential gene expression, cellular swelling, lifting off from the basement membrane, and attachment of white blood cells to the cell surface (Carden and Granger, 2000). In mammals, the arterioles, capillaries, and venules respond to I/R somewhat differently:

- the main response of arterioles is an impaired ability to export nitric oxide (NO) to the smooth muscle for vasodilation (Carden and Granger, 2000). As a result, any endothelium-dependent mechanism of vasodilation (e.g. acetylcholine) cannot work, resulting in vasoconstriction and restricted blood flow to the organ.
- the main responses of capillaries are increased fluid filtration and reduction in capillary perfusion (Carden and Granger, 2000).
  - The increased fluid filtration may at least in part be due to the suppression of nitric oxide export from the endothelia.
  - The reduction in capillary perfusion seems to be due to a mixture of
    - clogging of capillaries with white blood cells (WBCs) and platelets
    - flow reduction from the swollen and partially detached vascular endothelia
    - WBC-dependent stimulation of interstitial fluid accumulation, which builds pressure that compresses the capillaries
- the main responses of venules are inflammation and oxidative stress (Carden and Granger, 2000)(subsection 51.8.3).
  - The inflammation results in increased leakiness.
  - The venules have a greater oxidative stress than arterioles or capillaries, because WBCs accumulate in the venules, and they (along with the endothelia themselves) produce ROS. Vascular endothelia are rich in xanthine oxidase, which can produce large amounts of ROS during reperfusion, due to hypoxanthine accumulation during ischemia (see (subsubsection 53.6.3.7)).

In cephalopods, however, the large vessels (e.g. dorsal aorta) and smallest vessels have incomplete or a complete lack of endothelial cells (Wells, 1983; Abbott and Miyan, 1995), and they do not have white blood cells (WBCs) so their blood vessels could be more hypoxic resistant than in mammals.

53.6.6.4 Cutaneous respiration

Unlike the whole animal, cephalopod skin is oxyconforming (at least in vitro), with a decreased MO_2 with decreasing P_{O_2} (Madan and Wells, 1996).

53.6.6.5 Chromatophore expression

While the metabolic cost of chromatophore expression has never been assessed to date, there is some evidence that their activity is impacted by environmental O_2. *Octopus bimaculoides* and *Octopus californicus* both turn completely white under anoxia exposure (Seibel and Childress, 2000). Though, chromatophore expression was still possible when disturbed even in anoxia. This suggests that the chromatophores are able to get at least some of their O_2 from the blood (rather than solely through cutaneous respiration). Similarly, *Octopus vulgaris* has been documented to change from brown to pale grey under hypoxia (Wells and Wells, 1983).

53.6.6.6 Vision

Paralarval octopus and squid as well as larval arthropods show a decline in retinal sensitivity to light under hypoxia (McCormick et al., 2019).

At least in snapper, hypoxia impairs visual acuity (Robinson et al., 2013).

53.6.6.7 Nervous system function

Impacts on hypoxia-sensitive taxa At least in mammalian brain neurons, hypoxia causes an initial hyperpolarization (caused by K_{ATP} channels; see subsubsection 30.2.2.6) followed by a depolarization (caused by inhibition of K_v channels, an influx of Na^+, and fall in ATP-dependent NKA activity) and rise in $[Ca^{2+}]$ levels (caused by Ca_v channels) (Shimoda and Polak, 2011).

Additionally, glutamate uptake proteins that are normally powered by the transmembrane ion gradient begin to shut down, allowing extracellular glutamate to accumulate and activate glutamate receptors that, in turn, allow Ca^{2+} influx. All this intracellular Ca^{2+} can trigger proteases, nucleases, and cell death (section 39.10).

Independently of the Ca^{2+} influx problem, triggering of glutamate receptors as well as failure of NKA causes a rise in $[Na^+]$ and concomitant loss in membrane potential, which triggers a voltage-gated Cl^- channel to open. The combined rise in Na^+ and Cl^- raises osmolarity sufficiently to cause water to enter the cell, leading to neuronal swelling through cytotoxic edema (Rungta et al., 2015).

Adaptations of hypoxia-tolerant taxa Hypoxic-adaptations may include the following:

- minimizing intracellular hypoxia (e.g. perfusion, globins)
- reducing energy consumption
- shifting metabolic demands among cell types
- exocytotic damage resistance
- necrosis/apoptosis resistance
- oxidative stress resistance
- facilitating re-establishment of homeostasis

Seals and whales have higher cerebral capillary density than non-diving species, which minimizes the diffusion distance and thus can provide sufficient oxygen to tissues for a longer time than otherwise (Larson et al., 2014).

Neuronal function (e.g. ability to fire) is longer under hypoxia in species that are adapted to hypoxia than those that are not. This has been demonstrated in seals (Mitz et al., 2009) and bivalves (Kraus and Colacino, 1986).

In hypoxia-tolerant brain neurons (such as in turtles), inhibitory neurotransmitters are upregulated and excitatory neurotransmitters are downregulated.

Both Arctic ground squirrel and naked mole-rat brains are adapted such that even when extracellular glutamate levels accumulate, this does not lead to excytotoxicity (Larson et al., 2014).

Seals express much more cytochrome c protein in astrocytes than terrestrial mammals, suggestive that they may have outsourced ATP production to astrocytes so that the neurons do not have as high of a metabolic load during hypoxic dives (Mitz

et al., 2009). If so, the neurons would be more anaerobic and the astrocytes could process lactate production from the neurons (Mitz et al., 2009).

Some seals have been demonstrated to cool their brains by 3-4°C during dives, which should lower metabolic demand (Larson et al., 2014).

Epaulette sharks reduce metabolic rate and whole brain cytochrome c oxidase activity. These responses combined with others allows their brains to maintain ATP levels for an hour in anoxia (Gillian Renshaw's work).

Neuroglobin See subsection 34.1.2.

Hypoxia-mediated miRNA induction Comparative analysis of miRNAs in hypoxia- and anoxia-tolerant vertebrates (crucian carp, painted turtle, leopard frog, and epaulette shark) demonstrates that in tolerant lower vertebrates, the differentially expressed miRNAs are each unique in each species, evolving in its own divergent way to attain similar characteristics (e.g. metabolic suppression) (Riggs et al., 2018). Similar lack of commonality occurs across animals (Hadj-Moussa and Storey, 2020). Therefore, miRNA responses in one species may not be any indicator of how any other species will respond.

With that being said, in *Dosidicus gigas*, the following miRNAs are upregulated in the whole brain after a few hours of whole-animal hypoxic exposure (Hadj-Moussa et al., 2018):

miR-33 In human liver cells, miR-33 has been shown to regulate both glucose and lipid metabolism (Ramírez et al. 2013). In human melanocytes, miR-33 targets the 3' UTR of HIF – 1α (Zhao et al. 2017). Similarly, in hypoxia-tolerant crayfish muscle, hypoxia downregulates miR-33, which should ameliorate HIF – 1α degradation and allow the HIF-1 dimer to form (English et al., 2018).

miR-67

miR-133 In mammalian cardiomyocytes, transfection with miR-133a reduces apoptosis during I/R (Li et al 2015). Also upregulated in periwinkle foot muscle in response to hypoxia (Hadj-Moussa and Storey, 2020) and in altitude-adapted great tits (Hadj-Moussa and Storey, 2020).

miR-1175

Additionally, in non-cephalopod taxa, the following miRNAs have also be demonstrated to upregulate under brain hypoxia (Hadj-Moussa and Storey, 2020):

miR-10 crucian carp

miR-17 epaulette shark (not sure if brain)

miR-20a epaulette shark (not sure if brain)

miR-24 naked mole rat

miR-27 naked mole rat

miR-92 epaulette shark (not sure if brain)

miR-138 epaulette shark (not sure if brain)

miR-140 epaulette shark (not sure if brain)

miR-143 epaulette shark (not sure if brain)

miR-146b epaulette shark (not sure if brain)

miR-181a epaulette shark (not sure if brain)

miR-182 crucian carp, red-eared slider turtle

miR-207 naked mole rat

miR-592 naked mole rat

miR-6497 crucian carp, red-eared slider turtle

Differential expression of miR-210 is also a common response (Hadj-Moussa and Storey, 2020) because it affects HIF (subsection 39.4.1).

In general, across multiple animal comparisons, less hypoxia-tolerant taxa have more responsive miRNA profiles (i.e. more miRNAs are differentially expressed) (Hadj-Moussa and Storey, 2020).

53.6.7 Impact on behavior

Since all cephalopods are mobile, they will likely seek to migrate out of hypoxic waters, when possible (Wu, 2002).

When exposed to hypoxia, most ectotherms (cephalopods likely included) prefer a cooler habitat to lower oxygen demands (Boutilier, 2001).

Lolliguncula brevis have been observed to migrate in and out of hypoxic regions. This may be an excellent hunting strategy since many burrowing animals are known to come out of their burrows and stay on top of the benthos under hypoxia, easy prey items for squids (Wu, 2002).

Schooling squids are likely similar to herring which spread out in their school formations under extreme hypoxia, maintaining the school shape, but increasing inter-individual distances (Domenici et al., 2002).

Many animals reduce feeding under prolonged hypoxia, which (combined with the downregulation of protein synthesis) leads to reduced growth under hypoxia (Wu, 2002).

53.6.8 Biogeographic boundaries set by oxygen

Animals require oxygen to fuel metabolic production of ATP for maintenance, prey capture and consumption, locomotion, and growth (). Individual animals can survive for a limited time in very low oxygen (the survivable duration depending on species, temperature, and the magnitude of the hypoxic event) by lowering one or more of the above contributions to oxygen demand (e.g. moving less, fasting). Populations, however, require a higher O_2 threshold to be maintained than any given individual. Deutsch et al. (2015) developed a "metabolic index" to quantify how suitable a habitat is for aerobic metabolism. They found that populations of a variety of marine organisms require 2-5x the ambient O_2 as any given individual in those populations needs to survive. This extra oxygen provides an "aerobic scope" for activities such as locomotion, feeding, growth, and reproduction.

Cephalopods inhabit all oceans and seas except the Baltic and Black Seas (Nixon and Young, 2003). They are likely absent from these regions due to O_2 limitation. Other than OMZs, the Baltic and Black Seas are the only seas where P_{O_2} is quite low even as shallow as 100 m. According to the 2005 WOA, P_{O_2} is 40% saturated in both seas at 100 m. The Black Sea can even be anoxic as shallow as 100-200 m (Rabalais et al., 2010).

OMZ inhabiting cephalopods, fishes, and crustaceans tend to have lower M_{O_2} than their counterparts that inhabit surface waters. This has likely evolved due to light levels rather than P_{O_2}, however (see section 53.1), though it is certainly an exaptation (secondarily adaptive) in OMZs.

Additionally, coastal cephalopods may be limited in how long they can inhabit shallow tide pools. Some more hypoxia-tolerant species may be able to inhabit oxygen-poor tide pools longer than other species, as has been demonstrated in sculpins (Mandic et al., 2009) and triplefins (Devaux's SEB talk).

Artificial experiments with O_2 gradients have confirmed field behaviors in fishes of hypoxia avoidance (Burleson et al., 2001).

53.6.8.1 The metabolic index (Φ)

The metabolic index (Φ) is a ratio of O_2 supply in the environment to O_2 demand of an organism as follows:

$$\Phi = \frac{O_2\ \text{Supply}_{\text{env}}}{O_2\ \text{Demand}_{\text{organism}}} = \frac{\alpha_S B^{\delta} PO_2}{\alpha_D B^{\varepsilon} \exp(-E_0/k_B T)} = A_0 B^{n} \frac{PO_2}{\exp(-E_0/k_B T)}$$

where:

α_s per-mass rate of gas transfer between environment and organism (e.g. μmol $O_2 \cdot g^{-1} \cdot hr^{-1} \cdot kPa^{-1}$ O_2).

α_D organism's baseline metabolic rate (e.g. μmol $O_2 \cdot g^{-1} \cdot hr^{-1}$)

B body mass (e.g. g)

δ allometric scaling coefficient of α_S with body mass

ε allometric scaling coefficient of α_D with body mass

E_0 temperature dependence of A_0

k_B Boltzmann's constant

A_0 α_s/α_D, ratio of the rate coefficients for O_2 supply and metabolic rate

n $\delta - \varepsilon$, difference between allometric scaling of gas transfer and baseline metabolic rate

In practice, A_0, n, and E_0 can be calculated if Pcrit ($\Phi = 1$) at a variety of temperatures is known. This leaves B, PO_2, and T (all of which are known) to calculate Φ for an individual of a given body size. When $\Phi < 1$ then supply is less than demand and the organism must either utilize anaerobic metabolism or suppress metabolism. Deutsch et al. (2015) examined the distributions of 4 species of ectotherms in relation to Φ and found that species only inhabit geographic areas where Φ is at least between 2 and 5. Thus they defined Φ_{crit} for these species as 2-5. Therefore, Φ_{crit} defines the equatorward latitudinal range limit for a variety of ectotherms, potentially including cephalopods.

53.6.8.2 P_{50} depth

The P_{50} depth is a metric for estimating the depth limit of an organism before reaching hypoxic water (Mislan et al., 2015). It is based on the empirical relationship between P_{50} and P_{crit} in sculpins (though I cannot think of a reason why the principle would not apply to cephalopods) (Mislan et al., 2015). P_{50} depth is a function of P_{50}, temperature, and the heat of oxygenation (amount of heat released when O_2 binds Hc). In much of the pelagic ocean, P_{O_2} is high enough that no P_{50} depth occurs at all. They primarily occur in OMZs such as the ETP, Arabian Sea, Bay of Bengal, and North Pacific (Mislan et al., 2015). The breadth and depth of P_{50} depths are species-specific. For cephalopods, <30% of the pelagic ocean has a P_{50} depth that could be hypoxic (Mislan et al., 2015).

53.6.8.3 Habitat choice behavior influenced by O_2

Some species of cephalopods (notably *Lolliguncula brevis* as a good example) enter hypoxic water masses that are sub-Pcrit typically in search of prey or to avoid predation (Bartol et al., 2002). *Lolliguncula brevis* have excellent hypoxia tolerance that enables them to be one of the few nekton that inhabit the eutrophication-induced "dead zones" of the Gulf of Mexico. Based on experimental hypoxia tolerance tests (Zielinski et al., 2000), their metabolite levels reach their extremes within 15 minutes in extreme hypoxia (2.8 kPa O_2, 20 °C) which suggests that *L. brevis* must be utilizing O_2-rich microhabitats within the broader dead zones.

Cephalopods may behave similarly to cod by freely entering hypoxic regions when an O_2 refuge is nearby but, choosing instead to avoid these hypoxic regions when a normoxic O_2 refuge is not immediately available (Herbert et al., 2011).

53.7 pH

53.7.1 Historical perspective

Both ammonites and belemnites had calcareous planktonic stages. There is a correlation between ammonite and belemnite extinctions and OA events which suggests that their phragmocones were unable to be maintained in the OA conditions they faced (Arkhipkin and Laptikhovsky, 2012). This is concerning in light of modern-day OA because belemnites were relatively active predators (similar to cuttlefish or squids) and they had an internal phragmocone.

53.7.2 Metabolic suppression

Environmental decreases in pH can lead to metabolic depression. For example, *Dosidicus gigas* experienced a 10-30% metabolic depression as a result of a pH decrease from 7.93 to 7.62. This depression was observed in most but not all combinations of activity levels and temperatures ranging from 10 to 25 ^{o}C (Rosa and Seibel, 2008).

53.7.3 Impact on specific body systems

Embryonic *Sepioteuthis lessoniana* have been shown to increase the expression of a number of key acid-base regulatory enzymes in response to decreased seawater pH (Hu et al., 2013).

Increased ammonia excretion is a possible response to decreased pH due to its coupling to proton excretion (RhP are colocalized with NHE3) (Hu et al., 2013) but if true, the effect is small (Hu et al., 2014).

At least in mammalian systems, intracellular acidosis raises RNA editing activity (Malik et al., 2021).

53.7.3.1 Blood acid-base buffering

Cephalopod blood is buffered by both bicarbonate and non-bicarbonate buffering capacities. Non-bicarbonate buffering is achieved primarily via proteins in the blood, thus higher blood protein content increases non-bicarbonate buffering capacity. Non-bicarbonate buffering may be energetically more favorable (once the proteins are synthesized) under environmental acidosis because it does not depend upon the constant energy required to maintain blood [HCO_3^-] at up to 5x as high as seawater [HCO_3^-].

This may be particularly beneficial in environments with large frequent fluctuations in pH (as in coastal regions) (Small et al., 2015) because there is no lag in buffering response for non-bicarbonate buffers as there is in accumulating HCO_3^- which can take hours (Gutowska et al., 2010; Hu et al., 2014).

Blood HCO_3^- is primarily up- and down-regulated by acid-base balance proteins in the gills (e.g. NBC) (subsection 51.1.6).

53.7.3.2 O_2 delivery to tissues

At least at extreme pH values (<7 or >10), hemocyanin subunits can disassociate, but their sensitivity to pH is lessened by Mg^{2+} (Van Holde and Cohen, 1965).

An increase in seawater P_{CO_2} from 40 to 100 Pa would increase P_{50} by roughly 0.5 kPa when there's no compensation. So how would a 0.5 kPa increase in P_{50} affect metabolism? The answer to that question depends on the arterial P_{O_2} ($P_{O_{2a}}$). If $P_{O_{2a}}$ is near P_{100} (the minimal P_{O_2} required to fully saturate the hemocyanin) then a 0.5 kPa shift in the O_2-binding curve may be enough for $P_{O_{2a}}$ to fall along the steep slope of the curve (not fully saturate) and thus provide insufficient quantities of O_2 to the tissues resulting in metabolic suppression. If, on the other hand, $P_{O_{2a}} >> P_{100}$ then a 0.5 kPa shift in the curve would probably have little effect on O_2 delivery.

For blood pH = 7.4, P_{100} is about 10-13 kPa for both loliginids and ommastrephids (Pörtner, 1990; Seibel, 2013). If I use Redfield and Goodkind (1929)'s $P_{O_{2a}}$ measured from *Doryteuthis pealeii* (16 kPa) then a 0.5 kPa shift in the curve (or 0.04 pH unit shift) would have very little effect on saturation because 16 kPa >> P_{100}. Arterial P_{O_2} may be lower at times, however; it is poorly studied.

53.7.3.3 Gill morphology and ventilation

Some fishes are known to decrease diffusion distance across the gills and also hyperventilate due to hypercapnia on the order of 100 Pa (Esbaugh et al., 2016).

53.7.3.4 CO_2 excretion

Heightened P_{CO_2} in seawater lowers the P_{CO_2} gradient from the blood to seawater. At a seawater pH of 8.1, seawater P_{CO_2} is ~40 Pa. Resting squid blood typically has a pH of ~7.4 and P_{CO_2} near 300 Pa (Hu et al., 2014). For these conditions, the P_{CO_2} gradient is 260 Pa. However, when the pH lowers, seawater P_{CO_2} increases and can easily reach 100 Pa in oxygen minimum zones. Under these conditions, the P_{CO_2} gradient is only 200 Pa, or 23% lower. According to Fick's law (subsection 51.1.2), this will lower CO_2 diffusion across the gills by 23%. To alleviate this issue, cephalopods allow blood P_{CO_2} to increase to maintain the diffusion gradient and increase blood $[HCO_3^-]$ as well to maintain a stable blood pH (Hu et al., 2014; Gutowska et al., 2010).

53.7.3.5 Calcification

Cuttlefish exposed to high CO_2 (low pH) have been demonstrated to hypercalcify their cuttlebones through a currently-unknown mechanism. This is likely related to blood T_{CO_2} being raised so high. Mussels, in contrast, have been shown to have the internal sides of their shells dissolve when their blood is hypercapnic (Melzner et al. 2011).

53.7.3.6 Intracellular pH

Based on studies in fishes, it is likely that under hypercapnia intracellular P_{CO_2} and $[HCO_3^-]$ increase and thus seawater pH has little or no effect on intracellular pH (Heuer and Grosell, 2014).

53.7.4 Impact on behavior

Changes in environmental pH/CO_2 have been found to cause numerous changes in animal behavior (Regan et al., 2016) such as altered activity levels, olfactory and auditory responses, and impaired learning. In *Idiosepius*, hypercapnia has been shown to increase activity levels and preference to escape rather than defense responses to predatory stimuli (Spady et al., 2014).

When exposed to strong hypercapnia such that oxygen supply is limited, most ectotherms (cephalopods likely included) prefer a cooler habitat to lower oxygen demands (Boutilier, 2001).

53.7.4.1 GABA receptors

It is believed that behavioral alterations are due to acid-base compensation of the blood (subsection 51.1.6). At least in teleosts, acid-base compensation both increases HCO_3^- and reduces Cl^- concentrations in blood. These two ions are both regulated in neurons by GABA receptors (subsection 36.8.3). When GABA receptors are activated they normally cause Cl^- and/or HCO_3^-

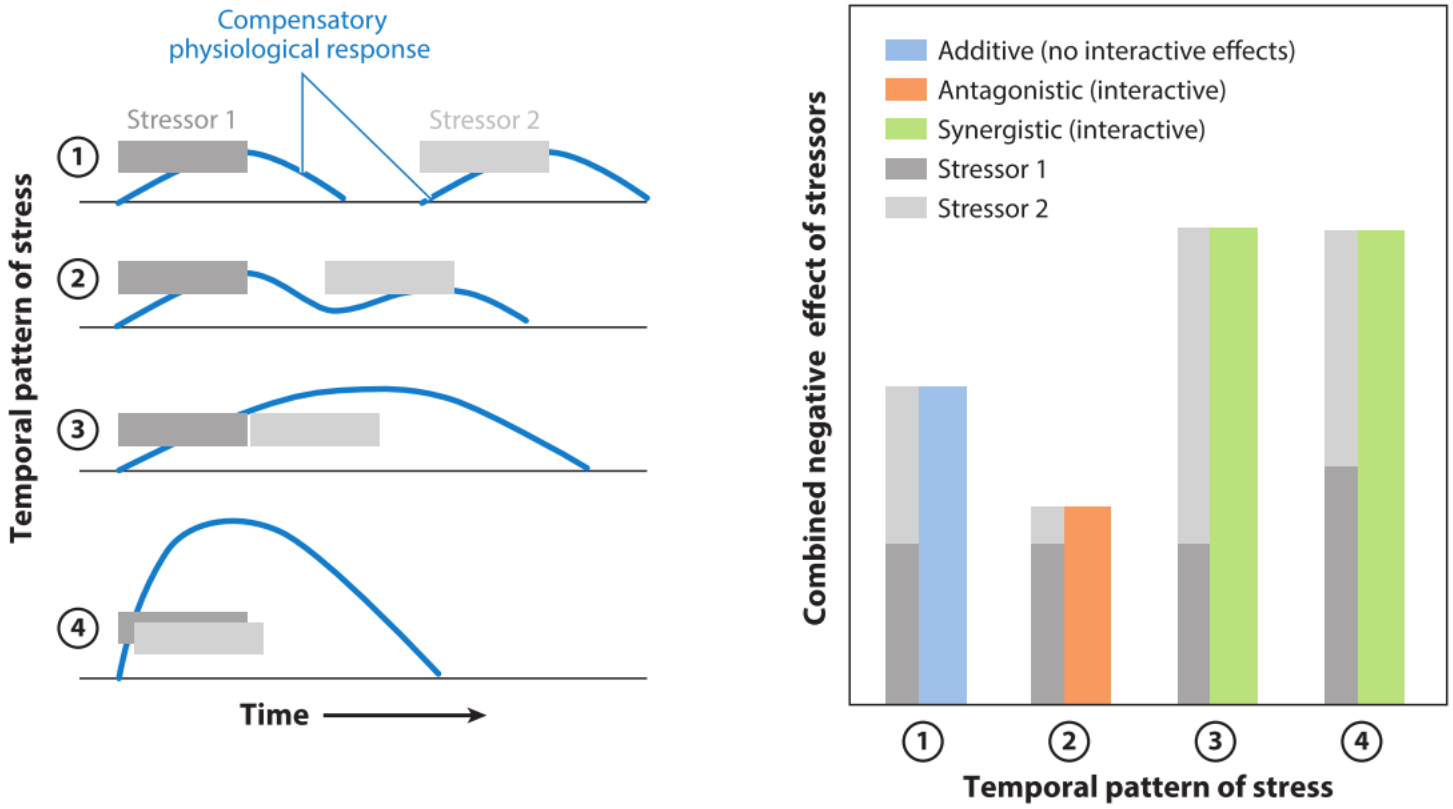

Figure 53.3: Theoretical effects of combined stressors depending on timing and interaction. Originally from Gunderson et al. 2016.

to enter the cell, hyperpolarizing it. When blood is acid-compensated, however, the electrochemical gradients can shift such that Cl^- and HCO_3^- now exit the cell upon activation, depolarizing it and making GABA now excitatory rather than inhibitory (Nilsson et al., 2012). This is quantitatively assessed by (Heuer and Grosell, 2014).

I am curious how this plays out in cephalopods. Unlike teleosts, which decrease blood Cl^- during compensation, I see no reason why cephalopod blood Cl^- should decrease (Hu and Tseng, 2017). Therefore, I am curious if an increase in blood HCO_3^- alone without any changes in Cl^- would affect the electrochemical gradients and whether the excitatory response would remain.

53.7.5 Biogeographic boundaries set by pH

53.7.5.1 Habitat choice behavior influenced by pH

53.8 Combined stressors

Cephalopods that inhabit tide pools at night, coral reefs, kelp forests, estuaries, or eastern boundary currents during upwelling events experience low pH simultaneously with low P_{O_2} (Gunderson et al., 2016).

53.8.1 Theory

All organisms, cephalopods included, have highly conserved cellular stress response pathways for acclimating to abiotic stressors (chapter 39). Thus, the physiological responses to multiple stressors may often interact to cause non-additive effects Figure 53.3.

Synergistic effects are most likely to occur when multiple stressors co-occur simultaneously. Antagonistic effects are most likely to occur when stressors are asynchronous but occur over a short timescale (this has been shown in tide pool sculpins which had better hypoxia tolerance if exposed to high temperature first). Finally, additive effects are most likely to occur when multiple stressors are asynchronous over long (e.g. seasonal) timescales (Gunderson et al., 2016).

If multiple stressors have a selective pressure on a trait in the same direction (e.g. temperature and hypoxia both encourage enhanced O_2 supply), then the selective force on that trait will be larger than due to just one stressor (Schulte's SEB talk).

53.8.2 Temperature and hypoxia

Cephalopods may alter their preferred habitat temperature due to hypoxia, preferring lower temperatures in hypoxic water (as has been demonstrated in trout (Schurmann et al., 1991)). Interspecific comparisons in fishes have shown that there is no relationship between adaptation temperature and P_{crit} (Rogers et al., 2016).

A recent experiment on red drum in a hypoxia shuttlebox demonstrated that the hypoxic threshold at which fish avoided the hypoxic side of the box was at a higher PO2 at warmer temperatures than cold temperature (Ern and Esbaugh 2021, J. of Fish Biol.).

Chapter 54

Responses to exercise

54.1 At rest

For reference to resting ventilation in cephalopods, see subsection 51.1.3.

54.2 Biomechanics of swimming

Pitch rotating around the left-right axis (angling up and down)

Yaw rotating around the dorsal-ventral axis (spinning in circles)

Roll rotating around the anterior-posterior axis (barrel rolling)

All aspects of locomotion are controlled by a neural circuit that is a central pattern generator (CPG).

Fishes have been shown to utilize existing water movement in their environment and actually take advantage of this to swim more efficiently in natural water than laminar flow (Liao, 2022). I am not aware that this has been assessed in squids.

54.2.1 Jet propulsion

Jet propulsion is a very inefficient technique for locomotion, particularly in a viscous medium like seawater. The jetting behavior is composed of two parts: filling the mantle with seawater, and expelling the water in the mantle cavity at high velocity through the funnel. Both of these parts are very inefficient: when a cephalopod fills its mantle with seawater before expelling it, it increases both mass and drag. When the water is expelled through the funnel, the cephalopod is limited compared to a fish in that it can only move the volume in its mantle cavity (O'Dor and Hoar, 2000). To get the same forward thrust as a fish which undulates a large volume of water at low velocity, a cephalopod must expel its small volume of water at high velocity (O'Dor, 2013). Jet propulsion decreases in efficiency with increasing size (O'Dor and Hoar, 2000; Bartol et al., 2008). This is likely why loliginids scale allometrically to favor fins over jetting as they grow (O'Dor and Hoar, 2000) and why *Vampyroteuthis infernalis* evolved a transition from jetting to fin-based locomotion during its metamorphosis (Seibel et al., 1998). Paralarval squids utilize jet propulsion exclusively rather than fin beating (Bartol et al., 2008).

While jetting, squids hold out their fins and arms III with keels to generate lift while swimming (Bartol et al., 2001).

The efficiency of a locomotion behavior can be quantified with the Froude number which is the ratio of power output to power input. As an example of how inefficient jet propulsion is compared to the undulatory fin movements of fishes, the Froude efficiency of *Doryteuthis opalescens* is less than 1/3rd of a similar sized trout (Alexander 1977 cited in (O'Dor and Webber, 1986). Additionally, *Illex illecebrosus* uses 6x as much energy per unit distance than a salmon of the same length (Webber and O'Dor, 1985). Cephalopod cost of transport does, however, seem to be lower than in crustaceans (O'Dor and Webber, 1986).

The efficiency of jet propulsion does vary among cephalopods. For example, cuttlefishes have an intermediate efficiency between *Nautilus* and squids (Gladman's SEB poster).

54.2.2 Fin beating

Fin beating is almost absent in paralarval squids due to their small fin size (Bartol et al., 2008).

Squids utilize their fins more at low speeds than high speeds (Bartol et al., 2001). This is for two reasons: 1. fin beating creates more drag at higher speeds than low speeds and thus is less efficient, and 2. fin beating creates more upward thrust

(by pushing water down) than jetting horizontally and thus is more efficient than jetting at low speeds when fighting negative buoyancy is required.

54.2.3 Medusoid contractions

54.2.4 Turning

Squids utilize their fins to help induce a roll during their turns (Bartol's 2022 CIAC talk).

54.3 Respiratory response

In *Octopus,* gill surface area limits aerobic scope for activity (Wells and Wells, 1984).

Oxygen consumption increases with exercise (Seguin and Lavoisier, 1789).

Ventilation rate (VR) increases with increasing speeds but in a non-linear fashion. VR increases up to its apparent peak rate (in order to allow time for the water to enter and exit the mantle cavity) of ~100 ventilations per minute (*Doryteuthis opalescens*; Shadwick et al., 1990).

Ventilatory stroke volume also increases with exercise relative to rest. This serves two functions: 1. it pushes more water out the funnel to provide thrust, and 2. it increases the volume of water in contact with the gills which increases O_2 uptake ability (Wells et al., 1988).

During mantle contraction, mantle cavity pressure increases greatly. Swimming jetting creates mantle cavity pressure ~2-6 kPa in squids and sepiids (Shadwick et al., 1990; Melzner et al., 2006b) and, interesting, a much higher 9 kPa in *Octopus* (Shadwick, 1994). Escape jetting, utilizing the giant axon, creates high pressure in the mantle cavity (~10-25 kPa in most cephalopods (Shadwick et al., 1990; Wells, 1990)).

The percentage of O_2 extracted from the water with each ventilation is quite low, at least in squids (Shadwick et al., 1990). Exercise jetting decreases percent extraction (Shadwick et al., 1990; Melzner et al., 2006b) and recovery after exercise increases extraction relative to a baseline resting extraction rate. *Lolliguncula brevis*, for example, extracts ~7% of O_2 from the water when at rest, extracts as little as 2% during swimming, and extracts at most 15% when recovering from exercise (Wells et al., 1988). Similarly, *Doryteuthis opalescens* extracts 11% at rest and as little as 5% when exercising (Shadwick et al., 1990).

54.4 Cardiovascular response

As exercise increases, heart rate (HR) increases as well up to a peak rate of ~120 bpm (*Doryteuthis opalescens*; Shadwick et al., 1990) at least in squids. Apparently, *Octopus* HR does not increase with exercise but instead blood pressure and stroke volume increase (Wells, 1983). In *Octopus,* systolic blood pressure in the dorsal aorta can commonly exceed 10 kPa when walking (compared to 3-7 kPa at rest)(Wells and Smith, 1987). This is likely indicative of their poor adaptation to constant active locomotion. In fact, the *Octopus* heart is impaired by each jet contraction, stopping aortic flow!

In squids, once HR begins to max out, cardiac stroke volume increases exponentially with exercise (Wells et al., 1988; Shadwick et al., 1990). Wells et al. (1988) calculate that the systemic heart must pump more than its own mass in blood with each contraction.

Together, the increased HR and stroke volume lead to an exponential increase in cardiac output (ml blood / min) with exercise. For example, *Doryteuthis opalescens* at 12 °C have a blood circulation time of 34 seconds at rest but a mere 3.4 seconds above their U_{crit} (Shadwick et al., 1990)! The cardiac output of active squids is much higher than octopuses, cuttlefishes, or nautiloids, closer to mammalian cardiac output (Shadwick et al., 1990). Similarly, fishes raise both HR and stroke volume during exercise (Priede and Tytler, 1977).

Exercise-induced cardiac responses are facilitated from CNS control through the visceral nerve (Wells, 1980).

At least in mammals, maximal heart rate (at MMR) is consistent in various species regardless of how active or sedentary they are, suggesting that active lifestyles in mammals are supported by changes in CSV and blood [O_2] rather than HR (Weibel et al., 1991).

54.5 Tissue response

In fatigued mantle muscle, the Arg-P to [Arg-P + Arg] ratio is only ~10-30%, down from 70% in resting mantle muscle (*Doryteuthis pealeii* and *Illex illecebrosus*; Pörtner et al., 1993).

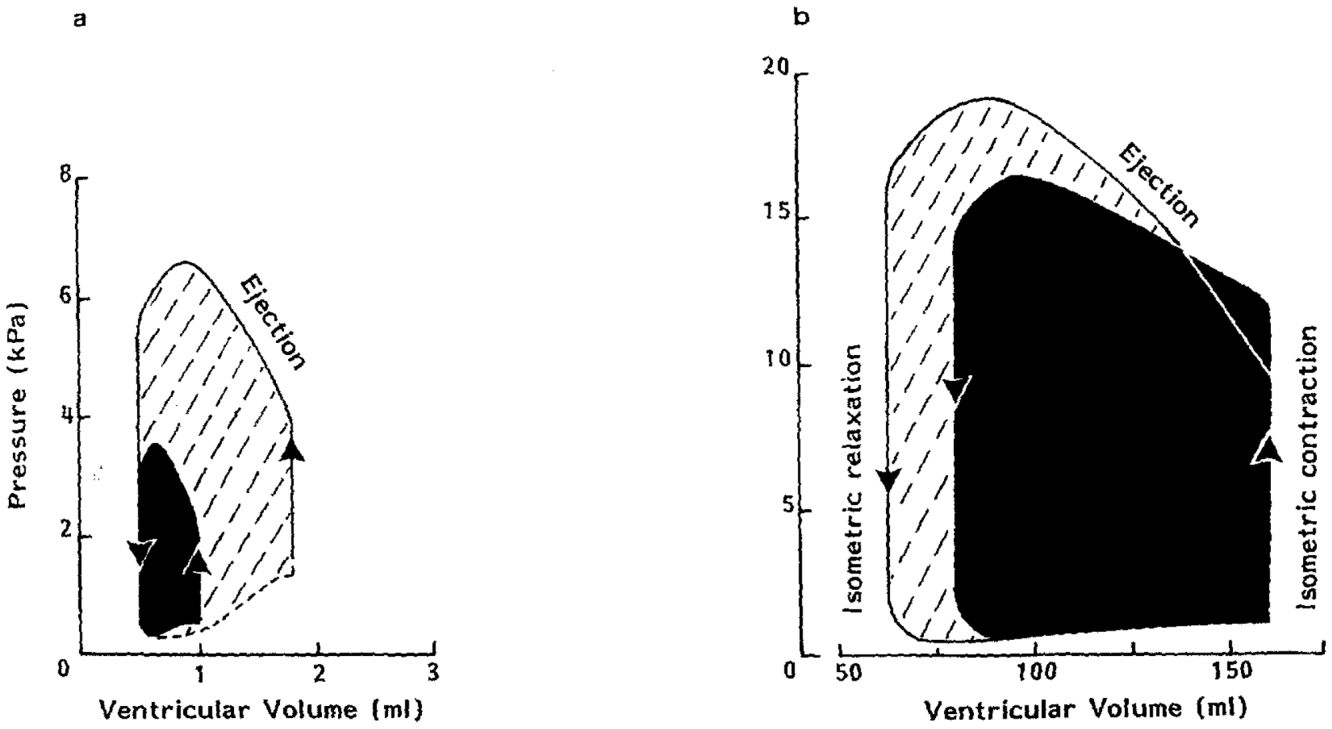

Figure 54.1: PV loops demonstrating the contrasting cardiovascular response to walking exercise of *Octopus* (left) vs humans (right). Figure from Wells and Smith, 1987. Notice that 1) the proportional increase in PV area (ventricular effort) is much greater in *Octopus.* 2) *Octopus* raises stroke volume by increasing end-diastolic volume (bottom right of loop), while humans raise stroke volume by decreasing end-systolic volume (top left of loop).

54.5.1 Octopine accumulation

$$\text{pyruvate} + \text{arginine} + \text{NADH} + \text{H}^+ \overset{\text{ODH}}{\rightleftharpoons} \text{octopine} + \text{NAD}^+ + \text{H}_2\text{O}$$

It seems likely that octopine built up in cephalopod mantle muscle during exercise is metabolized within the mantle tissue later during recovery, rather than some of the octopine leaving the mantle to the bloodstream to be oxidized by other tissues like the brain. For *Illex illecebrosus* and *Doryteuthis pealeii* under both exhaustion and recovery, arginine containing compounds remain at equal levels to resting conditions and blood [octopine] never changed, indicating that octopine is not released during exercise for these species (Pörtner et al., 1993). Likewise, isolated *Sepia* mantle muscle has been shown to not build up nor release any appreciable amount of octopine during exhaustive exercise, though some does build up during recovery (see below)(Sykes et al., in review). However, in adult *Sepia,* exhaustive exercise causes mantle octopine to rise from 0.2 to 8.6 μmol/g (Storey and Storey, 1979). A similar pattern has been documented in scallops where isolated muscle would not produce octopine but a whole animal swum to exhaustion would, suggesting that perhaps a blood-bourne signal stimulates octopine production.

Succinate concentrations increase in exhausted squids compared to resting levels (*Illex illecebrosus*; (Pörtner et al., 1993).

At least in mammals, changes in chronic activity levels can lead to changes in mitochondrial abundance and membrane composition due, in part, to upregulation of PGC-1α (Moyes, 2003).

54.6 Recovery

When scallops are forced to swim to exhaustion, octopine does not accumulate during the exercise, but only later during recovery (cited in Sykes et al, in review) although this seems different than occurs in squids (Pörtner et al., 1993).

After stressful exercise (capture), *D. pealeii* have been shown to require about 1 hour for blood pH to return to a pre-exercise level (Howell and Gilbert, 1976).

For an ommastrephid squid at 15 $^{\text{o}}$C, metabolite levels begin to return to normal 10 minutes after exhaustion and are back to normal within 60 minutes of recovery (Pörtner et al., 1993). Experiments from isolated *Sepia officinalis* mantle muscle suggest that the octopine produced by exhaustion is converted back to pyruvate and arginine locally within the muscle and is not appreciably extruded into the blood (Sykes et al., in review).

Global protein synthesis rates rise slightly in mantle muscle in the 1 hour of recovering from exhaustive exercise (Sykes et al., in review) as also occurs in mammalian muscle (cited in Sykes et al., in review).

54.6.0.1 Gluconeogenesis

Glycogen reserves are restored via gluconeogenesis. Based on the high enzymatic activity of PEPCK (the first enzyme in gluconeogenesis) in mantle muscle (Speers-Roesch et al., 2016), it seems likely that gluconeogenesis begins directly in the mantle muscle. But enzyme activities are not high for enzymes later in gluconeogenesis (Speers-Roesch et al., 2016). Thus, it may be that during recovery, gluconeogenesis begins directly in the mantle muscle and intermediate product(s) are sent to the digestive gland (where the remaining enzyme activities are high) to complete gluconeogenesis before returning the final glycogen product to the mantle tissues.

54.7 Integrated, whole-animal response

54.7.1 Metabolic rate and aerobic scope

Exercise typically increases an individual's oxygen requirement, utilizing the organism's aerobic scope (Fry, 1947). The breadth of an individual's aerobic scope is, in part, a function of environmental P_{O_2} (Figure 54.2) such that as environmental P_{O_2} decreases from air saturation down to Pcrit, aerobic scope decreases to zero (Claireaux and Chabot, 2016). However, for cephalopods which fight against their negative buoyancy to remain in the water column, swimming at an intermediate rate can require less oxygen than no or very little swimming due to the lift force generated by swimming (Bartol et al., 2001). Thus, MO_2 can scale with swimming speed not linearly, but rather in a J- or U-shape relationship.

Aerobic scope is rather low in cephalopods compared to vertebrates. Vertebrates often have factorial aerobic scopes ≈5-8 (Gillooly et al., 2017) while cephalopods are often lower. *Lolliguncula brevis* has been shown to have a factorial AS < 2 (Bartol et al., 2001). Terrestrial animals generally range from 1.5-7 (cited by Deutsch et al manuscript).

MMR can generally be very accurately estimated by $\text{BMR} \times 21/P_{\text{crit}}$, for species that do not encounter chronic hypoxia (for those that do, 21 should be adjusted to the hypoxic level in which they've evolved) (Seibel and Deutsch, 2020).

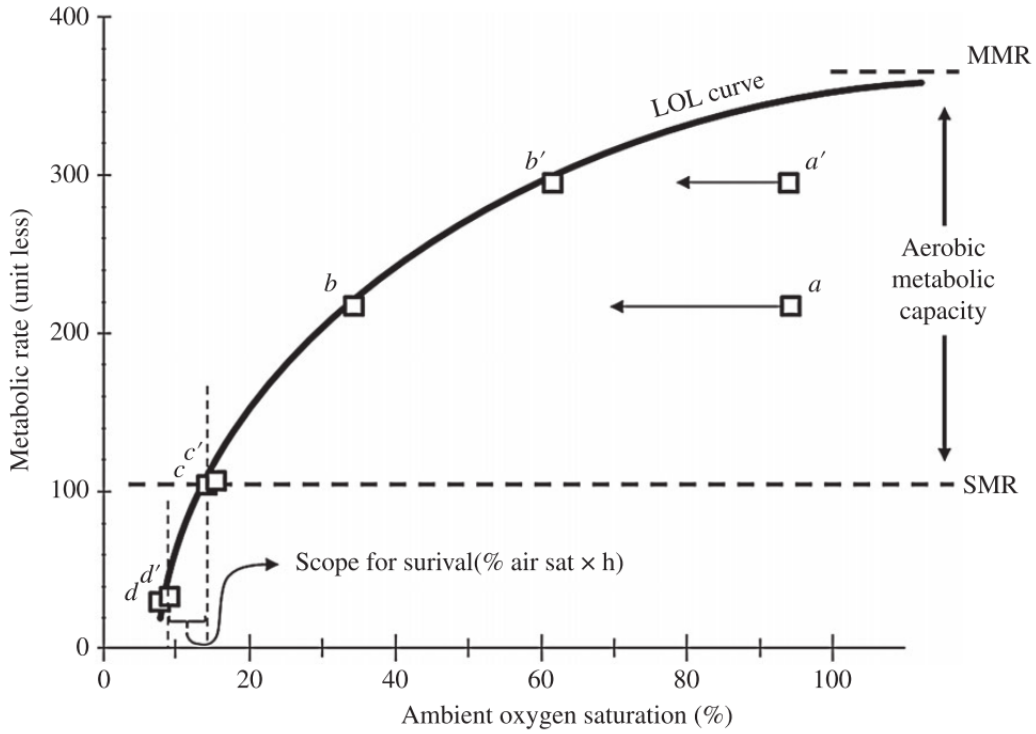

Figure 54.2: Theoretical limiting oxygen level (LOL) curve. *c* indicates Pcrit. Figure originally from (Claireaux and Chabot, 2016).

54.7.2 Critical swimming speed (U_{crit})

A cephalopod's exercise limit can be due to any process along the oxygen delivery pathway (e.g. getting O_2 from seawater to blood, getting O_2 from blood to tissues, getting O_2 to the heart).

Chapter 55

Responses to feeding and starvation

When food is sufficient, cephalopods fuel most of their metabolic demands via protein catabolism due to their predatory diet (Speers-Roesch et al., 2016; Lee, 1995). Despite this high proteinaceous metabolism, many cephalopods store large quantities of lipids in their digestive gland (Lee, 1995) that are the first fuel mobilized during fasting. Most cephalopods do not store much lipid reserves anywhere else in the body.

Among commonly studied shallow water cephalopods at moderate temperatures (10-30°C), the oro-anal transit time is 2-12 hours in teuthoid squids and 8-30 hours in octopus, *Sepia*, and *Nautilus* (Ponte et al., 2017).

In *S. officinalis* after 3-5 days starvation (T = 20°C), M_{O_2} was half the normal rate and NH_3 excretion a third (Lamarre et al., 2016). Fractional protein synthesis rate also fell to 25-50% of the rate in fed animals with a corresponding rise in the protease cathepsin expression (Lamarre et al., 2016) suggesting a strong shift towards net protein catabolism.

55.1 Specific dynamic action

After a meal, metabolic rate rises in under a few hours due to the metabolic demands of digestion (Rogers et al., 2016). To support SDA, *Octopus* have been shown to increase cardiac output by 50% when regularly fed, compared with 12 hour fasted animals (Wells et al., 1983).

55.2 Blood content

Within an hour or so of consumption, *Enteroctopus dofleini* blood glucose levels rise and remain high for at least 7 hours post-consumption (Goddard, 1968).

55.3 Cellular starvation progression

55.3.1 Step 1: Utilize lipids and ketone bodies from the digestive gland

During starvation, the digestive gland mass falls disproportionately to total body mass (Ponte et al., 2017). Well-fed *Sepia officinalis* maintain ~15 mg/g triacylglycerol (TAG) in their digestive gland. Within 3-5 days of starvation (T = 20 °C) however, TAG utilize much of this reserve, leaving only ~1/4 remaining. By 12 days, [TAG] is negligible (Speers-Roesch et al., 2016).

Sepia tissues possess some activity to catabolize the ketone body acetoacetate and this enzyme is maintained throughout starvation (Speers-Roesch et al., 2016). The acetoacetate is presumably released by the digestive gland along with TAG and other fatty acids, as is well understood in mammalian livers.

55.3.2 Step 2: Utilize protein from body tissues

Glycerol in mantle tissue is not utilized during starvation, being reserved instead for rapid locomotion when needed. Instead, protein catabolism fuels metabolism, as suggested by a lack of decrease in AspAT activity even after 12 days starvation in *Sepia* (Speers-Roesch et al., 2016).

Part IX

Their behavior and ecology

Packard (1972) proposed that cephalopods exist as they do today due to competition and inter-predation with fishes. This is likely given that these kind of interactions can lead to both species developing similar physiologies (e.g. Seibel et al., 2007).

Cephalopod behavior is a function of both internal physiological processes and external environmental factors with different behaviors relying more heavily on one, the other, or both (Clements and Hunt, 2015).

When the OMZ shoals, zooplankton and deep sea fishes are pushed into the photic zone (Wishner et al., 2013) and predation pressure increases which decreases populations Koslow et al. (2011).

55.3.3 Diel vertical migration

Many cephalopods are diel vertical migrators. Even nautiloids, with a more limited behavioral repertoire are diel vertical migrators (Nixon and Young, 2003). In most cases, this behavior seems driven by both predator avoidance and prey seeking.

Chapter 56

Cephalopods and their biogeography

56.1 Latitudinal effects

Biogeography is strongly impacted by not only the current abiotic and biotic conditions of a habitat, but also the historical conditions of that habitat and the evolutionary history of the taxon of interest (Rosa et al., 2008a).

As with many other taxa, coastal cephalopod diversity is highest at low latitudes and decreases towards the poles. Rosa et al. (2008a) found that cephalopod diversity on both the western and eastern margins of the Atlantic peak at 20 °N and 40 °N, respectively. The latitudinal range size (i.e. how many degrees of latitude a species inhabits) of a given species is function of the latitude it inhabits and its size at hatching. For example, Antarctic neritic cephalopods have a very small latitudinal range size (20^{o} or less) because their stenothermal habitat requirements do not let them expand beyond the Southern Ocean. Atlantic neritic cephalopods near the equator, however, have the largest latitudinal size range (up to 75^{o}) because they can survive in habitats both north and south of their ideal temperature (Rosa et al., 2008a). This pattern was not observed for pelagic or deep benthic cephalopods in the Atlantic, however. The richness of these taxa is more closely correlated to high net primary productivity (Rosa et al., 2008b). In general, large-sized hatchlings (benthic) have a smaller latitudinal range size than small-sized hatchlings (planktonic) (Villanueva's 2015 CIAC talk).

Cephalopod maximal body size also scales with latitude on a group-specific basis: in the Atlantic Ocean, cuttlefishes increase in body size from the Southern Ocean to the Arctic, teuthid body size is inversely related to temperature such that low-latitude species are smaller than high latitude species, and octopods on the eastern Atlantic follow a similar trend as teuthids (Rosa et al., 2012a).

56.2 Bathymetric effects

Bathymetric effects may be due to either light or pressure.

The diversity of pelagic cephalopods decreases with depth in the Atlantic Ocean starting at the meso-bathypelagic interface (Rosa et al., 2008b). Benthic cephalopod diversity in the Atlantic decreases with depth as well. Cuttlefishes are not found below 500 m and cirrate octopods are the only benthic cephalopods found deeper than 2000-3000 m (Rosa et al., 2008b).

Pterygioteuthis species are the most abundant cephalopods in the mesopelagic .

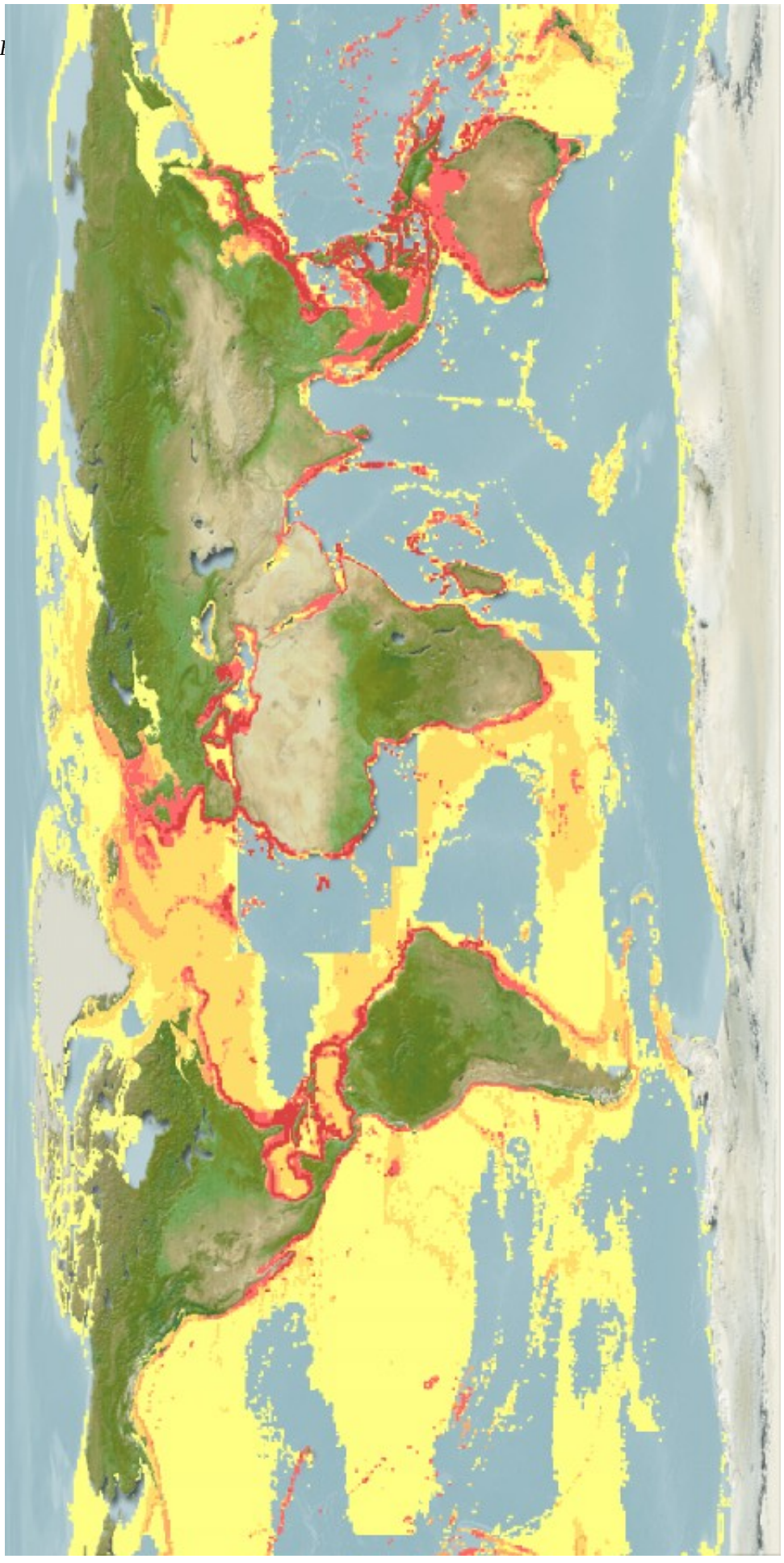

Figure 56.1: Cephalopod biodiversity map. Darkest red = 22-46 species. Created by AquaMaps. Last updated: 2016-09-07.

Chapter 57

Cephalopods and themselves

Polarization vision may be useful for navigation.

57.1 Locomotory behavior

Swimming behavior is ultimately controlled by the median basal lobe in the supra-esophageal mass of the brain (Budelmann, 1995).

57.1.1 Climb-and-glide swimming

Climb-and-glide locomotion is a behavior exhibited by many negatively buoyant flying and swimming animals. It is characterized by short active ascents followed by long passive descents. *Dosidicus,* for example, have been demonstrated to exhibit this behavior very frequently *in situ*. They angle upwards >45 ° fins first and jet up for about 10 seconds, gaining a few meters, before turning and gliding horizontally often for over a minute, slowly sinking at about 5-15 cm/s and moving forward around 30 cm/s for about 10 m or so (Gilly et al., 2012). This basic locomotory behavior can be adapted to, for example, rapidly climb >10 meters or slowly drift to greater depths. During the glides, the arms are flattened to utilize the keel on the arms III to stabilize. The same kind of behavior has been reported during DVM ascents by *Loligo forbesii* (Cones, et al. 2022, MEPS).

57.1.2 Walking/running

Octopus will "walk" or "run" along the substrate as a primary means of locomotion, unless rapid but short-term jetting is required. Rather large *Octopus* (~800 g) on exercise wheels have been demonstrated to run at up to 10 $cm \cdot s^{-1}$ (Wells and Smith, 1987). Generally, octopuses prefer to use arm pairs III and IV for walking and crawling (Bidel's 2022 CIAC talk).

57.1.3 Migrations

The maximum sustainable speed for *I. illecebrosus* is 75 $cm \cdot s^{-1}$ (Wells and Smith, 1987).

57.1.3.1 Diel vertical migrations

Many pelagic cephalopods, as well as many pelagic animals generally undergo diel vertical migrations in the open ocean. There are three patterns of DVM (Cohen and Forward, 2009):

1. the most common: ascending near sunset and descending near sunrise
2. twilight DVM: ascending near sunset, descending during the night, ascending again near sunrise, and descending again during the day
3. reverse DVM: ascending near sunrise and descending near sunset

There are three benefits to "normal" DVM behavior:

1. migrating to dark depths during the day avoids visually-oriented predators
2. migrating to cold depths during the day lowers metabolism and thus saves energy

3. migrating helps animals follow their migrating prey

Among these reasons, predator avoidance seems to be the most important. Reasons 2 and 3 do not apply to Antarctic fishes hunting krill yet they still migrate (Robison, 2004). In *Daphnia,* altering predator abundance alters the occurrence and depth of DVM (Loose and Dawidowicz, 1994). Indeed, predatory kairomones (chemicals released by one species to give advantageous information to another species) are a strong proximate driver of DVM (Cohen and Forward, 2009).

Many zooplankton and small fishes undergo diel vertical migrations often hundreds of meters. The most convincing hypothesis for this great energy expenditure is avoidance of visual predators during the day. In support of this idea, experiments in lakes as well as in-situ experiments on *Daphnia* have shown that DVM diminishes when predators are absent. This has also been demonstrated in marine zooplankton (Cohen and Forward, 2009).

These taxa will even DVM into shallow oxygen minimum zones (Wishner et al., 2013) in order to reach their preferred daytime light level.

DVM greatly enhances rates of the biological pump (Brierley, 2014).

The depth and timing of migration varies seasonally and by lunar phase (Ursella et al. 2021, Progress in Oceanography).

At least in the western Gulf of Mexico, shallow migrators (0-100 m) come up about an hour before sunset and descend again when the sun is about 20° below the horizon, while deeper migrators (400-600 m) migrate when the sun passes 35° above the horizon (Ursella et al. 2021, Progress in Oceanography).

In fishes, euphausiids, and copepods at least smaller individuals tend to be higher in the water column during the day than larger conspecifics (Cohen and Forward, 2009).

Aggregations of zooplankton can even produce vertically mixing eddies and produce instability in the water column when migrating (Houghton et al., 2018).

Light guide hypotheses There are 3 leading hypotheses for how animals sense when and how far to migrate daily (Cohen and Forward, 2009).

1. Animals follow an isolume as the isolume moves up at night and down during the day. This hypothesis is supported by a variety of field observations but variable behavior and technical challenges with quantifying isolume depths make this hypothesis less than 100% convincing.

2. Animals are triggered by an absolute intensity threshold. When light falls below a certain threshold, ascent begins. When light rises above a certain threshold, descent begins.

3. Animals are triggered by a rate-of-change of the light.

57.1.3.2 Ontogenetic migrations

Since most cephalopods have a lifespan of roughly one year, when cephalopods migrate annually it is often for both seasonal and ontogenetic purposes. Many squids migrate annually between feeding grounds and spawning grounds (Arkhipkin, 2013; Hixon, 1980). These migrations can be driven by a number of factors such as temperature, food availability, and appropriate spawning habitat.

Ommastrephid squids are known to migrate rather long distances, but they may use a swim-glide behavior to make the migration much less energetically costly than constant swimming (O'Dor, 1988; Gilly et al., 2012). *Dosidicus* have been tracked to travel on average 30 km / day in the Gulf of California (Gilly et al., 2006) though most squid move slower, between 3 and 30 km / day.

57.1.4 Emersion

The following octopods have been documented to emerse themselves in the wild: *Octopus vulgaris, Abdopus aculeatus, O. tetricus, O. rubescens*, and probably others.

57.2 Cognition

The historical view of the evolution of intelligence (based on vertebrate systems such as apes, cetaceans, elephants, birds) contends that intelligence evolves due to 1) long life histories and 2) complex social interactions (Amodio et al., 2019). Coleoids, however, lack both traits yet are highly intelligent. Intelligence is hard to quantify but can be estimated by neurological morphology and behavioral flexibility (Amodio et al., 2019). Cephalopod intelligence likely evolved due to a combination of the need for complex foraging behavior (Ecological Intelligence Hypothesis) and the need to avoid predation (Amodio et al., 2019).

57.2.1 Learning and memory

Octopuses have been demonstrated to improve foraging techniques on bivalves with experience (cited in (Amodio et al., 2019)).

57.2.1.1 Neurological basis

Learning and memory are often possible through increased synaptic strength between neurons that are repeatedly stimulated. This is known as long term potentiation (Brown and Piscopo, 2013). See section 36.9.

The vertical lobe is thought to be the brain region that stores memories.

57.2.1.2 Behavior

Octopuses can learn by observing the behavior of conspecifics (Fiorito talk at CIAC). Even *Nautilus* have been demonstrated to form short- and long-term memories.

Cuttlefish have been demonstrated to have episodic memory (as opposed to general "textbook knowledge") based on their avoiding a previously foraged area for some hours so it can be replenished (all demonstrated in behavioral experiment setups) (Jozet's 2022 CIAC talk).

57.2.2 Personalities

Octopuses have "personalities" defined as differences in individual behavior that are stable over time and in different contexts. When reaching for something, different individuals have a preferred reaching arm (Mather and Kuba, 2013).

57.2.3 Play and fun

Octopuses have often been observed to play in captivity.

57.2.4 Sleep

Cephalopods sleep and even have REM cycles (Frank et al., 2012; Iglesias et al., 2019). During their sleep, they alternate between quiet and active sleep phases, like humans do (Lima de Souza Medeiros et al. 2021, iScience).

57.2.5 Tool use

Octopuses have been demonstrated to use water (through jetting at things), rocks to form dens, coconuts and shell hash for protection (Amodio et al., 2019).

57.2.6 Pain

It seems that octopuses at least can feel pain (Crook, 2021).

Chapter 58

Cephalopods and their prey

58.1 Diet

58.1.1 Composition

Doryteuthis pealeii change their dietary composition throughout ontogeny. As paralarvae, they primarily consume copepods. This shifts to larger crustaceans as juveniles, and finally they prey upon fishes and other squids (including conspecifics) as adults (Rosa et al., 2013a). As an individual squid grows, however, its trophic niche widens as it continues to consume small prey such as copepods but also consumes larger prey such as fishes and squids due to its allometric growth of its buccal crown. They are highly opportunistic predators, changing their feeding preferences based on prey availability (Macy III, 1982b).

Unlike in loliginids, the trophic position of most oceanic cephalopods is invariant of body size (Murphy's 2018 CIAC talk).

Apparently rather rare among cephalopods, *Haliphron atlanticus* feeds on jellyfish and siphonophores (Hoving and Haddock, 2017).

Because most cephalopods are rather generalist predators, they can consume many different prey species, funneling lots of energy into one species. This leads to decreased food for more specialized competitors. The end result is that cephalopods may decrease biodiversity. This is why jellyfish blooms are problematic for biodiversity; they are generalists as well.

Newly settled juveniles on the Mediterranean coast of northern Spain feed on amphipods as a huge proportion of their prey (Escolar's 2022 CIAC talk).

Individual cuttlefish in the lab have been shown to have stable food preferences (Jozet's 2022 CIAC talk).

Cephalopods can often consume prey much larger relative to body size than most fishes. When cephalopods do this, they are lengthening the food chain and thus decreasing trophic efficiency (Barnes et al., 2010).

58.1.2 Frequency

Captive studies on *Illex illecebrosus* have demonstrated that a minimum diet of 1-3% body weight is required to maintain body weight, but this is heavily dependent on activity and temperature (O'Dor et al., 1980; Wells and Clarke, 1996). Similarly, coastal octopuses seem to need ≈1-2% body weight in food per day to maintain body weight (Wells and Clarke, 1996). More typical daily food intake rates in the wild were 3-7% body weight or even more (e.g. 15-18% for *Doryteuthis opalescens* (Yang et al., 1986)). For every 1 g of prey consumed, ~0.25-0.33 g of weight was gained.

58.2 Predatory behavior

Octopuses have been observed to bob their heads when detecting prey likely to judge distance with monocular parallax (Hanlon and Messenger, 1996).

Some cephalopods utilize dynamic coloration for prey capture (Barbato et al., 2007). Cuttlefishes and octopods have been seen to use the "passing cloud" pattern to startle prey into moving and revealing its position (Adamo et al., 2006; Hanlon and Messenger, 1996). *Sepia latimanus* uses this technique quite dramatically.

The spatial scale of a "prey patch" has never been determined for any cephalopod (Birk and White, 2014).

From prey's perspective, the best indicator of a potential predator's distance is its cross-sectional area . As a predator gets closer, its cross sectional area at its widest point increases. The more posteriorly is the widest cross sectional area of a predator, the closer it can reach its anterior apex before the prey recognizes its proximity. This puts squids at an advantage over fishes given that the widest point on most squids is further back along the body than along a equivalent size fish predator.

Predator-prey dynamics are often modeled via Holling's functional response equations:

- Type I: as [prey] increases, prey caught per predator increases linearly until a saturation value and stays constant at that value.
- Type II: as [prey] increases, prey caught per predator increases in a Michaelis-Menten relationship until a saturation value and stays constant at that value.
- Type III: as [prey] increases, predators do not respond at first until [prey] reaches a notable value. Then predators switch to that prey. Thus prey caught per predator increases as a sigmoidal function.

Six stages of predatory behavior were defined by Endler (1986) and are described in cephalopods in the subsequent sections.

58.2.1 Encounter

Encounter The cephalopod predator moves within a distance from which it can potentially detect prey.

Abdopus aculeatus is the only cephalopod that is known to frequently cross over land between tide pools in search of prey.

Cuttlefish have been demonstrated to avoid a previously foraged area for some hours so prey stock can be replenished (Jozet's 2022 CIAC talk).

Octopuses generally prefer to use arm pairs I and II for searching and hunting for food (Bidel's 2022 CIAC talk).

58.2.2 Detection

Detection The cephalopod predator recognizes prey as objects distinct from the background.

Similarly to vertebrates with laterally-placed eyes, cephalopods predominantly use their left and right eyes for different priorities. *Sepia officinalis* focus on prey detection through their right eyes more than their left eyes (Schnell et al., 2016). In *Octopus vulgaris*, the preference seems to be individual-specific (Frasnelli et al., 2019).

Due to their polarized vision, cephalopods can easily detect things like fish scales to alter the polarized plane of light but still seem camouflaged to an animal without polarized vision (Budelmann, 1994).

58.2.3 Identification

Identification The cephalopod predator recognizes prey as edible or profitable.

The movement pattern of prey is an important component of prey recognition (Maegawa's 2015 CIAC talk).

58.2.4 Approach

Approach The cephalopod predator approaches and makes contact with the prey.

Decapodiforms typically attack their prey with a tentacle strike. *Doryteuthis pealeii* tentacles can reach over 2 $\mathrm{m \cdot s^{-1}}$ and strike within 20-40 ms, with the tentacles accelerating at 250 $\mathrm{m/s^2}$ (Kier, 2016).

Hatchling squids, however, do not use tentacle strikes as much but lunge with splayed arms at their prey. This is because their cross-striated tentacular ultrastructure has not yet developed (subsection 50.5.1).

Idiosepius paradoxus have been observed to use their ink for predation: they either eject ink between themselves and their prey as a "smokescreen" to move closer to the prey, or they use an ejected ink blob as a distraction and approach the prey from a different direction (Sato et al., 2016).

Octopods often attack with a "parachute attack" where they pounce on their prey with the interbrachial web extended (Hanlon and Messenger, 1996). They also attack by groping around rocks and corals (preferably with arm pair I and II) or extending a single arm rapidly towards the prey and bringing the prey item back under the web (Hanlon and Messenger, 1996). Sometimes they will wave an arm around seemingly aimlessly until finally grabbing the prey (Bidel's 2022 CIAC talk).

Cuttlefish have been observed in captivity and in the wild to putatively mimic crustaceans walking while approaching prey (van Elden and Meeuwig, 2020).

Cuttlefish, at least, have been demonstrated to use stereopsis with their eyes to judge prey distance and thus position their bodies to their prey before the tentacle strike (Wardill's 2022 CIAC talk).

58.2.5 Subjugation

Subjugation The cephalopod predator prevents prey escapement.

The interbrachial web of octopods is very effective at subjugating prey (Hanlon and Messenger, 1996). In addition, decapodiforms have muscles in their arms and tentacles that are oriented to prevent prey from twisting out of the arms (Kier, 2016). Octopodids possess cephalotoxin in their posterior salivary gland that they use to paralyze crabs very quickly (combined with overpowering muscles).

58.2.6 Consumption

Consumption The cephalopod predator ensures safe passage of the prey through the gut.

The feeding mechanics are controlled by the superior basal lobe in the brain (Budelmann, 1995).

58.3 Trophic position

The trophic level and diet of an individual cephalopod can be determined by examination of its δ^{13}C and δ^{15}N. For each increase in trophic level, the composition of the predator is +3.4 ‰, the δ^{15}N values in the prey. This is because the enzymes involved in metabolizing food fractionate (preferentially select) the lighter isotopes for excretion and the heavier isotopes for retention in new body mass. Chitinous tissues are apparently an exception, however, since they do not exhibit any enrichment from the prey (Cherel's 2018 CIAC talk).

δ^{34}S is identical in predators and their prey and thus the isotopic composition of a cephalopod is reflective of the basal food source for the ecosystem in which it is consuming its food.

Chapter 59

Cephalopods and each other

Social interactions between conspecifics are very important at some point in the life history of every cephalopod; some much more than other species. In fact, social constraints or interactions can cause individuals to behave very differently than predicted from merely their physiology alone (Killen's SEB talk).

Most octopods are solitary. An exception is the pelagic *Argonauta* in which females form chains (max observed = 18 individuals) as they swim at the surface (Rosa and Seibel, 2010c).

59.1 Conspecific communication

Signaling between conspecifics often involves simple, high-contrast patterns with the chromatophores. Pelagic squids actively use body patterns for communication. Most shallow pelagic squids are much more gregarious than benthic octopuses and cuttlefishes (Hanlon and Messenger, 1996) and thus have more opportunities for intraspecific communication. Adult *D. gigas* rapidly (2-4 Hz) change their entire body surface between red and light as a method of communication (Rosen et al., 2015). *D. gigas* changed its body pattern more frequently around conspecifics than when alone (Trueblood et al., 2015).

Octopuses can recognize conspecific individuals (which is surprising given their solitary life history) and learn by observing the behavior of conspecifics (Fiorito talk at CIAC). While they generally are solitary, they do not seem to be territorial, not defending their home range from nearby conspecifics (Alves et al., 2008). However, octopuses have been documented to have agonistic interactions. The approaching octopus turns uniformly dark as a sign of aggression. The responding octopus either turns dark as well and confronts the competitor, or it turns pale and evades confrontation (Scheel et al 2016). During these interactions, octopus physiology is likely similar to that in agonistic fishes. After an aggressive interaction between fishes, the subordinate leaves with a higher metabolic rate than the dominant individual due to social stress (Killen's SEB talk).

59.2 Shoaling

Many shallow-water squid species are very gregarious and form shoals ranging from two individuals to thousands. While isolated individuals may possess wide variation in a trait (e.g. routine activity), individuals must converge their behavioral tendencies together if the shoal is to stay intact (Killen's SEB talk). Innate variation can still affect the composition of the group, however. Squids may likely be similar to fishes in the tendency of individuals with higher aerobic scopes to maintain positions towards the front of the school with less aerobically capable individuals in the rear where they can take advantage of greater hydrodynamic efficiency (Killen et al., 2012). The individuals towards the front can benefit by having first access to food.

Squids may be similar to fishes in that schooling behavior emerges from all individuals following the same two rules: 1) stay close but not too close to your neighbor, and 2) keep swimming.

Shoaling also reduces metabolic rate in loliginids (Burford et al., 2019).

Environmental stressors can affect schooling behavior. Squids are likely similar to herring which spread out under extreme hypoxia (Domenici et al., 2002).

Cuttlefishes have recently been documented to shoal and putatively form defensive formations against scuba divers.

59.3 Reproductive behavior

Most loliginids in temperate regions migrate inshore to shallow waters to spawn and lay their eggs (Hixon, 1980).

Ommastrephid squids have been demonstrated to mate indiscremenantely with regards to gender (i.e. spermatangia found at similar rates on both males and females) (Hoving et al., 2019).

Mating is an important exception to the solitary life history that most cuttlefishes and octopuses have developed; dynamic coloration is used quite frequently during mating behaviors. In this respect, the dynamic camouflage used during the extravagant courtship aggregations and behaviors of *Sepia apama* has been best studied (Hall and Hanlon, 2002; Zylinski et al., 2011). In these aggregations, males utilize high contrast, bold patterns to fight competing males and attract receptive females (sometimes simultaneously on both sides of the body!).

59.3.1 Courtship and insemination

True courtship behavior is not well studied except in *Sepioteuthis sepioidea* and recently among some *Sepia* (Kubodera's 2018 CIAC talk). Many closely related species are sympatric, and species-specific courtship displays may provide a mechanism of genetic isolation (Kubodera's 2018 CIAC talk).

In some squid species, males begin mating with females before the female is sexually mature (Ikeda et al., 1993).

Male octopods can spend up to 3 hours with his hectocotylus inside the female (Hanlon, 1988).

Octopus chierchiae males vigorously shake the tips of their arms to attract females (known as tasseling) (Grearson's 2022 CIAC talk).

59.3.1.1 Consort versus sneaker males

Both *Sepia apama* and some loliginid males are known to utilize alternative reproductive tactics.

Male type	Male size	Mating position	Mating timing	Spermatophore placement	Spermatophore size
Consort	Large	Parallel	Shortly before fertilization	Near oviduct	Large
Sneaker	Small	Head-to-head	Longer before fertilization	Seminal receptacle in buccal mass	Small

Upon release of sperm in sneaker males, the sperm aggregate towards high CO_2 (Hirohashi's 2015 CIAC talk).

59.3.2 Post-mating behaviors

After mating with a female, male *Hapalochlaena* avoid physical contact with that female, possibly because females sometimes cannibalize males after mating or as sperm allocation (Morse and Huffard, 2022).

59.3.3 Male competition / sperm competition

Most cephalopods (in which much is known about reproductive behavior) are highly polygamous. As a result, male sperm delivery has undergone strong selection to ensure that the focal individual's sperm fertilizes the highest proportion of eggs. Females have multiple paternity within a single egg batch. In fact, a single egg batch from a female *Octopus oliveri* has been observed to contain eggs fertilized from 9+ males (Ylitalo-Ward's 2015 CIAC talk). This may be why many octopus species have very long reproduction behaviors (up to 3 hours in some cases!)(Hanlon, 1988). The male may mate rather early but then waits to ensure another male cannot replace his sperm. Males will also modulate how many spermatophores he spends on a female based on how many males she has recently mated with (Morse's 2022 CIAC talk).

Male loliginids do not place the spermatophore directly in the oviduct, but rather, on the female's body. Their placement depends both on species and male type (i.e. consort vs. sneaker). Consorts place the spermatophore in the mantle cavity near the oviducts, while sneaker males place their spermatophores on the buccal mass (Marian's 2015 CIAC talk). As a result, sneaker males generally have higher sperm competition than consort males and as a result, the sneaker male sperm can have longer flagella (at least in some species).

Males will sometimes implant their spermatangia in gashes and cuts made in the female. This may be a strategy of weakening the female so that she does not have as long to live and as many other males she could possibly mate with.

59.3.4 Egg laying

See section 47.4.

59.3.5 Egg brooding

Incirrate octopus females are known to "shut down" after spawning and guard the eggs until their death. This behavior is stimulated by the optic gland, such that when it is removed, the female does not display this behavior (Wang's 2015 CIAC talk).

Chapter 60

Cephalopods and their competitors and mutualists

Competition with fishes has driven many aspects of cephalopod evolution (Packard, 1972).

Octopuses have been demonstrated to hunt cooperatively with fishes (Amodio et al., 2019). Sometimes fish and sometimes the octopus will lead the group around searching for prey. This shows that hunting is cooperative, not just fish taking advantage of the octopuses successes. Between the two, the octopus tends to be the choosiest of the group and will follow the fishes often but sometimes will keep fishes back in an area it is interested in (Sampiao's 2022 CIAC talk). The fishes can signal the presence of prey by posturing so the octopus can find and reach hiding prey (Sampaio's 2018 CIAC talk). In order for these group dynamics to work, the octopus has to be similar size to the fishes, otherwise they will try to eat it (Sampiao's 2022 CIAC talk).

As an evolutionary generality, when competition is low in an ecosystem, there are many open niches that can be filled and so phenotypic evolution is fast. When competition is tight, there is no such room for mutational creativity and phenotypic evolution is slower. This is why adaptive radiations often happen after mass extinction events.

Chapter 61

Cephalopods and their predators

61.1 Predators

Dolphins have been shown to have complex foraging behaviors for cephalopods. In some cases, dolphins beat octopuses against the surface of the water or throw them through the air (Sprogis et al 2017). They have also been demonstrated to separate the palatable cuttlefish mantle from the head, ink, and cuttlebone before consuming the mantle (Smith and Sprogis 2017).

Other predators include fishes, and even polychaetes (see subsubsection 10.2.1.2).

61.2 Prey behavior

Six stages of predatory behavior were defined by Endler (1986) and are described in cephalopods in the subsequent sections.

61.2.1 Encounter

Encounter The cephalopod prey avoids moving within a distance from which it can potentially be detected by a predator.

Sepioteuthis sepioidea have on average 7 predatory encounters per hour during daylight hours. This encounter rate is much higher than average (Curio, 1976).

For pelagic cephalopods, they may be able to lessen encounter rates by entering hypoxic areas where their predators spend much less time foraging. Such a selection is likely driving *Dosidicus gigas* into the OMZ in the eastern tropical Pacific (ETP) (Seibel, 2013). This can be particularly advantageous when the predator has less hypoxia tolerance than the cephalopod. For example, the P_{50} depth (subsubsection 53.6.8.2) of many species of tuna in the ETP is 100-300 m shallower than the P_{50} depth for *D. gigas* (Mislan et al., 2015), thus providing 100-300 m of vertical habitat where *D. gigas* has a "hypoxia shelter" from tuna.

61.2.2 Detection

Detection The cephalopod prey avoids being recognized by a predator as an object distinct from the background.

The primary influence on the difference in dynamic coloration between pelagic and benthic cephalopods is habitat complexity. Benthic cephalopods live in an extremely complex visual environment with a diversity of colors, textures, shapes, and lighting conditions. In contrast, the visual habitat of pelagic cephalopods is extremely uniform: little to no structure (perhaps the floating sargassum now and again), uniform blue coloration, uniform (horizontally) downwelling light, and importantly, no places to hide. Presumably, since cephalopods use their body patterns to avoid predation, communicate with other individuals, and attract mates, they are essential for an individual's fitness and thus would be strongly selected to suit their habitat.

Similarly to their habitat, pelagic squids have a pretty limited diversity of body patterns (ethogram)(but see Trueblood et al., 2015). Most chromatic components of *Illex illecebrosus* or *Dosidicus gigas*, for example, are quite simple: all clear, all dark, dark fins, dark mantle bar, light dorsal stripe, etc. (Trueblood et al., 2015; Harrop et al., 2014).

Given that downwelling light is a consistent visual environment for pelagic squids, countershading is the most important body pattern for camouflage. This pattern consists of expanding the dorsal chromatophores to appear dark to predators from above and contracting ventral chromatophores to hide self-induced shading on the ventral surface when viewed laterally. Some pelagic squids (e.g. ommastrephids) even have ventral photophores to eliminate the shadow their bodies cast in the water column from predators below (Young and Roper, 1976). While chromatophores function well to adjust the individual's brightness, iridophores

are very important for hue matching: the iridophores reflect back the hue of the ambient lighting, thus allowing pelagic squids to always have a good match to the hue of their environment.

In contrast to the pelagic cephalopods described above, benthic cephalopods such as octopuses and cuttlefishes inhabit a much more complex environment which requires a more complex camouflage. Crypsis in this environment is conducted by more nuanced body patterns than in pelagic squids. *Sepia officinalis*, whose camouflage behavior has been extensively studied (Allen et al., 2009; Barbosa et al., 2008; Chiao and Hanlon, 2001a,b; Chiao et al., 2010; Hanlon and Messenger, 1988; Zylinski et al., 2009), hides successfully in a wide variety of habitats with three primary body pattern "templates": uniform, mottled, and disruptive (Hanlon, 2007) which are expressed based on their visual environment (subsubsection 52.1.3.1). Many cuttlefishes and octopuses can also modify the texture of their skin with muscular papillae to match the texture of objects in their environment like algae or coral (Allen et al., 2009).

S. officinalis in turbid water will express more papillae and show more disruptive skin patterning than in the same environment in clear water (Perkins' 2018 CIAC talk).

Cuttlefish (*Sepia officinalis*) seem not to make a complete decision on camouflage before starting the change, but rather make the first change and then fine tune to get them as close as possible (Liang's 2022 CIAC talk).

Sepioteuthis lessoniana have been demonstrated to change their body coloration to match nearby benthic coloration (Nakajima et al., 2022).

61.2.2.1 Camouflage patterns

Uniform

Mottle

Disruptive In addition to the standard 3 pattern types, *S. officinalis* also adjust their camouflage to to account for 3D objects and shadows (Nagar et al., 2021, JEB).

61.2.2.2 Pelagic camouflage

Predators with searchlight photophores can easily detect transparent animals and thus being red or black provides better camouflage. Therefore, meso- and bathypelagic cephalopods (*Japetella* and *Onychoteuthis*) have been demonstrated to maintain transparency under ambient light but to expand chromatophores to turn red under directed blue light (Zylinski and Johnsen, 2011) thus maintaining camouflage under both conditions.

61.2.2.3 Burrowing

Muusoctopus leioderma and *Euprymna* spp. have been shown to burrow in sand.

61.2.3 Identification

Identification The cephalopod prey avoids being recognized by a predator as edible or profitable.

Gonatus onyx approached by ROVs display a few typical teuthid defensive behaviors: the "J" curl, and "elk" posture (Hunt and Seibel, 2000).

In both pelagic and benthic cephalopods, dynamic coloration is also very important for responding to predators. If an individual's primary defenses (i.e. crypsis) fail and it is recognized as prey by a predator, secondary defenses are used to avoid the predator successfully catching it. In deimatic displays, the individual rapidly switches from its failed cryptic pattern to a body pattern with bright, high contrast chromatic components, often including eyespots (Hanlon and Messenger, 1996). This display is intended to startle the predator and inhibit the predator's prey-capture behavior. Other dramatic predator-escape behaviors like the blanch-ink-jet maneuver also involve rapid changes in the body pattern.

61.2.4 Approach

Approach The cephalopod prey avoids the predator's approaches and contact.

Similarly to vertebrates with laterally-placed eyes, *Sepia* (and likely other cephs as well) predominantly use their left and right eyes for different priorities. *Sepia officinalis* focus on predator detection through their left eyes more than their right eyes (Schnell et al., 2016).

All cephalopods which possess ink sacs can release their ink to deter predators. Interestingly, inking behavior is just as common in the bathypelagic as it is in the epipelagic (Bush and Robison, 2007).

Chromatophore changes are consistently faster for secondary defense than during primary defense (Hanlon's 2018 CIAC talk).

Squid and cuttlefish have been demonstrated to alter their approach avoidance based on the predatory strategy employed against them. They conceal on the substrate from pelagic fishes but leave the substrate from ambush predators (Staudinger et al., 2011, 2013).

61.2.5 Subjugation

Subjugation The cephalopod prey escapes from the predator's hold.

61.2.6 Consumption

Consumption The cephalopod prey ensures troublesome passage through the predator's gut.

Blue-ringed octopuses (*Hapalochlaena* spp.) tissues are rich in tetrodotoxin to prohibit consumption.

Chapter 62

Cephalopods and their parasites

Cephalopods possess many parasites. Parasite loads can affect performance by utilizing part of a cephalopod's energy budget for management (Binning's SEB talk). Additionally, as squids migrate, they provide pathways of connectivity for parasite populations and parasites may affect migratory behavior in squids as it does in other animals either causing them to migrate further to avoid parasite-infested regions or migrate less due to energy-limitation (Binning's SEB talk).

62.1 Common parasites

If cephalopods are wounded, they can easily obtain bacterial infection, commonly by *Vibrio* bacteria (Vidal et al., 2014; Castellanos-Martínez and Gestal, 2013).

Ommastrephid egg masses can be infected by ciliates and amphipods (Birk et al., 2017).

The caecum in cephalopods can be infected by *Aggregata* protozoans such that the host cannot absorb nutrients (Castellanos-Martínez and Gestal, 2013). Cestode and nematode worms and trematodes are also found in the digestive tracts of cephalopods, especially ommastrephids (Castellanos-Martínez and Gestal, 2013).

Parasitic copepods and occasionally isopods can also inhabit the mantle cavity and gills (Castellanos-Martínez and Gestal, 2013).

Dicyemids infest the renal appendages of benthic-associated cephalopods, though they have not been found in any oceanic species.

While it is currently unclear whether they are parasitic, cephalopod digestive systems are rich with *Mycoplasma* spp. and *Photobacterium* spp. bacteria (Kang et al., in prep 2021).

Chapter 63

Cephalopods and their population dynamics

Although individual cephalopods do not have asymptotic growth, at the population level, some cephalopod populations do average out to asymptotic growth since mean growth is driven initially by the fast growing individuals and later by the slow growing individuals (Wells and Clarke, 1996).

New recruitment also lowers the growth rate of the average animal size.

Microsatellite markers can reveal whether a species distribution has expanded or contracted recently (Pecl's 2018 CIAC talk).

Within a given population, there may be multiple seasonal cohorts based on multimodal spawning frequencies. When such population cohorts occur, they can be distinguished by trace metal concentrations in the statoliths. For example, Ba/Ca can be a marker of temperature history in different rings of the statolith (Hu's 2018 CIAC talk).

63.1 Paralarval settlement and recruitment

The success of paralarval recruitment into the next generation of adult marine animals is largely determined by Bakun's triad: enrichment, concentration, and retention.

Recruitment in a given area is heavily influenced by local current direction and strength.

Chapter 64

Cephalopods and biogeochemistry

Traditionally, nekton are not thought to contribute much to biogeochemical cycles because their total biomass is so dwarfed by the biomass of primary producers. Cephalopods that undergo diel vertical migration, however, are notable components of the carbon biological pump: they consume carbon at shallow depths (i.e. eat prey) and respire carbon at deep depths (Seibel and Dierssen, 2009). Horizontally migrating cephalopods are vectors in biogeochemical cycles, shifting the distributions of nutrients (Arkhipkin, 2013).

64.1 The carbon cycle

Cephalopods are efficient carbon vectors for a variety of reasons:

- They have high growth rates which make them rapid importers of carbon.
- They attain large sizes which makes them large reservoirs of carbon.
- Many species exhibit strong migratory behaviors (horizontal and vertical, ontogenetic and diel) which transfers carbon rapidly.
- They are semelparous which makes their carbon export rates (to predators or scavengers) high.
- When cetaceans eat them, they are often sloppy eaters and leave detritus to sink.

Migration of nekton is an important carbon vector in tropical estuaries and temperate saltmarshes (Hyndes et al., 2014).

As a very rough rule of thumb for organisms in general: 1 g C = 13 g wet weight.

64.2 The nitrogen cycle

All cephalopods are ammonotelic and as such they excrete nitrogen in the form of NH_4^+ into their environment. This N source likely increases primary productivity in N limited regions as occurs from fish nitrogen excretion (Layman et al., 2011; Burkepile et al., 2013).

Part X

Their fishery

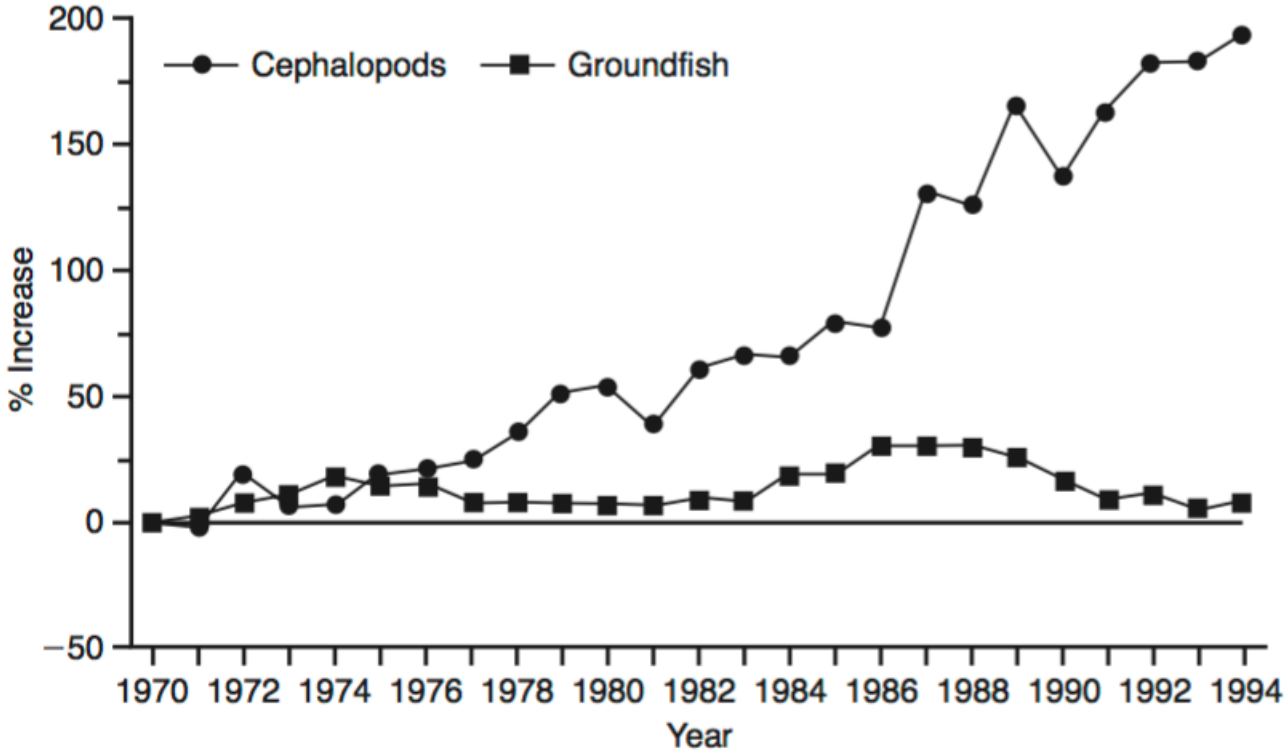

Fig. 1. Comparison of trends (% change from 1970 values) in total world catch of groundfish a cephalopods, 1970–1994.

Figure 64.1: Cephalopods are an increasingly popular fishery worldwide. Figure from (Caddy and Rodhouse, 1998, Fig. 1).

Among global cephalopod fisheries, ~80% target squid, 10% target octopods, and 10% target cuttlefish.

Cephalopods support the 3rd most valuable capture fishery in the world ($9.4 billion) behind tuna ($15.4 billion) and cods ($11.5 billion) (FAO Yearbook 2018).

Cephalopod flesh seems to be in general much safer parasite-wise compared to fishes (Gonzalez's 2022 CIAC talk).

64.3 Octopus fisheries

10% of global cephalopod fisheries target octopods.

Almost all octopodiforms fished are octopodids. *Enteroctopus* and *Eledone* are the only exceptions (Sauer's 2018 CIAC talk).

The US imports lots of octopuses but exports almost none (Gleadall's 2022 CIAC talk).

64.3.1 *Octopus cyanea* fishery

Off Madagascar is a very small-scale *Octopus cyanea* fishery that is run by women who hand-gather or dive/snorkel or harpoon to capture (Roumbedakis' 2022 CIAC talk).

64.3.2 *Octopus maya* fishery

The *Octopus maya* fishery is the largest octopus fishery in the Americas (Vidal et al., 2014). *Octopus maya* support a large fishery mainly around the northern coast of the Yucatan Peninsula in Mexico. The fishery is open from August through December each year (Avendaño's 2018 CIAC talk) and collects 20-30 thousand tons each year during that time (Rosas' 2022 CIAC talk).

Fishing is conducted with a drift rod and line off of boats (Roumbedakis' 2022 CIAC talk).

64.4 Squid fisheries

80% of global cephalopod fisheries target squids.

~3 million tonnes of loliginid and ommastrephid squids are caught globally annually by fisheries (FAO via FishStatJ). *Todarodes pacificus* is one of the most important fisheries in Japan (Ikeda et al., 1993).

At least for some squid fisheries, CPUE is lower during full moon than other moon phases probably because the lights from the jigging vessel aren't as contrasting with the rest of the surface (Kato's 2018 CIAC talk). CPUE when bottom trawling for loliginids is much higher during the day than at night (Hixon, 1980). Not all squids shoal to lights the same. *D. opalescens* rush the lights while *D. pealeii* and *S. sepioidea* approach in small numbers and *D. pleii* shoal along the periphery (Hanlon, 1988).

Commercial squid fishing effort can be measured via remote sensing of visual light detecting satellites (Maxwell et al., 2004). Japanese industrial squidding fleets use metal halide lights (Sadayasu's 2015 CIAC talk).

The most highly fished loliginids are *Doryteuthis gahi, D. opalescens, D. pealeii, Loligo forbesii, L. vulgaris*, and *L. reynaudii (Pecl and Jackson, 2007).*

64.4.1 *Berryteuthis magister* fishery

There is a notable trawl fishery for this gonatid species off the Pacific coast of Russia and northern Japan.

64.4.2 *Doryteuthis opalescens* fishery

This fishery is managed as one population, but there is actually two populations: one in Monterey Bay area and the other in the Southern California Bight (Cheng's 2018 CIAC talk).

64.4.3 *Doryteuthis pealeii* fishery

Doryteuthis pealeii have been commercially fished in the New England and George's Bank area since the 1800s (Hanlon et al., 2013). Currently, the commercial fishery predominantly targets squid when they are offshore in winter (Hanlon et al., 2013), however, there is a popular recreational fishery inshore such as in Narragansett Bay, RI. Commercial harvesting has traditionally been for the purpose of cod fishing bait on George's Bank. *Doryteuthis* support the second largest New York fishery by revenue.

The *Doryteuthis pealeii* fishery is managed as a single stock from the Gulf of Maine to Cape Hatteras (Peoples' 2022 CIAC talk).

64.4.4 *Dosidicus gigas* fishery

Squids are fished off Magdalena Bay, Baja California Sur, Mexico in spring and Santa Rosalia, Baja California, Mexico in summer and autumn (Gilly et al., 2006; Bazzino et al., 2010). Fishing grounds for *Dosidicus gigas* in the Gulf of California are off Santa Rosalia from May-October and Guaymas from November-May.

Dosidicus are the 13th largest single-species fishery worldwide (FAO 2018 report).

64.4.5 *Illex illecebrosus* fishery

Most squid are caught by otter trawl on the shelf edge and the biggest fishery focuses on the mid-Atlantic off VA and NC. June through September are the peak fishery months (until the quota is reached) (Hendrickson's 2018 CIAC talk, Bochenek & Powell 2021). The fishery is active during the day rather than at night (Bochenek & Powell 2021).

64.4.6 *Loligo reynaudii* fishery

This species supports the 4th largest fishery in South Africa (Gornall's 2018 CIAC talk).

64.4.7 *Loligo vulgaris* fishery

64.4.8 *Ommastrephes bartramii* fishery

100-300 kton/year are caught annually worldwide, mainly by Korean, Chinese, and Japanese fisheries (Kato's 2018 CIAC talk).

64.5 Cuttlefish fisheries

10% of global cephalopod fisheries target cuttlefish.

Part XI

Their aquaculture

Cephalopods have very high growth rates (5-10% wet weight/day) and high food conversion rates which make them very profitable for aquaculture.

64.6 Environmental requirements

Open aquaculture systems should be mindful of freshwater input from nearby rivers to avoid hyposaline conditions (Vidal et al., 2014).

[Sr] >= 8 mg/L is required for rearing cephalopod embryos (Hanlon et al., 1989).

Artemia are an insufficient diet for culturing paralarval cephalopods (Villanueva and Bustamante, 2006). This is likely because *Artemia* have quite a low Cu content and developing cephalopods require Cu for hemocyanin synthesis.

Bacteria in systems can be killed without causing harm to cephalopods by adding $KMnO_4$ to solution.

Ciliates are common issues with embryos and paralarvae. Water filtration and purification (e.g. UV sterilization) are important to avoid ciliates.

64.7 Feed requirements

Mysids are common prey items for paralarval cephalopods. However, sea roach isopods may be a good food source for hatchlings (Xu's 2018 CIAC talk). *Artemia* do not provide sufficient nutrients to support paralarval cephalopods' high growth rates (Grasse's 2022 CIAC talk). Once paralarvae have grown, they can be transitioned to live grass shrimp or frozen food (Grasse's 2022 CIAC talk).

Part XII

Their study by teuthologists

Table 64.1: Famous teuthologists

Name	Contribution(s)	Years
Aristotle	Described general morphology, behavior, and ecology	384-322 BCE
John Z. Young	Discovered the squid giant axon	
Naef	Proposed foundations of cephalopod phylogeny	

The first documentation of human interest in cephalopods comes from the 16th century BCE when octopuses, squids, and argonauts were painted on pottery.

Famously, Aristotle (384-322 BCE) documented Mediterranean cephalopods, noting their morphology, behavior, and ecology.

The term “Cephalopoda” was first coined in 1802 by Cuvier.

Chapter 65

Techniques for studying their environment

65.1 Measuring salinity

If salinity is measured electrically via conductivity, then the results are expressed as practical salinity units (psu). If, however, it is measured via chemical titration, then the results are expressed as ppt. Modern salinity measurements are conducted by comparing the conductivity of a seawater sample to the conductivity of a 0.435 molal solution of KCl. However, the relationship changes with pressure, such that deep water measurements must be adjusted. In addition, deep ocean interior water can accumulate high concentrations of silicic acid which is not ionic and therefore not detected by a salinometer. It is abundant enough, however, to increase seawater's density and therefore these deep samples must have their density adjusted.

65.2 Measuring pH

65.2.1 Spectrophotometric method with m-cresol purple (SOP 6b: Dickson et al., 2007)

When empirically determining the adjustment for the pH perturbation caused by dye addition, the spectrophotometer's integration time should not be altered, but rather averaging more scans will provide stable absorbance measurements even with dense dye.

Chapter 66

Techniques for studying their community

66.1 Measuring primary production

Primary production is typically measured by the ^{14}C method which involves collecting a water sample, labelling $NaHCO_3$ with ^{14}C, waiting for production to occur, then filtering the sample and measuring the quantity of ^{14}C on the filter. This measures particulate organic matter (POM) (i.e. phytoplankton) but cannot capture dissolved organic matter (DOM) (Pilson, 2013).

Sometimes PP is also quantified by measuring $\Delta[O_2]$ as well but not nearly as commonly as the ^{14}C method (Pilson, 2013).

Chapter 67

Techniques for studying cephalopods

NIRS is a technique to assess the elemental composition of a live animal without killing it (Moltsch's 2015 CIAC talk).

The Sr:Ca composition of statoliths is a metric of historic water temperatures experienced by an individual (Yamaguchi et al., 2015).

Measuring ^{13}C shows where a sample has been and measuring ^{15}N shows its trophic position. Classically, $\delta^{15}N$ increases 3.4 for every trophic level increase. The $\delta^{15}N$ of chitinous structures like beaks and gladii are lower than soft tissues in the same animal (Cherel et al. 2009).

The 38 kHz frequency on the EK60 is the best for detecting squid acoustically.

67.1 Preserving specimens / tissues

This is mainly advice from Mike Vecchione.

1. Take pictures of whole specimen, dorsal and ventral. Take pictures of arms and tentacles (if applicable) especially the sucker arrangements. Note funnel-locking apparatus and take pictures of photophores (if present).
2. Take tissue clip from the edge of the mantle or fin and place in 95% ethanol. Preserve at -80 °C.
3. Preserve in formalin diluted with seawater (100% formalin = 37% formaldehyde by mass in water = 40% formaldehyde by volume in water). According to Roper and Sweeney (1983):
   (a) 8-10% formalin for Loliginidae, Ommastrephidae, Onychoteuthidae, Gonatidae, Octopodidae
   (b) 6-8% formalin for Enoploteuthidae, Histioteuthidae, muscular Cranchiidae, Sepiolidae
   (c) 4-6% formalin for Cirrata, Bolitaeninae, gelatinous Cranchiidae
4. After 1 week in formalin, transfer for long-term storage to 50% isopropanol (preferred) or 70% ethanol.
5. If formalin is not available, place in air-tight bag and freeze as cold as possible and avoid freeze-thaw cycles.

67.2 RNASeq

RNA quality can be quantified with an RNA integrity number (RIN) (Schroeder et al., 2006). This ratio of 28S/18S rRNA peaks at ~2kb and 4kb band sizes, respectively. The RIN, developed for vertebrate samples, is a poor quality metric for molluscs because they consistently show only a peak at 2kb, corresponding to the 18S peak. This is because in protostomes, the 28S gene has a "hidden break" wherein two separate ORFs are transcribed and the two transcripts function by holding together through hydrogen bonds rather than a continuous RNA molecule (Adema, 2021). During purification, these segments separate and they are both ~2kb, which makes them blend into the 18S band.

RNA degradation within dying tissues has been shown to cause (Gallego Romero et al., 2014):

- differential expression of the majority of genes from a fresh sample vs a degraded one
- different rates of degradation in different genes, gene ontologies, and transcript sizes
- lower library complexity

However, RNA degradation of isolated RNA in a freezer has been shown to affect RNAs linearly and uniformly, such that typical library normalization will account for differences (Opitz et al. 2010, BMC Medical Genomics).

- How will I get rid of rRNA? polyA selection or rRNA depletion? - polyA selection depends on the mRNA being minimally degraded. The RIN can indicate the amount of degradation. - If mRNA is too degraded for polyA selection, then you can use rRNA depletion. - For prokaryotes, rRNA depletion is the only method available. - For ncRNA (such as miRNA), rRNA depletion is the way to go, but it's worth the money to get a really good kit to minimize rRNA as much as possible. - Strand-specific library prep? - useful if there is a chance that transcription is occurring on both strands of a given locus. - dUTP method is most common - SE vs PE reads - SE reads are cheaper but only worth it if it's a well-annotated organism. - Deeper coverage is better (most important for lowly expressed genes) except during de novo transcriptome assembly, where accumulated errors just make more contigs - How many replicates do we need? - dependent on technical noise and biological variation - Most of the technical variation occurs at RNA extraction and library prep stages rather than the sequencing itself - small RNASeq typically only has a read depth of 2-10 million reads because the complexity is rather low - Functional overrepresentation of DE genes (e.g. using DAVID) has bias because long genes are more likely to be sequenced than short genes. So long genes can make the cut just because they're long. - If RNA quality is poor, rRNA depletion can be used rather than polyA selection to avoid 3' bias. If really bad, consider using Illumina's FFPE kit rather than rRNA depletion. - Typically required # of reads is assuming polyA selection. If high quality RNA but using rRNA depletion, then you'll need 2x the reads of polyA. If low quality RNA (using rRNA depletion or FFPE samples), then you'll need 4x the reads of polyA. - Single end reads are more likely to have falsely labelled duplicate reads than PE reads because PE reads are much less likely for 2 reads to fall on the same places than single reads - For mammals, RIN > 8 is considered good. For other species, check the literature. - To quantify RNA going into a library prep, use a Qubit rather than NanoDrop since the later is too easily affected by DNA. - Use a denaturing agarose gel to get RNA to run well on the gel to assess RNA integrity

For library preps with very low input (e.g. single cell) or very deep coverage, unique molecular identifiers (UMIs) should be incorporated into library prep so that duplicated reads (which are much more likely in these kinds of experiments) can be accurately removed.

67.3 DNA barcoding

The following primers target the 18S rRNA gene of cephalopods from eDNA to make a ~200 bp amplicon of the V2 region of this gene (de Jonge et al., 2021):

fwd 5'-CGCGGCGCTACATATTAGAC-3'

rev 5'-GCACTTAACCGACCGTCGAC-3'

The following primers target cephalopods from animal diets by making a ~200-250 bp amplicon (Jarman et al., 2006):

fwd 5'-TGCGGTATTWTAACTGTACT-3'

rev 5'-TTATTCCTTRATCACCC-3'

The following primers target cephalopods from animal diets by making a 71 bp amplicon of the COI gene (Peters et al., 2015):

fwd 5'-CCCCTTTATCAAGTAACCTCTCACA-3'

rev 5'-AGCTAAGTGGAGGGAAAAAATGG-3'

67.4 Beaks

Beaks should be frozen (Arkhipkin et al., 2018).

The wandering albatross is the best biological sampler we have for beaks in the Southern Ocean now that we don't have sperm whales (Abreu's 2022 CIAC talk). But their squid consumption is mostly scavenging.

67.5 Gut content analysis

In addition to morphological determination, metabarcoding of gut contents can help determine prey identity.

67.6 Aging cephalopods

67.6.1 Statoliths

Statolith aging is easiest in squids and not possible in some cuttlefishes and all octopuses (Arkhipkin et al., 2018). Briefly, the statoliths are ground to a flat surface, polished, sometimes stained to enhance lines, then viewed under light microscopy.

The statoliths can record past stress history such as starvation. In ommastrephids, rings in the statoliths begin forming early in the paralarval stage; in loliginids they already started forming during late embryogenesis (Arkhipkin et al., 2018).

Temperature history of the individual can be tracked by $\delta^{18}O$ in the statoliths, but salinity and season also have modulating effects that should be considered (Chung 2020).

67.6.2 Beaks

See section 67.4.

Age increments can be measured either from the lateral wall surface (LWS) or rostral section (RSS).

67.6.3 Gladii

Gladii should be rinsed in fresh soapy water then stored in 4% formalin (Arkhipkin et al., 2018).

Daily periodicity has been confirmed in onychoteuthid gladii (Lui's 2018 CIAC talk).

67.6.4 Eye lenses

67.7 Anesthesia and euthanasia

67.7.1 Magnesium chloride

Magnesium ions have been demonstrated to block both afferent and efferent nerve transmission in cephalopods (Leary, 2020).

A stock solution of 7.5% (75 g/L, 370 mM of $MgCl_2 \cdot 6H_2O$) dissolved in DI is isosmotic with seawater and can be mixed 1:1 with seawater to result in euthanasia after immersion for 15 minutes (Leary, 2020).

$MgCl_2$ (55-73 mM; 5.237-6.8 g / L) has been demonstrated to be a good anesthetic for adult *Octopus maya* (Roumbedakis' 2015 CIAC talk) (Andrews et al., 2013).

Immersion in 330 mM $MgCl_2$ for 5-10 minutes is sufficient for octopus and cuttlefish to have no neural response to skin and cranial dissections (Butler-Struben et al., 2018).

67.7.2 Ethanol

In molluscs, ethanol inhibits neuronal sodium and calcium channels (Leary, 2020).

2% EtOH is a good anesthetic and 5% EtOH is lethal (Fiorito et al., 2015). Immersion should be at least 10 minutes (Leary, 2020).

Ethanol (30 $mL \cdot L^{-1}$) has been demonstrated to be a good anesthetic for adult *Octopus maya* (Roumbedakis' 2015 CIAC talk) (Andrews et al., 2013).

67.8 Histology

Light microscopy can (at best) distinguish particles that are at least 200 nm apart, while TEM can distinguish with 2 nm resolution.

To prepare tissues via the paraffin technique:

1. Tissues are often fixed in neutral buffered formalin.
2. Tissues are dehydrated in progressively concentrated alcohol baths and then once fully dehydrated are cleared in xylene (a paraffin solvent).
3. Tissues are embedded in warm paraffin wax and allowed to cool.
4. Tissues are sectioned on a microtome and mounted on a microscope slide.
5. To allow for staining, step 2 is reversed (rehydrated).

6. Tissues are stained.
7. Tissues are dehydrated to xylene again.
8. Mounting medium is added to secure the coverslip.

To prepare tissues via the frozen technique tissues are frozen in liquid nitrogen, and cut with a cold knife in a refrigerated chamber (cryostat). This is faster than the paraffin technique described above.

67.8.1 Stains

Acidophilic basic (cationic) components of the cell easily bind with acidic dyes. These include cytoplasmic proteins.

Basophilic acidic (anionic) components of the cell easily bind with basic dyes. These include nucleic acids.

67.8.1.1 H&E staining

The H&E staining method is the most commonly used stains (pink cytoplasm and purple nuclei). It is composed of haemotoxylin (basic; $dye^{+}Cl^{-}$) and eosin (acidic; $Na^{+}dye^{-}$) dyes.

Dye	Component	Ultrastructure
Haemotoxylin	Nucleic acids	Nucleus, ribosomes, rough ER
Eosin	Proteins	Cytoplasm

67.8.1.2 Other staining techniques

Staining technique	Molecule / Ultrastructure
Mallory	collagen, cytoplasm, red blood cells
Periodic acid-Schiff reaction (PAS)	carbohydrates (e.g. glycogen, mucus, basement membranes)
Masson's trichrome	nuclei, cytoplasm, muscle, red blood cells, keratin, collagen
Alcian blue	Mucin (mucus), cartilage
van Gieson	collagen, nuclei, erythrocytes, cytoplasm
Azan	nuclei, collagen, basement membrane, mucin, muscle, RBCs
Immunohistochemistry	Whatever target protein you have an antibody for

To stain freshly dissected tissue for nerve and/or muscle detection, make a 0.5% solution of methylene blue in 1% borax. Then dilute this 1:10 or 1:100 and soak tissue overnight (Steve Senft's advice).

Bibliography

Abbott, N. J. and Miyan, J. A. (1995). Cerebrovascular organization and dynamics in cephalopods. In Abbot, N. J., Williamson, R., and Maddock, L., editors, *Cephalopod Neurobiology: Neuroscience studies in squid, octopus and cuttlefish*, chapter 28, pages 459–476.

Adamo, S. A., Ehgoetz, K., Sangster, C., and Whitehorne, I. (2006). Signaling to the enemy? Body pattern expression and its response to external cues during hunting in the cuttlefish Sepia officinalis (Cephalopoda). *Biological Bulletin*, 210(3):192–200.

Adema, C. M. (2021). Sticky problems: extraction of nucleic acids from molluscs. *Philosophical Transactions of the Royal Society B: Biological Sciences*, 376:20200162.

Albertin, C. B., Simakov, O., Mitros, T., Wang, Z. Y., Pungor, J. R., Edsinger-Gonzales, E., Brenner, S., Ragsdale, C. W., and Rokhsar, D. S. (2015). The octopus genome and the evolution of cephalopod neural and morphological novelties. *Nature*, 524:220–224.

Alberts, B., Johnson, A., Lewis, J., Raff, M., Roberts, K., and Walter, P. (2008). *Molecular Biology of the Cell*. Garland Science, 5th edition.

Alexandrowicz, J. S. (1963). A pulsating ganglion in the Octopoda. *Proceedings of the Royal Society B: Biological Sciences*, 157(969):562–573.

Allen, J. J., Mäthger, L. M., Barbosa, A., and Hanlon, R. T. (2009). Cuttlefish use visual cues to control three-dimensional skin papillae for camouflage. *Journal of Comparative Physiology. A, Neuroethology, Sensory, Neural, and Behavioral Physiology*, 195:547–555.

Alon, S., Garrett, S. C., Levanon, E. Y., Olson, S., Graveley, B. R., Rosenthal, J. J. C., and Eisenberg, E. (2015). The majority of transcripts in the squid nervous system are extensively recoded by A-to-I RNA editing. *eLife*, 4:e05198.

Alves, C., Boal, J. G., and Dickel, L. (2008). Short-distance navigation in cephalopods: A review and synthesis. *Cognitive Processing*, 9(4):239–247.

Ameres, S. L. and Zamore, P. D. (2013). Diversifying microRNA sequence and function. *Nature Reviews Molecular Cell Biology*, 14(8):475–488.

Amodio, P., Boeckle, M., Schnell, A. K., Ostojíc, L., Fiorito, G., and Clayton, N. S. (2019). Grow Smart and Die Young: Why Did Cephalopods Evolve Intelligence? *Trends in Ecology & Evolution*, 34(1):45–56.

Andersen, Ø., Wetten, O. F., De Rosa, M. C., Andre, C., Alinovi, C. C., Colafranceschi, M., Brix, O., and Colosimo, A. (2009). Haemoglobin polymorphisms affect the oxygen-binding properties in Atlantic cod populations. *Proceedings of the Royal Society B: Biological Sciences*, 276:833–841.

Anderson, P. and Kedersha, N. (2006). RNA granules. *Journal of Cell Biology*, 172(6):803–808.

Andrews, P. L. R., Darmaillacq, A.-S., Dennison, N., Gleadall, I. G., Hawkins, P., Messenger, J. B., Osorio, D., Smith, V. J., and Smith, J. A. (2013). The identification and management of pain, suffering and distress in cephalopods, including anaesthesia, analgesia and humane killing. *Journal of Experimental Marine Biology and Ecology*, 447:46–64.

Arkhipkin, A. I. (1992). Reproductive System Structure, Development and Function in Cephalopods with a New General Scale for Maturity Stages. *Journal of Northwest Atlantic Fishery Science*, 12:63–74.

Arkhipkin, A. I. (2013). Squid as nutrient vectors linking Southwest Atlantic marine ecosystems. *Deep Sea Research Part II: Topical Studies in Oceanography*, 95:7–20.

Arkhipkin, A. I., Bizikov, V. A., Doubleday, Z. A., Laptikhovsky, V. V., Lishchenko, F. V., Perales-Raya, C., and Hollyman, P. R. (2018). Techniques for estimating the age and growth of molluscs: Cephalopoda. *Journal of Shellfish Research*, 37(4):783–792.

Arkhipkin, A. I. and Laptikhovsky, V. V. (2010). Observation of penis elongation in Onykia ingens: implications for spermatophore transfer in deep-water squid. *Journal of Molluscan Studies*, 76(3):299–300.

Arkhipkin, A. I. and Laptikhovsky, V. V. (2012). Impact of ocean acidification on plankton larvae as a cause of mass extinctions in ammonites and belemnites. *Neues Jahrbuch für Geologie und Paläontologie - Abhandlungen*, 266(1):39–50.

Arkhipkin, A. I. and Roa-Ureta, R. (2005). Identification of growth models for squids. *Marine and Freshwater Research*, 56:371–386.

Arnold, J. M. (1962). Mating behavior and social structure in Loligo pealii. *The Biological Bulletin*, 123(1):53–57.

Arnold, J. M. (1965). Normal embryonic stages of the squid, Loligo pealii (Lesueur). *The Biological Bulletin*, 128(1):24–32.

Arrigo, K. R. (2005). Marine microorganisms and global nutrient cycles. *Nature*, 437(7057):349–355.

Asbury, C. L., Fehr, A. N., and Block, S. M. (2003). Kinesin Moves by an Asymmetric Hand-Over-Hand Mechanism. *Science*, 302:2130–2135.

Atherton, J., Farabella, I., Yu, I.-M., Rosenfeld, S. S., Houdusse, A., Topf, M., and Moores, C. A. (2014). Conserved mechanisms of microtubule-stimulated ADP release, ATP binding, and force generation in transport kinesins. *eLife*, 3:e03680.

Avivi, A., Gerlach, F., Joel, A., Reuss, S., Burmester, T., and Nevo, E. (2010). Neuroglobin, cytoglobin, and myoglobin contribute to hypoxia adaptation of the subterranean mole rat Spalax. *Proceedings of the National Academy of Sciences*, 107(50):21570–21575.

Baik, A. H. and Jain, I. H. (2020). Turning the Oxygen Dial: Balancing the Highs and Lows. *Trends in Cell Biology*, 30(7):516–536.

Ballantyne, J. S., Hochachka, P. W., and Mommsen, T. P. (1981). Studies on the metabolism of the migratory squid, Loligo opalescens: enzymes of tissues and heart mitochondria. *Marine Biology Letters*, 2:75–85.

Barbato, M., Bernard, M., Borrelli, L., and Fiorito, G. (2007). Body patterns in cephalopods: "Polyphenism" as a way of information exchange. *Pattern Recognition Letters*, 28(14):1854–1864.

Barber, V. C. and Graziadei, P. (1967). The fine structure of cephalopod blood vessels II. The vessels of the nervous system. *Zeitschrift fur Zellforschung und Mikroskopische Anatomie*, 77(2):147–161.

Barbosa, A., Allen, J. J., Mäthger, L. M., and Hanlon, R. T. (2012). Cuttlefish use visual cues to determine arm postures for camouflage. *Proceedings of the Royal Society of London B: Biological Sciences*, 279:84–90.

Barbosa, A., Mäthger, L. M., Buresch, K. C., Kelly, J., Chubb, C. F., Chiao, C.-C., and Hanlon, R. T. (2008). Cuttlefish camouflage: the effects of substrate contrast and size in evoking uniform, mottle or disruptive body patterns. *Vision Research*, 48:1242–1253.

Barbosa, A., Mäthger, L. M., Chubb, C. F., Florio, C., Chiao, C.-C., and Hanlon, R. T. (2007). Disruptive coloration in cuttlefish: a visual perception mechanism that regulates ontogenetic adjustment of skin patterning. *Journal of Experimental Biology*, 210:1139–1147.

Bard, J. A. M., Goodall, E. A., Greene, E. R., Jonsson, E., Dong, K. C., and Martin, A. (2018). Structure and Function of the 26S Proteasome. *Annual Review of Biochemistry*, 87:697–724.

Barnes, C., Maxwell, D., Reuman, D. C., and Jennings, S. (2010). Global patterns in predator–prey size relationships reveal size dependency of trophic transfer efficiency. *Ecology*, 91(1):222–232.

Bartol, I. K., Krueger, P. S., Thompson, J. T., and Stewart, W. J. (2008). Swimming dynamics and propulsive efficiency of squids throughout ontogeny. *Integrative and Comparative Biology*, 48(6):720–733.

Bartol, I. K., Mann, R., and Patterson, M. R. (2001). Aerobic respiratory costs of swimming in the negatively buoyant brief squid Lolliguncula brevis. *The Journal of Experimental Biology*, 204(21):3639–3653.

Bartol, I. K., Mann, R., and Vecchione, M. (2002). Distribution of the euryhaline squid Lolliguncula brevis in Chesapeake Bay: effects of selected abiotic factors. *Marine Ecology Progress Series*, 226:235–247.

Bashford, D., Chothia, C., and Lesk, A. M. (1987). Determinants of a Protein Fold Unique Features of the Globin Amino Acid Sequences. *Journal of Molecular Biology*, 196(1):199–216.

Basil, J. A., Bahctinova, I., Kuroiwa, K., Lee, N., Mims, D., Preis, M., and Soucier, C. (2005). The function of the rhinophore and the tentacles of Nautilus pompilius L. (Cephalopoda, Nautiloidea) in orientation to odor. *Marine and Freshwater Behaviour and Physiology*, 38(3):209–221.

Basilio, C., Wahba, A. J., Lengyel, P., Speyer, J. F., and Ochoa, S. (1962). Synthetic polynucleotides and the amino acid code, V. *Proceedings of the National Academy of Sciences*, 48(4):613–616.

Bass, B. L. (2002). RNA editing by adenosine deaminases that act on RNA. *Annual Review of Biochemistry*, 71:817–846.

Bastiaanse, E. M. L., Hold, K. M., and Van der Laarse, A. (1997). The effect of membrane cholesterol content on ion transport processes in plasma membranes. *Cardiovascular Research*, 33:272–283.

Baumann, H., Wallace, R. B., Tagliaferri, T., and Gobler, C. J. (2015). Large Natural pH, CO2 and O2 Fluctuations in a Temperate Tidal Salt Marsh on Diel, Seasonal, and Interannual Time Scales. *Estuaries and Coasts*, 38(1):220–231.

Bazzino, G., Gilly, W. F., Markaida, U., Salinas-Zavala, C. a., and Ramos-Castillejos, J. (2010). Horizontal movements, vertical-habitat utilization and diet of the jumbo squid (Dosidicus gigas) in the Pacific Ocean off Baja California Sur, Mexico. *Progress in Oceanography*, 86(1-2):59–71.

Belcaid, M., Casaburi, G., McAnulty, S. J., Schmidbaur, H., Suria, A. M., Moriano-Gutierrez, S., Pankey, M. S., Oakley, T. H., Kremer, N., Koch, E. J., Collins, A. J., Nguyen, H., Lek, S., Goncharenko-Foster, I., Minx, P., Sodergren, E., Weinstock, G., Rokhsar, D. S., McFall-Ngai, M., Simakov, O., Foster, J. S., and Nyholm, S. V. (2019). Symbiotic organs shaped by distinct modes of genome evolution in cephalopods. *Proceedings of the National Academy of Sciences*, pages 1–6.

Belle, A., Tanay, A., Bitincka, L., Shamir, R., and O'Shea, E. K. (2006). Quantification of protein half-lives in the budding yeast proteome. *Proceedings of the National Academy of Sciences of the United States of America*, 103(35):13004–13009.

Belman, B. W. (1978). Respiration and the effects of pressure on the mesopelagic vertically migrating squid Histioteuthis heteropsis. *Limnology and Oceanography*, 23(4):735–739.

Ben-Zvi, M., Amariglio, N., Paret, G., and Nevo-Caspi, Y. (2013). F11R Expression upon Hypoxia Is Regulated by RNA Editing. *PLOS ONE*, 8(10):e77702.

Benjamin, E. J. (2017). Heart Disease and Stroke Statistics - 2017 Update A Report From the American Heart Association. *Circulation*, 135(10):e146–e603.

Bennice, C. O., Rayburn, A. P., Brooks, W. R., and Hanlon, R. T. (2019). Fine-scale habitat partitioning facilitates sympatry between two octopus species in a shallow Florida lagoon. *Marine Ecology Progress Series*, 609(4):151–161.

Berry, S. and Pelkmans, L. (2022). Mechanisms of cellular mRNA transcript homeostasis. *Trends in Cell Biology*, 32(8):655–668.

Beuerlein, K., Schimmelpfennig, R., Westermann, B., Ruth, P., and Schipp, R. (1998). Cytobiological studies on hemocyanin metabolism in the branchial heart complex of the common cuttlefish Sepia officinalis (Cephalopoda, Dibranchiata). *Cell Tissue Research*, 292:587–595.

Beuerlein, K., Westermann, B., Ruth, P., Schimmelpfennig, R., and Schipp, R. (2000). Hemocyanin re-uptake in the renal and branchial heart appendages of the coleoid cephalopod Sepia officinalis. *Cell Tissue Research*, 301:413–421.

Biagi, V. and Bello, G. (2009). Occurrence of an egg mass of Thysanoteuthis rhombus (Cephalopoda:Teuthida) in the Strait of Messina (Italy), locus typicus of the species. *Bollettino Malacologico*, 45:35–38.

Birk, M. A. (2018). *Ecophysiology of Oxygen Supply in Cephalopods*. Ph.d. dissertation, University of South Florida.

Birk, M. A., Dymowska, A. K., and Seibel, B. A. (2018). Do squids breathe through their skin? *Journal of Experimental Biology*, 221(19):jeb185553.

Birk, M. A., Paight, C., and Seibel, B. A. (2017). Observations of multiple pelagic egg masses from small-sized jumbo squid (Dosidicus gigas) in the Gulf of California. *Journal of Natural History*, 51(43-44):2569–2584.

Birk, M. A. and White, J. W. (2014). Experimental determination of the spatial scale of a prey patch from the predator's perspective. *Oecologia*, 174(3):723–729.

Bishop, R. E., Kakuk, B., and Torres, J. J. (2004). Life in the hypoxic and anoxic zones: metabolism and proximate composition of Caribbean troglobitic crustaceans with observations on the water chemistry of two anchialine caves. *Journal of Crustacean Biology*, 24(3):379–392.

Blainville, H. D. (1823). Memoire sur les especes du genre Calmar (Loligo, Lamarck). *Journal de Physique, de Chimie et d'Histoire Naturelle*, 96:116–135.

Blow, M. J., Grocock, R. J., van Dongen, S., Enright, A. J., Dicks, E., Futreal, P. A., Wooster, R., and Stratton, M. R. (2006). RNA editing of human microRNAs. *Genome Biology*, 7(4):R27.

Boggs, T. E., Friedman, J. S., and Gross, J. B. (2022). Alterations to cavefish red blood cells provide evidence of adaptation to reduced subterranean oxygen. *Scientific Reports*, 12(1):3735.

Bollati, E., D'Angelo, C., Alderdice, R., Pratchett, M., Ziegler, M., and Wiedenmann, J. (2020). Optical Feedback Loop Involving Dinoflagellate Symbiont and Scleractinian Host Drives Colorful Coral Bleaching. *Current Biology*, 30(13):2433–2445.

Bols, N. C., Mosser, D. D., and Steels, G. B. (1992). Temperature studies and recent advances with fish cells in vitro. *Comparative Biochemistry and Physiology*, 103A(1):1–14.

Bonaventura, C. and Bonaventura, J. (1983). Respiratory Pigments: Structure and Function. In Wilbur, K. M., editor, *The Mollusca*, volume 2: Environ, chapter 1, pages 1–50. Academic Press, Inc.

Bone, Q., Pulsford, A., and Chubb, A. D. (1981). Squid mantle muscle. *Journal of the Marine Biological Association of the United Kingdom*, 61:327–342.

Boucaud-Camou, E. and Boucher-Rodoni, R. (1983). Feeding and Digestion in Cephalopods. In Wilbur, K. M., editor, *The Mollusca*, volume 5, pages 149–187.

Boucher-Rodoni, R. and Mangold, K. (1989). Respiration and nitrogen excretion by the squid Loligo forbesi. *Marine Biology*, 103(3):333–338.

Boucher-Rodoni, R. and Mangold, K. (1994). Ammonia production in cephalopods, physiological and evolutionary aspects. *Marine and Freshwater Behaviour and Physiology*, 25:53–60.

Bourne, G. B. (1987). Hemodynamics in squid. *Experientia*, 43:500–502.

Boutilier, R. G. (2001). Mechanisms of cell survival in hypoxia and hypothermia. *The Journal of Experimental Biology*, 204:3171–3181.

Brahimi-Horn, M. C. and Pouysségur, J. (2009). HIF at a glance. *Journal of Cell Science*, 122(8):1055–1057.

Brierley, A. S. (2014). Diel vertical migration. *Current Biology*, 24(22):R1074–R1076.

Brix, O., Bårdgard, A., Cau, A., Colosimo, A., Condò, S. G., and Giardina, B. (1989). Oxygen-binding properties of cephalopod blood with special reference to environmental temperatures and ecological distribution. *Journal of Experimental Zoology*, 252(1):34–42.

Brix, O., Colosimo, A., and Giardina, B. (1995). Temperature dependence of oxygen binding to cephalopod haemocyanins: ecological implications. *Marine and Freshwater Behaviour and Physiology*, 25:149–162.

Brown, E. R. and Piscopo, S. (2013). Synaptic plasticity in cephalopods; more than just learning and memory? *Invertebrate Neuroscience*, 13:35–44.

Browning, J. (1982). The density and dimensions of exchange vessels in Octopus pallidus. *Journal of Zoology*, 196:569–579.

Buchumenski, I., Bartok, O., Ashwal-Fluss, R., Pandey, V., Porath, H. T., Levanon, E. Y., and Kadener, S. (2017). Dynamic hyper-editing underlies temperature adaptation in Drosophila. *PLOS Genetics*, 13(7):e1006931.

Budelmann, B. U. (1994). Cephalopod sense organs, nerves and the brain: Adaptations for high performance and life style. *Marine and Freshwater Behaviour and Physiology*, 25:13–33.

Budelmann, B. U. (1995). The cephalopod nervous system: What evolution has made of the molluscan design. In *The Nervous Systems of Invertebrates: An Evolutionary and Comparative Approach*, pages 115–138. Birkhäuser Basel.

Bullock, T. H. (1955). Compensation for temperature in the metabolism and activity of poikilotherms. *Biological Reviews*, 30(3):311–342.

Burford, B. P., Carey, N., Gilly, W. F., and Goldbogen, J. A. (2019). Grouping reduces the metabolic demand of a social squid. *Marine Ecology Progress Series*, 612:141–150.

Burkepile, D. E., Allgeier, J. E., Shantz, A. A., Pritchard, C. E., Lemoine, N. P., Bhatti, L. H., and Layman, C. A. (2013). Nutrient supply from fishes facilitates macroalgae and suppresses corals in a Caribbean coral reef ecosystem. *Scientific Reports*, 3:1–9.

Burleson, M. L., Wilhelm, D. R., and Smatresk, N. J. (2001). The influence of fish size on the avoidance of hypoxia and oxygen selection by largemouth bass. *Journal of Fish Biology*, 59(5):1336–1349.

Burmester, T., Ebner, B., Weich, B., and Hankeln, T. (2002). Cytoglobin: A Novel Globin Type Ubiquitously Expressed in Vertebrate Tissues. *Molecular Biology and Evolution*, 19(4):416–421.

Burmester, T., Weich, B., Reinhardt, S., and Hankeln, T. (2000). A vertebrate globin expressed in the brain. *Nature*, 407:520–523.

Burnett, L. E. and Stickle, W. B. (2001). Physiological Responses to Hypoxia. In Rabalais, N. N. and Turner, R. E., editors, *Coastal Hypoxia: Consequences for Living Resources and Ecosystems*, chapter 6, pages 101–114. American Geophysical Union.

Bush, S. L., Hoving, H. J. T., Huffard, C. L., Robison, B. H., and Zeidberg, L. D. (2012). Brooding and sperm storage by the deep-sea squid Bathyteuthis berryi (Cephalopoda: Decapodiformes). *Journal of the Marine Biological Association of the United Kingdom*, 92(7):1629–1636.

Bush, S. L. and Robison, B. H. (2007). Ink utilization by mesopelagic squid. *Marine Biology*, 152(3):485–494.

Butler-Struben, H. M., Brophy, S. M., Johnson, N. A., and Crook, R. J. (2018). In Vivo Recording of Neural and Behavioral Correlates of Anesthesia Induction, Reversal, and Euthanasia in Cephalopod Molluscs. *Frontiers in Physiology*, 9:109.

Caddy, J. F. and Rodhouse, P. G. (1998). Cephalopod and ground fish landings: evidence for ecological change in global fisheries? *Reviews in Fish Biology and Fisheries*, 8:431–444.

Cambridge, S. B., Gnad, F., Nguyen, C., Bermejo, J. L., Krüger, M., and Mann, M. (2011). Systems-wide Proteomic Analysis in Mammalian Cells Reveals Conserved, Functional Protein Turnover. *Journal of Proteome Research*, 10:5275–5284.

Campinho, M. A., Oliveira, A. R., and Sykes, A. V. (2018). Olfactory-like neurons are present in the forehead of common cuttlefish, Sepia officinalis Linnaeus, 1758 (Cephalopoda: Sepiidae). *Zoological Journal of the Linnean Society*, 183:338–346.

Carden, D. L. and Granger, D. N. (2000). Pathophysiology of ischaemia-reperfusion injury. *Journal of Pathology*, 190(3):255–266.

Carpenter, D. O. (1981). Ionic and metabolic bases of neuronal thermosensitivity. *Federation Proceedings*, 40(14):2808–2813.

Carreau, A., Hafny-Rahbi, B. E., Matejuk, A., Grillon, C., and Kieda, C. (2011). Why is the partial oxygen pressure of human tissues a crucial parameter? Small molecules and hypoxia. *Journal of Cellular and Molecular Medicine*, 15(6):1239–1253.

Castellanos-Martínez, S. and Gestal, C. (2013). Pathogens and immune response of cephalopods. *Journal of Experimental Marine Biology and Ecology*, 447:14–22.

Castillo, M. G., Salazar, K. A., and Joffe, N. R. (2015). The immune response of cephalopods from heat to foot. *Fish & Shellfish Immunology*, 46(1):145–160.

Castillo-Davis, C. I., Mekhedov, S. L., Hartl, D. L., Koonin, E. V., and Kondrashov, F. A. (2002). Selection for short introns in highly expressed genes. *Nature Genetics*, 31(4):415–418.

Castro, P. and Huber, M. E. (2019). *Marine Biology*. McGraw-Hill, 11th edition.

Chapman, E. R. (2002). Synaptotagmin: A Ca2+ sensor that triggers exocytosis? *Nature Reviews*, 3:1–11.

Charlton, M. P. and Atwood, H. L. (1979). Synaptic transmission: temperature-sensitivity of calcium entry in presynaptic terminals. *Brain Research*, 170:543–546.

Chiao, C.-C., Chubb, C., and Hanlon, R. T. (2015). A review of visual perception mechanisms that regulate rapid adaptive camouflage in cuttlefish. *Journal of Comparative Physiology A: Neuroethology, Sensory, Neural, and Behavioral Physiology*, 201(9):933–945.

Chiao, C.-C., Chubb, C. F., Buresch, K. C., Barbosa, A., Allen, J. J., Mäthger, L. M., and Hanlon, R. T. (2010). Mottle camouflage patterns in cuttlefish: quantitative characterization and visual background stimuli that evoke them. *Journal of Experimental Biology*, 213:187–199.

Chiao, C.-C., Chubb, C. F., Buresch, K. C., Siemann, L., and Hanlon, R. T. (2009). The scaling effects of substrate texture on camouflage patterning in cuttlefish. *Vision Research*, 49:1647–1656.

Chiao, C.-C. and Hanlon, R. T. (2001a). Cuttlefish Camouflage: Visual Perception of Size, Contrast, and Number of White Squares on Artificial Checkerboard Substrata Initiates Disruptive Coloration. *Journal of Experimental Biology*, 2125:2119–2125.

Chiao, C.-C. and Hanlon, R. T. (2001b). Cuttlefish Cue Visually on Area–Not Shape or Aspect Ratio–of Light Objects in the Substrate to Produce Disruptive Body Patterns for Camouflage. *Biological Bulletin*, 201:269 –270.

Childress, J. J. (1995). Are there physiological and biochemical adaptations of metabolism in deep-sea animals? *Trends in Ecology & Evolution*, 10(1):30–36.

Childress, J. J. and Seibel, B. A. (1998). Life at stable low oxygen levels: adaptations of animals to oceanic oxygen minimum layers. *The Journal of Experimental Biology*, 201:1223–1232.

Childress, J. J. and Somero, G. N. (1990). Metabolic scaling: a new perspective based on scaling of glycolytic enzyme activities. *American Zoologist*, 30(1):161–173.

Childress, J. J. and Thuesen, E. V. (1993). Effects of hydrostatic pressure on metabolic rates of six species of deep-sea gelatinous zooplankton. *Limnology and Oceanography*, 38(3):665–670.

Chowdhury, R., Leung, I. K. H., Tian, Y.-M., Abboud, M. I., Ge, W., Domene, C., Cantrelle, F.-X., Landrieu, I., Hardy, A. P., Pugh, C. W., Ratcliffe, P. J., Claridge, T. D. W., and Schofield, C. J. (2016). Structural basis for oxygen degradation domain selectivity of the HIF prolyl hydroxylases. *Nature Communications*, 7:12673.

Chubb, C., Chiao, C.-C., Ulmer, K., Buresch, K., Birk, M. A., and Hanlon, R. T. (2018). Dark scene elements strongly influence cuttlefish camouflage responses in visually cluttered environments. *Vision Research*, 149:86–101.

Church, M. J., Lomas, M. W., and Muller-karger, F. (2013). Sea change: Charting the course for biogeochemical ocean time-series research in a new millennium. *Deep-Sea Research Part II*, 93:2–15.

Chursov, A., Kopetzky, S. J., Bocharov, G., Frishman, D., and Shneider, A. (2013). RNAtips: analysis of temperature-induced changes of RNA secondary structure. *Nucleic Acids Research*, 41:W486–W491.

Claireaux, G. and Chabot, D. (2016). Responses by fishes to environmental hypoxia: integration through Fry's concept of aerobic metabolic scope. *Journal of Fish Biology*, 88:232–251.

Clarke, A. J. (2014). El Niño Physics and El Niño Predictability. *Annual Review of Marine Science*, 6:79–99.

Clarke, M. R. (1978). The cephalopod statolith - an introduction to its form. *Journal of the Marine Biological Association of the United Kingdom*, 58:701–712.

Clarke, M. R., Denton, E. J., and Gilpin-Brown, J. B. (1979). On the use of ammonium for buoyancy in squids. *Journal of the Marine Biological Association of the United Kingdom*, 59(2):259–276.

Clements, J. C. and Hunt, H. L. (2015). Marine animal behaviour in a high CO2 ocean. *Marine Ecology Progress Series*, 536:259–279.

Cloney, R. A. and Florey, E. (1968). Ultrastructure of cephalopod chromatophore organs. *Zeitschrift fur Zellforschung und Mikroskopische Anatomie*, 89(2):250–280.

Cohen, J. H. and Forward, R. B. (2009). Zooplankton Diel Vertical Migration - A Review of Proximate Control. *Oceanography and Marine Biology: An Annual Review*, 47:77–110.

Colin, S. P. and Costello, J. H. (2002). Morphology, swimming performance and propulsive mode of six co-occurring hydromedusae. *The Journal of Experimental Biology*, 205:427–437.

Colina, C., Palavicini, J. P., Srikumar, D., Holmgren, M., and Rosenthal, J. J. C. (2010). Regulation of Na+/K+ ATPase Transport Velocity by RNA Editing. *PLOS Biology*, 8(11):e1000540.

Collins, A. J., Fullmer, M. S., Gogarten, J. P., and Nyholm, S. V. (2015). Comparative genomics of Roseobacter clade bacteria isolated from the accessory nidamental gland of Euprymna scolopes. *Frontiers in Microbiology*, 6(February):123.

Collins, A. J., Schleicher, T. R., Rader, B. A., and Nyholm, S. V. (2012). Understanding the role of host hemocytes in a squid/Vibrio symbiosis using transcriptomics and proteomics. *Frontiers in Immunology*, 3:91.

Collins, M., Knutti, R., Arblaster, J., Dufresne, J.-L., Fichefet, T., Friedlingstein, P., Gao, X., Gutowski Jr., W. J., Johns, T., Krinner, G., Shongwe, M., Tebaldi, C., Weaver, A. J., and Wehner, M. (2013). Long-term Climate Change: Projections, Commitments and Irreversibility. In Stocker, T. F., Qin, D., Plattner, G.-K., Tignor, M., Allen, S. K., Boschung, J., Nauels, A., Xia, Y., Bex, V., and Midgley, P. M., editors, *Climate Change 2013: The Physical Science Basis. Contribution of Working Group I to the Fifth Assessment Report of the Intergovernmental Panel on Climate Change*, chapter 12, pages 1029–1136. Cambridge University Press, Cambridge, United Kingdom and New York, NY.

Collins, M. A. and Villanueva, R. (2006). Taxonomy, ecology and behaviour of the cirrate octopods. *Oceanography and Marine Biology: An Annual Review*, 44:277–322.

Conesa, A., Madrigal, P., Tarazona, S., Gomez-Cabrero, D., Cervera, A., McPherson, A., Szczesniak, M. W., Gaffney, D. J., Elo, L. L., Zhang, X., and Mortazavi, A. (2016). A survey of best practices for RNA-seq data analysis. *Genome Biology*, 17:13.

Connett, R. J., Honig, C. R., Gayeski, T. E. J., and Brooks, G. A. (1990). Defining hypoxia: a systems view of VO2, glycolysis, energetics, and intracellular PO2. *Journal of Applied Physiology*, 68(3):833–842.

Conti, L., Limon, A., Palma, E., and Miledi, R. (2013). Microtransplantation of cellular membranes from squid stellate ganglion reveals ionotropic GABA receptors. *Biological Bulletin*, 224(1):47–52.

Cossins, A. R. and Prosser, C. L. (1978). Evolutionary adaptation of membranes to temperature. *Proceedings of the National Academy of Sciences*, 75(4):2040–2043.

Coy, D. L., Hancock, W. O., Wagenbach, M., and Howard, J. (1999a). Kinesin's tail domain is an inhibitory regulator of the motor domain. *Nature Cell Biology*, 1:288–292.

Coy, D. L., Wagenbach, M., and Howard, J. (1999b). Kinesin Takes One 8-nm Step for Each ATP That It Hydrolyzes. *The Journal of Biological Chemistry*, 274(6):3667–3671.

Crook, R. J. (2021). Behavioral and neurophysiological evidence suggests affective pain experience in octopus. *iScience*, 24(3):102229.

Crowell, J. W. and Smith, E. E. (1967). Determinant of the optimal hematocrit. *Journal of Applied Physiology*, 22(3):501–504.

Curio, E. (1976). *The ethology of predation*, volume 7.

Cyran, N., Staedler, Y., Schönenberger, J., Klepal, W., and von Byern, J. (2013). Hatching glands in cephalopods - A comparative study. *Zoologischer Anzeiger*, 253(1):66–82.

Dabruzzi, T. F. and Bennett, W. A. (2014). Hypoxia effects on gill surface area and blood oxygen-carrying capacity of the Atlantic stingray, Dasyatis sabina. *Fish Physiology and Biochemistry*, 40:1011–1020.

Davletov, B. A. and Sudhof, T. C. (1993). A Single C2 Domain from Synaptotagmin I Is Sufficient for High Affinity Ca2+/Phospholipid Binding. *The Journal of Biological Chemistry*, 268(35):26386–26390.

de Jonge, D. S. W., Merten, V., Bayer, T., Puebla, O., Reusch, T. B. H., and Hoving, H.-J. T. (2021). A novel metabarcoding primer pair for environmental DNA analysis of Cephalopoda (Mollusca) targeting the nuclear 18S rRNA region. *Royal Society Open Science*, 8(2):201388.

De Rosa, M. C., Sanna, M. T., Messana, I., Castagnola, M., Galtieri, A., Tellone, E., Scatena, R., Botta, B., Botta, M., and Giardina, B. (1998). Glycated human hemoglobin (HbA1c): functional characteristics and molecular modeling studies. *Biophysical Chemistry*, 72:323–335.

De Silva-Dávila, R., Franco-Gordo, C., Hochberg, F. G., Godínez-Domínguez, E., Avendaño-Ibarra, R., Gómez-Gutiérrez, J., and Robinson, C. J. (2015). Cephalopod paralarval assemblages in the Gulf of California during 2004-2007. *Marine Ecology Progress Series*, 520:123–141.

De Silva-Dávila, R., Hochberg, F. G., Lindgren, A. R., and del Carmen Franco-Gordo, M. (2013). Paralarval development, abundance, and distribution of Pterygioteuthis hoylei (Cephalopoda: Oegopsida: Pyroteuthidae) in the Gulf of California, México. *Molluscan Research*, 33(1):50–64.

Deffit, S. N. and Hundley, H. A. (2016). To edit or not to edit: regulation of ADAR editing specificity and efficiency. *WIREs RNA*, 7:113–127.

Deffner, G. G. J. (1961). The dialyzable free organic constituents of squid blood: a comparison with nerve axoplasm. *Biochimica et Biophysica Acta*, 47(2):378–388.

DeFur, P. L., Mangum, C. P., and Reese, J. E. (1990). Respiratory Responses of the Blue Crab Callinectes sapidus to Long-Term Hypoxia. *The Biological Bulletin*, 178(1):46–54.

Deickert, A. and Bello, G. (2005). Egg masses of Sepietta oweniana (Cephalopoda: Sepiolidae) collected in the Catalan Sea. *Scientia Marina*, 69(2):205–209.

Denton, E. J., Gilpin-Brown, J. B., and Shaw, T. I. (1969). A buoyancy mechanism found in cranchid squid. *Proceedings of the Royal Society B: Biological Sciences*, 174(1036):271–279.

Denton, E. J. and Warren, F. J. (1968). Eyes of the Histioteuthidae. *Nature*, 219:400–401.

Derby, C. D. (2014). Cephalopod ink: production, chemistry, functions and applications. *Marine Drugs*, 12(5):2700–2730.

Deschamps-Francoeur, G., Simoneau, J., and Scott, M. S. (2020). Handling multi-mapped reads in RNA-seq. *Computational and Structural Biotechnology Journal*, 18:1569–1576.

Deutsch, C., Brix, H., Ito, T., Frenzel, H., and Thompson, L. (2011). Climate-forced variability of ocean hypoxia. *Science*, 333(6040):336–339.

Deutsch, C., Ferrel, A., Seibel, B. A., Pörtner, H.-O., and Huey, R. B. (2015). Climate change tightens a metabolic constraint on marine habitats. *Science*, 348(6239):1132–1135.

Devol, A. H. (1978). Bacterial oxygen uptake kinetics as related to biological processes in oxygen deficient zones of the oceans. *Deep-Sea Research*, 25(2):137–146.

Dewilde, S., Ebner, B., Vinck, E., Gilany, K., Hankeln, T., Burmester, T., Kreiling, J., Reinisch, C., Vanfleteren, J. R., Kiger, L., Marden, M. C., Hundahl, C., Fago, A., Doorslaer, S. V., and Moens, L. (2006). The Nerve Hemoglobin of the Bivalve Mollusc Spisula solidissima. *The Journal of Biological Chemistry*, 281(9):5364–5372.

Di Cosmo, A., Di Cristo, C., and Messenger, J. B. (2006). L-Glutamate and its Ionotropic Receptors in the Nervous System of Cephalopods. *Current Neuropharmacology*, 4:305–312.

Diaz, A. A., Tomba, E., Lennarson, R., Richard, R., Bagajewicz, M. J., and Harrison, R. G. (2010). Prediction of Protein Solubility in Escherichia coli Using Logistic Regression. *Biotechnology and Bioengineering*, 105(2):374–383.

Diaz, R. J. and Rosenberg, R. (2008). Spreading Dead Zones and Consequences for Marine Ecosystems. *Science*, 321:926–929.

Dickson, A. G., Sabine, C. L., and Christian, J. R. (2007). Guide to best practices for ocean CO2 measurements. *PICES Special Publication 3*, page 191.

Dilly, P. N. and Messenger, J. B. (1972). The Branchial Gland: A Site of Haemocyanin Synthesis in Octopus. *Zeitschrift fur Zellforschung und Mikroskopische Anatomie*, 132(2):193–201.

Divakaruni, A. S. and Brand, M. D. (2011). The Regulation and Physiology of Mitochondrial Proton Leak. *Physiology*, 26:192–205.

Doench, J. G. and Sharp, P. A. (2004). Specificity of microRNA target selection in translational repression. *Genes & Development*, 18(5):504–511.

Dolashka, P., Daskalova, A., Dolashki, A., and Voelter, W. (2020). De Novo Structural Determination of the Oligosaccharide Structure of Hemocyanins from Molluscs. *Biomolecules*, 10(11):1470.

Domenici, P., Ferrari, R. S., Steffensen, J. F., and Batty, R. S. (2002). The effect of progressive hypoxia on school structure and dynamics in Atlantic herring Clupea harengus. *Proceedings of the Royal Society B: Biological Sciences*, 269(1505):2103–2111.

D'Orbigny, A. D. (1835). *Voyage dans l'Amérique Méridionale*, volume t.5. Chez Pitois-Levrault et c.e., Paris.

Dörrbaum, A. R., Kochen, L., Langer, J. D., and Schuman, E. M. (2018). Local and global influences on protein turnover in neurons and glia. *eLife*, 7:e34202.

Dragovich, A. and Kelly Jr., J. A. (1964). Ecological observations of macro-invertebrates in Tampa Bay, Florida 1961-1962. *Bulletin of Marine Science*, 14(1):74–102.

Dragovich, A. and Kelly Jr., J. A. (1967). Occurrence of the squid, Lolliguncula brevis, in some coastal waters of western Florida. *Bulletin of Marine Science*, 17(4):840–844.

Driedzic, W. R. (1988). Matching of cardiac oxygen delivery and fuel supply to energy demand in teleosts and cephalopods. *Canadian Journal of Zoology*, 66:1078–1083.

Dubas, F., Hanlon, R. T., Ferguson, G. P., and Pinsker, H. M. (1986). Localization and stimulation of chromatophore motoneurones in the brain of the squid, Lolliguncula brevis. *The Journal of Experimental Biology*, 121:1–25.

Ekau, W., Auel, H., Pörtner, H.-O., and Gilbert, D. (2010). Impacts of hypoxia on the structure and processes in pelagic communities (zooplankton, macro-invertebrates and fish). *Biogeosciences*, 7(5):1669–1699.

Elliott, J. M. and Davison, W. (1975). Energy equivalents of oxygen consumption in animal energetics. *Oecologia*, 19(3):195–201.

Emery, W. J. (2003). Water Types and Water Masses. *Ocean Circulation*, pages 1556–1567.

Endler, J. A. (1986). *Natural selection in the wild*. Princeton University Press.

English, S. G., Hadj-Moussa, H., and Storey, K. B. (2018). MicroRNAs regulate survival in oxygen-deprived environments. *Journal of Experimental Biology*, 221(23):jeb190579.

Eno, N. C. (1994). The morphometrics of cephalopod gills. *Journal of the Marine Biological Association of the United Kingdom*, 74:687–706.

Eppley, R. W. and Peterson, B. J. (1979). Particulate organic matter flux and planktonic new production in the deep ocean. *Nature*, 282(5740):677–680.

Esbaugh, A. J., Ern, R., Nordi, W. M., and Johnson, A. S. (2016). Respiratory plasticity is insufficient to alleviate blood acid-base disturbances after acclimation to ocean acidification in the estuarine red drum, Sciaenops ocellatus. *Journal of Comparative Physiology B: Biochemical, Systemic, and Environmental Physiology*, 186(1):97–109.

Fabry, V. J., Seibel, B. A., Feely, R. A., and Orr, J. C. (2008). Impacts of ocean acidification on marine fauna and ecosystem processes. *ICES Journal of Marine Science*, 65:414–432.

Farhat, E., Turenne, E. D., Choi, K., and Weber, J. M. (2019). Hypoxia-induced remodelling of goldfish membranes. *Comparative Biochemistry and Physiology Part - B: Biochemistry and Molecular Biology*, 237:110326.

Feely, R. A., Alin, S. R., Carter, B., Bednaršek, N., Hales, B., Chan, F., Hill, T. M., Gaylord, B., Sanford, E., Byrne, R. H., Sabine, C. L., Greeley, D., and Juranek, L. (2016). Chemical and biological impacts of ocean acidification along the west coast of North America. *Estuarine, Coastal and Shelf Science*, 183:260–270.

Ferguson, G. P. and Messenger, J. B. (1991). A countershading reflex in cephalopods. *Proceedings of the Royal Society of London B: Biological Sciences*, 243(1306):63–67.

Ferguson, N., White, C. R., and Marshall, D. J. (2013). Competition in benthic marine invertebrates: the unrecognized role of exploitative competition for oxygen. *Ecology*, 94(1):126–135.

Fiedler, A. (1992). The Possible Role of Vena-Cava Peptides in Regulation of the Branchial Hearts of Sepia-Officinalis L. (Cephalopoda). *Journal of Experimental Zoology*, 264(2):136–143.

Fields, W. G. (1965). *The Structure, Development, Food Relations, Reproduction, and Life History of the Squid Loligo opalescens Berry*. Phd dissertation, Stanford University.

Fiorito, G., Affuso, A., Basil, J., Cole, A., de Girolamo, P., D'Angelo, L., Dickel, L., Gestal, C., Grasso, F., Kuba, M., Mark, F., Melillo, D., Osorio, D., Perkins, K., Ponte, G., Shashar, N., Smith, D., Smith, J., and Andrews, P. L. R. (2015). Guidelines for the Care and Welfare of Cephalopods in Research - A consensus based on an initiative by CephRes, FELASA and the Boyd Group. *Laboratory Animals*, 49:1–90.

Fornasiero, E. F., Mandad, S., Wildhagen, H., Alevra, M., Rammner, B., Keihani, S., Opazo, F., Urban, I., Ischebeck, T., Sakib, M. S., Fard, M. K., Kirli, K., Centeno, T. P., Vidal, R. O., Rahman, R.-U., Benito, E., Fischer, A., Dennerlein, S., Rehling, P., Feussner, I., Bonn, S., Simons, M., Urlaub, H., and Rizzoli, S. O. (2018). Precisely measured protein lifetimes in the mouse brain reveal differences across tissues and subcellular fractions. *Nature Communications*, 9:4230.

Fox, D. L. and Updegraff, D. M. (1943). Adenochrome, a glandular pigment in the branchial hearts of the octopus. *Archives of Biochemistry*, 1:339–356.

Franco, A. C., Hernández-Ayón, J. M., Beier, E., Carcon, V., Maske, H., Paulier, A., Färber-Lorda, J., Castro, R., and Sosa-Ávalos, R. (2014). Air-sea CO2 fluxes above the stratified oxygen minimum zone in the coastal region off Mexico. *Journal of Geophysical Research: Oceans*, 119(5):2923–2937.

Frank, M. G., Waldrop, R. H., Dumoulin, M., Aton, S., and Boal, J. G. (2012). A preliminary analysis of sleep-like states in the cuttlefish Sepia officinalis. *PLOS ONE*, 7(6):e38125.

Fraser, J., Vieira de Mello, L., Ward, D., Rees, H. H., Williams, D. R., Fang, Y., Brass, A., Gracey, A. Y., and Cossins, A. R. (2006). Hypoxia-inducible myoglobin expression in nonmuscle tissues. *Proceedings of the National Academy of Sciences*, 103(8):2977–2981.

Fraser, K. P. P. and Rogers, A. D. (2007). Protein Metabolism in Marine Animals: The Underlying Mechanism of Growth. *Advances in Marine Biology*, 52:267–362.

Frasnelli, E., Ponte, G., Vallortigara, G., and Fiorito, G. (2019). Visual Lateralization in the Cephalopod Mollusk Octopus vulgaris. *Symmetry*, 11:1121.

Frederico, L. (1878). La Physiologie Du Poulpe Commun (Octopus vulgaris). *Archives de Zoologie Expérimentale et Générale*, 7:535–583.

Friedman, D. S. and Vale, R. D. (1999). Single-molecule analysis of kinesin motility reveals regulation by the cargo-binding tail domain. *Nature Cell Biology*, 1:293–297.

Friedman, R. C., Farh, K. K.-h., Burge, C. B., and Bartel, D. P. (2009). Most mammalian mRNAs are conserved targets of microRNAs. *Genome Research*, 19:92–105.

Fry, F. E. J. (1947). *Effects of the environment on animal activity*, volume 68. University of Toronto Press.

Fujii, R. (2000). The regulation of motile activity in fish chromatophores. *Pigment Cell Research*, 13:300–319.

Fukuda, M., Moreira, J. E., Lewis, F. M. T., Sugimori, M., Niinobe, M., Mikoshiba, K., and Llinas, R. (1995). Role of the C2B domain of synaptotagmin in vesicular release and recycling as determined by specific antibody injection into the squid giant synapse preterminal. *Proceedings of the National Academy of Sciences of the United States of America*, 92:10708–10712.

Gai, Z., Matsuno, A., Kato, K., Kato, S., Khan, M. R. I., Shimizu, T., Yoshioka, T., Kato, Y., Kishimura, H., Kanno, G., Miyabe, Y., Terada, T., Tanaka, Y., and Yao, M. (2015). Crystal Structure of the 3.8-MDa Respiratory Supermolecule Hemocyanin at 3.0 Å Resolution. *Structure*, 23(12):2204–2212.

Gaikwad, S., De, K., Nanajkar, M., and Sautya, S. (2021). Octocoral colonies as spawning ground for the cuttlefish Sepiella inermis (Cephalopoda: Sepiidae). *Symbiosis*.

Gallego Romero, I., Pai, A., Tung, J., and Gilad, Y. (2014). RNA-seq: impact of RNA degradation on transcript quantification. *BMC Biology*, 12:42.

Garrett, S. and Rosenthal, J. J. C. (2012a). RNA Editing Underlies Temperature Adaptation in K+ Channels from Polar Octopuses. *Science*, 335:848–851.

Garrett, S. C. and Rosenthal, J. J. C. (2012b). A Role for A-to-I RNA Editing in Temperature Adaptation. *Physiology*, 27:362–369.

Garthwaite, R. L., Berg Jr, C. J., and Harrigan, J. (1989). Population Genetics of the Common Squid Loligo pealei LeSueur, 1821, from Cape Cod to Cape Hatteras. *Biological Bulletin*, 177:287–294.

Geffeney, S. L., Williams, B. L., Rosenthal, J. J. C., Birk, M. A., Felkins, J., Wisell, C. M., Curry, E. R., and Hani, C. T. (2019). Convergent and parallel evolution in a voltage-gated sodium channel underlies TTX-resistance in the Greater Blue-ringed Octopus: Hapalochlaena lunulata. *Toxicon*, 170:77–84.

Gillooly, J. F., Gomez, J. P., and Mavrodiev, E. V. (2017). A broad-scale comparison of aerobic activity levels in vertebrates: endotherms versus ectotherms. *Proceedings of the Royal Society B: Biological Sciences*, 284(1849):20162328.

Gilly, W. F., Beman, J. M., Litvin, S. Y., and Robison, B. H. (2013). Oceanographic and biological effects of shoaling of the oxygen minimum zone. *Annual Review of Marine Science*, 5:393–420.

Gilly, W. F. and Lucero, M. T. (1992). Behavioral Responses to Chemical Stimulation of the Olfactory Organ in the Squid Loligo Opalescens. *Journal of Experimental Biology*, 162:209–229.

Gilly, W. F., Markaida, U., Baxter, C. H., Block, B. A., Boustany, A., Zeidberg, L. D., Reisenbichler, K., Robison, B. H., Bazzino, G., and Salinas, C. (2006). Vertical and horizontal migrations by the jumbo squid Dosidicus gigas revealed by electronic tagging. *Marine Ecology Progress Series*, 324:1–17.

Gilly, W. F., Zeidberg, L. D., Booth, J. A. T., Stewart, J. S., Marshall, G., Abernathy, K., and Bell, L. E. (2012). Locomotion and behavior of Humboldt squid, Dosidicus gigas, in relation to natural hypoxia in the Gulf of California, Mexico. *The Journal of Experimental Biology*, 215(18):3175–3190.

Goddard, C. K. (1968). Studies on the blood sugar of Octopus dofleini. *Comparative Biochemistry and Physiology*, 27:275–285.

Goldman, D. (2008). Theoretical Models of Microvascular Oxygen Transport to Tissue. *Microcirculation*, 15(8):795–811.

Gonzalez-Bellido, P. T., Scaros, A. T., Hanlon, R. T., and Wardill, T. J. (2018). Neural Control of Dynamic 3-Dimensional Skin Papillae for Cuttlefish Camouflage. *iScience*, 1:24–34.

Gosline, J. M. and Shadwick, R. E. (1982). The biomechanics of the arteries of Nautilus, Nototodarus and Sepia. *Pacific Science*, 36(3):283–296.

Gou, Z.-H., Wang, X., and Wang, W. (2012). Evolution of neurotransmitter gamma-aminobutyric acid, glutamate and their receptors. *Zoological Research*, 33(E5-6):E75–81.

Graham, A. M. and Barreto, F. S. (2019). Loss of the HIF pathway in a widely distributed intertidal crustacean, the copepod Tigriopus californicus. *Proceedings of the National Academy of Sciences of the United States of America*, 116(26):12913–12918.

Graham, A. M. and Barreto, F. S. (2020). Independent Losses of the Hypoxia-Inducible Factor (HIF) Pathway within Crustacea. *Molecular Biology and Evolution*, 37(5):1342–1349.

Graham, A. M. and Presnell, J. S. (2017). Hypoxia Inducible Factor (HIF) transcription factor family expansion, diversification, divergence and selection in eukaryotes. *PLoS ONE*, 12(6):e0179545.

Gray, E. G. (1969). Electron microscopy of the glio-vascular organization of the brain of Octopus. *Philosophical Transactions of the Royal Society of London. Series B, Biological Sciences*, 255(797):13–32.

Gray, I. E. (1954). Comparative study of the gill area of marine fishes. *Biological Bulletin*, 107(2):219–225.

Grieshaber, M. K., Hardewig, I., Kreutzer, U., and Pörtner, H.-O. (1994). Physiological and Metabolic Responses to Hypoxia in Invertebrates. *Reviews of Physiology, Biochemistry, and Pharmacology*, 125:43–147.

Guderley, H. (2004). Metabolic responses to low temperature in fish muscle. *Biological Reviews*, 79:409–427.

Gunderson, A. R., Armstrong, E. J., and Stillman, J. H. (2016). Multiple Stressors in a Changing World: The Need for an Improved Perspective on Physiological Responses to the Dynamic Marine Environment. *Annual Review of Marine Science*, 8(1):357–378.

Gutowska, M. A. and Melzner, F. (2009). Abiotic conditions in cephalopod (Sepia officinalis) eggs: embryonic development at low pH and high pCO2. *Marine Biology*, 156(3):515–519.

Gutowska, M. A., Melzner, F., Langenbuch, M., Bock, C., Claireaux, G., and Pörtner, H.-O. (2010). Acid-base regulatory ability of the cephalopod (Sepia officinalis) in response to environmental hypercapnia. *Journal of Comparative Physiology: B, Biochemical, Systemic, and Environmental Physiology*, 180(3):323–335.

Hadj-Moussa, H., Logan, S. M., Seibel, B. A., and Storey, K. B. (2018). Potential role for microRNA in regulating hypoxia-induced metabolic suppression in jumbo squids. *Biochimica et Biophysica Acta (BBA) - Gene Regulatory Mechanisms*, 1861(6):586–593.

Hadj-Moussa, H. and Storey, K. B. (2020). The OxymiR response to oxygen limitation: a comparative microRNA perspective. *Journal of Experimental Biology*, 223(10):jeb204594.

Haefner Jr., P. A. (1964). Morphometry of the common atlantic squid, Loligo pealei, and the brief squid, Lolliguncula brevis in Delaware Bay. *Chesapeake Science*, 5(3):138–144.

Häfker, N. S. (2012). *Effects of hypoxia and hypercapnia on blood and tissue physiology of the common cuttlefish Sepia officinalis*. Master's thesis, University of Bremen.

Hall, K. C. and Hanlon, R. T. (2002). Principal features of the mating system of a large spawning aggregation of the giant Australian cuttlefish Sepia apama (Mollusca: Cephalopoda). *Marine Biology*, 140(3):533–545.

Hanke, F. D. and Kelber, A. (2020). The Eye of the Common Octopus (Octopus vulgaris). *Frontiers in Physiology*, 10:1637.

Hanlon, R., Buresch, K., Moustahfid, H., and Staudinger, M. (2013). Doryteuthis pealeii, Longfin Inshore Squid. In *Advances in Squid Biology, Ecology and Fisheries. Part I*, chapter 7.

Hanlon, R. T. (1988). Behavioral and body patterning characters useful in taxonomy and field identification of cephalopods. *Malacologia*, 29(1):247–264.

Hanlon, R. T. (2007). Cephalopod dynamic camouflage. *Current Biology*, 17:400–404.

Hanlon, R. T., Bidwell, J. P., and Tait, R. (1989). Strontium is required for statolith development and thus normal swimming behaviour of hatchling cephalopods. *The Journal of Experimental Biology*, 141:187–195.

Hanlon, R. T., Maxwell, M. R., Shashar, N., Loew, E. R., and Boyle, K.-L. (1999). An ethogram of body patterning behavior in the biomedically and commercially valuable squid Loligo pealei off Cape Cod, Massachusetts. *Biological Bulletin*, 197(1):49–62.

Hanlon, R. T. and Messenger, J. B. (1988). Adaptive Coloration in Young Cuttlefish (Sepia officinalis L.): The Morphology and Development of Body Patterns and their Relation to Behaviour. *Philosophical Transactions of the Royal Society of London. Series B, Biological Sciences*, 320:437–487.

Hanlon, R. T. and Messenger, J. B. (1996). *Cephalopod behaviour*. Cambridge University Press.

Harrop, J., Vecchione, M., and Felley, J. D. (2014). In situ observations on behaviour of the ommastrephid squid genus Illex (Cephalopoda: Ommastrephidae) in the northwestern Atlantic. *Journal of Natural History*, pages 1–16.

Head, J. M. (2010). The effects of hypoxia on hemocyanin regulation in Cancer magister: Possible role of Hypoxia-Inducible Factor-1. *Journal of Experimental Marine Biology and Ecology*, 386(1-2):77–85.

Heine, K. B. and Hood, W. R. (2020). Mitochondrial behaviour, morphology, and animal performance. *Biological Reviews*, 95(3):730–737.

Heisler, N. (1986). Buffering and Transmembrane Ion Transfer Processes. In *Acid-Base Regulation in Animals*, chapter 1, pages 3–47. Elsevier Science Publishers B.V.

Heisler, N. (1989). Interactions between gas exchange, metabolism, and ion transport in animals: an overview. *Canadian Journal of Zoology*, 67:2923–2935.

Heming, T. A., Vanoye, C. G., Brown, S. E. S., and Bidani, A. (1990). Cytoplasmic pH recovery in acid-loaded haemocytes of squid (Sepioteuthis lessoniana). *The Journal of Experimental Biology*, 148:385–394.

Herbert, N. A., Skjæraasen, J. E., Nilsen, T., Salvanes, A. G. V., and Steffensen, J. F. (2011). The hypoxia avoidance behaviour of juvenile Atlantic cod (Gadus morhua L.) depends on the provision and pressure level of an O2 refuge. *Marine Biology*, 158(4):737–746.

Herke, S. W. and Foltz, D. W. (2002). Phylogeography of two squid (Loligo pealei and L. plei) in the Gulf of Mexico and northwestern Atlantic Ocean. *Marine Biology*, 140(1):103–115.

Herring, P. J., Dilly, P. N., and Cope, C. (1987). The morphology of the bioluminescent tissue of the cephalopod Japetella diaphana (Octopoda: Bolitaenidae). *Journal of Zoology*, 212(2):245–254.

Heuer, R. M. and Grosell, M. (2014). Physiological impacts of elevated carbon dioxide and ocean acidification on fish. *American Journal of Physiology: Regulatory, Integrative, and Comparative Physiology*, 307:R1061–R1084.

Hirokawa, N. (1998). Kinesin and Dynein Superfamily Proteins and the Mechanism of Organelle Transport. *Science*, 279:519–526.

Hixon, R. F. (1980). *Growth, reproductive biology, distribution and abundance of three species of loliginid squid (Myopsida, Cephalopoda) in the Northwest Gulf of Mexico*. PhD thesis, University of Miami.

Hochachka, P. W., Buck, L. T., Doll, C. J., and Land, S. C. (1996). Unifying theory of hypoxia tolerance: molecular/metabolic defense and rescue mechanisms for surviving oxygen lack. *Proceedings of the National Academy of Sciences*, 93(18):9493–9498.

Hochachka, P. W., Clark, C. M., Brown, D., Stanley, C., Stone, C. K., Nickles, R. J., Zhu, G. G., Allen, P. S., and Holden, J. E. (1994). The Brain at High Altitude: Hypometabolism as a Defense Against Chronic Hypoxia? *Journal of Cerebral Blood Flow and Metabolism*, 14(4):671–679.

Hochachka, P. W., French, C. J., and Meredith, J. (1978). Metabolic and ultrastructural organization in Nautilus muscles. *Journal of Experimental Zoology*, 205:51–62.

Hochachka, P. W., Moon, T. W., Mustafa, T., and Storey, K. B. (1975). Metabolic sources of power for mantle muscle of a fast swimming squid. *Comparative Biochemistry and Physiology*, 52B:151–158.

Hochachka, P. W. and Somero, G. N. (2002). *Biochemical Adaptation: Mechanism and Process in Physiological Evolution*. Oxford University Press.

Hochberg, F. G., Norman, M. D., and Finn, J. (2006). Wunderpus photogenicus n. gen. and sp., a new octopus from the shallow waters of the Indo-Malayan Archipelago (Cephalopoda: Octopodidae). *Molluscan Research*, 26:128–140.

Hodgkin, A. L. and Keynes, R. D. (1955). Active transport of cations in giant axons from Sepia and Loligo. *Journal of Physiology*, 128:28–60.

Hoeger, U., Mommsen, T. P., O'Dor, R., and Webber, D. (1987). Oxygen uptake and nitrogen excretion in two cephalopods, octopus and squid. *Comparative Biochemistry and Physiology Part A: Physiology*, 87(1):63–67.

Hofmann, G. E., Smith, J. E., Johnson, K. S., Send, U., Levin, L. A., Paytan, A., Price, N. N., Peterson, B., Takeshita, Y., Matson, P. G., Crook, E. D., Kroeker, K. J., Gambi, M. C., Rivest, E. B., Frieder, C. A., Yu, P. C., and Martz, T. R. (2011). High-Frequency Dynamics of Ocean pH: A Multi-Ecosystem Comparison. *PLOS ONE*, 6(12):e28983.

Holmgren, M. and Rosenthal, J. J. C. (2015). Regulation of Ion Channel and Transporter Function Through RNA Editing. *Current Issues in Molecular Biology*, 17:23–36.

Hon, W.-C., Wilson, M. I., Harlos, K., Claridge, T. D. W., Schofield, C. J., Pugh, C. W., Maxwell, P. H., Ratcliffe, P. J., Stuart, D. I., and Jones, E. Y. (2002). Structural basis for the recognition of hydroxyproline in HIF-1α by pVHL. *Nature*, 417(June):975–978.

Houghton, I. A., Koseff, J. R., Monismith, S. G., and Dabiri, J. O. (2018). Vertically migrating swimmers generate aggregation-scale eddies in a stratified column. *Nature*, 556:497–500.

Houlihan, D. F., Duthie, G., Smith, P. J., Wells, M. J., and Wells, J. (1986). Ventilation and circulation during exercise in Octopus vulgaris. *Journal of Comparative Physiology. B, Biochemical, Systemic, and Environmental Physiology*, 156:683–689.

Houlihan, D. F., Innes, A. J., Wells, M. J., and Wells, J. (1982). Oxygen Consumption and Blood Gases of Octopus vulgaris in Hypoxic Conditions. *Journal of Comparative Physiology: B, Biochemical, Systemic, and Environmental Physiology*, 148:35–40.

Houlihan, D. F., McMillan, D. N., Agnisola, C., Genoino, I. T., and Foti, L. (1990). Protein synthesis and growth in Octopus vulgaris. *Marine Biology*, 106(2):251–259.

Hoving, H. J. T., Fernández-Álvarez, F., Portner, E. J., and Gilly, W. F. (2019). Same-sex sexual behaviour in an oceanic ommastrephid squid, Dosidicus gigas (Humboldt squid). *Marine Biology*, 166:33.

Hoving, H.-J. T. and Haddock, S. H. D. (2017). The giant deep-sea octopus Haliphron atlanticus forages on gelatinous fauna. *Scientific Reports*, 7:44952.

Hoving, H.-J. T. and Robison, B. H. (2017). The pace of life in deep-dwelling squids. *Deep-Sea Research Part I: Oceanographic Research Papers*, 126:40–49.

Hoving, H. J. T., Zeidberg, L. D., Benfield, M. C., Bush, S. L., Robison, B. H., and Vecchione, M. (2013). First in situ observations of the deep-sea squid Grimalditeuthis bonplandi reveal unique use of tentacles. *Proceedings of the Royal Society B*, 280:20131463.

Howell, B. J. and Gilbert, D. L. (1976). pH-temperature dependence of the hemolymph of the squid, Loligo pealei. *Comparative Biochemistry and Physiology*, 55A:287–289.

Hoyle, W. E. (1885). Diagnoses of new species of Cephalopoda collected during the cruise of H.M.S. Challenger - Part 1. The Octopoda. *The Annals and Magazine of Natural History: Zoology, Botany, and Geology*, 15(5):222–236.

Hu, M. and Tseng, Y.-C. (2017). Acid-Base Regulation and Ammonia Excretion in Cephalopods: An Ontogenetic Overview. In Weihrauch, D. and O'Donnell, M., editors, *Acid-Base Balance and Nitrogen Excretion in Invertebrates*, chapter 11, pages 275–298. Springer International.

Hu, M. Y., Guh, Y.-J., Stumpp, M., Lee, J.-R., Chen, R.-D., Sung, P.-H., Chen, Y.-C., Hwang, P.-P., and Tseng, Y.-C. (2014). Branchial NH4+-dependent acid-base transport mechanisms and energy metabolism of squid (Sepioteuthis lessoniana) affected by seawater acidification. *Frontiers in Zoology*, 11(1):55.

Hu, M. Y., Hwang, P.-P., and Tseng, Y.-C. (2015). Recent advances in understanding trans-epithelial acid-base regulation and excretion mechanisms in cephalopods. *Tissue Barriers*, 3(4):e1064196.

Hu, M. Y., Sung, P. H., Guh, Y. J., Lee, J. R., Hwang, P. P., Weihrauch, D., and Tseng, Y. C. (2017). Perfused gills reveal fundamental principles of pH regulation and ammonia homeostasis in the cephalopod Octopus vulgaris. *Frontiers in Physiology*, 8:162.

Hu, M. Y. A., Lee, J.-R., Lin, L.-Y., Shih, T.-H., Stumpp, M., Lee, M.-F., Hwang, P.-P., and Tseng, Y.-C. (2013). Development in a naturally acidified environment: Na+/H+-exchanger 3-based proton secretion leads to CO2 tolerance in cephalopod embryos. *Frontiers in Zoology*, 10(1):51.

Hu, M. Y. A., Tseng, Y.-C., Stumpp, M., Gutowska, M. A., Kiko, R., Lucassen, M., and Melzner, F. (2011). Elevated seawater PCO2 differentially affects branchial acid-base transporters over the course of development in the cephalopod Sepia officinalis. *American Journal of Physiology: Regulatory, Integrative, and Comparative Physiology*, 300:1100–1114.

Huang, Z., Huang, W., Liu, X., Han, Z., Liu, G., Boamah, G. A., Wang, Y., Yu, F., Gan, Y., Xiao, Q., Luo, X., Chen, N., Liu, M., You, W., and Ke, C. (2022). Genomic insights into the adaptation and evolution of the nautilus, an ancient but evolving "living fossil". *Molecular Ecology Resources*, 22(1):15–27.

Hughes, D. J., Alexander, J., Cobbs, G., Kühl, M., Cooney, C., Pernice, M., Varkey, D., Voolstra, C. R., and Suggett, D. J. (2022). Widespread oxyregulation in tropical corals under hypoxia. *Marine Pollution Bulletin*, 179:113722.

Hughes, G. M. (1973). Respiratory Responses to Hypoxia in Fish. *American Zoology*, 13:475–489.

Hunt, J. C. and Seibel, B. A. (2000). Life history of Gonatus onyx (Cephalopoda: Teuthoidea): ontogenetic changes in habitat, behavior and physiology. *Marine Biology*, 136(3):543–552.

Hüttelmaier, S., Zenklusen, D., Lederer, M., Dictenberg, J., Lorenz, M., Meng, X., Bassell, G. J., Condeelis, J., and Singer, R. H. (2005). Spatial regulation of B-actin translation by Src-dependent phosphorylation of ZBP1. *Nature*, 438:512–515.

Huxtable, R. J. (1992). Physiological Actions of Taurine. *Physiological Reviews*, 72(1):101–163.

Hyndes, G. A., Nagelkerken, I., Mcleod, R. J., Connolly, R. M., Lavery, P. S., and Vanderklift, M. A. (2014). Mechanisms and ecological role of carbon transfer within coastal seascapes. *Biological Reviews*, 89(1):232–254.

Ibáñez, C. M., Sepúlveda, R. D., Ulloa, P., Keyl, F., and Pardo-Gandarillas, M. C. (2015). The biology and ecology of the jumbo squid Dosidicus gigas (Cephalopoda) in Chilean waters: a review. *Latin American Journal of Aquatic Research*, 43(3):402–414.

Iglesias, T. L., Boal, J. G., Frank, M. G., Zeil, J., and Hanlon, R. T. (2019). Cyclic nature of the REM sleep-like state in the cuttlefish Sepia officinalis. *Journal of Experimental Biology*, 222:jeb174862.

Ikai, A. (1980). Thermostability and Aliphatic Index of Globular Proteins. *Journal of Biochemistry*, 88:1895–1898.

Ikeda, T. (2016). Routine metabolic rates of pelagic marine fishes and cephalopods as a function of body mass, habitat temperature and habitat depth. *Journal of Experimental Marine Biology and Ecology*, 480:74–86.

Ikeda, Y., Sakurai, Y., and Shimazaki, K. (1993). Maturation process of the Japanese common squid Todarodes pacificus in captivity. *Recent Advances in Cephalopod Fisheries Biology.*

Imperadore, P., Parazzoli, D., Oldani, A., Duebbert, M., Büschges, A., and Fiorito, G. (2019). From injury to full repair: nerve regeneration and functional recovery in the common octopus, Octopus vulgaris. *Journal of Experimental Biology*, 222:jeb209965.

Ingolia, N. T., Lareau, L. F., and Weissman, J. S. (2011). Ribosome Profiling of Mouse Embryonic Stem Cells Reveals the Complexity and Dynamics of Mammalian Proteomes. *Cell*, 147(4):789–802.

IPCC (2014). *Climate Change 2014: Synthesis Report. Contribution of Working Groups I, II and III to the Fifth Assessment Report of the Intergovernmental Panel on Climate Change.* IPCC, Geneva, Switzerland.

Jaakkola, P., Mole, D. R., Tian, Y.-M., Wilson, M. I., Gielbert, J., Gaskell, S. J., von Kriegsheim, A., Hebestreit, H. F., Mukherji, M., Schofield, C. J., Maxwell, P. H., Pugh, C. W., and Ratcliffe, P. J. (2001). Targeting of HIF-α to the von Hippel-Lindau Ubiquitylation Complex by O2-Regulated Prolyl Hydroxylation. *Science*, 292:468–472.

Jackson, G. D., Finn, J., and Nicol, S. (2002). Planktonic cephalopods collected off East Antarctica during the 'BROKE' survey. *Deep-Sea Research Part I: Oceanographic Research Papers*, 49(6):1049–1054.

Jamieson, A. J. and Vecchione, M. (2020). First in situ observation of Cephalopoda at hadal depths (Octopoda: Opisthoteuthidae: Grimpoteuthis sp.). *Marine Biology*, 167:82.

Jarman, S. N., Redd, K. S., and Gales, N. J. (2006). Group-specific primers for amplifying DNA sequences that identify Amphipoda, Cephalopoda, Echinodermata, Gastropoda, Isopoda, Ostracoda and Thoracica. *Molecular Ecology Notes*, 6(1):268–271.

Jereb, P. and Roper, C. F. E., editors (2005). *Cephalopods of the World. An annotated and illustrated catalogue of species known to date. Volume 1. Chambered nautiluses and sepioids (Nautilidae, Sepiidae, Sepiolidae, Sepiadariidae, Idiosepiidae and Spirulidae)*, volume 1. FAO, Rome, 4 edition.

Jereb, P. and Roper, C. F. E., editors (2010). *Cephalopods of the world. An annotated and illustrated catalogue of cephalopod species known to date. Volume 2. Myopsid and Oegopsid Squids*, volume 2. FAO, Rome, 4 edition.

Jereb, P., Roper, C. F. E., Norman, M. D., and Finn, J. K., editors (2013). *Cephalopods of the world. An annotated and illustrated catalogue of cephalopod species known to date. Volume 3. Octopods and Vampire Squids*, volume 3. FAO, Rome, 4 edition.

Jiang, B.-H., Rue, E., Wang, G. L., Roe, R., and Semenza, G. L. (1996). Dimerization, DNA binding, and transactivation properties of hypoxia-inducible factor 1. *The Journal of Biological Chemistry*, 271(30):17771–17778.

Johansen, K., Brix, O., and Lykkeboe, G. (1982). Blood gas transport in the cephalopod, Sepia officinalis. *The Journal of Experimental Biology*, 99:331–338.

Johansen, K. and Weber, R. E. (1976). On the adaptability of haemoglobin function to environmental conditions. *Perspectives in Experimental Biology*, 1:219–234.

Johnsen, S., Balser, E. J., Fisher, E. C., and Widder, E. A. (1999). Bioluminescence in the deep-sea cirrate octopod Stauroteuthis syrtensis Verrill (Mollusca: Cephalopoda). *Biological Bulletin*, 197(1):26–39.

Joyner, R. W. (1981). Temperature effects on neuronal elements. *Federation Proceedings*, 40(14):2814–2818.

Judkins, H., Vecchione, M., Cook, A., and Sutton, T. (2017). Diversity of midwater cephalopods in the northern Gulf of Mexico: comparison of two collecting methods. *Marine Biodiversity*, 47(3):647–657.

Kang, W., Kim, P. S., Tak, E. J., Sung, H., Shin, N.-R., Hyun, D.-W., Whon, T. W., Kim, H. S., Lee, J.-Y., Yun, J.-H., Jung, M.-J., and Bae, J.-W. (2022). Host phylogeny, habitat, and diet are main drivers of the cephalopod and mollusk gut microbiome. *Animal Microbiome*, 4(1):30.

Kardong, K. V. (2012). *Vertebrates: Comparative anatomy, function, and evolution.* McGraw-Hill, 6th edition.

Kassahn, K. S., Crozier, R. H., Pörtner, H.-O., and Caley, M. J. (2009). Animal performance and stress: responses and tolerance limits at different levels of biological organisation. *Biological Reviews*, 84:277–292.

Kato, S., Matsui, T., Gatsogiannis, C., and Tanaka, Y. (2018). Molluscan hemocyanin: structure, evolution, and physiology. *Biophysical Reviews*, 10:191–202.

Katz, B. and Miledi, R. (1965). The effect of temperature on the synaptic delay at the neuromuscular junction. *Journal of Physiology*, 181:656–670.

Kawahara, Y., Megraw, M., Kreider, E., Iizasa, H., Valente, L., Hatzigeorgiou, A. G., and Nishikura, K. (2008). Frequency and fate of microRNA editing in human brain. *Nucleic Acids Research*, 36(16):5270–5280.

Kawahara, Y., Zinshteyn, B., Sethupathy, P., Iizasa, H., Hatzigeorgiou, A. G., and Nishikura, K. (2007). Redirection of Silencing Targets by Adenosine-to-Inosine Editing of miRNAs. *Science*, 315:1137–1140.

Keeling, R. F., Körtzinger, A., and Gruber, N. (2010). Ocean Deoxygenation in a Warming World. *Annual Review of Marine Science*, 2(1):199–229.

Kern, D. M. (1960). Hydration of Carbon Dioxide. *Journal of Chemical Education*, 37(1):14–23.

Kerwin, A. H., Gromek, S. M., Suria, A. M., Samples, R. M., Deoss, D. J., O'Donnell, K., Frasca, S., Sutton, D. A., Wiederhold, N. P., Balunas, M. J., and Nyholm, S. V. (2019). Shielding the Next Generation: Symbiotic Bacteria from a Reproductive Organ Protect Bobtail Squid Eggs from Fungal Fouling. *mBio*, 10(5):e02376–19.

Keys, A. B. (1930). The relation of the oxygen tension in the external respiratory medium to the oxygen consumption of fishes. *Science*, 71(1833):195–196.

Khan, A., Paro, S., Mcgurk, L., Sambrani, N., Hogg, M. C., Brindle, J., Pennetta, G., Keegan, L. P., and O'Connell, M. A. (2020). Membrane and synaptic defects leading to neurodegeneration in Adar mutant Drosophila are rescued by increased autophagy. *BMC Biology*, 18:15.

Kidder, D. L. and Worsley, T. R. (2004). Causes and consequences of extreme Permo-Triassic warming to globally equable climate and relation to the Permo-Triassic extinction and recovery. *Palaeogeography, Palaeoclimatology, Palaeoecology*, 203(3-4):207–237.

Kiel, S., Goedert, J. L., and Tsai, C.-H. (2022). Seals, whales and the Cenozoic decline of nautiloid cephalopods. *Journal of Biogeography*, page jbi.14488.

Kier, W. M. (2016). The Musculature of Coleoid Cephalopod Arms and Tentacles. *Frontiers in Cell and Developmental Biology*, 4:10.

Kier, W. M. and Thompson, J. T. (2003). Muscle arrangement, function and specialization in recent coleoids. *Berliner Paläobiologische Abhandlungen*, 3:141–162.

Killen, S. S., Marras, S., Steffensen, J. F., and McKenzie, D. J. (2012). Aerobic capacity influences the spatial position of individuals within fish schools. *Proceedings of the Royal Society B: Biological Sciences*, 279(1727):357–364.

Kingston, A. C. N., Kuzirian, A. M., Hanlon, R. T., and Cronin, T. W. (2015). Visual phototransduction components in cephalopod chromatophores suggest dermal photoreception. *Journal of Experimental Biology*, 218(10):1596–1602.

Kinsey, S. T., Hardy, K. M., and Locke, B. R. (2007). The long and winding road: influences of intracellular metabolite diffusion on cellular organization and metabolism in skeletal muscle. *Journal of Experimental Biology*, 210(20):3505–3512.

Kiss, T. (2010). Apoptosis and its functional significance in molluscs. *Apoptosis*, 15(3):313–321.

Knoll, A. H., Bambach, R. K., Payne, J. L., Pruss, S., and Fischer, W. W. (2007). Paleophysiology and end-Permian mass extinction. *Earth and Planetary Science Letters*, 256(3-4):295–313.

Kölsch, A., Hörnemann, J., Wengenroth, C., and Hellmann, N. (2013). Differential regulation of hexameric and dodecameric hemocyanin from A. leptodactylus. *BBA - Proteins and Proteomics*, 1834(9):1853–1859.

Koslow, J. A., Goericke, R., Lara-Lopez, A., and Watson, W. (2011). Impact of declining intermediate-water oxygen on deepwater fishes in the California Current. *Marine Ecology Progress Series*, 436:207–218.

Kraus, D. W. and Colacino, J. M. (1986). Extended Oxygen Delivery from the Nerve Hemoglobin of Tellina alternata (Bivalvia). *Science*, 232:90–92.

Kröger, B., Vinther, J., and Fuchs, D. (2011). Cephalopod origin and evolution: A congruent picture emerging from fossils, development and molecules. *Bioessays*, 33(8):602–613.

Krogh, A. (1919). The rate of diffusion of gases through animal tissues, with some remarks on the coefficient of invasion. *The Journal of Physiology*, 52(6):391–408.

Kubodera, T. and Mori, K. (2005). First-ever observations of a live giant squid in the wild. *Proceedings of the Royal Society B: Biological Sciences*, 272:2583–2586.

Kukita, F. (1982). Properties of sodium and potassium channels of the squid giant axon far below 0Â°C. *The Journal of Membrane Biology*, 68(1):151–160.

Kültz, D. (2005). Molecular and evolutionary basis of the cellular stress response. *Annual Review of Physiology*, 67:225–257.

Kurth, J. A., Thompson, J. T., and Kier, W. M. (2014). Connective Tissue in Squid Mantle Is Arranged to Accommodate Strain Gradients. *Biological Bulletin*, 227:1–6.

Lacoste, A., Malham, S. K., Cueff, A., Jalabert, F., Gelebart, F., and Poulet, S. A. (2001). Evidence for a form of adrenergic response to stress in the mollusc Crassostrea gigas. *The Journal of Experimental Biology*, 204:1247–1255.

Lamarre, S. G., MacCormack, T. J., Sykes, A. V., Hall, J. R., Speers-Roesch, B., Callaghan, N. I., and Driedzic, W. R. (2016). Metabolic rate and rates of protein turnover in food-deprived cuttlefish, Sepia officinalis (Linnaeus 1758). *American Journal of Physiology: Regulatory, Integrative, and Comparative Physiology*, 310:R1160–R1168.

Lane, S. J., Moran, A. L., Shishido, C. M., Tobalske, B. W., and Woods, H. A. (2018). Cuticular gas exchange by Antarctic sea spiders. *Journal of Experimental Biology*.

Lang, W. H. and van Holde, K. E. (1991). Cloning and sequencing of Octopus dofleini hemocyanin cDNA: Derived sequences of functional units Ode and Odf. *Proceedings of the National Academy of Sciences of the United States of America*, 88:244–248.

Lapennas, G. N. (1983). The magnitude of the Bohr coefficient: optimal for oxygen delivery. *Respiration Physiology*, 54:161–172.

Laptikhovsky, V. V. and Nigmatullin, C. M. (1993). Egg size, fecundity, and spawning in females of the genus Illex (Cephalopoda: Ommastrephidae). *ICES Journal of Marine Science*, 50:393–403.

Laptikhovsky, V. V., Nigmatullin, C. M., Hoving, H. J. T., Onsoy, B., Salman, A., Zumholz, K., and Shevtsov, G. A. (2008). Reproductive strategies in female polar and deep-sea bobtail squid genera Rossia and Neorossia (Cephalopoda: Sepiolidae). *Polar Biology*, 31(12):1499–1507.

Larcombe, M. F. and Russell, B. C. (1971). Egg laying behaviour of the broad squid, Sepioteuthis bilineata. *New Zealand Journal of Marine and Freshwater Research*, 5(1):3–11.

Larson, J., Drew, K. L., Folkow, L. P., Milton, S. L., and Park, T. J. (2014). No oxygen? No problem! Intrinsic brain tolerance to hypoxia in vertebrates. *Journal of Experimental Biology*, 217:1024–1039.

Lasek, R. J. and Brady, S. T. (1985). Attachment of transported vesicles to microtubules in axoplasm is facilitated by AMP-PNP. *Nature*, 316:645–647.

Lau, G. Y., Mandic, M., and Richards, J. G. (2017). Evolution of Cytochrome c Oxidase in Hypoxia Tolerant Sculpins (Cottidae, Actinopterygii). *Molecular Biology and Evolution*, 34(9):2153–2162.

Laughlin, R. A. and Livingston, R. J. (1982). Environmental and trophic determinants of the spatial/temporal distribution of the brief squid (Lolliguncula brevis) in the Apalachicola Estuary (North Florida, USA). *Bulletin of Marine Science*, 32(2):489–497.

Lavery, T. J., Roudnew, B., Gill, P., Seymour, J., Seuront, L., Johnson, G., Mitchell, J. G., and Smetacek, V. (2010). Iron defecation by sperm whales stimulates carbon export in the Southern Ocean. *Proceedings of the Royal Society B: Biological Sciences*, 277(1699):3527–3531.

Lawrence, C. J., Dawe, R. K., Christie, K. R., Cleveland, D. W., Dawson, S. C., Endow, S. A., Goldstein, L. S. B., Goodson, H. V., Hirokawa, N., Howard, J., Malmberg, R. L., McIntosh, J. R., Miki, H., Mitchison, T. J., Okada, Y., Reddy, A. S. N., Saxton, W. M., Schliwa, M., Scholey, J. M., Vale, R. D., Walczak, C. E., and Wordeman, L. (2004). A standardized kinesin nomenclature. *The Journal of Cell Biology*, 167(1):19–22.

Layman, C. A., Allgeier, J. E., Rosemond, A. D., Dahlgren, C. P., and Yeager, L. A. (2011). Marine fisheries declines viewed upside down: Human impacts on consumer-driven nutrient recycling. *Ecological Applications*, 21(2):343–349.

Leary, S. L., editor (2020). *AVMA Guidelines for the Euthanasia of Animals: 2020 Edition*. American Veterinary Medical Association, Schaumburg, IL, 2020 edition edition.

Lee, M. T., Bonneau, A. R., and Giraldez, A. J. (2014). Zygotic Genome Activation During the Maternal-to- Zygotic Transition. *Annual Review of Cell and Developmental Biology*, 30:581–613.

Lee, P. G. (1995). Nutrition of cephalopods: fueling the system. *Marine and Freshwater Behaviour and Physiology*, 25:35–51.

Lefevre, S. (2016). Are global warming and ocean acidification conspiring against marine ectotherms? A meta-analysis of the respiratory effects of elevated temperature, high CO2 and their interaction. *Conservation Physiology*, 4.

Lefevre, S., McKenzie, D. J., and Nilsson, G. E. (2017). Models projecting the fate of fish populations under climate change need to be based on valid physiological mechanisms. *Global Change Biology*, pages 1–11.

Lesueur, C. A. (1821). Descriptions of several new species of Cuttle-fish. *Journal of the Academy of Natural Sciences of Philadelphia*, 2:86–101.

Leuenberger, P., Ganscha, S., Kahraman, A., Cappelletti, V., Boersema, P. J., von Mering, C., Claassen, M., and Picotti, P. (2017). Cell-wide analysis of protein thermal unfolding reveals determinants of thermostability. *Science*, 355:eaai7825.

Li, L., Qian, G., Zuo, Y., Yuan, Y., Cheng, Q., Guo, T., Liu, J., Liu, C., Zhang, L., and Zheng, H. (2016). Ubiquitin-dependent Turnover of Adenosine Deaminase Acting on RNA 1 (ADAR1) Is Required for Efficient Antiviral Activity of Type I Interferon. *Journal of Biological Chemistry*, 291(48):24974–24985.

Li, R., Xu, Z., Mu, C., Song, W., and Wang, C. (2017). Molecular cloning and characterization of a hemocyanin from Sepiella maindroni. *Fish and Shellfish Immunology*, 67:228–243.

Liao, J. C. (2022). Fish swimming efficiency. *Current Biology*, 32(12):R666–R671.

Liao, M.-l., Somero, G. N., and Dong, Y.-w. (2019). Comparing mutagenesis and simulations as tools for identifying functionally important sequence changes for protein thermal adaptation. *Proceedings of the National Academy of Sciences*, 116(2):679–688.

Lieb, B. and Markl, J. (2004). Evolution of molluscan hemocyanins as deduced from DNA sequencing. *Micron*, 35:117–119.

Lindsay, D. J., Hunt, J. C., McNeil, M., Beaman, R. J., and Vecchione, M. (2020). The First In Situ Observation of the Ram's Horn Squid Spirula spirula Turns "Common Knowledge" Upside Down. *Diversity*, 12(12):449.

Lipiński, M. R. and Underhill, L. G. (1995). Sexual maturation in squid: quantum or continuum? *South African Journal of Marine Science*, 15:207–223.

Liscovitch-Brauer, N., Alon, S., Porath, H. T., Elstein, B., Unger, R., Ziv, T., Admon, A., Levanon, E. Y., Rosenthal, J. J. C., and Eisenberg, E. (2017). Trade-off between Transcriptome Plasticity and Genome Evolution in Cephalopods. *Cell*, 169(2):191–202.e11.

Liu, Y.-C., Liu, T.-H., Su, C.-H., and Chiao, C.-C. (2017). Neural Organization of the Optic Lobe Changes Steadily from Late Embryonic Stage to Adulthood in Cuttlefish Sepia pharaonis. *Frontiers in Physiology*, 8:538.

Llinas, R. R., Sugimori, M., Moran, K. A., Moreira, J. E., and Fukuda, M. (2004). Vesicular reuptake inhibition by a synaptotagmin I C2B domain antibody at the squid giant synapse. *Proceedings of the National Academy of Sciences*, 101(51):17855–17860.

Logan, C. A. and Buckley, B. A. (2015). Transcriptomic responses to environmental temperature in eurythermal and stenothermal fishes. *The Journal of Experimental Biology*, 218:1915–1924.

Long, M. H., Mooney, T. A., and Zakroff, C. (2016). Extreme low oxygen and decreased pH conditions naturally occur within developing squid egg capsules. *Marine Ecology Progress Series*, 550:111–119.

Loose, C. J. and Dawidowicz, P. (1994). Trade-offs in diel vertical migration by zooplankton: the costs of predator avoidance. *Ecology*, 75(8):2255–2263.

Low, N. H. N., Micheli, F., Aguilar, J. D., Arce, D. R., Boch, C. A., Bonilla, J. C., Bracamontes, M. Á., De Leo, G., Diaz, E., Enríquez, E., Hernandez, A., Martinez, R., Mendoza, R., Miranda, C., Monismith, S., Ramade, M., Rogers-Bennett, L., Romero, A., Salinas, C., Smith, A. E., Torre, J., Villavicencio, G., and Woodson, C. B. (2021). Variable coastal hypoxia exposure and drivers across the southern California Current. *Scientific Reports*, 11:10929.

Lucero, M. T., Farrington, H., and Gilly, W. F. (1994). Quantification of L-Dopa and Dopamine in Squid Ink: Implications for Chemoreception. *Biological Bulletin*, 187:55–63.

Lykkeboe, G. and Johansen, K. (1982). A Cephalopod Approach to Rethinking about the Importance of the Bohr and Haldane Effects. *Pacific Science*, 36(3):305–313.

MacDonald, R. (1977). Red cell 2,3-diphosphoglycerate and oxygen affinity. *Anaesthesia*, 32:544–553.

Macy III, W. K. (1982a). Development and application of an objective method for classifying long-finned squid, Loligo pealei, into sexual maturity stages. *Fishery Bulletin*, 80(3):449–459.

Macy III, W. K. (1982b). Feeding patterns of the long-finned squid, Loligo pealei, in New England waters. *Biological Bulletin*, 162:28–38.

Madan, J. J. and Wells, M. J. (1996). Cutaneous respiration in Octopus vulgaris. *The Journal of Experimental Biology*, 199:2477–2483.

Madan, J. J. and Wells, M. J. (1997). A 'hyaline' layer in the skin of squids. *Journal of the Marine Biological Association of the United Kingdom*, 77(4):1247–1250.

Mahon, P. C., Hirota, K., and Semenza, G. L. (2001). FIH-1: a novel protein that interacts with HIF-1α and VHL to mediate repression of HIF-1 transcriptional activity. *Genes & Development*, 15:2675–2686.

Malik, T. N., Doherty, E. E., Gaded, V. M., Hill, T. M., Beal, P. A., and Emeson, R. B. (2021). Regulation of RNA editing by intracellular acidification. *Nucleic Acids Research*, page gkab157.

Mandic, M., Todgham, A. E., and Richards, J. G. (2009). Mechanisms and evolution of hypoxia tolerance in fish. *Proceedings of the Royal Society B: Biological Sciences*, 276(1657):735–744.

Mangum, C. P. (1990). Gas Transport in the Blood. In Gilbert, D. L., Adelman Jr., W. J., and Arnold, J. M., editors, *Squid as Experimental Animals*. Plenum Press.

Mangum, C. P. (1991). Salt sensitivity of the hemocyanin of eury- and stenohaline squids. *Comparative Biochemistry and Physiology*, 99A(1/2):159–161.

Mangum, C. P. (1997). Invertebrate blood oxygen carriers. In *Handbook of Physiology*, chapter 15, pages 1097–1135. Oxford University Press.

Marian, J. E. A. R. (2015). Evolution of spermatophore transfer mechanisms in cephalopods. *Journal of Natural History*, 49(21-24):1423–1455.

Markl, J. (2013). Evolution of molluscan hemocyanin structures. *Biochimica et Biophysica Acta*, 1834(9):1840–1852.

Marthy, H.-J. (1976). Natural tranquilliser in cephalopod eggs. *Nature*, 261:496–497.

Martin, R. and Voigt, K. H. (1987). The neurosecretory system of the octopus vena cava: A neurohemal organ. *Experientia*, 43(5):537–543.

Maselli, V., Xu, F., Syed, N. I., Polese, G., and Cosmo, A. D. (2018). A Novel Approach to Primary Cell Culture for Octopus vulgaris Neurons. *Frontiers in Physiology*, 9:220.

Masson, N., Willam, C., Maxwell, P. H., Pugh, C. W., and Ratcliffe, P. J. (2001). Independent function of two destruction domains in hypoxia-inducible factor-α chains activated by prolyl hydroxylation. *The EMBO Journal*, 20(18):5197–5206.

Mather, J. A. and Kuba, M. J. (2013). The cephalopod specialties: complex nervous system, learning, and cognition. *Canadian Journal of Zoology*, 91:431–449.

Mathieson, T., Franken, H., Kosinski, J., Kurzawa, N., Zinn, N., Sweetman, G., Poeckel, D., Ratnu, V. S., Schramm, M., Becher, I., Steidel, M., Noh, K.-M., Bergamini, G., Beck, M., Bantscheff, M., and Savitski, M. M. (2018). Systematic analysis of protein turnover in primary cells. *Nature Communications*, 9:689.

Matthews, M. M., Thomas, J. M., Zheng, Y., Tran, K., Phelps, K. J., Scott, A. I., Havel, J., Fisher, A. J., and Beal, P. A. (2016). Structures of human ADAR2 bound to dsRNA reveal base-flipping mechanism and basis for site selectivity. *Nature Structural and Molecular Biology*, 23(5):426–433.

Maxwell, M. R., Henry, A., Elvidge, C. D., Safran, J., Hobson, V. R., Nelson, I., Tuttle, B. T., Dietz, J. B., and Hunter, J. R. (2004). Fishery dynamics of the California market squid (Loligo opalescens), as measured by satellite remote sensing. *Fishery Bulletin*, 102:661–670.

McCormick, L. R. and Cohen, J. H. (2012). Pupil light reflex in the Atlantic brief squid, Lolliguncula brevis. *Journal of Experimental Biology*, 215(15):2677–2683.

McCormick, L. R. and Levin, L. A. (2017). Physiological and ecological implications of ocean deoxygenation for vision in marine organisms. *Philosophical Transactions of the Royal Society A*, 375:20160322.

McCormick, L. R., Levin, L. A., and Oesch, N. W. (2019). Vision is highly sensitive to oxygen availability in marine invertebrate larvae. *Journal of Experimental Biology*, 222:jeb200899.

McCoy, M. J. and Fire, A. Z. (2020). Intron and gene size expansion during nervous system evolution. *BMC Genomics*, 21:360.

McGuinness, T. L., Brady, S. T., Gruner, J. A., Sugimori, M., Llinas, R., and Greengard, P. (1989). Phosphorylation-Dependent Inhibition by Synapsin I of Organelle Movement in Squid Axoplasm. *The Journal of Neuroscience*, 9(12):4138–4149.

McMahon, B. R. (2001). Respiratory and circulatory compensation to hypoxia in crustaceans. *Respiration Physiology*, 128(3):349–364.

Melzner, F., Bock, C., and Pörtner, H.-O. (2006a). Critical temperatures in the cephalopod Sepia officinalis investigated using in vivo 31P NMR spectroscopy. *The Journal of Experimental Biology*, 209:891–906.

Melzner, F., Bock, C., and Pörtner, H.-O. (2006b). Temperature-dependent oxygen extraction from the ventilatory current and the costs of ventilation in the cephalopod Sepia officinalis. *Journal of Comparative Physiology B: Biochemical, Systemic, and Environmental Physiology*, 176:607–621.

Melzner, F., Gutowska, M. A., Langenbuch, M., Dupont, S., Lucassen, M., Thorndyke, M. C., Bleich, M., and Pörtner, H.-O. (2009). Physiological basis for high CO2 tolerance in marine ectothermic animals: pre-adaptation through lifestyle and ontogeny? *Biogeosciences*, 6(10):2313–2331.

Melzner, F., Mark, F. C., and Pörtner, H.-O. (2007). Role of blood-oxygen transport in thermal tolerance of the cuttlefish, Sepia officinalis. *Integrative and Comparative Biology*, 47(4):645–655.

Messenger, J. B. (1996). Neurotransmitters of cephalopods. *Invertebrate Neuroscience*, 2:95–114.

Messenger, J. B. (2001). Cephalopod chromatophores: neurobiology and natural history. *Biological Reviews of the Cambridge Philosophical Society*, 76(4):473–528.

Messenger, J. B., Muzii, E. O., Nardi, G., and Steinberg, H. (1974). Haemocyanin synthesis and the branchial gland of Octopus. *Nature*, 250:154–155.

Messerli, M. A., Raihan, M. J., Kobylkevich, B. M., Benson, A. C., Bruening, K. S., Shribak, M., Rosenthal, J. J. C., and Sohn, J. J. (2019). Construction and Composition of the Squid Pen from Doryteuthis pealeii. *Biological Bulletin*, 237(August):1–15.

Michinomae, M., Masuda, H., Seidou, M., and Kito, Y. (1994). Structural basis for wavelength discrimination in the banked retina of the firefly squid Watasenia scintillans. *Journal of Experimental Biology*, 193:1–12.

Miller, K. I. (1985). Oxygen Equilibria of Octopus dofleini Hemocyanin. *Biochemistry*, 24(17):4582–4586.

Miller, K. I. (1995). Cephalopod haemocyanins. A review of structure and function. *Marine and Freshwater Behaviour and Physiology*, 25(1-3):101–120.

Miller, K. I. and Mangum, C. P. (1988). An investigation of the nature of Bohr, Root, and Haldane effects in Octopus dofleini hemocyanin. *Journal of Comparative Physiology B*, 158(5):547–552.

Milligan, B. J., Curtin, N. A., and Bone, Q. (1997). Contracticle properties of obliquely striated muscle from the mantle of squid (Alloteuthis subulata) and cuttlefish (Sepia officinalis). *The Journal of Experimental Biology*, 200:2425–2436.

Min, J.-H., Yang, H., Ivan, M., Gertler, F., Kaelin Jr, W. G., and Pavletich, N. P. (2002). Structure of an HIF-1α-pVHL Complex: Hydroxyproline Recognition in Signaling. *Science*, 296(June):1886–1889.

Minakata, H. (2006). Neuropeptides and peptide hormones in cephalopods. In Satake, H., editor, *Invertebrate neuropeptides and hormones: basic knowledge and recent advances*, chapter 5, pages 1–15.

Miserez, A., Schneberk, T., Sun, C., Zok, F. W., and Waite, J. H. (2008). The transition from stiff to compliant materials in squid beaks. *Science*, 319(5871):1816–1819.

Mislan, K. A. S., Dunne, J. P., and Sarmiento, J. L. (2015). The fundamental niche of blood oxygen binding in the pelagic ocean. *Oikos*, 125:938–949.

Mitchell, G. S. and Johnson, S. M. (2003). Neuroplasticity in respiratory motor control. *Journal of Applied Physiology*, 94:358–374.

Mitz, S. A., Reuss, S., Folkow, L. P., Blix, A. S., Ramirez, J.-M., Hankeln, T., and Burmester, T. (2009). When the brain goes diving: glial oxidative metabolism may confer hypoxia tolerance to the seal brain. *Neuroscience*, 163(2):552–560.

Mole, D. R., Blancher, C., Copley, R. R., Pollard, P. J., Gleadle, J. M., Ragousis, J., and Ratcliffe, P. J. (2009). Genome-wide association of hypoxia-inducible factor (HIF)-1α and HIF-2α DNA binding with expression profiling of hypoxia-inducible transcripts. *Journal of Biological Chemistry*, 284(25):16767–16775.

Moltschaniwskyj, N. A. (2004). Understanding the process of growth in cephalopods. *Marine and Freshwater Research*, 55(4):379–386.

Mommsen, T. P., Ballantyne, J., Macdonald, D., Gosline, J. M., and Hochachka, P. W. (1981). Analogues of red and white muscle in squid mantle. *Proceedings of the National Academy of Sciences of the United States of America*, 78(5):3274–3278.

Montana, J., Norman, M. D., and Finn, J. K. (2015). Liquid sand burrowing and mucus utilisation as novel adaptations to a structurally-simple environment in Octopus kaurna Stranks, 1990. *Behaviour*, 152:1871–1881.

Montgomery, J. C. and MacDonald, J. A. (1990). Effects of temperature on nervous system: implications for behavioral performance. *American Journal of Physiology - Regulatory, Integrative and Comparative Physiology*, 28:R191–R196.

Moore, C. M., Mills, M. M., Arrigo, K. R., Berman-Frank, I., Bopp, L., Boyd, P. W., Galbraith, E. D., Geider, R. J., Guieu, C., Jaccard, S. L., Jickells, T. D., Roche, J. L., Lenton, T. M., Mahowald, N. M., Marañón, E., Marinov, I., Moore, J. K., Nakatsuka, T., Oschlies, A., Saito, M. A., Thingstad, T. F., Tsuda, A., and Ulloa, O. (2013). Processes and patterns of oceanic nutrient limitation. *Nature Geoscience*, 6(9):701–710.

Morse, P. and Huffard, C. L. (2022). Chemotactile social recognition in the blue-ringed octopus, Hapalochlaena maculosa. *Marine Biology*, 169(8):99.

Moyes, C. D. (2003). Controlling muscle mitochondrial content. *The Journal of Experimental Biology*, 206:4385–4391.

Murai, R., Shiomi, M., Yoshida, M.-a., Tomano, S., Iwata, Y., Sugai, K., and Hirohashi, N. (2021). All the spermatangia on a female were implanted by single-pair copulation in giant squid Architeuthis dux. *Deep Sea Research Part I: Oceanographic Research Papers*, 175(June):103585.

Muzii, E. (1981). Intracellular polymerized haemocyanin in the branchial gland of a cephalopod. *Cell Tissue Research*, 220:435–438.

Nahmad-Rohen, L. and Vorobyev, M. (2019). Contrast sensitivity and behavioural evidence for lateral inhibition in octopus. *Biology Letters*, 15:20190134.

Nakajima, R., Lajbner, Z., Kuba, M. J., Gutnick, T., Iglesias, T. L., Asada, K., Nishibayashi, T., and Miller, J. (2022). Squid adjust their body color according to substrate. *Scientific Reports*, 12(1):5227.

Nayak, G., Prentice, H. M., and Milton, S. L. (2009). Role of neuroglobin in regulating reactive oxygen species in the brain of the anoxia-tolerant turtle Trachemys scripta. *Journal of Neurochemistry*, 110:603–612.

Naylor, G. J. P. and Gerstein, M. (2000). Measuring Shifts in Function and Evolutionary Opportunity Using Variability Profiles: A Case Study of the Globins. *Journal of Molecular Evolution*, 51:223–233.

Neumeister, H., Ripley, B., Preuss, T., and Gilly, W. F. (2000). Effects of temperature on escape jetting in the squid Loligo opalescens. *The Journal of Experimental Biology*, 203:547–557.

Nigmatullin, C. M., Nesis, K. N., and Arkhipkin, A. I. (2001). A review of the biology of the jumbo squid Dosidicus gigas (Cephalopoda: Ommastrephidae). *Fisheries Research*, 54:9–19.

Nilsson, G. E. (2007). Gill remodeling in fish-a new fashion or an ancient secret? *The Journal of Experimental Biology*, 210(14):2403–2409.

Nilsson, G. E., Dixson, D. L., Domenici, P., McCormick, M. I., Sørensen, C., Watson, S. A., and Munday, P. L. (2012). Near-future carbon dioxide levels alter fish behaviour by interfering with neurotransmitter function. *Nature Climate Change*, 2(3):201–204.

Nilsson, G. E. and Östlund-Nilsson, S. (2008). Does size matter for hypoxia tolerance in fish? *Biological Reviews*, 83(2):173–189.

Nishikura, K., Yoo, C., Kim, U., Murray, J. M., Estes, P. A., Cash, F. E., and Liebhaber, S. A. (1991). Substrate specificity of the dsRNA unwinding/modifying activity. *EMBO Journal*, 10(11):3523–3532.

Nixon, M. and Young, J. Z. (2003). *The Brains and Lives of Cephalopods*. Oxford University Press, New York.

Norin, T. and Clark, T. D. (2016). Measurement and relevance of maximum metabolic rate in fishes. *Journal of Fish Biology*, 88:122–151.

Norman, M. D. and Hochberg, F. G. (2005). The "Mimic Octopus" (Thaumoctopus mimicus n. gen. et sp.), a new octopus from the tropical Indo-West Pacific (Cephalopoda: Octopodidae). *Molluscan Research*, 25:57–70.

Nyack, A. C., Henry, R. P., and Seibel, B. A. Characterization of carbonic anhydrase activity in gill and mantle tissue of Dosidicus gigas, Lolliguncula brevis, and Doryteuthis pealeii.

O'Carroll, D. and Schaefer, A. (2013). General principals of miRNA biogenesis and regulation in the brain. *Neuropsychopharmacology*, 38(1):39–54.

O'Dor, R. K. (1988). The forces acting on swimming squid. *The Journal of Experimental Biology*, 137:421–442.

O'Dor, R. K. (2013). How squid swim and fly. *Canadian Journal of Zoology*, 91:413–419.

O'Dor, R. K., Durward, R. D., Vessey, E., and Amaratunga, T. (1980). Feeding and growth in captive squid, Illex illecebrosus, and the influence of food availibility on growth in the natural population. In *International Commission for the Northwest Atlantic Fisheries Selected Papers*, number 6, pages 15–21.

O'Dor, R. K. and Hoar, J. A. (2000). Does geometry limit squid growth? *ICES Journal of Marine Science*, 57(1):8–14.

O'Dor, R. K. and Webber, D. M. (1986). The constraints on cephalopods: why squid aren't fish. *Canadian Journal of Zoology*, 64(8):1591–1605.

O'Dor, R. K. and Webber, D. M. (1991). Invertebrate athletes: trade-offs between transport efficiency and power density in cephalopod evolution. *Journal of Experimental Biology*, 160:93–112.

O'Dor, R. K. and Wells, M. J. (1984). Circulation time, blood reserves and extracellular space in a cephalopod. *Journal of Experimental Biology*, 113:461–464.

Oellermann, M., Lieb, B., Pörtner, H.-O., Semmens, J. M., and Mark, F. C. (2015a). Blue blood on ice: modulated blood oxygen transport facilitates cold compensation and eurythermy in an Antarctic octopod. *Frontiers in Zoology*, 12(1):6.

Oellermann, M., Strugnell, J. M., Lieb, B., and Mark, F. C. (2015b). Positive selection in octopus haemocyanin indicates functional links to temperature adaptation. *BMC Evolutionary Biology*, 15(1):133.

Okutani, T. and Osuga, K. (1986). A peculiar nesting behavior of Ocythoe tuberculata in the test of a gigantic salp, Tethys vagina. *Venus*, 45(1):67–69.

O'Leary, T. and Marder, E. (2016). Temperature-Robust Neural Function from Activity-Dependent Ion Channel Regulation. *Current Biology*, 26(21):2935–2941.

Ortega, A. and Olivares-Bañuelos, T. N. (2020). Neurons and Glia Cells in Marine Invertebrates: An Update. *Frontiers in Neuroscience*, 14:121.

O'Shea, S. (2004). The giant octopus Haliphron atlanticus (Mollusca: Octopoda) in New Zealand waters. *New Zealand Journal of Zoology*, 31:7–13.

Ota, H., Sakurai, M., Gupta, R., Valente, L., Wulff, B.-e., Ariyoshi, K., Iizasa, H., Davuluri, R. V., and Nishikura, K. (2013). ADAR1 Forms a Complex with Dicer to Promote MicroRNA Processing and RNA-Induced Gene Silencing. *Cell*, 153(3):575–589.

Pace, C. N., Grimsley, G. R., and Scholtz, J. M. (2009). Protein Ionizable Groups: pK Values and Their Contribution to Protein Stability and Solubility. *The Journal of Biological Chemistry*, 284(20):13285–13289.

Packard, A. (1972). Cephalopods and fish: the limits of convergence. *Biological Reviews*, 47(2):241–307.

Packard, A. (1988). The Skin of Cephalopods (Coleoids): General and Special Adaptations. In Trueman, E. R., editor, *The Mollusca, Volume 11: Form and Function*, chapter 3, pages 37–67. Academic Press, Inc.

Palavicini, J. P., O'Connell, M. A., and Rosenthal, J. J. C. (2009). An extra double-stranded RNA binding domain confers high activity to a squid RNA editing enzyme. *RNA*, 15:1208–1218.

Passarella, K. C. and Hopkins, T. L. (1991). Species composition and food habits of the micronektonic cephalopod assemblage in the eastern Gulf of Mexico. *Bulletin of Marine Science*, 49(1-2):638–659.

Patton, D. E., Silva, T., and Bezanilla, F. (1997). RNA editing generates a diverse array of transcripts encoding squid Kv2 K+ channels with altered functional properties. *Neuron*, 19(3):711–722.

Paulmier, A. and Ruiz-Pino, D. (2009). Oxygen minimum zones (OMZs) in the modern ocean. *Progress in Oceanography*, 80(3-4):113–128.

Pauly, D. (1981). The relationships between gill surface area and growth performance in fish: a generalisation of von Bertalanffy's theory of growth. *Berichte der Deutschen Wissenchaftlichen Kommission fur Meeresforschung*, 28(4):251–282.

Paxton, C. G. M. (2016). Unleashing the Kraken: on the maximum length in giant squid (Architeuthis sp.). *Journal of Zoology*, (Ml):1–7.

Pecl, G. T. and Jackson, G. D. (2007). The potential impacts of climate change on inshore squid: biology, ecology and fisheries. *Reviews in Fish Biology and Fisheries*, 18(4):373–385.

Pelechano, V., Chavez, S., and Perez-Ortin, J. E. (2010). A Complete Set of Nascent Transcription Rates for Yeast Genes. *PLOS ONE*, 5(11):e15442.

Pennisi, E. (2012). Light in the Deep. *Science*, 335:1160–1163.

Perry, S. F. and Gilmour, K. M. (2002). Sensing and Transfer of Respiratory Gases at the Fish Gill. *Journal of Experimental Zoology*, 293:249–263.

Peters, K. J., Ophelkeller, K., Herdina, Bott, N. J., and Goldsworthy, S. D. (2015). PCR-based techniques to determine diet of the Australian sea lion (Neophoca cinerea): A comparison with morphological analysis. *Marine Ecology*, 36(4):1428–1439.

Piantadosi, C. A. (2003). *The Biology of Human Survival: Life and Death in Extreme Environments*. Oxford University Press.

Pickford, G. E. and McConnaughey, B. H. (1949). The Octopus bimaculatus problem: a study in sibling species. *Bulletin of the Bingham Oceanographic Collection*, 12(4):1–66.

Pierce, N. T. (2017). *Developmental Transcriptomics of the California Market Squid, Doryteuthis opalescens*. Phd dissertation, University of California, San Diego.

Pilson, M. E. (2013). *An Introduction to the Chemistry of the Sea*. Cambridge University Press, 2nd edition.

Pinto, L. H. and Brown, J. E. (1977). Intracellular Recordings from Photoreceptors of the Squid (Loligo pealii). *Journal of Comparative Physiology*, 122(2):241–250.

Polese, G., Bertapelle, C., and Di Cosmo, A. (2016). Olfactory organ of Octopus vulgaris: morphology, plasticity, turnover and sensory characterization. *Biology Open*, 5:611–619.

Polglase, J. L., Bullock, A. M., and Roberts, R. J. (1983). Wound healing and the haemocyte response in the skin of the Lesser octopus Eledone cirrhosa (Mollusca: Cephalopoda). *Journal of Zoology*, 201:185–204.

Ponte, G., Sykes, A. V., Cooke, G. M., Almansa, E., and Andrews, P. L. R. (2017). The Digestive Tract of Cephalopods: Toward Non-invasive In vivo Monitoring of Its Physiology. *Frontiers in Physiology*, 8:403.

Porath, H. T., Knisbacher, B. A., Eisenberg, E., and Levanon, E. Y. (2017). Massive A-to-I RNA editing is common across the Metazoa and correlates with dsRNA abundance. *Genome Biology*, 18:185.

Porter, R. K. and Brand, M. D. (1993). Body mass dependence of H+ leak in mitochondria and its relevance to metabolic rate. *Nature*, 362:628–630.

Portner, E. J., Markaida, U., Robinson, C. J., and Gilly, W. F. (2019). Trophic ecology of Humboldt squid, Dosidicus gigas, in conjunction with body size and climatic variability in the Gulf of California, Mexico. *Limnology and Oceanography*, pages 1–17.

Pörtner, H.-O. (1990). An analysis of the effects of pH on oxygen binding by squid (Illex illecebrosus, Loligo pealei) haemocyanin. *The Journal of Experimental Biology*, 150:407–424.

Pörtner, H.-O. (1994). Coordination of metabolism, acid-base regulation and haemocyanin function in cephalopods. *Marine and Freshwater Behaviour and Physiology*, 25:131–148.

Pörtner, H.-O. and Grieshaber, M. K. (1993). Critical PO2 (s) in oxyconforming and oxyregulating animals: gas exchange, metabolic rate and the mode of energy production.

Pörtner, H.-O. and Reipschläger, A. (1996). Ocean disposal of anthropogenic CO2: physiological effects on tolerant and intolerant animals. In Ormerod, W. and Angel, M., editors, *Ocean Storage of Carbon Dioxide Workshop 2 - Environmental Impact*, chapter Appendix B, pages 57–81. International Energy Agency Greenhouse Gas R&D Program, Cheltenham, UK.

Pörtner, H.-O., Webber, D. M., Boutilier, R. G., and O'Dor, R. K. (1991). Acid-base regulation in exercising squid (Illex illecebrosus, Loligo pealei). *American Journal of Physiology*, 261:R239–R246.

Pörtner, H.-O., Webber, D. M., O'Dor, R. K., and Boutilier, R. G. (1993). Metabolism and energetics in squid (Illex illecebrosus, Loligo pealei) during muscular fatigue and recovery. *American Journal of Physiology*, 265:R157–R165.

Prahlad, V., Helfand, B. T., Langford, G. M., Vale, R. D., and Goldman, R. D. (2000). Fast Transport of Neurofilament Protein along Microtubules in Squid Axoplasm. *Journal of Cell Science*, 113:3939–3946.

Priede, I. G. and Tytler, P. (1977). Heart rate as a measure of metabolic rate in teleost fishes; Salmo gairdneri, Salmo trutta and Gadus morhua. *Journal of Fish Biology*, 10:231–242.

Puneeta, P., Vijai, D., Yoo, H.-K., Matsui, H., and Sakurai, Y. (2015). Observations on the spawning behavior, egg masses and paralarval development of the ommastrephid squid Todarodes pacificus in a laboratory mesocosm. *The Journal of Experimental Biology*, 218:3825–3835.

Purser, A., Marcon, Y., Hoving, H.-J. T., Vecchione, M., Piatkowski, U., Eason, D., Bluhm, H., and Boetius, A. (2016). Association of deep-sea incirrate octopods with manganese crusts and nodule fields in the Pacific Ocean. *Current Biology*, 26(24):R1268–R1269.

Rabalais, N. N., Díaz, R. J., Levin, L. A., Turner, R. E., Gilbert, D., and Zhang, J. (2010). Dynamics and distribution of natural and human-caused hypoxia. *Biogeosciences*, 7(2):585–619.

Rädle, B., Rutkowski, A. J., Ruzsics, Z., Friedel, C. C., Koszinowski, U. H., and Dölken, L. (2013). Metabolic Labeling of Newly Transcribed RNA for High Resolution Gene Expression Profiling of RNA Synthesis, Processing and Decay in Cell Culture. *Journal of Visualized Experiments*, 78:e50195.

Redfield, A. C., Coolidge, T., and Hurd, A. L. (1926). The transport of oxygen and carbon dioxide by some bloods containing hemocyanin. *Journal of Biological Chemistry*, 69(2):475–509.

Redfield, A. C. and Goodkind, R. (1929). The significance of the Bohr effect in the respiration and asphyxiation of the squid, Loligo pealei. *The Journal of Experimental Biology*, 6(4):340–349.

Reeves, R. B. (1977). The interaction of body temperature and acid-base balance in ectothermic vertebrates. *Annual Review of Physiology*, 39:559–586.

Regan, M. D., Turko, A. J., Heras, J., Andersen, M. K., Lefevre, S., Wang, T., Bayley, M., Brauner, C. J., Huong, D. T. T., Phuong, N. T., and Nilsson, G. E. (2016). Ambient CO2, fish behaviour and altered GABAergic neurotransmission: exploring the mechanism of CO2-altered behaviour by taking a hypercapnia dweller down to low CO2 levels. *Journal of Experimental Biology*, 219(1):109–118.

Reichow, D. and Smith, M. J. (2001). Microsatellites reveal high levels of gene flow among populations of the California squid Loligo opalescens. *Molecular Ecology*, 10:1101–1109.

Richards, J. G. (2009). Chapter 10: Metabolic and Molecular Responses of Fish to Hypoxia. *Fish Physiology*, 27(C):443–485.

Riggs, C. L., Summers, A., Warren, D. E., Nilsson, G. E., Lefevre, S., Dowd, W. W., Milton, S., and Podrabsky, J. E. (2018). Small Non-coding RNA Expression and Vertebrate Anoxia Tolerance. *Frontiers in Genetics*, 9:230.

Rinne, J. N., Holand, B., and Sundnes, G. (2001). Comparison of Heart Rate in Fishes: Cold, Temperate Sea Water Versus Warm, Desert Rivers. In *Proceedings of the International Congress on the Biology of Fish*, pages 13–26.

Rizo, J. and Sudhof, T. C. (1998). C2-domains, Structure and Function of a Universal Ca2+-binding Domain. *Journal of Biological Chemistry*, 273(26):15879–15882.

Robertson, C. E., Wright, P. A., Koblitz, L., and Bernier, N. J. (2014). Hypoxia-inducible factor-1 mediates adaptive developmental plasticity of hypoxia tolerance in zebrafish, Danio rerio. *Proceedings of the Royal Society B: Biological Sciences*, 281:20140637.

Robinson, C. (2008). Heterotrophic bacterial respiration. In Kirchman, D. L., editor, *Microbial Ecology of the Oceans*, chapter 9, pages 299–334. John Wiley & Sons, Inc., 2 edition.

Robinson, E., Jerrett, A., Black, S., and Davison, W. (2013). Hypoxia impairs visual acuity in snapper (Pagrus auratus). *Journal of Comparative Physiology A: Neuroethology, Sensory, Neural, and Behavioral Physiology*, 199(7):611–617.

Robison, B., Seibel, B. A., and Drazen, J. C. (2014). Deep-Sea Octopus (Graneledone boreopacifica) Conducts the Longest-Known Egg-Brooding Period of Any Animal. *PLOS ONE*, 9(7):e103437.

Robison, B. H. (2004). Deep pelagic biology. *Journal of Experimental Marine Biology and Ecology*, 300(1-2):253–272.

Robison, B. H. and Young, R. E. (1981). Bioluminescence in Pelagic Octopods. *Pacific Science*, 35(1):39–44.

Rocha, F., Guerra, A., and González, Á. F. (2001). A review of reproductive strategies in cephalopods. *Biological Reviews of the Cambridge Philosophical Society*, 76(3):291–304.

Rodhouse, P. G. (1998). Physiological Progenesis in Cephalopod Molluscs. *Biological Bulletin*, 195:17–20.

Roesner, A., Mitz, S. A., Hankeln, T., and Burmester, T. (2008). Globins and hypoxia adaptation in the goldfish, Carassius auratus. *FEBS Journal*, 275:3633–3643.

Rogers, N. J., Urbina, M. A., Reardon, E. E., Mckenzie, D. J., and Wilson, R. W. (2016). A new analysis of hypoxia tolerance in fishes using a database of critical oxygen level (Pcrit). *Conservation Physiology*, 4:1–19.

Root, R. W. (1931). The respiratory function of the blood of marine fishes. *The Biological Bulletin*, 61(3):427–456.

Roper, C. F. E. (1969). Systematics and zoogeography of the worldwide bathypelagic squid Bathyteuthis (Cephalopoda: Oegopsida). *Bulletin of the United States National Museum*, 291:1–210.

Roper, C. F. E. and Sweeney, M. J. (1983). Techniques for fixation, preservation, and curation of cephalopods. *Memoirs of the National Museum Victoria*, 44:28–47.

Roper, C. F. E. and Young, R. E. (1975). Vertical distribution of pelagic cephalopods. *Smithsonian Contributions to Zoology*, 209:1–51.

Rosa, R., Dierssen, H. M., Gonzalez, L., and Seibel, B. A. (2008a). Ecological biogeography of cephalopod molluscs in the Atlantic Ocean: historical and contemporary causes of coastal diversity patterns. *Global Ecology and Biogeography*, 17(5):600–610.

Rosa, R., Dierssen, H. M., Gonzalez, L., and Seibel, B. A. (2008b). Large-scale diversity patterns of cephalopods in the Atlantic open ocean and deep sea. *Ecology*, 89(12):3449–3461.

Rosa, R., Gonzalez, L., Dierssen, H. M., and Seibel, B. A. (2012a). Environmental determinants of latitudinal size-trends in cephalopods. *Marine Ecology Progress Series*, 464:153–165.

Rosa, R., Lopes, V. M., Guerreiro, M., Bolstad, K., and Xavier, J. C. (2017). Biology and ecology of the world's largest invertebrate, the colossal squid (Mesonychoteuthis hamiltoni): a short review. *Polar Biology*, 40(9):1871–1883.

Rosa, R., O'Dor, R., and Pierce, G. J., editors (2013a). *Advances in Squid Biology, Ecology and Fisheries: Part I - Myopsid Squids*. NOVA.

Rosa, R., Pimentel, M. S., Boavida-Portugal, J., Teixeira, T., Trübenbach, K., and Diniz, M. (2012b). Ocean warming enhances malformations, premature hatching, metabolic suppression and oxidative stress in the early life stages of a keystone squid. *PLOS ONE*, 7(6):e38282.

Rosa, R. and Seibel, B. A. (2008). Synergistic effects of climate-related variables suggest future physiological impairment in a top oceanic predator. *Proceedings of the National Academy of Sciences of the United States of America*, 105(52):20776–20780.

Rosa, R. and Seibel, B. A. (2010a). Metabolic physiology of the Humboldt squid, Dosidicus gigas: Implications for vertical migration in a pronounced oxygen minimum zone. *Progress in Oceanography*, 86(1-2):72–80.

Rosa, R. and Seibel, B. A. (2010b). Slow pace of life of the Antarctic colossal squid. *Journal of the Marine Biological Association of the United Kingdom*, 90(7):1375–1378.

Rosa, R. and Seibel, B. A. (2010c). Voyage of the argonauts in the pelagic realm: physiological and behavioural ecology of the rare paper nautilus, Argonauta nouryi. *ICES Journal of Marine Science*, 67:1494–1500.

Rosa, R., Trueblood, L. A., and Seibel, B. A. (2009). Ecophysiological influence on scaling of aerobic and anaerobic metabolism of pelagic gonatid squids. *Physiological and Biochemical Zoology*, 82(5):419–429.

Rosa, R., Yamashiro, C., Markaida, U., Rodhouse, P. G. K., Waluda, C. M., Salinas-Zavala, C. A., Keyl, F., O'Dor, R. K., Stewart, J. S., and Gilly, W. F. (2013b). Dosidicus gigas, Humboldt Squid. In Rosa, R., Pierce, G. J., and O'Dor, R. K., editors, *Advances in Squid Biology, Ecology and Fisheries. Part II*, chapter 6, pages 169–206. Nova Science Publishers, Inc.

Rosen, H., Gilly, W., Bell, L., Abernathy, K., and Marshall, G. (2015). Chromogenic behaviors of the Humboldt squid (Dosidicus gigas) studied in situ with an animal-borne video package. *The Journal of Experimental Biology*, 218:265–275.

Rosenthal, J. J. C. (2015). The emerging role of RNA editing in plasticity. *Journal of Experimental Biology*, 218(12):1812–1821.

Rosenthal, J. J. C. and Bezanilla, F. (2000). Seasonal Variation in Conduction Velocity of Action Potentials in Squid Giant Axons. *Biological Bulletin*, 199:135–143.

Rosenthal, J. J. C. and Bezanilla, F. (2002). Extensive Editing of mRNAs for the Squid Delayed Rectifier K+ Channel Regulates Subunit Tetramerization. *Neuron*, 34:743–757.

Rungta, R. L., Choi, H. B., Tyson, J. R., Malik, A., Dissing-Olesen, L., Lin, P. J., Cain, S. M., Cullis, P. R., Snutch, T. P., and MacVicar, B. A. (2015). The cellular mechanisms of neuronal swelling underlying cytotoxic edema. *Cell*, 161(3):610–621.

Ruvolo, P. P., Deng, X., and May, W. S. (2001). Phosphorylation of Bcl2 and regulation of apoptosis. *Leukemia*, 15(4):515–522.

Samson, J. E., Mooney, T. A., Gussekloo, S. W. S., and Hanlon, R. T. (2016). A Brief Review of Cephalopod Behavioral Responses to Sound. In *The Effects of Noise on Aquatic Life II*, chapter 120, pages 969–975. Springer, New York.

Sanchez, G., Fernández-Álvarez, F. Á., Taite, M., Sugimoto, C., Jolly, J., Simakov, O., Marlétaz, F., Allcock, L., and Rokhsar, D. S. (2021). Phylogenomics illuminates the evolution of bobtail and bottletail squid (order Sepiolida). *Communications Biology*, 4:819.

Sato, N., Takeshita, F., Fujiwara, E., and Kasugai, T. (2016). Japanese pygmy squid (Idiosepius paradoxus) use ink for predation as well as for defence. *Marine Biology*, 163(3):56.

Saugstad, O. D. (1975). Hypoxanthine as a measurement of hypoxia. *Pediatric Research*, 9(4):158–161.

Savva, Y. A., Jepson, J. E., Sahin, A., Sugden, A. U., Dorsky, J. S., Alpert, L., Lawrence, C., and Reenan, R. A. (2012). Auto-regulatory RNA editing fine-tunes mRNA re-coding and complex behaviour in Drosophila. *Nature Communications*, 3:790.

Schipp, R. (1987). General morphological and functional characteristics of the cephalopod circulatory system: An introduction. *Experientia*, 43:474–477.

Schmidt, M., Giessl, A., Laufs, T., Hankeln, T., Wolfrum, U., and Burmester, T. (2003). How Does the Eye Breathe? Evidence for neuroglobin-mediated oxygen supply in the mammalian retina. *The Journal of Biological Chemistry*, 278(3):1932–1935.

Schnell, A. K., Hanlon, R. T., Benkada, A., and Jozet-Alves, C. (2016). Lateralization of eye use in cuttlefish: Opposite direction for anti-predatory and predatory behaviors. *Frontiers in Physiology*, 7:620.

Schneuer, M., Flachsbarth, S., Czech-Damal, N. U., Folkow, L. P., Siebert, U., and Burmester, T. (2012). Neuroglobin of seals and whales: evidence for a divergent role in the diving brain. *Neuroscience*, 223:35–44.

Scholander, P. F., Flagg, W., Walters, V., and Irving, L. (1953). Climatic Adaptation in Arctic and Tropical Poikilotherms. *Physiological Zoology*, 26(1):67–92.

Schroeder, A., Mueller, O., Stocker, S., Salowsky, R., Leiber, M., Gassmann, M., Lightfoot, S., Menzel, W., Granzow, M., and Ragg, T. (2006). The RIN: An RNA integrity number for assigning integrity values to RNA measurements. *BMC Molecular Biology*, 7:1–14.

Schulte, P. M. (2004). Changes in gene expression as biochemical adaptations to environmental change: A tribute to Peter Hochachka. *Comparative Biochemistry and Physiology - B Biochemistry and Molecular Biology*, 139:519–529.

Schulte, P. M. (2015). The effects of temperature on aerobic metabolism: towards a mechanistic understanding of the responses of ectotherms to a changing environment. *Journal of Experimental Biology*, 218(12):1856–1866.

Schurmann, H., Steffensen, J. F., and Lomholt, J. P. (1991). The influence of hypoxia on the preferred temperature of rainbow trout Oncorhynchus mykiss. *Journal of Experimental Biology*, 157:75–86.

Schwarz, R., Piatkowski, U., and Hoving, H. J. T. (2018). Impact of environmental temperature on the lifespan of octopods. *Marine Ecology Progress Series*, 605:151–164.

Scott, G. R. (2011). Elevated performance: the unique physiology of birds that fly at high altitudes. *The Journal of Experimental Biology*, 214:2455–2462.

Seguin, A. and Lavoisier, A. (1789). Premier memoire: Sur la respiration des animaux. In *Memoires de l'Academie des sciences, annee*, page 185.

Seibel, B. A. (2007). On the depth and scale of metabolic rate variation: scaling of oxygen consumption rates and enzymatic activity in the Class Cephalopoda (Mollusca). *The Journal of Experimental Biology*, 210:1–11.

Seibel, B. A. (2011). Critical oxygen levels and metabolic suppression in oceanic oxygen minimum zones. *The Journal of Experimental Biology*, 214:326–336.

Seibel, B. A. (2013). The jumbo squid, Dosidicus gigas (Ommastrephidae), living in oxygen minimum zones II: Blood-oxygen binding. *Deep Sea Research Part II: Topical Studies in Oceanography*, 95:139–144.

Seibel, B. A. (2015). Environmental physiology of the jumbo squid, Dosidicus gigas (d'Orbigny, 1835) (Cephalopoda: Ommastrephidae): Implications for changing climate. *American Malacological Bulletin*, 33(1):161–173.

Seibel, B. A. (2016). Cephalopod Susceptibility to Asphyxiation via Ocean Incalescence, Deoxygenation, and Acidification. *Physiology*, 31(6):418–429.

Seibel, B. A. and Carlini, D. B. (2001). Metabolism of pelagic cephalopods as a function of habitat depth: a reanalysis using phylogenetically independent contrasts. *Biological Bulletin*, 201(1):1–5.

Seibel, B. A., Chausson, F., Lallier, F. H., Zal, F., and Childress, J. J. (1999). Vampire blood: respiratory physiology of the vampire squid (Cephalopoda: Vampyromorpha) in relation to the oxygen minimum layer. *Experimental Biology Online*, 4(1):1–10.

Seibel, B. A. and Childress, J. J. (2000). Metabolism of benthic octopods (Cephalopoda) as a function of habitat depth and oxygen concentration. *Deep Sea Research Part I: Oceanographic Research Papers*, 47(7):1247–1260.

Seibel, B. A. and Deutsch, C. (2020). Oxygen supply capacity in animals evolves to meet maximum demand at the current oxygen partial pressure regardless of size or temperature. *Journal of Experimental Biology*, 223:jeb210492.

Seibel, B. A. and Dierssen, H. M. (2009). Animal Function at the Heart (and Gut) of Oceanography. *Science*, 323(January):343–344.

Seibel, B. A. and Drazen, J. C. (2007). The rate of metabolism in marine animals: environmental constraints, ecological demands and energetic opportunities. *Philosophical Transactions of the Royal Society of London. Series B, Biological Sciences*, 362(1487):2061–2078.

Seibel, B. A., Dymowska, A., and Rosenthal, J. (2007). Metabolic temperature compensation and coevolution of locomotory performance in pteropod molluscs. *Integrative and Comparative Biology*, 47(6):880–891.

Seibel, B. A., Goffredi, S. K., Thuesen, E. V., Childress, J. J., and Robison, B. H. (2004). Ammonium content and buoyancy in midwater cephalopods. *Journal of Experimental Marine Biology and Ecology*, 313(2):375–387.

Seibel, B. A., Häfker, N. S., Trübenbach, K., Zhang, J., Tessier, S. N., Pörtner, H.-O., Rosa, R., and Storey, K. B. (2014). Metabolic suppression during protracted exposure to hypoxia in the jumbo squid, Dosidicus gigas, living in an oxygen minimum zone. *The Journal of Experimental Biology*, 217(14):2555–2568.

Seibel, B. A., Hochberg, F. G., and Carlini, D. B. (2000a). Life history of Gonatus onyx (Cephalopoda: Teuthoidea): deep-sea spawning and post-spawning egg care. *Marine Biology*, 137:519–526.

Seibel, B. A., Robison, B. H., and Haddock, S. H. D. (2005). Post-spawning egg care by a squid. *Nature*, 438(7070):929.

Seibel, B. A., Thuesen, E. V., and Childress, J. J. (1998). Flight of the vampire: ontogenetic gait-transition in Vampyroteuthis infernalis (Cephalopoda: Vampyromorpha). *The Journal of Experimental Biology*, 201:2413–2424.

Seibel, B. A., Thuesen, E. V., and Childress, J. J. (2000b). Light-Limitation on Predator-Prey Interactions: Consequences for Metabolism and Locomotion of Deep-Sea Cephalopods. *Biological Bulletin*, 198:284–298.

Seibel, B. A., Thuesen, E. V., Childress, J. J., and Gorodezky, L. A. (1997). Decline in Pelagic Cephalopod Metabolism with Habitat Depth Reflects Differences in Locomotory Efficiency. *Biological Bulletin*, 192:262–278.

Seibel, B. A. and Walsh, P. J. (2001). Potential impacts of CO2 injection on deep-sea biota. *Science*, 294(5541):319–320.

Semmens, J. M., Pecl, G. T., Villanueva, R., Jouffre, D., Sobrino, I., Wood, J. B., and Rigby, P. R. (2004). Understanding octopus growth: patterns, variability and physiology. *Marine and Freshwater Research*, 55(4):367–377.

Shadwick, R. E. (1994). Mechanical organization of the mantle and circulatory system of cephalopods. *Marine and Freshwater Behaviour and Physiology*, 25:69–85.

Shadwick, R. E., O'Dor, R. K., and Gosline, J. M. (1990). Respiratory and cardiac function during exercise in squid. *Canadian Journal of Zoology*, 68(4):792–798.

Shea, E. K., Ziegler, A., Faber, C., and Shank, T. M. (2018). Dumbo octopod hatchling provides insight into early cirrate life cycle. *Current Biology*, 28(4):R144–R145.

Sheumack, D. D., Howden, M. E. H., Spence, I., and Quinn, R. J. (1978). Maculotoxin: A Neurotoxin from the Venom Glands of the Octopus Hapalochlaena maculosa Identified as Tetrodotoxin. *Science*, 199:188–189.

Shigeno, S., Andrews, P. L. R., Ponte, G., and Fiorito, G. (2018). Cephalopod Brains: An Overview of Current Knowledge to Facilitate Comparison With Vertebrates. *Frontiers in Physiology*, 9:952.

Shimoda, L. A. and Polak, J. (2011). Hypoxia. 4. Hypoxia and ion channel function. *American Journal of Physiology - Cell Physiology*, 300:C951–C967.

Shoukimas, J., Adelman Jr., W. J., and Sege, V. (1977). Cation concentrations in the hemolymph of Loligo pealei. *Biophysical Journal*, 18:231–234.

Sigwart, J. D., Lyons, G., Fink, A., Gutowska, M. A., Murray, D., Melzner, F., Houghton, J. D. R., and Hu, M. Y.-a. (2015). Elevated pCO2 drives lower growth and yet increased calcification in the early life history of the cuttlefish Sepia officinalis (Mollusca: Cephalopoda). *ICES Journal of Marine Science*, pages 1–11.

Singh, J. and Padgett, R. A. (2009). Rates of in situ transcription and splicing in large human genes. *Nature Structural & Molecular Biology*, 16(11):1128–1133.

Small, D. P., Milazzo, M., Bertolini, C., Graham, H., Hauton, C., Hall-Spencer, J. M., and Rastrick, S. P. S. (2015). Temporal fluctuations in seawater pCO2 may be as important as mean differences when determining physiological sensitivity in natural systems. *ICES Journal of Marine Science*, pages 1–9.

Smith, P. J. S. and Boyle, P. R. (1983). The Cardiac Innervation of Eledone cirrhosa (Lamarck) (Mollusca: Cephalopoda). *Philosophical Transactions of the Royal Society of London B: Biological Sciences*, 300(1101):493–511.

Snyder, L. R. G. (1985). Low P50 in deer mice native to high altitude. *Journal of Applied Physiology*, 58(1):193–199.

Somero, G. N. (2004). Adaptation of enzymes to temperature: searching for basic "strategies". *Comparative Biochemistry and Physiology Part B*, 139:321–333.

Somero, G. N. (2018). RNA thermosensors: how might animals exploit their regulatory potential? *Journal of Experimental Biology*, 221:jeb162842.

Song, Y., Kang, M., Morfini, G., and Brady, S. T. (2016). Fast axonal transport in isolated axoplasm from the squid giant axon. In *Methods in Cell Biology*, volume 131, chapter 16, pages 331–348. Academic Press.

Spady, B. L., Watson, S.-A., Chase, T. J., and Munday, P. L. (2014). Projected near-future CO2 levels increase activity and alter defensive behaviours in the tropical squid Idiosepius pygmaeus. *Biology Open*, 2:1–8.

Speers-Roesch, B., Callaghan, N. I., MacCormack, T. J., Lamarre, S. G., Sykes, A. V., and Driedzic, W. R. (2016). Enzymatic capacities of metabolic fuel use in cuttlefish (Sepia officinalis) and responses to food deprivation: insight into the metabolic organization and starvation survival strategy of cephalopods. *Journal of Comparative Physiology B*, 186(6):711–725.

Speers-Roesch, B., Richards, J. G., Brauner, C. J., Connolly, S. R., Hickey, A. J. R., Wang, Y. S., and Renshaw, G. M. C. (2012). Hypoxia tolerance in elasmobranchs. I. Critical oxygen tension as a measure of blood oxygen transport during hypoxia exposure. *Journal of Experimental Biology*, 215(1):93–102.

Spicer, J. I. (1995). Oxygen and acid-base status of the sea urchin Psammechinus miliaris during environmental hypoxia. *Marine Biology*, 124:71–76.

Staaf, D. (2017). *Squid Empire: The rise and fall of the cephalopods*. ForeEdge.

Staaf, D. J., Camarillo-Coop, S., Haddock, S. H. D., Nyack, A. C., Payne, J., Salinas-Zavala, C. A., Seibel, B. A., Trueblood, L., Widmer, C., and Gilly, W. F. (2008). Natural egg mass deposition by the Humboldt squid (Dosidicus gigas) in the Gulf of California and characteristics of hatchlings and paralarvae. *Journal of the Marine Biological Association of the United Kingdom*, 88(4):759–770.

Staudinger, M. D., Buresch, K. C., Mäthger, L. M., Fry, C., McAnulty, S., Ulmer, K. M., and Hanlon, R. T. (2013). Defensive responses of cuttlefish to different teleost predators. *The Biological Bulletin*, 225(3):161–174.

Staudinger, M. D., Hanlon, R. T., and Juanes, F. (2011). Primary and secondary defences of squid to cruising and ambush fish predators: variable tactics and their survival value. *Animal Behaviour*, 81(3):585–594.

Stephens, P. J. and Atwood, H. L. (1982). Thermal acclimation in a crustacean neuromuscular system. *Journal of Experimental Biology*, 98:39–47.

Stocker, T. F. and Schmittner, A. (1997). Influence of CO2 emission rates on the stability of the thermohaline circulation. *Nature*, 388(6645):862–865.

Storey, K. B. and Storey, J. M. (1978). Energy Metabolism in the Mantle Muscle of the Squid, Loligo pealeii. *Journal of Comparative Physiology: B, Biochemical, Systemic, and Environmental Physiology*, 123:169–175.

Storey, K. B. and Storey, J. M. (1979). Octopine metabolism in the cuttlefish, Sepia officinalis: Octopine production by muscle and its role as an aerobic substrate for non-muscular tissues. *Journal of Comparative Physiology: B, Biochemical, Systemic, and Environmental Physiology*, 131(4):311–319.

Storey, K. B., Storey, J. M., Johansen, K., and Hochachka, P. W. (1979). Octopine metabolism in Sepia officinalis: effect of hypoxia and metabolite loads on the blood levels of octopine and related compounds. *Canadian Journal of Zoology*, 57:2331–2336.

Stramma, L., Johnson, G. C., Sprintall, J., and Mohrholz, V. (2008). Expanding oxygen-minimum zones in the tropical oceans. *Science*, 320(5876):655–658.

Strugnell, J., Norman, M., Drummond, A. J., and Cooper, A. (2004). Neotenous origins for pelagic octopuses. *Current Biology*, 14(8):300–301.

Strugnell, J. M., Norman, M. D., Vecchione, M., Guzik, M., and Allcock, A. L. (2014). The ink sac clouds octopod evolutionary history. *Hydrobiologia*, 725(1):215–235.

Suarez, R. K., Lighton, J. R. B., Brown, G. S., and O., M.-C. (1991). Mitochondrial respiration in hummingbird flight muscles. *Proceedings of the National Academy of Sciences of the United States of America*, 88:4870–4873.

Sunday, J. M., Bates, A. E., and Dulvy, N. K. (2011). Global analysis of thermal tolerance and latitude in ectotherms. *Proceedings of the Royal Society B: Biological Sciences*, 278(1713):1823–1830.

Sutton, M., Perales-Raya, C., and Gilbert, I. (2015). A phylogeny of fossil and living neocoleoid cephalopods. *Cladistics*, pages 1–11.

Tan, M. H., Li, Q., Shanmugam, R., Piskol, R., Kohler, J., Young, A. N., Liu, K. I., Zhang, R., Ramaswami, G., Ariyoshi, K., Gupte, A., Keegan, L. P., George, C. X., Ramu, A., Huang, N., Pollina, E. A., Leeman, D. S., Rustighi, A., Goh, Y. P. S., Consortium, G., Chawla, A., Sal, G. D., Peltz, G., Brunet, A., Conrad, D. F., Samuel, C. E., O'Connell, M. A., Walkley, C. R., Nishikura, K., and Li, J. B. (2017). Dynamic landscape and regulation of RNA editing in mammals. *Nature*, 550(7675):249–254.

Tanner, A. R., Fuchs, D., Winkelmann, I. E., Gilbert, M. T. P., Pankey, M. S., Ribeiro, Â. M., Kocot, K. M., Halanych, K. M., Oakley, T. H., da Fonseca, R. R., Pisani, D., and Vinther, J. (2017). Molecular clocks indicate turnover and diversification of modern coleoid cephalopods during the Mesozoic Marine Revolution. *Proceedings of the Royal Society of London B: Biological Sciences*, 284(1850).

Terwilliger, N. B. (1998). Functional adaptations of oxygen-transport proteins. *The Journal of Experimental Biology*, 201(Pt 8):1085–1098.

Thomas, J. M. and Beal, P. A. (2017). How do ADARs bind RNA? New protein-RNA structures illuminate substrate recognition by the RNA editing ADARs. *BioEssays*, 39(4):1600187.

Thompson, J. T. and Kier, W. M. (2006). Ontogeny of mantle musculature and implications for jet locomotion in oval squid Sepioteuthis lessoniana. *Journal of Experimental Biology*, 209(3):433–443.

Thonig, A., Oellermann, M., Lieb, B., and Mark, F. C. (2014). A new haemocyanin in cuttlefish (Sepia officinalis) eggs: sequence analysis and relevance during ontogeny. *EvoDevo*, 5(1):6.

Thore, S. (1949). Investigations on the "Dana" Octopoda. *Dana-Report No. 33*, pages 1–85.

Thurman, C. L. (1988). Rhythmic physiological color change in crustacea: A review. *Comparative Biochemistry and Physiology, Part C: Comparative Pharmacology*, 91(1):171–185.

Thurtle-Schmidt, D. M. and Lo, T.-W. (2018). Molecular Biology at the Cutting Edge: A Review on CRISPR/Cas9 Gene Editing for Undergraduates. *Biochemistry and Molecular Biology Education*, 46(2):195–205.

Thuy-Boun, A. S., Thomas, J. M., Grajo, H. L., Palumbo, C. M., Park, S., Nguyen, L. T., Fisher, A. J., and Beal, P. A. (2020). Asymmetric dimerization of adenosine deaminase acting on RNA facilitates substrate recognition. *Nucleic Acids Research*, 48(14):7958–7972.

Tomaselli, S., Bonamassa, B., Alisi, A., Nobili, V., and Locatelli, F. (2013). ADAR Enzyme and miRNA Story: A Nucleotide that Can Make the Difference. *International Journal of Molecular Sciences*, 14:22796–22816.

Tomita, A., Kreutzer, U., Adachi, S.-I., Koshihara, S.-y., and Jue, T. (2010). 'It's hollow': the function of pores within myoglobin. *The Journal of Experimental Biology*, 213:2748–2754.

Tommerdahl, A. P., Burnett, K. G., and Burnett, L. E. (2015). Respiratory properties of hemocyanin from wild and aquacultured penaeid shrimp and the effects of chronic exposure to hypoxia. *Biological Bulletin*, 228(3):242–252.

Trübenbach, K., Teixeira, T., Diniz, M., and Rosa, R. (2013). Hypoxia tolerance and antioxidant defense system of juvenile jumbo squids in oxygen minimum zones. *Deep Sea Research Part II: Topical Studies in Oceanography*, 95:209–217.

Trueblood, L. A., Onthank, K., Bos, N., Buller, L., Coast, A., Covrig, M., Edwards, E., Fratianni, S., Gano, M., Iwakoshi, N., Kim, E., Moss, K., Personius, C., Reynoso, S., and Springbett, C. (2022). Bathyal octopus, Muusoctopus leioderma, living in a world of acid: First recordings of routine metabolic rate and critical oxygen partial pressures of a deep water species under elevated pCO2. *Frontiers in Physiology*, 13:1039401.

Trueblood, L. A., Zylinski, S., Robison, B. H., and Seibel, B. A. (2015). An ethogram of the Humboldt squid Dosidicus gigas Orbigny (1835) as observed from remotely operated vehicles. *Behaviour*, pages 1–29.

Turner, C. (2015). *Verification of pH fluctuations in Narragansett Bay*. Master's thesis, University of Rhode Island.

Ubach, J., Zhang, X., Shao, X., Sudhof, T. C., and Rizo, J. (1998). Ca2+ binding to synaptotagmin: how many Ca2+ ions bind to the tip of a C2-domain? *The EMBO Journal*, 17(14):3921–3930.

Vaghy, P. L. (1979). Role of mitochondrial oxidative phosphorylation in the maintenance of intracellular pH. *Journal of Molecular and Cellular Cardiology*, 11:933–940.

Vale, R. D. and Fletterick, R. J. (1997). The design plan of kinesin motors. *Annual Review of Cell and Developmental Biology*, 13:745–777.

Vale, R. D. and Milligan, R. A. (2000). The way things move: Looking under the hood of molecular motor proteins. *Science*, 288(5463):88–95.

Vale, R. D., Reese, T. S., and Sheetz, M. P. (1985). Identification of a Novel Force-Generating Protein, Kinesin, Involved in Microtubule-Based Motility. *Cell*, 42(August):39–50.

Vallecillo-Viejo, I. C., Liscovitch-Brauer, N., Diaz Quiroz, J. F., Nemes, S., Rangan, K. J., Levinson, S. R., Eisenberg, E., and Rosenthal, J. J. C. (2020). Spatially regulated editing of genetic information within a neuron. *Nucleic Acids Research*, pages 1–13.

van der Lee, R., Lang, B., Kruse, K., Gsponer, J., de Groot, N. S., Huynen, M. A., Matouschek, A., Fuxreiter, M., and Babu, M. M. (2014). Intrinsically disordered segments affect protein half-life in the cell and during evolution. *Cell Reports*, 8(6):1832–1844.

van Elden, S. and Meeuwig, J. J. (2020). Wild observation of putative dynamic decapod mimicry by a cuttlefish (Sepia cf. smithi). *Marine Biodiversity*, 50:93.

van Giesen, L., Kilian, P. B., Allard, C. A., and Bellono, N. W. (2020). Molecular Basis of Chemotactile Sensation in Octopus. *Cell*, 183(3):594–604.e14.

Van Holde, K. E. and Cohen, L. B. (1965). Physical Studies of Hemocyanins. I. Characterization and Subunit Structure of Loligo peleai Hemocyanin. *Biochemistry*, 3(12):1803–1808.

Vidal, É. A. G. and Haimovici, M. (1998). Feeding and the possible role of the proboscis and mucus cover in the ingestion of microorganisms by rhynchoteuthion paralarvae (Cephalopoda: Ommastrephidae). *Bulletin of Marine Science*, 63(2):305–316.

Vidal, É. A. G., Villanueva, R., Andrade, J. P., Gleadall, I. G., Iglesias, J., Koueta, N., Rosas, C., Segawa, S., Grasse, B., Franco-Santos, R. M., Albertin, C. B., Caamal-Monsreal, C., Chimal, M. E., Edsinger-Gonzales, E., Gallardo, P., Le Pabic, C., Pascual, C., Roumbedakis, K., and Wood, J. (2014). Cephalopod culture: current status of main biological models and research priorities. In *Advances in Marine Biology*, volume 67, chapter 1, pages 1–98. Elsevier Ltd.

Villanueva, R. and Bustamante, P. (2006). Composition in essential and non-essential elements of early stages of cephalopods and dietary effects on the elemental profiles of Octopus vulgaris paralarvae. *Aquaculture*, 261:225–240.

Vitturi, R., Rasotto, M. B., and Farinella-Ferruzza, N. (1982). The chromosomes of 16 molluscan species. *Bollettino di zoologia*, 49(1-2):61–71.

Voight, J. R. (1995). Sexual dimorphism and niche divergence in a mid-water octopod (Cephalopoda: Bolitaenidae). *Biological Bulletin*, 189(2):113–119.

von Boletzky, S. (1987). Ontogenetic and phylogenetic aspects of the cephalopod circulatory system. *Experientia*, 43(5):478–483.

von Boletzky, S. and Hanlon, R. T. (1983). A review of the laboratory maintenance, rearing and culture of cephalopod molluscs. *Memoirs of the National Museum Victoria*, 44:147–187.

Von Brand, T., Rakestraw, N. W., and Renn, C. E. (1937). The experimental decomposition and regeneration of nitrogenous organic matter in sea water. *Biological Bulletin*, 72(2):165–175.

Walker, G. T. (1924). Correlation In Seasonal Variations Of Weather IX - A Further Study of World Weather. *Memoirs of the India Meteorological Department*, 24:275–333.

Wang, G. L., Jiang, B.-H., Rue, E. A., and Semenza, G. L. (1995). Hypoxia-inducible factor 1 is a basic-helix-loop-helix-PAS heterodimer regulated by cellular O2 tension. *Proceedings of the National Academy of Sciences*, 92(June):5510–5514.

Wang, Z. Y., Pergande, M. R., Ragsdale, C. W., and Cologna, S. M. (2022). Steroid hormones of the octopus self-destruct system. *Current Biology*, page S0960982222006613.

Wang, Z. Y. and Ragsdale, C. W. (2018). Multiple optic gland signaling pathways implicated in octopus maternal behaviors and death. *Journal of Experimental Biology*, 221(19):jeb185751.

Wang, Z. Y. and Ragsdale, C. W. (2019). Cephalopod Nervous System Organization.

Wanninger, A. and Wollesen, T. (2019). The evolution of molluscs. *Biological Reviews*, 94:102–115.

Warnke, K. M., Meyer, A., Ebner, B., and Lieb, B. (2011). Assessing divergence time of Spirulida and Sepiida (Cephalopoda) based on hemocyanin sequences. *Molecular Phylogenetics and Evolution*, 58(2):390–394.

Watanabe, K., Sakurai, Y., Segawa, S., and Okutani, T. (1996). Development of the ommastrephid squid Todarodes pacificus, from fertilized egg to rhynchoteuthion paralarva. *American Malacological Bulletin*, 13(1/2):73–88.

Watanabe, K. I., Bessho, Y., Kawasaki, M., and Hori, H. (1999). Mitochondrial genes are found on minicircle DNA molecules in the mesozoan animal Dicyema. *Journal of Molecular Biology*, 286(3):645–650.

Watson, J. D. and Crick, F. H. C. (1953). Molecular structure of nucleic acids: a structure for deoxyribose nucleic acid. *Nature*, 171(4356):737–738.

Webb, P. *Introduction to Oceanography*.

Webber, D. M. and O'Dor, R. K. (1985). Respiration and Swimming Performance of Short-finned Squid (Illex illecebrosus). *NAFO Sci. Coun. Studies*, 9:133–138.

Weber, R. E. and Vinogradov, S. N. (2001). Nonvertebrate Hemoglobins: Functions and Molecular Adaptations. *Physiological Reviews*, 81(2):569–628.

Weibel, E. R. and Hoppeler, H. (2005). Exercise-induced maximal metabolic rate scales with muscle aerobic capacity. *The Journal of Experimental Biology*, 208:1635–1644.

Weibel, E. R., Taylor, C. R., and Hoppeler, H. (1991). The concept of symmorphosis: A testable hypothesis of structure-function relationship. *Proceedings of the National Academy of Sciences of the United States of America*, 88:10357–10361.

Weight, F. F. and Erulkar, S. D. (1976). Synaptic transmission and effects of temperature at the squid giant synapse. *Nature*, 261:720–722.

Weiss, R. F. (1970). The solubility of nitrogen, oxygen and argon in water and seawater. *Deep-Sea Research and Oceanographic Abstracts*, 17(4):721–735.

Wells, M. J. (1980). Nervous control of the heartbeat in Octopus. *Journal of Experimental Biology*, 85:111–128.

Wells, M. J. (1983). Circulation in Cephalopods. In Saleuddin, A. S. M. and Wilbur, K. M., editors, *The Mollusca*, volume 5, chapter 5, pages 239–290. Academic Press, Inc.

Wells, M. J. (1990). Oxygen extraction and jet propulsion in cephalopods. *Canadian Journal of Zoology*, 68:815–824.

Wells, M. J. (1992). The cephalopod heart: The evolution of a high-performance invertebrate pump. *Experientia*, 48(9):800–808.

Wells, M. J. and Clarke, A. (1996). Energetics: the costs of living and reproducing for an individual cephalopod. *Philosophical Transactions of the Royal Society of London. Series B, Biological Sciences*, 351(1343):1083–1104.

Wells, M. J., Hanlon, R. T., Lee, P. G., and Dimarco, F. P. (1988). Respiratory and cardiac performance in Lolliguncula brevis (Cephalopoda, Myopsida): the effects of activity, temperature and hypoxia. *The Journal of Experimental Biology*, 138:17–36.

Wells, M. J., O'Dor, R. K., Mangold, K., and Wells, J. (1983). Feeding and metabolic rate in Octopus. *Marine Behaviour and Physiology*, 9:305–317.

Wells, M. J. and Smith, P. J. S. (1985). The ventilation cycle in Octopus. *Journal of Experimental Biology*, 116:375–383.

Wells, M. J. and Smith, P. J. S. (1987). The performance of the octopus circulatory system: A triumph of engineering over design. *Experientia*, 43:487–499.

Wells, M. J. and Wells, J. (1982). Ventilatory currents in the mantle of cephalopods. *The Journal of Experimental Biology*, 99:315–330.

Wells, M. J. and Wells, J. (1983). The circulatory response to acute hypoxia in Octopus. *The Journal of Experimental Biology*, 104:59–71.

Wells, M. J. and Wells, J. (1984). The effects of reducing gill area on the capacity to regulate oxygen uptake and on metabolic scope in a cephalopod. *Journal of Experimental Biology*, 108:393–401.

Wells, M. J. and Wells, J. (1985). Ventilation frequencies and stroke volumes in acute hypoxia in Octopus. *Journal of Experimental Biology*, 118:445–448.

Wells, M. J. and Wells, J. (1986). Blood flow in acute hypoxia in a cephalopod. *Journal of Experimental Biology*, 122:345–353.

Wells, M. J. and Wells, J. (1995). The control of ventilatory and cardiac responses to changes in ambient oxygen tension and oxygen demand in Octopus. *The Journal of Experimental Biology*, 198:1717–1727.

Wenger, R. H., Stiehl, D. P., and Camenisch, G. (2005). Integration of Oxygen Signaling at the Consensus HRE. *Science Signaling*, 306:re12.

Williams, L. W. (1902). The vascular system of the common squid, Loligo pealii. *The American Naturalist*, 36(430):787–794.

Williams, L. W. (1909). *The Anatomy of the Common Squid Loligo pealii, Lesueur*. Brill.

Williams, R. G. and Follows, M. J. (2011). *Ocean Dynamics and the Carbon Cycle: Principles and Mechanisms*. Cambridge University Press.

Williams, T. L., Senft, S. L., Yeo, J., Martín-Martínez, F. J., Kuzirian, A. M., Martin, C. A., Dibona, C. W., Chen, C.-T., Dinneen, S. R., Nguyen, H. T., Gomes, C. M., Rosenthal, J. J. C., MacManes, M. D., Chu, F., Buehler, M. J., Hanlon, R. T., and Deravi, L. F. (2019). Dynamic pigmentary and structural coloration within cephalopod chromatophore organs. *Nature Communications*, 10:1004.

Williamson, R. and Chrachri, A. (2004). Cephalopod neural networks. *Neurosignals*, 13(1-2):87–98.

Winslow, R. M. (2007). The role of hemoglobin oxygen affinity in oxygen transport at high altitude. *Respiratory Physiology & Neurobiology*, 158:121–127.

Wishner, K. F., Outram, D. M., Seibel, B. A., Daly, K. L., and Williams, R. L. (2013). Zooplankton in the eastern tropical north Pacific: Boundary effects of oxygen minimum zone expansion. *Deep Sea Research Part I: Oceanographic Research Papers*, 79:122–140.

Wittenberg, B. A., Briehl, R. W., and Wittenberg, J. B. (1965). Haemoglobins of Invertebrate Tissues: Nerve haemoglobins of Aphrodite, Aplysia and Halosydna. *Biochemical Journal*, 96:363–371.

Wolter, K. and Timlin, M. S. (1998). Measuring the strength of ENSO events: How does 1997/98 rank? *Weather*, 53(9):315–324.

Wozniak, M. J. and Allan, V. J. (2006). Cargo selection by specific kinesin light chain 1 isoforms. *The EMBO Journal*, 25:5457–5468.

Wright, P. A. (1995). Nitrogen excretion: three end products, many physiological roles. *The Journal of Experimental Biology*, 281(2):273–281.

Wright, T. J. and Davis, R. W. (2015). Myoglobin oxygen affinity in aquatic and terrestrial birds and mammals. *The Journal of Experimental Biology*, 218:2180–2189.

Wu, L., Fan, J., and Belasco, J. G. (2006). MicroRNAs direct rapid deadenylation of mRNA. *Proceedings of the National Academy of Sciences of the United States of America*, 103(11):4034–4039.

Wu, R. S. S. (2002). Hypoxia: from molecular responses to ecosystem responses. *Marine Pollution Bulletin*, 45:35–45.

Wuchter, C., Abbas, B., Coolen, M. J., Herfort, L., Van Bleijswijk, J., Timmers, P., Strous, M., Teira, E., Herndl, G. J., Middelburg, J. J., Schouten, S., and Damsté, J. S. S. (2006). Archaeal nitrification in the ocean. *Proceedings of the National Academy of Sciences of the United States of America*, 103(33):12317–12322.

Wyman, J. (1964). Linked functions and reciprocal effects in hemoglobin: a second look. *Advances in Protein Chemistry*, 19:223–286.

Xavier, J. C., Peck, L. S., Fretwell, P., and Turner, J. (2016). Climate change and polar range expansions: Could cuttlefish cross the Arctic? *Marine Biology*, 163(4):78.

Xu, G. and Zhang, J. (2014). Human coding RNA editing is generally nonadaptive. *Proceedings of the National Academy of Sciences*, 111(10):3769–3774.

Yablonovitch, A. L., Deng, P., Jacobson, D., and Li, J. B. (2017). The evolution and adaptation of A-to-I RNA editing. *PLoS Genetics*, 13(11):e1007064.

Yahalomi, D., Atkinson, S. D., Neuhof, M., Sally Chang, E., Philippe, H., Cartwright, P., Bartholomew, J. L., and Huchon, D. (2020). A cnidarian parasite of salmon (Myxozoa: Henneguya) lacks a mitochondrial genome. *Proceedings of the National Academy of Sciences of the United States of America*, 117(10):5358–5363.

Yamaguchi, T., Kawakami, Y., and Matsuyama, M. (2015). Migratory routes of the swordtip squid Uroteuthis edulis inferred from statolith analysis. *Aquatic Biology*, 24(1):53–60.

Yan, Y., Lu, Z., Wang, T., Chen, Y., Yang, J., Guo, B., Jiang, L., Wu, C., and Liu, L. (2018). Determination and Analysis of the Complete Mitochondrial DNA Sequence of Octopus dollfusi (Mollusca: Cephalopoda: Octopodidae) from China. *Pakistan Journal of Zoology*, 50(2):463–472.

Yang, W., Chendrimada, T. P., Wang, Q., Higuchi, M., Seeburg, P. H., Shiekhattar, R., and Nishikura, K. (2006). Modulation of microRNA processing and expression through RNA editing by ADAR deaminases. *Nature Structural & Molecular Biology*, 13(1):13–21.

Yang, W. T., Hixon, R. F., Turk, P. E., Krejci, M. E., Hulet, W. H., and Hanlon, R. T. (1986). Growth, behavior, and sexual maturation of the market squid, Loligo opalescens, cultured through the life cycle. *Fishery Bulletin*, 84(4):771–798.

Yoshida, M.-a., Shigeno, S., Tsuneki, K., and Furuya, H. (2010). Squid vascular endothelial growth factor receptor: A shared molecular signature in the convergent evolution of closed circulatory systems. *Evolution & Development*, 12(1):25–33.

Young, J. Z. (1963). The number and sizes of nerve cells in Octopus. *Proceedings of the Zoological Society of London*, 140(2):229–254.

Young, R. E. (1972). Brooding in a Bathypelagic Octopus. *Pacific Science*, 26:400–404.

Young, R. E. (1978). Vertical distribution and photosensitive vesicles of pelagic cephalopods from Hawaiian waters. *Fishery Bulletin*, 76(3):583–615.

Young, R. E. and Mencher, F. M. (1980). Bioluminescence in mesopelagic squid: Diel color change during counterillumination. *Science*, 208(4449):1286–1288.

Young, R. E. and Roper, C. F. (1976). Bioluminescent countershading in midwater animals: evidence from living squid. *Science*, 191(4231):1046–1048.

Young, R. E., Vecchione, M., and Donovan, D. T. (1998). The evolution of coleoid cephalopods and their present biodiversity and ecology. *South African Journal of Marine Science*, 20(1):393–420.

Zachar, P. C. and Jonz, M. G. (2012). Neuroepithelial cells of the gill and their role in oxygen sensing. *Respiratory Physiology & Neurobiology*, 184(3):301–308.

Zakon, H. H. (2012). Adaptive evolution of voltage-gated sodium channels: The first 800 million years. *Proceedings of the National Academy of Sciences*, 109(1):10619–10625.

Zakroff, C., Mooney, T. A., and Wirth, C. (2017). Ocean acidification responses in paralarval squid swimming behavior using a novel 3D tracking system. *Hydrobiologia*.

Zeebe, R. E. (2012). History of Seawater Carbonate Chemistry, Atmospheric CO2, and Ocean Acidification. *Annual Review of Earth and Planetary Sciences*, 40(1):141–165.

Zeidberg, L. D. and Robison, B. H. (2007). Invasive range expansion by the Humboldt squid, Dosidicus gigas, in the eastern North Pacific. *Proceedings of the National Academy of Sciences of the United States of America*, 104(31):12948–12950.

Zhang, Q., Dai, X., Cong, Y., Zhang, J., Chen, D.-H., Dougherty, M. T., Wang, J., Ludtke, S. J., Schmid, M. F., and Chiu, W. (2013). Cryo-EM Structure of a Molluscan Hemocyanin Suggests Its Allosteric Mechanism. *Structure*, 21(4):604–613.

Zhang, X., Mao, Y., Huang, Z., Qu, M., Chen, J., Ding, S., Hong, J., and Sun, T. (2012). Transcriptome Analysis of the Octopus vulgaris Central Nervous System. *PLOS ONE*, 7(6):e40320.

Zhang, X., Rizo, J., and Südhof, T. C. (1998). Mechanism of Phospholipid Binding by the C2A-Domain of Synaptotagmin I. *Biochemistry*, 37:12395–12403.

Zhong, P. and Huang, H. (2017). Recent progress in the research of cold-inducible RNA-binding protein. *Future Science OA*, 3(4):FSO246.

Zhou, W., Chung, I., Liu, Z., Goldin, A. L., and Dong, K. (2004). A Voltage-Gated Calcium-Selective Channel Encoded by a Sodium Channel-like Gene. *Neuron*, 42:101–112.

Zhu, Y. C. and Cooper, R. L. (2018). Cold Exposure Effects on Cardiac Function and Synaptic Transmission at the Neuromuscular Junction in Invertebrates. *International Journal of Zoological Research*, 14:49–60.

Zielinski, S., Lee, P. G., and Pörtner, H.-O. (2000). Metabolic performance of the squid Lolliguncula brevis (Cephalopoda) during hypoxia: an analysis of the critical PO2. *Journal of Experimental Marine Biology and Ecology*, 243(2):241–259.

Zwiazek, J. J., Xu, H., Tan, X., Navarro-Ródenas, A., and Morte, A. (2017). Significance of oxygen transport through aquaporins. *Scientific Reports*, 7:40411.

Zylinski, S., How, M. J., Osorio, D., Hanlon, R. T., and Marshall, N. J. (2011). To Be Seen or to Hide: Visual Characteristics of Body Patterns for Camouflage and Communication in the Australian Giant Cuttlefish Sepia apama. *The American Naturalist*, 177(5):681–690.

Zylinski, S. and Johnsen, S. (2011). Mesopelagic cephalopods switch between transparency and pigmentation to optimize camouflage in the deep. *Current Biology*, 21:1937–41.

Zylinski, S., Osorio, D., and Shohet, A. J. (2009). Perception of edges and visual texture in the camouflage of the common cuttlefish, Sepia officinalis. *Philosophical Transactions of the Royal Society of London. Series B, Biological Sciences*, 364:439–448.